Cellular targets of HIV-1 VPU

Vigan, Raphael

Awarding institution:
King's College London

Title: Cellular targets of HIV-1 VPU

Author: Raphaël Vigan

CELLULAR TARGETS OF HIV-1 VPU

Raphaël Vigan

A thesis submitted to the University of London for the degree of Doctor of Philosophy

Department of Infectious Diseases
King's College London
School of Medicine
London - SE1 9RT

- February 2013 -

Declaration

I, Raphaël Vigan, confirm that the work presented in this thesis is my own. Where information has been derived from other sources, I confirm that this has been indicated in the thesis.

London, 08.08.2012
Raphaël Vigan

“ The scientist is not a person who gives the right answers, he's one who asks the right questions. ”

Claude Lévi-Strauss

Acknowledgements

The work presented in this thesis was carried out between February 2009 and April 2012 in the department of infectious diseases at King's college London.

In my daily work I have been blessed with a friendly and cheerful group of brilliant scientists. I would like to express my deepest gratitude to all members of Stuart Neil's group; Tonya Kueck (Kück) for her constant attention and help. Suzy Willey/Pickering and Rui Pedro Galão for their experience, wisdom and encouragement. I would also like to thank Julia Weinelt, Toshana Foster and Grégory Berger.

I am especially grateful to Dr Anna Le Tortorec who helped me considerably at the beginning of my project.

I also thank the members of Juan Martin-Serrano's group for their precious feedbacks in lab meetings.

I am extremely grateful to my thesis committee, Michael Malim, Juan Martin-Serrano, Stipo Jurcevic and Michael Linden for having monitored my progression over these four years.

I would like to express my sincerest gratitude to my supervisor, Dr Stuart Neil, who has supported me throughout my thesis with his patience and knowledge. On his side I have learnt so much about science and " life " in general. I dedicate this thesis to his commitment, I could not hope for a better and friendlier supervisor.

I would particularly like to acknowledge my partner Claire Péan. She has been a constant source of support-emotional and moral, and she gave me useful guidance.

My family has been a constant source of support; In particular, I would like to thank my mother who has always believed in me and encouraged me all these years since I left home.

Abstract

Aside from the typical retroviral *gag*, *pol*, and *env* genes, HIV-1 encodes a set of accessory proteins. Amongst those, Vpu modulates the expression of several cell surface receptors within the infected cell to promote HIV-1 replication. Particularly, Vpu enhances virus release by overcoming the antiviral action of tetherin.

HIV-1 is not the only virus to have evolved countermeasures to inactivate tetherin. Here we have investigated the strategy employed by Kaposi's sarcoma-associated herpesvirus (KSHV) to escape from tetherin-mediated restriction of virus particle release. We have found that KSHV encodes a ubiquitin ligase, K5, that ubiquitinates tetherin on its cytoplasmic tail to target it for endolysosomal degradation.

We then assessed the determinants in the Vpu transmembrane domain required to antagonize tetherin. Three amino acid residues that form one face of the transmembrane region of Vpu were found to be important for the interaction with tetherin. In contrast to Vpu from HIV-1 Group M, those encoded by Group O have not acquired the capacity to counteract tetherin. The defects map to the transmembrane domain and the membrane-proximal hinge region of the first alpha helix of the cytoplasmic tail; both are respectively defective for tetherin binding and trans-Golgi network-associated subcellular localization.

As the panel of Vpu's targets is increasing, we have collaborated with Paul Lehner's group to identify new cellular substrates of Vpu. The glutamine transporter, SNAT-1, was identified by proteomic screening (SILAC). SNAT-1 is downregulated and degraded in HIV-1 infected $CD4^+$ T cells. We are currently investigating the effects of Vpu-mediated SNAT-1 degradation and glutamine limitation on virus growth and cell proliferation/survival in primary $CD4^+$ infected T cells. In parallel, we have investigated the molecular mechanism by which Vpu achieves SNAT-1 depletion.

Table of Contents

List of Figures

Chapter 1

Chapter 4

Chapter 5

Chapter 6

Chapter 7

List of Tables

Chapter 1

Chapter 3

Chapter 7

Abbreviations

AAV	Adeno-associated virus
Ab	Antibody
agm	African green monkey
AGS	Aicardi-Goutières syndrome
AICD	Activation-induced cell death
AIDS	Acquired immunodeficiency syndrome
AP-1/2	Adaptor protein complex 1/2
APC	Antigen-presenting cell
APOBEC3	Apolipoprotein B mRNA-editing enzyme polypeptide like
ATP	Adenosine triphosphate
AZT	Azidothymidine
BCN	Broadly cross-neutralizing antibody
bp	Base pair(s)
BSA	Bovine serum albumin
BST-2	Bone marrow stromal cell antigen 2
CA	Capsid
cDNA	Complementary DNA
CFSE	Carboxyfluorescein succinimidyl ester
cpz	Chimpanzee
CsA	Cyclosporine
CT	Cytoplasmic tail
CTD	C-terminal domain
CTL	Cytotoxic T lymphocytes
CypA	Cyclophilin A
DC	Dendritic cell
DMEM	Dulbecco's modified eagle medium
DMSO	Dimethyl sulfoxide
DNA	Deoxyribonucleic acid
dNTP	Deoxyribonucleotide triphosphate
DTT	Dithiothreitol
E.*coli*	*Escherichia coli*
ECL	Enhanced chemiluminescence
EDTA	Ethylenediaminetetraacetic acid
Env	Envelope
ER	Endoplasmic reticulum
ERAD	Endoplasmic-reticulum-associated protein degradation
ESCRT	Endosomal sorting complex required for transport
EST	Expression sequence tag
FACS	Fluorescence-activated cell sorting
FBS	Fetal bovine serum
FDA	Food and drug administration
FIV	Feline immunodeficiency virus
FRET	Fluorescence resonance energy transfer
Fv1	Friend virus susceptibility 1
GABA	γ-Aminobutyric acid
Gag	Group-specific antigen
GALT	Gut-associated lymphoid tissue
GFP	Green fluorescent protein
Gln	Glutamine
gor	Gorilla
gp	Glycoprotein
GPI	Glycosylphosphatidylinositol
gsn	Greater spot-nosed monkey
HA	Hemagglutinin (Influenza A)
HAART	Highly active antiretroviral therapy
HHV-8	Human herpesvirus 8
HIV-1	Human immunodeficiency virus type 1

HIV-2	Human immunodeficiency virus type 2
HLA	Human leukocyte antigen
HRP	Horseradish peroxidase
HSC	Hematopoietic stem cell
Hsp90	Heat shock protein 90
HTLV	Human T-lymphotropic virus
hu	Human
IFN	Interferon
Ig	Immunoglobulin
IN	Integrase
IRES	Internal ribosome entry site
ISG	Interferon-stimulated gene
IU	Infectious unit
kb	Kilobase
kDa	Kilo Dalton
KSHV	Kaposi's sarcoma-associated herpesvirus
LAV	Lymphadenopathy-associated virus
LB	Luria Broth
LEDGF	Lens epithelium derived growth factor
LTR	Long terminal repeat
MA	Matrix
mAb	Monoclonal antibody
mac	Macaque
MARCH	Membrane-associated RING-CH
MFI	Mean fluorescence intensity
mg	Milligram
MHC	Major histocompatibility complex
ml	Milliliter
MLV	Murine leukemia virus
mM	Millimolar
MOI	Multiplicity of infection
mRNA	Messenger RNA
mTOR	Mammalian target of rapamycin
MVB	Multivesicular body
NC	Nucleocapsid
NES	Nuclear export signal
NFAT	Nuclear factor of activated T-cell
NF-κB	Nuclear factor kappa B
ng	Nanogram
NK	Natural killer
NKT	Natural killer T
NLS	Nuclear localization signal
nM	Nanomolar
NMR	Nuclear magnetic resonance
NNRTI	Non-nucleoside reverse transcriptase inhibitor
NPC	Nuclear pore complex
NRTI	Nucleoside reverse transcriptase inhibitor
NWM	New world monkey
OD	Optical density
ORF	Open reading frame
OWM	Old world monkey
PAMP	Pathogen-associated molecular pattern
PBMC	Peripheral blood mononuclear cell
PBS/pbs	Phosphate-buffered saline / Primer binding site
PCR	Polymerase chain reaction
pDC	Plasmacytoid dendritic cell
PDI	Protein disulphide-isomerase
PE	Phycoerythrin
PEI	Polyethylenimine
pH	Potential hydrogen
PIC	Pre-integration complex
PM	Plasma membrane

Pol	Polymerase
PPT	Polypurine tract
PR	Protease
PRR	Pattern-recognition receptor
Pts	Pan troglodytes schweinfuthii
Ptt	Pan troglodytes troglodytes
rcm	Red-capped mangabey
rh	Rhesus
RING	Really interesting new gene
RLU	Relative light unit
RNA	Ribonucleic acid
rpm	Revolution per minute
RRE	Rev response element
RT	Reverse transcriptase
SAMHD1	Sterile alpha motif- and metal-dependent phosphohydrolase domain-containing protein 1
SDS-PAGE	Sodium dodecyl sulfate polyacrylamide gel electrophoresis
SEM	Standard error of the mean
shRNA	Small hairpin RNA
SILAC	Stable isotope labeling by amino acids in cell culture
siRNA	Small interfering RNA
SIV	Simian immunodeficiency virus
SLC	Solute carrier
sm	Sooty mangabey
SNAT-1	Sodium coupled neutral amino acid transporter 1
SU	Surface
tan	Tantalus monkey
TAR	Trans-activation response
Tat	Trans-activator of transcription
TCR	T-cell receptor
TEM	Transmission electron microscopy
TGN	Trans-Golgi network
THN	Tetherin
TLR	Toll-like receptor
TM	Transmembrane
TRIM	Tripartite motif
Tsg101	Tumor susceptibility gene 101
Ub	Ubiquitin
UBAP1	Ubiquitin-associated protein 1
UPS	Ubiquitin-proteasome system
v/v	Volume/volume
Vif	Viral infectivity factor
VLP	Virus-like particle
Vpr	Viral protein R
Vpu	Viral protein U
VS	Virological synapse
VSV-G	Vesicular stomatitis virus G glycoprotein
w/v	Weight/volume
Wt	Wild-type
YFP	Yellow fluorescent protein
µg	Microgram
µl	Microliter
µM	Micromolar

Chapter 1 Introduction

1.1 Discovery and Origins of HIV

Acquired Immune Deficiency Syndrome (AIDS) was the name given to a new disease that caused loss of $CD4^+$ T lymphocytes in increasing numbers of young homosexual men in the early 1980's in the United States. These patients displayed a severely compromised immune system that led to unusual opportunistic infections such as *Pneumocystis carinii* pneumonia. At the time, the syndrome did not match with any of the diseases listed in the medical literature indicating that a new pathogenic agent was responsible. Epidemiologic analyses suggested that this new pathogen was sexually transmitted.

In 1983, Luc Montagnier and Françoise Barré-Sinoussi reported the detection of reverse transcriptase activity in a culture of lymph node cells taken from a patient with AIDS-related-lymphadenopathy (1). They suggested that the etiologic agent was a retrovirus immunologically different from the only other known human retrovirus, HTLV. One year later, a research group led by Robert C. Gallo isolated and characterized a retrovirus from numerous AIDS patients (2, 3). Later studies revealed that those two viruses were identical, and ultimately, human immunodeficiency virus type 1 (HIV-1) was chosen to designate the cause of AIDS. In 2008, Françoise Barré-Sinoussi and Luc Montagnier received the Nobel Prize in Physiology/Medicine for the discovery of HIV-1.

In 1986, a morphologically similar but antigenically distinct virus was found to cause AIDS in patients in western Africa (4). This new virus, termed human immunodeficiency virus type 2 (HIV-2) was closely related to a simian virus that infected captive macaques (5, 6). From this observation came the idea that additional AIDS-causing viruses could exist in non-human primate hosts. Several simian immunodeficiency viruses (SIVs) were isolated from various different primates from sub-Saharan Africa, including African green monkeys, sooty mangabeys, mandrills, chimpanzees and many others. In contrast to HIV-1, these SIVs were found to be non-pathogenic in many of their natural hosts despite high plasma viral loads. Through comparison with sequences of SIVs, HIV-1 was proposed to result from the transmission of a sub-lineage of SIVcpz infecting chimpanzees from south-eastern Cameroon (SIVcpz Ptt-Pan troglodytes troglodytes) (7-10). The other SIVcpz lineage infecting chimpanzees from eastern Africa, SIVcpz Pts, displays a high degree of divergence from SIVcpz Ptt, and has not been transmitted to humans. Presumably, SIVcpz Ptt might have been better equipped to adapt to the human host than SIVcpz Pts, particularly in overcoming restriction factors such as tetherin (11).

Geographical and genetic evidence suggest that SIVcpz in chimpanzees is derived from two different lineages of infected monkeys, the red-capped mangabeys and various Cercopithecus species (greater spot-nosed, mustached and mona monkeys) (12). Since chimpanzees are known to hunt and kill other mammals, including monkeys, it is likely that they acquired SIVs in the context of predation. It is also presumably the same way that humans have acquired the

ape precursor, through bushmeat hunting. But whatever the circumstances, it seems that human-ape encounters in west central Africa resulted in four independent cross-species transmission events giving rise to distinct lineages, termed groups M, N, O and P. Group M (Major) was the first to be discovered and it represents the most virulent form of HIV at the origin of the worldwide pandemic. Group O (Outlier) was discovered in 1990 and is much less prevalent than group M (13, 14). It represents less than 1% of global HIV-1 infections, and is largely restricted to Cameroon, Gabon, and neighbouring countries (15). Group N (non-M and non-O) was isolated in 1998 and is even more rare than group O with only 13 documented cases in total (16). Finally, group P was discovered in 2009 in a Cameroonian woman living in France (17).

The probable location of the early pandemic has been identified in the area around Kinshasa, then called Léopoldville (18). In that region, a human sample dating to 1959 and containing HIV-1 was found (19). Based on phylogenetic and statistical analyses, the last common ancestor of HIV-1 group M was extrapolated to around 1910-1930 (20). Léopoldville was the largest city in the region at that time and thus a likely destination for a newly emerging infection. Rivers, which served as major routes of travel and commerce, would have provided a link between the chimpanzee reservoir of HIV-1 group M in south-eastern Cameroon and Léopoldville on the banks of the Congo (21).

HIV-1 group M is classified into nine subtypes or clades (A-D, F-H, J, K) that result from transmission of the founder HIV-1 group M into different human populations (18). It is likely that HIV-1 group M has diversified in the Democratic Republic of the Congo and then has spread worldwide. For instance, subtype B, which accounts for the majority of HIV- infections in Europe and the Americas, arose from a single African strain that appears to have first spread to Haiti in the 1960s and then onward to the US and other western countries (22). Clades A and C account for the majority of infections worldwide. Clade C is mainly found in southern Africa and India, whereas clades A and D are frequent in central and eastern Africa.

While HIV-1 has infected millions of people worldwide, HIV-2 has remained largely restricted to West Africa, mainly in Guinea-Bissau and Senegal. HIV-2-infected patients tend to have lower viral loads than HIV-1, which may explain the lower transmission rate of HIV-2 and the near absence of mother-to-infant transmissions (23). In fact, most individuals infected with HIV-2 do not progress to AIDS. HIV-2 originates from multiple cross-species transmissions of SIVsmm from sooty mangabeys (24-26). SIVsmm also gave rise to pathogenic SIVmac. SIVsmm was found to be non-pathogenic in its natural host but was accidentally transmitted to macaques in captivity through inoculation of various species of macaques with blood/tissues from naturally infected sooty mangabeys (27).

1.2 The AIDS Pandemic

1.2.1 Report

Since its identification almost thirty years ago, HIV-1 has infected approximately 60 million people and caused more than 30 million deaths (UNAIDS 2010, Global Report). The most recent report on the AIDS epidemic, based on data collected from 182 countries, was conducted by UNAIDS and published in 2010. In this study, it is reported that an estimated number of 33.3 million people were living with HIV at the end of 2009 compared with 26.2 million in 1999 (27 % increase), despite a decrease of the annual number of new infections per year. In 2009, an estimated 2.6 million people became newly infected with HIV and 1.8 million people died of AIDS-related illness (Figure 1.1).

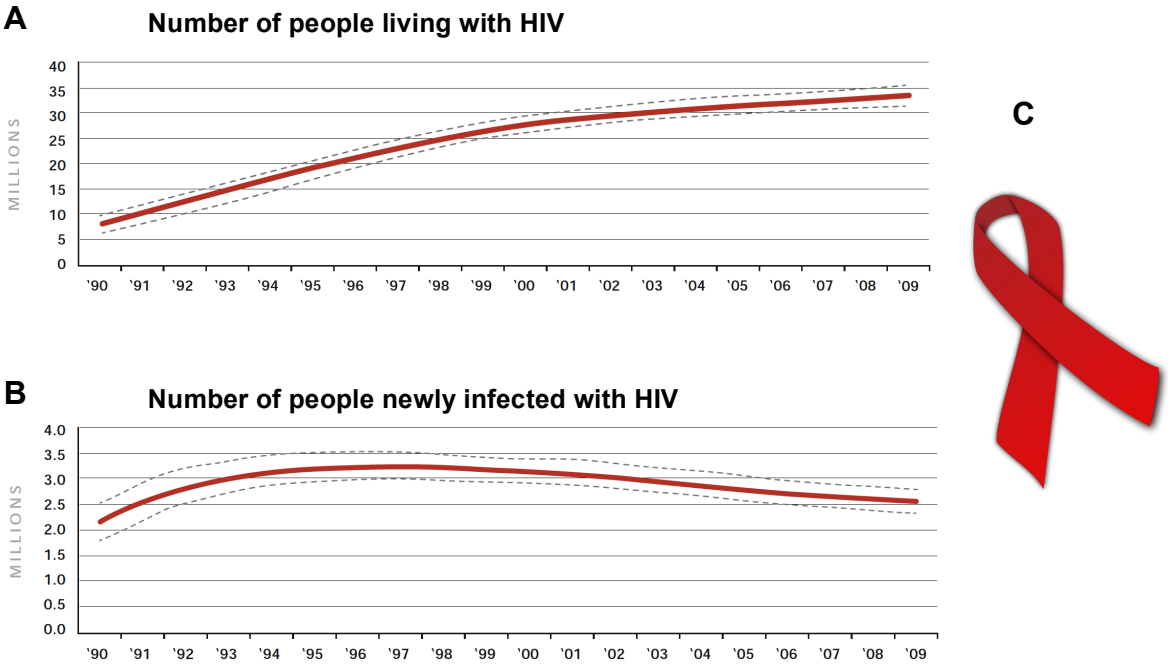

Figure 1.1: HIV infections from 1990 to 2009.

A: Number of people living with HIV-1 from 1990 to 2009. **B:** Number of people newly infected with HIV per year between 1990 and 2009. Source: The 2010 UNAIDS Report on the global AIDS epidemic. **C:** The red ribbon is the universal symbol of awareness and support for those living with HIV. The idea of the red ribbon comes from a New York arts organisation including photographers, painters, filmmakers and costume designers sat around in a gallery space in New York' s East Village in 1991 to discuss a new project for Visual AIDS.

Although HIV/AIDS is found in all parts of the world, some areas are more afflicted than others. The worst affected region is sub-Saharan Africa, where in a few countries more than one in five adults is infected with HIV (Figure 1.2).

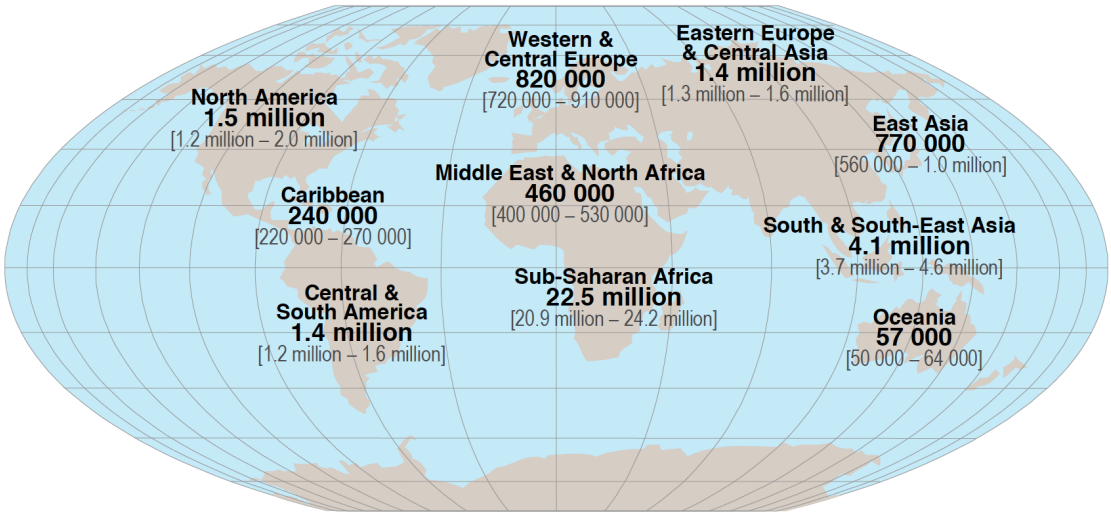

Figure 1.2: Global view of HIV infection.

This maps displays by geographical zones the number of people (adults and children) estimated to be living with HIV at the end of 2009 out of a total of 33.3 million HIV-infected individuals worldwide. Source: The 2010 UNAIDS Report on the global AIDS epidemic.

1.2.2 HIV-1 Transmission and Pathogenesis

The major mode of HIV transmission is through mucosal surfaces during sexual contact. HIV can also be transmitted by exposure to infected body fluids or tissues and from mother to child during delivery, and after delivery via breastfeeding, and in rare cases during pregnancy. Many HIV-1 infections also occur amongst intravenous drug users.

Dissemination of HIV through the body is believed to originate from a single infected cell. Initially, the founder virus preferentially infects $CD4^+$ T cells present at sites of infection with high levels of CD4 and expressing the CCR5 co-receptor. Mucosal $CD4^+$ memory T cells constitute the primary cells targeted by HIV-1. In approximately 50% of cases, at some point during infection, the virus evolves to infect a broader range of T cell subsets including naive $CD4^+$ T cells by switching its co-receptor usage from CCR5 to CXCR4, and this is generally associated with a faster disease progression (28).

The time course of HIV infection can be divided into four different phases based on the measurement of two markers, the $CD4^+$ T cell count in the blood and viremia (reviewed in (29)) (Figure 1.3). During the first phase, called eclipse, the founder virus starts replicating at the initial site of infection. As the virus multiplies, it gradually spreads to other tissues and organs. At that time, the viremia and immune responses directed against HIV are still low. It is believed

that it is during this short period of time, the first few weeks post-exposure, that the virus causes most of its irreversible damages to the host. This damage occurs predominantly in tissues other than the peripheral blood, particularly the gastrointestinal tract where massive depletion of $CD4^+$ T cells is observed. The eclipse phase is then followed by a phase where high levels of viral load are detected in the blood accompanied by high levels of infected $CD4^+$ T cells in the blood and in the lymph nodes. It is during this period that the viremia reaches its peak and that immune responses specifically directed against HIV start to be detected. This includes both the detection of HIV-1 Gag^{p24} antibodies defining seroconversion and $CD8^+$ T cells specific to HIV viral antigens. As a result of theses responses, the peak of viremia then declines and from this point a longer phase of HIV infection establishes. This phase, called "chronic", is characterized by a gradual fall of $CD4^+$ T cells while plasma viral loads persist slowly at increasing levels (30). Over the years, as $CD4^+$ T cells decline, their number becomes so low that the immune system is too compromised to cope with other infectious agents. In that context, opportunistic infections begin to appear and ultimately lead to the patient death.

Therefore, the hallmark of HIV infection is the depletion of $CD4^+$ T cells and subsequent loss of immune competence. However, the factors that cause this massive depletion are still debated (reviewed in (31, 32)). The first explanation is that HIV causes loss of $CD4^+$ T lymphocytes by directly infecting and killing those cells. But this does not account for the death of bystander cells that are not productively infected. In many of these cells, particularly naive $CD4^+$ T cells, HIV infection is aborted after viral entry as reverse transcription is initiated but fails to reach completion (33). As a result these cells accumulate reverse transcripts in their cytoplasm that activate a host defence program that elicits pro-apoptotic and pro-inflammatory response leading to cell death. Various factors have been proposed to account for the death of bystander cells including the action of host derived factors like TNF, Fas ligand and viral factors like Tat, Vpr and Nef released from productively infected cells. Finally, high level of immune activation is also a major cause of $CD4^+$ T cells depletion. This constitutes a major outcome of pathogenic HIV infection whereas non-pathogenic SIV infections lack this exaggerated immune activation (reviewed in (34, 35)).

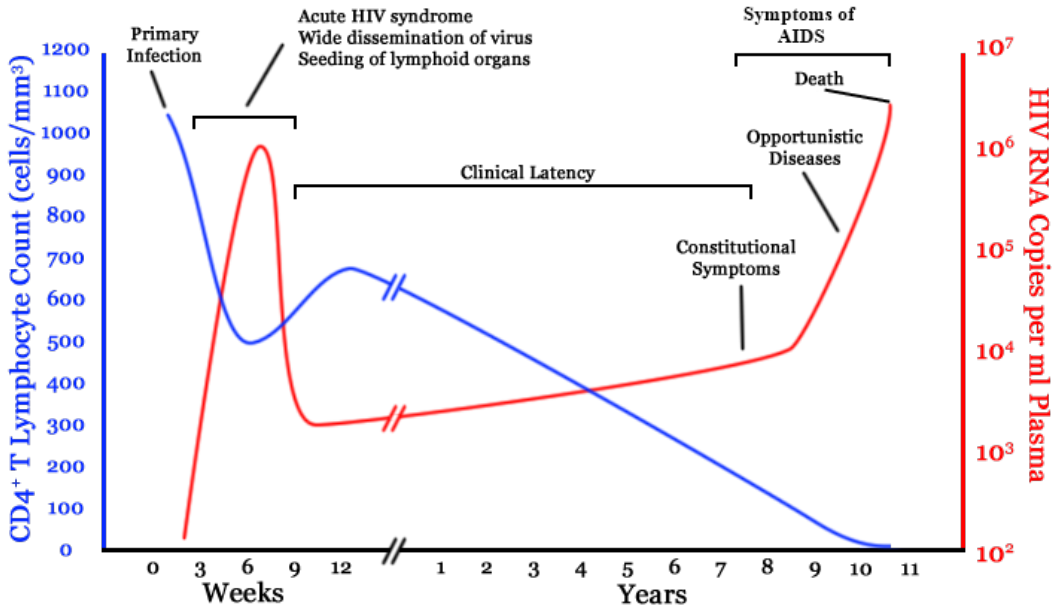

Figure 1.3: Time course of HIV infection.

Evolution of $CD4^+$ T lymphocytes count and levels of HIV RNA copies in the blood over the course of untreated HIV infection. Figure adapted from (30).

1.2.3 Treatment and Prevention

In the fight against the AIDS pandemic, research aiming to find preventive or curative medicines has been extensively studied. Measures for treatment of HIV-1 infections are represented by a panoply of twenty-four FDA-approved antiviral drugs that can suppress HIV-1 replication *in vivo* to undetectable levels when used in combination. A better understanding of the HIV-1 replication cycle has been essential in the development of such antiviral drugs. These drugs can be classified into several groups based on which phase of the virus life cycle they target (reviewed in (36)): nucleoside-analogue reverse transcription inhibitors (NRTIs), non-nucleoside reverse transcriptase inhibitors (NNRTIs), integrase inhibitors, protease inhibitors, fusion inhibitors, and co-receptor antagonists. Combination anti-retroviral therapy, also known as HAART (Highly Active Anti-Retroviral Therapy) has been shown to dramatically suppress viral replication and reduce the plasma HIV viral load to below the limits of detection (< 50 RNA copies/ml). HIV-1-infected individuals on HAART display significant reconstitution of their immune system, an increase but not complete reconstitution of $CD4^+$ T cells, and their life expectancy is increased (37, 38). However, even after several years of treatment, HAART fails to eradicate HIV-1 infection because viruses can persist as a reservoir of latent/inactive forms (reviewed in (39)). Latently infected cells are generated when activated $CD4^+$ T cells, the major target cells for HIV-1, are infected and survive long enough to revert back to a resting memory

state. In this state, $CD4^+$ T cells are not permissive for viral gene expression, and thus remain protected from immune recognition and drug therapy. The absence of Tat expression in these cells may contribute to maintain the reservoir. Once antiviral drugs are stopped these latent viruses are re-activated and can establish chronic infection again.

In many cases, long-term therapy with HAART induces toxicities, persisting inflammation and immune activation in treated-patients. The other reason for treatment failure is due to the ability of HIV-1 to develop drug-resistant escape mutants. Even though the Pol polyprotein is the most conserved across HIV strains, Pol enzymes targeted by antiviral drugs (protease, reverse transcriptase, integrase) display a high degree of inherent plasticity that confers the capacity to generate compensatory changes in response to drug pressure.

Given the limitations and the potential complications of HAART, there has been interest in novel approaches to control or preferably cure HIV infection. For instance, cell and gene therapies aiming to modify host cells to resist HIV infection have also provided promising perspective, especially with the case of the "Berlin patient" (40). This HIV-1 infected patient received a hematopoietic stem cell transplant from a donor carrying a homozygous CCR5Δ32 mutation in the CCR5 gene. Three and half years post-transplant and in the absence of HAART, no traces of HIV were detected in this patient (41). Several gene therapy strategies are currently being investigated aiming to either reduce or disrupt CCR5 expression by zinc-finger nucleases (42).

In parallel to these studies, considerable efforts have been carried out to create a suitable HIV vaccine. The lack of a relevant animal model for HIV-1 infection has rendered difficult the development and screening of vaccines. Macaques infected with SIVmac or chimeric HIV/SIV viruses (SHIVs) have so far provided the best model of HIV infection. Experimental preventive HIV vaccines have been administered to more than 44,000 human volunteers in more than 187 separate trials since 1987. Initially, studies were aimed at eliciting neutralizing antibodies. Based on that approach, two phase III gp120 vaccine trials were conducted each with a bivalent formulation of two strains of recombinant gp120 (AIDSVAX), but they showed no significant impact on acquisition of HIV-1 infection and had no effect on viremia or peripheral $CD4^+$ T-cell counts. The error-prone nature of RT, the strain diversity, the low spike density on the virion surface, the highly glycosylated nature of the envelope protein and its conformational flexibility, all render difficult the induction of neutralizing antibodies.

Due to disappointing efforts to induce neutralizing antibodies, and based on the observation that $CD8^+$ T cells play an important role in immune control of HIV-1 replication, several products were developed aiming to stimulate $CD8^+$ T-cell responses. This strategy requires antigen expression within the host cell, and its processing/presentation on MHC class I molecules for CTL recognition. In the phase III human trial RV144, a canary pox-based vector (ALVAC) was used to deliver HIV genes to host cells in combination with a boost of recombinant glycoprotein gp120 (AIDSVAX). This study showed 31% efficacy in protection from infection amongst community-risk Thai participants, and was shown to elicit non-neutralizing envelope-specific antibodies associated with $CD4^+$ T-cell but no $CD8^+$ T-cell responses (43).

1.3 HIV-1 Structure and Genome

HIV-1 is a retrovirus of the lentivirus subfamily. As such, it has an ssRNA genome that during the life cycle is reverse transcribed to a DNA form. The DNA is then incorporated into the host's genome, and acts as template to allow virus multiplication within the infected cell. Reverse transcription and integration are the two characteristics that distinguish retroviruses from others viruses.

The HIV-1 genome contains nine open reading frames (ORF) (Figure 1.4) (44). From the 5' to 3' ends of the genome are found the *gag*, *pol* and *env* genes. The *gag* (group-specific antigen) gene encodes a polyprotein precursor designated as $Pr55^{Gag}$ to refer to its molecular weight. $Pr55^{Gag}$ is cleaved by the viral protease (PR) into MA (matrix-p17), CA (capsid-p24), NC (nucleocapsid-p7) and p6. Two spacer peptides, sp1 and sp2, are also generated upon Gag processing. The *pol*-encoded enzymes including PR (protease), RT (reverse transcriptase) and IN (integrase) are initially synthesized as part of a large polyprotein precursor, $Pr160^{GagPol}$, whose synthesis results from a frame-shifting event during $Pr55^{Gag}$ translation. The subunits of Pol are subsequently generated by PR cleavage. The *env* ORF also encodes for a polyprotein precursor. Unlike Gag and Pol precursors, which are cleaved by the viral PR, the Env precursor, known as gp160, is processed by cellular proteases of the furin family during its trafficking to the cell surface. This results in the generation of the surface (SU) Env glycoprotein gp120 and the transmembrane (TM) glycoprotein gp41.

The four Gag proteins and the two Env proteins are the structural components that make up the core of the virion and the outer membrane envelope (Figure 1.5). The external lipid membrane is taken from the infected cell when a newly formed virus particle buds out of the plasma membrane. Between 10-20 spikes composed of trimers of gp120/gp41 heterodimers stud the surface of each particle. The three Pol products provide essential enzymatic functions and are encapsulated within the viral particle.

While Gag, Pol and Env encode the major structural and non-structural proteins common to all replication-competent retroviruses, HIV-1 also encodes six additional proteins. Amongst these, Tat and Rev are regulatory proteins, essential to control viral gene expression. Finally, Vpu, Nef, Vif and Vpr, referred to as accessory proteins, are not packaged into the virion with the exception of Vpr, and perform essential functions at various steps to facilitate HIV-1 replication *in vivo* (reviewed in (45)).

The retroviral genome is encoded by a ≈ 9.5kb RNA. Two copies of this positive sense single-stranded RNA are packaged within the virion core. The RNA genome contains several *cis* acting elements that are important at different stages of HIV-1 replication cycle. Beginning at the 5' end, the *cis* elements include the TAR (trans-activating response region) hairpin region that serves as binding site for Tat, a primer-binding site (pbs) that enables cellular $tRNALys^3$ to anneal for initiation of reverse transcription, the packaging signal ψ for viral RNA incorporation into the virion through interaction with NC, a dimerization site, a major splice donor site for generating all subgenomic spliced mRNAs, a Gag-Pol frame-shifting region, the polypurine

tracts (PPT) for plus strand DNA synthesis, the Rev-response element (RRE) involved in nuclear export, and several splice acceptor sites.

Like cellular mRNAs, viral RNA molecules are capped at their 5' end with 7-methylguanosine and polyadenylated (polyA tail) at their 3' end. Once released into the target cell, the genomic RNA serves as a template for reverse transcription, whereby a dsDNA copy is produced, delivered into the nucleus and integrated into the host genome. This copy of integrated viral DNA is referred to as a provirus. The provirus is flanked by two long terminal repeat (LTR) regions, which are essential to mediate integration of viral DNA into the host genome. In addition to the TAR motif, the 5' LTR also contains a promoter region that regulates transcription initiation. Viral RNA transcripts are then generated by the host cellular machinery, exported into the cytoplasm for translation into proteins or for packaging into virions.

Thus, the HIV-1 genome represents a molecular entity consisting of only 15 proteins and one RNA, but despite this apparent simplicity HIV-1 possesses all the information needed to actively multiply in the human host (reviewed in (46)).

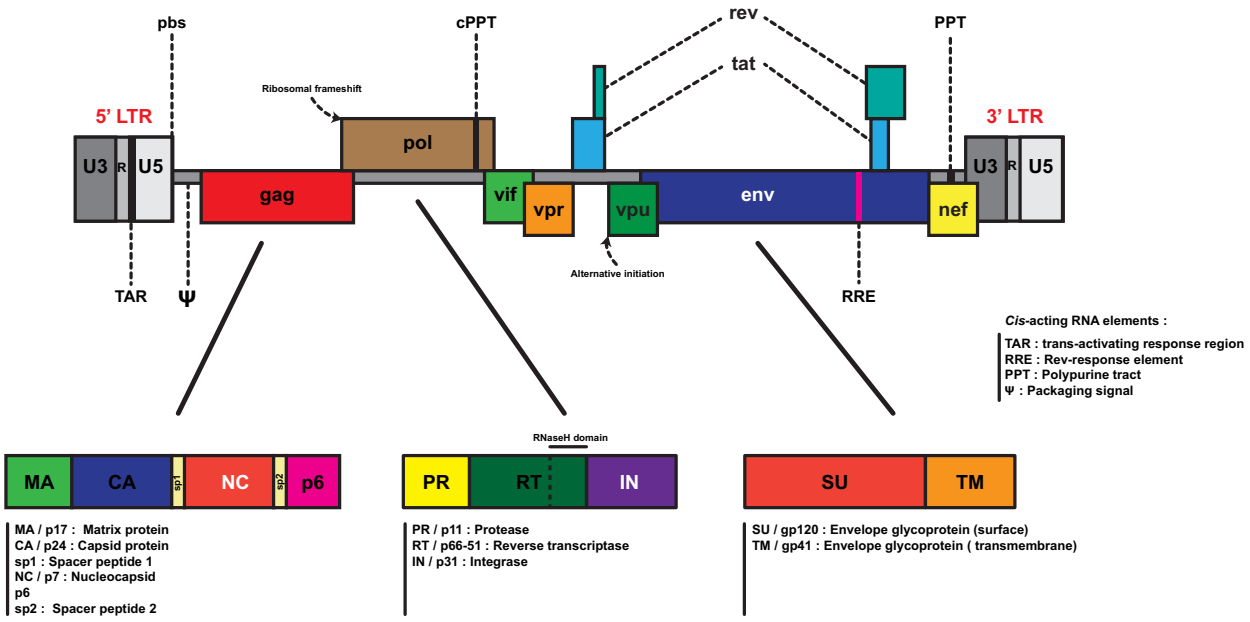

Figure 1.4: Landmarks of the HIV-1 genome.

This figure displays the nine open frames *gag*, *pol*, *env*, *vif*, *vpr*, *vpu*, *nef*, *tat* and *rev* of HIV-1 genome in its proviral form. The LTR regions are indicated at both extremities of the provirus. The LTR sequence contains the regions U3, R and U5. The ψ symbol indicates the position of the RNA packaging signal that binds to Gag-NC. The *gag* open reading frame consists of four domains MA, CA, NC and p6, which are generated from $Pr55^{Gag}$ by protease cleavage. The Gag spacer peptides sp1 and sp2 are also indicated. At the 3' end of p6, a slippery sequence allows the ribosome to skip gag's stop codon to generate the Gag-Pol polyprotein. The *pol* gene encodes three enzymes, PR, RT and IN. RT contains two subdomains, p66 and p51. The SU (surface-gp120) and TM (transmembrane-gp41) glycoproteins are encoded by the *env* gene. The Tat binding motif, TAR is also indicated. RRE, the motif recognized by Rev to mediate nuclear export, is located in the *env* region.

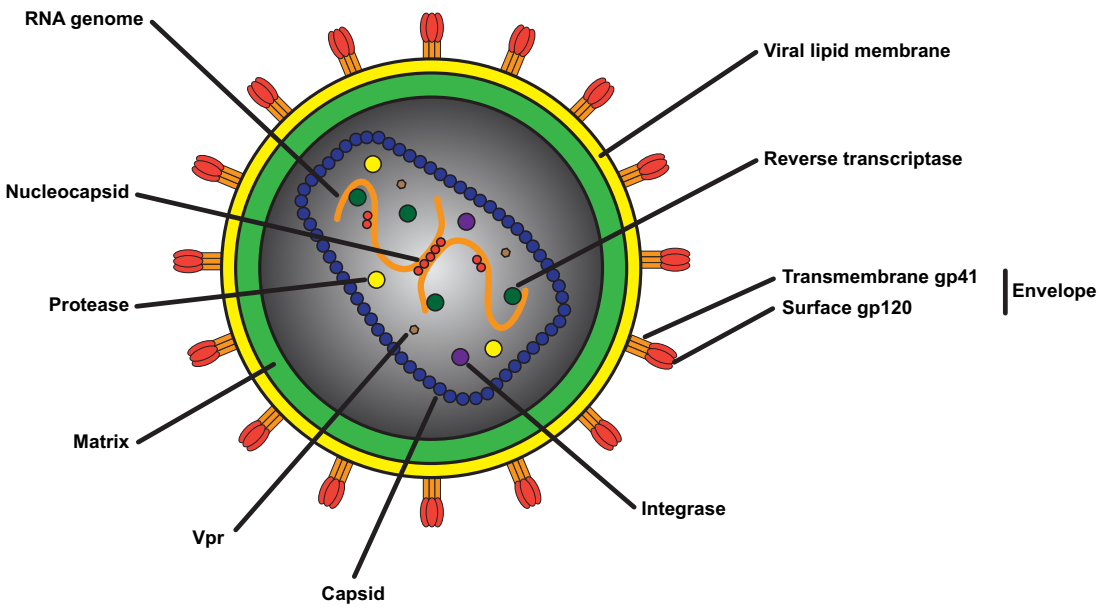

Figure 1.5: Structure of a mature HIV-1 virion.

The size of a virion is approximately 0.1 micron (1 seventieth of the diameter of a human $CD4^+$ T cell). HIV-1 produces 15 proteins that combine to make the infectious virion. The virion is spherical in shape. All the parts of the virion are made by the virus itself with the exception of the lipid membrane, which is taken from the infected cell during budding. Cellular components such as tRNA, cyclophilin A and APOBEC3G/F can also be packaged into HIV-1 virus particle (not indicated).

1.4 HIV-1 Replication Cycle

Following the attachment of HIV-1 virions to the host cell, a succession of complex events occurs within the cell before newly fully competent viral particles are produced (Figure 1.6) (reviewed in (47)). Binding and fusion of HIV particles with the target cell constitute the first steps of HIV-1 replication. The virus, then, releases its RNA and other viral proteins into the cytoplasm to initiate reverse transcription from which the single-stranded HIV RNA will be converted into double-stranded DNA. The newly formed HIV DNA enters the nucleus and integrates into the host genome. This copy of viral DNA, called a provirus, is then transcribed to mRNA, which is exported out of the nucleus and translated by the cellular machinery into proteins. HIV-1 proteins and genomic RNA copies are then directed to the plasma membrane, assembled into an immature virion that buds out of the plasma membrane before being released into the extracellular milieu. Nascent virions then undergo protease cleavages leading to formation of mature virions able to establish another round of replication. This constitutes the last step of HIV-1 replication cycle.

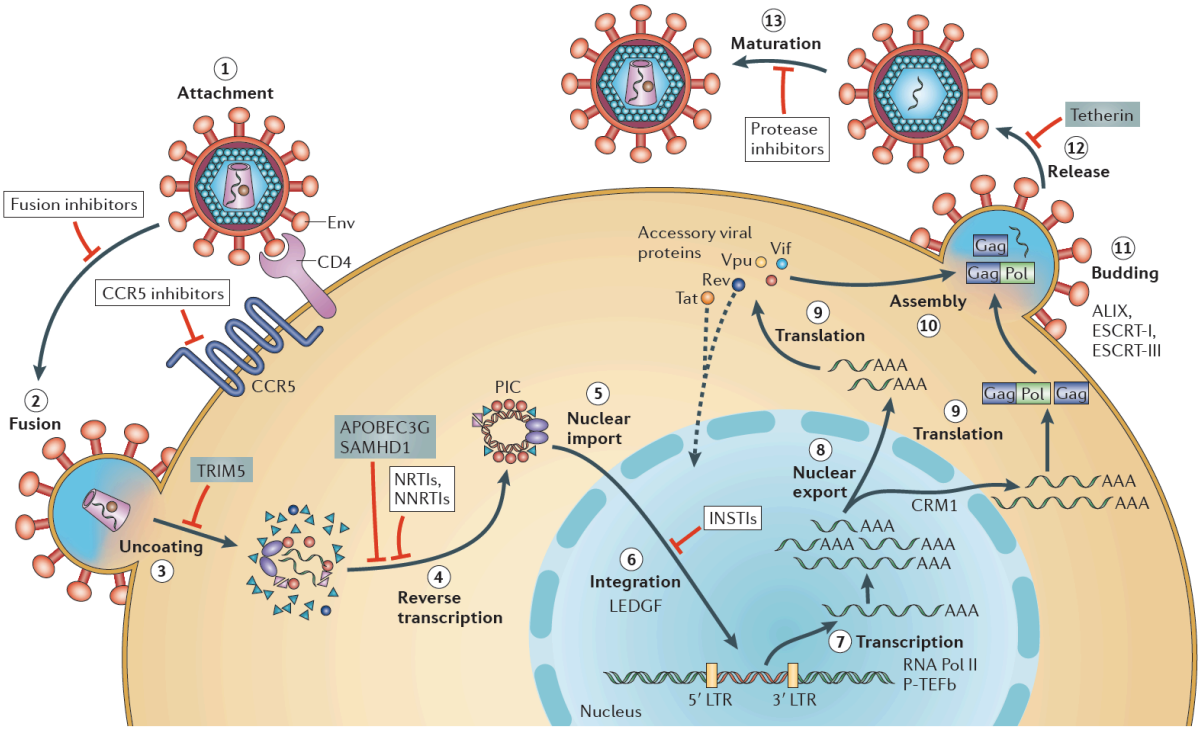

Figure 1.6: HIV-1 replication cycle.

This is an overview of HIV-1 life cycle showing the different processes that the incoming virus undergoes within the infected cell to ultimately lead to the production of a new HIV-1 virion. The host proteins involved in the replication cycle are also indicated. These proteins include essential proteins for virus replication designated as co-factors, and restriction factors (grey boxes), which act at various stages to interfere and limit virus production. Drugs inhibiting essential steps of the replication cycle are also indicated (white boxes). In this picture, the replication cycle begins with the recognition of the CD4 receptor on the surface of the target cell by the envelope glycoprotein of the incoming virion (step 1: attachment). This interaction induces a conformational change that allows the surface subunit gp120 of Env to bind the chemokine co-receptor CCR5 (CXCR4 can also be used as co-receptor depending the tropism of the viral strain). Spatial rearrangement of the transmembrane unit gp41 of Env allows the virus to fuse with the host cell membrane and to introduce its viral core into the cytoplasm of the target cell (step 2: fusion). Inside the cell, the viral core shaped by the capsid proteins, undergoes a poorly characterized process called uncoating (step 3: uncoating), which is then followed by the reverse transcription (step 4: reverse transcription). During this process, the viral RNA is converted into double-stranded DNA by the reverse transcriptase (RT). Associated within a pre-integration complex (PIC), the viral DNA shuttles from the cytoplasm to the nucleus by crossing nuclear pores (step 5: nuclear import). Insertion of viral DNA into the host genome is catalysed by the integrase (IN) and facilitated by the host protein LEDGF (step 6: integration). Cellular RNA polymerase II transcribes the integrated provirus but the success of this process depends on the ability of the viral protein Tat to recruit the P-TEFb complex to boost the elongation efficiency of RNA Pol II (step 7: transcription). Unspliced and partially spliced mRNA encoding the polyproteins Gag, Gag-Pol and Vif, Env, Vpr, Vpu, respectively, are exported out of the nucleus in a Rev and Crm1 dependent manner, while completely spliced mRNA encoding Rev, Tat and Nef are exported by the normal export pathway (step 8: nuclear export). Cytoplasmic viral mRNAs then serve as templates for protein production (step 9: translation) while genome full length RNA is incorporated into viral particle through its interaction with the Gag-NC domain. At the plasma membrane Gag multimerizes and orchestrates the assembly of the different viral components into an immature spherical virion (step 10: assembly). During this process, Gag recruits ESCRT-I and ALIX through its late domains in p6 (step 11: budding). In turn, this attracts ESCRT-III, the membrane fission machinery that cuts the thin membrane neck

between the cell and the immature virion (step 12: release). Thereby the immature virion separates from the producer cell and is released into the extracellular environment. After this, the viral particle undergoes a process called maturation driven by the protease (PR) (step 13: maturation). PR cleaves at several sites the Gag and Gag-Pol polyproteins and thus allows the viral components to reorganize in a way that ultimately forms a mature and infectious virion. Figure adapted from (47).

1.4.1 Attachment and Entry

The first step of the HIV-1 life cycle is mediated by the binding of virions to the target cells, a process depending on the interaction between the envelope glycoprotein (Env) on the virus and the CD4 receptor at the surface of the host cell. CD4 is a glycoprotein expressed on the surface of T helper lymphocytes, monocytes, macrophages and dendritic cells. In T cells, CD4 serves as a co-receptor that assists the T cell receptor to amplify the signal generated upon antigen recognition. Consistent with the observation that AIDS patients were reported to have a decline of $CD4^+$ T cells, it was shown that HIV-1 preferentially infected $CD4^+$ T cells (48, 49) and that infection was inhibited by CD4 antibody treatment (reviewed in (50)). However, CD4 expression in mouse cells could only restore binding of virus to the cell surface but not entry, suggesting that an additional component was required (51). Later, the chemokine receptors CCR5 and CXCR4 were isolated as secondary receptors (co-receptors) required for full entry of HIV-virion into host cell (52-57).

Env is a heavily glycosylated protein displayed at the surface of the virion as trimers of gp120 and gp41 heterodimers ("spikes"). A specific region within gp120 referred to as the CD4 binding site (CD4bs) initiates the entry process by interacting with the CD4 receptor (Figure 1.7) (58, 59). CD4 constitutes the primary entry receptor of HIV and is absolutely required for further steps; Env binding to CD4 causes rearrangements of gp120 allowing it to bind the co-receptor. HIV-1 strains can be classified into two groups based on their co-receptor affinity either for CCR5 or CXCR4 (60). Originally, viruses using CCR5 were designated as macrophage-tropic viruses to differentiate them from viruses only able to infect $CD4^+$ T cell lines. Later on, this classification was changed since primary $CD4^+$ T cells can express either CXCR4, CCR5 or both receptors on their cell surface, depending on their activation state, whereas derived $CD4^+$ T cell lines only express CXCR4. To alleviate this ambiguity, viruses that use CCR5 are called R5 and those using CXCR4 are termed X4. Some viruses have been found to be able to use both chemokine receptors to gain entry into the host cell and are called dual tropic of R5X4. X4 viruses are found at later stage during disease progression and may be more virulent, but the mechanism by which the virus switches from one co-receptor to the other is unclear. Co-receptor binding induces structural changes in gp41, which allow it to insert its fusion peptide into the host cell membrane (61, 62). The fusion peptide of each gp41 in the trimer fold, bringing the two terminal regions from each gp41 subunit together. This results in the formation of a six-helix bundle between gp41 monomers, that brings the viral and host membranes into close proximity. In such configuration, a fusion pore is generated between the two membranes whereby the viral core can enter into the host cell cytoplasm.

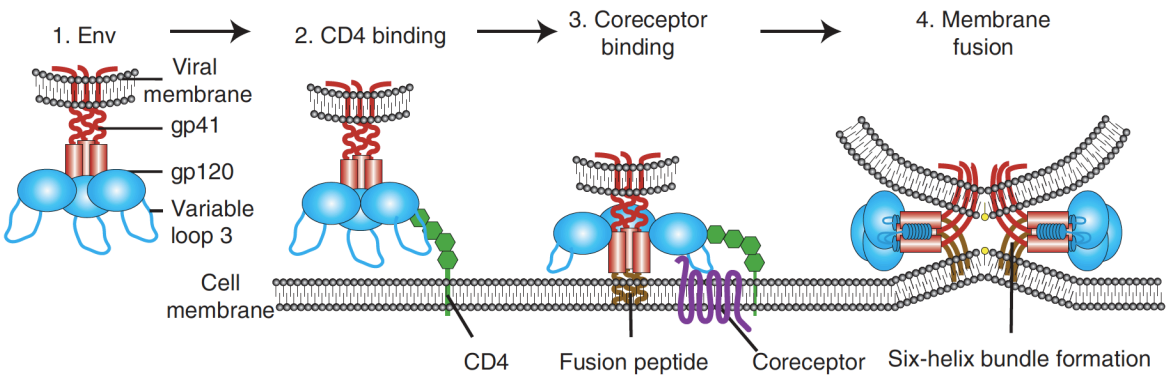

Figure 1.7: Early contacts between HIV-1 and its target cell.

Entry of HIV-1 into the target cell is an ordered multistep process mediated by HIV Env, which is composed of two subunits, gp120 and gp41 (step 1). Firstly, Env binds to the CD4 receptor (step 2: CD4 binding) expressed at the cell surface of $CD4^+$ T cells, macrophages, and dendritic cells through interactions with the surface subunit gp120 of the viral envelope protein. This interaction triggers a conformational change in the structure of gp120 that allows the protein to interact with a secondary receptor or co-receptor (step 3: co-receptor binding). In turn, the transmembrane unit of Env gp41 undergoes a conformational change and inserts its fusion peptide into the cellular membrane. This results in the formation of a six-helix bundle, which brings into close proximity the viral and the cellular membranes, thereby allowing the two membranes to fuse with each other. Figure adapted from (63).

1.4.2 From RNA to DNA: Reverse Transcription

Following the fusion of HIV-1 with the host cell membrane, the core of the virion is then introduced into the cytoplasm of the cell. Shortly after, reverse transcription is initiated and ensures the conversion of single-stranded viral RNA into a linear double-stranded DNA. This viral DNA product then constitutes the substrate for the integration process. Although only reverse transcriptase (RT) and viral RNA are required for synthesis of ds DNA *in vitro*, this process in infected cells is much more complicated and occurs within an entity called the reverse transcription complex (RTC). In addition to RT and RNA, multiple viral proteins, including MA, CA, NC, IN, and Vpr have been reported to be associated with the RTC (64, 65).

The role of MA in the RTC is unclear. While some studies suggest that MA might direct the nuclear import of RTC and allows HIV-1 to infect non-dividing cells (66, 67), this conclusion was disproved by others (68, 69). CA most likely provides the overall structure of the RTC, whereas NC acts as a nucleic acid chaperone by assisting DNA elongation in regions where secondary structures form, and by facilitating strand transfer (70-72). Vpr is also present in the RTC but its contribution is still a matter of debate. In addition to these viral components, the RTC can also contain host restriction factors such as APOBEC3G, which have been incorporated into virions from the virus-producer cell, and cause mutations during DNA synthesis (cf. section 1.7.2).

The nature of the RTC is still unclear. One model predicts that the structure of the core evolves along with the on-going reverse transcription through a process called uncoating that

ultimately transforms the RTC into a pre-integration complex (PIC) (73, 74). The RTC is a target for TRIM5α and TRIMCyp because they can interact with hexameric CA protein and interfere with the uncoating process in a way that blocks reverse transcription (cf. section 1.7.4). Another model proposes that the RTC maintains the same structure as the viral core within which DNA synthesis occurs. Once reverse transcription is completed, this core-like structure is transported to the nuclear pores and converted into PICs before they enter the nucleus (75).

Whatever the composition of the RTC is, within this entity RT mediates two essential enzymatic activities during the reverse transcription reaction: a DNA polymerase that can copy either DNA or RNA templates into DNA, and a RNase H that degrades RNA from the RNA-DNA duplex (reviewed in (76)). RT is produced from a Gag-Pol polyprotein by cleavage with the viral protease PR, ensuring that the Pol portion of Gag-Pol including RT is assembled into virions. RT is a heterodimer composed of two subunits: the larger p66 and the smaller, p51. The p66 subunit consists of two domains: polymerase and RNase H while the p51 subunit corresponds closely, but not exactly, to the polymerase domain of p66. The p66 domain has a catalytic role, whereas the p51 subunit plays a structural role. The high error frequency of RT, due to its lack of proofreading function, is one of the major factors responsible for the sequence variation of the HIV-1 genome even within an individual patient initially infected with a single virus. Through this mechanism, HIV-1 can rapidly adapt to avoid the adaptive immune response and escape antiviral drugs. Reverse transcription is an essential step in the HIV-1 life cycle and for this reason constitutes a primary target for anti-HIV drugs. The first approved anti-HIV drug, AZT, targets RT and of the 26 drugs currently approved to treat HIV-1 infections, 14 are RT inhibitors.

The process of reverse transcription starts with the host tRNA Lys3 incorporated from the virus producer cell that acts as a primer by annealing to a complementary sequence near the 5' end of the viral RNA (Figure 1.8) (reviewed in (76)). From this sequence, called the primer binding site (pbs), the synthesis of the minus-strand DNA is initiated. The RNA-DNA duplex is recognized by RT, which uses its RNase H domain to remove the 5' end of the viral RNA, exposing the newly synthesized minus-strand DNA. This minus-strand DNA is then transferred to the direct repeat sequence (R) at the 3' end of the viral RNA and serves as a primer for a second round of DNA synthesis. Since there are two copies of the viral RNA genome, this transfer or jump can also involve the R sequence at the 3' ends of the second copy of viral RNA. Then the corresponding minus-strand DNA of the rest of the viral genome is generated until the 5' pbs sequence is reached. As DNA synthesis proceeds, RNase H degradation removes the RNA fragments from RNA-DNA complexes but leaves intact portions of RNA that are purine-rich. These sequences are called polypurine tracts (ppt) and serve as primers for the initiation of the plus-strand DNA synthesis. The HIV-1 genome contains two ppt sequences, one near the 3' end of the RNA (ppt) and the other near the middle of the genome (cppt). The 3' ppt is essential for viral replication, while the central ppt probably increases the ability of the virus to complete plus-strand DNA synthesis but is not essential ((77)). When RT generates the plus-strand DNA that is initiated from the 3' ppt, it not only copies the minus-strand DNA, but also the nucleotides of the Lys3 tRNA which then become a new substrate for RNase H. Then RNase H does not cleave entirely the tRNA and leaves a single A ribonucleotide at the 5' end of the minus-strand

DNA. Removal of the tRNA primer allows the second transfer (" jump ") of the plus-strand DNA from the 5' end to the 3' end of the minus-strand DNA where the pbs sequences from both DNA strands hybridize with each other. Both DNA strands are then extended to the ends of both templates, generating a complete double-stranded linear viral DNA. Thus, the reverse transcription creates a DNA product that is longer than the initial RNA template genome from which it is derived because both ends of the DNA contain sequences from each end of the RNA: U3 from the 3' end and U5 from the 5' end. Each end of the viral DNA has the same sequence, U3-R-U5 called the long terminal repeats (LTRs), which will be, after integration, the extremities of the provirus. At some point late in the reverse transcription process, the RTC transitions into a pre-integration complex or PIC, which is then transported into the nucleus.

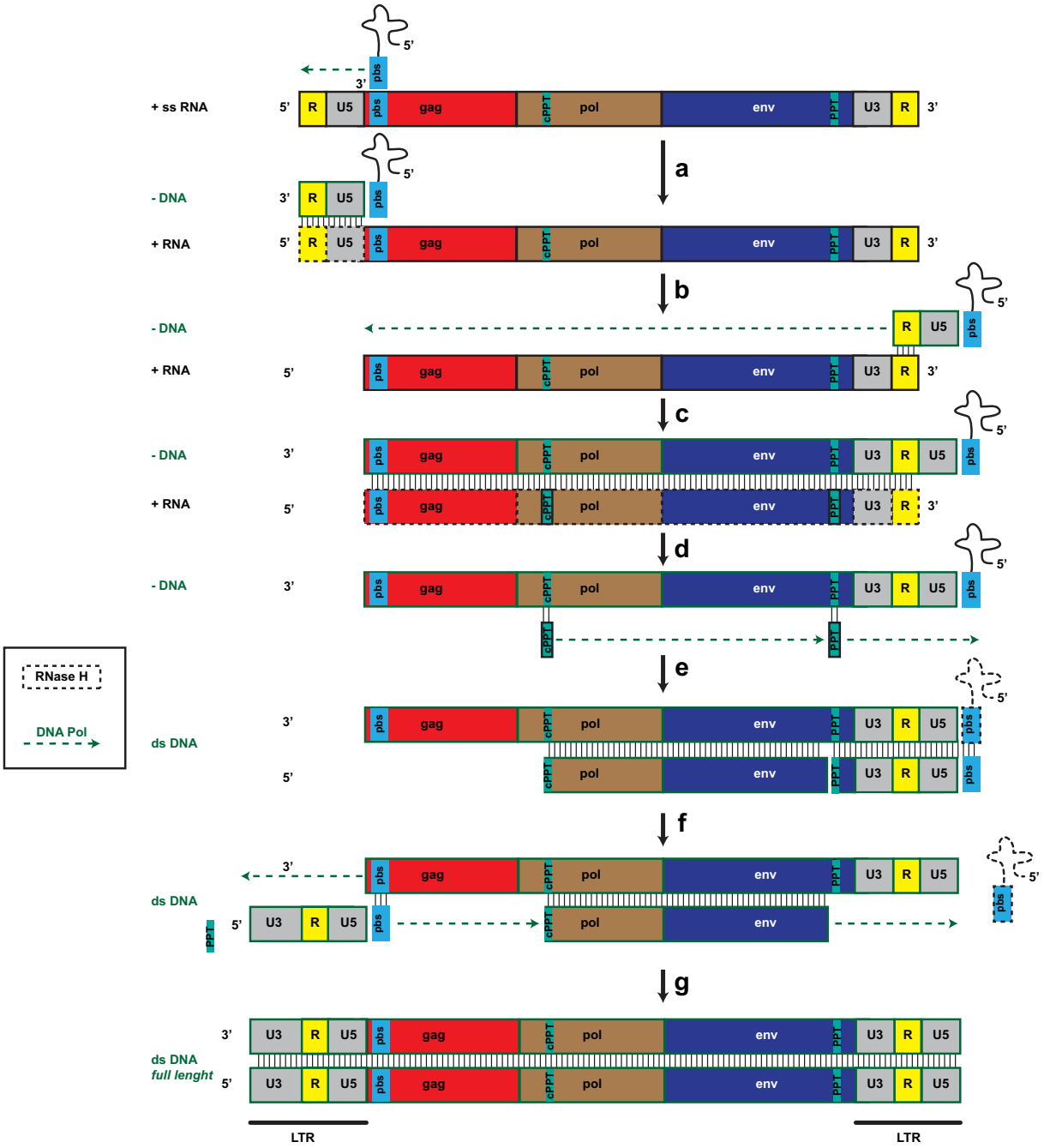

Figure 1.8: Conversion of viral RNA into DNA via the process of reverse transcription.

Reverse transcription begins with the annealing of the cellular tRNA on the primer binding site (pbs) located at the 5' end of the positive sense single stranded viral RNA (+ ss RNA). From this point, RT through its DNA polymerase domain generates the minus-strand DNA while its RNase H domain degrades the RNA template (step: a). This newly synthesized minus-strand DNA is then transferred to the opposite end in 3' of the + ss RNA by complementarity between the repeated sequences (R) (step: b), and serves as primer to direct the elongation of the minus-strand DNA (step: c). RNAse H removes the initial plus-strand RNA (step: d) with the exception of two regions, cppt and ppt, which then serve as primers for the synthesis of plus-strand DNA (step: e). Plus-strand DNA continues until the tRNA is copied, allowing RNAse H cleavage to remove the tRNA primer. This second round of DNA amplification is then followed by a second jump or strand transfer of the positive-strand DNA which hybridizes with the complementary pbs on the minus strand DNA (step: f). Both strands are extended leading to the synthesis of the complete double-stranded linear viral DNA (step: g). The ds DNA is longer than the initial + ss RNA template and contains two long terminal repeat sequences (LTR) at its both ends.

1.4.3 Nuclear Import and Integration

As described above, reverse transcription generates a linear double-stranded DNA copy of the retroviral genome. This viral DNA is associated with integrase (IN) and other proteins to form the pre-integration complex (PIC). In contrast to oncoretroviruses, lentiviruses can replicate in non-dividing cells. The pre-integration complex of lentiviruses must therefore be transported through the nuclear pores via an active nuclear import mechanism in order to penetrate the nucleus. Oncoretroviruses, by contrast, cannot cross the nuclear pore and therefore require nuclear membrane breakdown to enter the nucleus.

The exact mechanism by which the PIC gains entry to the nucleus is still unclear. One of the reasons that render this field complicated is the difficulty of isolating large amounts of PICs functional for integration. The viral determinants for nuclear import have been subject to much controversy over the years (reviewed in (78)). In addition to proviral DNA, MA, CA, NC, IN and Vpr were also found associated with the PIC (reviewed in (79)). Their participation in nuclear import pathway was suggested since several of these proteins exhibit karyophilic properties and localize to the nucleus when expressed alone. However, none have specifically been shown to play a role in viral nuclear entry. Current evidence suggests that CA is the principal determinant of whether HIV-1 can infect non-dividing cells. Exchange of HIV-1 MA and CA with those from MLV abolish the ability of HIV-1 to infect non-dividing cells, however, addition of HIV-1 MA alone is not sufficient to restore viral infection (80). Furthermore, MLV, that cannot infect non-dividing cells, contains capsid in its PICs (81), whereas CA is below the limit of detection in purified HIV-1 PICs (64). However, the labile nature of mature HIV-1 CA lattices may confound these observations.

Recent studies on the cellular factors involved in the early steps of HIV-1 infection have been more informative as to the mechanism of nuclear entry. Studies using an *in vitro* nuclear import assay reported the importance of importin-β/7, an import receptor for ribosomal proteins and histone H1, and the Ran GTPase for mediating nuclear import of purified PICs (82). Further studies by the same group indicated that damaged tRNAs with defective 3'CCA tails were associated with purified PICs and promoted nuclear transit (83). To identify HIV-1 cofactors, several genome-wide siRNA screens were performed (reviewed in (84)). Among the candidates, knockdown of the nuclear import receptor transportin 3 (TNPO3/transportin-SR2) and several nuclear pore proteins including Nup358/RanBP2 and Nup153, were found to inhibit HIV-1 infection and induced 2-LTR circle accumulation (85). 2-LTR circles are covalently closed circular forms of DNA that can form when HIV-1 cDNA enters the nucleus. Such a structure is unable to support integration. TNPO3 was initially identified in a yeast two-hybrid screen as a binding partner for integrase (86). TNPO3 and Nup358 also appeared in a second RNAi screen for HIV-1 co-factors (87). Furthermore, TNPO3 was also proposed to regulate nuclear export of tRNAs and capsid from the nucleus (88), suggesting a specific nuclear import/export pathway that regulates HIV-1 infection. Finally, screening of cDNA libraries for post-entry inhibitors of viral infection identified a fragment of Cleavage and Polyadenylation Factor 6, CPSF6 (89). When enriched in the cytoplasm, a CPSF6 fragment prevents HIV-1 nuclear entry by targeting CA. Importantly, HIV-1 viruses resistant to overexpression of this fragment CPSF6 were found

to contain a mutation in CA (N74D). This mutant is defective for CPSF6 binding, but was found to efficiently infect cycling cells in a manner dependent on Nup155 rather than Nup153, suggesting that HIV-1 PICs may be transported into the nucleus through several alternative import pathways. However, the N74D mutant was unable to infect macrophages, implying that this may not be true in primary HIV-1 target cells. In accordance with this notion, a recent study showed that interactions between CA and the cyclophilin domain of Nup358 could dictate the use of Nup358/Nup153 for HIV-1 nuclear entry (90). Importantly, failure to engage the Nup358 pathway impairs HIV infection of non-dividing macrophages.

Once in the nucleus, IN catalyses the covalent attachment of proviral DNA to the host cells DNA (reviewed in (91)). The integration reaction starts in the cytoplasm with the removal of two nucleotides from each 3' end of the blunt-ended linear viral DNA, a process called 3' end-processing, and then carries on into the nucleus. The 3' ends generated by 3' processing attack a pair of phosphodiester bonds in the target DNA. The sites of attack on the two target DNA strands are separated by five nucleotides. The 3' ends of the viral DNA are then joined to the 5' ends of the target DNA at the site of integration. Completion of integration requires removal of the two unpaired bases at the 5' ends of the viral DNA, the filling in the single-strand DNA gaps between viral and target DNA and then the ligation of the 5' ends of the viral DNA to target DNA. Among all these steps, IN catalyses the 3' processing and DNA-strand transfer to form the integration intermediate while the subsequent steps are catalysed by cellular DNA repair enzymes.

Integration can take place at many locations in the host genome, but preferentially in transcriptionally active regions (92). These sites are likely to promote efficient viral gene expression after integration. Some features characterize these regions such as high G/C content and high gene density. The selection for integration sites has been proposed to be linked to the ability of IN to interact with the cellular factor LEDGF/p75 (lens epithelium growth factor) which itself binds to regions within transcription units ("LEDGF islands") (93-95). LEDGF/p75 was initially found by affinity-based screening performed to identify cellular proteins bound to IN (96, 97). LEDGF contains a PWWP chromatin-binding domain, an A/T hook domain likely involved in DNA binding, a nuclear localization signal and the domain that binds to IN. Depletion of LEDGF results in the loss of much of the targeting to transcription units and causes reduction of infectivity. An increase in formation of 2-LTR circles is also observed when LEDGF expression is silenced (98) or in the presence of IN inhibitors.

Overall, the data support a model in which LEDGF boosts the efficiency of integration by binding to IN and to chromatin at active transcription units and mediates integration at these locations. The cellular DNA condensing protein BAF is also required for efficient integration as it blocks 'suicidal' auto-integration events (99).

1.4.4 Transcription and Nuclear Export

After integration into the host genome, the HIV-1 provirus acts as a host gene. Transcription is initiated at the 5' LTR, which contains several DNA regulatory elements that serve as binding sites for cellular transcription initiation factors and control the level of viral transcription (100). The core promoter consists of three tandem SP1 binding sites (101), an efficient TATA element (102) and a highly active initiator sequence (103) (Figure 1.9A). Together these elements participate in the binding of the initiation factors TFIID and its associated TAF co-factors to the TATA box and actively recruit RNA polymerase II (RNA Pol II). In addition to the core promoter, the 5'-LTR also contains an enhancer region that provides two binding motifs for NK-κB and NFAT (104-106). While the HIV-1 LTR appears to be an extremely potent promoter to initiate transcription, the efficiency of transcription is impaired by the low processivity of RNA Pol II. As a result, in the absence of the viral transcriptional activator Tat, most viral transcripts terminate prematurely at many positions throughout the 9.5 kilobase proviral genome. Tat does not enhance the frequency of transcriptional initiation but rather stimulates RNA polymerase II processivity causing an increase in the amount of transcripts generated that extend all the way to the 3' end of the provirus (reviewed in (107, 108)). Tat recognizes a hairpin loop structure, known as the TAR (transactivating responsive region), near the 5' end of the viral RNA in the LTR region (109, 110) and recruits components of the positive acting elongation factor complex P-TEFb (Figure 1.9B). In this complex Tat binds with high affinity to Cyclin T1 (CycT1) (111). Since the Cyclin T1-Tat complex binds the TAR with higher affinity than Tat alone, it contributes to enhance Tat binding to TAR. In turn, CycT1 recruits and activates the cyclin-dependent kinase 9 (CDk9), which phosphorylates the carboxy-terminal heptad-repeat domain (CTD) of the RNA polymerase II large subunit. CTD phosphorylation of RNA Pol II enhances its elongation capacity. In line with this model, CDk9 protein kinase inhibitors were shown to block HIV-1 transcription (112). Tat is inactive in murine cells because the murine Cyclin T1 sequence differs from the human sequence by a single amino acid difference. Replacement of Y261 into the human CycT1 blocked Tat-mediated HIV-1 transactivation in transfected cells whereas introduction of C261 into the murine CycT1 restored Tat's activity (113).

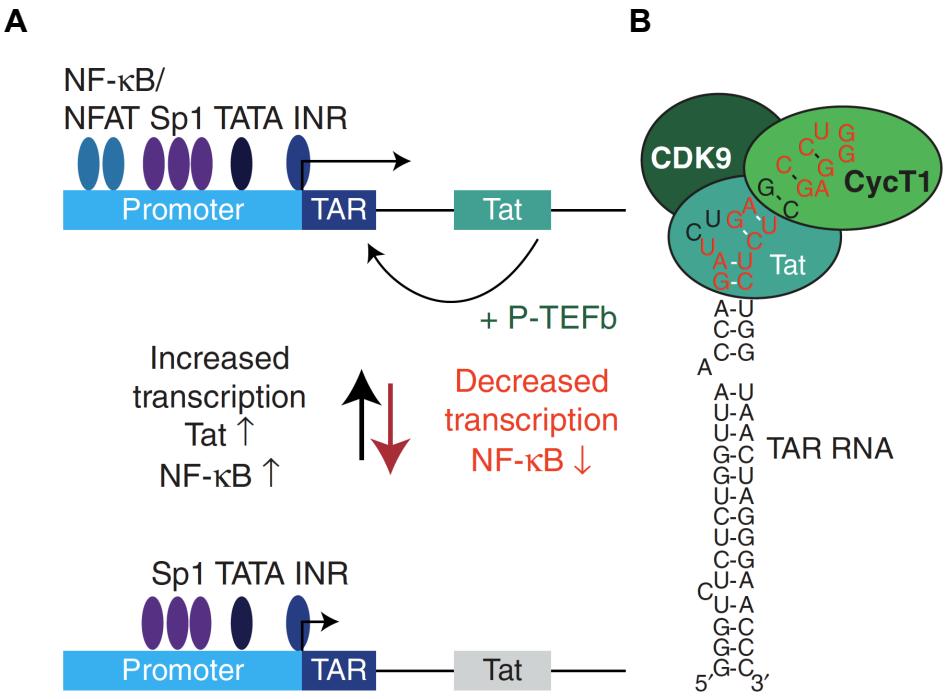

Figure 1.9: Tat-mediated HIV-1 transcriptional activation.

A: Tat regulates HIV-1 transcriptional elongation by binding to the TAR RNA sequence in HIV-1 RNA and recruits the P-TEFb complex. In this complex, Tat binds to cyclin T1 which itself is associated to the protein kinase CDk9. This association induces a conformational change in CDk9 that activates its enzymatic function. This leads to hyperphosphorylation of the CTD of RNA polymerase II and, thus, stimulates its elongation capacity to extend the full HIV-1 genome. The LTR region acts as a promoter region of the HIV-1 provirus. It contains binding motifs for the transcription factors Sp1, TFIID that are required to initiate the transcription reaction. The HIV-LTR has also motifs for recognition by NF-KB and NFAT. Recognition of these motifs by NF-KB enhances transcription initiation and thus increases Tat expression levels, which in turn positively regulates HIV-1 gene expression. Therefore, NF-KB can also indirectly influences HIV-1 transcription efficiency. Low levels of Tat drive the HIV-1 provirus into latency. **B:** Recognition of TAR by Tat and Cyclin T1. Figure adapted from (108).

Once transcribed, nascent viral pre-mRNAs are processed by the spliceosome. This complex contains an array of small nuclear ribonucleoproteins (snRNPs) that remove introns and join the exons from pre-mRNA. This process is called splicing and in general only spliced mRNAs can be exported out of the nucleus into the cytoplasm for translation. RNA splicing constitutes an obstacle for HIV-1 because all HIV viral proteins with the exception of Tat, Rev and Nef are translated from incompletely spliced or unspliced transcripts (reviewed in (108)). For this reason, Tat and Rev are the first viral proteins to be expressed and their presence is essential for expression of the other viral proteins. While Tat, as described above, stimulates transcription elongation, Rev protects unspliced and incompletely spliced transcripts from degradation by mediating their export out of the nucleus. The completely spliced ≈ 1.8kb mRNA transcripts which encode Tat, Rev and Nef are exported to the cytoplasm by an endogenous

cellular pathway used by cellular mRNAs (Figure 1.10A), while the ≈ 9kb unspliced mRNA and the ≈ 4kb incompletely spliced mRNAs which encode the polyproteins Gag, Gag-Pol and the proteins Env, Vpu, Vif, Vpr, respectively, require Rev for their transport and expression (Figure 1.10B).

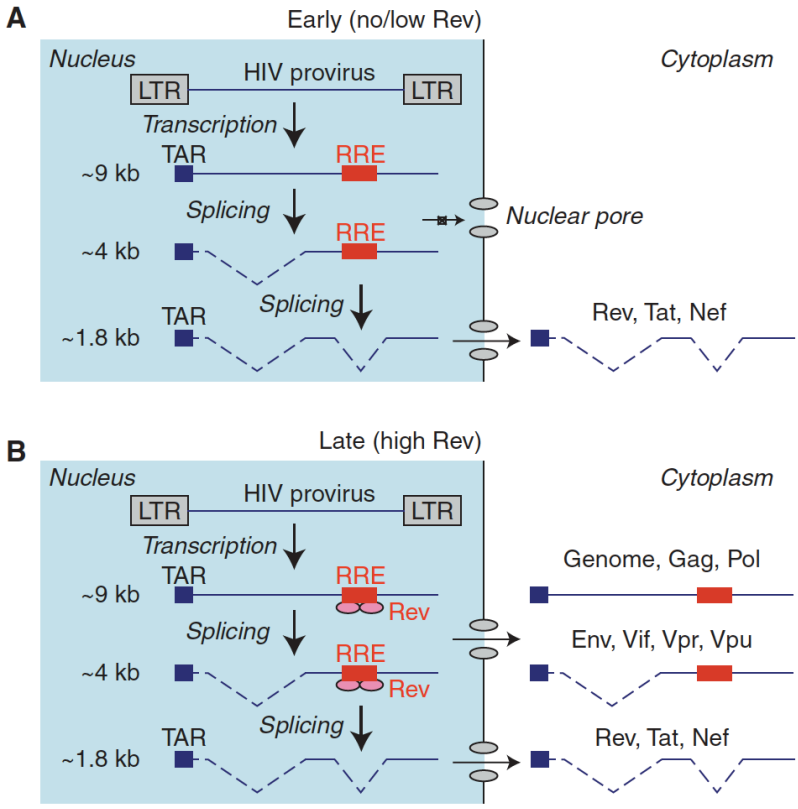

Figure 1.10: Rev mediates the nuclear export of partially spliced and unspliced HIV-1 mRNAs.

A: At the early stages of HIV-1 transcription, only the completely spliced mRNAs (~ 1.8 kb) encoding the Tat, Rev and Nef proteins are exported to the cytoplasm while the other unspliced (~ 9 kb) and partially spliced (~ 4 kb) transcripts are restricted to the nucleus for subsequent splicing or degradation. Completely spliced transcripts are then exported to the cytoplasm by the normal nuclear export cellular pathway and then translated into Tat, Rev or Nef proteins. **B:** By virtue of its NLS, Rev can penetrate back into the nucleus to assist the nuclear export of larger unspliced mRNAs (~ 9 kb) and partially spliced (~ 4 kb) encoding the polyproteins Gag, Gag-Pol and Env, Vif, Vpr, Vpu, respectively. Therefore, Rev bypasses the default nuclear export pathway in which mRNAs are spliced prior to nuclear export, allowing the subsequent translation of the full-length HIV-1 genome. The Rev-response element (RRE) is shown as a red rectangle. Figure adapted from (114).

Rev facilitates the transport of intron-containing viral RNA out of the nucleus by interacting with a highly structured RNA segment in the *env* coding region of unspliced and partially spliced viral mRNAs (115, 116). This sequence is referred as the Rev-responsive element (RRE) and adopts an elongated stem-loop structure of 351 nucleotides. Multimers of Rev bound to the RRE interact with the karyopherin family member Crm1 (also referred to as exportin 1) through a 10 amino acid leucine-rich nuclear export signal (NES) near its carboxyl terminus (Figure

1.11) (117, 118). Crm1 interacts with a small guanine nucleotide binding protein, Ran which facilitates binding between Crm1 and Rev. In the nucleus, Ran is bound to GTP while in the cytoplasm it associates with GDP. The relative abundance between nuclear pools of GTP and cytoplasmic GDP generates a gradient that provides the driving force to direct transport into and out of the nucleus. Rev associated to this export machinery complex is then transported out of the nucleus via the nuclear pore complex (NPC). After export to the cytoplasm, the bound GTP is hydrolysed to GDP by the proteins RanGAP (Ran GTPase-activating protein) and RanBP1. This reaction destabilizes the Rev complex and releases factors from the RRE (119). Crm1 is then transported back into the nucleus and Rev gains entry back to the nucleus by binding to the nuclear import factor, importin-β, where it can oligomerize and mediate another cycle of RNA export (120).

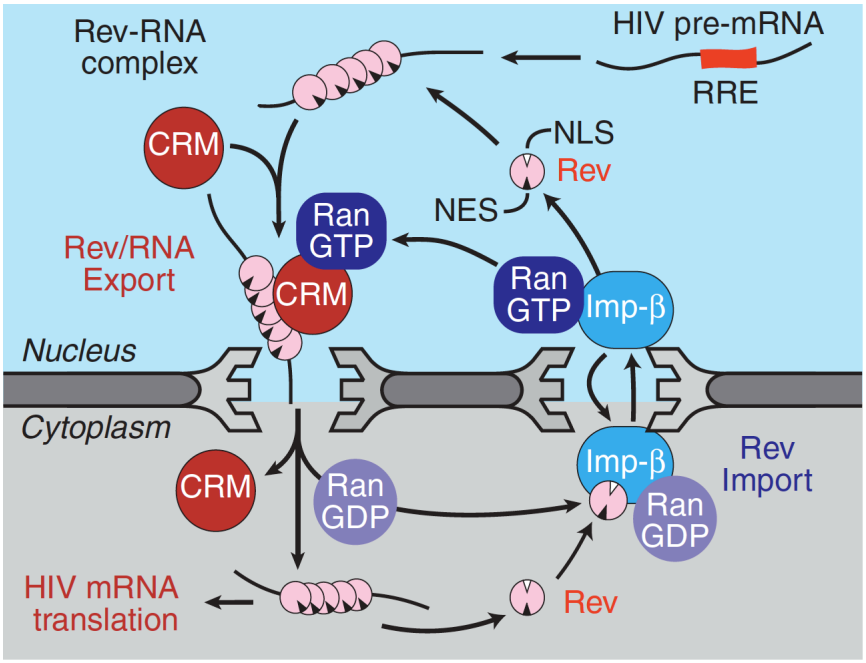

Figure 1.11: Rev-mediated HIV-1 nuclear export.

Rev interacts with unspliced and partially spliced transcripts containing a RRE element. Rev associated to RRE binds Crm1 through the nuclear export sequence (NES) and together cross the nuclear membrane through interactions with the nuclear pore proteins. Once in the cytoplasm Ran-GTP is converted into Ran-GDP which leads to destabilization of the complex and ultimately releases Rev, HIV-1 RNA and Crm1. Crm1 is then imported back to the nucleus. Rev binds to importin-β through its NLS and with Ran-GDP to mediate import into the nucleus. In the nucleus, conversion of Ran-GDP into Ran-GTP, allows Rev to dissociate from the complex and bind HIV-1 pre-mRNA to mediate another cycle of nuclear export. Figure adapted from (114).

1.4.5 Translation and Assembly of viral proteins

Once in the cytoplasm, HIV-1 mRNAs are scanned by ribosomes from the 5' cap until an initiation AUG with an appropriate Kozak consensus sequence is detected. In some cases the initiation of the translation can be rendered difficult. For example, the *gag* ORF contains multiple highly structured regions such as the TAR sequence, the primer binding site or the RNA packaging signal that potentially interfere with the ribosomal scanning. Moreover, some coding sequences can contain an AUG motif upstream of the authentic initiator start codon that can mislead the translation initiation at the authentic AUG. To circumvent these issues, it is thought that HIV-1 might include an internal ribosome binding site (IRES) to facilitate the recognition of the *gag* initiation codon, but this remains unclear (reviewed in (121)). Post-transcriptional elements (PCEs) along the HIV-1 RNA can bind to cellular RNA binding proteins to facilitate translation initiation. For instance, the binding of the cellular proteins SRp40 and SRp55 can enhance Gag translation (122). Since Vpu and Env are translated from the same bicistronic mRNA, additional components are also likely to be required to bypass the *vpu* open reading frame to start instead the translation at the *env* AUG (123). To add further complexity, HIV-1 also contains *cis*-acting sequence elements ("slippery" sequence: UUUUUUA) upstream of the *gag* termination codon required for frame shifting. When ribosomes encounter these elements the reading frame shifts from the *gag* reading frame to the *pro* and *pol* reading frame. This frame shift occurs ~ 5% of the time and allows the production of the Gag-Pro-Pol precursor polyprotein. Individually produced in the cytoplasm, Gag, Gag-Pro-Pol, Env, Vpr and the viral genomic RNAs are then directed to the plasma membrane for assembly.

Viral assembly is entirely orchestrated by the Gag polyprotein at the plasma membrane, and this allows the virus to assemble all of its components using a single targeting signal (Figure 1.12) (124-127). Gag is the main constituent of the virion providing ~ 50% of the entire virion mass. All the Gag subunits have a specific role and altogether they assemble the viral components at the plasma membrane into a spherical immature particle. In this structure, the membrane-bound Gag molecules are oriented radially with their amino-terminal MA domains bound to the inner membrane leaflet and their carboxy-terminal p6 domain facing the interior of the virion.

Since the assembly occurs at the plasma membrane, the viral proteins need to traffic from their point of synthesis in the cytoplasm to sites of virus assembly (128). Gag has been reported to interact with various components of intracellular vesicle trafficking pathways but the mechanism by which Gag and Gag-Pro-Pol polyproteins reach the plasma membrane is still poorly understood. Gag membrane targeting requires myristoylation of the MA domain and the presence of the lipid phosphatidyl inositol (4,5) biphosphate ($PI(4,5)P_2$) in the composition of the plasma membrane (129, 130). The interaction between MA domain and $PI(4,5)P_2$ exposes the amino-terminal myristoyl group which then stabilizes the anchoring of Gag on the inner leaflet. En route to the PM, Gag-NC packages the dimeric genomic RNA via its two zinc fingers that can recognize the packaging signal sequence (Ψ) (131, 132). This sequence consists of four stable stem loop structures. The two RNA strands are non-covalently dimerized in their 5' UTR. In the cytoplasm Gag poorly polymerizes but when it arrives at the plasma membrane

associated with genomic RNA, it can form high-order multimers (133). At the PM, Gag and Gag-Pol polyproteins are sorted into detergent-resistant membrane microdomains, also called lipid rafts (134). The capsid (CA) domain organizes the interaction between Gag monomers required for the formation of the Gag lattice in immature virions (135). The carboxy-terminal Gag p6 subunit contains a binding site for Vpr and thereby packages it into immature virions (136). In addition to the viral proteins encoded by the HIV-1 genome, small cellular RNAs and most notably tRNAs required for priming the reverse transcription are also packaged into virions (137).

Env is inserted into ER membranes during its translation and then travels through the cellular secretory pathway where it is glycosylated, assembled into trimeric complexes, processed into the transmembrane (gp41-TM) and the surface (gp120-SU) subunits by the cellular protease furin and delivered to the PM via vesicular transport (reviewed in (138)). Env trafficking to the PM does not rely on Gag and requires its intracellular tail to be directed into raft-like domains. This tail is then thought to interact with MA at the plasma membrane to promote Env incorporation into assembling virions.

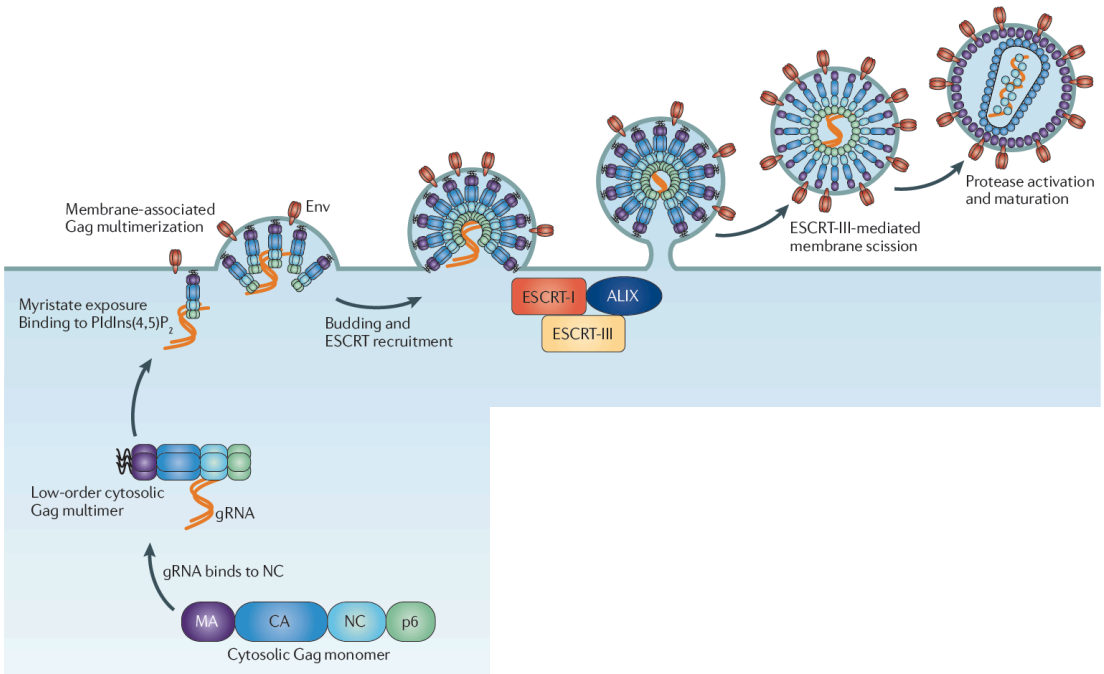

Figure 1.12: Gag orchestrates assembly of viral components at the plasma membrane.

The polyprotein Gag produced in the cytosol can only form low-order multimers. During its trafficking to the plasma membrane, Gag packages dimeric genomic RNA through recognition of the packaging signal ψ by its NC domain. At the plasma membrane MA domain interacts with $PI(4,5)P_2$ which results in exposure of its myristoyl group. This allows Gag to remain embedded in the membrane. MA also recruits Env glycoproteins. At the plasma membrane Gag polymerizes at several nucleation sites. During the budding process, ESCRT-I is engaged through interactions between regions of Gag-p6 domain called the late domains with the subunits Tsg101 and ALIX. This leads to the recruitment of the CHMP proteins from ESCRT-III and VSP4, which together mediate the final membrane scission event that releases the budding virion from the producer cell. Later on, final maturation of the virion is driven by the viral protease PR that catalyses a series of proteolytic cleavages. Figure adapted from (139).

1.4.6 Budding and Release

Although Gag mediates virion assembly, the budding event that allows the immature virion to be released from the producer cell is mediated by the host ESCRT machinery (endosomal sorting complex required for transport) (Figure 1.13). Gag recruits the ESCRT machinery through interactions between its p6 domain and ESCRT-I subunits. p6 contains two different late domain motifs that bind ESCRT. The Pro-Thr-Ala-Pro (PTAP) late domain binds the Tsg101 subunit of ESCRT-I complex (140, 141). Each of the four residues of this late domain makes specific contact within an extended groove on the amino-terminal E2 variant (UEV) domain of Tsg101. The second late domain called YPXL (Tyr-Pro-X-Leu with X being variable in sequence and length) binds the V domain of the ESCRT-associated factor ALIX (142).

CA interacts with NEDD4L, a member of the human NEDD4 ubiquitin E3 ligase protein family (143). However, this interaction does not appear to be absolutely required for HIV-1 budding suggesting that NEDD4-mediated Gag ubiquitination might help the p6 late domains at recruiting the ESCRT machinery. Budding of PTAP or YPXL mutated HIV-1 can be rescued by overexpression of this ubiquitin ligase.

Thus, Gag acts an adaptor to link the future virion membrane with the ESCRT machinery. These interactions lead to the recruitment of ESCRT-III proteins of the CHMP1, CHMP2, CHMP4 families (CHromatin Modifying Protein) and the VPS4 ATPase. These ESCRT-III subunits are then believed to polymerize into a dome that promotes closure of the membrane neck (Figure 1.13B) (144). This mechanism is topologically equivalent to the membrane fission events occurring during the release of vesicles into endosomal multivesicular bodies (MVB) or during the abscission stage of cytokinesis (Figure 1.13A) (139, 145). CHMP4 subunits are thought to form spiralling filaments around the inside of the neck of the budding virus. As the filaments spiral inward, they may create closed domes that constrict the opposing membranes until they separate from each other. VPS4 is also required for membrane fission, possibly by helping the dome formation and in the final stage, VPS4 uses the energy of ATP hydrolysis to disassemble the filaments and release the ESCRT-III subunits back into the cytoplasm as soluble, auto-inhibited proteins (146).

The membrane fission event completes assembly and the immature virion is released into the extracellular environment. At this final stage, the interferon-inducible restriction factor tetherin can interfere and block virus release. Its role in restricting virus particle release will be extensively described later in this chapter.

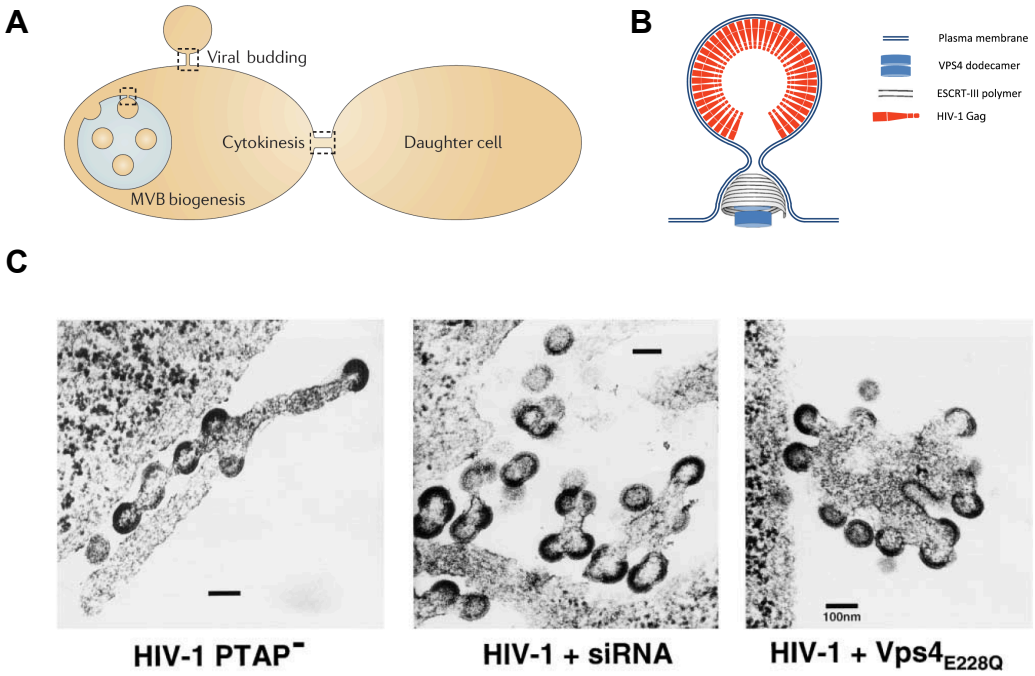

Figure 1.13: Role of ESCRT machinery in HIV-1 budding and release.

A: The membrane fission machinery mediated by ESCRT is required for three different cellular pathways. During cytokinesis ESCRT resolves the membrane neck at the midbody to separate the daughter cell. Fusion of late endosomes within multivesicular bodies (MVBs) also requires the ESCRT scission machinery. Finally, ESCRT mediates the budding of enveloped viruses at the plasma membrane. Figure adapted from (139). **B:** CHMP4 and CHMP2, components of ESCRT-III as well as the ATPase VPS4 are recruited by Gag-p6 at site of assembling virion. It is thought that ESCRT-III subunits assemble into filaments to form a dome-like structure, which ultimately constricts the junction between the cell membrane and the virion. This process is then accelerated and finalized by action of VPS4 through its ATPase activity to release the virion. Figure adapted from (147). **C:** Electron micrographs showing the effects of p6 PTAP mutation, depletion of Tsg101 and over-expression of the dominant negative Vps4 E228G on HIV-1 budding. In those conditions, virus budding is arrested at late stage with immature particles remaining connected to the plasma membrane via membrane stalks or to other budding particles to form clusters of inter-connected particles. Figure adapted from (140).

1.4.7 Maturation

While the HIV-1 virion is budding through the plasma membrane, the process of maturation begins. Gag and Gag-Pol multimerization triggers the activation of the viral protease PR, which then processes Gag into its constituent subunits. Once cleaved, the Gag domains undergo a series of conformational rearrangements that ultimately lead to the formation of a mature infectious viral particle. The most visible characteristic of HIV-1 maturation is the morphology conversion of capsid from spherical-shaped into a conical core (Figure 1.14).

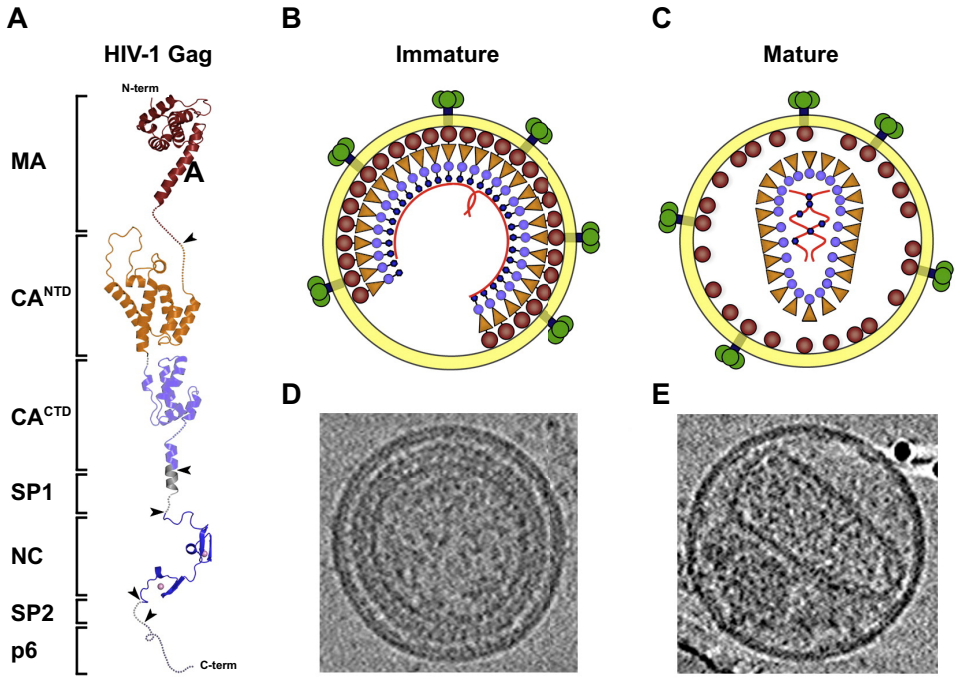

Figure 1.14: HIV-1 virion maturation.

A: Representation of the tertiary structure model of full-length HIV-1 Gag. Gag domains are displayed in different colours and the cleavage sites of PR are indicated by arrowheads. **B:** Representation of the organization of viral Gag proteins in an immature virion. **C:** Spatial arrangement of Gag proteins in a mature HIV-1 virion. **D:** Central section from a cryo-EM tomographic reconstruction of an immature HIV-1 virion. **E:** Same than E for a mature virion. Figure adapted from (148).

Maturation is driven by the viral protease PR. PR cleaves Gag at five different sites, ultimately producing the fully processed MA, CA, NC, and p6 proteins (Figure 1.15A). These cleavages occur in sequential order beginning with the cleavage between NC and sp1 followed by sp2/NC cleavage (149). Once released, NC stabilizes the genomic RNA as a dimer. MA/CA cleavage disassembles the immature lattice and releases CA-sp1. MA remains anchored with the inner leaflet of the viral membrane forming a discontinuous layer that covers the internal lipid envelope. The final stage of PR-mediated Gag processing is accomplished by cleavage between CA and sp1. This releases the CA proteins, which then assemble into hexamers to form the core structure. Occasionally, CA can associate into pentamers causing irregularities in the hexameric organisation. As a result, a cone structure is generated that closely resembles the fullerenes formed by elemental carbon (Figure 1.15B) (135, 150, 151). PR also cleaves at five different sites within the Gag-Pol polyprotein to generate IN, RT and PR proteins. Owing its crucial role in the HIV-1 replication cycle, several PR inhibitors have been designed and applied for the treatment of HIV-infected individuals.

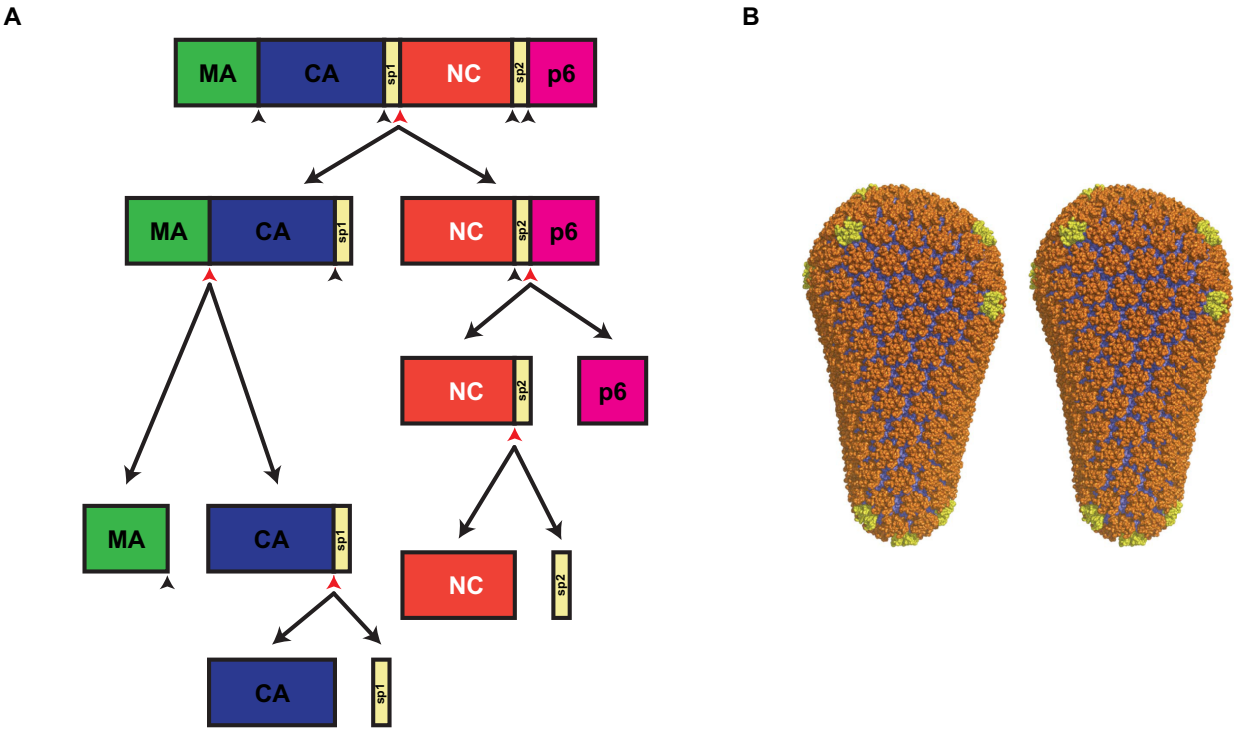

Figure 1.15: PR-mediated processing of Gag polyprotein.

A: Schematic representation of the proteolytic cleavages catalysed by PR during the HIV-1 maturation process. Arrowheads indicate proteolytic sites before cleavage. The order of cleavage events shown is based on the rates of cleavage: rapid (sp1/NC), intermediate (sp2/p6, MA/CA), and slow (NC/sp2, CA/sp1). **B:** Model of the HIV-1 capsid. Stereo view of a backbone-only fullerene cone model composed of 1,056 CA subunits. The hexamers, pentamers and dimers are coloured in orange, yellow and blue, respectively. This structure encloses the viral genome and facilitates its delivery into new host cells. Figure adapted from (152).

1.5 Immune Responses to HIV-1 Infection

HIV-1 infection elicits strong immune responses in patients, especially during the acute phase. However, they fail to eradicate the virus. The immune system harbours two different lines of defences that intervene at different stage during infection and are complementary with each other. The first line of defence, called innate immunity, involves the non-specific, and thus rapid intervention of immune cells, molecules, cellular pathways, all unified to react against a broad range of infectious agents. In this section we will discuss how intrinsic immunity factors called restriction factors and cellular sensors can elicit innate immune responses during HIV-1 infection. The second line of defence is represented by the adaptive immune system, which is antigen-specific and involves recognition and processing of antigens by the immune system. Once generated, adaptive immune responses are much more efficient at clearing traces of external agents than innate responses. The adaptive immunity can be classified into two types depending on the type of components that are involved, humoral or cellular mediated-immunity.

1.5.1 The Antibody Response

The adaptive (or acquired) humoral immune response involves B lymphocytes, which upon antigen-specific activation differentiate into plasma cells to secrete antibodies (reviewed in (153)). Neutralizing antibodies (NAbs) are able to directly bind to HIV-1 envelope glycoprotein and block the interaction of viral particles with CD4 and CCR5, or fusion by gp41. Non-neutralizing antibodies may also inhibit infection through recruitment of effector cells such as NK cells or the complement system.

At early times post-HIV-1 infection, antigen-antibody interactions result in the secretion of anti-gp41 and anti-gp120 non-neutralizing antibodies that do not reduce circulating viral loads. Months later, autologous NAbs appear but their spectrum of action is limited; they generally only recognize the specific invading viral strain since they tend to target specific variable regions of the envelope glycoprotein (154-156). These autologous NAbs drive the evolution of the envelope protein to escape from neutralizing responses. Escape variants emerge through single amino acid substitutions, insertions, and deletions or through changes in the glycan shield in which shifting N-linked glycans prevents access of NAbs to their cognate epitopes (156). In some individuals, autologous NAbs develop the ability to recognize more conserved viral regions thus rendering them able to neutralize heterologous HIV-1 variants. The reasons why some individuals (≈ 30%) develop these broadly cross neutralizing (BCN) antibodies is unclear but these responses seem to be related to the duration of infection and viral levels suggesting that years of persistent viral stimulation are necessary for their generation (reviewed in (157)).

BCN antibodies target conserved envelope regions; IgG1b12 targets the CD4 binding site in gp120 (anti-CD4bs), the antibodies 4E10 and 2F5 bind to conserved epitopes within the membrane-proximal external region of gp41. The investigation of such antibodies and their targets is important to develop potential immunogens that could serve as candidates for

vaccines (158). HIV-1 might have more difficulty to develop mutants able to escape from such BCN antibodies. The CD4 binding site represents one of the most attractive targets because it is a highly conserved site present on all HIV-1 genetic subtypes, and mutations into this region are likely to impair virus fitness.

Despite the establishment of an antibody response against HIV-1 infection, the results generated so far seem to indicate that the role of NAbs in controlling established infection is limited due to viral escape (reviewed in (157)). Human vaccine trials that focused on envelope immunogens failed to elicit strong NAbs. But the considerable technical improvements might allow in the future to identify new sites of vulnerability in the HIV-1 envelope.

1.5.2 The T-Cell Response

Cellular immunity is mainly mediated by cytotoxic T lymphocytes (CTLs) that directly kill infected cells upon recognition of MHC Class I-peptide complexes presented on their surface. During the acute phase of HIV-1 infection, $CD8^+$ T-cell responses are generated and play an important role in controlling initial viremia. $CD8^+$ T cells that develop during this phase tend to react against a narrow range of epitopes mainly derived from Env and Nef, regions that are amongst the most variable in the virus (159-161). Following acute infection, CTLs evolve to extend their repertoire of epitopes. Most chronically infected individuals target more than a dozen $CD8^+$ epitopes simultaneously and in some instances up to 19% of $CD8^+$ T cells are specific for HIV, yet control of viremia is not achieved. Without ruling out the contribution of cytokine and chemokine production (interferon-γ, IL-2, TNFα, etc.), it is through their lytic ability that CTLs mainly modulate disease progression.

Some individuals control HIV better than others, and this was shown to be related to certain HLA-B alleles (162-164). Some protective HLA-B class I alleles have been identified such as B57, B58, B81, B14 and HLA-B27 that target conserved epitopes in Gag. In most cases, these protective HLA-B alleles are associated with a decrease of disease progression. The determinants of this influence on HIV control map to residues within the HLA binding groove that bind to the viral peptide (165). Presumably, certain amino acids are preferential to provide a stronger association with the viral peptide, and thus promote a better presentation to CTLs. Protective HLA alleles may also function in part through induction of fitness-impairing mutations. For instance, escape mutations within Gag that arise to avoid recognition by HLA B57 impair the capacity of the virus to replicate (166). This might explain the reason why $CD8^+$ T-cell responses targeting conserved Gag epitopes are associated with lower viral loads, whereas $CD8^+$ T-cell responses targeting Env that can readily be tolerated by the virus without affecting its fitness are associated with higher viral loads. Although $CD8^+$ T cells from infected patients display robust responses to inhibit viral replication *in vivo*, the individuals can still progress to AIDS. $CD4^+$ T-cell responses are much more attenuated since they are constantly damaged by viral replication and impaired considerably in their proliferative capacity.

1.5.3 Innate Immune Control of HIV-1 and Restriction factors

The first line of defence of the immune system upon HIV-1 entry into the human host involves an array of cell subsets, intracellular antiviral proteins, inflammatory cytokines and the complement system, which altogether constitute the arsenal of the innate immune system. Innate immune cells include phagocytes (monocytes, macrophages, dendritic cells), cytolytic cells (NK cells and neutrophils) and professional antigen-presenting cells such as dendritic cells (DCs). Each of these cells express distinct innate immune receptors called pattern recognition receptors (PRRs) (reviewed in (167)). Unlike the antigen-specific receptors of the adaptive immune system, PRRs are able to directly detect small molecular motifs common to pathogens called PAMPs (pathogen associated molecular patterns). PRRs include the toll-like receptors (TLRs), C-type lectin receptors (CLRs) and the cytoplasmic PRRs (RIG-I like helicases, NOD-like receptors, DNA sensors). The recognition of PAMPs is then followed by an intracellular signalling cascade that ultimately leads to the transcription of pro-inflammatory genes and generates an antiviral state. Two classes of transcription factors are mobilized upon PRR engagement: interferon regulatory factors (IRFs), which activate transcription of type I interferon, and NF-κB essential for expression of pro-inflammatory cytokines and chemokines.

HIV-1 particles can induce expression of IFNα from plasmacytoid dendritic cells (pDCs) through engagement with TLRs, particularly via the recognition of viral genomic single-stranded RNA by TLR7 and TLR9 from endocytosed virions (168-171). TLRs are transmembrane proteins, and the TLRs that recognize nucleic acids (TLR3, TLR7, TLR8 and TLR9) are located in endosomes of antigen-presenting cells. Whereas the endosomal TLRs detect nucleic acids after internalization, specialized cytosolic nucleic acid sensors detect RNA or DNA derived from infection.

In T cells and macrophages, HIV-1 infection does not induce a strong antiviral interferon response *in vitro*. A reason for this is the presence of a cytosolic exonuclease, TREX1, that hides HIV-1 from cytosolic nucleic acid sensors by degrading cytoplasmic HIV-1 ssDNA (172). In the absence of TREX1, HIV-1 infection leads to the accumulation of HIV-1 DNA in the cytosol, which triggers DNA sensors and interferon responses. The cytoplasmic DNA sensors involved in this pathway have not been identified yet. Triggering of this unknown sensor by HIV-1 DNA activates STING, activating TBK1, which phosphorylates IRF3. Phosphorylated IRF3 dimerizes and translocates into the nucleus, where it interacts with the promoters of interferon genes.

In quiescent $CD4^+$ T cells, accumulation of incomplete reverse transcripts that fail to integrate elicit pro-apoptotic and pro-inflammatory responses leading to cell death (33).

Monocytic-derived DCs are relatively refractory to HIV-1 infection and produce low levels of IFN when encountering HIV-1. The reason for that has been attributed to the newly identified restriction factor SAMHD1 (173). But when resistance to infection with HIV-1 is circumvented, the virus induces DC maturation and type I IFN production (174). This process might rely on the interaction of newly synthesized viral capsid (CA) with cellular cyclophilin A. The protein sensor that triggers this IFN production has not yet been identified.

Among the innate immune cells involved in the control of HIV, evidence indicates a central role for NK cells (175). NK cells are a subset of large granular lymphocytes that are able to sense viral infections bypassing the antigen presentation process. When NK cells bind to MHC class I molecules on the surface of uninfected cells, NK receptors called killer immunoglobulin-like receptors (KIRs) provide a negative or inhibitory signal to the NK cells, preventing them from mediating killing. HIV-1 infection reduces the expression of certain MHC class I alleles at the surface of infected cells, thus allowing the activation of NK cells. But loss of MHC class I expression is not sufficient to trigger NK-cell destruction of an HIV-infected cell, and requires a second activating signal through recognition of a stress-ligand. For instance, HIV-1 infection often results in the upregulation of the stress-inducible ligands for the activating c-type lectin NK-cell receptor NKG2D. MIC-A, ULBP-1/2 are examples of those ligands and their expression may be downregulated by Nef in infected cells (176).

While *in vitro* HIV-1 infection does not trigger a strong IFN production, acutely infected patients present high levels of plasma type I interferon (177). Production of interferon released into the extracellular environment serves as a stimulatory signal to induce expression of more than a hundred IFN-stimulated genes (ISGs). Amongst the genes upregulated upon interferon production, those encoding for cellular factors called restriction factors provide direct resistance to HIV-1 and other viral infections. These factors possess intrinsic immune functions and can be seen as an extension of the innate immune system. To date four restrictions factors have been identified: APOBEC3G, Tetherin, SAMHD1 and TRIM5α (cf. Figure 1.6). They all directly interfere with the virus life cycle at a different stage through distinct mechanisms. The notion that specific cellular proteins could be entirely devoted to block retroviral replication emerged following the identification of Fv1 (Friend virus susceptibility 1). Fv1 was found to block the replication of MLV (murine leukaemia virus) in mice by targeting viral capsid proteins. For years the efforts were focused on identifying cellular molecules, called co-factors, recruited by the virus to perform its functions but this concept could not explain the cell-tropism of retroviruses. Importantly, restriction factors share common features. Firstly, they can be constitutively expressed in certain cell types and they are induced or upregulated by type I interferon. Sequence analyses reveal that restriction factors have undergone strong positive selection during mammalian evolution as a result of viral pressure. Viruses and host have co-evolved over millions of years. Evolution of a given restriction factor is followed by adaption of its viral countermeasure. Both sides rapidly evolve to gain an advantage (reviewed in (178)). HIV-1 has developed a countermeasure for all the restriction factors identified either through a specific protein dedicated to this function or by mutating its structural components.

In the next section we will provide an overview of the findings concerning tetherin and its antiviral function.

1.6 Tetherin

1.6.1 Tetherin, the last block before virus escape

The antiviral activity of tetherin was identified through the investigation of the HIV-1 accessory protein Vpu. Vpu was known to be required to enhance virus particle release from HIV-1 infected cells in a cell-type dependent manner, but the reasons for this phenotype remained to be solved (179, 180). HeLa were an example of human cells that were not permissive (or restrictive) to HIV-1 release in the absence of Vpu (181). By contrast, other human cells such as 293T, HT1080 or African green monkey cell lines COS-7 allowed viral egress independently of Vpu expression (182-184). Infection of non-permissive cells with HIV-1 lacking Vpu resulted in newly assembled virions that remained attached to the cell surface and accumulated in endosomal vesicles ($CD63^+$ late endosomes), rather than being released into the supernatant (183). This phenotype could be induced in permissive COS-7 cells by fusing them with restrictive HeLa cells, suggesting the existence of a dominant inhibitor expressed by HeLa cells but not by COS-7 cells that was antagonized by Vpu (184). Importantly, permissive cells treated with type I interferon could also become restrictive to Vpu-defective HIV-1 release (185).

It was also known that, beyond its ability to enhance HIV-1 release, Vpu could also promote the release of other retroviruses such as Murine Leukaemia virus (MLV), or VLPs from Ebola virus, indicating that the unknown viral inhibitor could function in a non-specific way to block enveloped-virus particle release (181, 185). Additional experiments revealed that fully mature virions retained at the surface of cells infected with Vpu-deleted HIV-1 could be released by proteolysis, particularly when their endocytosis was blocked using a dominant negative form of Rab5 (183, 185). Therefore based on these data, the inhibitor candidate was predicted to be a cellular interferon-induced protein constitutively expressed in HeLa cells but not in 293T cells, that could block virus release and that was antagonized by HIV-1 Vpu. Then, in early 2008, two independent groups attributed the restriction of the release of HIV-1 virions to BST-2 (186, 187). Neil et al renamed BST-2 " tetherin " to refer to its potential mode of action consisting of tethering the nascent virions to the cell surface. In cells where HIV-1 virion release required Vpu expression, siRNA depletion of tetherin rescued Vpu-deficient HIV-1 particle release. Tetherin was identified by microarray analyses of messenger RNAs between cells that required Vpu for HIV-1 release and those that did not. In this screening, tetherin mRNA was 20-fold higher in HeLa than in HOS cells and upregulated with the same magnitude by IFN-α in 293T and HT1080 cells. At that time, tetherin was designated BST-2 (bone marrow stromal antigen 2 or CD317) and described as expressed on terminally differentiated B cells (188), bone marrow stromal cells (hence the name BST-2) (189), and plasmacytoid dendritic cells (190). Its expression on B cells supposed a potential role in B cell development. Tetherin was also previously identified as the most downregulated cell-surface protein by KSHV-K5 from a quantitative proteomics SILAC screening (191).

Since then, tetherin has become a novel component of the innate immune response against HIV-1 infection. Even if later studies revealed the broad range of tetherin against other

enveloped viruses, HIV-1 Vpu historically remains the prototype viral antagonist of tetherin. For the last four years tetherin has been extensively studied, and, beyond the restriction of virus particle release, additional studies suggest that tetherin might have a wider role in the antiviral immune response (reviewed in (192)).

1.6.2 Tetherin: Features of a unique protein

Tetherin is expressed in plasmacytoid dendritic cells, some cancer cells, terminally differentiated B cells, macrophages, T cells and in bone marrow stromal cells. However, it becomes generally expressed in many cell types and tissues after treatment with type I interferon underscoring its crucial role in the innate immune response to virus infections (190).

Tetherin is a glycosylated type II integral membrane protein whose the molecular weight can vary from 28 kDa to 36 kDa depending on its glycosylation profile (190, 193, 194). In the literature tetherin is often qualified as '' unusual '' due to its topology that so far is shared with only one variant of the prion protein (Figure 1.16A) (195). Tetherin is anchored in the plasma membrane via two types of membrane anchors at the N- and C-terminal regions (193). Tetherin is composed of a short N-terminal cytoplasmic tail linked to a transmembrane region that is predicted to be a single alpha-helix followed by a coiled-coil structure in the extracellular domain, and a C-terminal glycophosphatidyl-inositol (GPI) lipid anchor that links the protein back to the cellular membrane. The GPI anchor is added post-translationally by the ER-resident enzyme PIGL. In the absence of PIGL, proteins such as tetherin harbouring a GPI modification signal are inserted into the ER membrane but remain trapped and fail to enter the secretory pathway (196, 197). The ectodomain contains two N-linked glycosylation sites (N-65 and N-92) and three cysteine residues (C-53, C-63 and C-91) that mediate disulfide bond formation (Figure 1.16A) (197, 198). The extracellular core region forms a single long helix that associates as a parallel dimeric disulphide-linked coiled-coil domain (residues 47-152), and adopts a 17 nm long rod-like structure that displays flexibility at the N-terminus (Figure 1.17) (199-202). The N-terminus of the extracellular domain can also form an anti-parallel four-helix bundle through association with another tetherin dimer, creating a global tetrameric structure. However, mutagenesis studies indicate that the tetrameric form of tetherin might not be essential for its antiviral activity and is likely to be an artefact resulting from production of tetherin in bacteria under reducing conditions.

Although tetherin glycosylation has been shown to positively contribute to its transport and folding, it seems to be dispensable for its antiviral function (197). Mutations of all three cysteine residues abolish tetherin antiviral function despite expression being maintained at the cell surface. Interactions within the coiled-coil region and at least one of out the three cysteine residues in the extracellular domain are required to allow disulphide bond formation, promote dimer stability and consequently support antiviral function.

Tetherin localizes to sites of HIV-1 assembly at the plasma membrane (186, 193, 203, 204). Super-resolution microscopy analysis showed the presence of tetherin clusters containing on

average 4 to 7 tetherin dimers at HIV-1 assembly sites (205). Interestingly, a tetherin mutant lacking the C-terminal GPI anchor (tetherin delGPI) but not tetherin delTM (deletion of the C-transmembrane anchor) has been found associated with Gag-containing budding sites indicating that the tetherin transmembrane domain might drive tetherin localization to HIV-1 budding sites. At the plasma membrane, tetherin is inserted into cholesterol-rich micro-domains (also called lipid rafts) via its GPI lipid anchor (193). In addition to its localization at the cell surface, tetherin is also expressed in intracellular compartments, particularly in the TGN and in early/recycling endosomes.

Unlike other known GPI-anchored proteins, tetherin is endocytosed from the cell surface in a clathrin-dependent manner. This internalization appears to rely on the interaction between the clathrin adaptor protein AP-2 subunit and a non-canonical, highly conserved dual tyrosine motif within the tetherin cytoplasmic tail (YxYxxϕ) (206, 207). Tetherin is then transported from the endosomes to the TGN through recognition of the cytoplasmic domain by the AP-1 complex. Therefore, the trafficking of tetherin from the plasma membrane to the TGN requires a sequential action of AP-2 and AP-1 adaptor proteins. Additionally, tetherin localizes at the apical surface of polarized epithelial cells where it interacts with the underlying actin cytoskeleton through association with RICH-2, EBP50 and ezrin, thus providing a physical link between lipid rafts and the apical actin network in these cells (203). The potential contribution of these properties for tetherin's antiviral action has yet to be evaluated.

A

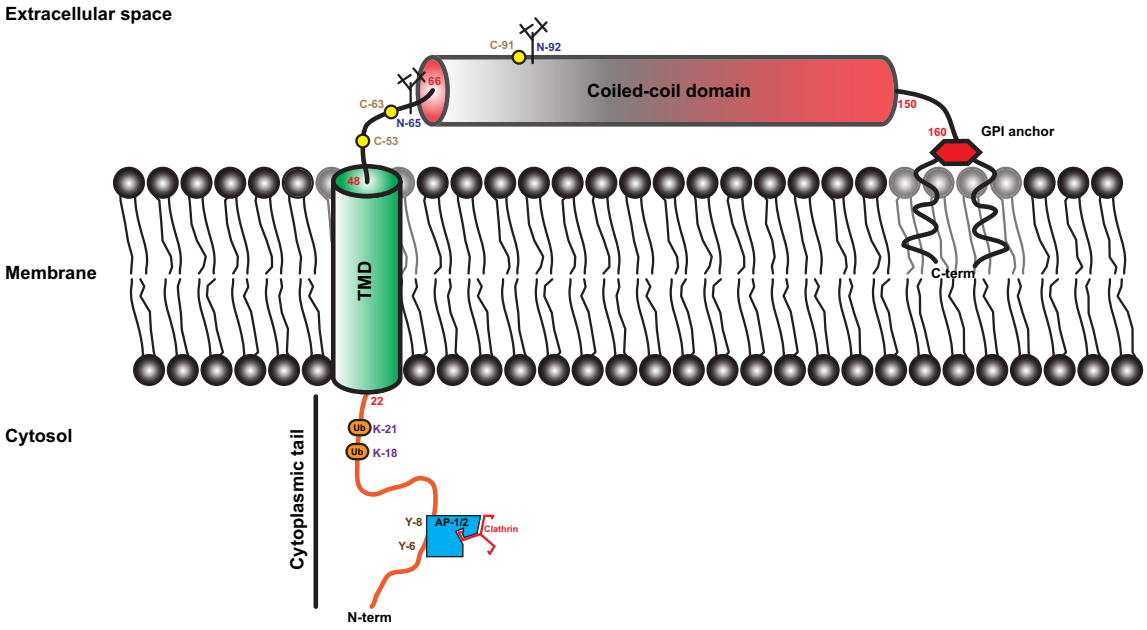

B

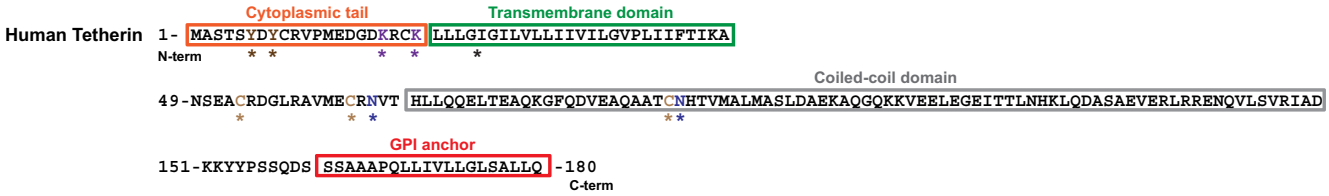

Figure 1.16: Topology and features of tetherin.

A: Predicted secondary structure of tetherin monomer. The tyrosine-based endocytic motif (YxYxxϕ) and the potential ubiquitin-acceptor lysine residues (K18 and K21) are indicated on the cytoplasmic tail. Three cysteine residues at position 53, 63 and 91 involved in dimerization and the two N-glycosylation sites (N-65 and N-92) are indicated in the extracellular domain. The core region of the ectodomain forms a coiled-coil domain composed of two α-helical regions followed by a GPI anchor that links back the protein to the membrane. **B:** Primary structure of tetherin. On the sequence are displayed the features indicated in panel A.

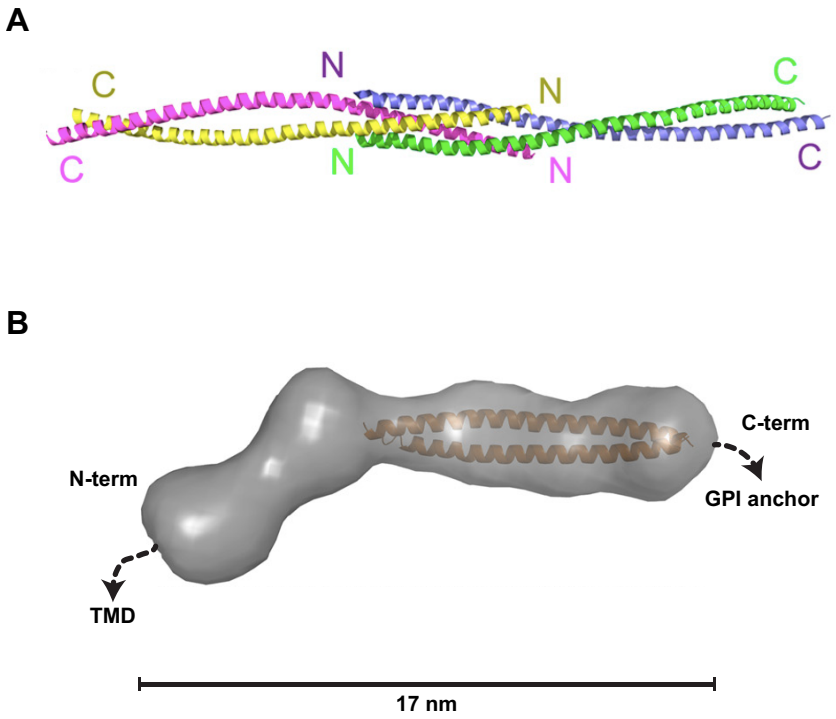

Figure 1.17: Structure of tetherin ectodomain.

A: Tertiary structure of reduced tetherin (residues 47-152) based on X-ray crystallographic studies. The structure forms a single long helix that associates as a parallel dimeric coiled coil over its C-terminal two-thirds (yellow/magenta and blue/ green dimers), while the N-terminal third forms an anti-parallel four-helix bundle with another dimer, creating a global tetramer. Figure adapted from (200). **B:** Model of the global rod-like structure adopted by the entire extracellular domain (residues 47-159). The parallel dimeric α-helical coiled-coil domain (residues 80-147) is indicated. Figure adapted from (199).

1.6.3 Tetherin ties up a broad range of enveloped viruses: Antiviral activities

The inhibitory mechanism is relatively non-specific, as tetherin can restrict the release of a broad range of viruses that all share a lipid envelope derived from host cells. Initially, tetherin was identified as the inhibitor of HIV-1 virus release, but further studies revealed the ability of tetherin to restrict many other retroviruses (alpha-retrovirus, beta-retrovirus, delta-retrovirus, lentivirus, spumaretrovirus), filoviruses (Ebola and Marburg viruses), arenaviruses (Lassa and Machupo viruses), paramyxovirus, gamma-herpesvirus (KSHV) and rhabdoviruses (vesicular stomatitis virus) (204, 208-211). Because tetherin restricts such a wide spectrum of viruses, it is unlikely that the mechanism requires specific interactions with viral proteins. Presumably, tetherin could trap any enveloped virus that buds from the cellular membrane by interacting with the virion lipid envelope, unless the virus buds from a region devoid of tetherin. This notion, however, was recently challenged by a study showing that influenza A virus was insensitive to tetherin expression (212). In contradiction to this, Mangeat et al. showed that expression of tetherin strongly inhibited fully replicative influenza virus with the same potency as other anti-

influenza cellular factors such as MxA, ADAR1, ISG15 and viperin (213). These results combined with the fact that tetherin is largely expressed upon interferon stimulation, indicate that tetherin may be an effective component of innate immune defence against pathogens.

1.6.4 Tetherin, an aptly named protein: Mode of action

In the absence of counteracting factors like Vpu, tetherin restricts retroviral particle release by trapping nascent virions at the cell surface. Aggregated virions at the plasma membrane are subsequently internalized into endosomes and directed to lysosomes for destruction. Dominant-negative mutants of Rab5a, the early endocytic GTPase, can inhibit this process (186). So far, studies performed to elucidate the mechanism by which tetherin retains viral particles at the cell surface suggest that it, as implied by its name, directly tethers/cross-links the virions to the host-cell membrane (Figure 1.18A). This model is supported by the observation that Vpu-defective particles can be released from the cell surface by protease treatment (186). Tetherin colocalization with the HIV-1 structural protein Gag along the plasma membrane has been observed in immunofluorescence assays. Consistent with a direct tethering mechanism, immunoelectron microscopy showed that tetherin was detected between virions and the plasma membrane and intercalated within clusters of virions (Figure 1.18B-C-D) (214, 215).

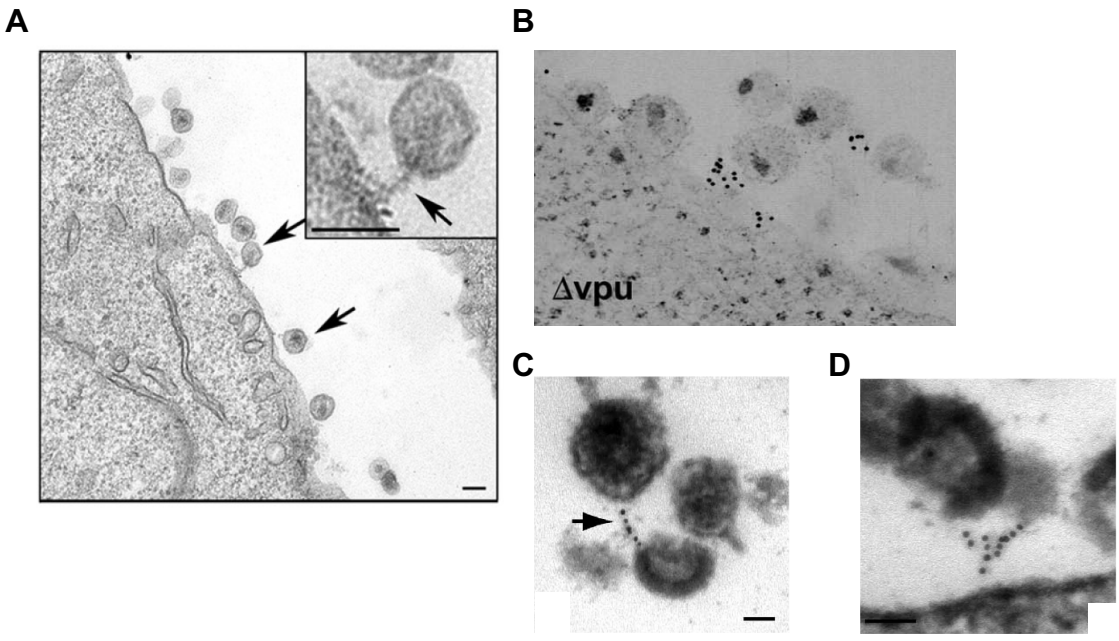

Figure 1.18: Tetherin functions as a physical bridge between virions and the plasma membrane.

A: Virions tethered to the plasma membrane. Ultrathin sections of HIV-1 delVpu infected Jurkat cells and processed for TEM. Tethered virions are indicated with arrows. Bar=100 nm. These Vpu-defective particles appear to be connected by a membrane stalk. Such a stalk could be lined with multiple tetherin molecules. Figure adapted from (216). **B:** Visual evidence of direct virion tethering and virion-incorporation of tetherin. HeLa cells were transfected to express a

Vpu-defective HIV-1 and stained for cell surface tetherin (antibody against tetherin ectodomain) and processed for electron microscopy. Figure adapted from (215). **C:** Immunoelectron micrographic of indinavir-treated Vpu-defective infected A3.01 cells. Detection of linear tetherin filament bridging virions demonstrating inter-virion connections. Bar=50 nm. Figure adapted from (214). **D:** immuno-electron micrographic analysis of Vpu-defective-infected A3.01 cells treated with indinavir. Immunogold labelling of tetherin localized to particle budding sites on the plasma membrane of IFN-α stimulated cells. Bar=50nm. Figure adapted from (214).

Beyond the visual evidence, biochemical studies also revealed that tetherin was physically incorporated into HIV-1 particles in the absence of Vpu (197). Importantly, tetherin's unusual configuration rather than its primary sequence seems to determine its antiviral function. Indeed, a complete artificial tetherin-like protein composed of unrelated protein subunits (TMD from the transferrin receptor, a coiled-coil domain from distrophia myotonica protein kinase, and a GPI anchor from urokinase plasminogen activator receptor), thus mimicking tetherin topology, inhibited the release of HIV-1 and Ebola virus particles almost as efficiently as the native protein (197). This result suggests that tetherin acts on its own as a cross-linker and does not require a cellular co-factor to achieve its function. Altogether these data support a model in which tetherin serves as physical bridge between nascent virions and host cell membrane, however the precise configuration adopted by tetherin molecules in this context is still unclear. The ability of tetherin molecules to form dimers is required for its restriction activity and this conformation implies the integrity of at least one of the three cysteine residues to mediate disulphide bonds (197, 198). Studies performed on the crystal structure of the extracellular core of tetherin reveals a parallel dimeric disulphide-linked α-helical coiled coil structure (199-201). Weak interactions exist between the coiled-coil domain of each monomer but because of irregularities in the sequence, the disulphide bonds are thought to provide dimer stability. Actually, the weak coiled-coil interactions through salt bridges together with the stabilizing disulphide bonds generate a dynamic structure, which confers a controlled-flexibility of the coiled-coil essential during dynamic processes such as virus particles budding from the plasma membrane. Indeed this dynamic feature would be essential to allow tetherin to maintain its links with both the cellular membrane and the newly forming virus membrane. This model might explain the fact that treatment of infected cells with a reducing agent such as DTT fails to release trapped virions from the cell surface indicating that interactions might subsist within the coiled-coil regions.

The dimerization state of tetherin is required for its antiviral activity but the precise configuration adopted by the dimers remains to be clarified. Indeed, several models of possible direct tethering mechanisms have been proposed. For instance, tetherin might be anchored in a single membrane either from the virus or the host cell, and virions would be retained through the interaction between the ectodomains (Figure 1.19A). Alternatively, both tetherin anchor regions might be incorporated into different membranes, one end in the cellular membrane and the other end in the viral membrane, and in that configuration, ectodomains interaction would consolidate virion trapping (Figure 1.19B). Based on the X-ray structure study of the coiled-coil domain, it is predicted that the two tetherin monomers face each other in a parallel orientation.

Finally, to add more complexity, the parallel dimers could be arranged either with the GPI anchors in the viral membrane or in the cellular membrane. The discrimination between the three models proposed has not been fully solved, disrupted by contradictory results. Elimination of either the N-terminal transmembrane region (TM) or the C-terminal GPI anchor abolishes the ability of the molecule to tether virions supporting the model in which tetherin is a parallel homodimer with one set of anchors in the host membrane while the other set is embedded in the virion membrane (197). But both inactive-tetherin mutants are efficiently incorporated into released virions. Virions recovered from restriction at the cell-surface by protease stripping contained N-terminal tetherin fragments suggesting that tetherin might insert its TM anchor into virus membranes (197). Paradoxically, treatment of retained virions with the GPI anchor cleavage enzyme, phosphatidyl inositol-specific phospholipase C (Pi-PLC) did not entirely released virions from the cell surface (215). Crystal structure analysis revealed that the complete extracellular domain of tetherin formed an extended 170Å long structure (199-201) inconsistent with EM studies detecting distances larger than that between cellular membranes and retained-virions (214, 215). Potentially, retention of virus particles involves the formation of more complex structures such as clusters of tetherin dimers similar to those observed by super resolution microscopy (205). Therefore, more studies will need to be done to fully understand the spatial arrangement of tetherin dimers required to capture and retain virus particles at the plasma membrane.

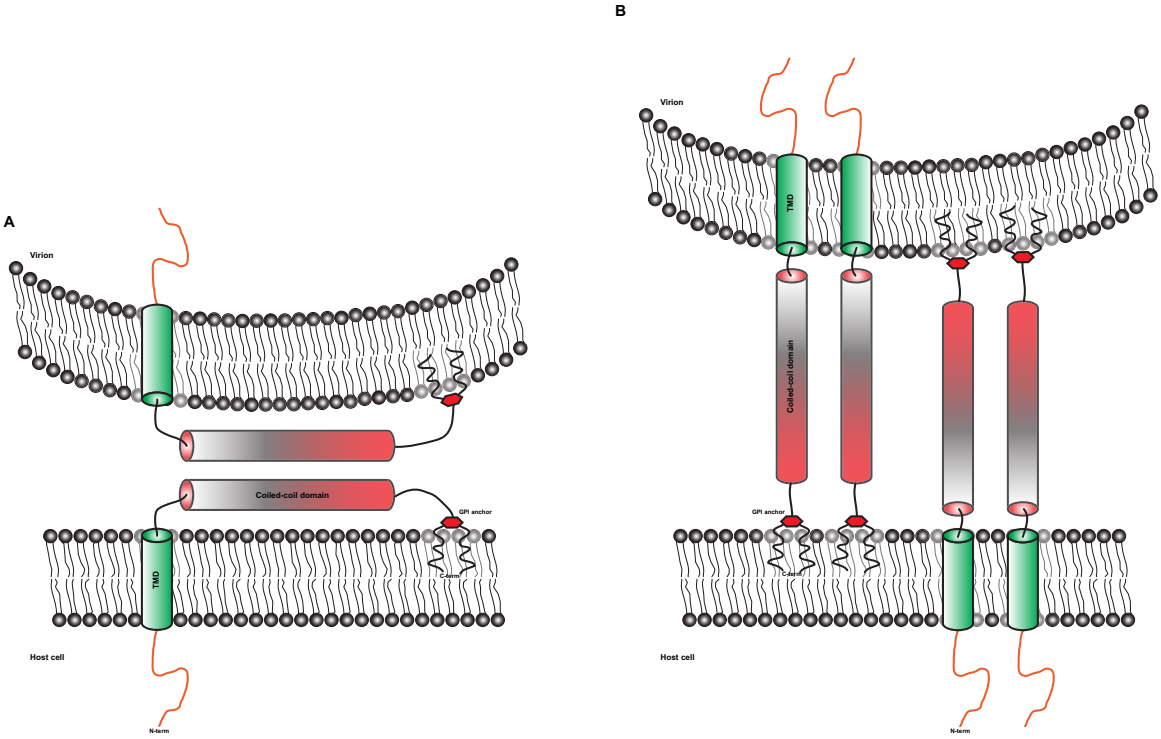

Figure 1.19: Models of tetherin-mediated retention of virus particle.

A: In this model, virions are retained through interactions of the ectodomains of each tetherin monomer. One monomer is anchored, via both ends, in the host cell membrane while the other monomer is inserted in the virion. **B:** Each monomer is inserted in both membranes. Monomers are arranged in a parallel orientation, and either the GPI anchors or the N-TM domains can span the cellular membrane.

1.6.5 Tetherin, a common enemy: Viral countermeasures

By the nature of its mode of action, tetherin can restrict many enveloped viruses. Tetherin reflects the capacity of the host cellular machinery to react against invading pathogens and, thus, may constitute a mandatory target for enveloped viruses. As membranes of viruses are immutable, this has led several viruses to develop their own countermeasures to overcome tetherin's function (reviewed in (217)). Specific proteins encoded by diverse viruses have been identified that share the ability to inactivate tetherin's function. In addition to the prototype tetherin antagonist, Vpu, six other mammalian virus-encoded proteins have been characterized so far: SIV Nef, HIV-2 Env, SIVtan Env, SIV Vpu, KSHV-K5 and Ebola-GP (Table 1.1).

Tetherin species	Restricted virus	Viral antagonist	Mechanism of counteraction
Human	HIV-1	Vpu (Group M)	Cell-surface downregulation Alteration of cellular trafficking Lysosomal degradation
	HIV-2	Env	Intracellular sequestration / No degradation AP-2 dependent
	Ebola	GP	? No cell-surface downregulation or degradation
	KSHV	K5	Cell-surface downregulation Lysosomal degradation
Chimpanzee	SIVcpz	Nef	
Gorilla	SIVgor	Nef	
Old World monkeys			
Rhesus macaque	SIVmac	Nef	Stimulation of internalization from the cell-surface
African green	SIVagm	Nef	AP-2 dependent mechanism
Sooty mangabey	SIVsmm	Nef	
Blue monkey	SIVblu	Nef	
Red capped monkey	SIVrcm	Nef	
Moustached monkey	SIVmus	Vpu	Cell-surface downregulation?
Mona monkey	SIVmon	Vpu	
Greater spot-nosed	SIVgsn	Vpu	
Tantalus monkey	SIVtan	Env	Intracellular sequestration / No degradation Similar to HIV-2 Env

Table 1.1: Viral antagonists of tetherin.

This table summarizes the mechanisms employed by viral countermeasures from primate lentiviruses and other enveloped viruses to overcome tetherin-mediated restriction from their corresponding host.

HIV-1 Vpu

Vpu reduces tetherin expression on the cell-surface (187) and directs it towards a lysosomal compartment for degradation (Figure 1.20) (218-220). Vpu targets tetherin by interacting with its transmembrane domain. Some of the determinants required for this interaction have been mapped and form a single face of both proteins' respective TM domains (221, 222). Vpu displays species-specificity governed by these TM domain interactions (223, 224). For this reason, HIV-1 Vpu can only counteract human, chimpanzee, and gorilla tetherins. The mechanism by which Vpu neutralizes tetherin has been extensively studied for the last four years. Several hypotheses have been proposed to explain how Vpu induces tetherin downregulation from the cell surface, and as a result inactivates its antiviral activity on HIV-1 release. The molecular mechanism of Vpu-mediated tetherin antagonism will be discussed in depth later (cf. section 1.8.2.2).

SIV Nef

Most of the SIV strains that do not encode a Vpu gene have acquired anti-tetherin activities in their Nef proteins (225-227). Specifically, the SIVmac (macaque/rhesus), SIVagm (African green monkey), SIVsmm (sooty mangabey), SIVblu (blu monkey), SIVrcm (red capped monkey) Nef proteins can suppress tetherin activity in a species-specific manner. Indeed, all these Nefs only efficiently counteract the tetherin proteins from their natural host, but they fail to target human tetherin. This specificity is governed by the deletion of a motif in the human cytoplasmic tail of tetherin (-GDIWK-). The tryptophan residue of this motif has been under high selective pressure in primates potentially imposed by viruses, and this may have forced the protein to mutate into a resistant form. Interestingly, insertion of this motif into the human tetherin cytoplasmic domain confers sensitivity to SIV Nef proteins (227). For the same reason, HIV-1 and HIV-2 Nef proteins are unable to antagonize human tetherin but retain some activity against rhesus and sooty mangabey tetherins but are less potent than SIV Nefs. In contrast to the SIV strains mentioned above, SIVcpz (chimpanzee) and SIVgor (gorilla), which do encode Vpu proteins, also use their Nef proteins to overcome tetherin's function.

Like Vpu, SIVmac Nef downregulates rhesus tetherin from the cell surface (Figure 1.20). The myristoylation site and a putative cholesterol recognition motif within Nef sequence are required for tetherin downregulation, thus highlighting the importance of Nef membrane localization. This is consistent with recent findings suggesting that Nef increases the internalization of tetherin from the cell surface (228). Depletion of the clathrin adaptor AP-2 using RNA interference, and mutations in an AP-2 binding site in Nef impair its ability to antagonize tetherin, demonstrating that AP-2 recruitment is required for Nef proteins to counteract tetherin. This suggests that Nef uses the same mechanism to downregulate CD4 and tetherin: recruitment of AP-2 and stimulation of clathrin-mediated endocytosis.

HIV-2 and SIVtan Envelope glycoproteins

It was long known that HIV-2 Env had a Vpu-like activity in that it could enhance the virus particle release from certain cell types and could substitute for Vpu in rescuing HIV-1 particle release from HeLa cells (229). HIV-2 Env was shown to act as a human tetherin antagonist (230). The envelope protein from the human $CD4^+$ T cell-line passaged tantalus SIV (SIVtan) has a similar activity against tetherin (231). In addition to the ability to antagonize tetherin from their natural host, HIV-2 Env and SIVtan Env also display activity against rhesus tetherin.

Studies showed that, similar to Vpu, HIV-2 Env and SIVtan Env could interact and reduce tetherin expression at the cell surface (Figure 1.20). HIV-2 Env requires an intact GYxxθ endocytic sorting motif in the cytoplasmic domain of gp41 to mediate cell-surface tetherin downregulation (230, 232, 233). This motif binds to the clathrin adaptor complex AP-2, suggesting a mechanism in which Envs might promote tetherin internalization by recruiting the endocytic machinery. Importantly, only mature Env proteins, processed into gp105 and gp41 by furin digestion, are able to antagonize tetherin. The ability of Env to overcome tetherin may rely on mutual interactions through the ectodomains. This was illustrated by studies showing that substitution of a single amino acid (A100D), found in the porcine protein, in the extracellular domain of human tetherin could confer resistance to HIV-2 Env and SIVtan Env (231). Interestingly, this residue was found to be under positive selection in mammals.

Unlike Vpu, Env proteins do not reduce total tetherin cellular levels but rather induce accumulation of tetherin in intracellular compartments, preventing it from localizing to the cell surface and virus assembly sites.

Finally, Nef-deleted SIVmac viruses are attenuated in macaques and maintain persistent low-level replication without generally causing disease in their host (234). But, occasionally, Nef-deleted SIVmac reverts to pathogenicity inducing severe effects *in vivo*. Isolation of these pathogenic revertants revealed that activity against rhesus tetherin had been developed by the envelope protein (235). The genetic changes associated with pathogenic Nef-deleted SIVmac included five amino acid substitutions in the cytoplasmic tail of the gp41 subunit of Env. The resulting envelope protein was found to interact with rhesus tetherin and its activity relies on the presence of the membrane-proximal GYXXθ sorting signal in gp41 cytoplasmic tail in combination with the new five amino acids. Unlike HIV-2 and SIVtan Envs, the ectodomain of Nef-deleted SIVmac Env was dispensable for overcoming tetherin. Therefore, there are several ways for Env to evolve into a tetherin antagonist.

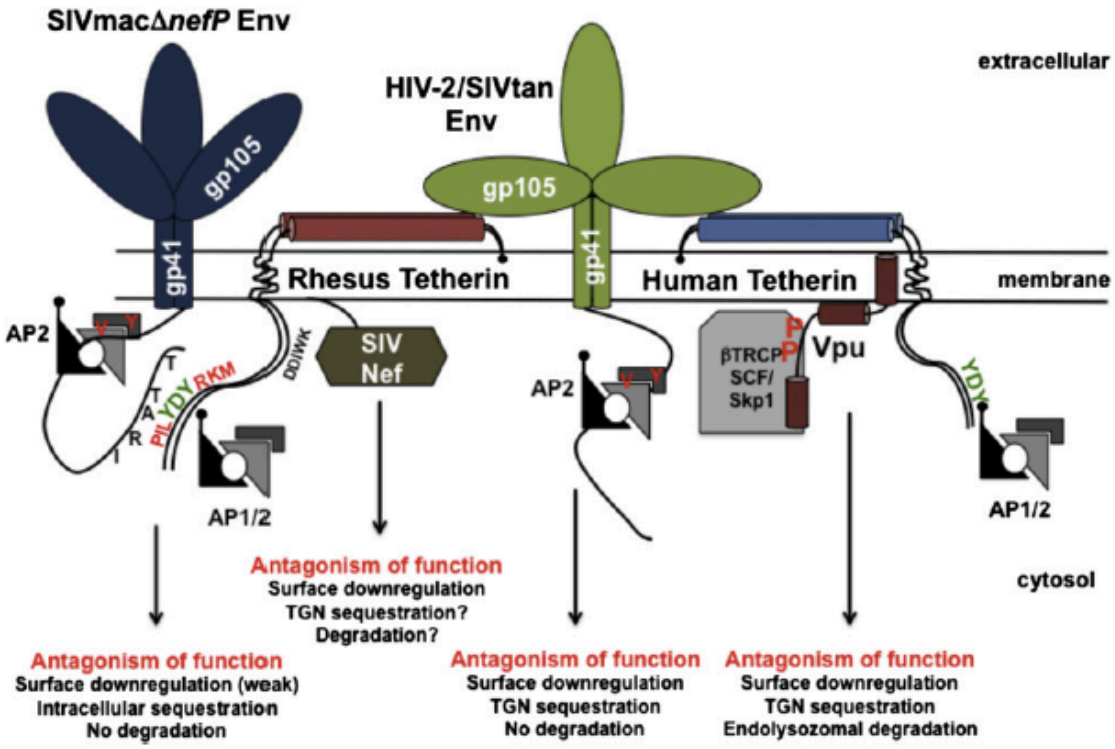

Figure 1.20: Mechanisms of tetherin antagonism in primate lentiviruses.

Env, Vpu and Nef are all tetherin antagonists. The mechanisms by which they neutralize tetherin's antiviral action is indicated and differ between Env, Vpu and Nef. Figure adapted from (236).

SIV Vpu

SIVmus (moustached monkey)/mon (Mona monkey)/gsn (greater spot-nosed monkey) and the SIVden (Dent's mona) isolate are members of the SIVsyk lineage, and encode Nef and Vpu in their genome. But only Vpu has activity against macaque tetherin with their Nef proteins being limited to CD4 targeting (226).

Interestingly, Vpu from SIVgsn was found to also suppress human tetherin activity suggesting that the presence of Vpu in the ancestral SIVmus/mon/gsn virus has contributed to HIV-1 Vpu evolution/adaptation (237). SIVmon, SIVden and SIVmus Vpus could also counteract human tetherin when its transmembrane domain was replaced by the TMD from macaque tetherin indicating that similar to the situation with HIV-1 Vpu, the specificity of the interaction between SIVsyk Vpu proteins and tetherin also maps to the transmembrane domain.

Ebola GP

Ebola virus (EBOV) is a highly pathogenic negative-sense RNA virus first described in 1976 that causes severe haemorrhagic disease in humans and nonhuman primates. It belongs to the

family of Filoviridae, whose members, the Ebola and Marburg viruses, produce filamentous virions. Tetherin has been shown to restrict the release of Ebola virus-like particles, generated by the expression of the matrix protein VP40 (204). Because HIV-1 Vpu could efficiently circumvent tetherin-mediated restriction of Ebola VLPs, it was proposed that Ebola may encode a protein with a Vpu-like function in its genome (185). Within the Ebola genome, four proteins out of seven have been previously shown to influence virus release (GP, NP, VP24 and VP35), but only expression of GP correlates with restoration of VLP release in the presence of tetherin (208). GP is the glycoprotein spike in the viral envelope membrane used by the virus to promote entry in the target cells. The mechanism by which Ebola GP counteracts tetherin is unclear. Co-immunoprecipitation studies show that Ebola GP interacts with tetherin (208). In contrast to Vpu, Nef and Env, GP mediated tetherin antagonism does not rely on specific determinants in tetherin sequence since GP can successfully overcome the restriction of a complete artificial tetherin protein (238). Ebola GP can also antagonize the murine tetherin that shares only ≈36% protein sequence analogy, but the main features with the human orthologue are conserved (N-terminal TMD, C-terminal GPI anchor, and 3 cysteines in the extracellular domain). Although tetherin retains Ebola particles on the cell surface, studies so far show that Ebola GP inactivates tetherin without removing it from the plasma membrane (238). This is especially surprising since early reports showed that EBOV GP leads to a general downregulation of cell surface molecules (239, 240). The intracellular levels of tetherin are not reduced under GP expression indicating that it is unlikely that GP diverts tetherin toward a degradative pathway. Altogether these observations suggest a novel mechanism to circumvent tetherin restriction that implies neither downregulation from the cell surface nor specific molecular interactions. Hypothetically, Ebola GP might physically interfere with the retention mechanism of tetherin at the plasma membrane. Clearly, more studies are required to fully understand this unusual way of neutralizing tetherin's function.

KSHV K5

Kaposi's sarcoma-associated herpesvirus (KSHV or HHV-8) release is blocked by tetherin in the absence of its K5 protein (209, 210). K5 is an E3-ubiquitin ligase described in the literature as a viral immune modulator due to its ability to downregulate a large panel of cell surface receptors involved in immune recognition (reviewed in (241)). MHC class I molecules are the best described targets of K5. K5 is derived from the cellular homologue MARCH proteins found in mammals. MARCH proteins represent a family of transmembrane ubiquitin ligases modulating intracellular trafficking and turnover of transmembrane protein targets. K5 induces tetherin ubiquitination on its cytoplasmic tail resulting in delivery to late endosomes and subsequent degradation in lysosomes in an ESCRT-dependent manner. The mechanistic details employed by K5 to abrogate tetherin-mediated restriction of HIV-1 and KSHV particle release will be addressed more extensively in the results section (cf. Chapter 4).

1.6.6 Tetherin-driven remodelling of primate lentiviruses: Adaptation of Vpu, Nef and Env

Evolutionary data indicate that SIVcpz is a recombinant virus (12) that received its Vpu from the precursor of the SIVgsn/mus/mon lineage, whereas its Nef is derived from the SIVrcm lineage. Each protein is able to antagonize the tetherins from their corresponding host and other monkey-related tetherins (Figure 1.21) (226). Thus, initially the resulting SIVcpz virus issued from both lineages contained two candidates to counteract chimpanzee tetherin. It is likely, however, that they both had weak activity against cpz tetherin as Nef and Vpu have been shown to antagonize tetherin in a host-specific manner (223-225, 227). The acquisition of a competent cpz tetherin antagonist might have been a requirement for the cross-species transmission of monkey SIVs to chimpanzees. Ultimately, function against cpz tetherin emerged in the Nef protein rather than Vpu.

However, upon zoonotic transfer to humans, SIVcpz Nef became inefficient due to the deletion of its target motif in the cytoplasmic tail of tetherin (G/DIWKK). This deletion occured at least 800,000 years ago before the separation between *Homo neanderthalensis*, *Homo sapiens* and *Homo denisovans*. Since the cpz tetherin transmembrane (TM) domain displays high sequence homology with human tetherin TM domain, it might have been easier for SIVcpz to adapt against the tetherin TM domain rather than the cytoplasmic region. Vpu was presumably the best candidate to adapt to the human tetherin TM domain.

Transmission of SIVcpz to humans occurred at least four independent times, giving rise to HIV-1 group M, N, O and P. Only Vpus from group M and N successfully adapt to overcome human tetherin (226). Consistent with that notion, SIVcpz Vpu does not antagonize human tetherin unless its TM domain is replaced by that from HIV-1 M Vpu. HIV-1 Nef had completely lost its activity against human tetherin (226), but its function could be restored by inserting the ancestral five amino acids into human tetherin (225, 227).

Vpu from HIV-1 group M shows species specificity, in that HIV-1 Vpu can only counteract human and ape tetherins including chimpanzees, gorilla, but not the monkey tetherins or those from other mammals (mouse, rat or pig). The specificity of HIV-1 Vpu and other SIV Vpus maps to the transmembrane domain of tetherin. An exchange of the TM domain in human tetherin with that of monkey tetherin (agm or rh) renders it resistant to HIV-1 Vpus (224), but conferred sensitivity to SIV Vpus. A mutation of a single amino acid found in the TMD of monkey tetherins into human tetherin can confer resistance against HIV-1 Vpu (223). These findings suggest that the tetherin TMD has been under positive selection pressure during primate evolution from monkeys to chimpanzees and finally to humans, forcing it to modify its sequence. In turn, this has forced primate lentiviruses to adapt to these changes through acquisition of new functions either in their Nef or Vpu proteins, to constantly maintain tetherin antagonism. In other words, tetherin, because of its sequence variation, has driven the evolution and adaptation of primate lentiviruses, in particular Nef and Vpu proteins. Overall these adaptations have been successful since tetherin antagonism is conserved in many primate lentiviruses tested so far. This flexibility of lentiviruses to switch between Nef and Vpu to counteract tetherin might have been a key determinant for cross-species transmission events.

Finally, Nef-deleted SIVmac and HIV-2 viruses are additional illustrations of the selective pressure that tetherin can exert on lentiviruses and the importance of maintaining tetherin antagonism. Nef-deleted SIVmac and HIV-2 derive from SIV strains lacking Vpu, hence the necessity to acquire a tetherin antagonist in another viral component. In the case of Nef-deleted SIVmac virus, the absence of Nef has forced the acquisition of an anti-tetherin activity in its envelope protein (235). Whether this adaptation to tetherin by Nef-deleted SIVmac contributed to the gain of pathogenicity is unknown. For HIV-2, anti-tetherin function in its envelope must have been the preferential option due to the inability of Nef to target the missing five amino acids in the human tetherin cytoplasmic tail. Whether this adaptation has impaired the primary function of the envelope protein is unknown, but we can speculate that this might be a reason why HIV-2 is less virulent than HIV-1.

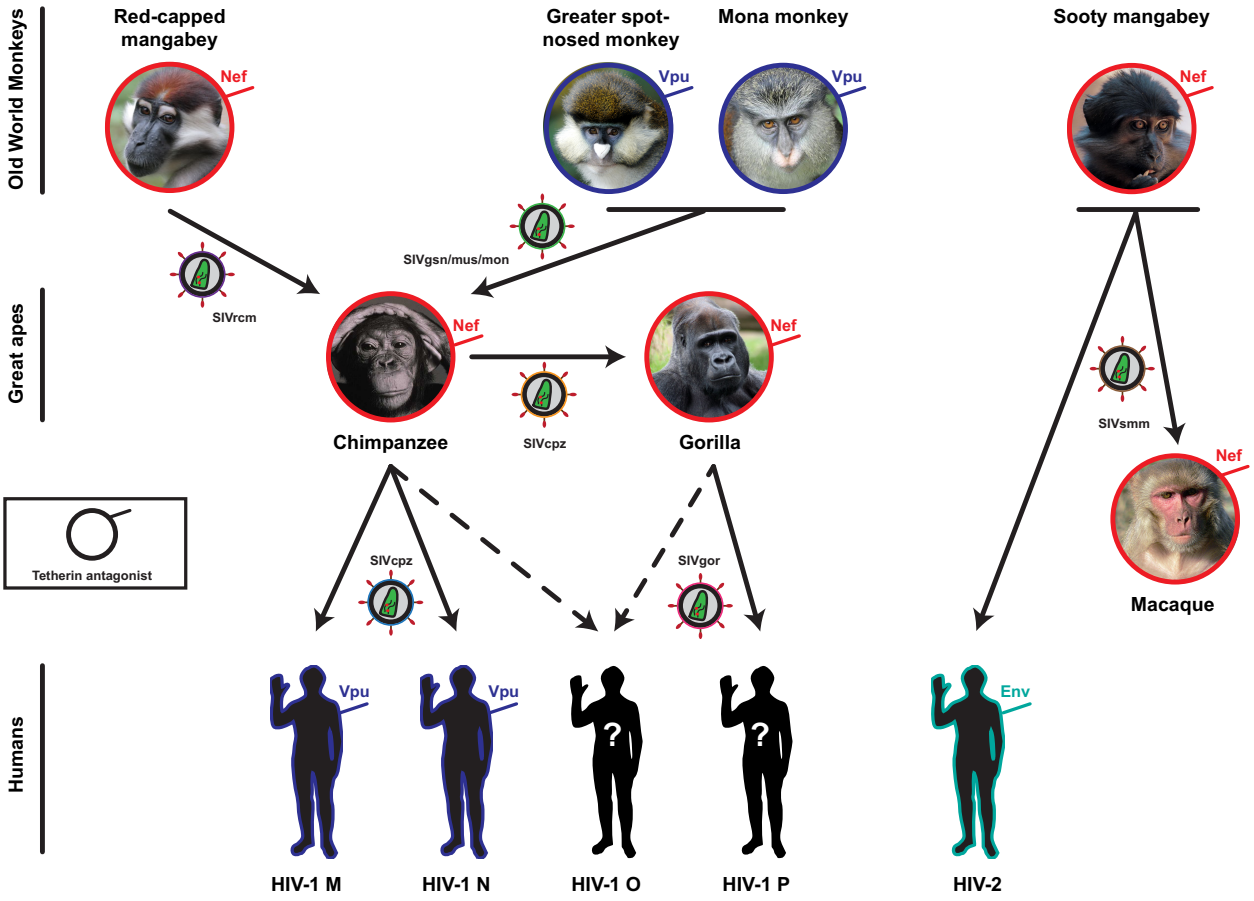

Figure 1.21: Co-evolution of tetherin and Vpu/Nef/Env proteins.

Arrows represent cross-species transmission events, and the viral gene product that antagonizes tetherin from the corresponding host is displayed in color. The simian immunodeficiency virus of chimpanzees (SIVcpz) is believed to be the result of a recombination between viruses infecting red-capped mangabeys (SIVrcm) and those infecting Greater spot-nosed (SIVgsn), mustached (SIVmus), and Mona monkeys (SIVmon). SIVrcm uses its Nef protein to overcome tetherin from its host while Vpus from SIVgsn, SIVmus and SIV mon possess the anti-tetherin activity. Presumably, chimpanzees in contact in the wild with these

monkeys became co-infected with both simian viruses. In SIVcpz, Nef rather than Vpu targets tetherin. SIVcpz was then transmitted to gorillas and to humans evolving to SIVgor and HIV-1 respectively. Vpus from HIV-1 Group N and M are tetherin antagonists while Vpus from HIV-1 Group O and P are not. At present it is unclear whether HIV-1 Group O derives from SIVgor or from SIVcpz (dashed lines). It is unknown whether HIV-1 Group O and P have acquired the capacity to neutralize tetherin in one of their others encoded viral proteins. HIV-2 and SIVmac reflect the cross-species transmission of SIVsmm from sooty mangabeys to humans and from sooty mangabey to macaques respectively. In HIV-2, the anti-tetherin function has been acquired in its envelope protein presumably because Nef failed to adapt due to deletion of a motif in tetherin cytoplasmic tail. This graph also highlights the fact that the tetherin antagonists vary from one species to another.

1.6.7 Tetherin and HIV-1 transmission between cells

HIV-1 can be transmitted between cells by two mechanisms (Figure 1.22). The first one involves the release of cell-free virions. In that scenario, nascent virions diffuse into the extracellular environment until they reach cells bearing the receptors they need for entry. In the second scenario, nascent virions are directly transferred from infected cells to uninfected cells. This second mode of transmission is called cell-to-cell transmission and is in general, more rapid and efficient than cell-free virus spread (reviewed in (242)). It is unclear whether the direct cell-cell spread also allows the virions to remain unseen and protected from patrolling immune cells (macrophages, dendritic cells) or from immune components such as neutralizing antibodies and complement molecules. While studies using matrix-GFP viral constructs have suggested that transfer of virions via the VS is less sensitive to antibodies (243, 244), there are concerns about the assembly of these viral constructs (139). Studies using the full-length virus have contradicted this and reconstruction of cryo-electron microscopy images reveals that the VS should be permeable to antibodies (245). This mode of transmission requires the same determinants for viral entry as cell-free virus transmission; both modes of HIV-1 transmission require the engagement of envelope protein with its receptors on the target cell and a fully assembled virion. The relative contribution of each of these modes of transmission in the context of *in vivo* HIV-1 infection is still unclear, but a recent study showing that HIV-infected T cells were migratory vehicles for viral dissemination strongly suggests that cell-to-cell transfer is likely to be the predominant mode of HIV-1 transmission between T cells (246).

Cell-to-cell transmission of HIV-1 is initiated at the interface between HIV-infected cells and target cells via the formation of virological synapses (VS) (247). The VS was first described for HTLV-1 (248). VSs are multi-molecular structures generated by binding of the HIV-1 envelope glycoprotein Env, expressed at the surface of infected cell, to its entry receptor (CD4 and either CXCR4 or CCR5) displayed on the target cell membrane (243, 247, 249). Additional components are required to maintain the cell-junction and VS stability such as adhesion molecules (interactions between LFA-1 and ICAM-1 and ICAM-3) (247, 250). This configuration allows a close intercellular contact whereby viral particles can be transferred. But the cell-cell spread would not be functional in the absence of a dynamic cellular process that directs intracellular HIV-1 proteins towards the VS (251). Indeed, remodelling of the cytoskeleton from

the donor-infected cell, in particular actin and tubulin networks, regulates polarization of HIV-1 components at the cell-cell interface, thus forcing HIV-1 assembly and egress to take place at the VS for subsequent passage into the engaged target cell. Viral particles are then transferred by budding into the synaptic cleft and virions attach to the target cell membrane to trigger entry. In this configuration, the VSs promote more rapid round of infections and ultimately contribute to increase HIV-1 pathogenesis.

Since tetherin traps nascent virions at the surface of the infected cell, thereby inhibiting cell-free virus release, it was asked whether, in addition to blocking cell-free virus dissemination, tetherin could also influence cell-to-cell virus spread. These questions can be addressed by analysing the fate of membrane-trapped virions and the effects of tetherin expression on VS formation.

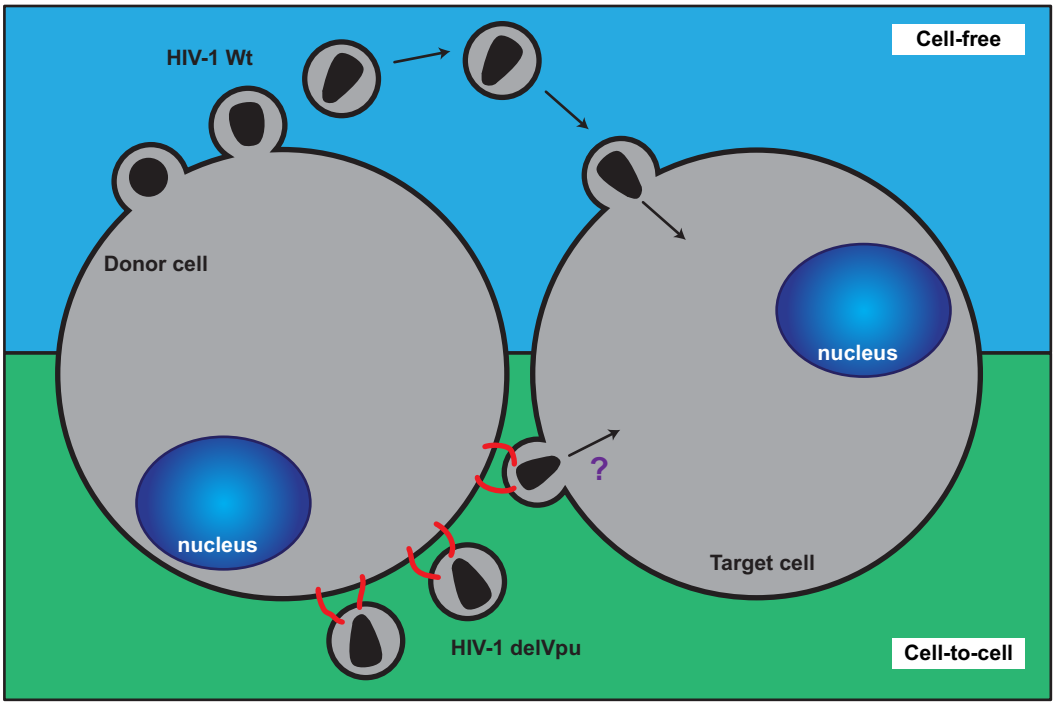

Figure 1.22: Cell-free versus cell-to-cell transmission of HIV-1 in the presence of tetherin.

In the top half of the figure, HIV-1 Wt virus particles are not restricted by tetherin and can be released from the infected cell (or donor cell) into the extracellular environment to infect a new target cell. Alternatively, HIV-1 Wt particles can also be transmitted by direct cell-cell dissemination. In contrast, Vpu-defective HIV-1 particles (bottom half of the figure) are retained by tetherin (red) at the plasma membrane and they can be transmitted to a donor cell via cell-to-cell transfer. Whether these tethered particles are fusion competent and fully infectious is still a matter of debate (question mark).

The contribution of tetherin to HIV-1's mode of transmission remains unclear, as opposing results have been described (216, 252, 253). The studies are based on the quantification of

target cells that become Gag positive when co-cultured, for a short period of time, with HIV-1 Wt or delVpu infected cells. One study reported that tetherin inhibited productive cell-to-cell transmission of Vpu-defective virus to target cells (252). This result was tested using several types of donor cells expressing tetherin either endogenously (HeLa cells) or expressed by transient transfection in 293T cells, while primary lymphocytes and Jurkats served as target cells. Importantly, tetherin was found to colocalize with Gag at the contact zone between infected and target cells, but did not alter the formation of the VS. However, in the presence of tetherin in the donor cell, delVpu viruses form large patches on the target cell after transfer whereas small puncta are observed with Wt virus. This observation may be cofounded by the fact that Gag-GFP constructs, such as those used in this study, have assembly defects and as a result often induce artefacts. These viral aggregates were found to be defective for second round replication because they were impaired in their fusion capacities.

By contrast, a parallel study revealed that Vpu-defective HIV-1 disseminated more efficiently by cell-to-cell contact between Jurkat cells (donor cells) and primary $CD4^+$ T cells (target cells) than Wt virus, under conditions where tetherin restricted cell-free virion release (216). In the same study the authors showed that small interfering RNA-mediated depletion of tetherin affected VS formation and cell-to-cell transmission of Vpu-defective HIV-1. Presumably, tetherin might promote more Env-CD4 interactions to occur by concentrating clusters of virions at the assembly site and as a consequence increase the formation of VS. In contrast to the previous study, virions produced from T cells expressing endogenous tetherin did not lose infectivity. This result raises the intriguing question of what are the benefits to the virus of inhibiting its most efficient mode of transmission. In line with this study, early reports indicate that Vpu-deficient HIV-1 could replicate at the same rate as wild-type virus even though less Vpu-deficient free virions were released into the supernatant (179, 180).

The contradictory results between the two studies might be explained by the variable tetherin expression levels between cell types. T cells and Jurkat express comparatively less tetherin than HeLa cells or transiently transfected-293T, and it is possible that the outcome of HIV-1 cell-to-cell spread varies with tetherin expression levels. At high tetherin levels, cell-to cell transfer might be impaired whereas at low levels the opposite effect occurs. However, this hypothesis is in contradiction with data from Jolly et al. showing that cell-to-cell transmission of HIV-1 delVpu particles was not affected even after tetherin upregulation by IFN. Alternatively, the ultimate goal of Vpu might be to reduce tetherin expression on the cell surface to such levels where its most efficient mode of HIV-1 transmission, cell-to-cell transfer, is promoted. This might explain why HIV-1 bearing a Vpu S52-56A mutant, impaired in its capacity to degrade tetherin, replicates much less efficiently in macrophages than in primary $CD4^+$ T cells (254). Importantly, macrophages express high levels of tetherin compared to T lymphocytes.

HIV-1 might also employ tetherin to switch between the cell-free and cell-cell transmission modes. Thus, tetherin offers an opportunity for the virus to orientate its mode of transmission and potentially control the propagation of the virus over the body. Cell-free virus transmission is likely to favour rapid dissemination of the virus throughout the host while cell-cell transmission favours localized virus spread within a tissue.

1.6.8 Tetherin, more than just an inhibitor of virus release?

By virtue of its mode of action, tetherin labels the surface of infected cells with virions, and thus enhances the potential targets for antibody deposition. This might facilitate the recruitment of molecules from the complement system, which in turn mediate the destruction of the infected cell. Alternatively, recognition of antibodies bound to virions on the target cell activates patrolling NK cells via Fc receptors leading to the lysis of the infected cell. This last process is called antibody-dependent cell-mediated cytotoxicity (ADCC). Subsequent internalization of retained virus particles might induce several biological effects. In antigen presenting cells, such as macrophages or dendritic cells, internalized tetherin-trapped virions are processed into small peptides that can serve as antigens for presentation. This function would place tetherin at the interface of the innate and adaptive immune responses. Endocytosis of viral particles might also contribute to enhance the intracellular pool of PAMPs, such as viral nucleic acids, available to activate endosomal TLRs, cytoplasmic PRR, and DNA sensors. For this reason, tetherin might control a positive feedback loop of interferon response.

As described above, exposure of pDCs to HIV-1 products is sensed by endosomal TLR7 and TLR9, which in turn activate transcription of type I interferon (Figure 1.23) (170, 171). This leads to the expression of several IFN-stimulated genes, including tetherin. Studies showed that tetherin could act as a negative feedback regulator of interferon production by pDCs. Tetherin has been found to be the natural ligand for the receptor ILT7 that is expressed exclusively on pDCs (255). Interaction between tetherin and ILT7-FcεRIγ complex triggers a signalling pathway that ultimately leads to repression of TLR7 or TLR9-mediated type I interferon and pro-inflammatory cytokine secretion.

Therefore, tetherin might be involved in the modulation of the interferon response following infection, either by downregulating the inflammatory response to avoid immune hyper-activation or by upregulating an inflammatory response if a more robust immune intervention is required.

Finally, tetherin might itself serve as a signalling receptor. In a large-scale study aiming to identify human genes that activate NF-κB and MAPK signalling pathways, tetherin was one of those (256).

Therefore, tetherin might have a wider role in the antiviral innate immune response, but whether these functions are just "side effects" of viral retention or whether they are real intrinsic functions of tetherin has yet to be determined (Figure 1.23). Tetherin might be versatile, harbouring different functions depending on the type of immune cell in which it is expressed.

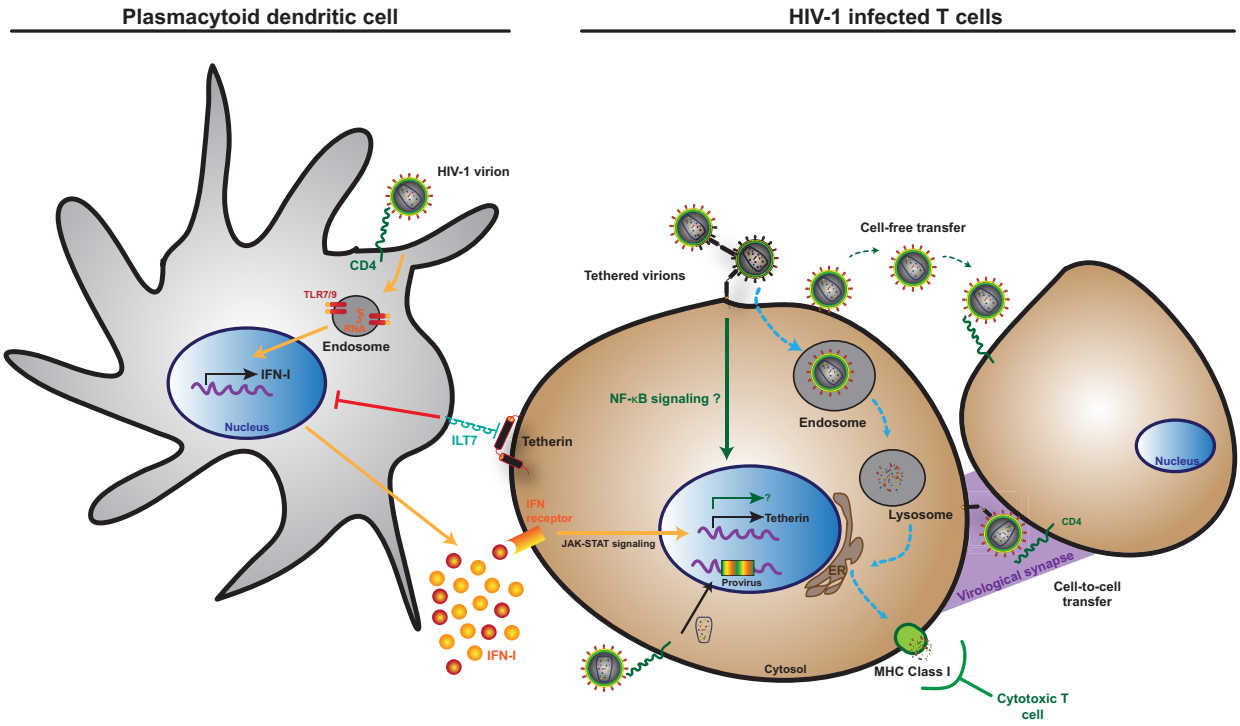

Figure 1.23: Tetherin is at the center of the antiviral response.

HIV-1 virions bind to CD4 on the surface of plasmacytoid dendritic cells. Virions are then endocytosed. In the endosomes, recognition of viral genomic RNA by TLR7/9 triggers the transcription of interferon type I gene. IFN-I interacts with their receptor on the surface of T cell. This signal is then transduced to the nucleus via the JAK-STAT pathway leading to the expression of several interferon-stimulated genes such as tetherin. At the cell surface of the infected T cell, tetherin bridges the nascent virions with the host plasma membrane. This results in the internalization and most likely lysosomal degradation of virions. Hypothetically, peptides derived from endocytosed-virions could be loaded on MHC class I complexes and then displayed on the cell surface for recognition by cytotoxic $CD8^+$ T lymphocytes. Retention of virions by tetherin might also activate the NF-KB signaling pathway. Finally, tetherin can interact with ILT7 expressed on the surface of pDCs and induces a negative feedback of interferon production to prevent overproduction of pro-inflammatory cytokines.

1.6.9 Evidence of tetherin's antiviral effect in mouse models

The role of tetherin as a key antiviral determinant *in vivo* is best evidenced by infection of tetherin-deficient mice with MLV (257). In this study the authors showed that tetherin restricts Moloney Murine Leukemia virus (Mo-MLV) and a pathogenic MLV complex known as LP-BM5 *in vivo*. Treatment of mice with IFN-α was required to reveal the anti-Mo-MLV activity of tetherin. Tetherin-deficient mice infected with the MLV strain LP-BM5 showed more pathologic effects than the control mice. The ability of tetherin to inhibit retroviral replication *in vivo* was also illustrated through the identification of a single nucleotide polymorphism (SNP) in the tetherin sequence of NZW/LacJ mice (258). In those mice, the canonical ATG start site is mutated to GTG, and as a result the translation is initiated later in the sequence. This leads to a tetherin

protein that lacks the N-terminal 12 amino acids (designated as NZW tetherin), and in particular the endosomal recycling motif, resulting in higher cell-surface expression and more potent inhibition of Friend retrovirus release compared to C57BL/6 (full length) tetherin *in vitro*. Furthermore, NZW tetherin expression correlates with a decrease of Friend retrovirus replication and pathogenesis *in vivo*.

Altogether, these observations demonstrate that tetherin is is a bona fide antiviral protein, which plays a major role *in vivo* by reducing retroviral replication and disease.

1.7 Mechanisms of Evasion and Accessory Viral Proteins

One striking contrast between Gammaretroviruses and HIV-1 is the relative simplicity of the MLV genome. MLV only encodes the proteins that will be assembled into the progeny virus particles, whereas HIV-1 encodes four additional, so-called "accessory proteins". These accessory proteins include Vpr, Nef, Vpu and Vif. The SIVsm lineage from which HIV-2 derives, shares the same array of accessory proteins with the exception of Vpu, but additionally encodes Vpx. Although these proteins are dispensable for HIV-1 replication *in vitro* in many cases, *in vivo*, they contribute, to varying degrees, to efficient virus spread and disease induction. Their importance was first illustrated by the fact that SIVmac lacking a functional *nef* gene replicated poorly and did not cause disease in adult macaque monkeys (259). Furthermore, humans infected with nef-defective HIV-1 exhibit a slow/nonprogressor phenotype (260, 261). It is becoming clear that these proteins perform essential functions to ensure viral survival in a host(-ile) environment (reviewed in (45)). They act by modulating various cellular pathways, host protein expression levels and immune responses, in order to create a cellular environment favourable for viral persistence, replication, transmission, dissemination and immune evasion (Table 1.2). Vpu and Nef can be associated in the same group because they both have effects on host cell surface molecules whereas Vif, Vpr and Vpx modulate cytoplasmic and nuclear proteins. These accessory proteins are a perfect example to illustrate the high degree of interaction between the virus and its host.

In this section, we will address the biological effects of these viral proteins on the host cell, and how they adapted to counteract cellular barriers. Despite not being an accessory protein, the structural protein capsid will also be mentioned given its ability to escape cellular recognition.

1.7.1 Vpr and Vpx

While Vpr is highly conserved in primate lentiviruses, Vpx is only encoded by the HIV-2/SIVsm/SIVmac lineage. Vpr and Vpx share a high degree of sequence homology suggesting that they probably arose through either a gene duplication or homologous recombination. Both

are required for pathogenesis in rhesus macaques (262-265), and are incorporated into viral particles.

Vpr is packaged into virions at high levels, via interaction with the p6 subunit of Gag (136), and localizes to the nucleus of infected cells where it is believed to cause direct cytopathic effects. Expression of Vpr in dividing cells can block progression of the cell cycle in the G2 phase after most or all of the cellular chromatin has been replicated. HIV-1 infected people display more $CD4^+$ T cells in G2 phase than healthy uninfected controls (266). In vitro analyses showed that this effect was dependent on the ability of Vpr to interact with the cullin4A-DDB1 E3 ubiquitin ligase complex through the adaptor protein DCAF1 (also referred to as VprBP) (267-271). Cell-cycle progression could be restored when interaction between DCAF1 and Vpr was disrupted, or when expression of DCAF1 or DDB1 was inhibited by siRNA. DDB1 (DNA damage-binding protein1) is not only a component of the cullin4A E3 ligase but also mediates the repair of DNA lesions generated during the S phase. Presumably by forming DCAF1/cullin4A-DDB1 complexes, Vpr prevents DDB1 from performing its DNA-repair function leading to an accumulation of damaged DNA. This, then, triggers the activation of the DNA damage-sensing kinase ATR (ataxia telangiectasia and Rad3 related) leading to G2 arrest followed by apoptosis (272). Therefore, Vpr mimics intracellular conditions that are similar to those encountered after DNA stress/damage. The benefits for HIV in stopping cell cycle is not fully understood but studies revealed that HIV-1 transcription is enhanced under such conditions. The uracil DNA glycosylases UNG2 and SMUG, involved in DNA repair, have been found to be sensitive to Vpr-mediated proteasomal degradation via the cullin4A complex but none have been linked to Vpr-mediated G2 arrest. Clearly Vpr-induced G2 arrest requires the cullin4 ubiquitin ligase complex but the substrate targeted for ubiquitination has not been identified yet. Based on the discovery that Vpx could recruit the same cullin4A E3 ligase as Vpr to degrade SAMHD1 (173, 273), it was thought that SAMHD1 was the substrate targeted by Vpr. But this was not the case, at least for HIV-1 Vpr.

In addition to G2 arrest, HIV-1 Vpr also facilitates infection of macrophages. But the levels of HIV-1 infection remain low in comparison to infection with HIV-2 or SIVmac. Adding Vpx *in trans* in HIV-1 infected macrophages and dendritic cells significantly increased their susceptibility to HIV-1 infection (274, 275) suggesting that these cells expressed an antiviral factor that was antagonized by Vpx. SAMHD1 (sterile alpha motif and HD domain 1) was recently identified as the cellular factor responsible for the inhibition of HIV-1 infection of dendritic and myeloid cells. SAMHD1 was identified using tandem affinity chromatography purification coupled with mass spectrometry. The lack of a monocytic cell line model in which HIV-1 infection was restricted has made the identification of the Vpx' s target difficult. The authors identified SAMHD1 in PMA-differentiated THP1 monocytic cells (173). SAMHD1 was initially identified as the human ortholog of the mouse gene Mg11, which is induced by interferon treatment of macrophages and dendritic cells (276).

To counteract SAMHD1, Vpx, like the other accessory proteins, serves as an adaptor protein bridging its substrate with the cellular ubiquitin machinery. Vpx interacts with SAMHD1 and recruits the same E3 ubiquitin ligase complex as Vpr, the cullin4A-DDB1-DCAF1, to mediate

SAMHD1 ubiquitination and subsequent degradation via the proteasomal pathway (273, 277). Silencing of SAMHD1 in non-permissive cell lines alleviates HIV-1 restriction, and addition of SAMHD1 to cells in which HIV-1 normally could replicate rendered them resistant to infection unless Vpx was expressed.

In the absence of Vpx *in trans*, HIV-1 reverse transcription is blocked in myeloid cells. This observation appears to be a consequence of the hydrolase activity of SAMHD1. SAMHD1 has been found to be a potent dGTP-stimulated triphosphohydrolase that converts deoxynucleoside triphosphates to the constituent deoxynucleoside and inorganic triphosphate (278). The crystal structure of the catalytic core of SAMHD1 (from residues 120 to 626) reveals that the protein is dimeric and indicates a molecular basis for dGTP stimulation of catalytic activity against dNTPs. Presumably, SAMHD1, which is highly expressed in dendritic cells, restricts HIV-1 replication by hydrolysing the majority of cellular dNTPs, thus inhibiting reverse transcription and viral complementary DNA synthesis. Therefore, SAMHD1 might be involved in regulating the cytoplasmic nucleic acid metabolism. It is for this reason that SAMHD1 has been referred to as a negative regulator of the innate immune response to interferon stimulatory DNA. This function has also been attributed to the cellular DNase TREX1 that degrades cytoplasmic nucleic acids (172). In the absence of TREX1, the resulting accumulation of cytosolic HIV DNA triggers IFN release and auto-immune responses that inhibit HIV replication and spreading. It is surprising that SAMHD1 degradation is not conserved in HIV-1, but hypothetically the inability of HIV-1 Vpr to degrade SAMHD1 may represent an advantage in that it would otherwise elicit strong antiviral interferon-induced immune responses by dendritic cells (174).

The discovery of SAMHD1 has provided evidence that accounts for the different degrees of permissiveness of human cells to HIV-1 infection. SAMHD1 is highly expressed by monocytes and monocyte-derived DCs (MDDC), and less well expressed in monocyte-derived macrophages (MDM) and absent from HIV-1 sensitive T cell lines suggesting a direct correlation between SAMHD1 expression levels and permissiveness of the cell types to HIV-1 infection.

The SAMHD1 gene is mutated in a subset of patients suffering from Aicardi-Goutières syndrome (AGS), an early-onset disease that resembles a congenital viral infection (279). This syndrome is characterized by familial encephalopathy with predominantly neurologic symptoms and increased production of interferon alpha in the brain (280). In accordance with the results above, $CD14^{+}$ monocytes isolated from AGS patients lack endogenous SAMHD1 and can support HIV-1 replication while the same cell subset from healthy donors cannot (281).

Vpx is not expressed in all lineages of primate lentiviruses and in those devoid of Vpx, it is Vpr that degrades SAMHD1 (282, 283). Based on evolutionary analyses and Vpr/Vpx' species-activities against the different SAMHD1 proteins, the appearance of SAMHD1-antagonistic function is predicted to be the result of neo-functionalization of Vpr that preceded the acquisition of Vpx in primate lentiviruses. Many lentiviral lineages leading to HIV-1 never acquired this function and only conserved the predicted ancestral function of cell cycle arrest. This ancestral function, then, disappeared from Vpx.

1.7.2 Vif and APOBEC3G

Viral infectivity factor (Vif) is a 192 amino acid protein that allows HIV-1 replication by targeting the cellular restriction factor APOBEC3G (A3G or CEM15) (284) and others including APOBEC3B, D, E, F, H of debatable importance (Figure 1.24). Vif-defective HIV-1 can replicate in some permissive cells such as Jurkat and SupT1 cells because they are A3G negative, but cannot replicate in other non-permissive cells such as macrophages and primary human T cells. In the absence of Vif expression in restrictive cell lines, HIV-1 viral particles package APOBEC3G molecules through interactions with Gag nucleocapsid NC and viral RNA (285). The mechanistic details allowing this incorporation have not been fully established, but once in the cytoplasm of the newly infected cell, A3G through its association with the RTC deaminates cytidine residues in nascent minus-strand viral cDNA into uridine residues (286-288). The direct consequence is the generation of guanosine-to-adenosine hypermutation of the viral plus strand sequence encoding for non-functional viral proteins. However, A3G's ability to edit viral DNA does not appear to be the only mechanism of restriction since A3G mutants that have lost their enzymatic-editing function are still able to inhibit viral infectivity (289). Importantly, in the presence of A3G the levels of cDNA accumulating during HIV-1 infection are also diminished. Based on this observation, it was initially thought that the recognition of uridine-containing DNA by host DNA repair enzymes could then trigger DNA degradation. However, this hypothesis was discounted because inhibition of uracil-DNA-glycosidase fails to enhance the DNA levels in the presence of A3G (290, 291). It was then proposed that A3G bound to viral RNA might sterically hinder the translocation of RT along the viral RNA template and thus inhibiting cDNA synthesis (292).

Vif enables HIV-1 to evade the antiviral activities of APOBEC3G by targeting it for proteasomal degradation (293, 294). Vif has been shown to interact with APOBEC3G and recruit the cullin5-elonginB/C-Rbx2 E3 ubiquitin ligase complex via its SOCS box (suppressor of cytokine signalling box) (295). This SOCS box contains an elongin C binding helix (the BC-box), a conserved HCCH Zn binding motif and a short Cullin Box. Recently, the transcription cofactor CBF-β has been identified as an additional component recruited by Vif to the E3 ligase complex and important to promote HIV-1 infection (296). In such configuration, ubiquitin molecules are transferred from an, as yet unknown, E2 ubiquitin-conjugating enzyme to APOBEC3G (poly-ubiquitination), thus marking it for degradation via the 26S proteasome. Through the depletion of APOBEC3G enzymes from the cytoplasm of infected cells, Vif prevents their incorporation into viral particles.

The mode of action of Vif is species-specific in that HIV-1 Vif can only counteract human but not agm APOBEC3G (297), whereas SIVagm Vif is able to counteract agm APOBEC3G but not the human version. This species-specificity correlates with the ability of Vif to only bind and prevent encapsidation of the APOBEC3G from its corresponding host. A single mutation in human A3G found in agm A3G (D128K) is sufficient to confer resistance to HIV-1 Vif and sensitivity to SIVagm Vif (298).

In addition to APOBEC3G, APOBEC3F can also restrict the replication of Vif-deficient virus and is counteracted by Vif in a similar way to APOBEC3G (299). APOBEC3G and APOBEC3F

belong to the mammalian APOBEC (*apo*lipoprotein *B* mRNA-*e*diting enzyme *c*atalytic polypeptide 1-like) family of cytidine deaminases, of which at least nine other members appear to be expressed in humans. As expected, these proteins are expressed in the natural targets of HIV-1 infection, T cells and macrophages. APOBEC3 genes are unique to mammals and are believed to play an important role in the innate host immune response illustrated by A3G's activity against HIV-1 mentioned above. In the mouse genome, at the equivalent locus to A3G, is located Rfv3, a host resistance gene for Friend murine retrovirus. Not only HIV-1 is sensitive to restriction by APOBEC3 proteins, other types of viruses such as hepadnaviruses (hepatitis B), adeno-associated virus (AAV) and foamy viruses are also inhibited by APOBEC3 proteins.

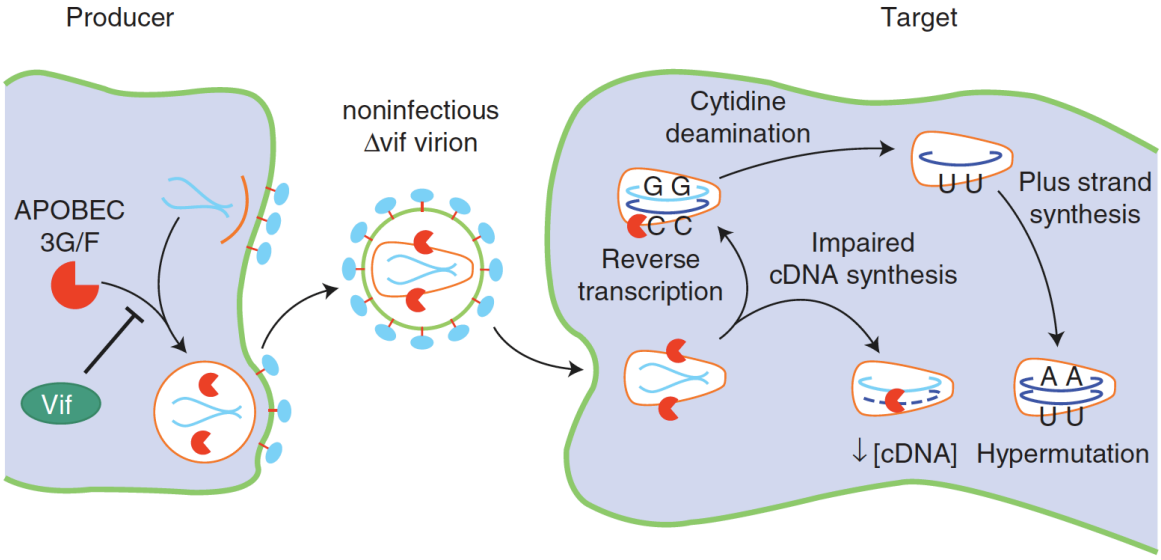

Figure 1.24: APOBEC3G/F inhibit HIV-1 infection and are antagonized by Vif.

Vif-deleted HIV-1 particles from the producer cell (left side) are packaged with the cellular factors APOBEC3G/F and infect a target cell (right side). In the target cell, A3G/F associate with the reverse transcription complex and induce two effects: deamination of cytidine residues into uridine residues in minus reverse strand transcripts causing hypermutation of the viral DNA, and reduction of the levels of viral cDNA by physically interfering with the reverse transcription process. In the presence of Vif in the producer cell, A3G/F are degraded and cannot be incorporated into viral particles. Figure adapted from (300).

1.7.3 Nef and Cell Surface Receptors

Nef is a myristoylated protein encoded by all primate lentiviruses that binds to the inner leaflet of cellular membranes. Many functions have been attributed to Nef for infectivity and pathogenicity due to its ability to modulate the expression of a large range of cell surface receptors and molecules in T cells and antigen-presenting cells (reviewed in (45)). Overall, the downregulation of Nef-targeted proteins leads to enhancement of infectivity, reduction of super-infection,

disruption of immunological responses and regulation of T cell activation, thus creating the perfect environment for viral replication and persistence.

The effect of Nef on viral pathogenicity can be illustrated by the fact that defective forms of *nef* were found in HIV-1 infected individuals termed long-term nonprogressors (261). Furthermore, while SIVmac is usually highly pathogenic, macaques inoculated with Nef-deleted SIVmac have extremely low viral loads, resulting in either no pathogenicity or a markedly long disease course (259).

All HIV/SIV Nef alleles can downregulate the levels of CD4 in infected cells. Nef binds to CD4 and recruits the clathrin adaptor AP-2, which leads to the formation of clathrin-coated pits (301, 302). Clathrin-coated vesicles containing CD4 are then endocytosed and sorted to the lysosomes via the ESCRT machinery for degradation. Thereby, Nef-mediated CD4 cell-surface downregulation prevents infected T cells from undergoing a second round of infection which might be deleterious for the cell viability and consequently for viral replication. The removal of CD4 from the cell surface might also stabilize the envelope proteins and facilitate their incorporation into nascent virions resulting in higher infectivity and replication of HIV-1 (303, 304). By comparison, Vpu also causes a decrease of CD4 levels on the cell surface, but Vpu targets CD4 molecules earlier in the secretory pathway through interactions occurring in the endoplasmic reticulum.

The MHC class I molecules, HLA-A and HLA-B but not HLA-C, are also downmodulated by Nef. MHC class I molecules are expressed at the surface of most cells and can be loaded with viral antigens. Cytotoxic T cells (CTLs) can then recognize infected cells via a specific TCR that together with CD8 interact with the MHC class I molecule associated with the antigen peptide. This recognition elicits the lysis of the infected cell. Thus, Nef-mediated MHC class I downregulation enables infected cells to escape from adaptive immune responses (305). With regards to the mechanistic aspects, two pathways have been proposed. First, Nef binds to the cytoplasmic tail of MHC class I early in the secretory pathway, and recruits AP-1 complex to deliver its substrate to endosomes (306-308). Alternatively, Nef activates a signalling cascade leading to the endocytosis of MHC class I from the cell surface (309). Additionally, Nef suppresses MHC class II expression from the cell surface of professional APCs, thus impairing activation of naïve $CD4^+$ T cells and subsequent T-helper cells-mediated immune responses (310-312).

Nef has also been shown to modulate infectivity of viral particles by facilitating viral core penetration of the cortical actin network during the initial phases of infection. By pseudotyping with VSV-G, the infectivity of Nef-deleted virus could be restored. Furthermore, recent studies showed that Nef interacts with dynamin 2, a GTPase that is required for clathrin-mediated endocytosis, to enhance infectivity of virions (313). Based on these observations, it was proposed that Nef through the recruitment of dynamin 2 might modify the composition of viral membranes to enhance their infectivity.

Nef also interacts with a serine/threonine kinase, member of the p21-activated kinase (PAK) family (314). Once Nef binds to PAK, the kinase is activated and this ultimately leads to inactivation of a pro-apoptotic Bad protein.

Nef expression was also shown to increase DC-SIGN levels on the cell surface of dendritic cells (315). In the context of HIV-1 infection, cells expressing DC-SIGN are able to retain attached virions in an infectious state for several days and transmit them to T cells through a process called transinfection.

While Nef alleles from the great majority of primates lentiviruses, including HIV-2, downmodulate cell surface TCR-CD3 (316) and reduce TCR-induced NFAT activation, HIV-1 Nef is devoid of this attribute and this difference has been proposed to govern the pathogenic outcome of lentiviral infections. However, this notion is debated since SIVmac causes disease in infected monkeys while being able to downregulate CD3 through its Nef protein. Natural SIV infections are usually not pathogenic for their primary host and this correlates with low levels of T cell activation and apoptosis. However, pathogenic HIV infections are associated with high levels of immune activation causing cell death (AICD). The ability of SIVs to downregulate TCR-CD3 to limit T cell activation is intriguing since generally this process contributes to replenish the pool of infectable cells and stimulates virus replication. It is possible that by doing so, Nef might adjust T cell activation to an optimal level where viral replication is promoted and AICD avoided.

Finally, as mentioned previously, most of SIV Nefs target a conserved motif in tetherin cytoplasmic tail and bind the clathrin adaptor complex AP-2 to stimulate tetherin internalization from the cell-surface. This function is not conserved in HIV-1 Nef.

Recently, the NK cell activating ligand PVR was also found to be downregulated by HIV-1 Nef (317). This contributes to the avoidance of recognition and lysis of infected cells by NK cells.

Accessory Protein	Cellular Target	Co-factor	Mechanism	Biological effect / Benefit to Virus
Vpr **HIV-1** **HIV-2**	Unknown	Cullin 4A-DDB1-DCAF1 ATR	Unknown	- G2 cell-cycle arrest --> HIV-1 transcription increased - Facilitates infection of macrophages - Stimulation of PIC nuclear import?
Vif **HIV-1**	APOBEC3G/F*	Cullin5-elongB/C-Rbx2 CBF-β	Proteasomal degradation	Protection from APOBEC-mediated HIV DNA hypermutation
Vpx **HIV-2** **SIVsm** **SIVmac**	SAMHD1*	Cullin4A-DDB1-DCAF1	Proteasomal degradation	Alleviate HIV-1 restriction in myeloid cells (Dendritic cells and macrophages)
Vpu **HIV-1**	CD4	SCF β-TrCP	Proteasomal degradation (ERAD)	- Avoid super-infection of $CD4^+$ T cells - Maturation and trafficking of Env
	Tetherin*	SCF β-TrCP	- Reduction of cell-surface tetherin levels - Lysosomal degradation	Enhancement of virus release
	NTB-A	Unknown	Cell-surface downregulation	Avoid NK-cell-mediated killing
	CD1d	Unknown	"	Escape from NKT cells recognition
	PVR	Unknown	"	Avoid NK-cell-mediated killing
Nef **HIV-1** **HIV-2** **SIV**	CD4	Clathrin adaptor AP-2	- Stimulation of endocytosis - Lysosomal degradation	- Prevent super-infection - Facilitate Env incorporation into nascent virions - Disruption of CD4-based immune responses
	MHC Class I	Clathrin adaptor AP-1	Lysosomal degradation	Escape from CTLs recognition
	MHC Class II	Clathrin adaptor AP-1	Lysosomal degradation	Reduce antigen presentation
	PVR NKG2D ligands	Unknown Unknown	Unknown Unknown	Avoid cytotoxic function of NK cells Avoid cytotoxic function of NK cells
	DC-SIGN	Unknown	Upregulation	Promote transinfection between DCs and T cells
Nef **SIV**	CD3/CD28	Unknown	Unknown	Block responsiveness of infected T cell to activation **-->** Avoid AICD

Table 1.2: Four accessory proteins devoted to create the ideal cellular environment for viral replication.

This table displays the host molecules and cellular pathways targeted by accessory proteins encoded by primate lentiviruses HIV and SIV. Restriction factors are indicated with an asterisk.

1.7.4 HIV-1 Capsid and TRIM5α

Tripartite motif-containing protein 5 alpha (TRIM5α) was isolated as the cellular factor responsible for blocking HIV-1 infection in Old World Monkey (OWM) cells (318). TRIM5α is expressed in the cytoplasm and recognizes specific motifs within the incoming retroviral capsid proteins, thus providing species-specific retrovirus restriction at the stage of reverse transcription. TRIM5α blocks infection before the establishment of a provirus in the target cell. The human orthologue of TRIM5α, initially designated Ref1, cannot target HIV-1 CA but can mediate restriction of several strains of MLV (319-321).

TRIM5α comprises an N-terminal RBCC domain made up of RING (R), B-box (B), and coiled-coil (C) modules and a C-terminal B30.2 domain. The B30.2 domain mediates virus binding and determines antiviral specificity, whereas the RBCC domain is important for TRIM5α multimerization and appears responsible for recruiting the proteasome.

The molecular details by which TRIM5α blocks virus replication are not well understood. TRIM5α is auto-ubiquitinylated in a RING dependent way and rapidly turned over by the proteasome (Figure 1.25). Presumably, when incoming sensitive retroviral cores encounter ubiquitinated-TRIM5α, they also become recruited to the proteasome and destroyed before the reverse transcription process takes place. Proteasomal inhibitor treatment allows the virus to reverse transcribe, however, the infection is not rescued because reverse transcripts fail to integrate. This suggests that TRIM5α-virus complexes remain uninfectious even when protected from degradation. It is thought that the formation of such complexes disrupts the reconfiguration and uncoating steps necessary to ensure the transition of RTC into PIC and subsequent nuclear import. Therefore, TRIM5α mediates an early block in the HIV-1 replication cycle that appears to occur before and after reverse transcription.

Among New World primates, only owl monkeys exhibit post-entry restriction of HIV-1 (322). This block in owl monkeys results from the retrotransposition of cyclophilin A encoding sequence into TRIM5α gene giving rise to a TRIM5-CypA (TRIM-Cyp) fusion protein (323). A similar protein has also been identified in several species of macaques via a similar retrotransposition event. HIV-1 restriction by TRIMCyp is capsid-specific illustrated by the inability of TRIMCyp to block SIVmac infection. HIV-1 restriction in owl monkeys is completely abrogated when the interaction between HIV-1 CA and CypA is disrupted, either by mutations altering capsid or by treatment of targets cells with the cyclophilin-binding drug, cyclosporine (CsA). In HIV-restricted owl monkey cells, cyclophilin A helps TRIM5 restriction by facilitating its binding to the CA. But the role of CypA is not clear; because for instance in human cells CypA has the opposite effect, its binding with CA seems to inhibit restriction by TRIM5α and is required for maximal infectivity.

Importantly, the HIV-1 genome does not encode a protein whose the function is to target TRIM5α like it is the case with APOBEC3G, Tetherin and SAMHD1 through respectively the accessory proteins, Vif, Vpu and Vpx. Instead, sequence variations within the CA sequence combined with the recruitment of the cellular protein CypA appear to allow HIV-1 to escape from TRIM5α-mediated restriction.

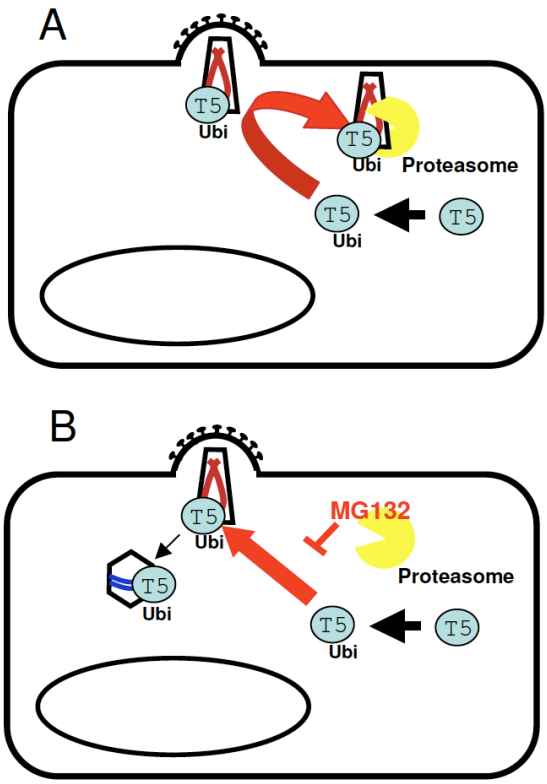

Figure 1.25: Model of TRIM5α-mediated post-entry restriction of HIV-1.

A: By virtue of its RING domain, TRIM5α is auto-ubiquitinated and as a result becomes a substrate for the proteasome. Incoming viral capsids interact with ubiquitinated-TRIM5α and become also part of the complex targeted for proteasomal degradation. In that case TRIM5α induces a block before the reverse transcription occurs. **B:** In the absence of proteasomal degradation (inhibition by MG132), reverse transcripts can be generated but fail to integrate. This suggests that TRIM5α bound to viral capsid induce an additional blockage. Figure adapted from (324).

1.8 HIV-1 Vpu

In 1988, two independent groups, led by William A. Haseltine and Malcolm A. Martin reported the identification of an additional gene encoded by the HIV-1 genome (325, 326). The open reading frame from which this protein is synthesized was originally designated U, and so they proposed to call the new gene *vpu*, for viral protein Unique. Importantly, antibodies against this novel protein were detected in the sera of people infected with HIV-1. This protein distinguished HIV-1 isolates from the other human and simian immunodeficiency viruses (HIV-2 and SIVmac/sm) that do not encode a similar protein. Later on, SIV strains encoding homologues of Vpu were identified (SIVcpz, SIVgsn, SIV mon, SIVmus, SIVden, SIVgor). Early after its discovery, studies revealed a key role of Vpu for efficient virus replication. A five-to-ten fold reduction in progeny virions was observed after the infection of T lymphocytes with a mutant virus bearing a frame-shift mutation into the *vpu* open reading frame. Subsequently, Vpu has been considerably studied to better understand its role in HIV-1 replication and pathogenesis.

1.8.1 The Vpu protein of HIV-1: Structure and Characteristics

Vpu is a 16-kDa type I integral membrane protein consisting of an N-terminal transmembrane anchor (residues 1-27) followed by a C-terminal hydrophilic region that protrudes into the cytoplasm (28-81) (Figure 1.26A) (327). The transmembrane segment adopts an alpha-helical secondary structure anchored in the membrane lipid bilayer with a tilt angle of 13 degrees (328, 329) (330). In addition to its role in mediating interactions with Vpu's targets, the transmembrane domain serves as a signal peptide that remains uncleaved and is thought to interact with other Vpu molecules to form pentameric structures (327, 331). Based on structural similarity with the M2 protein from the influenza A virus, and on the fact that it induced Na^+ and K^+ flux in Xenopus Oocytes, it was thought that Vpu TM domain could form cation-selective ion channels (332). This was also confirmed by introduction of purified Vpu, expressed from Escherichia coli, in planar lipid bilayers (333). In both experiments, Vpu increased membrane conductance to sodium and potassium cations but not to anions. This was dependent on the TM domain since a scrambled TM sequence into full-length Vpu abrogated its capacity to increase membrane conductance in oocytes. But whether the ion channel activity is required for Vpu function is still under debate. In that regard, while substitution of the serine residue (S23) into alanine abrogates ion channel function, Vpu remains able to enhance virus release in the presence of tetherin (cf. Chapter 5). The cytoplasmic region is formed of two alpha helices (designated as αH-1 and αH-2) linked by a conserved DSGNES motif that includes a pair of serine residues (S52 and S56) phosphorylated by casein kinase II (334-337). The Vpu cytoplasmic tail contains a high proportion of charged residues which include a membrane proximal stretch of positively charged basic residues followed by a series of negatively charged acidic residues in the C-terminal part of the protein that confer an overall negative electrostatic charge to the molecule (Figure 1.26B) (338). In more detail, the membrane-spanning N-terminal

domain is connected to the cytoplasmic tail by a short positively charged linker that is predicted to interact with the negatively charged heads of the lipid surface. This small flexible arm is then followed by the helix 1 composed of an alternance of hydrophobic (uncharged residues), basic and acidic residues rendering the region amphipathic (Figure 1.26). Potentially, the hydrophobic side of the helix 1 would be buried in the lipid bilayer, exposing the hydrophilic (charged residues) side to the cytoplasm. The flexible portion interconnecting the two cytoplasmic alpha helices is likely to form a loop pointing away from the membrane due to the polar nature of the two highly conserved phosphorylated serine residues. However, these conformations are, at present, just models of the tertiary structure of Vpu based on highly purified segments of Vpu proteins. The configuration adopted by Vpu might be completely different in the context of an infected cell. In that regard, Vpu's interactions with several host factors, notably CD4 or tetherin, might result in a profound modification of its tertiary structure, in particular, the orientation of the cytoplasmic helices.

Vpu is synthesized late in HIV-1 replication cycle, from a Rev-dependent bicistronic mRNA that also encodes the envelope glycoprotein (cf. section 1.4.4) (339). This allows Vpu and Env expression to be coordinated during HIV-1 infection. While Env incorporation into the viral particle is essential to generate infectious virus, Vpu protein is not incorporated into HIV-1 virions and therefore performs its function within the infected cell.

Vpu proteins from subtype B strains, which is the version of Vpu most commonly studied since its identification, localize predominantly to internal cellular membranes, including the *trans*-Golgi network (TGN) and endosomes but only a minor localization at the plasma membrane has been detected (340, 341). Recent studies indicate that a fraction of Vpu was associated in raft-membrane (342), although the relevance of this for counteracting the particle release restriction imposed by tetherin is still unclear (343, 344). Vpus from HIV-1 Group M clade C and SIVcpz have been found to accumulate mainly at the cell surface (345, 346). Interestingly, this divergence in the Vpu cellular localization might be driven by putative trafficking signals in the cytoplasmic tail since these regions are not conserved among Vpu alleles from different HIV-1 subtypes. These putative localization motifs include a tyrosine (YxxΦ in which Φ refers to a hydrophobic residue) sorting motif in the hinge region that links the transmembrane domain to the cytosolic tail and an acidic/dileucine based ([D/E]xxxl[l/I/V]) signal in the second alpha helix (Figure 1.26B).

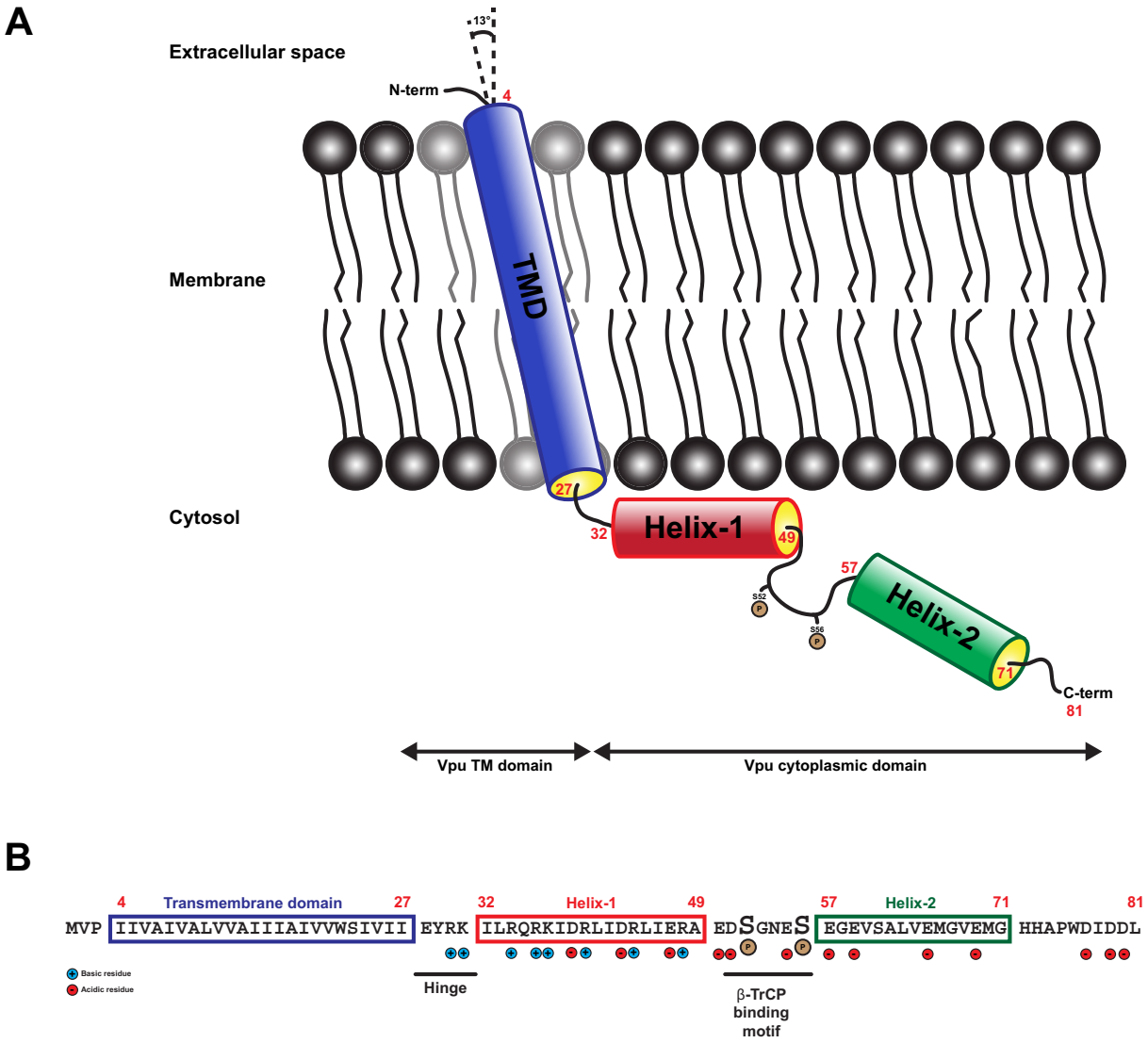

Figure 1.26: Schematic representations of Vpu.

A: Secondary structure of Vpu. This model is based on NMR studies and modelling data performed from fragments of Vpu. To date the full-length protein has not been successfully crystallized. The Vpu transmembrane domain is tilted at 13° degrees. In this model, the first alpha helix is aligned with the lipid bilayer and the two phospho-serine residues protrude into the cytoplasm. The numbers in red indicate amino acid positions of the NL4.3 prototypical Vpu allele. **B:** Amino acid sequence of NL4.3 Vpu annotated with structural features described in panel A. Acidic residues negatively charged are indicated in red and basic residues positively charged are annotated in blue. The conserved β-TrCP binding motif in the cytoplasmic tail that contains the two phosphorylation sites (S52 and S56) is also indicated.

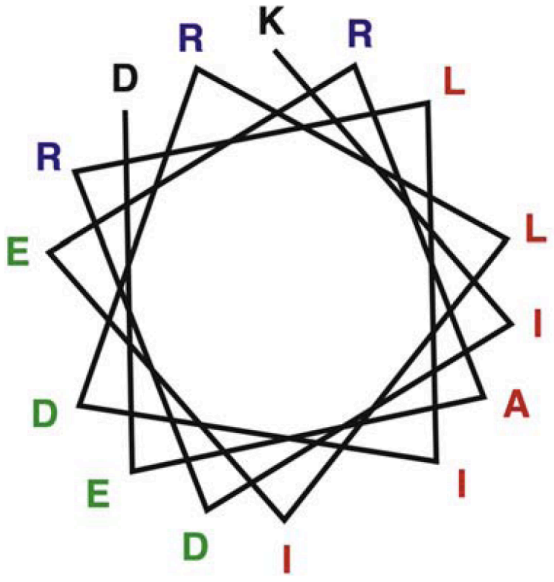

Figure 1.27: Wheel diagram of residues 37-51 from Vpu cytoplasmic tail showing the amphipathic nature of the first alpha helix.

Negatively charged residues are depicted in green, positively charged residue in blue and hydrophobic residues in red. The hydrophobic residues form one side of the first alpha helix and are predicted to be submerged in the lipid bilayer, while the opposite side bearing the charged residues may be in contact with the phospholipid heads and facing the cytoplasm. Figure adapted from (338).

To date, four main functions have been associated with Vpu (Table 1.3) (reviewed in (347)). Firstly, Vpu induces a rapid degradation of newly synthesized CD4 molecules within the ER via a proteasomal pathway. Secondly, Vpu enhances HIV-1 particle release by counteracting tetherin. Vpu also inhibits the surface expression of the lipid antigen receptor, CD1d, in productively infected DCs to avoid recognition by the NKT cells (348). Finally, HIV-1 Vpu might ensure protection of infected cells from lysis by NK cells through the downmodulation of NTB-A (349) and PVR (317). Additionally, as an indirect consequence of Vpu interacting with β-TrCP, Vpu may interfere with essential cellular processes resulting in cell death via apoptosis (350).

Function	Mechanism	Biological effect(s)
CD4 degradation	- Interaction through TM and cytoplasmic domains - Connects the E3 ubiquitin ligase SCF via recruitment of β-TrCP for proteasomal degradation (ERAD)	- Prevention of super-infection - Release of Env precursor from the ER - Efficient virion release - Maintenance of infectivity - Avoid constant $CD4^+$ T cell activation
Tetherin inactivation	- Prevents tetherin from being expressed on the cell surface - β-TrCP and ESCRT-dependent lysosomal degradation	- Enhancement of virus release - Inhibition of tetherin-mediated NFκB signalling
NTB-A downregulation from the cell surface	- Inhibition of cell surface expression - No degradation - No enhancement of endocytosis - Interaction with Vpu TM domain required - Alteration of the cellular trafficking?	- Protection of infected cells from NK-cell-mediated killing by hindering NK-cell degranulation
PVR downregulation	Not defined	- Prevent NK cell-mediated lysis of infected cells
CD1d downregulation	- Suppress CD1d recycling from endosomal compartments to the PM - Retention into intracellular compartment - No degradation - No enhancement of endocytosis	- Avoid recognition of APCs (monocytes, macrophages, DCs) by NKT cells
MHC Class I	Not defined	- Escape recognition of infected cells by CTLs

Table 1.3: Activities of Vpu and their biological effects on HIV-1 replication.

Vpu was also shown to induce $CD4^+$ T cell death by apoptosis but this effect is not mentioned in this table because it is considered as being an indirect consequence of Vpu-binding to β-TrCP rather than a direct biological function of Vpu.

1.8.2 Vpu, a multifunctional protein

1.8.2.1 Vpu induces CD4 degradation

Although HIV-1 penetrates the host cell by interacting with the CD4 surface receptor, the virus encodes two proteins out of fifteen, Nef and Vpu, which both target CD4 for degradation. Early after infection, expression of Nef accelerates the endocytosis of mature cell surface CD4 by a clathrin/AP-2 dependent pathway followed by delivery to the multivesicular bodies for subsequent degradation in lysosomes (301, 351). Unlike Nef, Vpu is translated at later stages of

infection in a Rev-dependent manner, and targets newly synthesized CD4 in the ER for degradation by cytosolic proteasomes. The fact that two proteins are devoted to the same function suggests that suppression of CD4 expression must be important for the HIV-1 infectious cycle. First, downregulation of CD4 from the cell surface of infected cells prevents further super-infections by new virions (352). Superinfected primary T cells show enhanced levels of apoptosis, so by reducing the levels of CD4 on the cell surface, Vpu may prevent premature cell death and expand the period of effective virus production. Vpu also prevents CD4 from interfering with the production of infectious virus particles (303, 353-356). CD4 can form complexes in the ER with newly synthesized Env precursor gp160, thus blocking the transport of Env towards the plasma membrane. But, in that scenario, Env proteins trapped in the endoplasmic reticulum would also result in the production of Env-deficient and non-infectious virions. Therefore, Vpu intervenes to release trapped-Env proteins from gp160-CD4 complexes and allow them to resume maturation, and trafficking towards the cell surface for their incorporation into nascent virions. Similarly, CD4 can also interact with Env glycoproteins at the site of viral assembly, at the plasma membrane, preventing them from being incorporated into progeny virions. Alternatively, CD4 can be incorporated into nascent virions along with Env but viral infectivity consequently would also be reduced. Altogether, these effects of Vpu on CD4 expression predispose the infected cell for optimal production of fully competent infectious virus particles.

The ability of Vpu to mediate the degradation of CD4 is linked to its capacity to physically interact with it. Mutagenesis studies have mapped the region from residues 414 to 419 (LSEKKT) in the CD4 cytoplasmic domain, as crucial to allow Vpu binding and degradation (357-361). For Nef-targeting of CD4, the determinants in CD4 are distinct and involve a dileucine motif. The domains in Vpu required for CD4 binding are less defined but several studies tend to support that these binding determinants are likely to be present in the cytoplasmic region of Vpu. Firstly, a randomized Vpu TMD was still able to bind and induce CD4 degradation as comparable levels than the wild type protein (362). Furthermore, Vpu and CD4 cytoplasmic domains were found to interact in a yeast two-hybrid assay in the absence of their membrane anchor domains (363). In line with this, mutational analysis of the Vpu cytoplasmic tail revealed the importance of the first alpha helix for CD4 binding and degradation (364). A panel of mutations in the Vpu cytoplasmic region were generated to affect the integrity of the two alpha helices. It was found that both C-terminal alpha-helices were required for degradation of CD4, but only the first alpha helix located in the membrane-proximal region was required for mediating interaction with CD4.

Although the binding of Vpu to CD4 is necessary to induce CD4 downregulation, it is not sufficient. This is best evidenced by experiments using the Vpu mutant in which the two conserved phospho-serine residues at positions 52 and 56, within the region DSpGxxSp, are mutated into asparagines. This phosphorylation-defective mutant retained the capacity to interact with CD4 but cannot induce final depletion of CD4 molecules (365), (363), (366). This partial phenotype was attributed to the inability of phospho-defective Vpu mutant to bind the F-box containing proteins β-TrCP1 and β-TrCP2. β-TrCP is one of the subunits of the multi-protein

E3 ubiquitin ligase complex, $SCF^{\beta\text{-}TrCP}$. In that complex, Vpu's phosphorylated serine residues bind to the C-terminal WD repeats of β-TrCP while the F-box domain mediates the connection with the other components of the E3 ubiquitin ligase complex (Skp1, Cullin-1) (367). Recruitment of this $SCF^{\beta\text{-}TrCP}$ complex triggers the poly-ubiquitination of the CD4 cytosolic tail on lysines (368, 369) and serine/threonine residues (370), marking CD4 for degradation by the cytosolic proteasome (371), (372). Vpu itself appears to escape from ubiquitination and degradation. Therefore Vpu acts as an adaptor protein between its substrate, CD4, and the E3 ubiquitin ligase complex.

While the first helix of Vpu seems to play a crucial role in mediating CD4 binding, the importance of the second alpha helix has yet to be determined. But it appears that some determinants in the second helix are required for CD4 degradation but not interaction. Deletion of the C-terminal 23 amino-acid residues or substitution of residues Val 64 to Met 70 impairs Vpu-mediated CD4 degradation without, yet, affecting CD4 binding (345, 364). Furthermore, an alanine scan of the entire second alpha helix revealed the requirement of two residues, Leu 63 and Val 68 for CD4 downregulation by Vpu (373). Substitution of Leu 63 into alanine or valine residue did not affect binding to CD4 or β-TrCP suggesting that Vpu-mediated CD4 downregulation might involve, in addition to CD4-interaction and β-TrCP recruitment, other processes.

Although most studies have focused on experiments demonstrating the role of Vpu and CD4 cytosolic domains, the importance of the transmembrane domains for Vpu-mediated CD4 downregulation cannot be excluded. This was illustrated in a recent study. Replacement of the vesicular stomatitis virus G glycoprotein (VSV-G) TMD for the CD4 TMD abolished Vpu-induced CD4 degradation (374). In the same study, a cluster of amino acids on the Vpu TMD (Val 20, Trp 22, Ser 23), centred on Trp 22, was identified as crucial for CD4 downregulation. Therefore the transmembrane domains of both CD4 and Vpu play important roles in the process of Vpu-induced CD4 downregulation. However, the fact that a scrambled Vpu transmembrane domain is still able to interact and mediate CD4 degradation indicates that this interaction may not be dependent on the primary sequence of the Vpu transmembrane domain but rather on non-specific interactions.

Vpu mediated CD4-ubiquitination in the ER suggests a subsequent degradation via the ER-associated degradation (ERAD) machinery. ERAD generally ensures the removal of abnormal (misfolded or unassembled) proteins from the endoplasmic reticulum (375). ERAD targets are selected by a quality control system within the ER lumen and are ultimately destroyed by the cytoplasmic ubiquitin-proteasome system (UPS). The spatial separation between substrate selection and degradation in ERAD requires substrate transport from the ER to the cytoplasm by a process termed dislocation. ERAD substrates dislocated into the cytosol are then degraded by the 26S proteasome. Several lines of evidence distinguish the mechanism of Vpu-mediated CD4 degradation from the classical ERAD process (368). On one hand, the cytosolic E3 ubiquitin ligase $SCF^{\beta\text{-}TrCP}$ complex does not normally function in ERAD, but is responsible for the ubiquitination and degradation of cytoplasmic substrates such as IκBα and β-catenin. Instead, the ERAD pathway employs several membrane-bound ubiquitin ligases, including the HRD1-

SEL1L complex, TEB4/MARCH-VI and the GP78-RMA1 complex. On the other hand, genetic analysis involving expression of CD4 and Vpu in a yeast system showed that CD4 degradation could persist even in the absence of key ERAD components such as Hrd1p, Hrd3p and Ubc7p, which are orthologous to the mammalian proteins HRD1, SEL1L and UBC7 respectively. These results suggest that the mechanism by which Vpu triggers CD4 degradation is fundamentally distinct from ERAD. This notion was tested by Magadan and colleagues, and interestingly they found additional components of the ERAD machinery required for Vpu-induced CD4 degradation (370). They reported that siRNA depletion of the valosin-containing (VCP) protein AAA ATPase p97 and its associated co-factors UFD1L and NPL4 blocked CD4 degradation by Vpu. They showed that the VCP-UFD1L-NPL4 complex provided the machinery to extract CD4 molecules from the ER into the cytosol; the UFD1L co-factor binds ubiquitinated CD4 through recognition of K48-linked polyubiquitin chains while the NPL4 subunit stabilizes the complex, and the valosin-containing (VCP) protein AAA ATPase p97 provides energy for the dislocation process through ATP binding and hydrolysis. Although VCP-UFD1L-NPL4 depletion abolished CD4 degradation, the bulk of CD4 molecules was still retained in the ER. They showed that this retention was dependent on interactions between Vpu and CD4 transmembrane domains but not on the cytoplasmic tail of CD4.

The data from Magadan and colleagues support a model in which Vpu would exert two temporally separable effects on CD4: ER retention followed by targeting to late stages of ERAD (Figure 1.28) (370). First, Vpu might retain CD4 in the ER compartment via transmembrane interactions, although this hypothesis is in contradiction with previous data showing that the majority of CD4 proteins, in an Env-deficient context, acquired an Endo-H resistance in the presence of Vpu suggesting trafficking through the Golgi apparatus. Then, the cytosolic domain of Vpu interacts with the cytoplasmic tail of CD4 and recruits the E3 ubiquitin ligase $SCF\beta^{-TrCP}$ complex, which mediates the polyubiquitination of lysine and serine/threonine residues. Ubiquitination may further contribute to CD4 retention in the ER, and additionally marks CD4 for delivery to proteasomes. This last process involves the recruitment of the VCP-UFD1L-NPL4 complex through recognition by UFD1L of K48-linked poly Ub chains on the CD4 cytosolic tail. The ATPase activity of VCP then drives dislocation of CD4 from the ER membrane into the cytosol for eventual degradation in proteasomes. Thus, Vpu appears to bypass the early stages of ERAD, including substrate recognition and ubiquitination by ERAD machinery components, but joins in the later stages, beginning with dislocation by the VCP-UFD1L-NPL4 complex (347).

In conclusion, the mechanism by which Vpu depletes the infected cells from CD4 expression at the cell surface involves a complex succession of events closely linked rendering the understanding difficult. In any case, Vpu-mediated CD4 degradation must be efficient and rapid since the half-life of CD4 drops from 6 hours to approximately 25 minutes in the presence of Vpu. Through this process, Vpu maintains viral infectivity during replication.

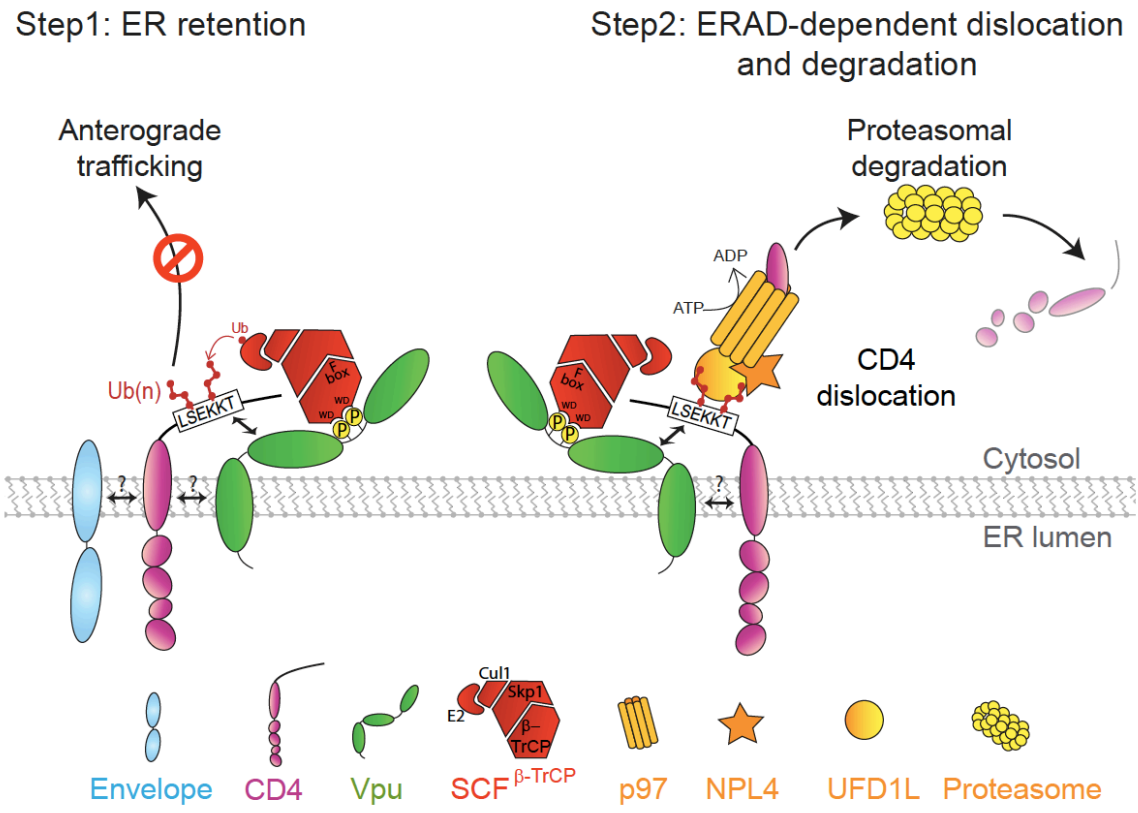

Figure 1.28: Model of Vpu-mediated CD4 degradation.

The first step involves the retention of CD4 in the ER through TM domains interactions. Formation of Env/CD4 complexes could also contribute to this retention. The cytosolic domain of Vpu (likely to be mediated by the first alpha helix) then interacts with CD4 (region 414-LSEKKT-419) and recruits the SCFβ-TrCP E3 Ub ligase complex, which mediates the addition of multiple moieties to lysine and serine/threonine residues in the cytosolic tail of CD4. Ubiquitination further contributes to CD4 retention in the ER, and additionally marks CD4 for delivery to proteasomes. This delivery involves recruitment of the p97(VCP)-UFD1L-NPL4 complex through recognition by UFD1L of K48-linked poly-Ub chains on the CD4 cytosolic tail. Then, the ATPase activity of p97(VCP) drives dislocation of CD4 from the ER membrane to the cytosol for eventual degradation in proteasomes. Figure adapted from (347).

1.8.2.2 Vpu inactivates tetherin's antiviral function

Vpu counteracts tetherin to prevent it from trapping nascent retroviral particles at the cell surface, and as a result allows efficient cell-free virion release into the extracellular milieu. Since its discovery several groups have tried to understand the mechanism employed by Vpu to achieve complete inactivation of tetherin molecules. Vpu has been shown to exert several effects on tetherin: degradation, interaction, cell-surface downregulation, trafficking alteration and intracellular sequestration (reviewed in (192)). After four years of extensive publications on the molecular mechanism of Vpu-mediated tetherin antagonism, we now better understand how Vpu overcomes tetherin, and despite some question marks persisting in this area, we can begin to establish one unified model that encompasses all the phenotypes described so far.

a) Vpu prevents tetherin from being expressed at the site of virus assembly

The first striking effect of Vpu on tetherin appeared from the observation that tetherin expression at the plasma membrane was reduced in the presence of Vpu (187). Since HIV-1 assembly, budding and release occur at the cell surface it was thought that by mediating tetherin downregulation from its site of action, Vpu could abolish the antiviral activity. But this notion was challenged when Vpu was shown to enhance HIV-1 virus release in the absence of tetherin cell surface downregulation (376). Indeed, in CEMx174 and H9 cells (T cell lines), virus replication was Vpu-dependent but cell-surface tetherin levels were not affected by Vpu expression. However, this phenotype has never been reproduced in any other studies (220, 377, 378).

Tetherin is believed to restrict viral particle release by physically cross-linking the cell membrane and the virus membrane together (cf. section 1.6.4) (197). Consistent with this, tetherin is incorporated into virions (214, 215, 379). In the presence of Vpu, tetherin packaging into viral particles is reduced suggesting that Vpu might directly block tetherin incorporation into virions at the site of viral assembly. But this conclusion is cofounded by the fact that Vpu leads to a reduction of tetherin levels at the cell surface. Other studies have shown that Vpu association in membrane rafts was required for enhanced virus release (342). Since tetherin also localized to the lipid rafts at the plasma membrane through its GPI lipid anchor, it was proposed that Vpu displaced tetherin out of the raft domains to inactivate its antiviral function. But again this notion is not supported by more recent studies (343, 344).

Several studies have investigated the mechanism by which Vpu induces tetherin cell-surface downregulation and some determinants have been identified. Firstly, the cellular protein β-TrCP from the E3 ubiquitin ligase complex is required for optimal cell-surface downregulation of tetherin by Vpu (220). Indeed, Vpu-mediated tetherin cell surface downregulation is severely impaired when a dominant negative form of β-TrCP (ΔF-box β-TrCP) is expressed. ΔF-box β-TrCP can mediate interactions with Vpu but cannot link it to the other components of the ubiquitin machinery, and this mutant also inhibits degradation of CD4 by Vpu. Similarly, Vpu-mediated tetherin downregulation is affected when expression of β-TrCP-1 and β-TrCP-2 are simultaneously depleted by shRNA. Moreover, when the DSGxxS β-TrCP binding motif in Vpu is mutated, tetherin downregulation is also compromised. In accordance with the notion that tetherin downregulation is the mechanism by which Vpu counteracts tetherin, ΔF-box β-TrCP over-expression and mutation in the β-TrCP binding motif also affects the enhancement of virion release by Vpu. These data suggest that Vpu might recruit the ubiquitin ligase machinery via interaction with the cellular co-factor β-TrCP to downregulate tetherin from the cell surface and allow enhancement of particle release. However, in all cases where the recruitment of β-TrCP by Vpu was affected, the inhibition of tetherin restriction was not completely abolished, suggesting that another mechanism was also involved. In other words, despite the importance of β-TrCP for Vpu-mediated tetherin downregulation, it was unclear how much the recruitment of this co-factor by Vpu contributed to the antagonistic process. We now know that β-TrCP is essential for lysosomal degradation of tetherin and consequently for optimal cell-surface

downregulation. But it is the commitment into that degradative pathway which is thought to be the major cause of tetherin counteraction rather than the β-TrCP dependent degradation *per se.*

Tetherin is internalized from the plasma membrane and delivered back to the plasma membrane through a clathrin-dependent pathway that involves the sequential action of AP2 and AP1 adaptor complexes (206, 207). Early studies showed that the clathrin adaptor protein complex AP-2 was also found to be required for Vpu-mediating tetherin cell-surface downregulation (220). Similar effects were observed in cells transfected with the dominant negative mutant of dynamin 2, which inhibits the membrane scission of endocytic vesicles (218, 380). Based on these observations, it was proposed that Vpu might stimulate/accelerate clathrin-dependent endocytosis of tetherin from the cell surface. But this was contradicted by reports showing that in fact the rate of internalization of tetherin was not enhanced by Vpu expression (377, 381, 382). Alternatively, since inhibition of endocytosis through AP-2 knockdown or dominant-negative dynamin 2 (K44A), can also lead to a reduction of the pools of tetherin in recycling vesicles, it could not be excluded that Vpu might prevent endocytosed tetherin from recycling back to the plasma membrane. This scenario was ruled out by experiments showing that Vpu still actively counteracted and depleted cell-surface levels of a tetherin mutant, in which the residues Y6 and Y8 required for endocytosis were mutated (377).

We now know that cell-surface tetherin downregulation is a consequence of two additive effects of Vpu: Vpu first interacts with tetherin in the TGN by virtue of its transmembrane domain. Thereafter, Vpu/tetherin complexes are routed to late endosomes for subsequent degradation. Thus, AP2 being required for optimal tetherin cell-surface downregulation may be due to the fact that under condition where it is silenced, Vpu can only target newly synthesized tetherin molecules and not those being recycled. This is likely to be sufficient to overcome tetherin as suggested by a recent report showing that AP2 knockdown had no significant impact on Vpu-mediated tetherin antagonism (383). The partial cell-surface downregulation observed by β-TrCP depletion is likely to be a result of the non-commitment of tetherin molecules into the degradative pathway.

The next two paragraphs address in detail the two complementary effects of Vpu on tetherin that ultimately lead to an optimal reduction of tetherin levels on the plasma membrane.

b) Vpu physically associates with tetherin

Interactions between Vpu and tetherin were considered even before the direct evidence of physical interaction by co-immunoprecipitation studies. The first evidence was revealed by sequence analysis of tetherin showing that the protein had undergone strong positive selection in its TM domain during primate evolution (224). As commonly observed, these changes reflect the imprints resulting from pressures exerted by external agents such as viruses, suggesting that Vpu might have been one of those viral factors contributing to tetherin evolution. The evidence of interaction was revealed by studies showing that Vpu antagonized tetherin in a species-specific manner (223, 224). HIV-1 Vpu can only counteract closely related tetherin proteins from humans, chimpanzees and gorillas while other Vpus from SIVs infecting old world

monkeys can only overcome tetherin proteins from their corresponding host. Importantly this species-specificity is governed by the transmembrane domains of both proteins; exchange of human tetherin transmembrane domain by those from rhesus tetherin conferred resistance to Vpu. Likewise, a single mutation into human tetherin TMD by a residue found in monkey tetherin TMD could also confer resistance to HIV-1 Vpu. Later on, co-immunoprecipitation studies confirmed this species specificity by showing that Vpu and tetherin could interact with each other via their transmembrane domains (218, 377). In line with the genetic evidence, Vpu co-immunoprecipitates with human, but not monkey tetherin. Replacement of tetherin TMD by Tfr (transferrin receptor) TMD inhibited Vpu recognition, and chimeric Vpu proteins bearing CD4 TMD were also unable to bind tetherin molecules. In accordance with this, early data demonstrated that when Vpu TMD was modified either by deleting segments, scrambling or multiple amino acid replacements, the enhancement of virus release by Vpu was severely compromised (362, 384, 385). The determinants in Vpu TMD required for interaction with tetherin have been mapped. Three residues, A14, A18 and W22 that form one face of the transmembrane domain have been found to be essential for tetherin interaction and antagonism (cf. Chapter 5) (221). This observation was then confirmed by NMR spectroscopy studies that showed the importance of the conserved AxxxAxxxAxxxW face of Vpu TMD helix (386). The C-terminal region of tetherin TM domain helix was proposed to fit between the alanines on this interactive face of Vpu. In the tetherin TM domain, mutations on residues I34, L37 and L41 affect its sensitivity for Vpu (222). These aspects will be further expanded in Chapter 5.

Vpu-mediated tetherin interaction is required for all the effects identified so far (377). Modifications that disrupt this interaction prevent Vpu from inducing tetherin downregulation, degradation and antagonism. Although interaction in the TGN is the most advantageous scenario for Vpu because it can then access both to newly synthesized and recycled tetherins, interaction occurring early in the secretory pathway cannot be excluded (cf. Chapter 6).

c) Vpu induces tetherin degradation

Vpu not only leads to a reduction of tetherin levels at the plasma membrane but also induces a decrease of intracellular pools of tetherin (218-220, 387, 388). Under Vpu expressing conditions the half-life of tetherin molecules is shortened by approximately two fold.

Two main cellular degradation pathways have been investigated. Early studies reported a role of the proteasomal pathway in tetherin degradation by Vpu (387, 388). Firstly, tetherin levels could be restored by treatment with the proteasomal inhibitor MG132, but this observation does not exclude a role for lysosomes since both degradation pathways can be ubiquitin-dependent and long-term treatment with MG132 depletes pools of free ubiquitin. In support of tetherin degradation via the proteasome, the expression of a dominant negative form of ubiquitin (Ub-K48R) and the depletion of the ERAD component AAA-ATPase p97 partially inhibited Vpu-mediated tetherin degradation (388). However, this phenomenon was later shown to be an artefact of high levels of tetherin accumulating in the ER (381). Under conditions where tetherin is over-expressed, such as those existing in transient-transfection experiments, ERAD-

dependent degradation of tetherin by Vpu was detected, but not in infected cells with physiological levels of both Vpu and tetherin.

Alternatively, Bafilomycin A1 and lysosomal protease inhibitors have also been found to rescue tetherin expression levels from the cell lysates suggesting the implication of the lysosomal pathway (218-220). This was confirmed by the observation that essential components of the ESCRT machinery were required for Vpu-mediated tetherin degradation and optimal cell-surface downregulation. Knockdown of Tsg101, and the ESCRT-0 component HRS, or expression of the dominant negative form of Vps4 blocked Vpu-mediated tetherin degradation (389). However, since Tsg101 and Vps4 are also required for HIV-1 budding, and HRS is important for HIV-1 production, their role for Vpu-mediated enhancement of viral particle release could not be tested. This issue has been resolved through the identification of the ESCRT-I component UBAP1 (390). UBAP1 is specifically required for ESCRT-dependent endosomal degradation, but not for viral assembly or cytokinesis. While UBAP1 knockdown rescued tetherin levels from Vpu-mediated degradation it did not affect enhancement of virus release suggesting that Vpu induced an ESCRT-dependent lysosomal degradation of tetherin, but this was dispensable for inactivating tetherin's antiviral activity. Finally, siRNA-mediated depletion of Rab7a, which inhibits the early to late endosomal maturation, induced a " tetherin-like " phenotype on HIV-1 release in HeLa (391), suggesting that tetherin was likely targeted to the late endosomal compartment in the presence of Vpu.

β-TrCP, especially the β-TrCP-2 isoform, was also shown to be required for the degradation process (219, 220, 388) suggesting that Vpu might induce tetherin ubiquitination like it does to degrade CD4. In agreement with this, mutations on the potential ubiquitin-acceptors in tetherin cytoplasmic tail (K18 and K21) abolished Vpu-mediated mono-ubiquitination and degradation (210, 392). However, consistent with the notion that Vpu's ability to degrade tetherin is not strictly required for antagonism, the same study showed that tetherin mutants bearing those mutations were still sensitive to Vpu-mediated counteraction (cf. Chapter 4). β-TrCP-dependent ubiquitination on the cytoplasmic tail lysines was then confirmed by another group (393). Importantly, the authors also found that not only the lysines but also the serine/threonine motif (STS) was ubiquitinated in the presence of Vpu. In contrast to the lysines, this STS motif was essential for optimal tetherin cell-surface downregulation and antagonism by Vpu. These data indicate that the ubiquitination on lysine residues might be essential to engage the degradation machinery while ubiquitination on serine/threonine residues may participate more directly to the antagonistic process. Moreover, tetherin ubiquitination by Vpu may also be involved in diverting tetherin's natural cellular trafficking.

The Vpu S52,56A mutant provides another way to illustrate that Vpu-mediated tetherin degradation and inactivation are two separated effects. Vpu S52,56A cannot be phosphorylated by casein kinase II and as a consequence is unable to bind β-TrCP. For this reason, Vpu S52,56A does not lead to tetherin ubiquitination and degradation, however it still retains some levels of antagonism against tetherin. So once again, this suggests that the success of tetherin antagonism does not entirely rely on the ability of Vpu to mediate tetherin ubiquitin-ESCRT-dependent lysosomal degradation but involves additional mechanisms. However, under

conditions where tetherin is highly expressed, the degradation process might be more important. This is evidenced by studies showing that, in macrophages, Vpu S52,56A replication is severely impaired while in T cells it could replicate almost as efficiently as the wild-type (254). It is unlikely that Vpu acts in a cell-type dependent manner but instead, its activity might vary from one cell type to another depending on the levels of tetherin expressed in these cells. In macrophages, which express high levels of tetherin (394), Vpu's ability to degrade tetherin might be determinant for efficient counteraction, while in T cells, low amount of tetherin molecules might be easily neutralized by Vpu without the need of complete destruction.

Taken together, these data suggest that tetherin is degraded, most likely, in lysosomal compartments by an ubiquitin/β-TrCP and ESCRT-dependent mechanism. But it is unclear how much this mechanism contributes to the full antagonism of tetherin. Vpu exerts a primary effect on tetherin that leads to its inactivation and subsequently to its degradation. But it cannot be excluded that in certain circumstances degradation might be dispensable (392). However, if Vpu's primary function is saturated and some levels of tetherin are restored at the plasma membrane, then tetherin degradation becomes essential. A description of this primary mechanism mediated by Vpu is provided in the next paragraph.

d) Towards a unified model of Vpu-mediated tetherin antagonism

As tetherin degradation is not strictly required for Vpu activity and Vpu does not stimulate clathrin-mediated tetherin endocytosis, it was thought that Vpu interfered with tetherin trafficking to the cell-surface as a means to antagonize it. To investigate this scenario, Dube and colleagues established an assay to quantify the amount of tetherin re-expressed at the cell surface resulting from protein intracellular trafficking (377, 382). For this assay, cells were first treated with pronase to remove all the proteins at the plasma membrane. They found that the kinetics of tetherin re-expression at the cell surface was significantly delayed in the presence of Vpu. This suggests that Vpu interferes with tetherin trafficking along the secretory and/or recycling pathways. Since a large fraction of Vpu co-localizes with residual tetherin at steady state in the TGN, it was proposed that Vpu prevented tetherin from reaching the plasma membrane by retaining/sequestrating tetherin molecules in the TGN (378). In line with this hypothesis, mutations of conserved residues R30 and K31 within the hinge region that affect accumulation of Vpu in the TGN and consequently the degree of co-localization with tetherin, correlated with an attenuation of HIV-1 release (341). But at this point it was unclear why tetherin molecules accumulated in the TGN in the presence of Vpu. This was clarified by a recent study from Kueck et al, in which they proposed that Vpu did not directly mediate the sequestration of tetherin in the TGN *per se* but rather interacted with tetherin to commit it into a cellular pathway that led to degradation (Figure 1.29) (383). Therefore, retained tetherin observed in the TGN under Vpu expression is likely to be the result of the accumulation of molecules queuing for their delivery into endosomal compartments. At steady state, only the pools of tetherin and Vpu that accumulate in the slowest cellular pathway are visualized and this gives the impression that Vpu mediates an active sequestration of tetherin. In the same study,

the authors showed that the EXXXLV motif in the second alpha helix of Vpu cytoplasmic tail was the sorting signal that regulated the targeting of tetherin into a cellular pathway away from the plasma membrane. The EXXXLV motif resembles an acidic dileucine sorting signal (D/E)XXXL(L/I/V). Importantly, Vpu EXXXLV mutant was defective for tetherin cell-surface downregulation, degradation and efficient antagonism, but not for tetherin interaction. The evidence suggested that this motif acted as a sorting/trafficking signal that governed the post-binding routing of tetherin/Vpu complexes from the TGN and/or recycling vesicles to endosomal compartments, thus preventing the transit of tetherin molecules to the plasma membrane. However, the EXXXLV motif cannot be qualified as a bona fide sorting signal because the cargo adaptor that binds to it has not been identified. The fact that clathrin was required for Vpu-mediated antagonism and that EXXXLV motif could be substituted by the AP-2 binding motif from HIV-1 Nef to restore full tetherin antagonism, suggested that this motif acted as a clathrin-adaptor binding site. However, none of the clathrin-adaptor complexes tested in this study including AP1, AP2 and AP3 were found to be required for tetherin antagonism (383). In the same study, the authors showed that enhanced levels of tetherin expression required the ability of Vpu to mediate tetherin degradation. While in $CD4^+$ T cells Vpu ELV mutant is almost as functional as the wild-type to promote virus release, upon IFN-α treatment HIV-1 bearing Vpu ELV becomes as defective as Vpu-deleted virus.

In summary, the emerging consensus is that Vpu interacts with tetherin molecules through transmembrane interactions in the TGN and/or recycling endosomes. In the presence of ubiquitinated tetherin, the trafficking signal in the second alpha helix of Vpu drives Vpu/tetherin complexes towards the endosomal pathway. Tetherin molecules are then sorted by components of the ESCRT machinery that delivers it to lysosomal compartments for degradation. At present it is unknown whether Vpu recruits the E3 ubiquitin ligase SCFβ-TrCP to ubiquitinate tetherin in the TGN or in the recycling compartments. Ubiquitination might also further contribute to retain tetherin in the TGN and/or recycling vesicles. Presumably, since β-TrCP or ESCRT disruptions rescue tetherin at the cell surface we can speculate that in the absence of degradation some tetherin molecules can reach the plasma membrane as a result of their accumulation in the TGN. For this reason, Vpu S52-56D mutant defective for tetherin degradation causes a stronger re-localization of the cellular pool of tetherin in the TGN than the Wt Vpu (377).

In summary, Vpu-mediated block of tetherin incorporation into assembling virions seems to be the resulting effect of a complex intracellular mechanism exerted on tetherin by Vpu. Diversion of the cellular trafficking of tetherin toward the cell surface and subsequent degradation account for the total absence of tetherin expressed at the cell surface and allows the nascent viral particles to be released without any obstacles.

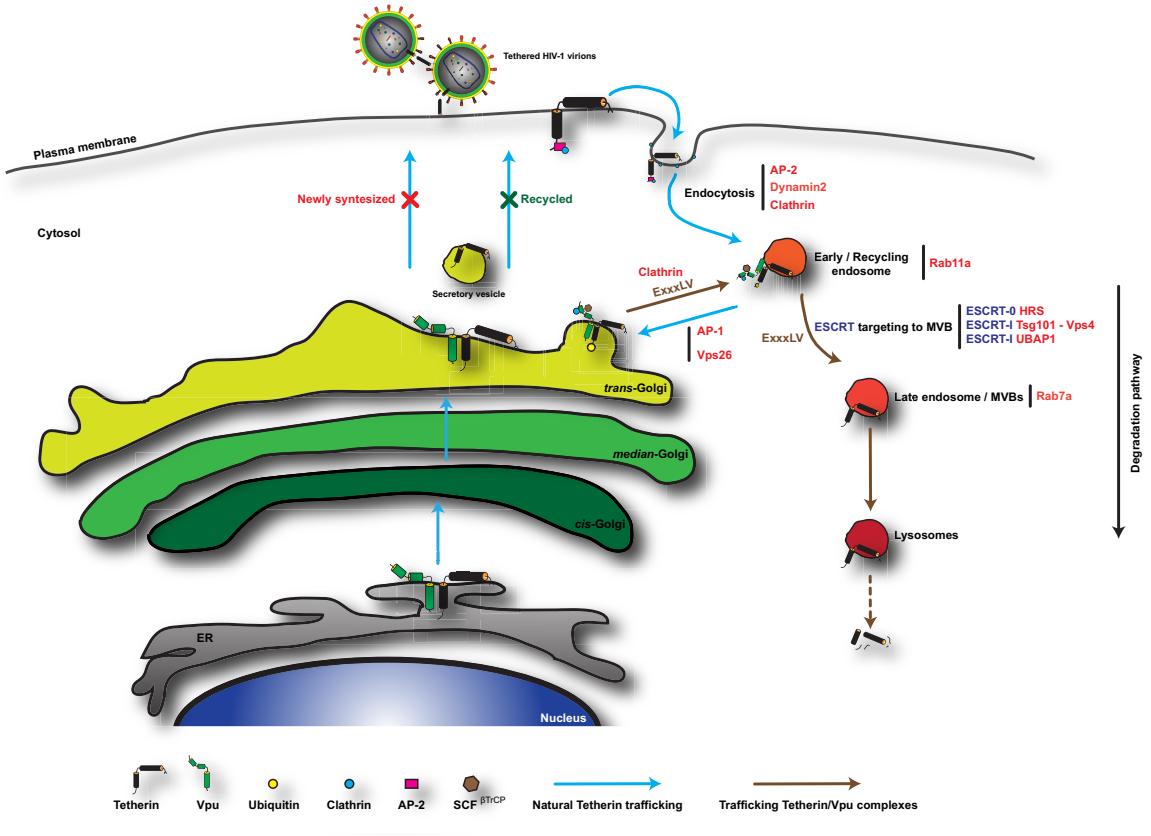

Figure 1.29: Model of Vpu-mediated tetherin antagonism.

Tetherin and Vpu are synthetized in the ER and then acquire maturation through trafficking into the Golgi apparatus. In the absence of Vpu, tetherin reaches the plasma membrane. The protein can then be endocytosed in clathrin-coated pits, transported to the TGN via recycling endosomes and probably recycles back to the cell surface. Tetherin endocytosis requires AP-2 that binds the tyrosine-based motif in tetherin cytoplasmic tail and acts as an adaptor protein to recruit clathrin. Dynamin 2 is also required for tetherin internalization from the plasma membrane. By virtue of their transmembrane domains, Vpu and tetherin interact with each other in the TGN. Thereafter, Vpu/tetherin complexes are routed to late endosomes bypassing the plasma membrane. This trafficking is thought to be governed by a sorting signal in Vpu second alpha helix (ExxxLV) and is clathrin-dependent. Recruitment of the E3 ubiquitin ligase complex SCFβ-TrCP by Vpu induces tetherin ubiquitination on its cytoplasmic tail. Ubiquitinated-tagged tetherin molecules are then sorted by components of the ESCRT machinery to the late endosomes for subsequent degradation in the lysosomes. HRS, Tsg101, Vps4 and UBAP1 are all required for Vpu-mediated tetherin degradation. Interference with late endosomes formation by mutants of Rab7 impact Vpu's ability to degrade tetherin, while disruption of the recycling compartment by a dominant Rab11a mutant compromises Vpu-mediated virus release. Knockdowns of AP-1 and Vps26 that regulate transport of cargo proteins from the endosomes to the Golgi do not affect Vpu-mediated tetherin antagonism. The blue arrow indicates the natural cellular trafficking of tetherin in the absence of Vpu expression, while the brown arrow indicates the cellular trafficking imposed by Vpu on tetherin. The cellular components required for the indicated pathways are written in red.

1.8.2.3 Vpu downmodulates NTB-A and CD1d

Natural killer (NK) cells constitute a major component of the innate immune system due to their ability to lyse virus-infected cells. They act as a first line in immune surveillance and defence against viruses before the establishment of antigen-specific adaptive immune responses (reviewed in (395)). NK cells mediate cell lysis through the release of cytoplasmic lytic granules such as perforins and granzymes into the target cell. This degranulation is triggered by interactions between NK cell surface receptors and their corresponding ligands on target cell. These receptor-ligand interactions are divided into three major categories depending on their effects on NK cell state: inhibiting, activating and co-activating. For instance, NKG2D is a potent NK-cell activation receptor (aNKR) able to recognize stress-induced molecules, such as ULBP-1/2 as ligands expressed at the surface of target cells. Although engagement of aNKR (signal 1: activation state) is necessary for NK-cell-mediated cell lysis of infected cells, this process also requires the simultaneous activation of co-receptors (signal 2) to trigger degranulation. One such factor that regulates NK-cell cytolysis is the NK-T and B cell antigen (NTB-A) co-activator receptor. NTB-A is a member of the signalling lymphocytic activation molecule (SLAM) family of receptors, and is found on all blood-derived NK, T, and B cells. It is a type 1 transmembrane protein of the immunoglobulin superfamily that functions as a homotypic ligand-coactivation NK receptor pair.

Early studies indicated that NK cells were ineffective at killing primary HIV-1 infected T cells (396). Surprisingly, examination of the infected cell surface receptors revealed that virus infection leads to a decrease in surface expression of HLA-A and -B inhibitory ligands through the action of HIV-1 Nef (397) and an increase in activating ligands for NKG2D through the action of Vpr (398-400). The downregulation of inhibitory ligands combined with the upregulation of activating ligands should make HIV-1 infected cells ideal targets for NK cell-mediated destruction. However, the ability of NK cells from even healthy uninfected individuals to destroy HIV-1 infected cells has been consistently characterized to be weak. For this reason it was thought that additional factors might be involved in regulating NK activity against HIV-1 infected cells.

A recent study reported the ability of HIV-1 Vpu to interfere with NK-cell degranulation by downmodulating NTB-A at the cell surface of infected cells (349). As a consequence, $CD4^+$ T cells infected with HIV-1 Vpu mutant elicited at least 50 per cent more NK cell degranulation than wild-type virus, resulting in an higher capacity to lyse HIV-infected cells. Thus Vpu dowmodulation of NTB-A protects the infected cell from lysis by NK cells (Figure 1.30). Interestingly, Vpu-targeting NTB-A involves distinct mechanisms to those used to downregulate CD4 and tetherin. Indeed, Vpu does not affect the intracellular levels of NTB-A and does not rely on the recruitment of β-TrCP to reduce cell surface NTB-A levels. Although Vpu does not accelerate NTB-A internalization as a means to deplete the coactivation NK receptor ligand from the cell surface, the viral protein interacts with NTB-A through its transmembrane domain and the Vpu TM region was found to be required for NTB-A downmodulation. Together, these results suggest that Vpu might interfere with NTB-A trafficking and/or recycling and as such sequester NTB-A in an intracellular compartment. So, Vpu mediating NTB-A downregulation

provides an explanation to account for the lack of killing of HIV-1 infected cells despite strong activation of NK cells. Similarly, Vpu also downmodulates another NK cell-activating ligand, PVR (317), however this appears to be in conjunction with Nef. More studies will need to be done to determine how the virus regulates the balance between activation and degranulation of NK cells.

Similar to NK cells, dendritic cells (DCs) also play an important role in viral infections as initiators of innate and adaptive immune responses. For instance, interaction between DCs and the innate-like CD1d-restricted natural killer T (NKT) cells results in the mutual activation of both cells and the subsequent initiation of cellular immune responses. Thus, NKT can rapidly secret T helper type 1 and 2 cytokines to activate and regulate a variety of other cell types, including DCs, NK cells, B cells and T cells. Recently, HIV-1 Vpu was found to inhibit the surface expression of CD1d in productively infected DCs (348). CD1d is a class I MHC-like membrane-associated protein expressed by antigen-presenting cells (APCs) and is involved in presenting exogenous pathogen-derived lipid antigens to NKT cells. Thus, by interfering with the CD1d antigen presentation pathway, Vpu prevents infected DCs from activating CD1d-restricted NKT cells (Figure 1.30). Considering its importance in early innate immune responses and presence at major HIV-1 transmission sites (mucosal surfaces), targeting the CD1d mediated lipid-antigen presentation may be an additional strategy for HIV-1 to evade innate cellular immune responses. Again, Vpu does not affect the rate of CD1d endocytosis or induce rapid CD1d degradation. Instead, Vpu co-localizes and interacts with CD1d in early endosomal compartments suppressing CD1d from recycling back to the plasma membrane. Hence, keeping CD1d away from the antigen-loading compartment (late endosomes) in combination with reducing its surface expression might be an efficient way for HIV-1 to avoid activation of NKT cells by infected DCs.

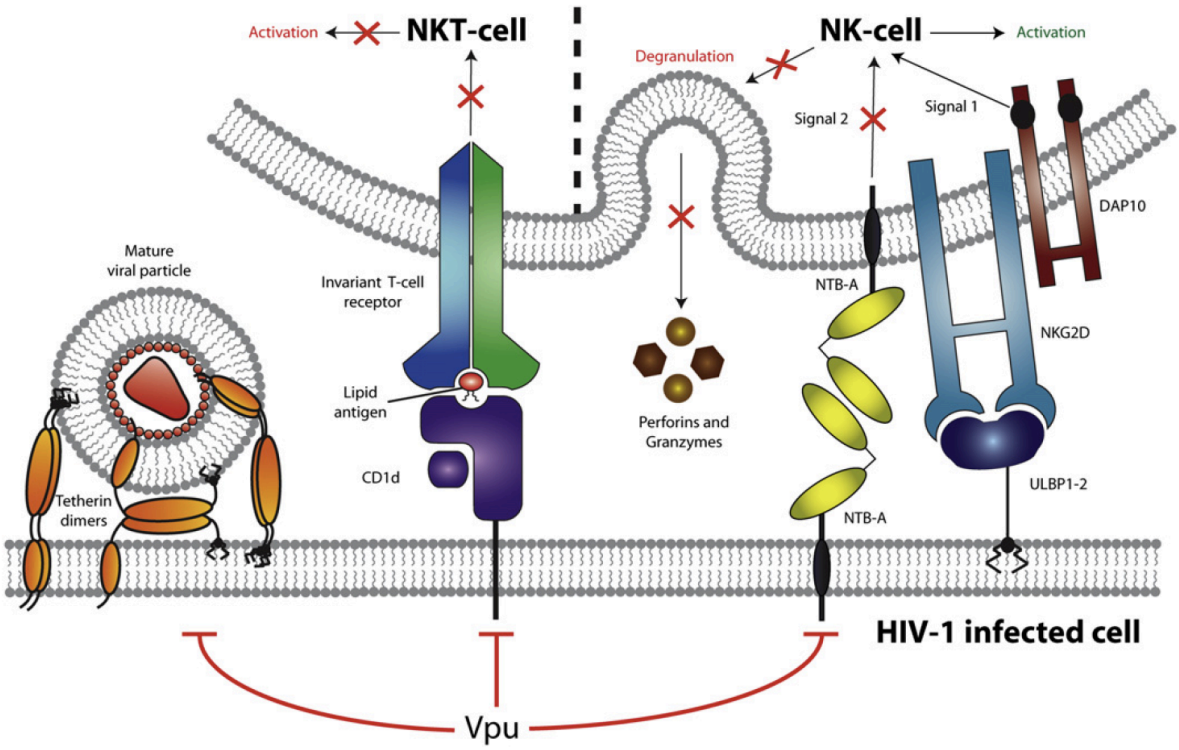

Figure 1.30: Vpu modulates the innate immune responses through the downregulation of NTB-A and CD1d.

Expression of HIV-1 Vpu in infected cells leads to cell-surface downregulation of CD1d and NTB-A (and also tetherin as described above). Reduction of CD1d cell-surface levels prevents presentation of lipid antigens to CD1d-restricted NKT cells, thereby avoiding their activation. Additionally, Vpu can also cause inhibition of cell surface expression of NTB-A to protect infected cells from NK-cell-mediated killing. Lysis of infected cell by NK cell requires both activation of NKG2D by its ligand ULBP1-2 and NTB-A to elicit degranulation (release of perforins and granzymes). On the overall, these effects of Vpu weaken the efficiency of the innate immune responses directed against HIV-1-infected cells. Figure adapted from (401).

1.8.2.4 Vpu induces cell death by apoptosis

As discussed above, one of the main pathologic characteristics in HIV-1 infected patients is the decrease of $CD4^+$ T lymphocytes. Uninfected bystander $CD4^+$ T cells die by apoptosis caused by aberrant T cell signalling, secretion of factors such as Tat, Nef, or Vpr or release from HIV-infected cells of cellular apoptosis-inducing factors (TNF-α). In productively HIV-infected $CD4^+$ T lymphocytes, viral replication can induce direct cytopathic effects leading to cell death by necrosis. In these cells, HIV-1 infection also causes through the action of Vpr, cell cycle arrest in G2/M phase leading to cell death by apoptosis. Although $CD4^+$ T cells infected with a Vpr-defective HIV-1 undergo less apoptosis than those infected with HIV-1 Wt, some annexin V positive cells can still be detected suggesting that another component of HIV-1 genome might contribute to the induction of apoptosis in infected cells (402).

Vpu has been proposed to induce apoptosis in infected cells as a consequence of its interaction with β-TrCP (Figure 1.31) (350, 403). Mechanistically, Vpu is thought to induce apoptosis by competitively binding with high affinity to β-TrCP, and thus interfering with the cellular functions in which the F-box protein is normally involved, in particular the degradation of β-catenin and IκB, or ubiquitination of the tumor suppressor p53. Accumulation of unprocessed IκB molecules further prevents activation of NF-κB, which as a result cannot trigger the transcription of genes involved in cell proliferation, cytokine production or in the regulation of apoptosis. In particular, reduction of NF-κB activity leads to an inhibition of expression of anti-apoptotic proteins such as the Bcl-2 family proteins (e.g. Bcl-x1 and A1/Bfl-1) or TNF-R complex proteins (e.g. TRAF1). TRAF1 plays an essential role in inhibiting caspase-8 activation but in Vpu-expressing cells the levels of TRAF1 are reduced and no longer sufficient to block the cytokine-induced activation of caspase-8. This results in the release of cytochrome c from the mitochondria, normally inhibited by the Bcl-2 family proteins, whose the expression is limiting in the presence of Vpu, and subsequent activation of caspase-3. Finally, active caspase-3 triggers the cleavage of a number of targets proteins leading to cell death.

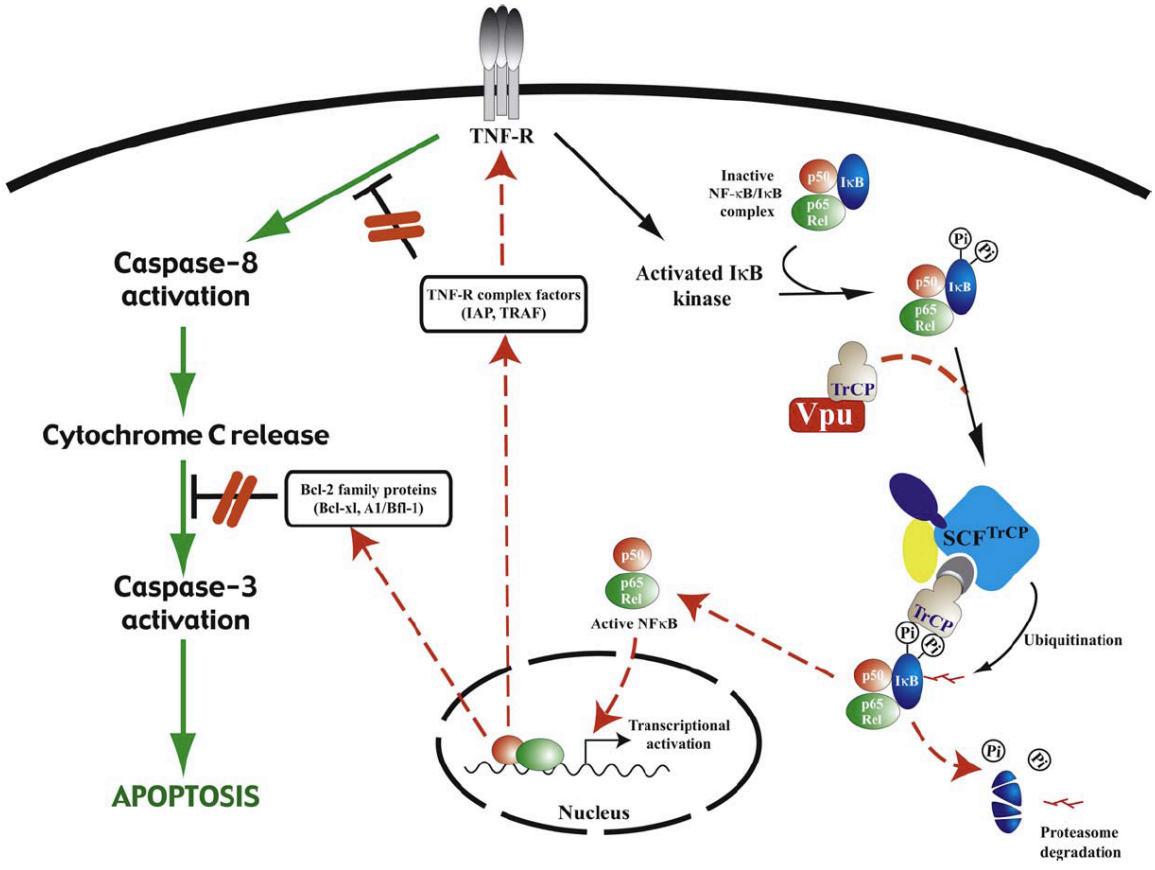

Figure 1.31: Model for Vpu-induced apoptosis through activation of the caspase pathway.

Upon stimulation of cells by cytokines such as TNF-α, IκB is rapidly phosphorylated by an IκB-specific kinase, resulting in a rapid degradation of IκB via a β-TrCP dependent pathway. Vpu by recruiting β-TrCP impedes on the proteasomal degradation of IκB resulting in the inhibition of NF-κB activation and subsequent NF-κB-dependent expression of anti-apoptotic Bcl-2 family proteins or TNF-R complex proteins (e.g. TRAF1). The steps inhibited by the action of Vpu are indicated with red arrows and steps activated by Vpu conditions are shown in green. Figure adapted from (338).

Chapter 2 Aim of Thesis

Vpu contributes to render the cellular environment less hostile for HIV-1 replication. This is achieved through the downregulation of several host proteins. In that regard, the aim of this thesis is to contribute to the understanding of the mechanism by which Vpu targets those cellular proteins. This thesis includes four chapters of experimental data that aim to demonstrate:

1. The viral protein K5, through its ubiquitin ligase activity, overcomes the antiviral restriction of tetherin imposed on the release of Kaposi's sarcoma-associated herpesvirus
2. The transmembrane domain of Vpu is an essential determinant for Vpu's ability to counteract tetherin
3. Intrinsic defects in Vpu from Group O HIV-1 account for its lack of tetherin antagonism
4. SNAT-1 is a new cellular target of HIV-1 Vpu

Chapter 3 Materials and Methods

3.1 Working with DNA

3.1.1 Amplification of DNA fragments by Polymerase Chain Reaction

- Synthesis of single M-Vpu transmembrane domain point mutants by single PCR:

All point mutations in the Vpu transmembrane domain were generated by site-directed mutagenesis PCR (QuickChange, Stratagene). The mammalian expression vector pCR3.1 encoding a codon-optimized version of HIV-1 NL4.3 Vpu tagged at the C-terminus with a hemagglutinin epitope (-HA) was used as template to initiate the polymerase chain reaction. PCR reactions were carried out in a total volume of 50 µl containing between 15 and 30 ng of DNA template, 0.2 µM of each primers (reverse and forward), 200 µM of each dNTP (dATP, dCTP, dGTP and dTTP), 1-2 units of Phusion® High-Fidelity DNA Polymerase (New England Biolabs), and 10 µl of 5X Phusion HF reaction buffer. The PCR can be divided into three phases characterized by a succession of different temperatures (Table 3.1). Besides the initial denaturation step performed at 95°C for 30 seconds, the sample was then subjected to 16-18 cycles with each cycle composed of a denaturation step at 95°C for 30 seconds during which the double strand DNA is separated into two single strands DNA, followed by an annealing step of 1 minute at 55°C which allows the primers to anneal to their complementary sequences and finally an elongation step performed at 68°C for 6 minutes (1 minute/kb of plasmid length). The forward and reverse oligonucleotide primers containing the desired point mutation were synthesized by MWG Eurofins, and each are complementary to opposite strands of the vector. The primers are between 25 and 45 bases in length with a melting temperature (Tm) of ≥78°C. The desired point mutation is located in the middle of the primer with approximately 10-15 bases of correct sequence on either side. Finally, the primers were designed with a minimum GC content of 40% and terminate in one or more C or G bases. Incorporation of the oligonucleotide primers generates a mutated plasmid containing staggered nicks.

The Vpu mutant A14L-W22A was generated by QuickChange site-directed mutagenesis as above using pCR3.1-Vpu W22A as plasmid template for the PCR.

- Synthesis of O-Vpu, chimeric genes and multiple point mutants by overlapping PCR:

Codon-optimized Vpu group O genes derived from HIV-1 group O strains 9435, HJ001 and a consensus sequence assembled from 32 full-length O-Vpu sequences available in the HIV sequence database were synthesized by multiple overlapping PCRs. In that case no DNA template was required since the succession of primers mimics the entire O-Vpu sequence. Two PCR reactions were required; in the first reaction all primers were added to the PCR mix and only a few temperature cycles were performed (x 10 cycles) to generate a small amount of the desired O-Vpu gene. 1 µl of the product from the first PCR was then amplified by a second round of PCR for 30 cycles in the presence of only the terminal primers. Standard PCR settings were used for the overlapping PCRs (Table 3.1).

The Vpu mutant A10,14,18L-W22A containing multiple mutations in its transmembrane domain was also synthesized by overlapping PCR using the same method than the one used to generate O-Vpu constructs.

Chimeric proteins bearing both sequences from O-Vpu and M-Vpu were also generated by overlapping PCR. In that scenario, M-Vpu and O-Vpu genes served as templates for two separated PCR reactions. The two resulting products were then mixed (1μl of each PCR products), used as templates and amplified after annealing with each other during the second PCR (x 30 cycles) in the presence of the corresponding primers. SNAT-1 and SNAT-2 constructs with the their cytoplasmic tails swapped were generated using the same method.

All the Vpu and SNAT-1 mutants were generated with a Kozak consensus sequence located upstream of their start codon (**GCCACC**-ATG). SNAT-1 and SNAT-2 genes were amplified from cDNA of 293T cells with primers bearing the flanking cloning sites EcoRI and XhoI.

Step	Time	Temperature	Cycles
Initial Denaturation	30 seconds	94°C-95°C	1 x
Denaturation	30 seconds	94°C-95°C	30 x (standard conditions) 16-18 x (QuickChange)
Annealing	30 seconds (standard conditions) 1 minute (QuickChange)	55°C	
Extension	30 seconds * 6 minutes	72°C (standard conditions) 68°C (QuickChange)	
Final extension	5-10 minutes *	72°C	1 x

* 1 minute/kb of insert or plasmid length

Table 3.1: Standard PCR thermal cycling conditions.

3.1.2 Extraction and Purification of DNA fragments

Amplified DNA resulting from the PCR was diluted in 10X DNA loading buffer (50% glycerol (v/v), 0.1 M EDTA, bromophenol blue (dye), in ddH_2O), loaded into a 1.5% agarose gel and subjected to electrophoresis. Agarose gels were made by melting powdered agarose (w/v) (UltraPure™ Agarose, Invitrogen) in 1X Tris-acetate running buffer (1X TAE: 40 mM Tris-acetate, 1 mM EDTA, 0.114% glacial acetic acid (v/v), pH 8.2-8.3), heated and supplemented at 0.5 μg/ml with a solution of ethidium bromide (Sigma). Gels at a lower percentage of agarose (0.7-1%) were used for separation of DNA fragments > 3kb. Gels were run at between 60 and 100 volts in 1X TAE buffer for approximately 1 hour, depending on the expected size of the bands. Band sizes were monitored by running the 2-log DNA ladder (range: 0.1-10.0 kb, New England Biolabs). DNA fragments were visualized on an ultra violet trans-illuminator using a CCD camera (BioRad). The DNA fragment band of interest (approximately 300 bp for Vpu and derived mutants; 1500 bp for SNAT-1) was excised from the gel, weighed and DNA was extracted and purified using QIAquick gel extraction kit protocol (QIAgen). 3 volumes of buffer QG were added to 1 volume of gel slice and incubated at 50°C for 10 minutes or more. After the gel slice has dissolved completely, one gel volume of isopropanol was added to the sample and mixed. The entire mix was then applied to the QIAquick column and centrifuged for 1 minute at

13,000 rpm in a top-bench centrifuge. The flow-through was discarded and 500 μl of buffer QG was added to the column to eliminate residual agarose gel and the sample was centrifuged for 1 minute at 13,000 rpm. The flow-through was discarded and the column was washed with 750 μl of buffer PE, centrifuged for 1 minute at 13,000 rpm and then for an additional minute to ensure the complete removal of ethanol. The column was then placed into a clean 1.5 ml microcentrifuge tube and the DNA-bound was eluted by adding 20-50 μl of ddH_2O. The column was left stand for 1 minute before being centrifuged for 1 minute at 13,000 rpm. The flow-through contains purified DNA.

3.1.3 DNA digestion by restriction endonucleases

Gel purified DNA fragments of Vpu, tetherin, SNAT-1 and derived mutants were then digested by the restriction enzymes EcoRI and XhoI or NotI (New England Biolabs) to generate DNA inserts with sticky ends. The expression vectors pCR3.1 (transient expression vector) and pCMS28 (derivative of the retroviral vector pMigR1, cf. section 3.2.3) were also digested with the same endonucleases in order to be linearized. The enzymatic reactions were performed in a 50 μl total volume. For plasmids digestion, 2 μg of DNA was digested with 10 units of each restriction enzyme (1 unit of enzyme is the quantity required to digest 1 μg of DNA), 5 μl of the appropriate 10X buffer, 5 μl of BSA 10X (5 μg) (if recommended) and the volume was completed to 50 μl with ddH_2O. Gel purified DNA inserts were digested similarly but the volume of water for the digestion reaction was adjusted depending on the volume of ddH_2O used for the elution step in the gel extraction protocol. DNA digestion by restriction endonucleases was also used for the screening of bacterial colonies from agar plates (cf. mini-prep).

For the QuickChange site-directed mutagenesis, the circular PCR product was digested with 1 μl of DpnI endonuclease to allow cleavage of the methylated parental DNA template (target sequence: 5'-Gm6ATC-3') in order to select the newly synthesized plasmid containing the desired mutation.

All restriction digest reactions were incubated for 2-3 hours at 37°C. The digestion products were then loaded into an agarose gel and purified using the technique described above (QIAquick gel extraction kit).

To prevent re-circularization of cloning vectors especially linearized vectors containing non-cohesive ends (pLHCX digested by HpaI), incubation with Antarctic Phosphatase (New England Biolabs) was performed for 30 minutes at 37°C to remove the 5´ phosphate groups from plasmid vector (dephosphorylation). The enzyme was then heat inactivated at 65°C for 10 minutes before proceeding to the ligation reaction. Tetherin mutants (THN-K18R, THN-K21R, THN-K18,21R) were digested with PmeI enzyme from the pCR3.1 and subcloned into the HpaI-digested pLHCX.

3.1.4 DNA Ligation

Vpu or SNAT-1 DNA inserts and other derived constructs digested with EcoRI/XhoI or EcoRI/NotI enzymes were cloned into a pCR3.1-HA expression vector, pCMS28 or pCMS28-GFP, previously linearized by digestion with the appropriate enzymes. Tetherin inserts were cloned into pLHCX vector. Ligation reactions were carried out in a total volume of 20 µl using 1 µl of T4 DNA ligase (= 400 units) in the presence of 3 times more insert than vector (≈ 100 ng of vector), 2 µl of 10X T4 DNA ligase buffer (1X T4 DNA ligase buffer contains: 50 mM Tris-HCl (pH 7.5), 10 mM $MgCl_2$, 10 mM dithiothreitol, 1 mM ATP, 25 µg/ml bovine serum albumin). Amount of insert was calculated with the following formula:

X ng of insert = 3 * [length of insert (bp) x mass of vector (ng)] / length of vector (bp)

A negative control was also made containing no insert in the reaction mixture. The reaction was incubated at room temperature (20-25°C) for at least 1 hour before transformation into chemically competent bacteria. For blunt-end ligation, the reactions were carried out at 16°C and incubated overnight.

3.1.5 Transformation of plasmid DNA into chemically competent bacteria

50 µl of chemically competent DH5α *E.coli* were thawed on ice for a few minutes before being incubated with 5-50 ng of plasmid DNA or with 2-3 µl of ligation product or PCR product. After 30 minutes incubation on ice, the cells were heat shocked at 42°C for 45 seconds. The bacteria were then allowed to recover on ice for 2 minutes before adding 100 µl of LB medium and incubated at 37°C for 30 minutes in a shaking incubator at 220 rpm. 150 µl of transformed cells were then plated onto LB-ampicillin (100 µg/ml) agar plates (LB-Agar Miller, Fisher) and incubated at 37°C or 30°C overnight. Retroviral vectors containing repetitive sequences were incubated at 30°C instead of 37°C to avoid genetic recombinations. Bacterial cells were grown in liquid phase Luria-Bertani Broth medium (LB) containing 1% tryptone (w/v), 0.5% yeast extract (w/v), and 1% NaCl (w/v) dissolved in ddH_2O, supplemented with ampicillin (100 µg/ml) or on LB-Agar (37 g/1L ddH_2O) poured into 10 cm sterile dishes for solid phase growth cultures.

Single colonies on agar plates were picked using a sterile tip, resuspended into 1-2 ml of LB/ampicillin medium and incubated at 37°C for a few hours or longer depending on the study. For the screening of colonies by PCR, cells were incubated until the medium became cloudy. 1 µl of this culture was then used to perform the PCR. For the screening of colonies by enzymatic digestion the cultures were left overnight before performing the mini-prep DNA extraction. Starter cultures used to inoculate larger volume of LB medium (100 ml) for plasmid amplification (midi-prep) were also incubated overnight in a shaking incubator.

3.1.6 Plasmid DNA Amplification and Purification

100 µl of a 2 ml starter culture grown overnight were inoculated in 100 ml of LB-Ampicillin medium and incubated overnight in a 250 ml flask at 37°C (or at 30°C for proviral plasmids) in a shaking incubator at 220 rpm. Bacterial cells were then harvested by centrifugation at 6000 x g for 15 minutes at 4°C. Plasmid DNA was extracted and purified using the QIAGEN plasmid midi kit (QIAGEN) whose the method is based on the principle of alkaline lysis. The bacterial pellet was resuspended in 4 ml of buffer P1 (50 mM Tris-Cl pH 8.0, 10 mM EDTA, 100 µg/ml RNase A). 4 ml of lysis buffer P2 (200 mM NaOH, 1% SDS (w/v)) were added to the sample, mixed and incubated at room temperature for 5 minutes. 4 ml of neutralization buffer P3 (3.0 M potassium acetate, pH 5.5) was added, mixed immediately and incubated on ice for 15 minutes. The sample was then centrifuged at 15,500 x g for 30 minutes at 4°C. The supernatant containing plasmid DNA was then applied to an equilibrated column (equilibrated by adding 4 ml of buffer QBT), and allowed to run through by gravity flow. The column was washed twice with 10 ml of buffer QC (1.0 M NaCl, 50 mM MOPS pH 7.0, 15% isopropanol (v/v)), and the DNA eluted with 5 ml of buffer QF (1.25 M NaCl, 50 mM Tris-Cl pH 8.5, 15% isopropanol (v/v)). Eluted DNA was then precipitated by adding 3.5 ml of isopropanol and centrifuged for 30 minutes at 15,500 x g. After centrifugation the DNA pellet was transferred into a microcentrifuge tube, resuspended into 1 ml of 70% ethanol and centrifuged at 14,000 rpm for 10 minutes at 4°C in a top-bench centrifuge. The ethanol was discarded and the tube placed on a heating block at 50°C for a few minutes to dry the DNA pellet and remove the residual ethanol. Finally the DNA was redissolved in 100 µl of ddH_2O.

Alternatively, plasmid DNA extraction was carried out from smaller cultures of 1-3 ml. The method is based on the same principle than the protocol mentioned above and only some buffers differ. Mini-preps were performed using the QIAprep Spin Miniprep kit (QIAGEN). The bacterial overnight culture was pelleted by centrifugation at 6000 rpm in a table-top microcentrifuge for 5 minutes at room temperature (15-25°C). The supernatant was then discarded and the pelleted bacterial cells were resuspended in 250 µl of buffer P1. Cells were lysed in 250 µl of buffer P2 and mixed by inverting the tube 4-6 times until the solution becomes clear. 350 µl of neutralization buffer N3 were added to the mixture and mixed immediately. The solution was then centrifuged for 10 minutes at 13,000 rpm and the resulting supernatant was applied to the QIAprep spin column and centrifuged for 1 minute at 13,000 rpm. The flow-through was then discarded and the column washed by adding 500 µl of buffer PB before the addition of 750 µl of buffer PE. This step was followed by two successive centrifugations of 1 minute each to completely remove the wash buffer. The column was then placed into a clean 1.5 ml microcentrifuge tube. To elute the DNA, 20-50 µl of ddH_2O were added to the center of the QIAprep spin column and the column was left stand for 1 minute before centrifugation.

3.1.7 Analysis and Sequencing of DNA

DNA concentrations were determined using a Nanodrop ND-100 Spectrophotometer (Labtech International), with optical density measurements at 260 nm. This method is based on the fact that 1 OD_{260} unit corresponds to 50 μg/ml of double strand (ds) DNA. On the average the DNA plasmids midi preparations give 0.1 mg of purified DNA. The quality of the DNA sample is assessed by the OD_{260}/OD_{280} ratio, which can be considered pure and relatively free from protein contamination for a ratio of 1.8. 1.5 μg of DNA preparations dissolved in 15 μl ddH_2O were sent for sequencing to Eurofins MWG Operon. Vpu, tetherin and SNAT-1 constructs were sequenced by MWG via the T7 forward primer site in pCR3.1.

Gene	Vector	Cloning sites	Resistance genes	Tag	Stable cell lines
YFP	pCR3.1		Ampicillin		
GFP	pCR3.1		Ampicillin		
Wild-Type Tetherin	pCR3.1 pLHCX	EcoRI/XhoI PmeI/HpaI	Ampicillin Ampicillin/hygromycin	HA (position 463[b]) * HA (position 463)	HT1080
K18R Tetherin	pCR3.1 pLHCX	EcoRI/XhoI PmeI/HpaI	Ampicillin Ampicillin/hygromycin	HA (position 463) * HA (position 463)	HT1080
K21R Tetherin	pCR3.1 pLHCX	EcoRI/XhoI PmeI/HpaI	Ampicillin Ampicillin/hygromycin	HA (position 463) * HA (position 463)	HT1080
K18-21R Tetherin	pCR3.1 pLHCX	EcoRI/XhoI PmeI/HpaI	Ampicillin Ampicillin/hygromycin	HA (position 463) * HA (position 463)	HT1080
Y6,8A Tetherin	pCR3.1 pLHCX	EcoRI/XhoI PmeI/HpaI	Ampicillin ampicillin/hygromycin	HA (position 463) * HA (position 463)	HT1080
Wild-Type M-Vpu	pCR3.1 pCMS28 pCMS28-GFP NL4.3 ** pCRV1	EcoRI/XhoI EcoRI/NotI EcoRI/XhoI	Ampicillin Ampicillin/puromycin Ampicillin/puromycin Ampicillin Ampicillin	HA (C-terminus) * Cherry	 Jurkat / HT1080 THN-HA
A14L M-Vpu	pCR3.1 pCMS28 pCMS28-GFP NL4.3 pCRV1	EcoRI/XhoI EcoRI/NotI EcoRI/XhoI	Ampicillin Ampicillin/puromycin Ampicillin/puromycin Ampicillin Ampicillin	HA (C-terminus)	 Jurkat / HT1080 THN-HA
W22A M-Vpu	pCR3.1 pCMS28 pCMS28-GFP NL4.3 pCRV1	EcoRI/XhoI EcoRI/NotI EcoRI/XhoI	Ampicillin Ampicillin/puromycin Ampicillin/puromycin Ampicillin Ampicillin	HA (C-terminus)	 Jurkat / HT1080 THN-HA
A14L-W22A M-Vpu	pCR3.1 pCMS28 pCMS28-GFP NL4.3 pCRV1	EcoRI/XhoI EcoRI/NotI EcoRI/XhoI	Ampicillin Ampicillin/puromycin Ampicillin/puromycin Ampicillin Ampicillin	HA (C-terminus)	 Jurkat / HT1080 THN-HA
A10-14-18L /W22A M-Vpu	pCR3.1	EcoRI/XhoI	Ampicillin	HA (C-terminus)	
TMD Mutants M-Vpu	pCR3.1 pCMS28-GFP	EcoRI/XhoI EcoRI/XhoI	Ampicillin Ampicillin/puromycin	HA (C-terminus)	
S52,56A M-Vpu	pCR3.1 pCMS28 pCMS28-GFP NL4.3	EcoRI/XhoI EcoRI/NotI EcoRI/XhoI	Ampicillin Ampicillin/puromycin Ampicillin/puromycin Ampicillin	HA (C-terminus)	 Jurkat / HT1080 THN-HA
Wild-Type O-Vpu 9435	pCR3.1	EcoRI/XhoI	Ampicillin	HA (C-terminus)	
Wild-Type O-Vpu HJ001	pCR3.1	EcoRI/XhoI	Ampicillin	HA (C-terminus)	
Wild-Type O-Vpu Consensus	pCR3.1	EcoRI/XhoI	Ampicillin	HA (C-terminus)	
O-Vpu Chimera	pCR3.1	EcoRI/XhoI	Ampicillin	HA (C-terminus)	
SNAT-1	pCR3.1 pCMS28	EcoRI/XhoI EcoRI/XhoI	Ampicillin Ampicillin/puromycin	HA (C-terminus) * HA (C-terminus)	 293T / HeLa
SNAT-2	pCR3.1 pCMS28	EcoRI/XhoI EcoRI/XhoI	Ampicillin Ampicillin/puromycin	HA (C-terminus) HA (C-terminus)	 293T / HeLa
SNAT 1-2	pCR3.1 pCMS28	EcoRI/XhoI EcoRI/XhoI	Ampicillin Ampicillin/puromycin	HA (C-terminus) HA (C-terminus)	 293T / HeLa
SNAT 2-1	pCR3.1 pCMS28	EcoRI/XhoI EcoRI/XhoI	Ampicillin Ampicillin/puromycin	HA (C-terminus) HA (C-terminus)	 293T / HeLa
K5	pCR3.1 pCMS28	EcoRI/XhoI EcoRI/NotI	Ampicillin Ampicillin/puromycin	HA 	 HT1080/THN-HA
K5 delRING	pCR3.1 pCMS28	EcoRI/XhoI EcoRI/NotI	Ampicillin Ampicillin/puromycin	HA 	 HT1080/THN-HA
VSV-G	pCMV		Ampicillin		
MLVgag-pol			Ampicillin		

♭In tetherin sequence the HA tag is inserted at the amino acid position 463 with the numbering starting from the N-terminus. The HA tag is localized between the extracellular coiled-coil domain and the GPI anchor.
* Untagged versions of these proteins were also cloned (presence of a stop codon at the C-terminus) into the pCR3.1 expression vector.
** The pNL4.3delVpu was generated by replacing the ATG start codon of vpu ORF by a BamHI site (ggATccCAA) generating also one frame shift.

Table 3.2: List of plasmid DNA constructs generated for transient expression of proteins, production of VLPs and associated stable cell lines synthesized.

3.2 Working with Cells

3.2.1 Cell Culture

All adherent cells were maintained at 37°C/5% CO_2 in Dulbecco's modified Eagle's medium (DMEM, Invitrogen) supplemented with 10% heat inactivated fetal bovine serum (v/v) (FBS, Invitrogen - inactivation for 30 minutes at 56°C) and gentamicin (0.02 mg/ml, Invitrogen) and cell density was monitored daily. For suspension cells such as Jurkat, RPMI 1640 medium (Invitrogen) was used as a culture medium instead of DMEM. All procedures were performed using sterile techniques in a laminar flow hood. HEK-293T cells, HeLa cells, HT1080 and Jurkat cells were obtained from the American Type Culture Collection (ATCC) and the HIV-1 reporter cell line HeLa-TZMbl was kindly provided by John Kappes through the NIH AIDS Reagents Repository Program (ARRP). HeLa cells modified to only express CD4 were provided by A. Akrigg through the National Institute of Biological Standards and Controls (NIBSC) Centre for AIDS Reagents. All cell lines were passaged at least every two days or more if needed for experimental purposes. Adherent cells were first washed with 3 ml of 1X phosphate buffered saline (1X PBS, Invitrogen) and dissociated from the tissue culture plate by addition of 2 ml of Trypsin (TrpLE Express + phenol red, Invitrogen) and then incubated for a few minutes at 37°C until the cells were detached. Cells were then resuspended into fresh pre-warmed DMEM.

HEK-293T cell line is a variant of HEK-293 cells that contains, in addition, the SV40 Large T-antigen, that allows for episomal replication of transfected plasmids containing the SV40 origin of replication. Alternatively to HEK-293T cells (often designated as 293T), HeLa and HT1080 were also used for this study (Table 3.3). HeLa cells are constitutively CXCR4 positive but do not express CD4 and CCR5. TZMbl cells are HeLa cells modified to express these lacking HIV-1 entry receptors rendering them permissive to infection by HIV-1. These cells were further engineered to contain integrated reporter genes for firefly luciferase and Escherichia coli β-galactosidase (lacZ) under the control of an HIV long-terminal repeat (LTR) promoter. In this configuration reporter gene expression is induced *in trans* by expression of the viral protein Tat soon after infection. β-galactosidase activity is quantified as relative luminescence units (RLU) and is directly proportional to the number of infectious virus particles present in the initial inoculum and by extension proportional to the number of virus particles.

Stocks of frozen cells were kept in liquid nitrogen. Cells were pelleted by centrifugation at 1,200 rpm for 5 minutes and resuspended into DMEM supplemented with 20% FBS (v/v) (Invitrogen) and 10% DMSO (v/v) (Sigma). The cells were cooled down at -80°C for a few days before being transferred to liquid nitrogen for long-term storage.

Cell Line	Origin	Culture Medium	Features
HEK-293T	Human embryonic kidney cells	DMEM Adherent cells	Do not endogenously express tetherin Tetherin expression induced by IFN Absence of HIV-1 entry receptors
HT1080	Fibrosarcoma	DMEM Adherent cells	Do not endogenously express tetherin Absence of HIV-1 entry receptors
HeLa	Cervical cancer	DMEM Adherent cells	Endogenously express tetherin Absence of HIV-1 entry receptor CD4
HeLa-TZMbl	Cervical cancer	DMEM Adherent cells	Endogenously express tetherin Expression of HIV-1 entry receptors CD4 and CCR5 β-galactosidase reporter gene under the control of HIV-1 promoter
Jurkat	$CD4^+$ T lymphocyte (leukemia)	RPMI Suspension cells	Endogenously express tetherin Expression of HIV-1 entry receptors CD4 and CXCR4 but not CCR5

Table 3.3: List of cell lines used for this study.

3.2.2 Transient transfection

Cells were seeded a day prior to transfection. For indication, cells were plated at a density of 3-4x10^5 in a well of a 6-well plate and at 10^5 cells per well of a 24-well plate. For each transfection sample, the appropriate amount of pCR3.1 vector encoding a given protein was diluted in DMEM without serum and mixed gently. Then, the transfection reagent was prepared in serum free medium and combined after 5 minutes incubation at room temperature with the diluted DNA. 293T cells were transfected with polyethylenimine (PEI solution prepared in ddH_2O at 1 mg/ml, 0.22 μm filtered and pH 7.0, Polysciences) whereas for HeLa cells, Lipofectamine 2000 (2 mg/ml, Invitrogen) was used as a transfection reagent. In both cases, the transfection reagents facilitate entry of exogenous DNA into cell cytoplasm through endocytosis or membranes fusion. The solution was then mixed gently, incubated for 20 minutes at room

temperature and added dropwise to the cells. Cells were then incubated for 48 hours prior to testing for protein expression, and medium was replaced 16 hours post-transfection.

3.2.3 Generation of stable cell lines using retroviral vector transduction

293T cells plated into a 6-well plate were transfected with expression vectors encoding MLV gag-pol proteins (1 μg), the VSV-G (0.2 μg) envelope protein and an MLV-based retroviral vector (1 μg), either the pCMS28 or the pLHCX. In this system, 293T cells serve as a packaging cell line. The retroviral vector pCMS28 is derived from pMigR1 and encodes a puromycin resistance gene. The resistance gene is linked via an internal ribosomal entry site (IRES) to the multi-cloning site, thereby coupling antibiotic selection to mRNA synthesis of the gene of interest. The multiple cloning site of this vector contains the restriction sites of the enzymes EcoRI, NotI and XhoI via which K5, Vpu and SNAT-1 genes were inserted. The pLHCX contains elements derived from Moloney murine leukemia virus and Moloney murine sarcoma virus. The 5' viral LTR in this vector contains promoter/enhancer sequences that control expression of the hygromycin resistance gene for antibiotic selection in eukaryotic cells. In this construct, tetherin and the derived cytoplasmic tail tetherin mutants were cloned into the multiple cloning site immediately downstream of the human cytomegalovirus (CMV) promoter. Once in the cell, mRNA from the retroviral vectors is packaged via the packaging signal ψ into replication-incompetent retroviral particles. This leads to the production of virus like particles (VLPs) containing the retroviral vector packaged into the structural proteins of MLV and bearing the VSV-G envelope protein at their surface. Importantly, for VLP production with pLHCX-THN, 100 ng of pCR3.1-Vpu were added to inhibit restriction of particle release mediated by tetherin. 48 hours post-transfection the virus like particles were harvested, 0.22 μm filtered and used to transduce 293T, HT1080 or HeLa cells. In most cases, spinoculation was used as a mean to increase delivery of virus particles into target cells (404). The spinoculation consists of centrifuging the plate for 2 hours at 3000 rpm at 20°C. By pseudotyping the VLPs with the VSV-G envelope protein, these retroviral particles can infect and deliver the gene of interest into the host genome of a broad range of target cells. 48 hours later, transduced cells were split into a larger well format and placed under antibiotic selection (hygromycin at 100 μg/ml or puromycin at 1-2 μg/ml) and incubated at 37°C until all untransduced control cells had died.

3.2.4 Preparation of replication-competent HIV-1 virus stocks and Infection

Semi-confluent HEK-293T cells on 6-well dishes were transfected with 2 µg of pNL4.3 or pNL4.3 (delVpu) and 0.2 µg of pCMV-VSV-G when necessary. This leads to the production of replication-competent HIV-1 virus particles that have both VSV-G and gp160 envelope proteins on their surface to allow infection of CD4 negative cells. Alternatively non-VSV-G pseudotyped HIV-1 virus stocks were also produced. 24 hours post-transfection, the medium was replaced and the cells were left in culture at 37°C for 24 more hours before being harvested. Then, supernatants containing viral particles were filtered 0.22 µm, aliquoted, stored at -80°C and subsequently titers determined on HeLa-TZMbl (cf. 3.3.1). Cells were infected with different multiplicities of infection (MOI) depending on the assay. For detection of tetherin or SNAT-1 degradation mediated by Vpu, cells were infected with a MOI of 2. This multiplicity of infection ensures that approximately 90% of the cells were infected. To measure the production of virus particles released from a single round of infection through HeLa, 293T or HT1080 cells, MOIs of 0.2-0.5-1 were used. MOIs lower than 0.2 were used to study virus replication (multiple cycles of infection) through the culture over time (MOI=0.1) in human primary $CD4^+$ T cells. In that system, several rounds of replication are possible since these cells express all the HIV-1 entry receptors. For indication, a multiplicity of infection of 1 means that the amount of infectious virus particles (titrated on HeLa-TZMbl cells) added is the same than the amount of cells present in the culture, however the proportion of resulting infected cells is defined by the Poisson distribution indicated below:

$P(k) = e^{-m}m^k/k!$

In this equation, P(k) is the fraction of cells infected by k virus particles, and m is the MOI.

3.2.5 HIV-1 virus release assay

Subconfluent HEK-293T cells seeded at a density of 10^5 cells per well in a 24-well plate were transfected with 500 ng of HIV-1 proviral plasmid (pNL4.3, pNL4.3 delVpu) in combination with 50 ng of pCR3.1-huTetherin and variable concentrations of pCR3.1-Vpu-HA or mutants thereof using PEI (5 µg/sample). The medium was replaced 16 hours after transfection, and viral supernatants and cell lysates were harvested 48 hours post-transfection. The infectivity of viral supernatants was determined by infecting HeLa-TZMbl and analyzing chemiluminescent β-galactosidase activity 48 hours later (cf. section 3.3.1). Alternatively, to analyze physical particle release, 0.22 µm filtered supernatants were pelleted through a 20% sucrose-PBS cushion in a bench-top microcentrifuge at 14,000 x rpm for 90 minutes at 4°C, and pellets were resuspended in SDS-PAGE loading buffer. Virions and cell lysates were then subjected to SDS-PAGE and Western Blotting for HIV-1 p24-CA.

3.2.6 Gene expression knockdown by siRNA

293T cells stably expressing SNAT-1/HA were seeded at a density of $1.5x10^5$ cells per well in a 12-well plate. After 3-4 hours, the first transfection was performed. Cells were transfected with Dharmafect transfection reagent (Dharmacon) with 100 pmoles of the corresponding siRNA (non-targeting control, UBAP1 or Tsg101 - QIAGEN) (Table 3.4) diluted in Optimem (Invitrogen). Medium was replaced 16 hours later. 48 hours post-transfection, 1/8 of the cells from one well of 12-well plate was reseeded into a 24-well plate and the second transfection was performed as before with 50 pmoles of siRNA oligo. 3-4 hours later, the cells were infected at a MOI of 2 with VSV-G pseudotyped HIV-1 particles and incubated for two days before being harvested.

Silenced-Gene	Type	Target sequence
UBAP1	siRNA	5'-CTCGACTATCTCTTTGCACAT-3'
Tsg101	siRNA	5'-CCUCCAGUCUUCUCUCGUC-3'

Table 3.4: Sequences of siRNA oligomers used to silence UBAP1 and Tsg101 expressions in 293T SNAT-1/HA cells.

3.2.7 Isolation of Peripheral Blood Mononuclear Cells (PBMC)

Mononuclear cells (lymphocytes and monocytes) from human peripheral blood were isolated by a density gradient centrifugation method. Fresh blood taken from healthy donors was collected into heparin-coated tubes. The blood was then diluted by addition of an equal volume of 1X PBS (without Mg^{2+} and Ca^{2+}). 30 ml of diluted blood was layered over 15 ml of Lymphoprep (Axis-Shield, sodium diatrizoate 9.1% (w/v); polysaccharide 5.7% (w/v)) in a 50 ml conical tube and centrifuged at room temperature (approximately 20°C) for 30 minutes at 1000 x g in a swinging-bucket rotor without brake. After centrifugation the mononuclear cells forming a distinct band (also called buffy coats) at the sample/medium interface were removed using a disposable Pasteur pipette without removing the upper layer. The harvested fraction was then diluted with a large volume of 1X PBS and the cells were pelleted by centrifugation for 10 minutes at 300 x g. This washing step was repeated until the supernatant became completely clear. PBMCs count was determined using a haemocytometer. For indication, on average $2x10^6$ PBMCs should be isolated per ml of blood.

3.2.8 Isolation and Purification of $CD4^+$ T lymphocytes

$CD4^+$ T lymphocytes were isolated from PBMCs using Dynabeads Untouched human CD4 T cells kit (Invitrogen). This method allows the negative selection of $CD4^+$ T cells by depletion of B

cells, NK cells, monocytes, platelets, dendritic cells, $CD8^+$ T cells, granulocytes and erythrocytes from PBMCs leaving intact the wanted $CD4^+$ T cells. Isolated $CD4^+$ T cells are therefore bead- and antibody-free. PBMCs were resuspended in isolation buffer (Ca^{2+} and Mg^{2+} free 1X PBS supplemented with 2% FBS (v/v) and 2 mM EDTA). After addition of heat inactivated FBS, a mixture of mouse IgG antibodies against the non-$CD4^+$ T cells was added to the sample and incubated for 20 minutes at 2-8°C. Cells were then washed with isolation buffer and pelleted by centrifugation at 300 x g for 8 minutes at 2-8°C. The supernatant was discarded and the cells were resuspended into fresh isolation buffer and incubated for 15 minutes at 18-25°C in the presence of pre-washed Depletion MyOne Dynabeads. This step allows the antibody-labelled cells to bind to the magnetic beads. The bead-bound cells were subsequently separated on a magnet for 1 minute and discarded. The supernatant contains the negatively isolated human $CD4^+$ T cells. At this stage, a $CD4^+$ T cells count was performed. For indication, 1/4 of PBMCs should be $CD4^+$ T cells giving a total number of $2.5x10^7$ $CD4^+$ T cells in 50 ml blood. A fraction of isolated $CD4^+$ T cells is conserved to check the purity. This fraction was stained with an anti-CD4 antibody coupled to an APC fluorochrome before being analyzed by flow cytometry. 10^6 $CD4^+$ T cells were then plated into a well of a 24-well plate in a seeding volume of 1 ml pre-warmed RPMI-1mM glutamine (supplemented with 10% heat inactivated dialyzed FBS (v/v), Invitrogen) in the presence of 25 µl of Dynabeads Human T-Activator CD3/CD28 (Invitrogen) in order to obtain a bead-to-cell ratio of 1:1. These beads mimic *in vivo* T cell activation from antigen-presenting cells by utilizing the two activators signals CD3 and CD28, bound to a three-dimensional bead similar in size to the antigen-presenting cells. Cells were activated for 48 hours with anti-CD3/anti-CD28 magnetics beads before HIV-1 infection. The beads were then removed and the cells were maintained in rhIL-2 (20 U/ml)(Roche). Alternatively, $CD4^+$ T cells were stained with CellTrace Violet dye (Invitrogen) before addition of CD3/CD28 Dynabeads.

3.2.9 Cell Proliferation

CellTrace™ Violet Cell proliferation kit (Invitrogen) was used to label $CD4^+$ T cells with a dye-marker that allows monitoring of cell proliferation. This dye diffuses into cells where it is cleaved by intracellular esterases to yield a highly fluorescent compound. This compound covalently binds to intracellular amine and is inherited by daughter cells after cell division. Primary human $CD4^+$ T lymphocytes were resuspended in a final concentration of 10^6 cells/ml in 1X PBS-5% dialyzed FBS. Cells were then mixed with a final CellTrace Violet concentration of 5 µM and incubated for 20 minutes at 37°C, protected from light. Any unbound dye was quenched by adding 5 times the original staining volume of RPMI-1mM glutamine to the cells. Cells were then incubated for 5 minutes at 4°C, pelleted via centrifugation and resuspended in fresh pre-warmed RPMI-1mM glutamine at a final concentration of 10^6 cells/ml. Violet-labeled $CD4^+$ T cells were then activated as above with CD3/CD28 Dynabeads (Invitrogen). A sample of violet-labeled $CD4^+$ T cells was maintained without CD3/CD28 stimulation in order to detect the generation 0.

3.3 Working with Viruses

3.3.1 β-Galactosidase reporter assay: virus stock titration and virus release quantification

- Absolute titration of virus stocks:

HIV-1 virus stocks and those pseudotyped with VSV-G prepared as described in part 3.2.4 were titrated on HeLa-TZMbl cells. TZMbl cells were seeded at a density of 10^4 per well in a flat bottom 96-well plate (or $5x10^4$ cells per well for a 48-well plate format) and infected 24 hours later with 25 µl input of serial dilutions from 10^{-1} to 10^{-6} of the initial virus stock. Two days post-infection, cells were fixed with 0.5% glutaraldehyde/PBS for 15 minutes at room temperature, washed twice with 1X PBS and incubated with X-Gal substrate (solution at 1 mg/ml X-gal-dimethylformamide in 5 mM K ferrocyanide, 5 mM K ferricyanide, 2 mM $MgCl_2$, 0.02% NP40, 0.01% Triton-X100 in 1X PBS) overnight at 37°C. Infected cells should turn blue as a result of the β-galactosidase activity induced by Tat expression. Blue colonies were then counted with a light microscope and the end point titer of virus (IU/ml) determined.

- Relative titration for virus release:

Alternatively, infected TZMbl cells were lyzed 48 hours post-infection in 50-100 µl of Tropix Galacto-*Star* Lysis Solution (100 mM potassium phosphate (pH 7.8), 0.2% Triton X-100, Applied Biosystems) for 10 minutes at room temperature. 10 µl of cell lysates were then transferred to a white luminescence microplate well and incubated for 10-15 minutes in the dark with 45 µl of Tropix Galacton-*Star* substrate diluted at 1:50 in Reaction Buffer Diluent (100 mM sodium phosphate (pH 7.5), 1 mM magnesium chloride, 5% Sapphire-II enhancer, Applied Biosystems). The light signal was then measured using a luminescence counter (Victor Light 1420-Perkin Elmer) and Wallac 1420 workstation software. In that system, HeLa-TZMbl cells serve as a HIV-1 reporter cell line and allow to quantify the infectivity of viral supernatants, which in that case, reflects the absolute amount of virions.

3.3.2 Intracellular p24 staining

Infected primary human $CD4^+$ T cells or Jurkat cells were fixed in 4% paraformaldehyde solution at 4°C for 10-20 minutes, washed 2 times in cold staining buffer (1X PBS, 2 mM EDTA, 2% FBS (v/v)) and stored at 4°C for up to 3-4 days in staining buffer before FACS analysis. Cells were then pelleted to remove the staining buffer and permeabilized for 15 minutes with BD Perm/Wash buffer (saponin and FBS diluted in ddH_2O, BD Cytofix/Cytoperm fixation/permeabilization kit; BD Biosciences). Cells were then pelleted by centrifugation, resuspended in 50 µl of BD Perm/Wash buffer containing HIV-1 Gag antibody diluted at 1:100

(KC57 antibody conjugated to phycoerythrin (PE), Beckman-Coulter) (Table 3.5) and incubated at 4°C for 1 hour in the dark. The cells were then washed 2 times with BD Perm/Wash buffer and resuspended in staining buffer prior to flow cytometry analysis. Uninfected cells were also stained and used as negative controls to detect non-specific staining.

3.3.3 HIV-1 replication in primary $CD4^+$ T lymphocytes

CD3/CD28-activated $CD4^+$ T lymphocytes were infected with HIV-1 Wt or delVpu at a multiplicity of infection of 0.1 for 3-4 hours in 1 ml total volume of glutamine-free RPMI medium. 10 ml of glutamine-free medium was then added to each sample (uninfected, HIV-1 Wt, HIV-1 delVpu) and cells were pelleted by centrifugation for 2 minutes at 2000 rpm. The supernatant was then discarded and replaced by 10 ml fresh glutamine-free medium. This washing step was then repeated one more time to ensure complete removal of glutamine. Cell pellets were resuspended in the appropriate volume of glutamine-free medium to obtain a density of $5x10^5$ cells/ml. 200 µl of this solution (= 10^5 cells) were then distributed into a 96-well plate. The plate was then centrifuged for 2 minutes at 2000 rpm, supernatants from each well removed and replaced with RPMI medium supplemented with IL-2 (30 units/ml), heat inactivated, dialyzed and treated FBS (Invitrogen) and the appropriate glutamine dilution (dilution range from 0 mM to 2 mM). Infected $CD4^+$ T cells were then incubated at 37°C. Cells and viral supernatants were harvested at several time points post-infection. A time point 24 hours post-infection was always taken in order to get a common and synchronous amount of virus for each conditions tested. The cells were stored at 4°C for p24 intracellular staining (cf. section 3.3.2) and viral supernatants titrated on HeLa-TZMbl cells (cf. section 3.3.1).

3.4 Working with Proteins

3.4.1 Co-immunoprecipitations

Subconfluent HEK-293T cells seeded at $3\text{-}4x10^5$ per well in a 6-well plate were transfected with 500-800 ng of Vpu expression vector (Vpu cloned into pCR3.1 or pCRV1), the appropriate Vpu mutant or pCR3.1-YFP, and 500-800 ng of pCR3.1-huTetherin or pCR3.1 SNAT-1/HA. At 48 hours post-transfection, the medium was removed and the cells were resuspended into 1 ml of cold lysis buffer (50 mM Tris-HCl (pH 7.4), 150 mM NaCl, complete protease inhibitors (Roche), and 1% digitonin (w/v) (Calbiochem)) and lysed for 30 minutes at 4°C on a rotational tumbler. The nuclei were then removed by centrifugation for 5 minutes at 10,000 x g and the supernatant was transferred into a new tube and pre-cleared for 30 minutes at 4°C on a rotator with 60 µl of pre-washed protein G-agarose beads (Invitrogen). The samples were then centrifuged for 5

minutes at 10,000 x g at 4°C and the supernatant transferred into a new tube. 80 μl of the cleared-supernatant serving as cell lysates control were taken and diluted in 2X SDS-PAGE loading buffer. The remaining supernatants (≈ 900 μl) were then incubated with 5 μg/ml mouse anti-HA antibody (Covance) for 2 hours at 4°C on a rotational tumbler before addition of 75 μl of fresh protein G-agarose. The samples were incubated for a further 3 hours at 4°C and then washed 4 times (4 cycles of centrifugation at 3500 x g of 1 minute at 4°C) in lysis buffer containing 0.1% digitonin (w/v). Finally, the last 100 μl were removed using a 26G needle and the beads resuspended in 100 μl of 2X SDS-PAGE loading buffer.

3.4.2 Detection of ubiquitinated tetherin

This assay was performed to detect ubiquitinated tetherin molecules in the presence of Vpu or K5 expression. HeLa cells seeded on 10cm plates were transiently transfected with a pCR3.1 THN-HA expression vector (5 μg) in combination with pCR3.1 K5, Vpu or GFP (2 μg) expression vectors and in the presence or absence of a 6-His-tagged ubiquitin encoding plasmid (2 μg). 48 hours after transfection, cells were treated for 8 hours with BafA1 (100 nM, Sigma) to prevent further tetherin degradation. Cells were lysed in buffer A (6 M guanidine-HCl, 0.1 M Na_2HPO_4/NaH_2PO_4, 10 mM imidazole and pH adjusted to 8.0 with NaOH), sonicated and ubiquitinated proteins were isolated by binding to 50 μl of Ni-NTA agarose beads (Invitrogen) for 3 hours at room temperature on a rotator. The resin was then washed twice with buffer A followed by two washes with buffer A/TI (1 volume of buffer A + 3 volumes of buffer TI) and washed one more time with buffer TI (25 mM Tris.Cl, 20 mM imidazole, pH 6.8). Finally, the bound ubiquitinated proteins were eluted from the resin by adding 100 μl of 2X SDS-PAGE loading buffer supplemented with 100 mM imidazole.

3.4.3 SDS-PAGE and Western blotting

Protein samples resuspended in 2X SDS-PAGE reducing loading buffer (20% (v/v) glycerol, 4% (w/v) SDS, 100 mM Tris-HCl (pH 6.8), 200 mM β-mercaptoethanol, 0.2% (w/v) bromophenol blue) were denatured for 10 minutes at 100°C before being loaded into a Sodium Dodecyl Sulphate PolyAcrylamide Gel Electrophoresis (SDS-PAGE). The purpose of SDS-PAGE is to separate proteins according to their molecular size. Denaturating separating gels (10% gels contain: 25% (v/v) of acrylamide 40% solution (acrylamide:BIS-acrylamide-29:1, Fisher), 0.1% (w/v) SDS, 0.1% (v/v) TEMED (N,N,N',N'-Tetramethyl-ethane-1,2-diamine, Sigma), 375 mM Tris-HCl (pH 8.8), 0.05% (w/v) ammonium persulphate in ddH_2O) were cast using the Mini-PROTEAN Tetra Cell electrophoresis system (Biorad). Gels of either 8% (proteins > 80 kDa) or 10-12% (20kDa < proteins < 80kDa) were also used. The separating gel was then overlaid with 1 ml of isopropanol and left for 30 minutes at room temperature until the gel was polymerized.

The isopropanol was then removed and the upper part of the gel washed several times with ddH_2O and dried with paper before layering the top with the stacking gel (9.3% (v/v) of acrylamide 40% solution (acrylamide:BIS-acrylamide, 29:1, Fisher), 0.1% (w/v) SDS, 0.1% (v/v) TEMED, 125 mM Tris-HCl (pH 6.8), 0.05% (w/v) ammonium persulphate in ddH_2O). Combs containing 15 spacers (0.75mm/well) were then inserted into the glass plates through the stacking gel and the solution was left at room temperature to allow it to polymerize. 10 μl of each protein sample was loaded per well. 5 μl of protein ladder (Prestained Protein Marker, broad range (7-175 kDa), New England Biolabs) solution was loaded in the first well of each gel. Gels were then placed into Biorad chambers into a tank filled with running buffer (0.1% (w/v) SDS, 25 mM Tris-Base, 200 mM glycine, pH 8.8). Gels were run at 80 volts for 15 minutes until the samples started to migrate through the separating gel, and then switched to 100 volts until the end of the run for approximately 1.5 hours.

Separated proteins were then transferred onto 0.45 μm nitrocellulose membrane (Hybond ECL nitrocellulose membrane, GE-Amersham Biosciences) in transfer buffer (20% ethanol (v/v), 25 mM Tris-Base, 200 mM glycine) at 18 volts overnight or at 100 volts for 1 hour. The nitrocellulose membrane was incubated with blocking buffer (5% milk (w/v) (dried skimmed milk, Marvel) in 0.1% (v/v) PBS-Tween 20) on a shaker for 1-2 hours at room temperature or overnight at 4°C to saturate non-specific binding sites. Membranes were incubated with the appropriate primary antibody (Table 3.5) diluted in blocking solution, for approximately 1-2 hours at room temperature, or overnight at 4°C. Membranes were then washed four times with washing buffer (0.1% (v/v) Tween 20 in 1X PBS) on the shaker for 5-10 minutes each time. Membranes were then incubated with the secondary antibody (Table 3.6) diluted into the milk solution, for 1 hour at room temperature. Depending on the nature of the detection method, membranes were incubated either with horseradish peroxidase (HRP) conjugated secondary antibodies for detection by enhanced chemiluminescence (ECL) method or with IRDye 800-700 conjugated secondary antibodies for detection with LI-COR Odyssey Infrared Imaging System. The membranes were then washed four times on the shaker for 5-10 minutes each time. For ECL development, activity of HRP-conjugated antibodies was detected by incubation of the membrane with SuperSignal West Pico Chemiluminescent solutions in a 1:1 ratio (2ml/membrane, Thermo Scientific) for 5 minutes and the resulting chemiluminescence signal visualized using an ImageQuant LAS 4000 mini system consisting of a Luminescent Image Analyser and a F0.85 43 mm LAS high sensitivity lens (GE Healthcare). For LI-COR detection, membranes were rinsed in 1X PBS and scanned at high resolution (169-84 μm) using the LI-COR Odyssey infrared imaging systems (LI-COR Biosciences).

Antibody	Source	Species	Antigen	Dilution	Application
α TGN46	AbD Serotec	Sheep	Human TGN46	1:100	IF (TGN marker)
α Vpu	NIH ARRP*	Rabbit	NL4.3 Vpu (amino acids 33-81- C terminus)	1:5000 1:1000	WB IF
α p24	Beckman Coulter	Mouse	HIV-1 proteins 55,39,33 &24kDa of core antigen	1:50-1:100	FC (Gag intracellular staining)
α p24 187	NIH ARRP*	Mouse Monoclonal	HIV-1 p24-CA (Hybridoma supernatant)	1:50	WB
α HA HA.11	Covance Clone 16B12 Flu tag	Mouse	Influenza hemagglutinin epitope CYP**YDVPDYA**SL	1:5000 1:150 1:1000	WB IP IF
α HA	Rockland	Rabbit	HA epitope tag	1:1000	WB / IF
α BST-2	NIH ARRP*	Rabbit	Human BST-2	1:1000	WB
α BST-2 M02	Abnova clone 3H4	Mouse Monoclonal	Human BST-2	1:200	FC
α Hsp90	Santa Cruz	Rabbit	Human Hsp90	1:5000	WB
α PDI	Invitrogen	Mouse	Protein disulfide isomerase (PDI)	1:1000	IF (ER marker)
α CD63	Biolegend	Mouse	CD63 (Hybridoma supernatant)	1:10	IF (Late endosome marker)
α CD4-APC	BD Biosciences	Mouse	Human CD4 receptor	1:100	FC
α SNAT-1	Santa Cruz	Rabbit	Amino acids 1-60 at the N-terminus of SNAT-1	1:1000	WB

* NIH AIDS Research & Reference Reagent Program
WB= Western Blot
IF= Immunofluorescence
FC= Flow Cytometry
IP= Immunoprecipitation

Table 3.5: List of primary antibodies used in this study.

Antibody	Source	Conjugation	Dilution	Application
Goat α-Mouse	Cell Signalling	HRP	1:5000	WB - ECL
Goat α-Rabbit	Cell Signalling	HRP	1:5000	WB - ECL
Goat α-Mouse	LI-COR Biosciences	IRDye 680	1:5000	WB - LICOR
Goat α-Rabbit	LI-COR Biosciences	IRDye 800	1:5000	WB - LICOR
Donkey α-Mouse	Molecular Probes - (Invitrogen)	Alexa Fluor 488	1:500	IF
		Alexa Fluor 647	1:500	FC
		Alexa Fluor 594	1:500	IF
Goat α-Mouse	Molecular Probes - (Invitrogen)	Alexa Fluor 488	1:500	IF
		Alexa Fluor 633	1:1000	FC
Donkey α-Rabbit	Molecular Probes - (Invitrogen)	Alexa Fluor 680	1:500	IF
		Alexa Fluor 488	1:500	IF
		Alexa Fluor 594	1:500	IF
Goat α-Rabbit	Molecular Probes - (Invitrogen)	Alexa Fluor 594	1:500	IF
Donkey α-Sheep	Molecular Probes - (Invitrogen)	Alexa Fluor 594	1:500	IF

* NIH AIDS Research & Reference Reagent Program
WB= Western Blot
IF= Immunofluorescence
FC= Flow Cytometry
IP= Immunoprecipitation

Table 3.6: List of secondary antibodies used in this study.

3.4.4 Imaging: immunofluorescence and confocal microscopy

Cells were plated on glass coverslips placed at the bottom of a well of a 24-well plate. To facilitate adhesion of 293T cells, the coverslips were pre-treated with poly-L-lysine (Sigma) for 10 minutes and washed with DMEM. 24 hours later, the cells were transfected with 100 ng of Vpu-HA expression vector, Vpu TM domain mutants or SNAT-1/HA. Alternatively, 293T-SNAT-1/HA and HT1080/THN-HA (+/- Vpu or K5) cells were plated on glass coverslips and infected 24 hours later with HIV-1 Wt or HIV-1 delVpu or Vpu mutants at an MOI of 0.2-1. At 24 hours post-transfection or 48 hours post-infection, the cells were fixed in 4% paraformaldehyde (formaldehyde 4% (v/v) in 1X PBS) for 15 minutes, washed in 1X PBS-10 mM glycine and permeabilized in 0.1% (v/v) Triton X-100 (in staining buffer: 1X PBS supplemented with 1% BSA (w/v)) for 15 minutes at room temperature. Cells were then washed with the staining buffer and incubated for 1 hour at room temperature with the primary antibody (Table 3.5) and agitated slowly on the shaker. Alternatively, cells were blocked for 0.5-1 hour in staining buffer before incubation with the primary antibody (for endoplasmic reticulum staining with PDI). The cells were washed 3 times in 1X PBS-1% BSA (w/v) and incubated at room temperature with the secondary antibody coupled to fluorophores in 1X PBS for 1 hour in the dark (Table 3.6). The cells were then washed 3 times with 1X PBS. The coverslips were then mounted on slides using ProLong Antifade (Molecular Probes, Invitrogen) containing DAPI (4',6- diamidino-2-phenylindole) for visualization of the nucleus, dried at 50°C for 20-30 minutes or overnight in the dark and examined on a Leica DM-IRE2 confocal microscope (63.0x oil immersion lens). Cells on coverslips can be stored at 4°C protected from the light.

3.4.5 Cell surface protein expression: Flow cytometry (FACS)

HeLa cells in 6-well dishes were transfected with 400 ng pCR3.1-enhanced green fluorescent protein (eGFP) and 400 ng pCR3.1-Vpu-HA or TM mutant. Alternatively, HT1080/THN-HA (+/- Vpu or K5) cells were treated with Bafilomycin A1 (100 nM), concanamycin A (100 nM) or MG132 (1 μg/ml) for 10-14 hours. 293T SNAT-1/HA cells seeded into a 24-well plate at a density of 10^5 cells per well were transduced with VLPs packaged with pCMS28 Vpu*-GFP vector whereas Jurkat cells were infected with vesicular stomatitis virus G (VSV-G)-pseudotyped HIV-1 Wt and HIV-1 delVpu (and derived Vpu TM domain mutants) at a multiplicity of infection of 1. At 48 hours post-transfection/transduction/infection, the cells were harvested and stained either for surface endogenous tetherin or surface SNAT-1/HA. Once the medium was removed from the plate, the cells were detached and resuspended into 1X PBS 5-10 mM EDTA. The cells were then transferred into a tube and pelleted by centrifugation at 3500 rpm for 1 minute at 4°C. During FACS staining, the cells were constantly kept at 4°C. The supernatant was then aspirated and the cells were incubated with the appropriate primary antibody (Table 3.5) diluted in FACS buffer (1X PBS- 1% BSA (w/v), 0.1% sodium azide (w/v)) for 1 hour on ice. Cells were then washed 3 times in 1X PBS-1% BSA before addition of the secondary antibody

(Table 3.6) and incubated for 1 hour at 4°C. Cells were then washed 3 times in FACS buffer and the last wash was performed with cold 1X PBS. At this step, the cells can be fixed with 2% paraformaldehyde (v/v) and stored at 4°C in the dark. Tetherin and SNAT-1/HA expressions on GFP^+ cells were then analyzed using a FACSCalibur flow cytometer (Becton Dickinson) and FlowJo software.

Chapter 4

Restriction of Kaposi's Sarcoma-associated Herpes Virus particle release by tetherin is antagonized by the RING-CH ubiquitin ligase K5

The study presented in this chapter was published in collaboration with Claire Pardieu from Greg J. Towers's group as " The RING-CH Ligase K5 Antagonizes Restriction of KSHV and HIV-1 Particle Release by Mediating Ubiquitin-Dependent Endosomal Degradation of Tetherin " (210).

4.1 Introduction

4.1.1 K5, a viral immune modulator

The human herpesvirus 8 (HHV-8) also known as Kaposi's sarcoma-associated herpesvirus (KSHV) belongs to the Rhadinovirus genera (or γ-2) of the γ-herpesvirus subfamily and is one of the seven currently known human cancer viruses (oncovirus) (reviewed in (405)/chapter 72). As its name implies, KSHV is associated with the development of a type of cancer, Kaposi's sarcoma, commonly occurring in AIDS patients. KSHV also causes B-cell neoplasms, multicentric castleman's disease and primary effusion lymphoma. KSHV is composed of a large double-stranded genomic DNA protected by two layers of viral proteins, a capsid and a matrix (or tegument), which are enclosed in a lipid envelope derived from the host cell membrane. KSHV entry occurs through macropinocytosis, a form of endocytosis for absorption of extracellular particles. Inside the infected cell, the viral life cycle proceeds through two distinct phases, either a latent or a lytic phase. During the latent phase, the expression of viral genes required for virus production and assembly is inhibited by the viral-latency-associated nuclear antigen (LANA) and only the viral DNA is replicated by the host cell machinery, whereas in the lytic phase these genes are activated to allow production of virus particles. Ultimately, thousands of virus particles can be made from a single cell, resulting in lysis of the infected cell. The primary viral protein responsible for the switch between latent and lytic replication is the ORF50 replication transactivation activator (RTA).

Inspired by studies which showed a downregulation of MHC class I molecules by mK3 from the murine Ƴ-herpesvirus 68 (MHV68) infection of murine fibroblasts, the KSHV genome was screened for gene products inhibiting MHC class I expression (406). Interestingly, two genes, K3 and K5 (also known as MIR1 and MIR2, respectively) were identified as immunomodulators able to reduce MHC class I expression in human cells. Immunomodulators of pathogens frequently target multiple cellular proteins, thus preventing recognition by different immune cells. One pathway targeted by KSHV via K3 and K5 is the antigen presentation by major histocompatibility complex class I molecules (reviewed in (241)). By interfering with MHC class I

expression, KSHV becomes less detectable by cytotoxic T cells. Additional cell surface targets of K5 were then identified, particularly those involved in T cell and NK cell recognition of virally infected cells. In addition to MHC class I molecules, K5 targets the HFE protein (human hemochromatosis protein related to MHC class I molecules) (407) and also adhesion molecules (ICAM-1, PECAM, ALCAM and VE-cadherin) (408), co-stimulatory molecules (B7.2) (409), ligands for NKT cells (CDd1) (410), ligands for NK cells (MICA, MICB, AICL) (411), cytokine receptors (IFN- γR1) (412), cellular restriction factors (tetherin or BST-2) (191), the plasma membrane t-SNARE syntaxin-4 (191) and a member of the TGF-beta family (BMPRII) (413). Tetherin, ALCAM (CD166) and syntaxin-4 were identified by a novel quantitative membrane proteomics approach termed SILAC (Stable Isotope Labelling with Amino acids in Cell culture) (191). In this screen, BST-2 (tetherin) was scored as the most highly under-represented protein in K5-expressing HeLa cells.

K5 belongs to a family of viral- and cellular-membrane-spanning RING E3 ubiquitin ligases found in mammals. K5 consists of a cytoplasmic amino-terminal RING-CH domain followed by two membrane-traversing domains, resulting in a type III transmembrane topology (Figure 4.1) (414). The RING domain binds an ubiquitin-conjugating enzyme (E2) and catalyses the transfer of the ubiquitin on its substrates. While E2 provides the ubiquitin, E3 confers the specificity for the target. K5, probably, derives from host genes since mammals encode similar proteins, termed membrane-associated RING-CH (MARCH) proteins whose role, mainly described through studies on viral proteins, is to modulate the intracellular trafficking and turnover of transmembrane protein targets (241). K5 is most closely related to MARCH-VIII. MARCH ligases mediate the ubiquitination of lysine or cysteine residues in the cytoplasmic tail of target transmembrane proteins. For most substrates, ubiquitination occurs in a post-endoplasmic reticulum compartment and ubiquitinated proteins are endocytosed, sorted to multivesicular bodies (MVB) in a clathrin-dependent process and degraded in lysosomes (415, 416). ER-associated proteasomal degradation (ERAD) has also been observed for some substrates of K5 (CD31/PECAM) (417). Although K5 is less effective at downregulating MHC class I, it does have a broader substrate specificity than K3 that seems to be conferred by the transmembrane regions since substitution of these domains of K3 by K5 was able to transfer substrate specificity of the proteins. However, the rules for target selection have yet to be established.

Therefore, the E3 ubiquitin ligase K5, enables KSHV viral survival and replication by inhibiting the immune response through the downregulation of a panel of cellular proteins. In the next section we will specifically study the role of K5 in targeting tetherin.

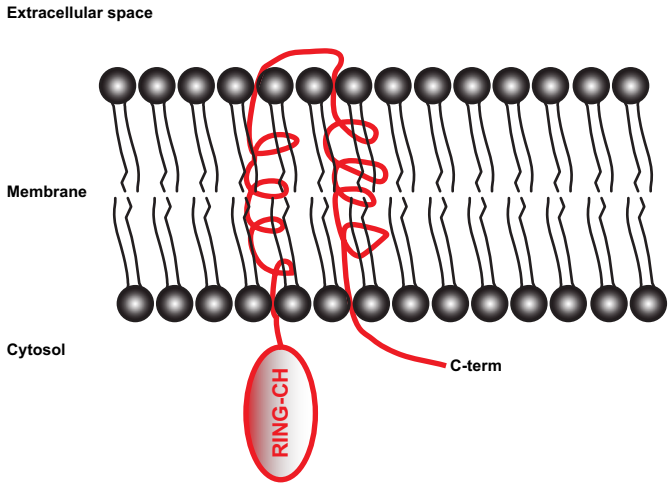

Figure 4.1: Structural features of K5 protein.

K5 is a membrane-anchored protein with two transmembrane domains. The RING-CH domain displayed at the N-terminus and the C-terminal region are cytoplasmic. The two transmembrane segments are linked via a short extracellular loop.

4.1.2 KSHV particle release is sensitive to tetherin-mediated restriction in a K5 dependent-manner

Previous studies have shown the broad spectrum of enveloped viruses restricted by tetherin (204, 208-211, 213). K5 targeting tetherin, therefore, led us to speculate the existence of an antiviral activity of tetherin against KSHV. To demonstrate a potential inhibition of KSHV particle release by tetherin, our collaborators Pardieu et al. measured KSHV production in the presence of increasing amounts of exogenous human tetherin (cf. published papers). Interestingly, a linear decrease in release of KSHV infectious virus was observed when increasing amounts of the tetherin-expressing plasmids were transfected. Further experiments showed that RNAi-depletion of K5 during lytic replication suppressed KSHV particle release in cells expressing constitutively tetherin. Therefore, K5 plays an important role in overcoming tetherin-mediated restriction of herpesvirus release.

4.2 Results: K5 is a potent tetherin antagonist

Having established the role of K5 for efficient KSHV particle release in tetherin-expressing conditions, we investigated the cellular and molecular biology of the mechanism by which K5 overcomes tetherin-mediated restriction.

4.2.1 K5 rescues Vpu-defective HIV-1 particles release from tetherin-mediated restriction

For HIV-1 it has been well documented that Vpu counteracts tetherin activity to allow efficient viral particle release (186). We asked whether K5 expression could substitute for Vpu and promote the release of tetherin-restricted HIV-1 delVpu particles. Firstly, HeLa cells were transfected with a NL4.3 proviral construct or a Vpu-defective counterpart in combination with HA-tagged K5 or Vpu expression vectors (Figure 4.2A-B-C). The presence of Vpu serves as a control in this experiment to monitor efficient tetherin counteraction. K5 expression *in trans* rescued HIV-1 delVpu release to levels achieved by Vpu, as evidenced either by titration of HIV-1 virions released into the supernatant onto the HIV-1 indicator cell line HeLa TZM-bl or measurement of HIV-1 p24 capsid protein in the supernatant by Western blot. Importantly, K5 expression had no effect on the processing of the gag precursor, Pr55, to the mature p24 capsid.

K5 acts as an E3 ubiquitin ligase to target several immune receptors (241). This function requires a functional RING-CH domain that recruits an E2-conjugating enzyme and catalyses the transfer of an ubiquitin moiety to its target protein (Figure 4.1). To test the importance of this ubiquitin ligase activity for K5 mediating tetherin counteraction, a RING deletion mutant of K5 (K5delRING) was generated, and tested for its ability to counteract tetherin-mediated HIV-1 delVpu restriction. Despite similar expression levels as K5 wild-type, K5delRING mutant failed to rescue the HIV-1 delVpu particle release from HeLa cells (Figure 4.2A-B-C).

Similar experiments were conducted in a tetherin-deficient cell line (HT1080) stably expressing an HA-tagged version of human tetherin (HT1080/THN-HA), and subsequently transduced with pCNCR retroviral vectors co-expressing DsRed and Vpu, or K5 or K5delRING (Figure 4.2D-E). 48 hours later, when more than 90% of the cells were DsRed positive, cells were infected with VSV-G pseudotyped HIV-1 Wt or HIV-1 delVpu at a multiplicity of infection of 0.2 (cf. Chapter 3). As expected, in HT1080/THN-HA, 20 fold less viral particles were released by HIV-1 delVpu compared to HIV-1 Wt. Furthermore, expression of K5 and Vpu but not K5delRING could rescue HIV-1 delVpu particles release from HT1080/THN-HA cells. Measurement of Gag levels in supernatants and extracts of infected cells by Western blot indicated that the effects of tetherin, Vpu and K5 were on HIV-1 release and not Gag protein expression.

Taken together, these data demonstrate the functional homology that KSHV-encoded K5 shares with HIV-1 Vpu in counteracting tetherin.

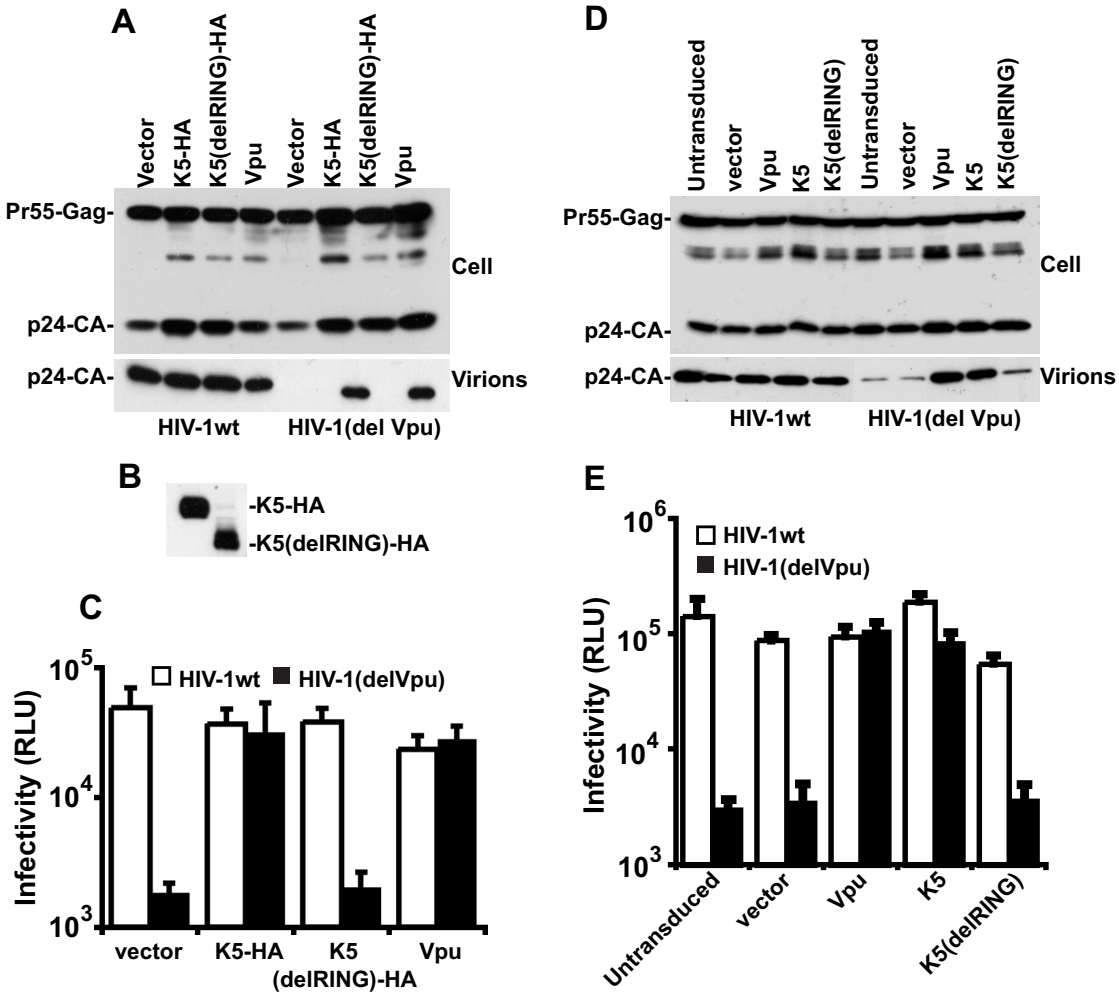

Figure 4.2: K5 rescues Vpu-defective HIV-1 particle release from tetherin-mediated restriction.

A and B: HeLa cells were co-transfected with HIV-1 Wt or HIV-1 delVpu proviral plasmids in combination with empty vector, or expression vector encoding Vpu, HA-tagged K5 or K5 lacking the N-terminal RING domain. 48 hours post-transfection, cell lysates and pelleted supernatants were analysed for HIV-1 Gag proteins by Western blot using an anti-p24CA monoclonal antibody (A) or an anti-HA monoclonal (B). **C:** Viral supernatants were also used to infect HeLa-TZM indicator cells and infectious viral release determined by relative β-galactosidase activity 48 hours later. Results are the mean of 3 independent experiments and errors are standard error of the mean. **D and E:** HT1080 cells stably expressing human tetherin (HT1080/THN-HA) were transduced with CNCR retroviral vectors encoding both dsRED and either Vpu, K5 or K5(del RING) at doses sufficient to give > 90% transduction as determined by flow cytometry. Cells were then infected with HIV-1 Wt or HIV-1 delVpu pseudotyped with VSV-G at an MOI of 0.2. Cell lysates and supernatants were processed as in (A) 48 hours later. Results are the mean of 3 independent experiments and errors are standard error of the mean.

K5 could not antagonize tetherin function in transiently-transfected 293T cells, even when tetherin expression was titrated to vary its expression level (Figure 4.3). Interestingly, 293T cells are also unable to support HIV-2 Env's anti-tetherin activity (230), suggesting that this particular cell line might be poorly suited for characterization of some tetherin antagonists. We propose

that 293T cells may lack a co-factor essential for K5's antagonism of tetherin, but not for Vpu function.

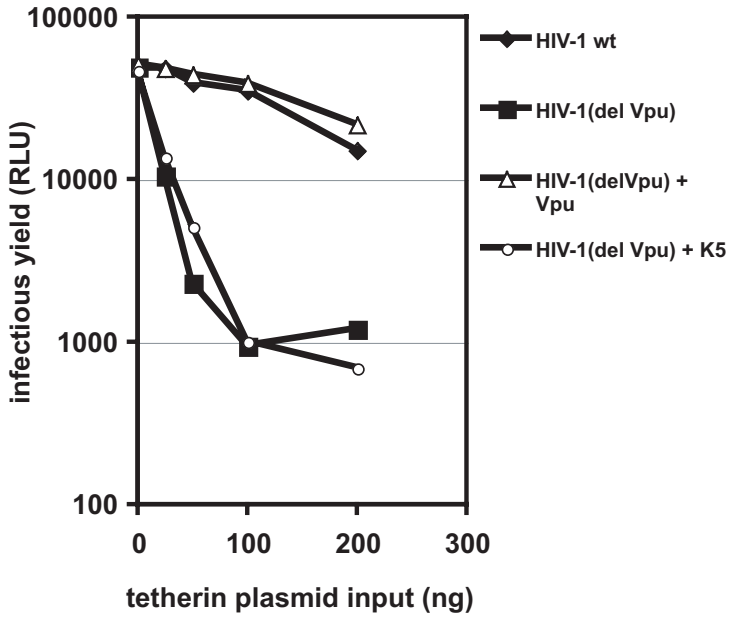

Figure 4.3: Lack of K5 activity against tetherin in 293T cells.

293T cells were co-transfected with HIV-1 Wt or HIV-1 delVpu proviral plasmids in combination with empty vector, or expression vector encoding Vpu, or K5 and increasing doses of tetherin plasmid. 48 hours post-transfection, infectivity of viral supernatants was titrated on HeLa-TZMbl cells as above. This result is a representative example of three independent experiments.

4.2.2 K5 depletes cell-surface human tetherin but not Rhesus macaque tetherin

Many studies have documented the ability of HIV-1 Vpu to reduce tetherin levels from the cell surface (187, 220, 376, 377). We therefore tested whether K5 could act in a similar way to counteract tetherin. HT1080/THN-HA cells were transduced with a retroviral vector encoding dsRED and either wild-type K5 or the RING-deleted K5 mutant (K5delRING). 48 hours post-transduction, cells were harvested, stained for tetherin-HA and surface expression levels in dsRED positive population were quantified by flow cytometry (Figure 4.4). As expected, K5 but not K5delRING expression resulted in the loss of tetherin levels at the cell-surface (Figure 4.4A). This result demonstrates that K5, like Vpu, mediates tetherin downregulation from the cell-surface and that this function requires a functional RING-CH domain. We then examined whether K5 could target another non-human primate orthologue of tetherin. Previous studies have shown that Vpu acts only against human, chimpanzee and Gorilla tetherins. Sensitivity of human tetherin can be abolished by mutation of a single amino acid in the transmembrane cap of human tetherin present in Old World monkeys (T45I) coupled with an in frame deletion of a GI pair at the N-terminus of the human tetherin TM domain (delGI) (224). In this assay we

tested whether K5 displayed such species-specificity in its mode of action. HT1080 cells stably expressing either the HIV-1 Vpu-resistant human tetherin (delGI,T45I) or Rhesus macaque tetherin, were transduced with a retroviral vector encoding K5 and assayed for expression of cell-surface tetherin levels. Interestingly, whilst K5 downregulates tetherin delGI-T45I, no appreciable reduction of cell-surface Rhesus macaque tetherin was detected after K5 expression (Figure 4.4B). Together these data suggest that K5 also displays species-specificity in its antagonism of primate tetherins similarly to HIV-1 Vpu but the determinants of this specificity are distinct. Further studies will be required to determine the residues in tetherin that govern its sensitivity for K5.

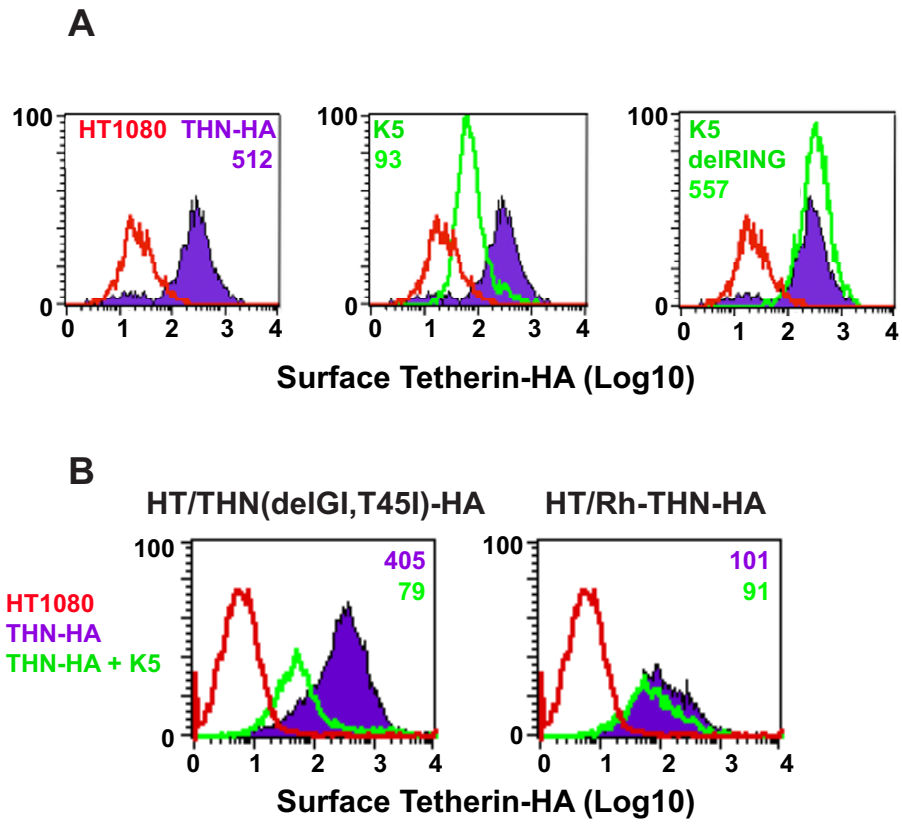

Figure 4.4: K5 mediates cell-surface downregulation of tetherin.

A: HT1080/THN-HA cells were transduced with retroviral vectors (pCNCR) encoding dsRED and either K5 or K5(del RING). 48 hours post-transduction, the cells were immunostained for surface tetherin using an anti-HA monoclonal antibody and an Alexa-488-conjugated goat-anti-mouse secondary antibody. Surface expression of tetherin was then analyzed in the dsRED positive population by flow cytometry. Parental HT1080 cells were used as a control for background antibody binding and are represented by the red line. Tetherin levels in HT1080 cells expressing tetherin alone are indicated by the purple line and levels of tetherin after K5 expression is represented by the green line. The median fluorescence intensities in the top corner of each histogram are representative examples of three independent experiments. **B:** The same analyses were performed on HT1080 cells stably expressing the HA-tagged Vpu-resistant human tetherin (delGI,T45I) and rhesus tetherin. Labelling is similar to panel A.

4.2.3 K5 induces endolysosomal degradation of tetherin

As Vpu mediates tetherin degradation, we then examined the fate of tetherin after K5 expression. HT1080/THN-HA cells were transduced to stably express K5 (HT1080/THN-HA K5) or Vpu (HT1080/THN-HA Vpu) and intracellular levels of tetherin were compared to levels in unmanipulated cells. Tetherin appears in Western blots as a heterogeneous smear of glycosylated species that varies between cell types (197, 376). After K5 and Vpu expression, tetherin levels in the modified cell lysates were decreased (to 4% of wild-type in the case of K5 and to 31% of wild-type for Vpu), suggesting that, like Vpu, K5 induces tetherin degradation (Figure 4.5). We then addressed the nature of the process by which K5 achieves tetherin depletion. For this purpose we examined the role of lysosomal degradation using the vacuolar ATPase inhibitor bafilomycin A1 (Baf A1) or by inhibiting proteasomal degradation using MG132. We then measured steady state levels of tetherin in K5 expressing cells in parallel with Vpu expressing cells to compare the two mechanisms. HT1080/THN-HA, HT1080/THN-HA K5 and HT1080/THN-HA Vpu were treated with Baf A1 or MG132 for 16 hours. Both Baf A1 and MG132 rescued tetherin levels in cells lysates from Vpu and K5 expression. Baf A1 treatment rescued not only mature tetherin species, but also lower molecular weight fragments presumably corresponding to partially degraded products of tetherin. This result suggests that K5 degrades tetherin via an endolysosomal process, similar to that by which it degrades Class I MHC. Furthermore, the rescue of tetherin degradation products in HT1080/THN-HA cells that do not express K5 or Vpu suggest that tetherin natural turnover involves the endosomal pathway. Treatment with bafilomycin A1 was more potent at rescuing tetherin levels than MG132. The fraction recovered after MG132 treatment in K5-expressing cells is likely due to depletion of free cytoplasmic ubiquitin interfering with the endolysosomal pathway rather than inhibition of the proteosome. In K5-expressing cells, MG132 treatment only rescues mature forms of tetherin suggesting that K5 mediating tetherin ubiquitination is upstream of lysosomal degradation. In contrast, in Vpu-expressing cells, MG132 appears much more efficient to restore tetherin levels than Baf A1 and again differential tetherin species were rescued by each inhibitor.

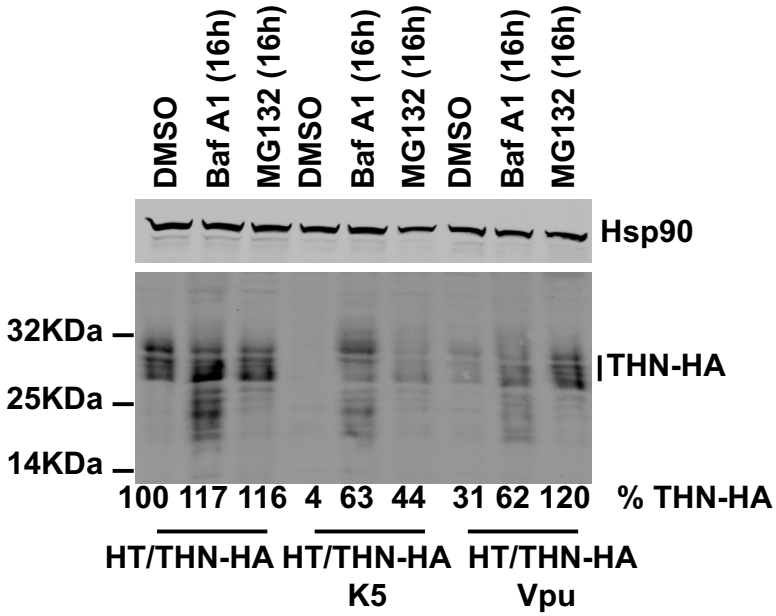

Figure 4.5: Effects of endosomal and proteasomal inhibitors on K5 inducing tetherin degradation.

Western blots of cell lysates from HT1080/THN-HA cells stably expressing K5 or Vpu from retroviral vectors. Cells were treated for 16 hours with Baf A1 (100 nM), MG132 (1mg/ml) or DMSO as a control, lysed and separated by SDS-PAGE. THN-HA expression was detected by Western blotting using an anti-HA antibody. Percentage of mature tetherin levels, normalized to Hsp90 loading are displayed below each lane.

Since K5 induces tetherin downregulation from the cell-surface, we next examined the effects of K5 expression on tetherin subcellular localization. HT1080/THN-HA +/- K5 cells were immunostained via the HA tag and observed by confocal microscopy (Figure 4.6A). Tetherin localizes predominantly to the plasma membrane with a minor fraction of the intracellular localization coincident with the late endosome marker CD63. This observation is consistent with the notion of natural tetherin turnover in endolysosomal compartments. As expected, K5 expression results in a loss of tetherin detectable at the cell-surface with the majority of residual tetherin relocalized into $CD63^+$ intracellular compartments, implicating K5-induced endosomal degradation. This observation correlates with the sensitivity of tetherin degradation to Baf A1. In contrast, in Vpu expressing cells, tetherin was never observed in $CD63^+$ endosomes, but instead localized predominantly to compartments that stain positive for the *trans*-golgi network marker TGN46 (Figure 4.6B). Of note, similar tetherin relocalization was observed after expression of the HIV-2 and SIVtan envelope glycoproteins, two other tetherin antagonists (230, 231). While Vpu and K5 both induce tetherin to be relocalized in intracellular compartments, the *trans*-Golgi network or late endosomes, the mechanisms by which they achieve tetherin degradation imply distinct pathways. Thus, the subcellular localization of tetherin after K5 expression suggests that K5 causes it to be delivered to late endosomes for degradation.

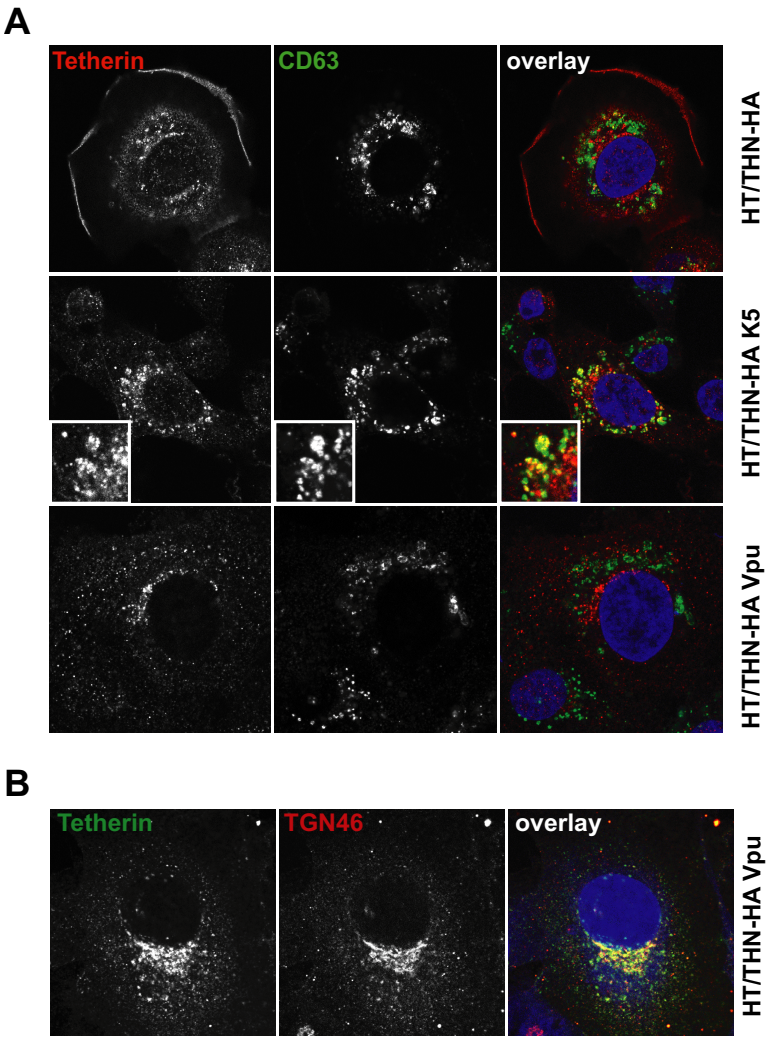

Figure 4.6: Subcellular localization of tetherin in K5 and Vpu-expressing cells.

A: Representative examples of HT1080/THN-HA, HT1080/THN-HA K5 and HT1080/THN-HA Vpu cells immunostained for tetherin with a rabbit anti-HA antibody (red) and an antibody for the late endosomal marker CD63 (green). Nuclei were counterstained with DAPI (blue) and cells examined by confocal microscopy. **B:** HT1080/THN-HA Vpu cells stained for THN-HA (green) and the *trans*-Golgi marker TGN46 (red) were processed as above.

4.2.4 K5-mediated tetherin degradation and cell-surface depletion requires lysine 18

The fact that both K3 and K5 target lysine residues in MHC class I molecules cytoplasmic tail (241) led us to examine the importance of the two lysine residues, in positions 18 and 21 in the cytoplasmic domain of tetherin for K5 mediated antagonism. Lysine 18 and 21 were mutated alone or in combination to arginine residues and cloned into a retroviral vector (pLHCX). HT1080 stably expressing these tetherin mutants (HT1080/THN-HA K18R; HT1080/THN-HA K21R; HT1080/THN-HA K18,21R) were then transduced with a puromycin-selective retroviral

vector encoding K5 or Vpu. Resistant cells were selected in order to maintain a steady expression level of these viral proteins. HT1080/THN-HA Wt, K18R, K21R or K18,21R cells expressing K5 or the corresponding empty vector where seeded at a density of $4x10^5$ and harvested one day later in SDS-PAGE loading buffer. Lysates were then blotted against the epitope HA for detection of intracellular levels of tetherin (Figure 4.7A). On the Western blot, tetherin appears as multiple bands, as described above. As expected, K5 expression reduced level of THN-HA Wt by 92%. Similar depletion of THN-HA K21R was detected in K5-expressing cells (90%) but levels of THN-HA K18R and THN-HA K18,21R were less affected by K5 expression with only 41% and 32% of tetherin depletion achieved respectively. In this system, the tetherin lysine mutants are expressed at higher levels than the wild-type protein suggesting a potential involvement of these residues for the natural tetherin turnover. Whereas in the similar system Vpu could cause 74% of tetherin Wt degradation, only 44% and 12% of tetherin K18R and K21R degradation respectively, were achieved by Vpu (Figure 4.7B). When both lysine mutations were combined, Vpu did not display any activity to induce tetherin depletion.

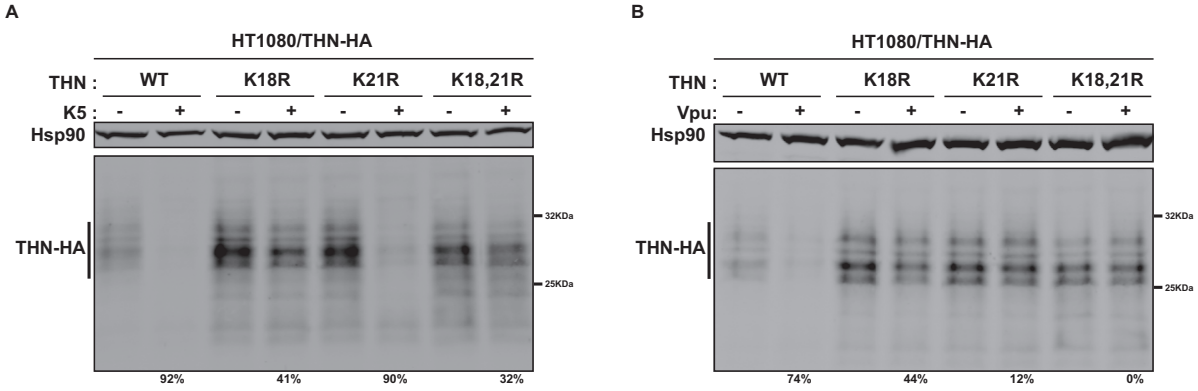

Figure 4.7: Lysine tetherin mutants are differentially affected by K5 and Vpu.

A: Western blots of cell lysates from HT1080/THN-HA cells and isogenic pools stably expressing K5 from retroviral vectors. Cells were seeded at a density of $4x10^5$, lysed 24 hours later in reducing loading buffer, separated by SDS-PAGE and subjected to Western blotting. THN-HA was detected by anti-HA antibody, with Hsp90 serving as a loading control and visualized using Licor fluorescently coupled 680 and 800 nm secondary antibodies. Percentage of tetherin degradation in K5 expressing cells was calculated by comparison to tetherin levels detected in K5 negative cells and normalized to Hsp90 loading and displayed below each lane. **B:** Same as in A but with HT1080/THN-HA stably expressing Vpu.

Consistent with the notion that K5 targets tetherin for its delivery to late endosomes, tetherin K21R but not tetherin mutants K18R and K18,21R resistant to K5-mediated degradation were redistributed to $CD63^+$ compartments upon K5 expression (Figure 4.8). Tetherin mutants bearing the K18 mutation were found to be predominantly localized at the plasma membrane upon K5 expression.

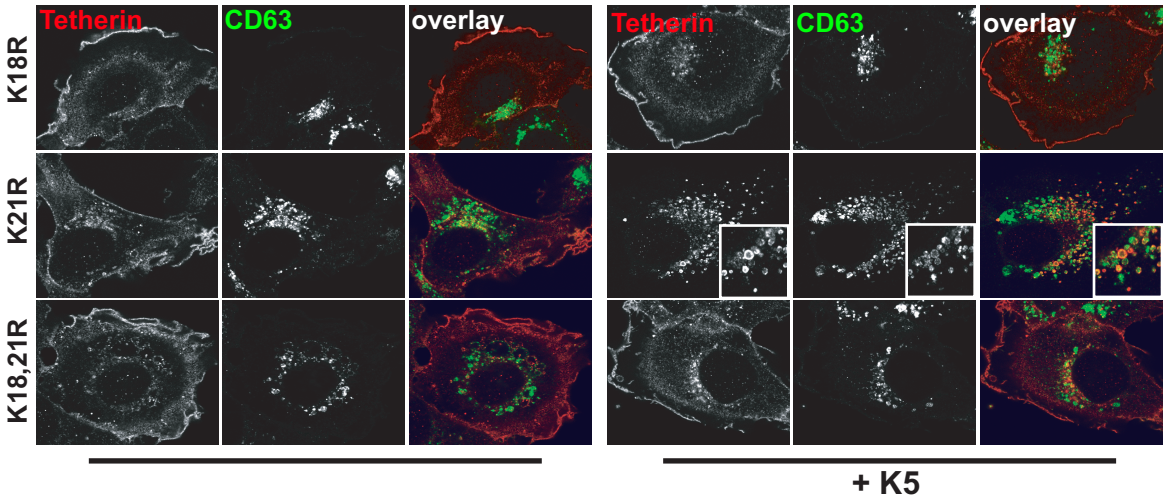

Figure 4.8: K18 in the tetherin cytoplasmic tail is required for K5-mediated delivery to late endosomes.

HT1080/THN-HA K18R, HT1080/THN-HA K21R and HT1080/THN-HA K18,21R expressing empty vector or K5 were co-stained for THN-HA (red) and CD63 (green). Cells were then observed by confocal microscopy. Images show representative examples of the subcellular localization of tetherin Wt or the indicated mutant observed in K5-expressing cells.

We then checked whether the inability of K5 to target the lysine 18 in the tetherin cytoplasmic tail to induce tetherin degradation was associated with a lack of THN-HA K18R cell-surface downregulation. HT1080/THN-HA Wt, K18R, K21R or K18,21R cells expressing K5 or the corresponding empty vector were stained for cell-surface tetherin via the HA tag and levels of tetherin measured by flow cytometry (Figure 4.9). All tetherin mutants were expressed at the cell surface, but the lysine mutants were expressed at higher levels than the wild-type protein as previously observed from expression in cell lysates. Unlike THN K21R, cell-surface levels of THN K18R and THN K18,21R were mostly unaffected by K5 expression.

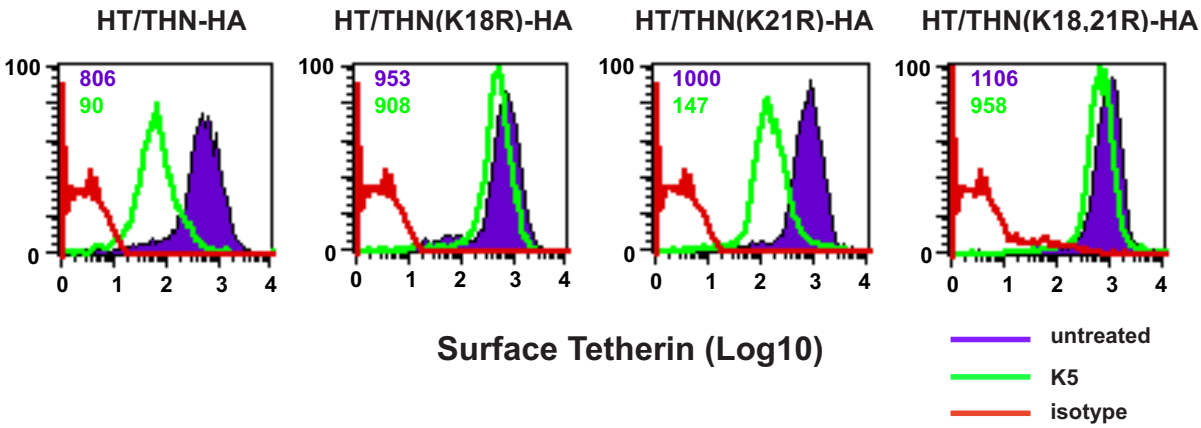

Figure 4.9: K18 in the tetherin cytoplasmic tail is required for K5-mediated cell surface downregulation.

Flow cytometry analyses of HT1080 cells expressing wild type tetherin or the indicated mutant. Purple histograms represent THN-HA levels on unmanipulated cells, with the green overlay showing tetherin levels in the equivalent cells stably expressing K5. Red histograms represent the antibody isotype control. The median fluorescence intensities in the top corner of each histogram are representative examples of three independent experiments.

4.2.5 Tetherin antagonism by K5 implies tetherin cell-surface downregulation and degradation

We then asked whether in the absence of cell-surface downregulation and degradation, K5 could still antagonize tetherin. HT1080/THN-HA Wt, K18R, K21R or K18,21R cells expressing K5, Vpu or the empty vector were infected with VSV-G pseudotyped HIV-1 wild-type or HIV-1 delVpu at a multiplicity of infection of 0.2. Two days later, cells were harvested and the infectivity of the supernatants determined on HeLa-TZM cells (Figure 4.10A). As expected, both K5 and Vpu expression rescue HIV-1 delVpu particle release from wild-type tetherin expressing cells. But in the context of K18R mutation alone or in combination with K21, K5 but not Vpu failed to rescue wild-type virus production. HT1080/THN-HA K21R also restricted HIV-1 delVpu virus production similarly to the wild-type protein and expression of K5 or Vpu *in trans* could restore virus release. These data suggest again that the determinants that confer sensitivity to Vpu or K5 are governed by different residues in the tetherin sequence. To further investigate the implication of the lysine residues in Vpu sensitivity for tetherin targeting, 293T cells were transiently transfected with HIV-1 Wt or HIV-1 delVpu proviruses in the presence of increasing doses of tetherin wild-type (THN-Wt), THN K18R, THN K21R or THN K18,21R. Two days post-transfection, viral supernatants were assayed for infectivity and cells lysates and pelleted virions analysed by Western blot for HIV-1 p24-CA and THN-HA expression (Figure 4.10B-C). As expected, in the presence of tetherin wild-type, HIV-1 delVpu particle release is strongly decreased. At high doses of tetherin wild-type, particle release of HIV-1 Wt tends toward levels

of HIV-1 delVpu virus production, presumably because of tetherin over-expression conditions saturating the ability of Vpu to overcome the cellular factor. Importantly, mutations on K18 and K21 residues, alone or combined, do not alter tetherin sensitivity to Vpu since the fold-ratio viral particle release between HIV-1 Wt and HIV-1 delVpu is similar to tetherin Wt for all tetherin mutants tested. These observations were confirmed by quantitative Western blot of pelleted virions released. Together these data suggest that K5 targets the lysine K18 but not K21 in the tetherin cytoplasmic tail to inactivate tetherin, but in the case of Vpu, those residues are dispensable to mediate tetherin antagonism. Similarly, Goffinet et al. also showed that steady-state levels of THN K18,21A were completely refractory to Vpu-induced depletion, despite efficient Vpu-mediated release enhancement (392). Thus, K5-mediated disruption of tetherin function requires the ability to target the lysine K18 in the tetherin cytoplasmic tail for subsequent cell-surface downregulation and degradation.

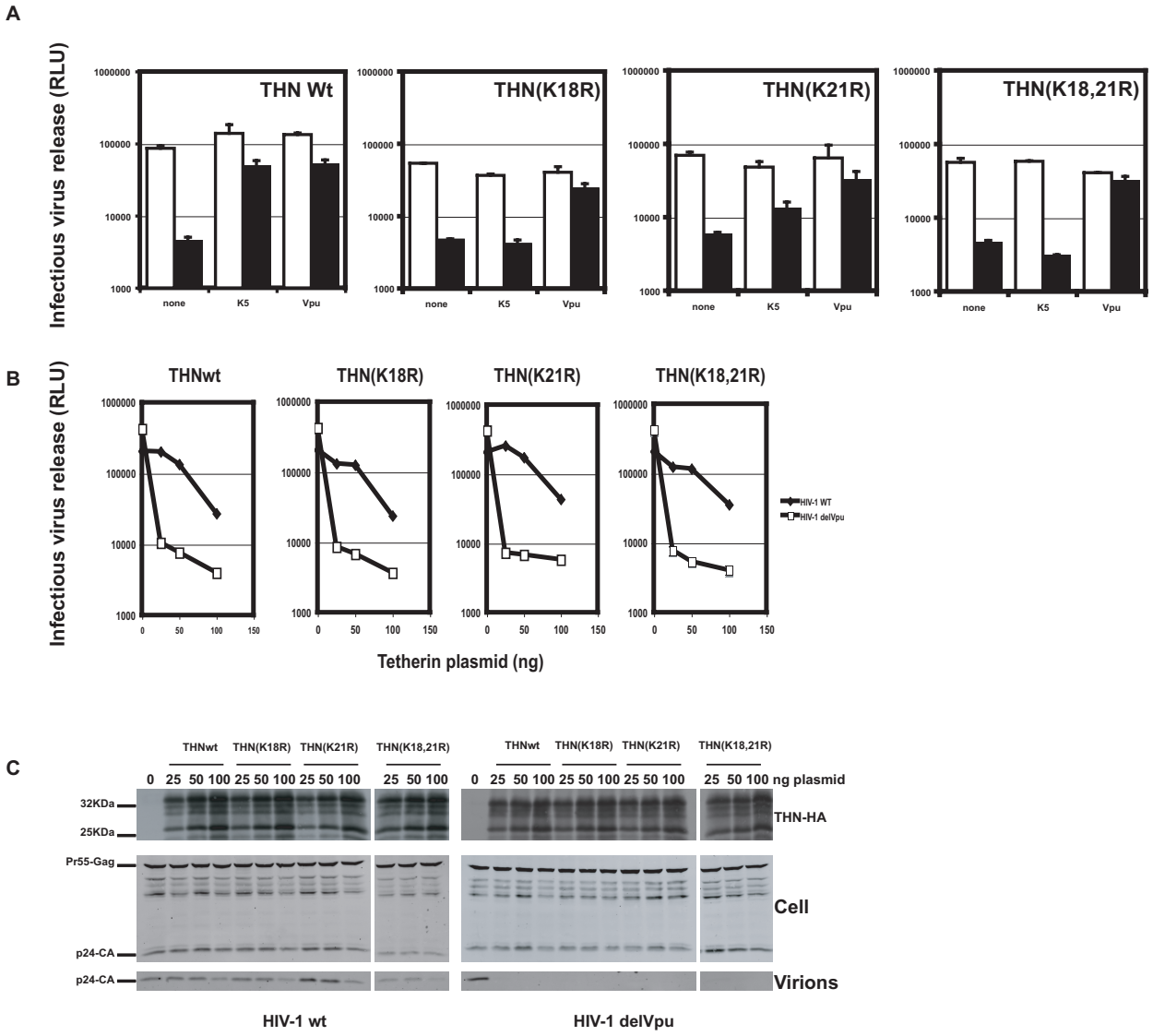

Figure 4.10: K18 is required for tetherin antagonism by K5 but both cytoplasmic tail lysines are dispensable for Vpu-mediated antagonism.

A: HT1080/THN-HA Wt, HT1080/THN-HA K18R, HT1080/THN-HA K21R, HT1080/THN-HA K18,21R or derivatives stably expressing K5 or Vpu were infected with wild type HIV-1 or HIV-1

delVpu VSV-G pseudotypes at an MOI of 0.2. 48 hours after infection, cell supernatants were harvested and the released infectivity determined on HeLa-TZM cells. Results are the mean of 3 independent experiments and errors are standard error of the mean. **B and C:** The effect of tetherin lysine mutants on HIV-1 release in 293T cells. Cells were transiently transfected with wild type HIV-1 or HIV-1 delVpu proviruses with increasing doses of the indicated THN-HA mutant. 48 hours after transfection, viral supernatants were assayed for infectivity on HeLa-TZM cells (B) and cell lysates and pelleted virions analyzed by Western blot for HIV-1 p24 CA and THN-HA expression (C).

As shown above, the determinants required for K5 and Vpu-mediated tetherin degradation are distinct, with K18 and K21 being preferentially targeted by K5 and Vpu respectively. While for K5 the residues involved for tetherin antagonism correlate with those required for degradation, for Vpu these two processes might not be as strictly linked. This observation can be exemplified by the ability of the Vpu S52,56A mutant to counteract tetherin's function while being ineffective at mediating tetherin degradation. Vpu S52,56A was initially described as inefficient at recruiting the β-TrCP, a substrate adaptor for an SCF (Skp Cullin- F-box) E3 ubiquitin ligase complex, to mediate CD4 degradation (cf. Chapter 1). Studies showed the requirement of β-TrCP1/2 for optimal downregulation and degradation of tetherin. Indeed, expression of dominant negative β-TrCP, or suppression of endogenous β-TrCP by RNA interference results in a significant decrease in tetherin degradation and downregulation. We tested the defect of Vpu S52,56A in mediating tetherin degradation by infecting HT1080/THN-HA and 293T/THN-HA with VSV-G pseudotyped HIV-1 Wt, HIV-1 delVpu or HIV-1 Vpu S52,56A at a MOI of 2. 48 hours later, cells were lysed and samples Western blotted with anti-HA for detection of THN-HA expression levels (Figure 4.11A). While both HT1080/THN-HA and 293T/THN-HA infected with HIV-1 Wt displayed a decrease of THN-HA expression in cell lysates, cells infected with HIV-1 Vpu S52,56A showed similar levels of tetherin expression as those infected with HIV-1 delVpu virus. Similarly, stable expression of Vpu S52,56A in HT1080/THN-HA did not impact upon intracellular level of THN-HA (Figure 4.11B). Together these data show that Vpu S52,56A fails to induce tetherin degradation.

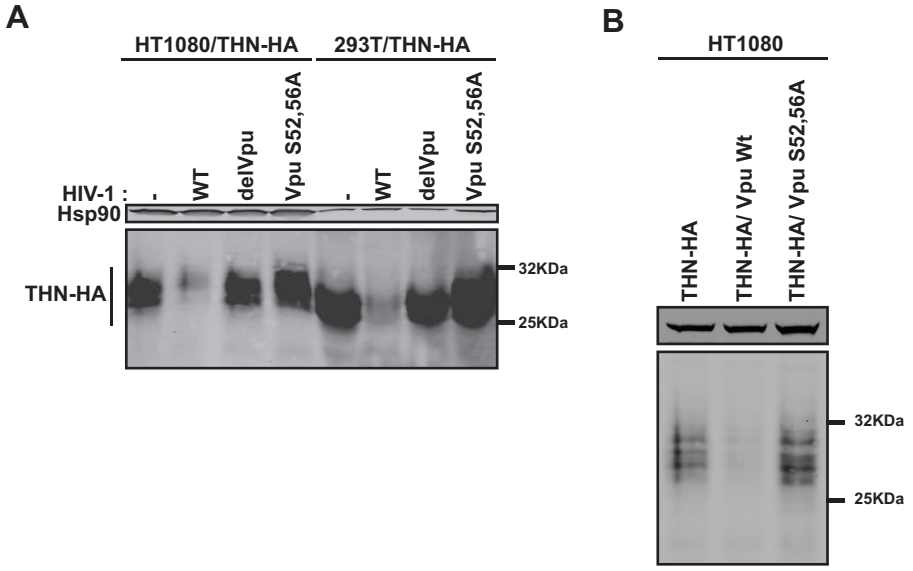

Figure 4.11: Vpu S52,56A fails to degrade tetherin.

A: HT1080 and 293T stably expressing THN-HA were infected with HIV-1 Wt, HIV-1 delVpu or HIV-1 Vpu S52,56A pseudotyped with VSV-G at an MOI of 2. 48 hours later, cell lysates were harvested and analysed on SDS-PAGE and THN-HA was detected using an anti-HA antibody. **B:** HT1080/THN-HA stably expressing Vpu Wt or Vpu S52,56A were Western-blotted for tetherin detection via the HA tag.

We then examined the anti-tetherin function of Vpu S52,56A in the absence of tetherin degradation. 293T cells were transfected with HIV-1 NL4.3 Wt, HIV-1 NL4.3 delVpu or HIV-1 NL4.3 Vpu S52,56A proviruses in the presence of increasing doses of a human tetherin expression vector. At 48 hours post-transfection, virus production was assessed by measuring infectivity of viral supernatants on HeLa-TZMbl sensitive cells (Figure 4.12A-top). As expected, production of HIV-1 delVpu virus was reduced in the presence of tetherin in a dose-dependent manner compared to HIV-1 Wt. HIV-1 Vpu S52,56A virus particle release showed an intermediate phenotype but retained significant activity to antagonize tetherin. This partial activity of Vpu S52,56A mutant was not due to a lack of expression as indicated by the expression levels on Western blot (Figure 4.12A-bottom). Virus particle release was similarly affected in HT1080/THN-HA cells infected with HIV-1 Vpu S52,56A (Figure 4.12B).

We then tested whether Vpu S52,56A displayed similar activity against endogenous levels of tetherin. HeLa cells were infected with VSV-G pseudotyped HIV-1 Wt, HIV-1 delVpu or HIV-1 Vpu S52,56A at a MOI of 0.2. After two days in culture, viral supernatants were harvested and virus production quantified as before (Figure 4.12C). We found that virus particle release of HIV-1 Vpu S52,56A was only approximately two fold lower than HIV-1 Wt and significantly higher than release of the Vpu-defective virus. These data suggest that Vpu S52,56A is more sensitive to higher expression levels of tetherin. In HeLa cells, in which the expression level of endogenous tetherin is lower than in 293T transiently-transfected or in HT1080/THN-HA, Vpu

S52,56A antagonizes tetherin almost as efficiently as the wild-type Vpu suggesting that degradation is more important in cells expressing high tetherin levels. Altogether, these data show that Vpu S52,56A does not induce tetherin degradation, but retains partial function to antagonize tetherin in a tetherin-dose dependent manner. Thus, Vpu can antagonize virion tethering in the absence of tetherin degradation. In contrast to K5, Vpu's ability to degrade tetherin does not entirely account for the full disruption of tetherin antiviral function and might be a consequence rather than the cause of tetherin inactivation.

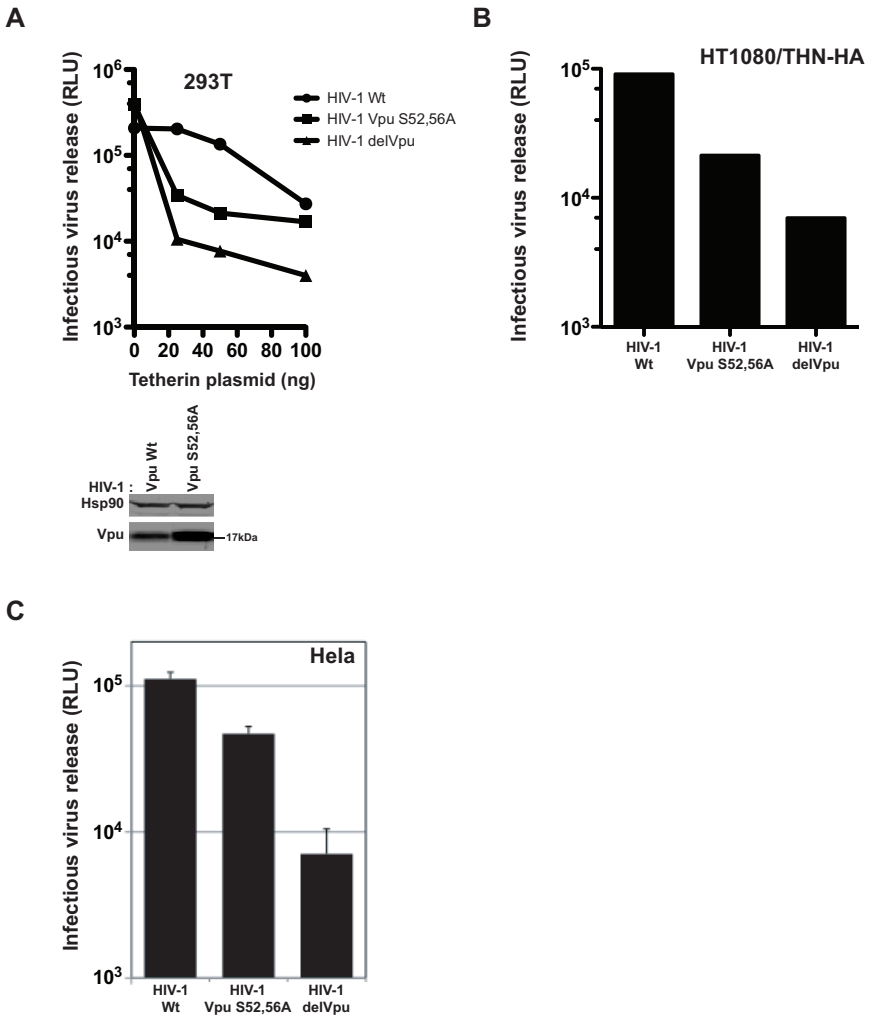

Figure 4.12: Vpu S52,56A fails to degrade tetherin but retains antagonism.

A: 293T cells were co-transfected with HIV-1 Wt, HIV-1 Vpu S52,56A or HIV-1 delVpu proviral plasmids in combination with an increasing amount of tetherin. 48 hours post-transfection, pelleted supernatants were used to infect HeLa-TZM indicator cells and infectious viral release determined by relative β-galactosidase activity. Western blot of 293T transfected by proviral plasmids NL4.3 HIV-1 Vpu or HIV-1 Vpu2/6. Vpu was detected using anti-Vpu antibody (rabbit polyclonal). **B:** HT1080/THN-HA cells were infected with HIV-1 Wt, HIV-1 delVpu or HIV- 1 Vpu S52,56A pseudotyped with VSV-G at an MOI of 0.2. 48 hours post-infection, viral release was determined as above. **C:** Same as B but with HeLa cells.

4.2.6 K5-mediated tetherin delivery to late endosomes is ubiquitin-dependent

Several lines of evidence suggest that K5 mediates ubiquitination of tetherin to deliver it to late endosomes. Firstly, the catalytic RING domain is required for removal of tetherin from the cell-surface. Secondly, lysine residues, which often serve as ubiquitin-acceptors, on tetherin cytoplasmic tail are required for K5-mediated tetherin counteraction. Finally, K5 mediated-tetherin degradation is sensitive to MG132 treatment, which is known to reduce the intracellular ubiquitin pool availability after prolonged exposure. We therefore examined the effects of proteasomal and endosomal inhibitors on cell-surface tetherin levels in K5 expressing cells. HT1080/THN-HA cells expressing either K5 or Vpu were stained for HA and levels of cell-surface tetherin measured by flow cytometry after a 16 hours treatment with the indicated drug (Figure 4.13A). Interestingly, although endosomal inhibition with Baf A1 treatment rescued tetherin proteins in the cell extracts of K5 expressing cells neither Baf A1 or Concanamycin A could rescue tetherin levels at the cell surface. However, with MG132 a consistent fraction of tetherin was rescued at the cell surface (Figure 4.13A-B). Presumably, ubiquitination of tetherin (reduced by prolonged MG132 treatment) results in its removal from the cell surface followed by endosomal sorting. Inhibition of endosome acidification induces tetherin to accumulate in intermediate endosomal compartments without being degraded. In contrast, none of the inhibitors significantly rescued tetherin surface expression in Vpu-expressing cells indicating again the divergence between K5 and Vpu mediating tetherin degradation. These observations coupled with the previous data demonstrate that K5 induces an ubiquitin-dependent endolysosomal degradation of tetherin.

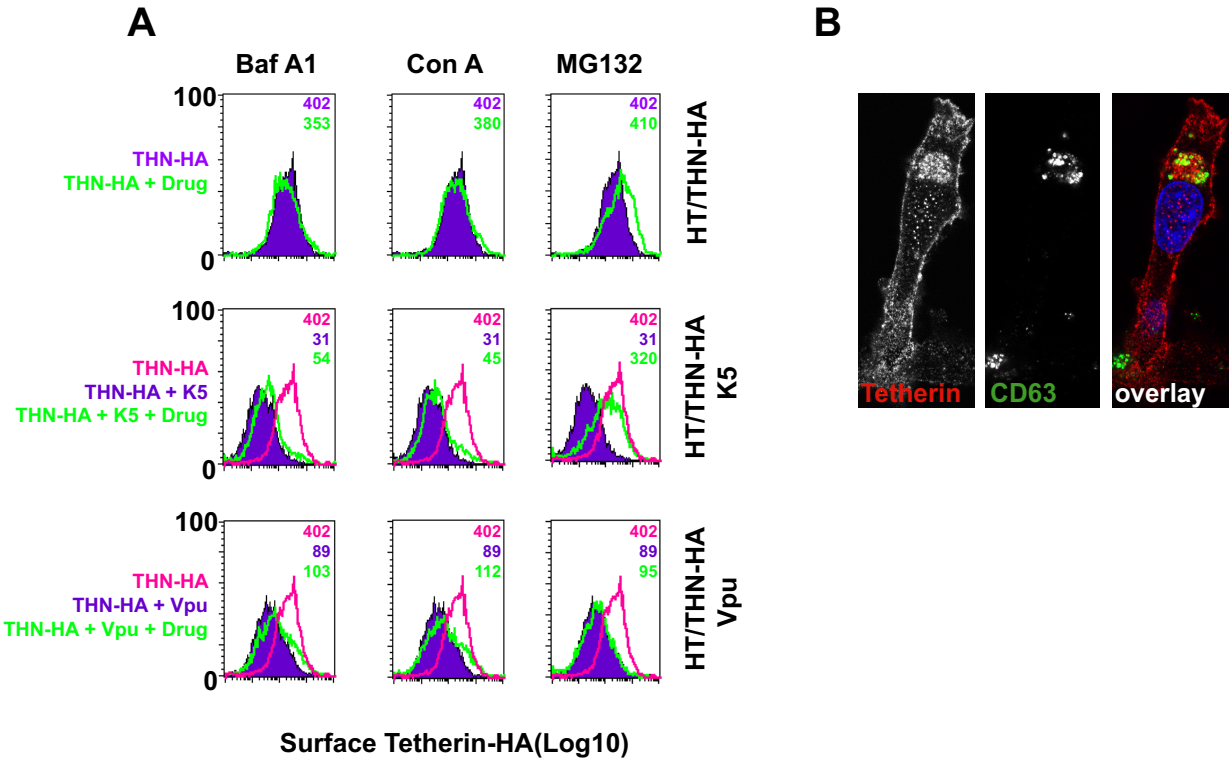

Figure 4.13: Effects of proteasomal and endosomal inhibitors on cell-surface tetherin levels in cells expressing K5 or Vpu.

A: HT1080/THN-HA, HT1080/THN-HA K5 and HT1080/THN-HA Vpu were surface stained for tetherin levels and analyzed by flow cytometry. Purple histograms represent tetherin levels on DMSO treated cells. Green overlays indicate tetherin levels after treatment with the indicated drug. The pink histogram overlays show the levels of tetherin on untreated HT1080/THN-HA from the upper row for comparison. The median fluorescence intensities in the top corner of each histogram are representative examples of three independent experiments. **B:** Confocal image of a representative HT1080/THN-HA K5 cell treated with MG132 and stained for THN-HA (red) and CD63 (green).

4.2.7 Ubiquitination of tetherin cytoplasmic tail lysine residues by K5

As lysine residues serve as targets for ubiquitination and the K18 mutant is resistant to K5-mediated tetherin downregulation and delivery to late endosomes, we next asked whether K5 could induce tetherin ubiquitination on its cytoplasmic lysine residues. HeLa cells were transiently transfected with a THN-HA Wt or THN-HA K18,21R expression vector in combination with a ubiquitin bearing a six-histidine tag (Figure 4.14). Cells were incubated for 48 hours and for the last 8 hours before harvest, cells were treated with Baf A1 to block tetherin degradation. Subsequently, ubiquitinated proteins were isolated by incubating whole cell lysates with nickel-agarose beads. Cell lysates and pull-downs were analysed by Western blot for THN-HA detection. In the presence of either co-transfected K5 or Vpu, THN-HA molecules could be isolated from the transfected cells. The ubiquitinated tetherin predominantly formed a single species at a size suggestive of mono-ubiquitination. Comparatively, K5 mediates polyubiquitination of MHC class I molecules via mixed Lys-63 and Lys-11 linkages on a single lysine acceptor residue (241). Interestingly, no ubiquitinated tetherin molecules were precipitated when their cytoplasmic lysine residues had been mutated, after either K5 or Vpu transfection. This implies the direct role of K5 and Vpu in mediating ubiquitination of the tetherin cytoplasmic tail. In the case of K5, this suggests that ubiquitination of K18 antagonizes tetherin-mediated restriction and directs it to endosomal compartments for lysosomal degradation. In contrast, the action of Vpu also leads to lysine ubiquitination but this process seems to be dispensable to antagonize tetherin's function suggesting that Vpu mediating tetherin antagonism and ubiquitin-dependent degradation are two separable events.

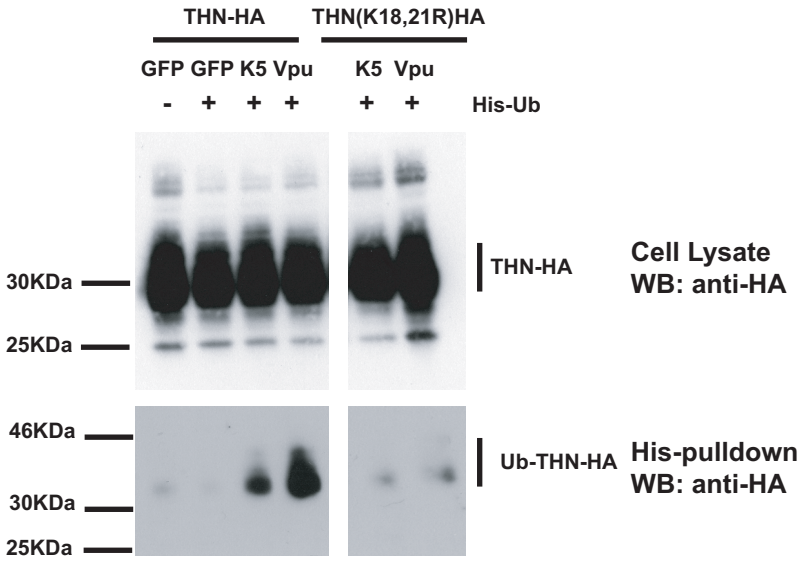

Figure 4.14: Tetherin cytoplasmic tail lysine residues are ubiquitinated in the presence of K5 and Vpu.

HeLa cells were transiently transfected with the indicated THN-HA expression vector in combination with K5, Vpu or GFP and in the presence or absence of 6His-tagged ubiquitin. 40 hours after transfection, cells were treated for 8 hours with Baf A1 (100 nM) to prevent tetherin degradation. Cell lysates were then harvested and ubiquitinated proteins were isolated by binding to Ni-Nti-agarose. Cell lysates and pull-downs were analyzed by Western blot for THN-HA using the HA antibody.

4.2.8 Tetherin's dual tyrosine-based endocytic motif is dispensable for K5 activity

Tetherin bears in its cytoplasmic tail a dual-tyrosine based endocytic motif, YxY. This motif binds to the clathrin adaptors AP1 and AP2 and has been reported to be important for tetherin endocytosis and recycling (cf. Chapter 1) (207). To test whether K5-mediated tetherin degradation required this endocytic motif, the two tyrosine residues in the cytoplasmic tail of tetherin (positions 6 and 8) were mutated into alanine. Corresponding HT1080 stably expressing those tyrosine mutants were generated (HT1080/THN-HA Y6,8A) and analysed by immunofluorescence microscopy for tetherin cellular localization (Figure 4.15A). As expected, this mutant tetherin was found almost exclusively at the plasma membrane. K5 expression was then introduced in these cells and tetherin levels analysed by flow cytometry and Western blot (Figure 4.15B-C). Expression of K5 leads to tetherin downregulation from the cell surface and degradation in cell lysates. Thus, tetherin trafficking rerouted by K5 to late endosomes is independent of its endocytic motif, implying that K5 overrides the normal trafficking machinery to modify the cellular fate of tetherin.

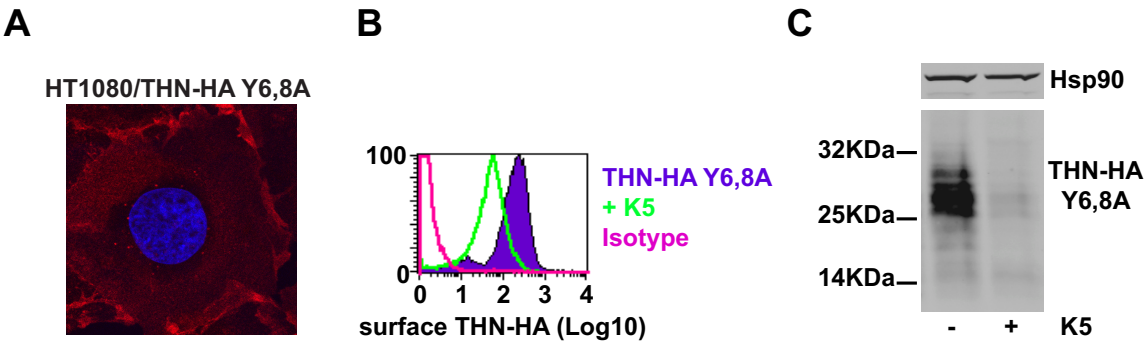

Figure 4.15: K5 mediated tetherin downregulation does not rely on the endocytic-based motif in tetherin cytoplasmic tail.

A: HT1080/THN-HA Y6,8A were imaged by confocal microscopy for tetherin (red). The cells were then manipulated to express K5 and analyzed by flow cytometry for surface tetherin (**B**) and by Western blot for total cellular tetherin levels (**C**).

4.2.9 K5 mediating tetherin cell-surface downregulation involves the ESCRT pathway

Components of the endosomal-sorting complex for transport (ESCRT) machinery are required for K3 targeting MHC class I molecules (416). Specifically, depletion of the ESCRT component Tsg101 leads to the recycling of MHC Class I molecules back to the cell surface in K3 positive cells because they can no longer be directed to MVBs. To examine the role of the ESCRT pathway in K5-mediated tetherin degradation, we tested whether downregulation of tetherin from the cell surface was affected by expression of a dominant negative form of VPS4 (dnVPS4). VPS4 is the essential AAA-ATPase that provides the energy for ESCRT disassembly and recycling during the final membrane scission event in the sorting of cell surface receptors for endosomal degradation. HeLa cells were co-transfected with a GFP-catalytically inactive form of VPS4 (E228Q) and a K5 or K5delRING expression vectors. Two days post-transfection, endogenous cell-surface tetherin levels in GFP positive cells were analysed by flow cytometry (Figure 4.16). Interestingly, the dominant negative form of VPS4 (dnVPS4) could restore cell-surface tetherin from K5 expression. Co-expression of K5delRING and dnVPS4 had no effect on tetherin cell surface levels. These results suggest that components of the ESCRT machinery are required for efficient tetherin downregulation from the cell surface. K5 induces a VPS4 dependent trafficking of tetherin to MVBs (late endosomes) for destruction. This mechanism is similar to that used by K3 to downregulate MHC class I molecules.

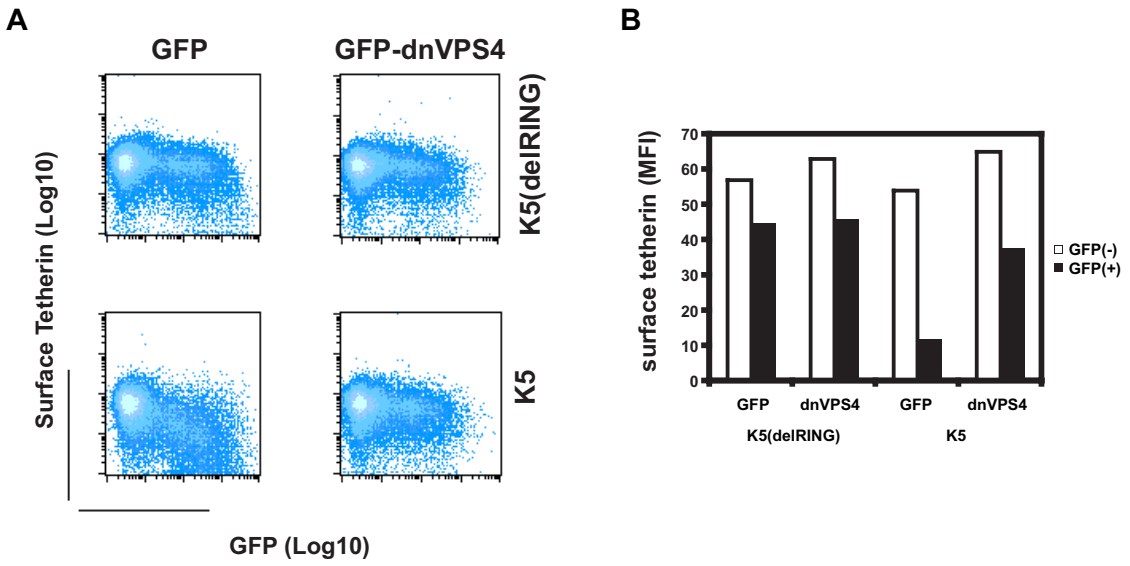

Figure 4.16: Cell-surface downregulation of tetherin by K5 is inhibited by dominant-negative VPS4.

A: HeLa cells were transfected with wild type K5 or K5(del RING) expression vectors in combination with either GFP or a dominant negative mutant of VPS4 fused to GFP (VPS4 E228Q). 24 hours later, cells were stained for cell surface tetherin using anti-BST2 monoclonal antibody and a goat-anti-mouse Alexa633 secondary antibody. Flow cytometry dot plots are shown. **B:** The mean florescent intensities (MFI) of surface tetherin expression in GFP positive and GFP negative populations from the samples in panel A are plotted.

4.3 Discussion

In this study we examined the molecular mechanism employed by K5 to overcome tetherin-mediated KSHV restriction. We found that by inducing tetherin ubiquitination, K5 triggers its removal from the cell surface and delivers it to late endosomes for destruction and this is sufficient to fully disrupt tetherin antiviral function. This mechanism is similar to that used by K5 to internalize MHC class I molecules from the cell surface for rapid degradation (241).

K5-mediated tetherin degradation is sensitive to endosomal inhibitors, and overnight MG132 treatment can rescue tetherin levels at the cell surface. For most of its substrates identified so far, K5 induces endolysosomal degradation with the exception of the target PECAM that is degraded via the ERAD pathway. In this study we identified a key residue in the cytoplasmic tail of tetherin required for K5 to antagonize tetherin‘s antiviral activity. Mutation of lysine 18 impairs the ability of K5 to induce tetherin ubiquitination and subsequent endosomal sorting for final destruction in lysosomes. It is surprising that K5 can target this membrane-proximal lysine (K18) which is so close to the membrane that the positively charged residue might be predicted to be embedded within the phospholipid bilayer so as not to be available for ubiquitination. However, one idea is that the proximity of K5, itself a membrane protein, may help expose the acceptor lysine for targeting. Interestingly, studies about ubiquitin-acceptor sites revealed that K5 not only prefers membrane proximal targets, as opposed to the more distal targets favoured by K3, but that the juxtamembrane cytoplasmic portions of K5 themselves contribute to this target preference (418).

KSHV encodes a E3 ubiquitin ligase to manipulate the ubiquitin pathway to further its own replication (419). Exploiting the ubiquitin pathway provides KSHV with a powerful mechanism for disposing of inhibitory elements of the immune system such as restriction factors. Moreover, ubiquitination is a dynamic process and enables KSHV to react rapidly to a hostile environment. Ubiquitination of tetherin by K5 may occur at the plasma membrane triggering its internalization, as K5 and K3 do with MHC class I molecules, but no evidence has been established to rule out a potential ubiquitination of tetherin molecules en route to the plasma membrane. Since K5 localizes predominantly to the endoplasmic reticulum at steady state (414, 417), it cannot be excluded that K5 might ubiquitin-tag tetherin early in the synthesis process, in the ER, for a degradation process initiated later in the secretory pathway. Comparatively, in the case of MHC class I, K3 and K5 can only ubiquitinate an EndoH resistant form of class I, suggesting targeting of MHC molecules in the late secretory pathway (post-ER). Alternatively, K5 might also traffic transiently to the TGN or the plasma membrane, or even act as a cargo loaded with its substrates until they reach the appropriate cellular compartment. This last scenario implies a retrieval signal in K5 sequence that would force the ubiquitin ligase to come back to the ER. More studies will need to be done to determine whether K5 stimulates tetherin internalization at the plasma membrane or reroutes tetherin to endosomes from the Golgi bypassing the cell surface.

We found that the RING domain was essential for K5 mediating tetherin antagonism since a RING deleted K5 protein lacked the ability to rescue HIV-1 delVpu particle release and was

defective for tetherin cell-surface downregulation. K5 is less effective at downregulating MHC class I molecules than K3, but has a broader substrate specificity. So far, this specificity has been mapped to the transmembrane regions but the determinants in the K5 sequence required for interaction with tetherin have yet to be determined. Without ruling out a direct interaction with tetherin, K5 could bind an adaptor protein, which would provide a platform for ubiquitination of several target proteins.

In this study we also demonstrated the importance of having an intact ESCRT pathway in K5-mediated cell-surface tetherin disposal. Indeed, compromising MVB formation using dnVPS4 resulted in a rescue of tetherin levels at the cell surface in K5 expressing cells. We also showed that K5 could fully substitute for Vpu in mediating the efficient release of HIV-1 particles from tetherin-expressing cells.

This study also showed the differences between the mechanisms by which K5 and Vpu disrupt tetherin's antiviral function. Both K5 and Vpu reduce tetherin expression from the cell surface and induce its degradation. In the case of K5, ubiquitination of tetherin triggers its delivery to late endosomes for destruction, and that is sufficient to overcome tetherin function and allow efficient virus particle release. For this reason, the molecular determinants required for K5 mediated-tetherin antagonism correlate with those involved in mediating tetherin ubiquitination and associated degradation or cell-surface downregulation. However, when tetherin degradation is prevented, either by mutating its cytoplasmic lysine residues or by mutating the phosphorylation site DSGNES, Vpu's ability to counteract tetherin is not completely abrogated. In line with this observation, Tokarev et al., subsequently showed that Vpu-stimulated tetherin ubiquitination could be abolished when all potential ubiquitination sites in the cytoplasmic domain, including lysines, cysteines, serines and threonines were mutated (393). Only a serine-threonine-serine (STS) sequence was shown to be specifically important for cell-surface tetherin downregulation and optimal relief of restricted virion release. These data suggest that degradation by itself does not account for the full anti-tetherin activity of Vpu. Since this study was published, several pieces of evidence showed that Vpu mediated tetherin degradation and antagonism were two separable events. This was best evidenced by silencing expression of an ESCRT-I component, UBAP1, required for tetherin depletion induced by Vpu but not for counteracting the antiviral activity (390). By re-routing the cellular trafficking of tetherin, Vpu prevents it from being expressed at the site of virus assembly. This is sufficient to overcome the antiviral activity and does not necessarily require the physical removal of tetherin (cf. Chapter 8).

Chapter 5
Determinants of Tetherin antagonism in the transmembrane domain of HIV-1 Vpu

The study presented in this chapter was published as " Determinants of tetherin antagonism in the transmembrane domain of the human immunodeficiency virus type 1 Vpu protein " (221).

5.1 Introduction

As discussed in the introduction, despite encoding Vpu, SIVcpz and SIVgor viruses rely on their Nef protein to counteract chimpanzee and gorilla tetherins while their Vpus are limited to CD4 degradation (226). However, in humans the situation is reversed with HIV-1 Vpu being a potent tetherin antagonist whereas Nef-targeting of tetherin was lost during primate evolution because of a deletion of five amino acids in tetherin cytoplasmic tail (225, 227). Selective pressure on SIVcpz resulted in the adaptation of Vpu to target the tetherin transmembrane domain and this was presumably an essential requirement for the virus zoonosis into the human host. Exchange of SIVcpz Vpu TM domain with those from HIV-1 Vpu can confer to SIVcpz Vpu antagonism against human tetherin (420), suggesting that the HIV-1 Vpu TM domain was the result of SIVcpz Vpu TM domain adaptation to human tetherin. For this reason, HIV-1 Vpu can only antagonize variants of tetherins from humans and chimpanzees but not those from old world monkeys. This situation can be reversed by reciprocal exchange of the transmembrane domains between human and monkey tetherins underscoring, once again, that the tetherin transmembrane domain was the region targeted by HIV-1 Vpu (224). Computational analysis of the tetherin TM domain predicted that some residues had been under positive selection. In line with the notion of co-evolution between host and pathogens, when those residues were replaced by their monkey homologues they could confer resistance to human tetherin against HIV-1 Vpu.

HIV-1 Vpu mediates interactions with tetherin through its transmembrane domain and this is a prerequisite to overcome tetherin's antiviral function (218, 377). Deletion of parts of the Vpu TM domain, scrambling or multiple amino acid replacements block Vpu-enhanced virus release (362, 384, 385). However, the determinants in the Vpu TM domain required for the interaction with tetherin have not been fully identified. In this study, we carried out mutagenesis of the HIV-1 NL4.3 Vpu TM domain to show that a conserved face of the HIV-1 group M Vpu transmembrane helix is required for tetherin interaction and antagonism.

5.2 Results

5.2.1 Screening of Vpu transmembrane domain for tetherin antagonism

To better characterize the determinants of tetherin antagonism in the Vpu TM domain, we conducted scanning mutagenesis through this region (residues 5 to 28) of a codon-optimized HIV-1 NL4.3 Vpu bearing a C-terminal HA tag (Figure 5.1A). All non-alanine residues were mutated individually to alanines, while bulkier hydrophobic leucine residues replaced those that were alanines. These Vpu TM mutants were then screened for their ability to rescue Vpu-defective HIV-1 from tetherin-mediated restriction. Human 293T cells, which lack endogenous tetherin expression, were transfected with HIV-1 NL4.3 delVpu proviruses in the presence of a fixed dose (50 ng) of a human tetherin expression vector and either a plasmid encoding HA-tagged wild-type (Wt) Vpu or the TM domain mutants. At 48 hours post-transfection, cell lysates and viral supernatants were harvested and analyzed by Western blotting or titrated on HeLa-TZM indicator cells (Figure 5.1B). As expected, in the presence of human tetherin, the release of infectious HIV-1 delVpu was reduced approximately 50-fold, as determined by the infectivity of harvested supernatants on HeLa-TZM indicator cells, and expression of wild-type Vpu *in trans* rescued the majority of this defect. Two mutants, the A14L and W22A mutants, were markedly defective in viral rescue compared to the control, with a third, the A18L mutant, displaying a minor defect. Interestingly, mutation of S23, which has been shown previously to completely abolish the ion channel activity of Vpu (421), or V13, I17, and V21, which would line the pore of a putative channel (329), conferred no defect in tetherin antagonism, suggesting that formation of an ion conducting pore may not be required to relieve the restriction.

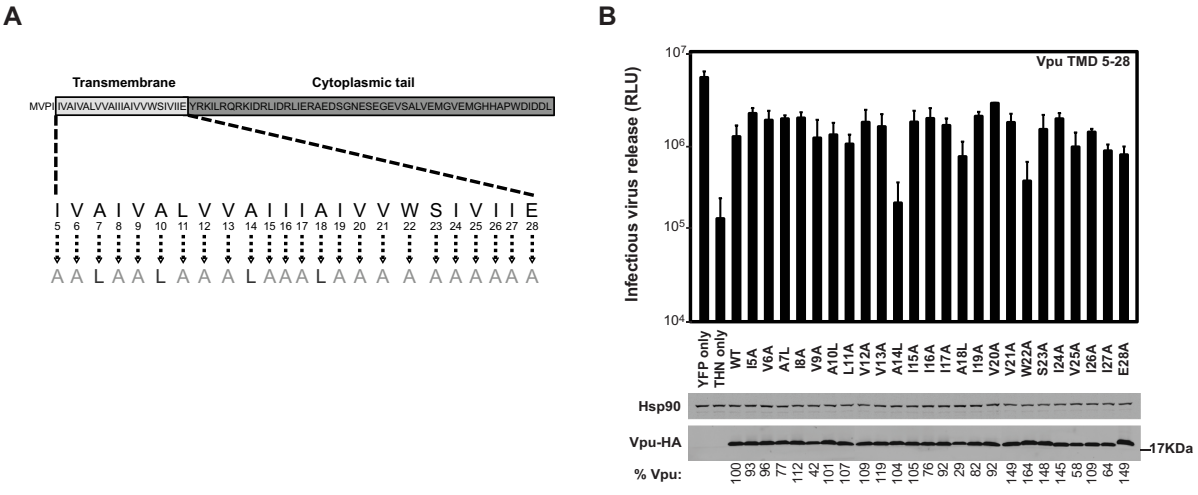

Figure 5.1: Scanning mutagenesis of the HIV-1 NL4.3 Vpu TM domain and tetherin antagonism.

A: A schematic representation of point mutations made in the TM domain of a codon-optimized HIV-1 NL4.3 Vpu protein. **B:** 293T cells were transiently transfected with 500 ng of HIV-1 delVpu provirus, 50 ng of tetherin plasmid, and 25 ng of the indicated Vpu expression vector. 48 hours after transfection, the resulting viral supernatants were assayed for infectivity on HeLa-

TZM indicator cells by measuring β-galactosidase activity (top). Error bars are +/- standard error of the mean (SEM) for three independent experiments. 293T cell lysates from one replicate of the assay were subjected to SDS-PAGE, blotted for Vpu-HA, with the 90-kDa heat shock protein (Hsp90) serving as a loading control (bottom), and analyzed by a LiCor quantitative imager. Numbers below the lanes indicate the percentages of relative Vpu expression compared to that of the wild-type protein.

To characterize the functional mutants further, the A14L, A18L, and W22A mutants or two combined mutants, the A14L/W22A and A10L/A14L/A18L/W22A mutants, were re-screened against a fixed dose of tetherin, but with varying levels of Vpu expression, and virus release characterized by both infectious titer release and physical particle yield by quantitative Western blotting (Figure 5.2A-B). Despite equivalent expression levels of Vpu and HIV-1 Gag in producer cells, neither the A14L mutant nor the W22A mutant could fully rescue HIV-1 delVpu from tetherin, and both remained defective compared to the wild-type Vpu, even at the highest inputs. The A18L mutant was the least defective and regained most of its function at higher plasmid concentrations. Combining the A14L and W22A mutants into a single mutant, either in the context of the A14L/W22A or A10L/A14L/A18L/W22A mutant, rendered Vpu effectively unable to counteract tetherin at any level of expression.

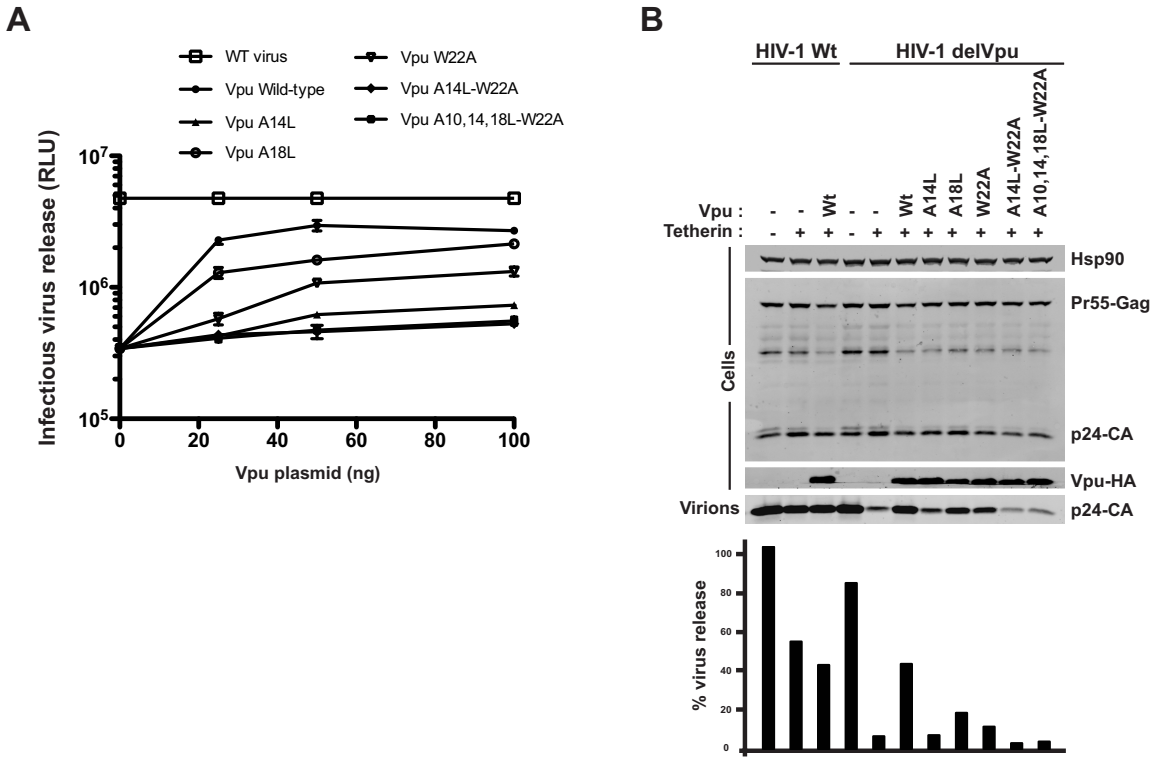

Figure 5.2: Vpu A14L and W22A are defective for tetherin antagonism.

A: 293T cells transfected with 500 ng of HIV-1 Wt or HIV-1 delVpu and 50 ng of tetherin expression vectors with increasing doses of the indicated Vpu-HA mutant. The resulting infectivity was determined as described before, and error bars represent +/- SEM for three independent experiments. **B:** Cell lysates and pelleted virions from one replicate of that shown

in panel A were subjected to SDS-PAGE and LiCor Western blotting was performed for HIV-1 p24-CA, Vpu-HA, and Hsp90 (top). The histogram (bottom) indicates supernatant virion yield (p24 band intensity) relative to the release of HIV-1 Wt in the absence of tetherin.

Finally, we engineered A14L and W22A mutants back into the HIV-1 NL4.3 genome to place them under wild-type viral Vpu expression conditions and tested virus release from 293T cells transfected with tetherin (Figure 5.3A-B). Consistent with expression of the mutants *in trans*, we found that the mutant carrying A14L alone and the combined mutant had a defect in release equivalent to a full Vpu deletion, whereas W22A retained a low level of tetherin antagonism. Thus, positions A14, W22, and, to a lesser extent, A18, appear to be key residues required for tetherin antagonism in the Vpu TM domain.

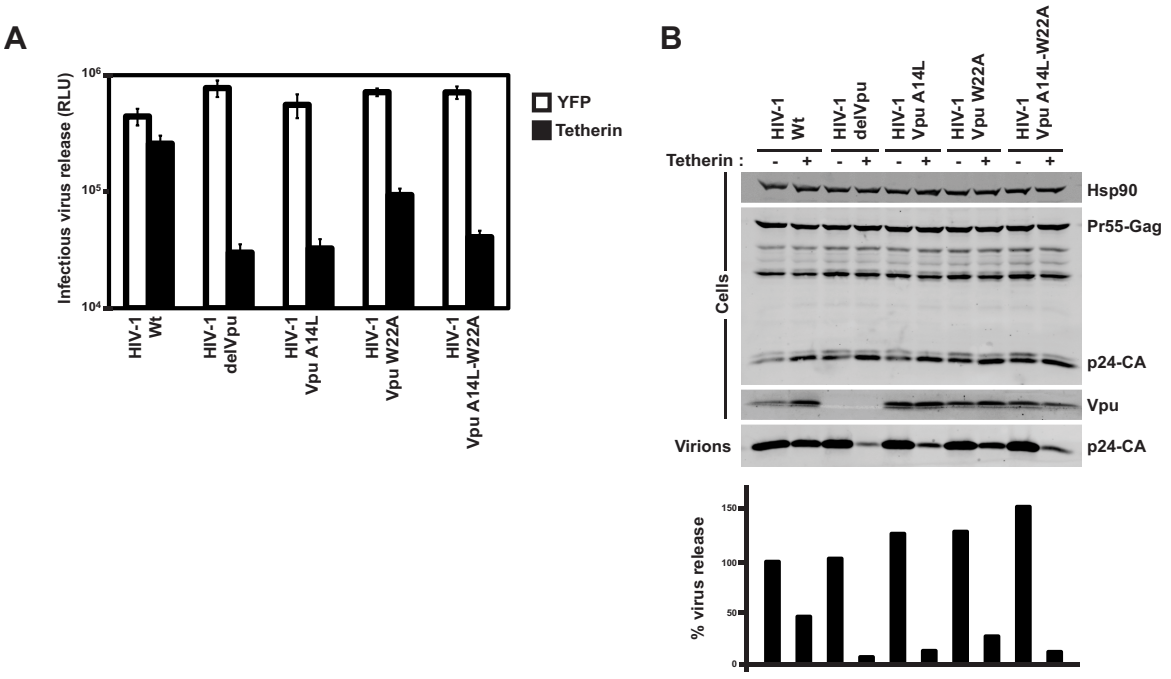

Figure 5.3: The effect of A14 and W22 mutations in the context of full-length proviral clones.

HIV-1 Wt, HIV-1 delVpu, HIV-1 Vpu A14L, HIV-1 Vpu W22A, and HIV-1 Vpu A14L-W22A proviral clones were transfected into 293T cells in the presence or absence of 50 ng of tetherin expression vector. Forty-eight hours later, the supernatants were assayed for infectivity on HeLa-TZM cells (**A**) and pelleted virions (**B**), and cell lysates were processed for Western blotting as described in the legend to Figure 5.2. Error bars are +/- standard error of the mean (SEM) for three independent experiments.

5.2.2 Mutants A14L and W22A fail to downregulate tetherin from the cell surface

To further characterize the nature of the defect in the Vpu TM mutants, we first determined their effects on cell surface tetherin levels. Vpu expression leads to a downregulation of cell surface tetherin and subsequently a degradation step which itself is dispensable for Vpu activity under certain circumstances (187, 376, 387). Tetherin-positive HeLa cells were co-transfected with an empty vector control or Vpu expression vector in combination with a GFP marker plasmid. At 48 hours post-transfection, the cells were harvested, stained for cell surface tetherin using a specific monoclonal antibody, and analyzed by flow cytometry (Figure 5.4). Tetherin was downregulated from the cell surface of GFP^+ cells expressing Vpu, and as expected, this downregulation was reduced in the presence of the Vpu S52,56A mutant that does not interact with β-TRCP1/2 (187, 220, 387). Both the A14L and W22A mutants failed to fully downregulate tetherin, and either multiple mutant containing both A14L and W22A mutations was completely defective for downregulation.

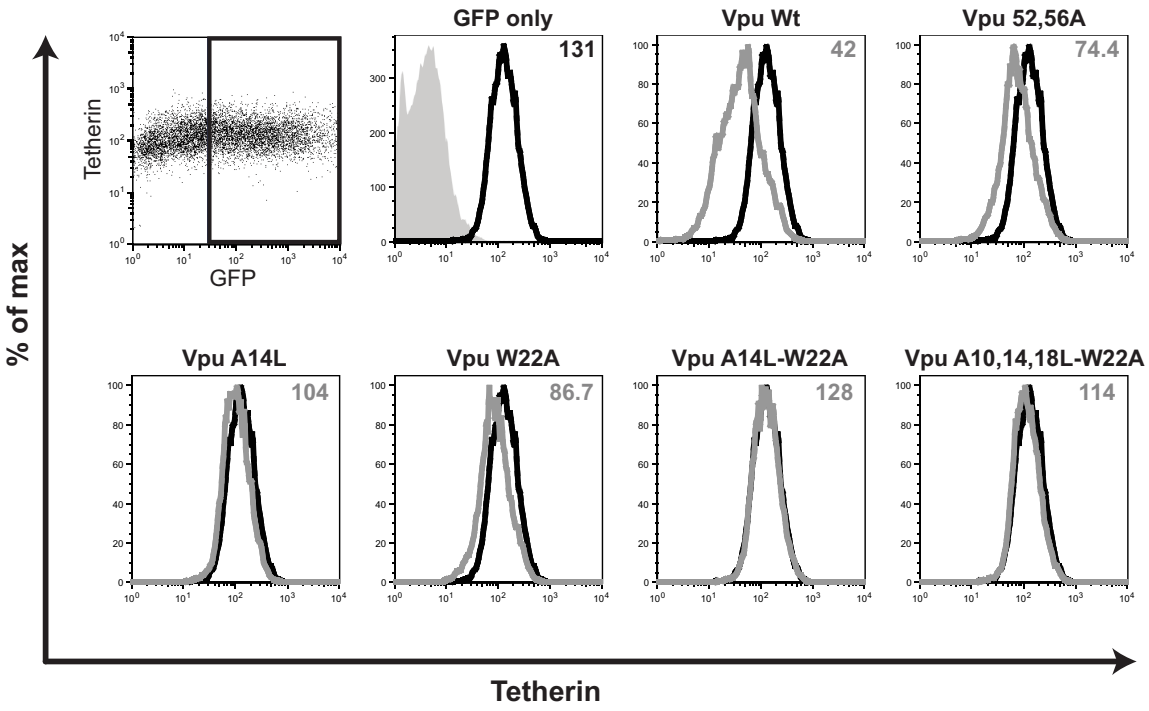

Figure 5.4: Effects of Vpu TM mutations on cell surface levels of tetherin in HeLa cells.

HeLa cells were transfected with a wild-type Vpu (Vpu Wt)-encoding vector or the indicated mutant and a GFP-expressing construct. Cell surface staining for endogenous tetherin was analyzed by flow cytometry 48 hours later. Histograms show the tetherin levels on GFP^+ cells in empty vector control cells (black) or in Vpu mutant-expressing cells (gray) and are representative examples of three independent experiments. The median fluorescence intensities are indicated in the top corner of each histogram. The solid peak histogram represents the binding of the isotype control.

To confirm this with a more physiologically relevant infected cell type, $CD4^+$ Jurkat T cells were infected with VSV-G-pseudotyped wild-type HIV-1, HIV-1 delVpu, HIV-1 Vpu S52,56A, HIV-1 Vpu A14L, HIV-1 Vpu W22A, or HIV-1 A14L/W22A, and 48 hours later, cells were stained for surface tetherin and intracellular Gag (p24-CA) (Figure 5.5). As expected, Gag-positive cells in cultures infected with wild-type HIV-1, but not with HIV-1 delVpu or HIV-1 Vpu S52,56A, showed loss of tetherin expression at the cell surface. However, in line with our findings for transfected cells, Jurkat cells infected with viruses bearing an A14L mutation showed little cell surface tetherin reduction. The W22A mutant retained a residual ability to downregulate cell surface tetherin, again consistent with our previous observations. Thus, Vpu TM mutants that cannot antagonize tetherin function are concomitantly defective for cell surface tetherin downregulation and, by extension, degradation.

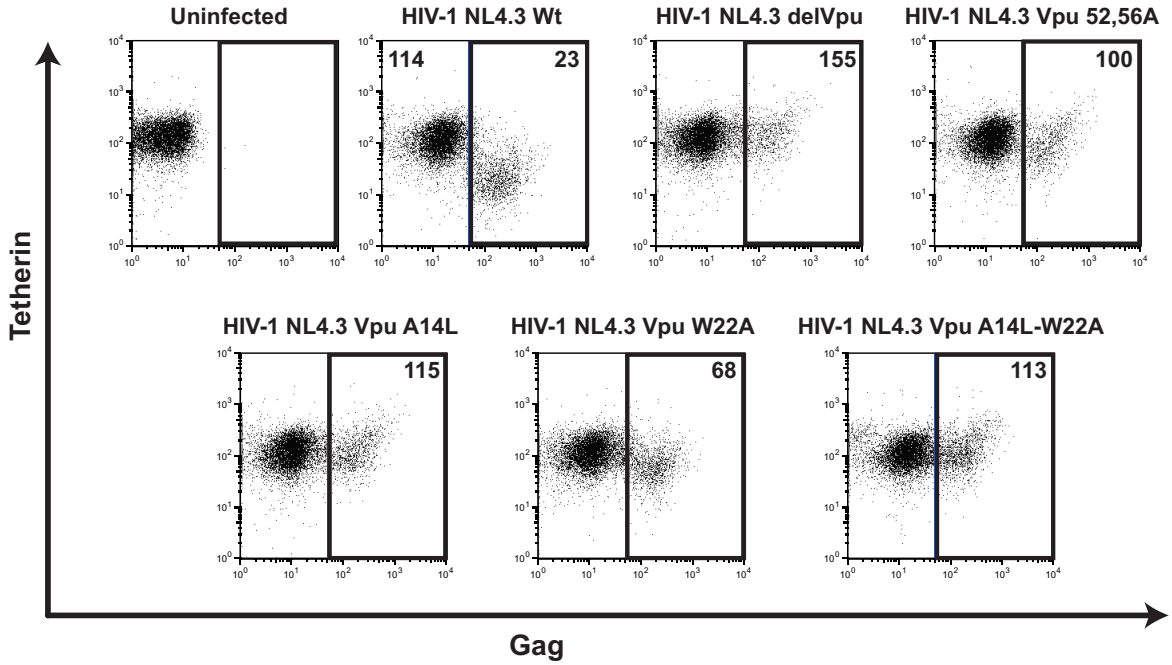

Figure 5.5: Effects of Vpu TM mutations on cell surface levels of tetherin in $CD4^+$ Jurkat T cells.

Jurkat cells were infected with the indicated VSV-G-pseudotyped viral stocks at an MOI of 0.2. Forty-eight hours later, cells were stained for surface tetherin expression and intracellular Gag and analyzed by flow cytometry. Gag-positive infected cells were gated (black square), and surface tetherin levels were compared. Numbers indicate median fluorescence intensities of surface tetherin on the infected cells.

We also tested our Vpu mutants for their ability to downregulate CD4. Although CD4 and Vpu have been shown to interact through cytoplasmic tail interactions, a role for the TM domain has been implicated by some (385), but not others (362). HeLa/CD4 cells were transfected as described above, and cell surface CD4 levels were measured 48 hours later (Figure 5.6). As

expected, Vpu expression led to a reduction in surface CD4 that again was blocked in the presence of an S52,56A mutant. Vpu A14L retained the ability to downregulate CD4, indicating that this mutant is specifically defective for tetherin antagonism. In contrast, and consistent with the work of Tiganos et al. (385), the Vpu W22A mutant and multiple mutants bearing this lesion were also defective for CD4 downregulation. This was further confirmed by work from Bonifacino's group showing that mutation of W22 did not prevent interaction of Vpu with CD4 but enhanced the oligomerization state of Vpu and reduced CD4 polyubiquitination leading to accumulation of CD4 molecules in the ER membrane (374). These retained CD4 molecules were found to be unable to be dislocated from the ER to the cytosol for degradation via the proteosome. Thus, both tetherin and CD4 downmodulation require residues in the Vpu TM, but these determinants only partially overlap.

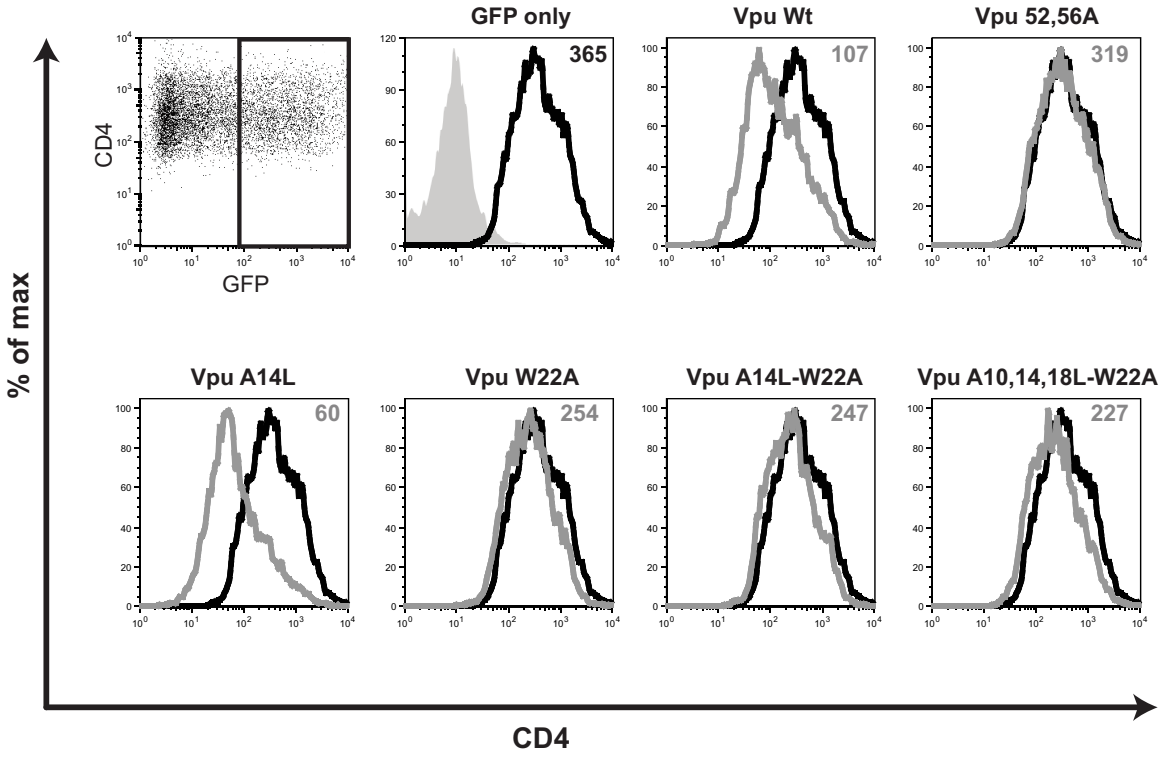

Figure 5.6: W22 but not A14 is required for Vpu-mediated CD4 downregulation.

HeLa/CD4 cells were transfected with a wild-type Vpu (Vpu Wt)-encoding vector or the indicated mutant and a GFP-expressing construct. Cell surface staining for endogenous CD4 was analyzed by flow cytometry 48 hours later. Histograms show the CD4 levels on GFP^+ cells in empty vector control cells (black) or in Vpu mutant-expressing cells (gray). The median fluorescence intensities indicated in the top corner of each histogram are representative examples of three independent experiments. The solid peak histogram represents the binding of the isotype control.

5.2.3 Defective Vpu TM mutants localize to the TGN

While CD4 degradation occurs in the endoplasmic reticulum (ER), Vpu-mediated virus release is sensitive to brefeldin A (365), suggesting that tetherin antagonism takes place outside the ER. Vpu localizes to the TGN and endosomal compartments, and the ability to localize to the TGN has been shown to be important for tetherin antagonism (341). Indeed, mutations in the hinge region (R30A, K31A) (341) or in the second alpha helix (motif EXXXLV) (383) cytoplasmic tail of Vpu that impair its TGN localization are associated with reduced virus release. It has been proposed that the TGN was the cellular compartment from where Vpu/tetherin complexes were committed to the endosomal pathway for degradation. Vpu localization to the TGN allows it to access both to pre-existing tetherin recycling via the TGN and to newly synthesized tetherin trafficking through the Golgi en route from the ER to the cell-surface. Since the TM domain(s) of integral membrane proteins may be involved in subcellular localization (422), we next sought to rule out whether our Vpu TM mutants were aberrantly localized. HeLa cells transfected with Vpu-HA or TM mutants were grown on coverslips, fixed 24 hours later, immunostained for Vpu (anti-HA) and the TGN marker TGN46, and examined by confocal microscopy (Figure 5.7). As expected, wild-type Vpu-HA localizes predominantly to perinuclear and punctate structures, with much of the perinuclear signal overlapping with the TGN, consistent with previous studies. We found that all of our Vpu TM mutants localized similarly, with TGN accumulation visible in all cases. These data suggest that Vpu localization to the TGN is independent of the ability to counteract tetherin.

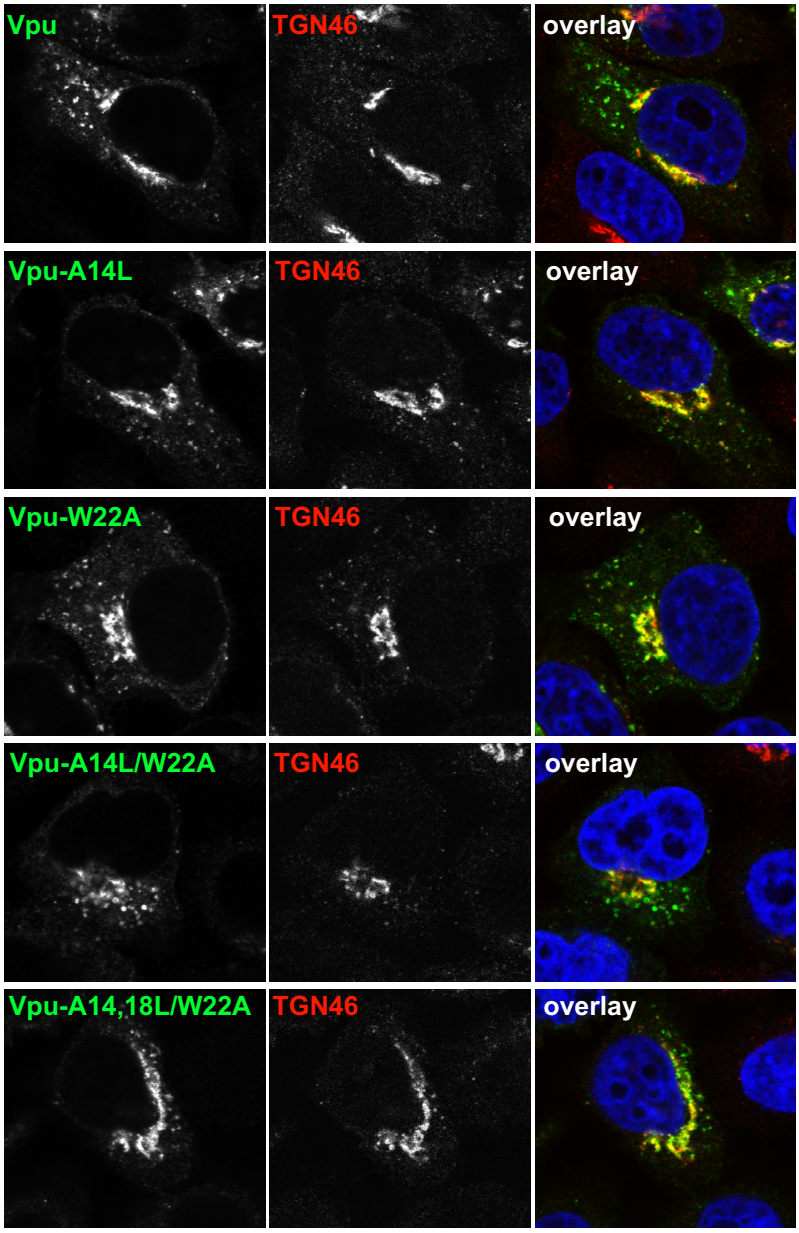

Figure 5.7: Subcellular localization of Vpu TM mutants in HeLa cells.

HeLa cells were transfected by either 100 ng Vpu Wt-HA or the indicated mutant. A total of 24 hours later, the cells were fixed and stained for Vpu localization with anti-HA antibody (green) and a TGN marker (TGN46; red) and examined by confocal microscopy. Images are representative examples of Vpu-expressing cells.

We then examined Vpu and tetherin localization in infected HT1080 cells expressing tetherin bearing an extracellular HA tag (HT1080/THN-HA, cf. Chapter 4) (Figure 5.8). As expected, in these cells tetherin localizes to the plasma membrane as well as the TGN since both newly synthesized tetherin and that which recycles passes through the Golgi network en route to the PM (193, 207). We found that wild-type Vpu and residual tetherin colocalized in the TGN with a concomitant reduction in cell surface expression. In contrast, and consistent with the flow cytometry data presented in Figure 5.4 and Figure 5.5, cells infected with a virus bearing the A14L/W22A mutation showed no evidence of tetherin relocalization from the PM to the TGN. This indicates that the defect in tetherin antagonism for A14L and W22A mutants of Vpu is likely not due to gross subcellular mislocalization, and that Vpu localization to the TGN and Vpu-induced accumulation of tetherin in TGN46-positive compartments are independent events.

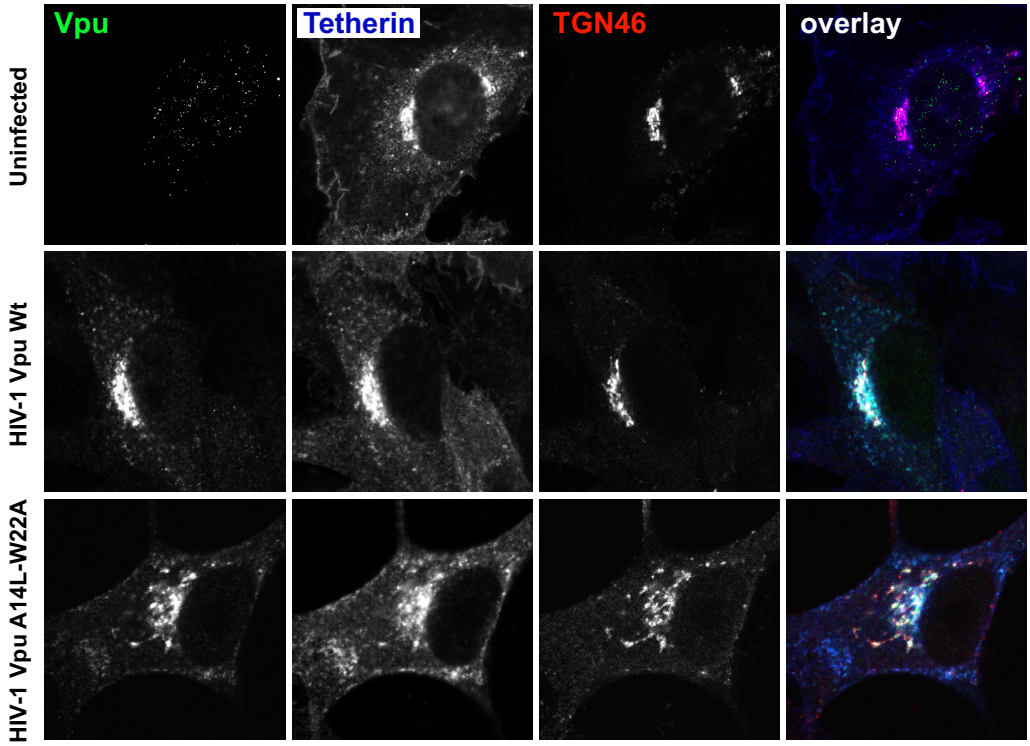

Figure 5.8: Subcellular localization of Vpu TM mutants in infected HT1080/THN-HA cells.

HT1080/THN-HA cells were infected with HIV-1 Wt or HIV-1 Vpu A14L/W22A at an MOI of 0.2. Forty-eight hours later, the cells were fixed and stained for Vpu (green), TGN46 (red), and tetherin-HA (blue) and examined by confocal microscopy. Images are representative examples of uninfected and HIV-1 Vpu A14L-W22A infected HT1080/THN-HA cells. Image of HIV-1 Vpu Wt infected HT1080/THN-HA is representative of cells in which residual tetherin could still be detected.

5.2.4 Vpu/tetherin interaction requires residues A14 and W22

We then assessed the ability of Vpu TM mutants to co-immunoprecipitate tetherin as an indicator of direct or indirect interaction between the proteins. 293T cells were transfected with a human tetherin expression vector and wild-type Vpu-HA or the TM mutant. 48 hours after transfection, cell lysates were immunoprecipitated with an anti-HA antibody. As shown in Figure 5.9, when transiently over-expressed in 293T cells, tetherin appears predominantly as a single species, likely to be a precursor mannosylated form, at a low molecular weight while higher molecular species running as a smear are only detected with long-exposure conditions. These latest forms are likely to be mature glycosylated species of tetherin. In contrast, in stable HT1080/THN-HA only the smear of high molecular species is mainly observed (cf. Chapter 4). This difference may reflect the fact that under conditions of transient expression in 293T cells, maturation through addition of carbohydrates to tetherin occurs more slowly than translation (197). As shown in Figure 5.9, tetherin (both low and high molecular species) was efficiently co-immunoprecipitated with wild-type Vpu, despite total cellular tetherin levels being lower in cell lysates due to Vpu-induced degradation (Figure 5.9, low-exposure lysate panel). The A14L and W22A mutants displayed little or no tetherin degradation and only poorly co-immunoprecipitated with the protein. Furthermore, combined mutants containing both A14L and W22A were further reduced in their ability to co-immunoprecipitate tetherin. Thus, the defect in tetherin antagonism in the A14L and W22A mutants correlates directly with their failure to interact with tetherin in co-IPs. Coupled with the observation that these mutants localize identically to wild-type Vpu, the data strongly suggest that these positions in the Vpu TM domain are critical for the interaction with tetherin. Interestingly, the fact that we co-immunoprecipitated the lower-molecular-weight, immature form of tetherin with Vpu suggests that while Vpu exerts its effect on tetherin in a post-ER compartment, interaction may occur prior to further carbohydrate modification (cf. Chapter 6).

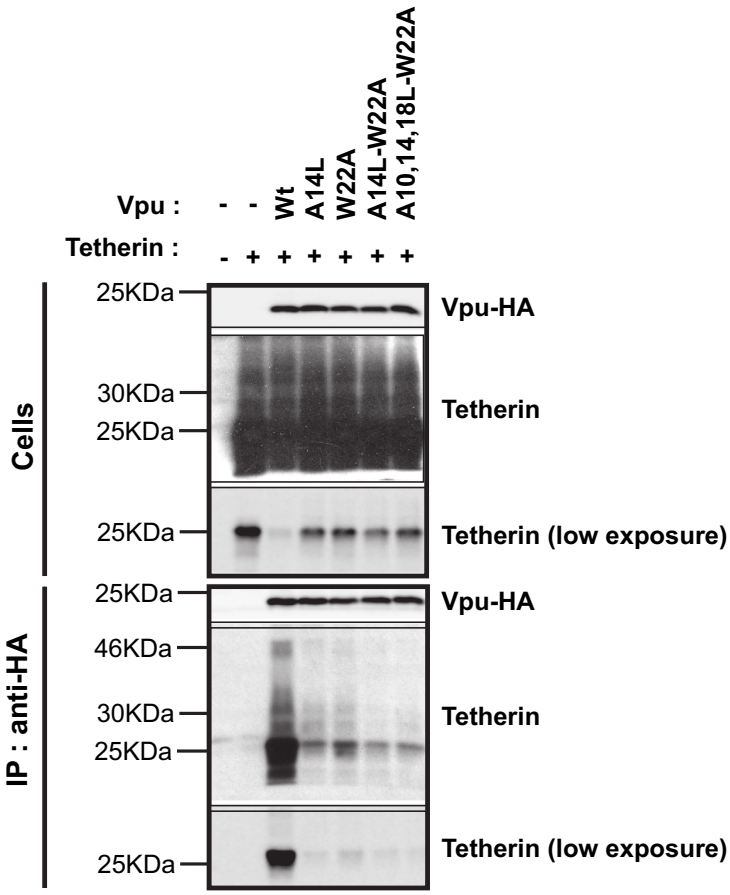

Figure 5.9: Vpu TM mutants are unable to co-immunoprecipitate tetherin.

293T cells were transfected with the indicated plasmid Vpu vectors or the indicated mutant and with tetherin. YFP only or tetherin only served as negative controls. Forty-eight hours later, Vpu was immunoprecipitated (IP) via the HA tag from cell lysates and subjected to SDS-PAGE. Total lysates and immunoprecipitates were then Western blotted for tetherin and Vpu-HA. Molecular mass markers are indicated, and blots are a representative example of three independent experiments.

5.2.5 Defective Vpu TM mutants retain the ability to form multimers

Oligomers of Vpu can be detected in infected cells (327, 331), although their functional significance for tetherin antagonism is not known. We then asked whether the ability of Vpu to form multimers was affected in the context of A14 and W22 residues mutated as a possible cause to account for a lack of interaction with tetherin. Western blots of post-nuclear lysates of Vpu-HA-transfected 293T cells run under non-reducing conditions without prior boiling displayed a higher-molecular-mass form of Vpu (approximately 80 kDa) in addition to a monomer (Figure 5.10), consistent with previous observations (327). This species of Vpu was also detected for the Vpu A14L/W22A mutant at enhanced levels, suggesting these mutations did not abolish Vpu multimerization and might even contribute to stabilize oligomeric forms. In addition, this mutant also formed a larger (approximately 100- to 120-kDa) form. In line with this observation,

a report from the Bonifacino group suggested that W22 was not required for Vpu-Vpu interactions and even prevented assembly of Vpu complexes into inactive oligomeric form (374). These data suggest that mutations on residues A14 and W22 do not compromise self-interaction.

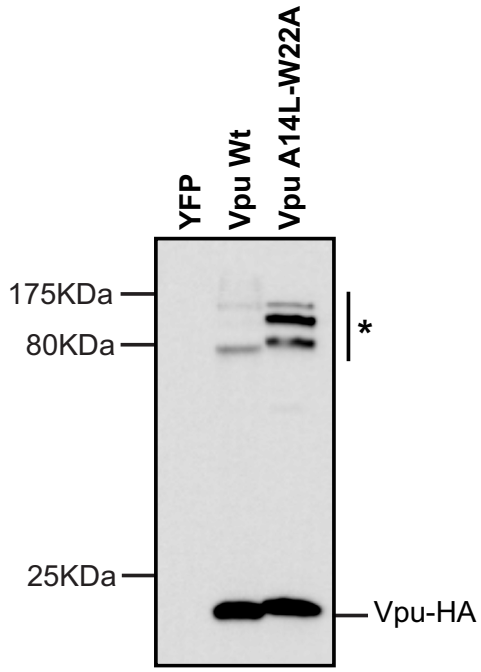

Figure 5.10: Vpu A14L-W22A mutant can self-associate.

293T cells transfected with HA-tagged Vpu or Vpu A14L/W22A were lysed in 1% digitonin after 48 hours, subjected to non-reducing SDS-PAGE without prior boiling, and Western blotted with an anti-HA monoclonal Ab. Higher molecular mass forms of Vpu are indicated with a star.

5.2.6 Oligomerization state of Vpu required for targeting tetherin

It has not been established whether Vpu targets tetherin as a monomer or if the multimerization state of Vpu is required to generate a functional binding interface with the tetherin transmembrane domain. To address this point, we first asked whether the Vpu A14L,W22A mutant could also form complexes with Vpu Wt proteins. 293T cells were transfected with Vpu-YFP and either Vpu-HA or Vpu A14L/W22A-HA. Under the same immunoprecipitation conditions, in which Vpu TM mutants failed to interact with tetherin (cf. Figure 5.9), we could show that wild-type Vpu tagged with YFP could co-immunoprecipitate with both Vpu-HA and Vpu A14L/ W22A-HA (Figure 5.11).

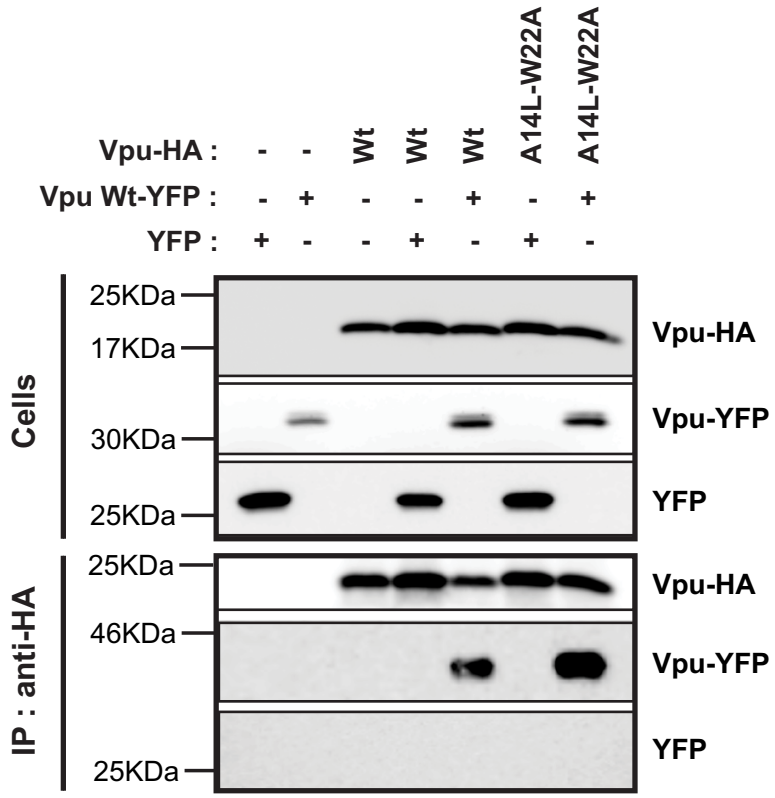

Figure 5.11: Vpu A14L-W22A mutant can multimerize with Vpu Wt.

293T cells were transfected with Vpu-YFP and either Vpu-HA or Vpu A14L/W22A-HA. Forty-eight hours later, cell lysates were immunoprecipitated with anti-HA Ab as described previously, and whole lysates and IP fractions Western blotted for Vpu-HA and Vpu-YFP with anti-HA and anti-GFP antibodies, respectively.

Based on the above observation, we reasoned that if tetherin antagonism was mediated by functional Vpu multimers, a Vpu A14L/W22A mutant might be a dominant-negative inhibitor of tetherin antagonism. However, titration of Vpu TM mutants into HIV-1 Wt viral release assays did not induce any enhanced sensitivity to tetherin, despite estimated mutant Vpu levels being 10-fold over that expressed from the provirus (Figure 5.12A-B). Thus, while not ruling out that Vpu acts as a multimer to target tetherin, these data show that the ability of Vpu TM mutants to associate with wild-type Vpu does not compromise its function. However, it cannot be excluded that a small fraction of functional Vpu might be sufficient to antagonize tetherin in a virus release assay, thus masking the potential dominant negative effect of the Vpu TM domain mutant. Consistent with these data, NMR studies suggest a monomeric interaction of Vpu with tetherin (386).

Further investigations will need to be performed to determine the exact stoichiometry of Vpu relative to tetherin required to achieve its anti-tetherin activity. Similarly to what has been

proposed in the case of CD4, a stock of Vpu monomers might be held under inactive multimeric forms before being engaged with tetherin molecules. In such a scenario, mutations on residues A14L-W22A might stabilize Vpu oligomerization, thus preventing Vpu monomers from targeting tetherin.

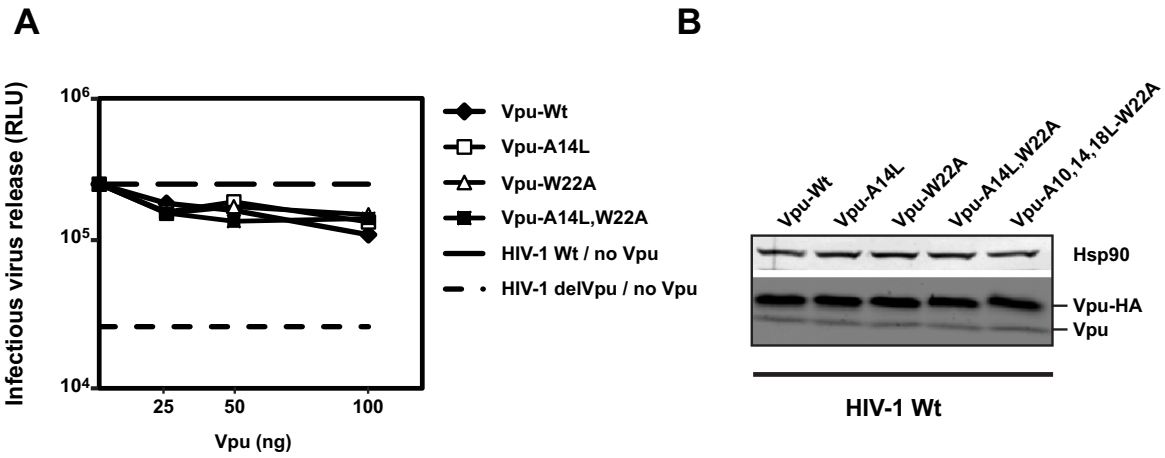

Figure 5.12: Vpu A14L-W22A mutant does not act as dominant-negative inhibitor of tetherin antagonism.

A: 293T cells were transfected with wild-type HIV-1 NL4.3 Wt proviral plasmid, 50 ng of tetherin, and the indicated amount of Vpu-HA or mutant, and infectious release was determined on HeLa-TZM cells 48 hours later. Dotted lines represent wild-type and Vpu-defective viral titers in the absence of any expression of Vpu *in trans*. **B:** Cell lysates of the 100-ng input described in the legend to panel A blotted with an anti-Vpu polyclonal Ab to allow simultaneous detection of the Vpu-HA expressed *in trans* and the wild-type Vpu expressed from the NL4.3 provirus.

5.2.7 Residues A14, A18 and W22 form a face of the Vpu transmembrane helix

A solid-state nuclear magnetic resonance (NMR) structure of the NL4.3 Vpu TM domain in lipid membranes has been determined previously (329, 423). The core TM domain (residues 8 to 25) forms a slightly kinked alpha helix tilted at approximately 13 degrees to the vertical. Residues A10, A14, A18, and W22 form one diagonal face of the helix (Figure 5.13). Because Vpu can form ion-permeable channels, this structure was further modeled to account for this, and the most favorable conformations that would allow channel function were predicted to be a tetramer or a pentamer (329). In this conformation, W22 is predicted to protrude outward from the pentamer and may give stability to the structure in the membrane. A14 and A18 are positioned at the interface with the adjacent monomers, and therefore, their replacement with bulkier leucine residues may impinge on this interaction and, although not sufficient to block Vpu multimerization, alter the conformation or stoichiometry of Vpu oligomers or segregate Vpu monomers into multimeric complexes. Alternatively, or in addition to contributing to interhelical contacts or stability, A14, A18, and W22 might also contribute to a conserved binding surface for interaction with another protein, potentially tetherin.

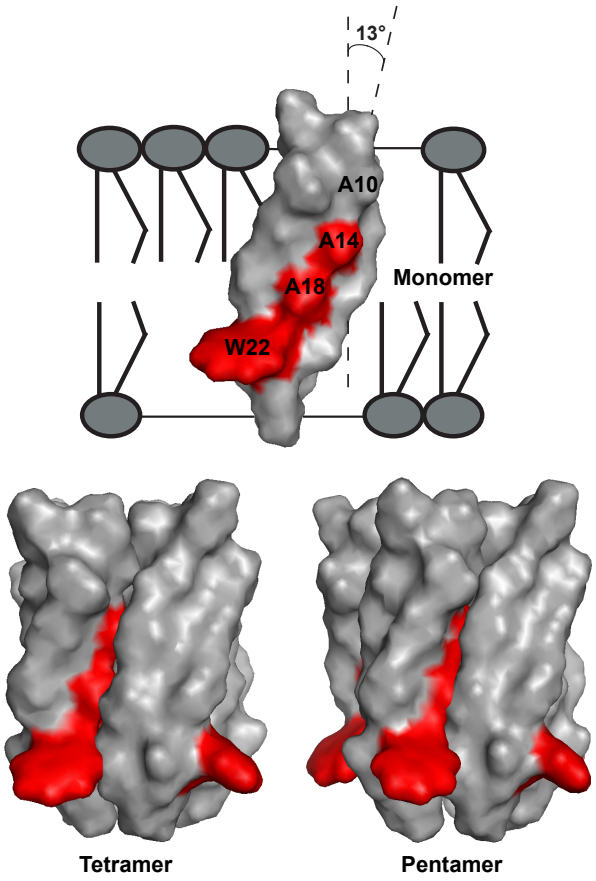

Figure 5.13: Residues A14, A18, and W22 form one face of the Vpu TM helix.

Positions of A14, A18, and W22 (red) in the solid-state NMR structure of the NL4.3 Vpu TM domain determined in membranes and the modeled tetrameric and pentameric assemblies based on it, as determined by Park et al. (329). Images were generated in PyMol from the RSCB protein database entries 1PI7 (pentamer) and 1PI8 (tetramer).

5.2.8 Residues A14, A18 and W22 are conserved in HIV-1 group M and N but not O

We next looked at the conservation of the above TM positions in Vpu sequences deposited in the HIV Sequence Database (www.hiv.lanl.gov). Alignment of the TM domains of 1,197 group M Vpu sequences showed that the positions equivalent to A18 and W22 are highly conserved (Figure 5.14A). The majority of sequences also have the equivalent of position 14 as A, but in many cases this can be V. Interestingly, we found that a valine in position 14 was also functional to counteract tetherin (Figure 5.14B). Notably, we did not find an L at this position in naturally occurring group M sequences. The same was observed with the small number of group N Vpu sequences available; the equivalents of positions 14, 18, and 22 were A, A, and W, respectively. Interestingly, this was not the case for HIV-1 group O Vpu proteins, which have been shown to be defective in tetherin antagonism (226). Here the position 14 equivalent is

almost always L, and the majority of sequences have an N at position 18. Again the W is invariant, which, since group O Vpu proteins retain CD4 degradation activity (226), is consistent with W22A mutants of NL4.3 Vpu being defective for both tetherin and CD4 downregulation. Thus, the residues we have identified as important for tetherin antagonism in HIV-1 NL4.3 Vpu are conserved in viruses that can antagonize human tetherin, but not in those that cannot.

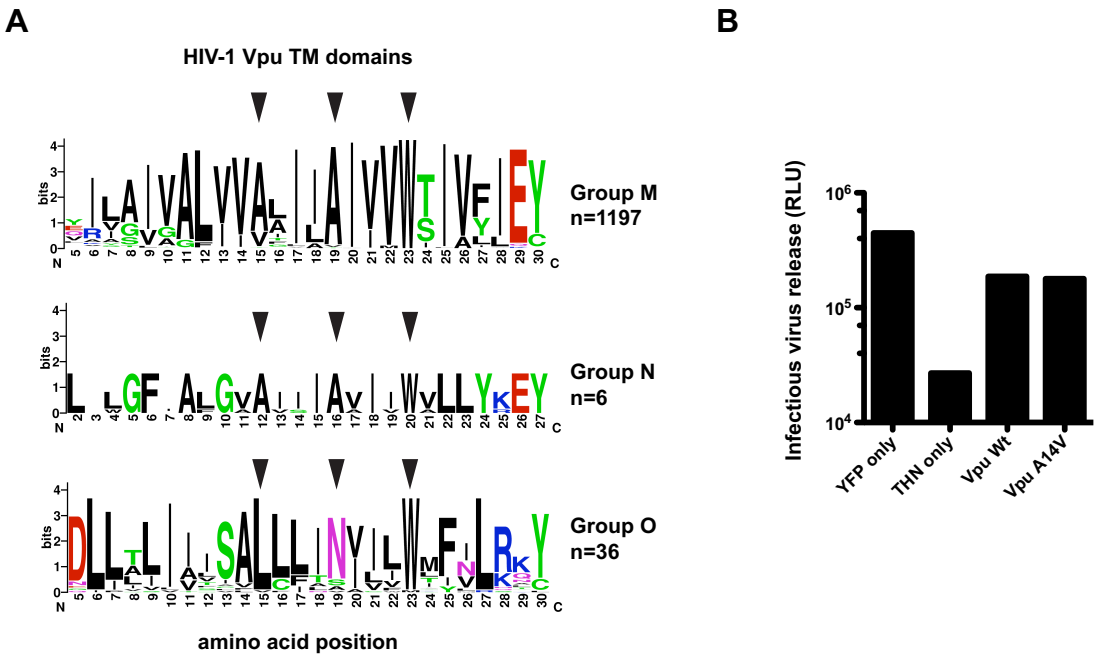

Figure 5.14: Residues A14, A18, and W22 are conserved in HIV-1 groups M and N, but not O.

A: Logo plots of the TM domains of Vpu sequences drawn from the HIV Sequence Database (www.hiv.lanl.gov). Group M comprises 500 clade B, 200 clade C, 200 clade A, 200 clade D, 42 clade F, 48 clade G, and 7 clade H TM sequences. Arrows indicate the equivalent positions of NL4.3 Vpu A14, A18, and W22 residues. **B:** 293T cells were transiently transfected with 500 ng of HIV-1 delVpu provirus, 50 ng of tetherin plasmid, and 25 ng of the indicated Vpu expression vector. 48 hours after transfection, the resulting viral supernatants were assayed for infectivity on HeLa-TZM indicator cells by measuring β-galactosidase activity.

5.3 Discussion

In this chapter we have identified two residues, A14 and W22 in the Vpu transmembrane domain, that are important for Vpu's ability to overcome tetherin antiviral function. We found that, despite localizing to similar cellular compartments as the wild-type protein, Vpu constructs bearing these mutations were defective in mediating interactions with tetherin. As a result, these mutations also impaired the ability of Vpu to reduce cell-surface tetherin levels and by extension tetherin degradation. We then investigated whether the oligomerization state of Vpu was affected by these mutations. We found that Vpu A14L-W22A mutant was able to self-associate to form multimers and was also functional to bind to the wild-type Vpu. These results suggest that these mutations compromised interactions with tetherin by means other than interfering with the formation of Vpu multimers. It is unknown whether Vpu acts on tetherin as a monomer or whether it needs to form multimeric complexes to be able to target tetherin. The Vpu A14L-W22A domain mutant binds the wild-type Vpu protein, we therefore reasoned that if Vpu acted as a multimer to target tetherin, Vpu TM domain mutant may have a dominant-negative effect on the HIV-1 Wt viral particle release. However, we found that HIV-1 Wt particle release was not affected by addition *in trans* of Vpu A14L-W22A despite expression levels of Vpu TMD mutant ten fold higher than Wt Vpu. These data tend to support a model in which monomeric form of Vpu binds to tetherin. More studies will need to be performed to determine the exact oligomerization state and the stoichiometry of Vpu required to target tetherin.

In this study we also addressed whether the residues required for tetherin counteraction corresponded to those required for CD4 degradation. Unlike W22, mutation on residue A14 did not impact on Vpu's ability to induce CD4 downregulation. Similarly, Vpu proteins from group O HIV-1, which are functional to target CD4, also have a tryptophan residue at the equivalent position but not an alanine in position 14. These results indicate that the determinants of Vpu-mediated CD4 degradation are not only located in the cytoplasmic tail but the Vpu TM domain might also have an important role. This idea was further supported subsequently by a recent study from the Bonifacino group in which they investigated the determinants in Vpu and CD4 TM domains required for CD4 downregulation (374). They found that the W22 was required to prevent assembly of Vpu into an inactive, oligomeric form, and to promote CD4 polyubiquitination and subsequent degradation via the proteasome. While Vpu W22 did not prevent interaction with CD4, its mutation led to the accumulation of CD4 molecules in the ER membrane instead of being dislocated in to the cytosol. In the same study, the authors also identified two residues, Val20 and Ser23, in the Vpu TM domain that mediated retention of Vpu and, by extension, CD4 in the ER. In our screen, when those residues were replaced by alanine they were still functional to antagonize tetherin and promote virus release. Based on these data, it is possible that mutation of W22 might stabilize the multimeric structure of Vpu preventing monomers from being released to target tetherin. This hypothesis is in agreement with our data, as we showed that the high molecular weight forms of Vpu A14L-W22A were detected on a non-reducing Western blot at higher levels than those from Vpu Wt.

Another important aspect of this study is the fact that the residue A14, identified to be important to mediate tetherin interaction, is highly conserved in all Vpus from HIV-1 group M and N that possess an anti-tetherin function, but not in Vpu proteins from group O HIV-1 or SIVcpz that are devoid of human tetherin antagonism (226). Interestingly, a recent study showed that anti-human tetherin activity could be conferred to SIVcpz Vpu by replacing parts of its TM domain by those from HIV-1 Vpu TM domain (420). Importantly, the residues identified in our study were present in the SIVcpz Vpu that gained function against human tetherin. These data indicate that adaptation of this region of Vpu TM domain, encompassing A14 and W22, might have been driven by the zoonosis of the virus into the human population. Predicted structures of the Vpu transmembrane domain based on solid-state NMR reveals that residues A14, A18 and W22 form one face of the helix, suggesting that they might be directly involved to generate a functional binding interface with tetherin (329). By mutating those positions in the transmembrane domain we may have affected the residues directly in contact with residues in tetherin transmembrane domain or disrupted the overall conformation of Vpu protein required to mediate tetherin interaction. In accordance with these data, subsequent NMR spectroscopy-based models revealed that the conserved AxxxAxxxAxxxW helix face of Vpu TM domain directed the interaction with tetherin (386). Alanine residues in the Vpu TM domain are predicted to fit into ridges formed by large hydrophobic residues in the tetherin TM domain and W22 ensures the correct positioning of the Vpu helix within the bilayer for interaction with tetherin. Alternatively, these mutations might stabilize the formation of Vpu multimers rendering the Vpu monomers unable to target tetherin. Of note, binding of Vpu induced a chemical shift in the NMR spectrum for several tetherin TM domain residues including V30, I34, L37 and L41 (386). Without dismissing the role of Vpu acting as ion-channel to promote virus release, we have not found residues that were both involved for ion channel activity and required for tetherin antagonism in our screening.

Chapter 6
Intrinsic defects of Group O HIV-1 Vpu in counteracting Tetherin

The study detailed in this chapter was published as " Separable determinants of subcellular localization and interaction account for the inability of Group O HIV-1 Vpu to counteract Tetherin " (424).

6.1 HIV-1 Group O, imperfect adaptation of SIVcpz to humans?

Chimpanzees from west central Africa infected with SIVcpz are believed to constitute the primary reservoir of HIV-1 pandemic (reviewed in (11)). This cross-species transmission must have happened at least four times, giving rise to HIV-1 group M (major), N (non-M and non-O), O (outlier) and P. HIV-1 group M (HIV-1 M) appears to be the most virulent form and is predominantly responsible for HIV-1 pandemic. HIV-1 group O is characterized by a high genetic divergence from HIV-1 group M and most cases of HIV-1 group O infection are detected in Cameroon, where the prevalence is estimated to be about 1% of all HIV infections (15). Cases of HIV-1 O infections have also been described in countries with previous colonial links to this region such as France. Later studies have reported the identification of HIV-1 group O-like viruses in wild gorillas (425). It has been proposed that chimpanzees transmitted HIV-1 group O-like viruses either to gorillas and humans independently, or to gorillas that then transmitted the virus to humans. While HIV-1 group O-infected individuals can progress to AIDS, the spread of this virus appears to be inefficient compared to group M. However, the reasons for the lower prevalence of group O remain unknown. Vpu proteins from group M (M-Vpu) can both antagonize tetherin efficiently and mediate the degradation of CD4 (226). The ability of M-Vpu to target human tetherin is an adaptation that presumably occurred during the zoonosis of the virus to humans because SIVcpz Vpu is defective for this attribute. In contrast, the Vpu proteins from Group O HIV-1 are unable to target tetherin but still retain the ability to degrade CD4, whereas this situation is reversed in HIV-1 group N, with Vpu retaining some level of tetherin antagonism but losing activity against CD4. It has been speculated that Vpu adaptation to human tetherin may have therefore been important for the pandemic spread of HIV/AIDS (426).

In this study, we characterized the cell biological basis for the defects in the Vpu proteins from HIV-1 group O (O-Vpu) that impair their ability to antagonize tetherin.

6.2 Results

6.2.1 Group O Vpu does not overcome tetherin's antiviral action

HIV-1 group O Vpu has been shown to lack the ability to counteract human tetherin but can still induce CD4 degradation (226). To confirm this, a Vpu gene from HIV-1 group O strain 9435 was synthesized with a C-terminal HA tag and tested for its ability to block tetherin's antiviral function. 293T cells were co-transfected with a fixed dose of tetherin plasmid, increasing amounts of Vpu expression vectors, and a proviral plasmid of HIV-1 NL4.3 deleted for the Vpu gene (HIV-1 delVpu). At 48 hours post-transfection, cells were lysed and supernatants were analyzed by Western blotting for p24 and Vpu detection or titrated on HeLa-TZMbl indicator cells (Figure 6.1). As expected, a prototype M-Vpu (NL4.3) efficiently rescues virus production in the presence of tetherin. In contrast, O-Vpu of strain 9435 (O-Vpu 9435 Wt) was unable to rescue particle release from tetherin restriction, even at higher plasmid inputs, and was equivalent to an M-Vpu A14L-W22A TM mutant that we have shown previously to be defective for tetherin antagonism (221) (cf. Chapter 5). All proteins were expressed at comparable levels in cell lysates, and O-Vpu 9435 expression did not affect intracellular Gag protein synthesis (Figure 6.1B). Whereas M-Vpu runs on a Western blot as a single species, O-Vpu 9435 appears as a doublet.

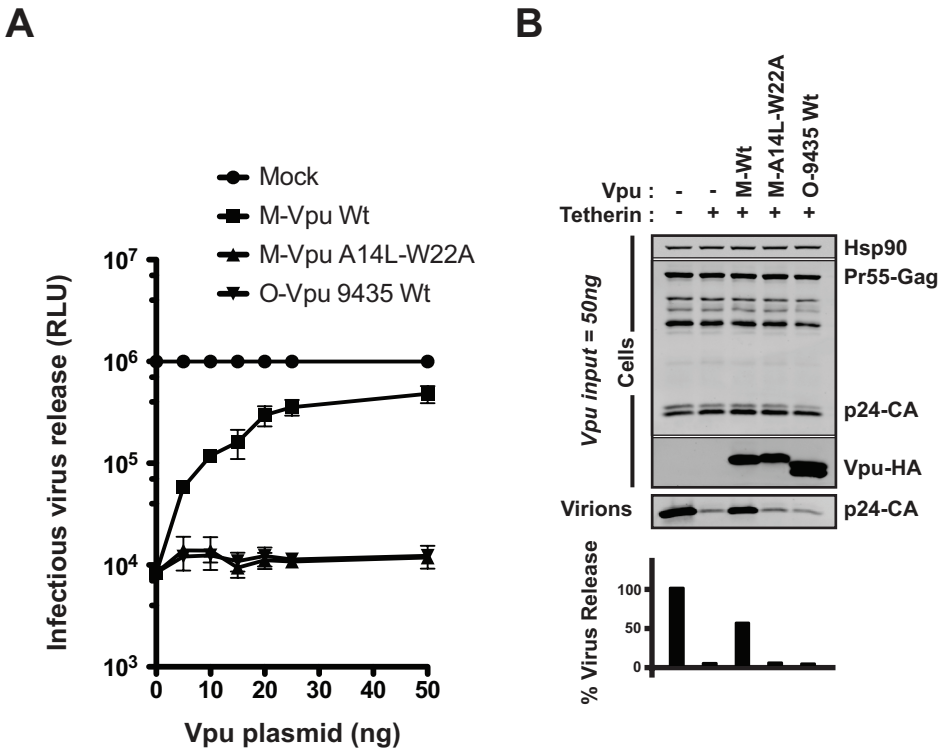

Figure 6.1: Defects in tetherin antagonism by O-Vpu 9435.

A: 293T cells were transiently transfected with 500 ng of HIV-1 delVpu provirus, 50 ng of tetherin plasmid, and increasing doses of the indicated Vpu expression vector or the empty vector control (mock). At 48 hours post-transfection, the resulting viral supernatants were

assayed for infectivity on HeLa-TZMbl indicator cells by measuring β-galactosidase activity at 48 hours post-infection. RLU, relative light units. Error bars are +/- standard error of the mean (SEM) for three independent experiments. **B:** Cell lysates and pelleted virions from cells transfected with 50 ng of Vpu plasmid were subjected to SDS-PAGE and blotted for Vpu-HA, p24-CA, and Hsp90 protein, which served as a loading control, and analyzed by a LiCor quantitative imager. Relative virus release was calculated as a percentage of the virion p24 band intensity of the no-tetherin control.

6.2.2 Lack of cell-surface tetherin downregulation by Group O Vpu

M-Vpu overcomes human tetherin by inducing its removal from the cell surface and blocking its incorporation into nascent virions. To address whether O-Vpu fails to antagonize tetherin because it cannot induce its downregulation, tetherin-positive HeLa cells were co-transfected with an empty vector control or a Vpu expression vector in combination with a GFP marker plasmid. At 48 hours post-transfection, cells were harvested and stained for surface tetherin levels (Figure 6.2). As expected in GFP-positive cells, expression of M-Vpu Wt but not M-Vpu A14L-W22A leads to a decrease of tetherin levels at the cell surface. Expression of O-Vpu 9435 had little effect on surface tetherin levels.

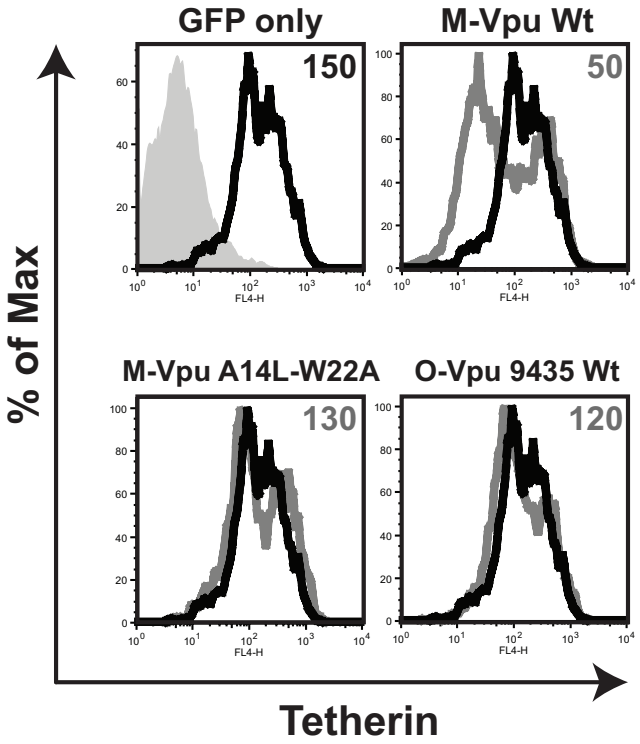

Figure 6.2: Defects in tetherin cell-surface downregulation by O-Vpu 9435.

HeLa cells were co-transfected with 400 ng of GFP marker plasmid and the indicated Vpu expression vector. At 48 hours post-transfection, endogenous surface tetherin was immunostained and expression levels were quantified by flow cytometry. Histograms represent the tetherin levels on GFP-positive gated cells in empty vector control cells (black peak) or in Vpu-expressing cells (overlaid gray peak) and are representative examples of three independent experiments. Median fluorescence intensities of the overlaid histogram are indicated in the top right corner. The solid peak histogram represents the binding of the isotype control.

6.2.3 Group O Vpu fails to interact with tetherin

M-Vpu mediates tetherin downregulation through interactions via their transmembrane domains. Mutations impairing this interaction render Vpu incapable of allowing co-immunoprecipitation of tetherin from cell lysates (221). We then assessed the ability of O-Vpu 9435 to interact with tetherin in this assay. 293T cells were co-transfected with tetherin and Vpu-HA expression vectors. Two days after transfection, cells were lysed and Vpu proteins were immunoprecipitated via the HA epitope and analyzed by Western blotting (Figure 6.3). As expected, tetherin co-immunoprecipitates with M-Vpu Wt and not with the transmembrane Vpu mutant (M-Vpu A14L-W22A). Similarly, tetherin also failed to co-immunoprecipitate with O-Vpu 9435, suggesting the lack of a direct or indirect interaction between the tetherin TMD and O-Vpu TMD.

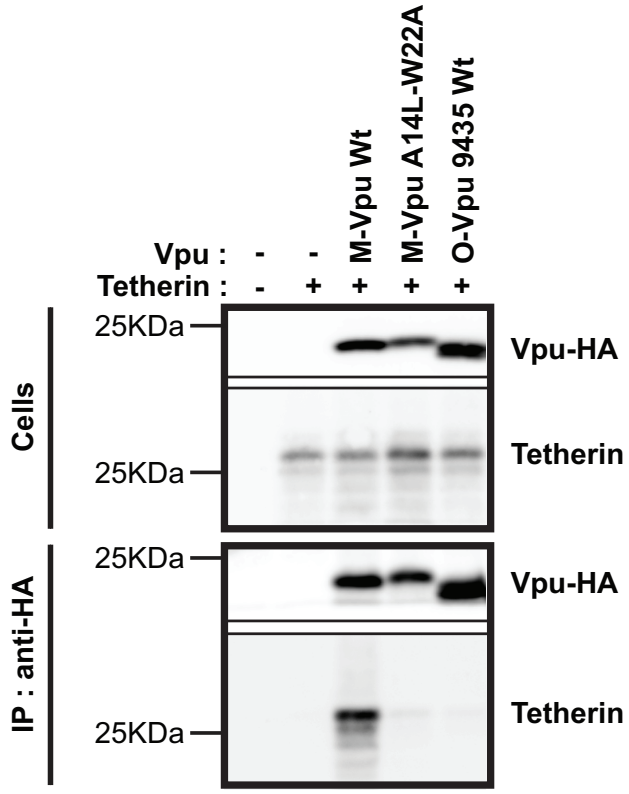

Figure 6.3: Defects in tetherin binding by O-Vpu 9435.

293T cells were transiently transfected with 500 ng of human tetherin-encoding plasmid and 500 ng of the indicated Vpu-HA expression vector. After 2 days of incubation, Vpu was immunoprecipitated (IP) via the HA tag from cell lysates and subjected to SDS-PAGE. Total cell lysates and immunoprecipitates were then Western blotted for tetherin and Vpu-HA. Molecular mass markers are indicated, and blots are a representative example of three independent experiments.

6.2.4 Group O Vpu retains the ability to downregulate CD4

Although O-Vpu bears in its sequence the key features required for CD4 downregulation, which are the tryptophan residue in the TMD (W22) and the β-TRCP binding site in the cytoplasmic tail, we tested whether our O-Vpu construct could mediate CD4 downregulation from the cell surface. CD4-positive HeLa cells were co-transfected with an empty vector control or a Vpu expression vector in combination with a GFP marker plasmid. At 48 hours post-transfection, cells were harvested and stained for surface CD4 levels (Figure 6.4). As expected in GFP-positive cells, expression of O-Vpu 9435 Wt leads to a decrease of CD4 levels at the cell surface. So, despite the defects in tetherin antagonism, this O-Vpu construct retained the ability to induce CD4 downregulation.

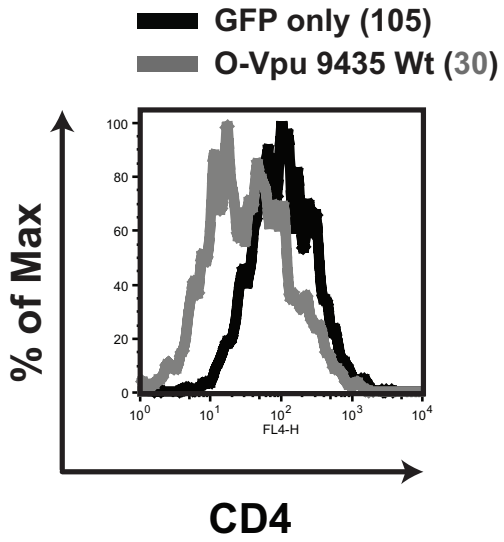

Figure 6.4: O-Vpu 9435 expression leads to a reduction of CD4 levels on the cell surface.

HeLa/CD4 cells were co-transfected with 400 ng of GFP marker plasmid and O-Vpu 9435 Wt expression vector. At 48 hours post-transfection, endogenous surface CD4 was immunostained and expression levels were quantified by flow cytometry. Histograms represent the CD4 levels on GFP-positive gated cells in empty vector control cells (black peak) or in Vpu-expressing cells (overlaid gray peak) and are representative examples of three independent experiments. Median fluorescence intensities of the overlaid histogram are indicated.

6.2.5 Group O Vpu localizes to ER-associated compartments

Group M Vpu localization in the TGN has been shown to be important to suppress tetherin restriction activity, consistent with Vpu inducing sequestration of tetherin in the TGN and preventing its transit to the plasma membrane (341, 377). Here we addressed whether the O-Vpu 9435 cellular localization accounts for its inability to block tetherin function. HeLa cells were transfected with a Vpu-HA-encoding vector. Twenty-four hours later, cells were fixed and

immunostained for Vpu-HA and either the ER marker, protein disulfide isomerase (PDI), or the *trans*-Golgi network marker, TGN46 (Figure 6.5). As expected, M-Vpu localized in perinuclear compartments that mainly overlay with TGN46-positive compartments but not with PDI. However, although a minor fraction of O-Vpu 9435 localizes in the TGN, the majority forms a reticular staining pattern that partially overlays with PDI-positive compartments, suggesting that, unlike M-Vpu, O-Vpu 9435 localizes to ER-associated compartments. Thus, the failure of O-Vpu 9435 to antagonize tetherin correlates both with its inability to interact directly with tetherin and with its lack of accumulation in the TGN.

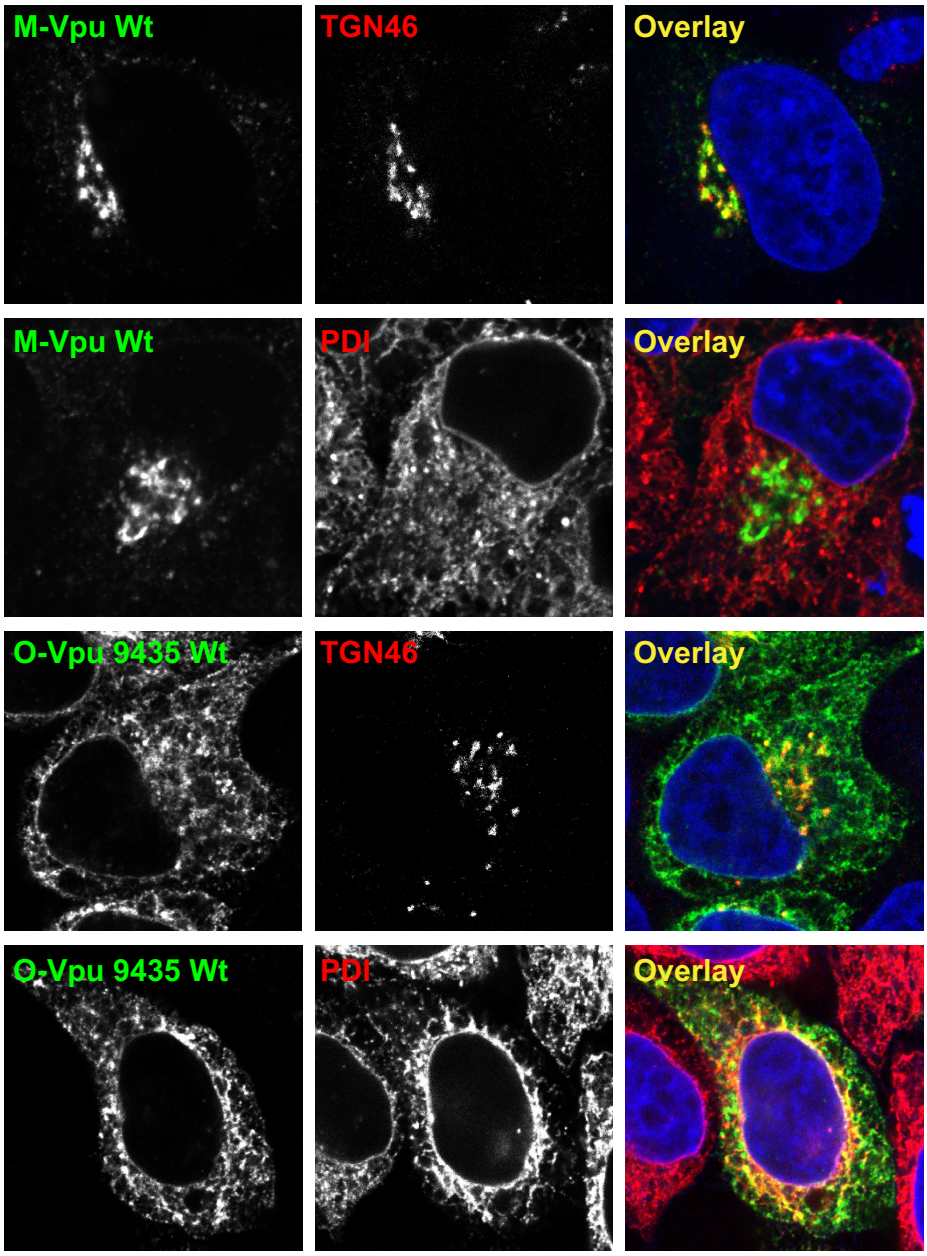

Figure 6.5: O-Vpu 9435 localizes to the ER.

HeLa cells were transfected by either 100 ng of M-Vpu Wt-HA or O-Vpu Wt-HA plasmid. Twenty-four hours later, the cells were fixed and stained for Vpu detection with anti-HA antibody (green), a TGN marker (TGN46; red), or an ER marker antibody (PDI; red) and examined by confocal microscopy. Images are representative examples of Vpu-expressing cells.

6.2.6 Retention of Vpu in the Endoplasmic Reticulum prevents tetherin antagonism

We next investigated the functional consequences of restricting Vpu expression to the ER. Vpu-induced virus release from $CD4^+$ T cells is sensitive to brefeldin A (365), suggesting that Vpu function requires post-ER trafficking. However, broad inhibition of the secretory pathway will also affect tetherin trafficking, potentially confounding this conclusion. To circumvent this, we made an M-Vpu protein bearing an ER retention signal derived from the bovine foamy virus envelope protein (-KKDQ) at the C-terminus (427). As expected, M-Vpu KKDQ shows a reticular staining overlapping with PDI-positive compartments, indicative of an ER localization (Figure 6.6A), with only a minor fraction of M-Vpu KKDQ proteins localizing with the TGN marker. M-Vpu KKDQ displays weak activity against tetherin restriction, despite increasing doses of plasmid (Figure 6.6B), indicating that post-ER trafficking of Vpu is essential for tetherin antagonism. Similarly, transfection of tetherin-positive HeLa cells reveals that M-Vpu KKDQ fails to downregulate tetherin from the plasma membrane (Figure 6.6C).

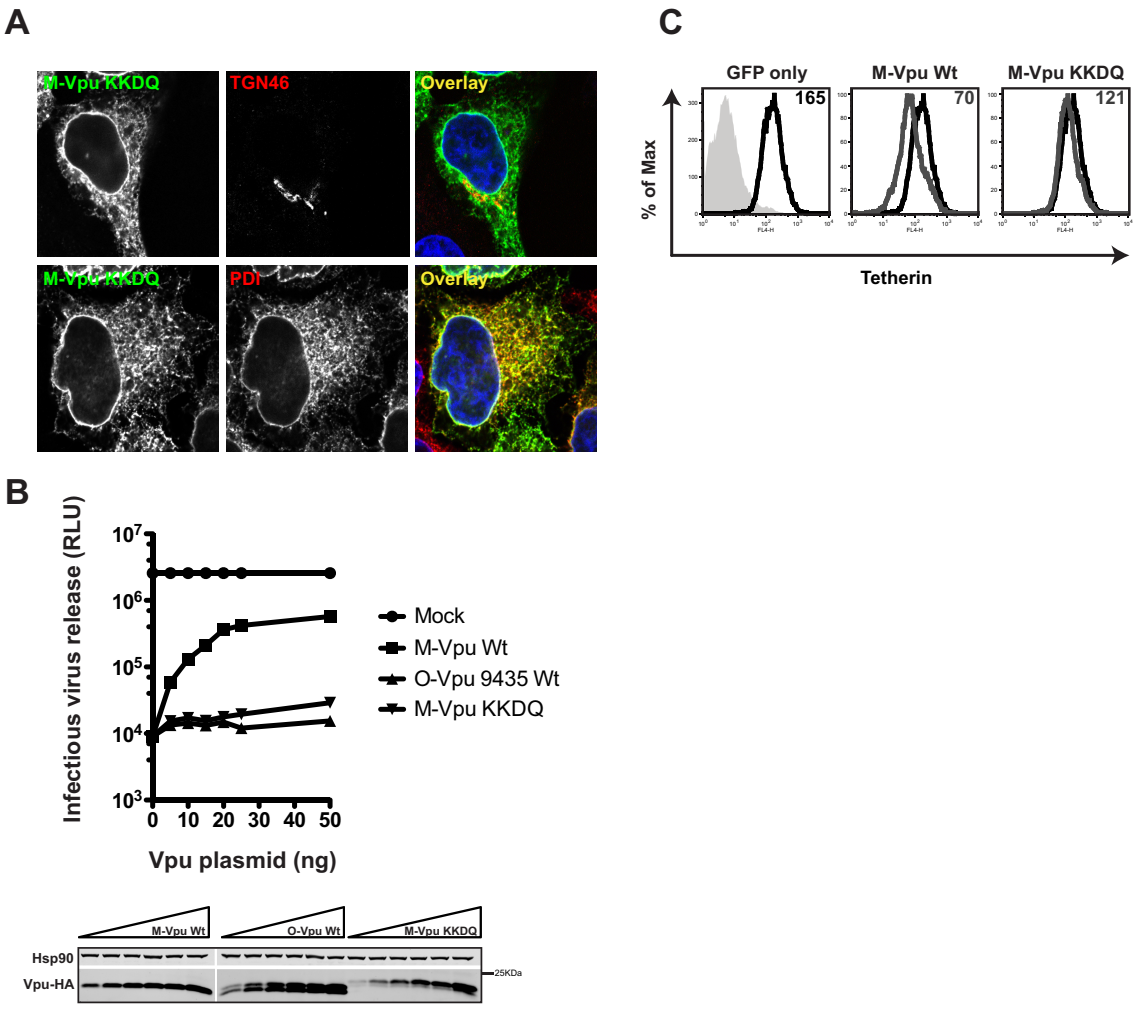

Figure 6.6: Retention of M-Vpu in the ER inhibits tetherin antagonism.

A: HeLa cells were transfected by 100 ng of M-Vpu KKDQ-HA plasmid. Twenty-four hours later, the cells were fixed and stained for Vpu detection with anti-HA antibody (green), a TGN marker (TGN46; red), or an ER marker antibody (PDI; red) and the appropriate secondary antibodies and examined by confocal microscopy. Images are representative examples of Vpu-expressing

cells. **B:** 293T cells were transiently transfected with 500 ng of HIV-1 delVpu provirus, 50 ng of tetherin-encoding plasmid, and increasing amounts of the indicated Vpu expression vector. Cells and supernatant-containing viral particles were harvested at 48 hours post-transfection. The resulting infectious virions in culture supernatants were titrated on HeLa-TZMbl indicator cells by measuring β-galactosidase activity at 48 hours post-infection. Vpu protein expression in cell lysates was analyzed by Western blotting using an anti-HA antibody. **C:** The indicated Vpu constructs were co-transfected in HeLa cells with a GFP-encoding vector, and surface tetherin levels were quantified by flow cytometry at 48 hours post-transfection. Histograms represent the tetherin levels on GFP-positive gated cells in empty vector control cells (black peak) or in Vpu-expressing cells (overlaid gray peak) and are representative examples of three independent experiments. Median fluorescence intensities of the overlaid histogram are indicated in the top right corner. The solid peak histogram represents the binding of the isotype control.

6.2.7 ER-retained Group M Vpu proteins can still interact with tetherin

M-Vpu KKDQ mimics O-Vpu cellular localization thus providing a useful tool to determine whether the inability of O-Vpu to interact with tetherin is related to its ER-cellular localization. Interestingly, preventing M-Vpu from leaving the ER does not impair its ability to interact with tetherin in co-immunoprecipitates from transient transfections (Figure 6.7A). This was not due to tetherin-Vpu interactions occurring during the immunoprecipitation, as subsequent mixing of cell lysates from 293T cells transfected with either Vpu or tetherin individually failed to yield tetherin co-immunoprecipitating with Vpu-HA (Figure 6.7B). Besides, in accordance with data from the chapter 5, in the presence of M-Vpu Wt it is mainly the low molecular weight species of tetherin that is immunoprecipitated from this transient expression system but traces of a smear of higher molecular weight can also be detected. However, with M-Vpu KKDQ only the low molecular weight forms of tetherin were pulled down. These data therefore suggest that Vpu and tetherin may interact early in the secretory pathway, but only after exit from the ER is Vpu able to exert its inhibitory effect on tetherin activity. Furthermore, these results suggest that O-Vpu 9435 localization in the endoplasmic reticulum may contribute to its deficiency in tetherin antagonism but does not account for its lack of tetherin interaction.

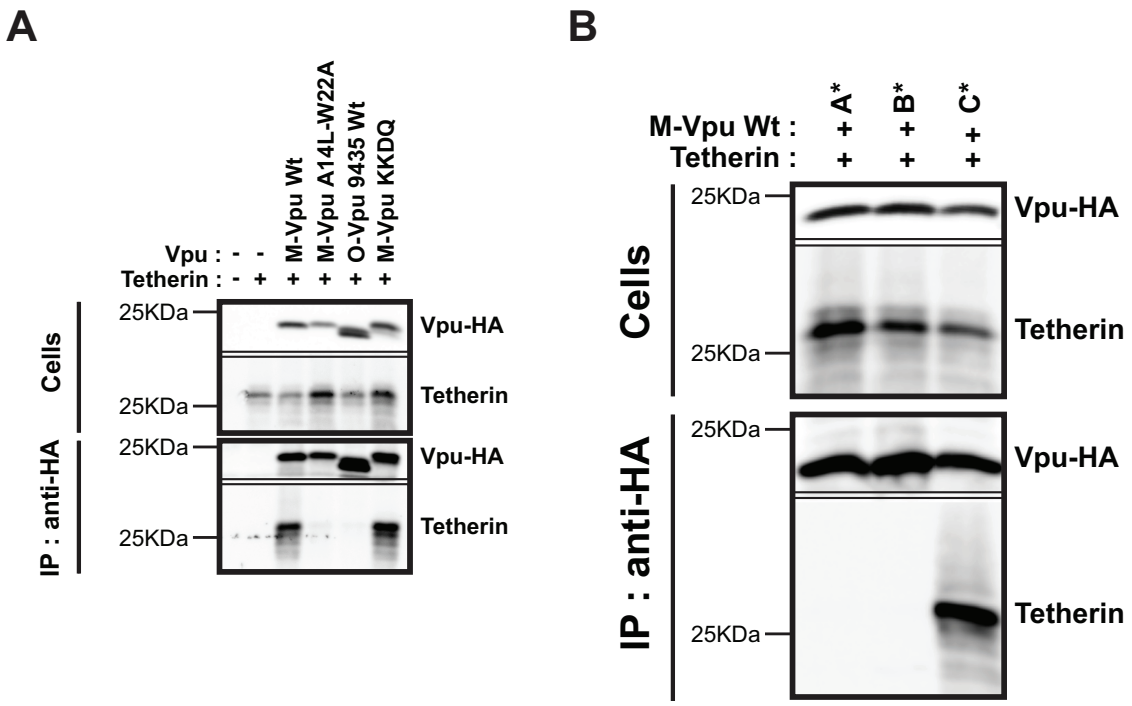

Figure 6.7: Retention of M-Vpu in the ER does not block interaction with tetherin.

A: 293T cells were transiently transfected with 500 ng of human tetherin-encoding plasmid and 500 ng of the indicated Vpu expression vector. After 2 days of incubation at 37°C, Vpu was immunoprecipitated via the HA tag from cell lysates and subjected to SDS-PAGE. Total cell lysates and immunoprecipitates were then Western blotted for tetherin and Vpu-HA detection. Molecular mass markers are indicated, and blots are a representative example of three independent experiments. **B:** Vpu and Tetherin do not interact in mixed cell lysates. 293T cells were transfected with either M-Vpu-HA or tetherin individually (samples A and B) or in combination (sample C). In sample A, the cells were removed from the plate and mixed prior to lysis, and in sample B the cells were lysed separately and post-nuclear supernatants mixed afterwards. Vpu-HA was immunoprecipitated from all three lysates as described before. Immunoprecipitates were then analyzed by Western blot using anti-HA and anti-tetherin antibodies, demonstrating that tetherin only co-immunoprecipitates with Vpu-HA from cells co-transfected with both proteins.

6.2.8 The defect in tetherin interaction maps to the transmembrane domain of Group O Vpu

We then went on to assess the minimal changes needed in O-Vpu 9435 to allow it to antagonize human tetherin. O-Vpu 9435 and M-Vpu proteins are derived from distinct SIVcpz zoonoses and as such are very diverse at the amino acid level. However, they do have basic features known to be important for CD4 degradation (Figure 6.8A): first, the conserved W residue in the TM domain and, second, the dual serine motif phosphorylated by CKII that binds to β-TrCP. After the TM domain in Vpu is a putative hinge region followed by an amphipathic alpha helix (H1), which has been proposed to lie along the face of the membrane with the

nonpolar residues partially submerged and the charged residues interacting with the polar phospholipid heads (338). In contrast, in H1 of O-Vpu the TM-proximal part of the helix is extended by a run of alternating basic and acidic residues that breaks its amphipathicity. As we identified two distinct functional defects in the O-Vpu protein, we aimed first to map the region that was responsible for the lack of interaction with tetherin. Chimeric proteins, combining M-Vpu TMD and O-Vpu CT or *vice versa*, were designed (Figure 6.8A) and tested for tetherin antagonism. We reasoned that if we found an O-Vpu chimera functional for tetherin counteraction they would be, by extension, able to mediate interaction with tetherin. 293T cells were co-transfected with a fixed amount of tetherin, Vpu, and the HIV-1 delVpu proviral plasmid. Forty-eight hours later, cells were analyzed by Western blotting and titrated on HeLa-TZMbl indicator cells (Figure 6.8B). Substitution of the two key residues from M-Vpu TMD, A14 and A18, essential for tetherin interaction (221), into O-Vpu TMD did not result in a functional O-Vpu mutant (O-Vpu B). Similarly, chimeras composed of O-Vpu TMD and M-Vpu CT (Vpu OTM-MCT) were unable to enhance particle release in tetherin-expressing cells. The opposite mutant designed by adding the equivalent determinants of M-Vpu TMD into O-Vpu TMD (Vpu OBTM-MCT) did not gain function to suppress tetherin restriction. However, two chimeras that were both composed of an intact M-Vpu TMD gained function against tetherin either in the context of the O-Vpu cytoplasmic tail (Vpu MTM-OCT) or with the M-Vpu first alpha helix (Vpu MTM-MH1-OH2). However, as the lack of antagonism might be due to additional defects and not only the inability to interact, we also checked the ability of the Vpu mutants mentioned above for interacting with tetherin. As expected, Vpu MTM-OCT and Vpu MTM-MH1-OH2 were effective at co-immunoprecipitating tetherin molecules (Figure 6.8C). However, O-Vpu B, Vpu OTM-MCT, Vpu OBTM-MCT failed to pull-down tetherin from cell lysates. Therefore, only O-Vpu mutants bearing the transmembrane from M-Vpu were functional to mediate tetherin interaction. Altogether these data suggest O-Vpu's incapacity to bind tetherin seems to be an intrinsic defect of its transmembrane domain.

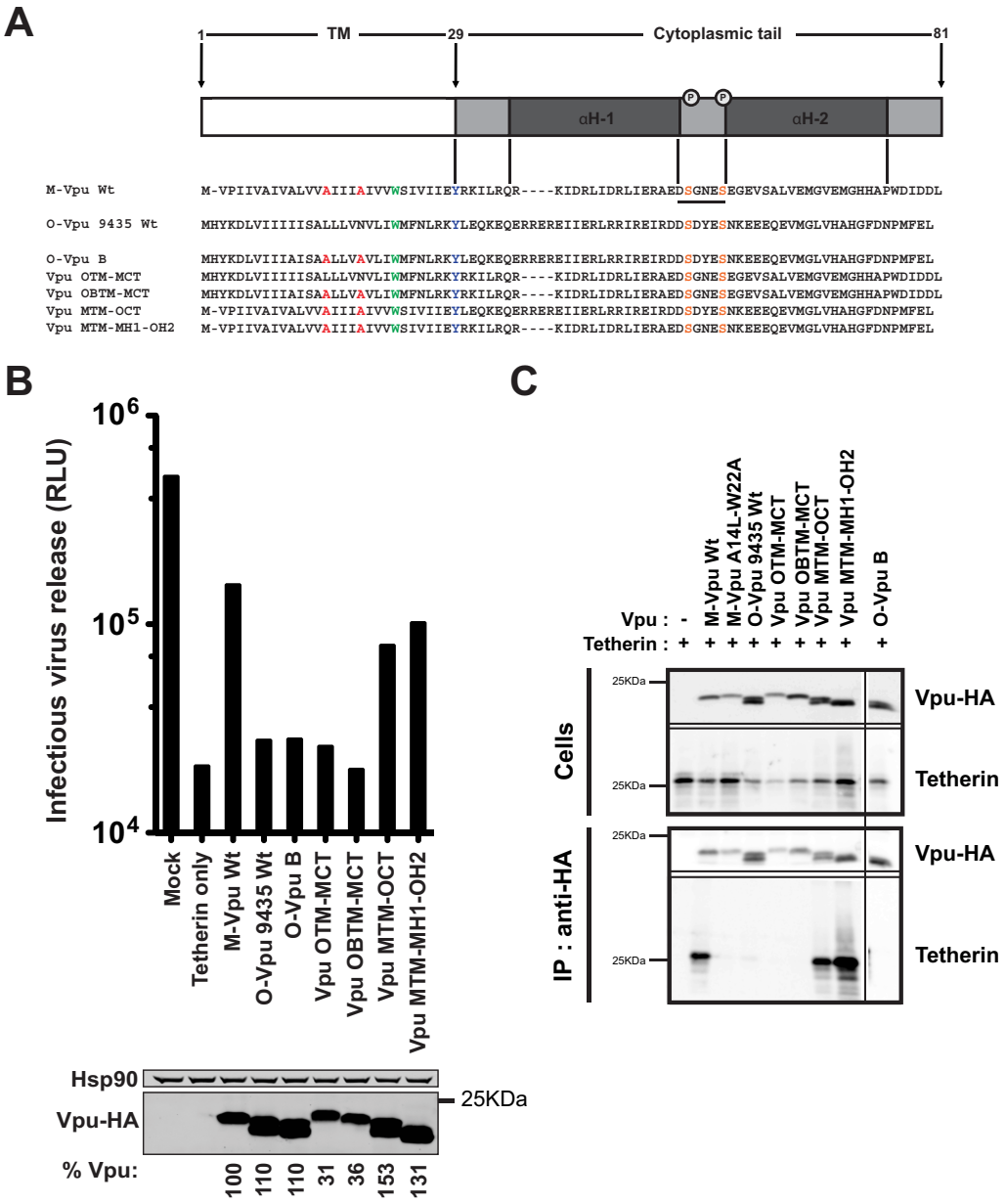

Figure 6.8: O-Vpu TMD accounts for the lack of tetherin interaction.

A: Schematic representation of the Vpu topology and alignments comparing Vpu sequences from HIV-1 group M and group O or the indicated mutants. **B:** 293T cells were transfected with the HIV-1 delVpu provirus, a fixed dose of tetherin plasmid, and the indicated Vpu construct. After 2 days, viral supernatants were assayed on HeLa-TZMbl indicator cells and cells lysates were analyzed by Western blotting for Vpu-HA and Hsp90. Numbers below indicate the Vpu expression levels normalized with Hsp90 expression levels compared to the M-Vpu Wt protein expression. **C:** The indicated Vpu construct was co-expressed in 293T cells with 500 ng of human tetherin-encoding plasmid. At 48 hours post-transfection, cells were lysed and Vpu proteins were isolated via immunoprecipitation and subjected to SDS-PAGE. Both tetherin and Vpu-HA expressions were visualized on a Western blot using the appropriate antibodies. Western blots are representative examples of three independent co-IP experiments.

6.2.9 The defect in TGN localization maps to the first alpha helix of Group O Vpu

We then investigated the region in the O-Vpu sequence that was responsible for its accumulation in the endoplasmic reticulum. We found that by adding the M-Vpu cytoplasmic tail into O-Vpu changed its ER-associated cellular localization to the TGN. Vpu OTM-MCT, Vpu OBTM-MCT displayed colocalization in HeLa-transfected cells with the TGN marker, TGN46 (Figure 6.9). These data suggest that the cytoplasmic tail of O-Vpu is involved in the retention of the protein in the ER.

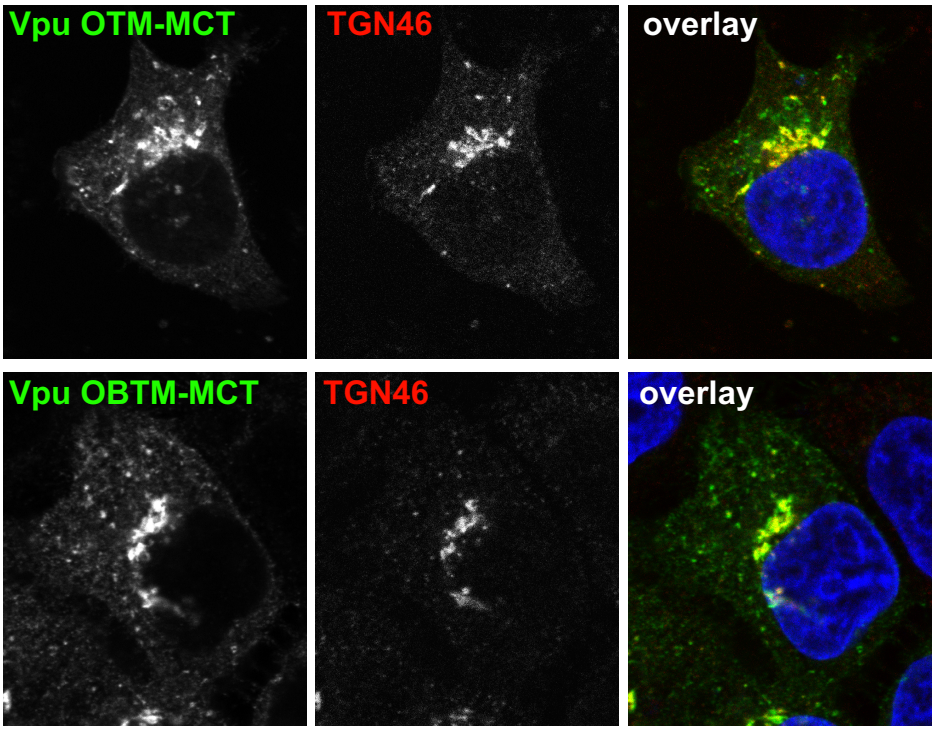

Figure 6.9: O-Vpu mutants bearing M-Vpu cytoplasmic tail localize to the TGN.

HeLa cells were transfected by 100 ng of Vpu OTM-MCT or Vpu OBTM-MCT. Twenty-four hours later, the cells were fixed and stained for Vpu detection with anti-HA antibody (green) and a TGN marker (TGN46; red), the appropriate secondary antibodies and examined by confocal microscopy. Images are representative examples of Vpu-expressing cells.

We then checked whether the first or the second alpha helix of the M-Vpu cytoplasmic tail conferred TGN localization. Interestingly, although they both were able to mediate tetherin interaction, only Vpu MTM-MH1-OH2 but not Vpu MTM-OCT was associated with TGN46 positive compartments suggesting that the O-Vpu first alpha helix was responsible for the cellular repartition in the ER (Figure 6.10A). Since these two mutants were both functional for tetherin antagonism despite distinct subcellular localization, we re-screened them against a fixed dose of tetherin but with various expression levels of Vpu (Figure 6.10B). Only Vpu MTM-

MH1-OH2 gained function against tetherin restriction at lower plasmid inputs and at higher expression had activity almost to the levels of M-Vpu Wt. In contrast, Vpu MTM-OCT achieved only a low efficiency of tetherin antagonism, even at the highest plasmid concentrations. This data is consistent with the importance of Vpu association with the TGN for tetherin counteraction (341). Therefore, only Vpu proteins bearing an intact M-Vpu TMD in the context of the first alpha helix of M-Vpu cytoplasmic tail can overcome tetherin's restriction. The simultaneous replacement of the tetherin interaction domain (TM) in the context of the first alpha helix (H1) of M-Vpu sequences that permit TGN localization is thus required for full antagonism of tetherin.

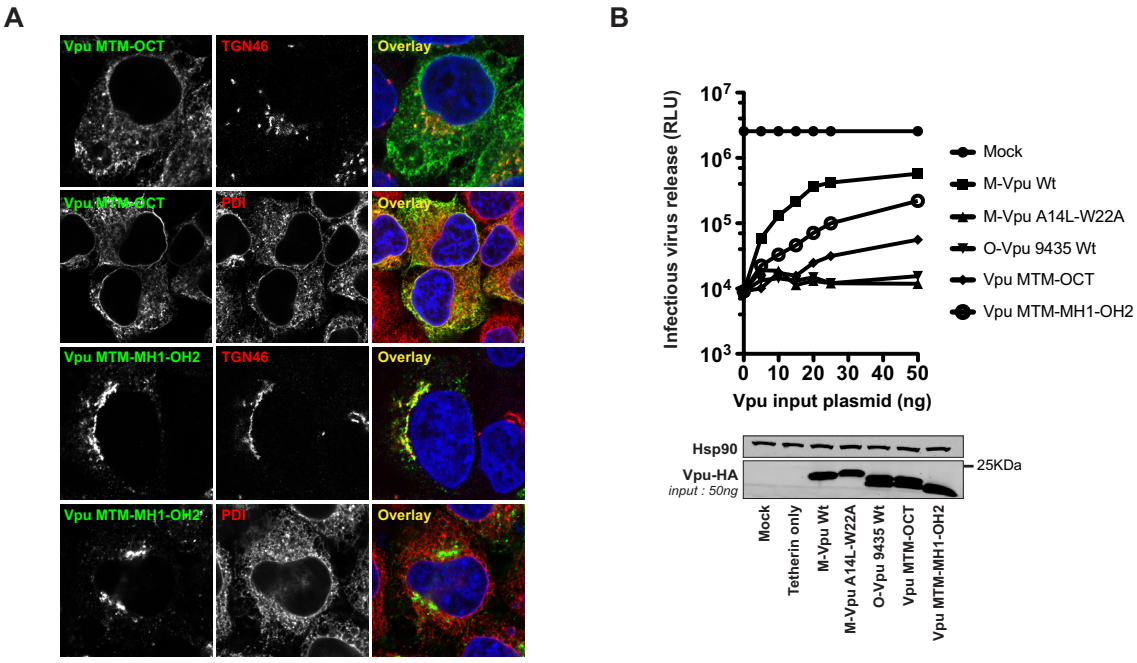

Figure 6.10: Defects in O-Vpu can be rescued by replacement of the TM domain in the context of the M-Vpu first alpha helix.

A: The indicated Vpu-HA chimeras (green) were transiently expressed in HeLa cells and co-immunostained either with a TGN marker (TGN46; red) or with an ER marker (PDI; red). Images are representative examples of Vpu-expressing cells. **B:** 293T cells were transfected with the HIV-1 delVpu provirus, a fixed dose of tetherin plasmid, and various doses of the indicated Vpu mutants added *in trans*. After 2 days, viral supernatants were assayed on HeLa-TZMbl indicator cells and cells lysates from cells transfected 50 ng of Vpu plasmid were subjected to SDS-PAGE and blotted for Vpu-HA and Hsp90.

6.2.10 A single glutamic acid-to-lysine change in the cytoplasmic tail confers Group O Vpu localization to the TGN

We next investigated the determinants in the H1 domain of O-Vpu that account for its localization to the ER. First, we assessed whether ER retention of our O-Vpu 9435 was representative of the known available sequences. To this end, we synthesized an HA-tagged

consensus O-Vpu (O-Vpu cons) from all the full-length sequences available in the HIV Sequence Database (http://www.hiv.lanl.gov) (n=32) and, additionally, the Vpu from the strain HJ001 (226). As expected, both proteins were defective for counteracting tetherin from transiently transfected 293T cells (Figure 6.11A) and failed to interact in co-immunoprecipitations (Figure 6.11B), consistent with our previous observations. When we examined their subcellular localization, however, we observed that while O-Vpu consensus was again retained in the ER, HJ001 Vpu displayed a more prominent localization to the TGN (Figure 6.11C).

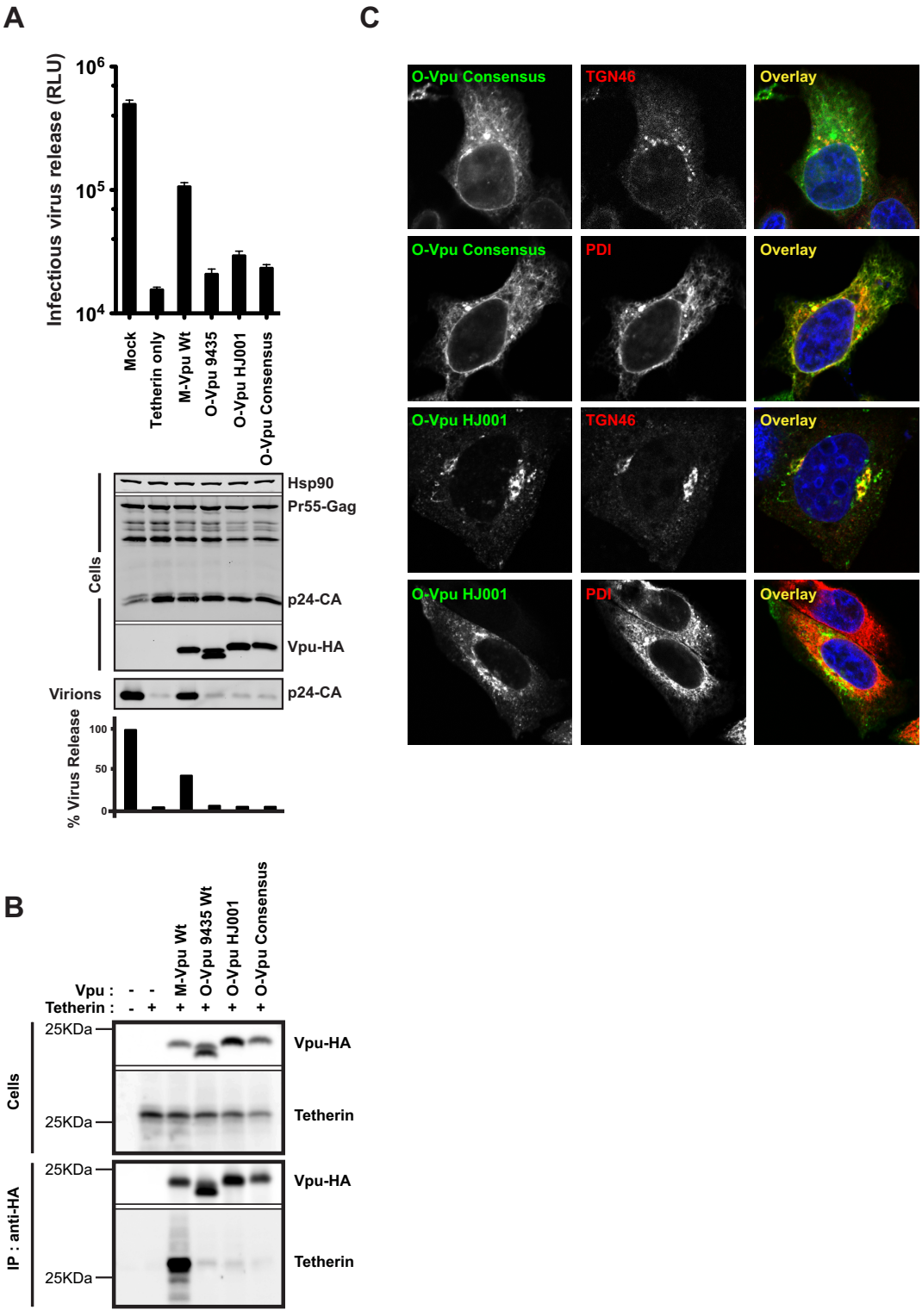

Figure 6.11: Anti-tetherin activities and subcellular localizations of a consensus O-Vpu and O-Vpu HJ001.

A: Counteraction of tetherin-mediated restriction of HIV-1 delVpu from transfected 293T cells by the indicated O-Vpu-HA construct and corresponding Western blots of cell lysates and pelleted virions. Error bars are +/- standard error of the mean (SEM) for three independent experiments. **B:** Co-immunoprecipitation of O-Vpu-HA proteins with tetherin from transiently transfected 293T cells as described previously. **C:** Subcellular localization of the indicated O-Vpu-HA (green) in transfected HeLa cells co-stained either with a TGN marker (TGN46; red) or with an ER marker (PDI; red). Images are representative examples of Vpu-expressing cells.

Alignment of the H1 domains of these proteins revealed that a major difference in HJ001 was a membrane-proximal K residue at position 32 instead of an E in O-Vpu cons and 9435 (Figure 6.12A). This lysine was present in only a minority of O-Vpu sequences, suggesting that the acidic residue is representative of HIV-1 group O. Interestingly, position 32 in O-Vpu is equivalent to K31 in M-Vpu, which is embedded within the putative membrane-proximal hinge YRKILR. Mutation of R30-K31 to alanines in HIV-1 NL4.3 Vpu was previously shown to lead to an endosomal localization and a concomitant decrease in anti-tetherin activity (341). To determine whether this residue also plays a role in O-Vpu localization, we replaced the hinge region with the equivalent part of M-Vpu in the context of the M-Vpu TM domain (MTM-RKILR-OCT). In addition, we also made the E32K point mutation in O-Vpu 9435 and MTM-OCT. Examination of the localization of these Vpu proteins revealed that unlike the parental O-Vpu, MTM-RKILR-OCT, MTM-OCT E32K, and O-Vpu E32K all displayed localization to TGN46-positive compartments (Figure 6.12B). These data suggest that a single point mutation in the first alpha helix of O-Vpu cytoplasmic tail is sufficient to abolish ER retention.

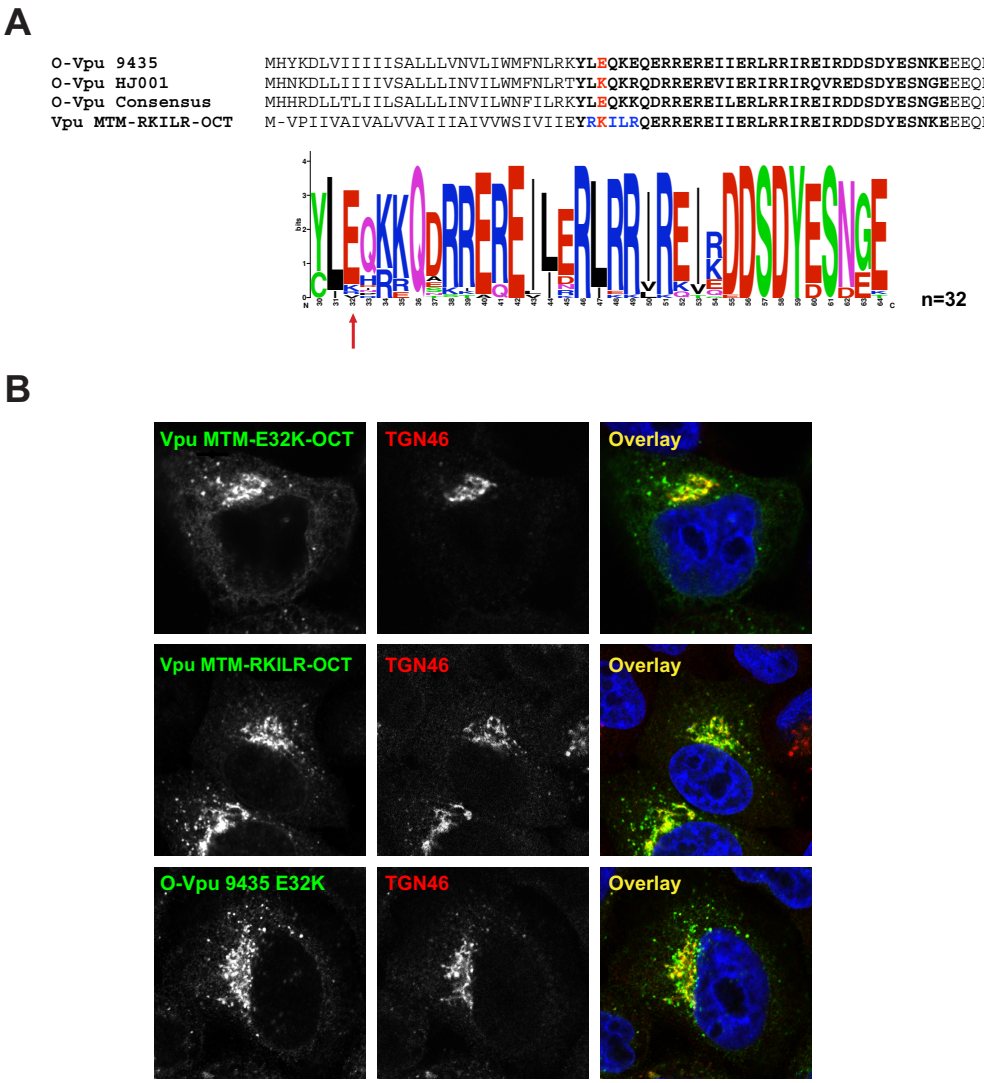

Figure 6.12: An E32K point mutation confers TGN localization to O-Vpu.

A: Alignment of the consensus O-Vpu, O-Vpu 9435, and O-Vpu HJ001 sequences (above) and expanded logoplot of the amino acid sequences of the first alpha helix of publicly available O-Vpu sequences (n=32) (below). Position E32 is indicated (red arrow). **B:** Subcellular localization of the indicated O-Vpu-HA (green) in transfected HeLa cells co-stained with a TGN marker (TGN46; red). Images are representative examples of Vpu-expressing cells.

6.2.11 Minimal changes to render Group O Vpu a tetherin antagonist

We established that O-Vpu was defective both for tetherin binding and also in its subcellular localization. These attributes are separable to the TM domain and the membrane-proximal hinge region of the first alpha helix of the cytoplasmic tail, respectively. We identified that O-Vpu binding to tetherin could be generated by replacing the entire TM domain from M-Vpu. As for the subcellular localization, substitution of the residue E32 in its first alpha helix by a lysine

could confer O-Vpu localization in the TGN. We then attempted to combine these modifications into a single O-Vpu mutant to see whether we could recapitulate tetherin antagonism in O-Vpu proteins. When transfected into 293T cells with tetherin, MTM-RKILR-OCT and MTM-OCT E32K both regained function equivalent to that of the MTM-MH1-OH2 chimera, indicating that this single amino acid change was sufficient to enhance tetherin antagonism (Figure 6.13). As expected, the E32K change on its own did not confer tetherin antagonism to O-Vpu due to its TM domain's inability to interact with tetherin. Therefore, an E32K point mutation confers TGN localization and tetherin antagonism to O-Vpu bearing the group M TM domain. A single acidic residue present in the hinge region of the majority of O-Vpu sequences precludes the protein from leaving ER-associated compartments and is responsible for their poor activity against human tetherin even when TM-mediated interaction is restored.

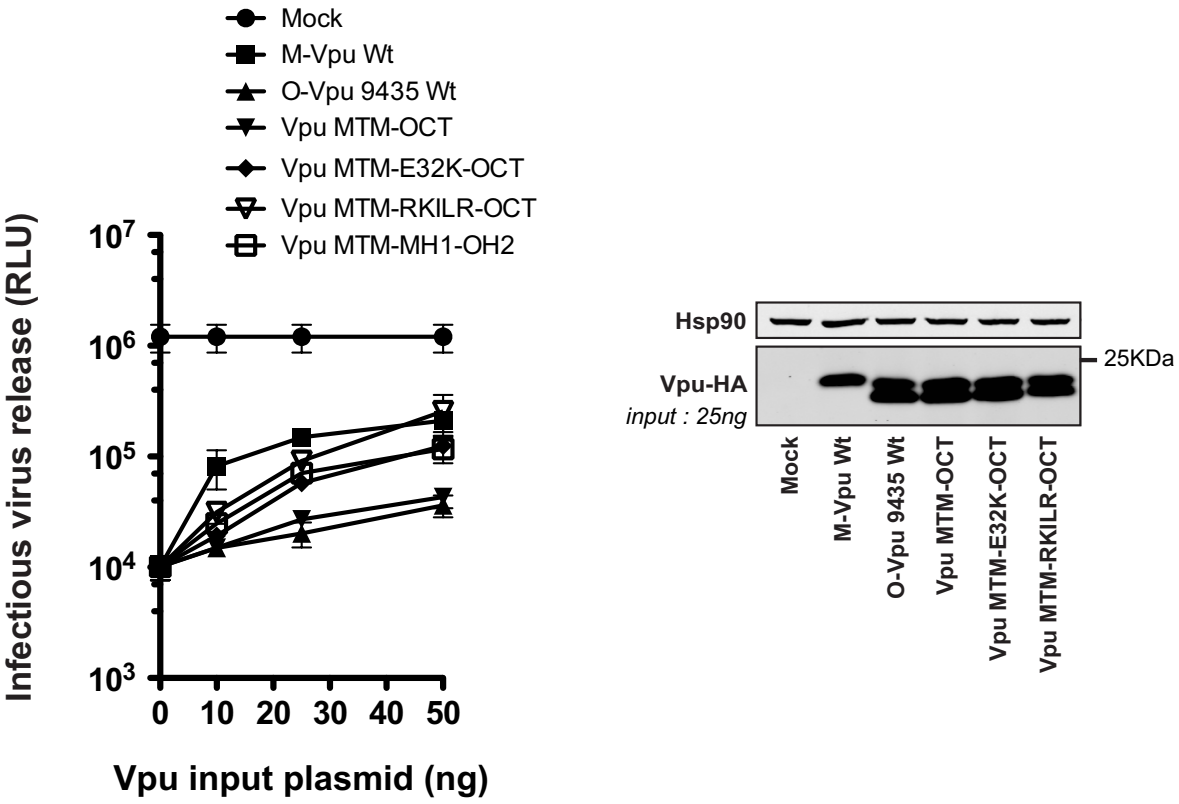

Figure 6.13: An E32K point mutation confers tetherin antagonism to O-Vpu bearing M-Vpu TM domain.

293T cells were transfected with 500 ng of HIV-1 delVpu, 50 ng of tetherin, and various doses of the indicated Vpu-HA construct and processed as described previously.

6.3 Discussion

The Vpu proteins of most group M viruses tested in a recent study can counteract human tetherin (226). By contrast, group O Vpu proteins are defective for this attribute, and in the few sequences from group N, Vpu counteraction of tetherin is variable. In this chapter, we have addressed the molecular and cell biological basis for the difference between M-Vpu and O-Vpu proteins. We have shown that O-Vpu is defective for tetherin antagonism for two reasons. First and most important, its TM domain lacks the capacity to interact with tetherin in co-immunoprecipitations. However, the ability to bind tetherin is not sufficient to confer antagonism to O-Vpu. Secondly, O-Vpu appears to be retained in the ER and fails to localize to the TGN. This maps to the first alpha-helix of the cytoplasmic tail, specifically, a glutamic acid residue at position 32, found in the majority of O-Vpu sequences. Replacement of this region is also required for efficient tetherin antagonism and TGN localization. We showed previously that mutation of conserved residues A14, A18, and W22, which form one face of the M-Vpu TM domain, impairs tetherin interaction and antagonism (221). The A14 and A18 positions are conserved in M- and N-Vpu proteins but not in group O or SIVcpz Vpu proteins, suggesting that changes to this face of the TM domain helix may have been driven by adaptation of HIV-1 Vpu to human tetherin. In line with this observation, a recent study showed the importance of the conserved face AxxxAxxxAxxxW of Vpu TM domain for directing tetherin binding (386). However, replacement of these residues is not sufficient to confer tetherin interaction to O-Vpu. Moreover, in attempts to delineate the minimal requirements to render the O-Vpu TM domain capable of mediating tetherin antagonism in the context of MTM-MH1, no chimeric TM domain gained function. These results suggest that the functional binding interface of Vpu with tetherin is likely to be contextually dependent on the entire conformation of the TM domain.

The retention of O-Vpu in ER-associated compartments confers a defect to antagonism even when interaction with tetherin is mediated through a chimeric TM domain. This can be partially overcome by increased Vpu expression, which we interpret as being due to minor amounts of O-Vpu being observable in the TGN at high expression levels. Several years ago Schubert and Strebel demonstrated that brefeldin A inhibited Vpu-mediated HIV-1 release from infected $CD4^+$ T cells (365), and the same laboratory has recently confirmed these data, in the light of the discovery of tetherin (381). However, because brefeldin A blocks the bulk flow of secretory proteins from the ER, including tetherin, we attempted to alleviate any potential confounding factors by appending a strong ER retention signal to M-Vpu. ER-retained M-Vpu was clearly defective for tetherin antagonism, but unlike O-Vpu, it was still able to interact with tetherin in co-immunoprecipitates, in contrast to a recent report (428). This suggests that while tetherin and Vpu can interact in the ER, antagonism of tetherin function requires trafficking of Vpu-tetherin complexes into TGN compartments. Recent data from the Strebel group have further shown that under overexpression conditions, Vpu can induce ER-associated degradation of newly synthesized tetherin, but this does not happen in virus-infected cells (381). Thus, if Vpu and tetherin do interact prior to ER exit, the appending of the KKDQ motif leads to disruption of this interaction when the Vpu is retrieved from the cis-Golgi network. However, to definitively

show whether this is the case will require further fluorescence resonance energy transfer-based microscopy studies of Vpu-tetherin interactions in living cells.

The inability of O-Vpu to exit the ER maps to the membrane-proximal region of the first alpha helix of the cytoplasmic tail. The amphipathic nature of helix 1 is thought to allow it to lie partially buried along the face of the membrane with the basic residues in contact with the phospholipid heads (338). Between the TM domain and the first alpha helix is a putative hinge region, the basic residues of which in subtype B Vpu proteins have been implicated in endosome-to-TGN localization when mutated to hydrophobic residues (341). We found that replacement of the hinge region in O-Vpu 9435 with the corresponding RKILR of M-Vpu conferred both TGN localization and efficient tetherin antagonism when combined with the M-Vpu TM domain. This phenotype mapped to an acidic residue (E32) in the position equivalent to M-Vpu K31 that is conserved in the majority of O-Vpu proteins. Since the reverse mutation in M-Vpu did not lead to its ER retention (not shown), these data suggest to us that it is unlikely that this is a specific TGN-targeting motif itself. Rather, we suggest that the distribution of basic and acidic residues in the membrane-proximal region of the O-Vpu may influence the overall conformation of the cytoplasmic tail in relation to the membrane and that the retention of O-Vpu in ER-associated compartments may be related to such a structural change. It is interesting to note that O-Vpu 9435 and chimeric molecules bearing its first alpha-helical region run as a doublet on SDS-polyacrylamide gels, perhaps suggesting potential differences in conformation or phosphorylation. Since O-Vpu still downmodulates CD4, a process that requires interaction with the Vpu cytoplasmic tail and its phosphorylation, such putative conformational differences do not affect this ER-associated process. However, they do preclude tetherin antagonism without high overexpression. Interestingly, while the majority of O-Vpu proteins have an E at position 32, a minority of sequences has K at this position and hence display increased TGN localization (exemplified by O-Vpu HJ001). The lack of a TMD-mediated interaction still precludes tetherin antagonism in this case.

In line with our findings, Petit et al, showed that both the transmembrane proximal domain and the TM domain of NL4.3 Vpu were essential for conferring anti-human tetherin activity to HIV-1 Group M Vpu (429). In this study they used different strains of O-Vpu (BCF06 and Ca9) and they could confer TGN localization to O-Vpu chimera bearing the TM domain from M-Vpu when residues I32 and L33 within the YXXφ motif of the M-Vpu proximal region were incorporated into O-Vpu BCF06. They hypothesized that one of the reason why O-Vpu BCF06 and Ca9 were defective was due to their ability to disrupt the TGN compartment.

The Vpu protein of SIVcpz is able to downregulate CD4 but cannot target tetherin, presumably because this function became redundant when the ancestral virus acquired a tetherin-antagonizing Nef protein from the SIVrcm lineage (226). Unlike the result with the TM domain of O-Vpu, replacement of the TM domain of consensus SIVcpzUS Vpu with that of HIV-1 M-Vpu is sufficient to confer tetherin antagonism (420). Groups M, N, O, and P represent four distinct zoonoses of SIVcpz strains to humans. Group O is also highly related to SIVgor, suggesting that both viruses have derived from the same SIVcpz strain relatively recently (less than 200 years) (430, 431). Whether group O was acquired directly from gorillas or whether

these are separate zoonoses of the same virus from chimpanzees is not clear. However, they were transmitted to humans, and in each case the zoonotic virus would have initially been unable to target human tetherin due to the loss of the Nef-targeting determinant in the human protein's cytoplasmic tail (225-227). In the case of groups M and N, it is likely that the TM adaptation of the SIVcpz Vpu proteins was sufficient to adapt to tetherin antagonism, although N-Vpu proteins appear to have lost the ability to degrade CD4, the reason for which is unclear at present. HIV-1 group N Vpu might have acquired additional functions at the expense of the ability to target CD4. CD4 targeting is conserved in all other known HIV-1/SIV Vpu proteins, indicating that this is also an essential function and is maintained, despite Nef performing a similar role, further suggesting spatial and temporal differences for CD4 targeting. It is interesting to speculate that the competing pressure to maintain CD4 degradation in the more distantly related SIVcpz that gave rise to HIV-1 group O precluded its adaptation to human tetherin because of its ER retention. In SIVcpz infections in chimpanzees, the requirement of the protein to leave the ER efficiently may have been under less pressure to be maintained because SIVcpz Nef antagonized tetherin in this species and was lost. Of note, HIV-1 group O Nef proteins seem to have lost some of their Nef-associated anti-CPZ-tetherin activity following transmissions to humans. Alternatively, if group O was primarily derived from SIVgor, these differences in Vpu may be a reflection of the SIVcpz Vpu adaptation to new hosts in relatively quick succession. To understand this further, more detailed molecular and cellular characterization of SIV Vpu proteins is required.

It has recently become clear that primate lentiviruses are under evolutionary pressure to maintain an activity that counteracts tetherin. That O-Vpu and at least some N-Vpu proteins have no such activity has led to speculation that this Vpu function may account for the lack of efficient spread of groups N and O in humans compared to group M (426). Furthermore, evidence from HIV-2 in human and Nef-defective SIVmac-infected macaques suggests that when tetherin antagonism is compromised, viruses that restore the activity in their envelope glycoproteins can emerge (230, 231, 235). It should be borne in mind that group N and O viruses still retain the capacity to cause AIDS in infected individuals, and at present, it is not known whether the failure of O-Vpu to adapt to human tetherin has forced the acquisition of tetherin antagonism on the O-group Env. This is all the more plausible given that there is at least one documented case of an HIV-1 envelope glycoprotein with Vpu-like activity (432). But it cannot be excluded that tetherin antagonism in certain HIV-1 strains might not be absolutely required for disease progression, as suggested by recent studies showing that HIV-1 group P was unable to antagonize human tetherin by Vpu, Env or Nef (433).

Chapter 7
Targeting of the glutamine transporter SNAT-1 by HIV-1 Vpu

7.1 Introduction

7.1.1 SNAT-1, a new cellular target of HIV-1 Vpu

In the past few years the accessory proteins and their associated functions have been extensively studied to better understand their importance for HIV-1 replication. In some cases, these accessory proteins are not limited to one single cellular target. The panel of Vpu's targets is increasing. Well known to downregulate CD4 receptor from infected T cells, Vpu came again into full focus with the discovery of tetherin as a novel target. Since then, Vpu has been extensively studied and the panel of Vpu's cellular targets expanded considerably with a total of 5 cellular proteins characterized so far (cf. Chapter 1).

For the purpose of finding new host proteins targeted by Vpu during HIV-1 infection, we have collaborated with Paul Lehner's group in Cambridge. To address this project, we have examined the effects of Vpu expression on the plasma membrane proteomic profile of a derived $CD4^+$ T-cell line (Jurkat). Protein abundance between cells stably expressing Vpu and control cells lacking Vpu expression was compared. Jurkat cells stably expressing the Vpu protein (Jurkat-Vpu) were generated by retroviral transduction using an MLV-based vector also conferring, once integrated into the host genome, resistance to puromycin. A control cell population (Jurkat-EV) was also made using the empty version of the vector used to express Vpu. The two cell populations mentioned above were subjected to SILAC (stable isotope labelling by amino acids in cell culture) analyses (Figure 7.1). This technique relies on the metabolic incorporation of light and heavy forms of specific amino acids. In our study, the Vpu positive cell line was grown in culture medium supplemented with isotopically labelled lysine and arginine resulting in the generation of ''heavy'' proteins. In contrast, cells lacking Vpu expression were cultivated in normal medium, and incorporated consequently ''light'' amino acids during protein synthesis. Then, cell extracts from both populations were treated in order to isolate plasma membrane proteins. The subsequent digestion of all membrane proteins with the serine protease, trypsin, generates a large panel of peptides, each of them corresponding to a unique protein. A unique protein can be identified by several peptides. The peptides are then separated and analysed by mass spectrometry (LC-MS: Liquid Chromatography and Mass Spectrometry). Pairs of identical heavy and light peptides can be differentiated via their mass difference and the height of the peak provides their corresponding abundance in the cell population. For instance, if the expression level of a given protein is not affected under Vpu expression the intensities of the light and heavy peaks will be equal. On the contrary, in conditions where Vpu induces changes in a protein's abundance, the height of the heavy peak will become either lower (Vpu inducing downregulation) or higher (Vpu inducing upregulation) compared to the control cells.

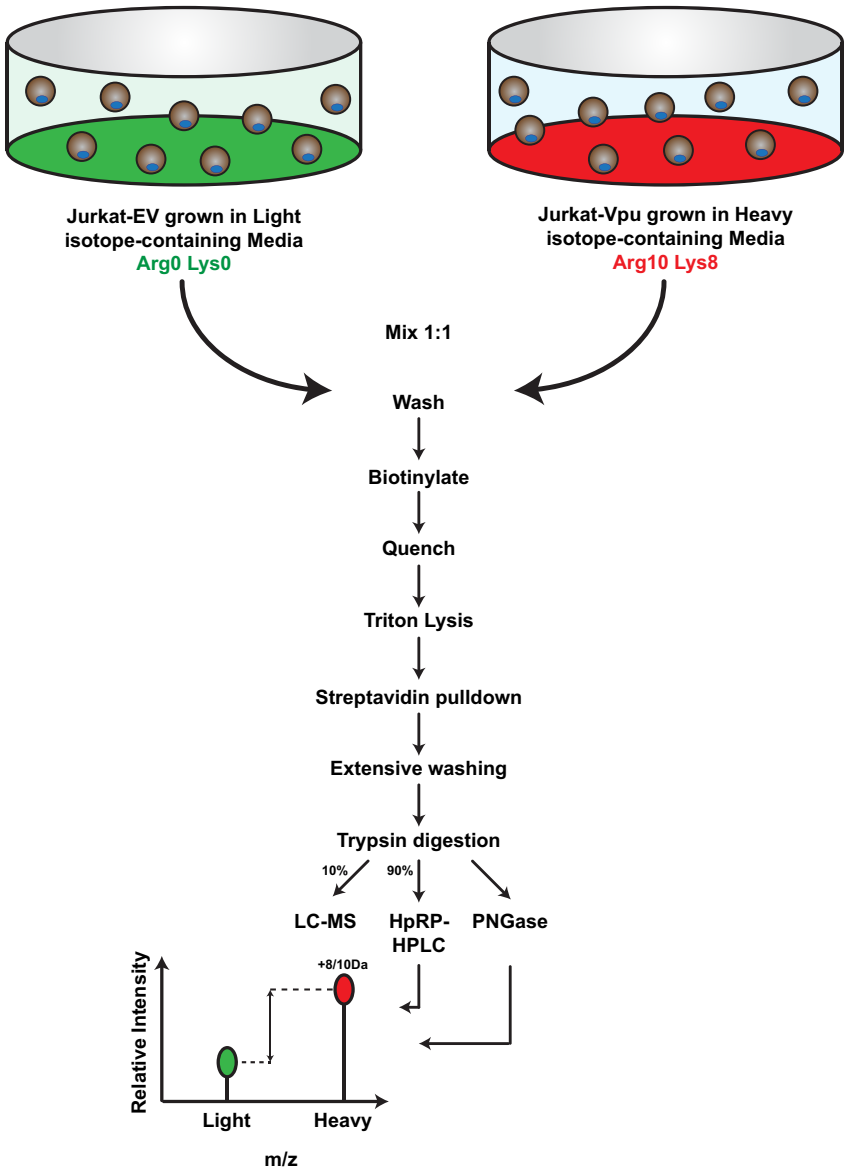

Figure 7.1: Schematic representation of the SILAC Labelling and Purification Protocol.

Experimental procedure used to identify plasma membrane proteins affected by Vpu expression. Method adapted from (434).

With this method, Paul Lehner's group identified 814 unique membrane proteins. Among those proteins, 226 were not affected by Vpu expression (ratio light/heavy =1), 270 were upregulated (ratio light/heavy <1) and 318 proteins were expressed at lower levels in the presence of Vpu (ratio light/heavy >1) (Figure 7.2). More precisely, from 318 proteins downregulated by Vpu, only 13 were found to have a 2 fold or more expression difference. At the top of the list, as expected, tetherin was found to be the most downregulated protein under Vpu expression with a ratio of 12. The T cell glycoprotein, CD4 was also downregulated by 3.6 fold. As an intermediate phenotype, the glutamine transporter SNAT-1 was downregulated approximately 10 fold (x9.9) in Vpu-expressing cells (Table 7.1).

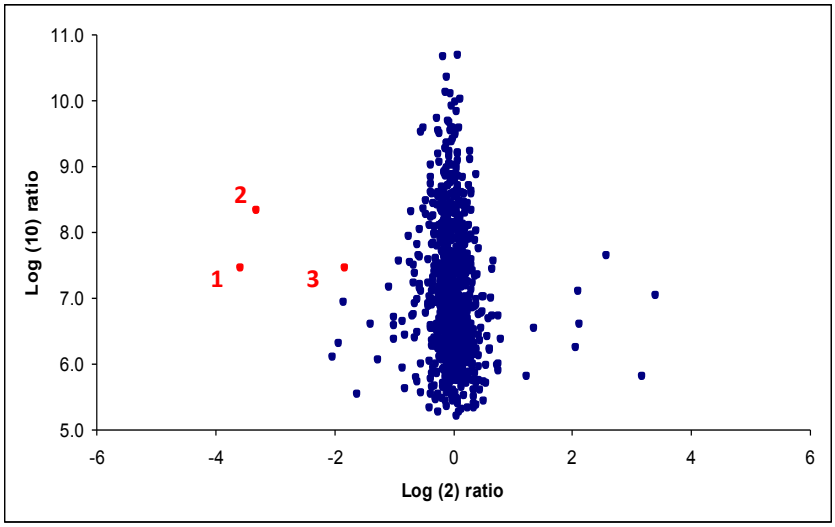

Figure 7.2: SILAC-based plasma membrane profiling of Vpu-expressing Jurkat cells.

Single blue dots indicate the differential abundance of a given protein under Vpu expression. Proteins upregulated in Vpu-expressing cells (ratio > 0) are plotted on the right part of the graph. Blue dots displayed on the left part (ratio <0) represent the proteins downregulated in Vpu-expressing cells. Three important substrates of Vpu are highlighted on the graph: **1**: Tetherin/BST-2; **2**: SNAT-1; **3**: CD4.

Protein	Unique Peptides	Ratio light/heavy	Function
Tetherin / BST-2	2	12	Antiviral restriction factor Viral sensor
SNAT-1 (SLC38A1)	8	9.9	Amino acid transporter
Glycerophosphodiester phosphodiesterase 2	1	4.1	Enzyme that breaks phosphodiester bonds
Transmembrane protein 63C	3	3.8	?
LMBR1 domain-containing protein 1	2	3.6	?
CD4	7	3.6	T-cell surface co-receptor

Table 7.1: Selection of plasma membrane proteins displaying a 3-fold cut-off level of downregulation under Vpu expression in the SILAC screening.

Candidates were identified by several unique peptides. Three additional Vpu substrates were identified but so far no functions have been associated with these proteins.

As a novel Vpu target, nothing is known about SNAT-1 in the context of HIV-1 infection. So far, as mentioned above, SNAT-1 (also known as SLC38A1) is a neutral amino acid transporter with high affinity for transport of glutamine. SNAT-1 plays an important role in the regulation of the glutamate/GABA-glutamine cycle in neurons (reviewed in (435)). Furthermore, SNAT-1, and its closest relative SNAT-2, have both been found to be upregulated upon T cell activation

concomitantly with increase in glutamine uptake (436). This project aims to investigate the physiological implications of SNAT-1 depletion by HIV-1 Vpu and the consequences of limited glutamine availability for HIV-1 replication in $CD4^+$ T cells, as well as the mechanistic aspects of Vpu-mediated SNAT-1 degradation.

7.1.2 SNAT-1, a glutamine transporter

SNAT-1 (sodium-coupled neutral amino acid transporter 1) was identified by screening a rat cDNA library from glutamatergic neuronal cultures (437). The screening was performed using a mouse EST (expression sequence tag) that displayed high sequence identity with vesicular GABA/glycine transporters from the AAAP (amino acid/auxin permease) found in yeast, plants and *C. elegans*. Subsequently, a cDNA clone with an open reading frame of 1455 base pairs was amplified and originally designated as GlnT (glutamine transporter).

SNAT-1 belongs to the SLC38 family of solute carriers (SLC38A1) and was the first member of the system A family of neutral amino acid transporters to be cloned. The system A (SNAT-1, SNAT-2, SNAT-4) and system N (SNAT-3, SNAT-5) transporters of the SLC38 family each mediate sodium-dependent transport of small, aliphatic amino acids and exhibit marked inhibition at low extracellular pH (435). Comparatively, system N subtypes have narrow substrate profiles (glutamine, histidine and asparagine) whereas system A subtypes accept a broader range of amino acids including alanine, asparagine, cysteine, glutamine, glycine, methionine and serine. SNAT-1 has been found to be preferentially associated with the unidirectional co-transport of glutamine and sodium ions with a stoichiometry of 1:1 (438). Interestingly, in Xenopus oocytes expressing SNAT-1, Na^+ binding is voltage-dependent and precedes the binding of amino acid and its simultaneous transport.

SNAT-1 is expressed in somata (cell bodies) and proximal dendrites of neurons (but not in the axon terminals) that use glutamine as a precursor for the synthesis of neurotransmitters such as glutamate and GABA (glutamatergic and GABAergic neurons) throughout the central nervous system (CNS) (Figure 7.3) (437, 438). In neurons, glutamine can be hydrolysed into glutamate by the mitochondrial enzyme phosphate-activated glutaminase (PAG). The converted glutamine can also serve as a direct precursor of GABA. Upon synaptic release, glutamate is then rapidly removed from the synaptic cleft by glutamate transporters that are located on surrounding astrocytes. There, the glutamine is synthesized back by conversion from glutamate catalysed by glutamine synthetase, an astrocyte specific enzyme. Then, the glutamine is exported from the astrocytes via SNAT-3 and possibly also SNAT-5, and then captured by SNAT-1 (and possibly also SNAT-2) for neuronal uptake. This mechanism explains the lack of SNAT-1 expression in astrocytes whereas SNAT-3 expression is largely confined to astrocytes. Therefore, the glutamine transporters from the SLC38 family play an important role in the glutamate/GABA-glutamine cycle.

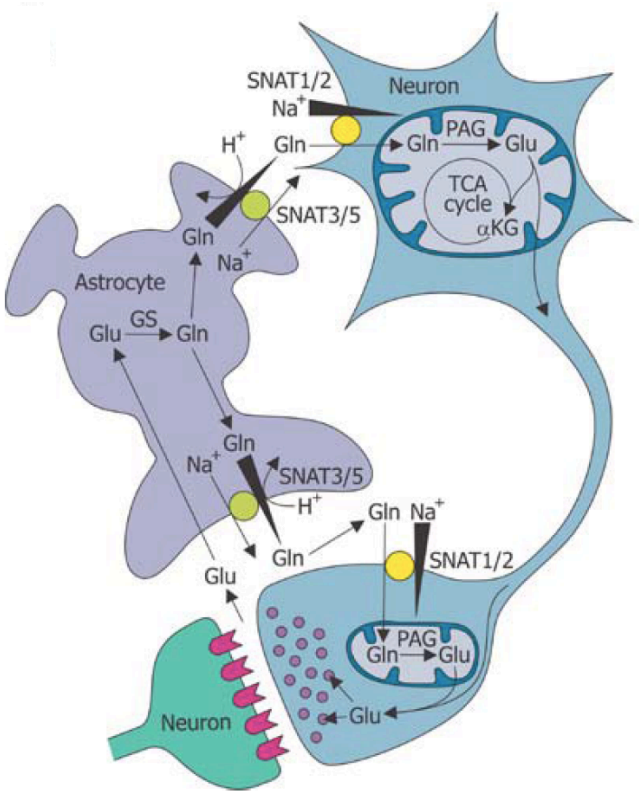

Figure 7.3: Role of SNAT-1 in the glutamate-glutamine cycling between central astrocytes and neurons.

An astrocyte is shown in contact with both the cell body and terminal of the neuron. SNAT1/2 are localized both at the cell body and terminal; SNAT3/5 are only localized within the astrocyte. Figure adapted from (435).

At a tissue level, the predominant expression of SNAT-1 is detected in the brain, spinal cord, retina, placenta, heart and traces were found in lung, skeletal muscle, spleen and intestine (437). Present at high concentrations in the rat brain and spinal cord, SNAT-1 is not only expressed in glutamatergic (excitatory neurons) and GABAergic (inhibitory neurons) neurons but also in dopaminergic and cholinergic neurons (438). Importantly, SNAT-1 may also contribute to providing metabolic fuel via conversion of glutamine into α-ketoglutarate (Figure 7.4) or in providing prerequisites (cysteine, glycine) for glutathione synthesis (439, 440).

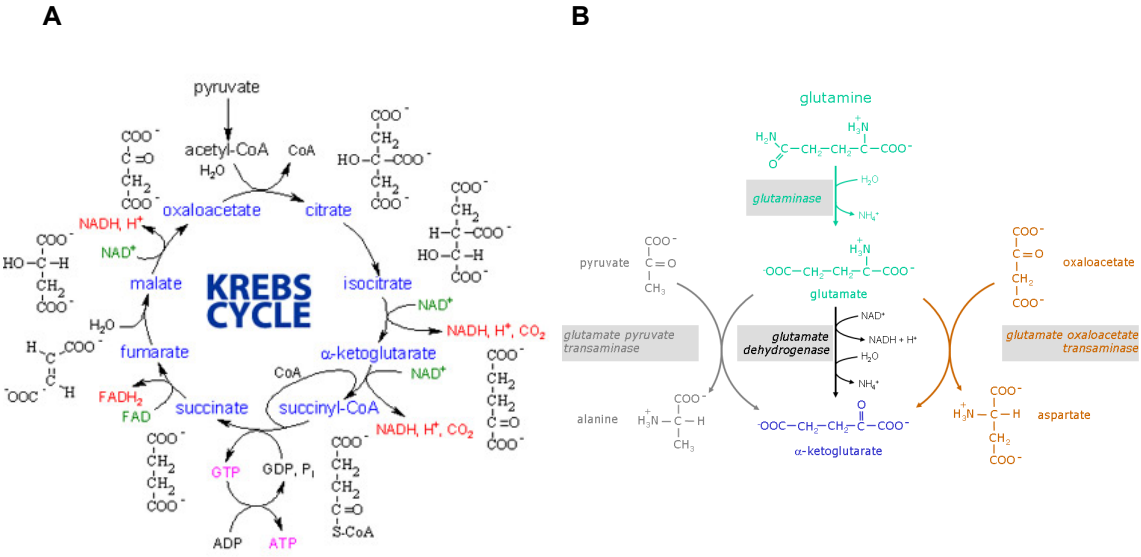

Figure 7.4: Glutaminolysis connects glutamine to the Krebs cycle.

A: Overview of the citric acid cycle (Krebs cycle). Entry of glutamine into the cycle involves its conversion into α-ketoglutarate. **B:** Conversion of glutamine into α-ketoglutarate involves two reactions. First, the hydrolysis of the amino group of glutamine yielding glutamate and ammonium is catalyzed by the glutaminase enzyme. Then, glutamate can be converted into α-ketoglutarate through 3 different catalyzing enzymes, glutamate dehydrogenase (GIDH) and glutamate pyruvate transaminase (GPT) or the glutamate oxaloacetate transaminase (GOT) that also require, in addition to glutamate, pyruvate and oxaloacetate, respectively.

SNAT-1 is a 485 amino-acid protein composed of eleven predicted hydrophobic membrane-spanning segments (Figure 7.5), mainly localized in intracellular compartments including endosomes (435). Although SNAT-1 must perform its function at the cell surface, only a minor fraction is detected on the plasma membrane. No signal sequence is detected to drive membrane insertion in the N-terminal part of the protein suggesting that this part is likely retained in the cytoplasm leaving the short C-terminal part in the extracellular compartment. Predictive analyses based on the primary structure reveal potential motifs, such as N-linked glycosylation sites and phosphorylated-residues by protein kinase C. These analyses also propose a configuration where the large glycosylated loop between TMD V and VI and the C-terminal part of the protein are extracellularly localized.

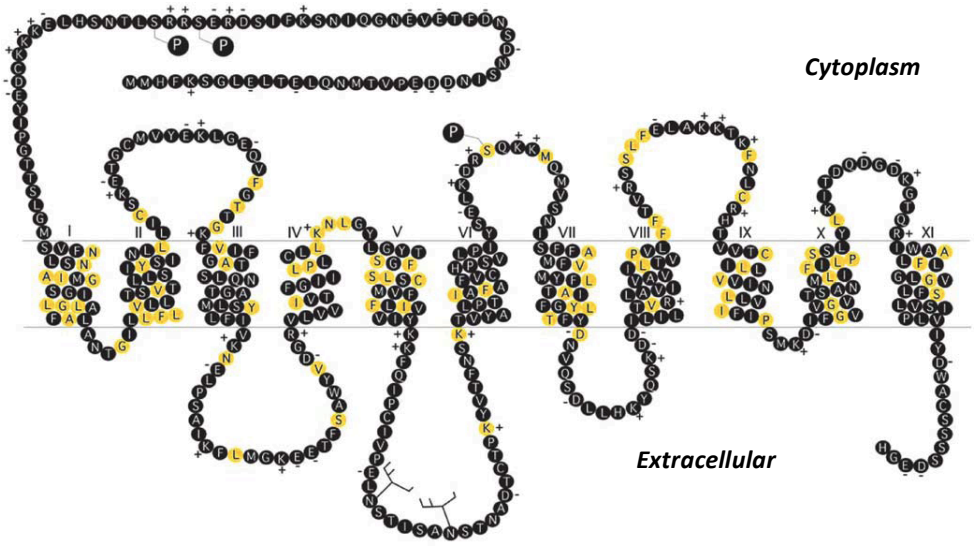

Figure 7.5: Primary amino acid sequence and proposed structure of human SNAT-1.

This spatial configuration is based on hydropathy analysis. The cytoplasm is shown above and the extracellular (or intraluminal) space below the membrane. Amino acid residues shared with the vesicular inhibitory amino acid transporter (VIAAT) are shown in yellow. Features such as potential sites for *N*-linked glycosylation (branches), acidic residues (-) and basic residues (+) are also displayed. Figure adapted from (435).

7.2 Results

7.2.1 SNAT-1 is degraded by HIV-1 Vpu

To test whether Vpu induces SNAT-1 degradation in the cell system used in the SILAC study, Jurkat-Vpu cells were lysed and cell extracts run on Western blot to measure SNAT-1 expression relative to the control cells (Jurkat-EV) (Figure 7.6A). Stable expression of Vpu results in a marked reduction of SNAT-1 expression levels in cell lysates suggesting that SNAT-1 was not a false-positive candidate in the proteomics screen. SNAT-1 runs on a Western blot at a molecular weight of approximately between 50-80 kDa. HeLa cells stably expressing Vpu were generated (HeLa-Vpu) by retroviral transduction. HeLa cells were transfected with either siRNA against SNAT-1 or control siRNA, in parallel with HeLa-Vpu. Two days post-transfection, the cells were lysed and cell extracts analysed by Western blot (Figure 7.6B). Interestingly, Vpu expression led to the depletion of SNAT-1 to levels comparable with siRNA-mediated SNAT-1 silencing. We then wanted to confirm whether we could still detect the effects of Vpu on SNAT-1 in a system where Vpu was expressed at a more physiological level, in the context of virus

infection. Jurkat cells were infected with VSV-G pseudotyped HIV-1 Wt or HIV-1 delVpu at a multiplicity of infection of 2. 48 hours later, cells were lysed in loading buffer and protein samples blotted for SNAT-1 and β-actin, serving as a loading control (Figure 7.6C). Infection with HIV-1 Wt but not HIV-1 delVpu decreases intracellular SNAT-1 expression levels.

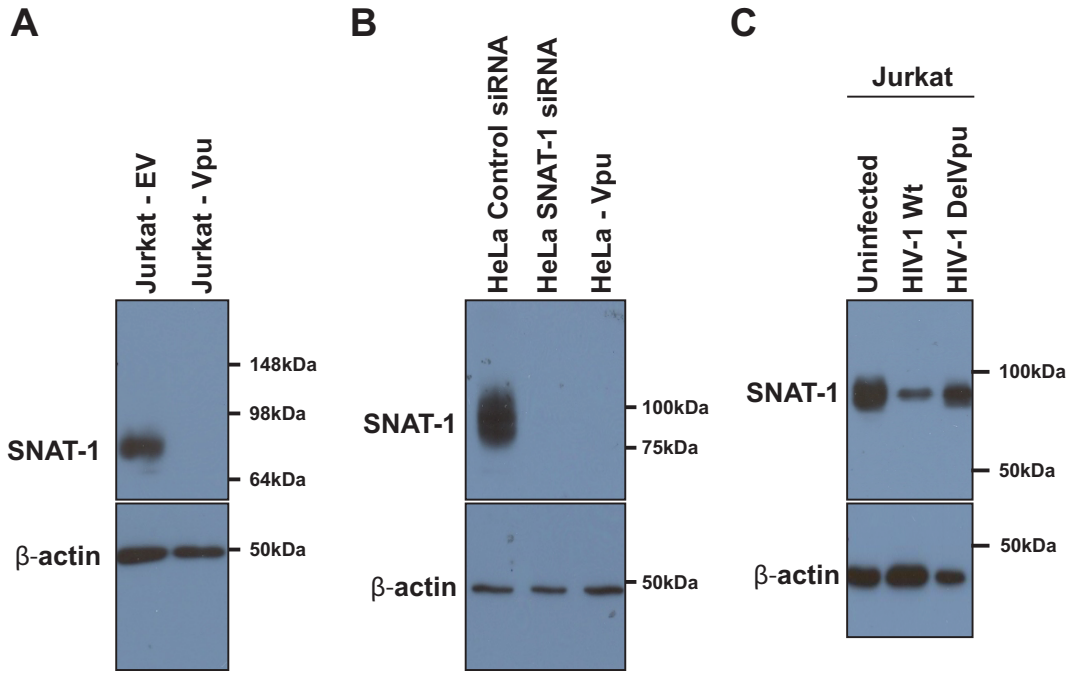

Figure 7.6: Vpu induces degradation of endogenous SNAT-1.

A: SNAT-1 degradation in Vpu-expressing Jurkat cells. **B:** SNAT-1 degradation in Vpu-expressing HeLa cells. HeLa cells were transfected with SNAT-1 siRNA 48 hours before lysis. Endogenous SNAT-1 expression was then quantified by Western blot with anti-SNAT-1 antibody. β-actin serves as loading control. **C:** SNAT-1 degradation in HIV-1 infected Jurkat cells. Cells were infected at a MOI of 2 with VSV-G pseudotyped HIV-1 Wt or delVpu and harvested 48 hours later. Stable cell lines from panels A, B and C were generated by Stuart Neil's lab and Western blots performed by our collaborators.

We then generated 293T cells stably expressing a C-terminally HA tag version of SNAT-1 (293T SNAT-1/HA). As the HA tag is located on the extracellular part, expression of SNAT-1/HA on the cell surface can be measured by flow cytometry (Figure 7.7A). We then examined whether in this system expression of SNAT-1 at the cell surface was decreased in the presence of Vpu. 293T SNAT-1/HA cells were transduced with MLV-based vectors encoding Vpu or an empty control coupled to an IRES-eGFP gene. Two days post-transduction, cells were immunostained for HA and analysed by flow cytometry to quantify surface SNAT-1/HA expression levels (Figure 7.7B). Consistent with the depletion of SNAT-1 levels in cell lysates, GFP positive cells displayed a markedly reduced expression of SNAT-1 at the cell surface in the presence of Vpu Wt in comparison to cells transduced with the empty-GFP vector. Alternatively,

293T SNAT-1/HA were infected with VSV-G pseudotyped HIV-1 Wt or HIV-1 delVpu at multiplicity of infection of 2. Two days post-infection, cells were harvested and analysed by Western blot for anti-HA for SNAT-1 detection (Figure 7.7C). In 293T SNAT-1/HA cells infected with HIV-1Wt, SNAT-1 expression levels were 3 fold lower compared to uninfected cells, whereas cells infected with the version of HIV-1 lacking the Vpu gene, SNAT-1/HA levels were similar to levels expressed in uninfected cells. Therefore, the HA epitope added at the C-terminus of SNAT-1 does not impair its sensitivity to Vpu. In this system SNAT-1 HA runs as a smear on a Western blot likely representing precursor and glycosylated forms. Altogether, these results demonstrate the ability of Vpu to induce SNAT-1 degradation in different cell types.

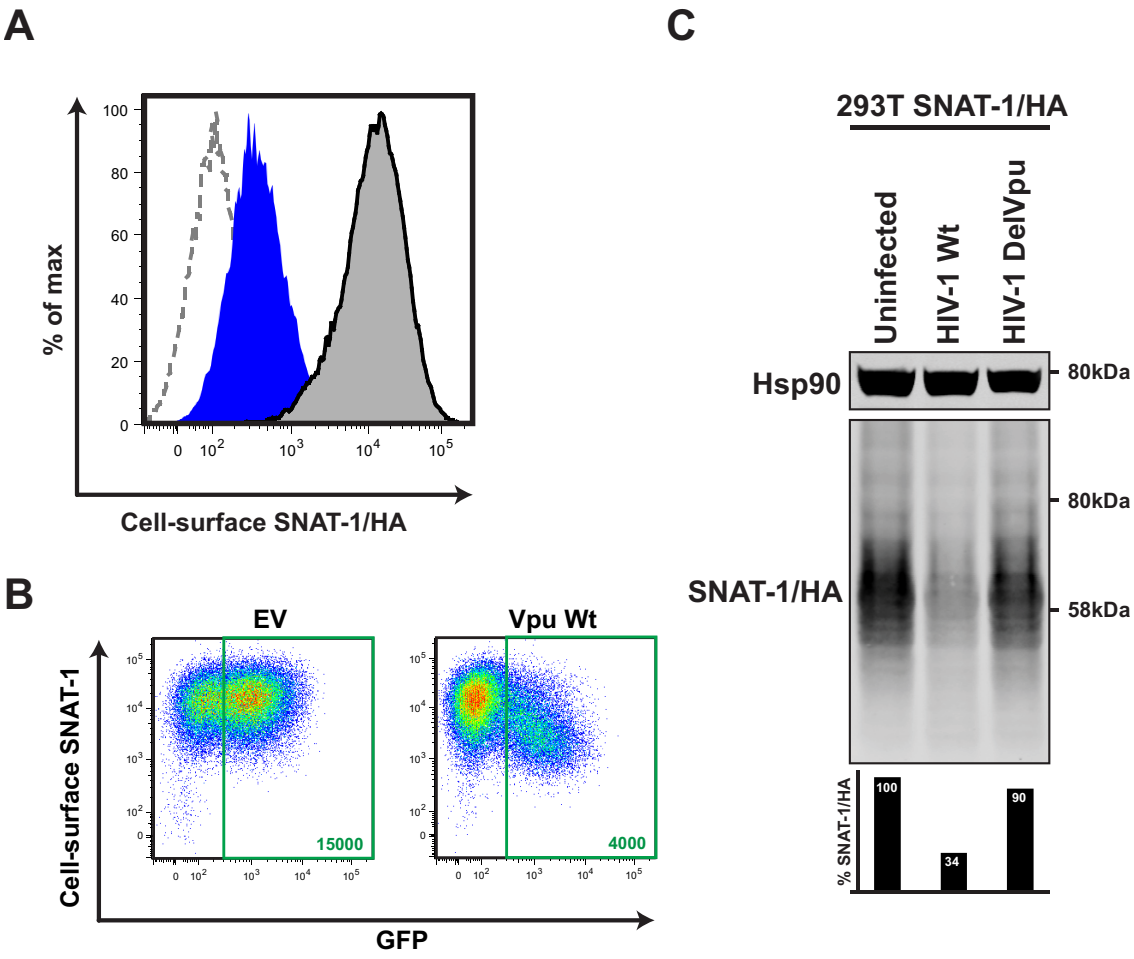

Figure 7.7: Vpu induces degradation of exogenous SNAT-1.

A: 293T SNAT-1/HA cells were immunostained with anti-HA antibody and levels of cell-surface SNAT-1/HA quantified by flow cytometry (grey histogram). The histogram with dashed line represents the binding of the isotype control. 293T were also stained with the anti-HA antibody and serve as background control (blue histogram). In SNAT-1 sequence the HA epitope is located at the short C-terminus extracellular part. **B:** 293T SNAT-1/HA cells were transduced with VLPs bearing Vpu Wt or the empty vector (EV). After two days in culture, cells were harvested and immunostained for surface SNAT-1 expression. Numbers indicate median fluorescence intensities of surface SNAT-1 in GFP^+ gate (green square). **C:** SNAT-1 degradation in infected 293T stably expressing SNAT-1/HA. Cells were infected at a MOI of 2 with VSV-G pseudotyped HIV-1 Wt or delVpu and harvested 48 hours later. Exogenous SNAT-1 expression was then quantified by Western blot with anti-HA antibody. The histograms represent the percentage of cell-surface SNAT-1/HA levels normalized to Hsp90.

We then tested whether SNAT-1 interfered with tetherin-mediated reduction of virus particle release. 293T, 293T SNAT-1/HA, HeLa and HeLa SNAT-1/HA were infected with HIV-1 Wt or HIV-1 delVpu viruses at a MOI of 2, and incubated for two days. The supernatants were then harvested and titrated on HeLa-TZMbl indicator cells (Figure 7.8). In both tetherin-negative (293T and 293T SNAT-1/HA) and positive (HeLa and HeLa SNAT-1/HA) cell lines, over-expression of SNAT-1 does not affect virus particle release resulting from one cycle of virus replication.

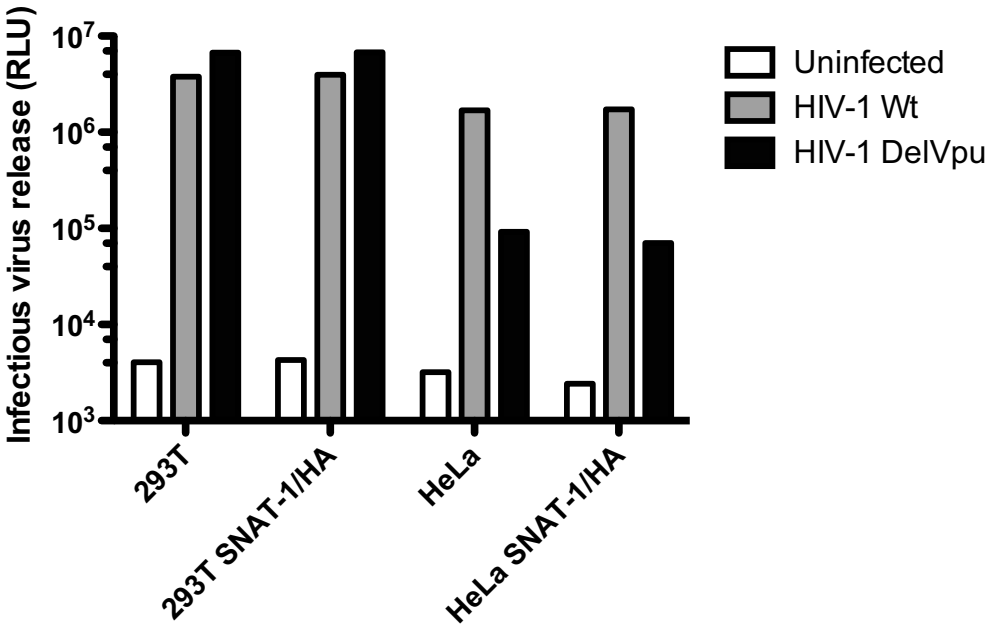

Figure 7.8: Virus particle release in SNAT-1 expressing cells is still sensitive to Vpu-mediated tetherin antagonism.

293T, 293T SNAT-1/HA, HeLa and HeLa SNAT-1/HA were infected with VSV-G pseudotyped HIV-1 Wt or HIV-1 delVpu at an MOI of 2. 48 hours post-infection, viral supernatants were assayed for infectivity using HeLa-TZMbl reporter cells. Infectious virus release plotted on a log-scale was determined by quantification of β-galactosidase activity in relative light units (RLU).

7.2.2 Determinants of SNAT-1 downregulation in Vpu

Vpu counteraction of tetherin requires the presence of intact key residues in the Vpu sequence. Mutations in the Vpu TMD domain impairing its ability to interact with tetherin, or modifications in its cytoplasmic tail altering its cellular trafficking, abolish the ability of Vpu to efficiently overcome tetherin-mediated restriction of virus particle release (221, 383). To identify whether residues in the transmembrane domain of Vpu were required to target SNAT-1, we tested the panel of Vpu TMD mutants (cf. alanine scan Vpu TMD mutants, chapter 5) for their capacity to downregulate SNAT-1 expression from the cell surface. 293T SNAT-1/HA cells were transduced with MLV-based vectors encoding Vpu Wt or Vpu TMD mutants coupled to an IRES-eGFP

gene. Two days post-transduction, cells were immunostained for HA and analysed by flow cytometry to quantify surface SNAT-1/HA expression levels (Figure 7.9). As expected, in GFP positive cells, the levels of cell-surface SNAT-1 were reduced in the presence of Vpu Wt. A five fold decrease in cell-surface levels of SNAT-1 is observed with Vpu-Wt compared to control cells transduced with the empty GFP vector. While Vpu I16A displayed a weaker ability to downregulate SNAT-1 expression than the wild type Vpu, the downregulation is completely abrogated by a Vpu construct bearing the W22A mutation. Additionally, we tested the importance of the two phosphorylated serine residues S52 and S56 in the conserved region of the Vpu cytoplasmic tail. Viral particles, bearing Vpu S52,56A changes transduced into 293T SNAT-1/HA cells failed to decrease SNAT-1 expression from the cell surface. Therefore, residue W22 and the dual serine motif S52,56 are required for Vpu-mediated SNAT-1 downregulation. Comparatively, these determinants are similar to those involved in tetherin and CD4 targeting by Vpu suggesting potential similarities between the mechanisms; Vpu might induce a β-TrCP-dependent degradation of SNAT-1. To confirm these data, the defective Vpu mutants W22A and S52,56A were stably expressed in Jurkat cells via retroviral transduction. Cells were then processed for Western blotting to measure intracellular SNAT-1 expression levels (Figure 7.10A). As expected, Vpu Wt and Vpu A14L but not Vpu W22, Vpu A14L-W22A or Vpu S52,56A reduced SNAT-1 expression in cell extracts. The Vpu A14L mutant was introduced in this experiment in order to rule out that Vpu/tetherin interactions could influence Vpu-mediated SNAT-1 degradation. Similar results were observed in 293T SNAT-1/HA cells infected with viruses bearing Vpu mutations mentioned above (Figure 7.10B). VSV-G pseudotyped HIV-1 Vpu Wt, Vpu A14L viruses but not Vpu W22, Vpu A14L-W22A and Vpu S52,56A efficiently depleted SNAT-1 expression from 293T SNAT-1/HA infected cells (MOI= 2) despite equivalent Vpu expression levels. The profile of Gag on Western blot indicates that Vpu-mediated SNAT-1 degradation does not affect the synthesis and further processing of structural viral proteins. These results provide useful tools to investigate further the molecular mechanism employed by Vpu to degrade SNAT-1. However, Vpu I16A introduced in the context of NL4.3 proviral plasmid achieves similar depletion levels of SNAT-1 HA to Wt Vpu (Figure 7.10C). In an attempt to map the residues in Vpu sequence required for SNAT-1 downregulation, we have not yet identified mutations in Vpu that render Vpu selectively defective for SNAT-1 downregulation without compromising its anti-tetherin function.

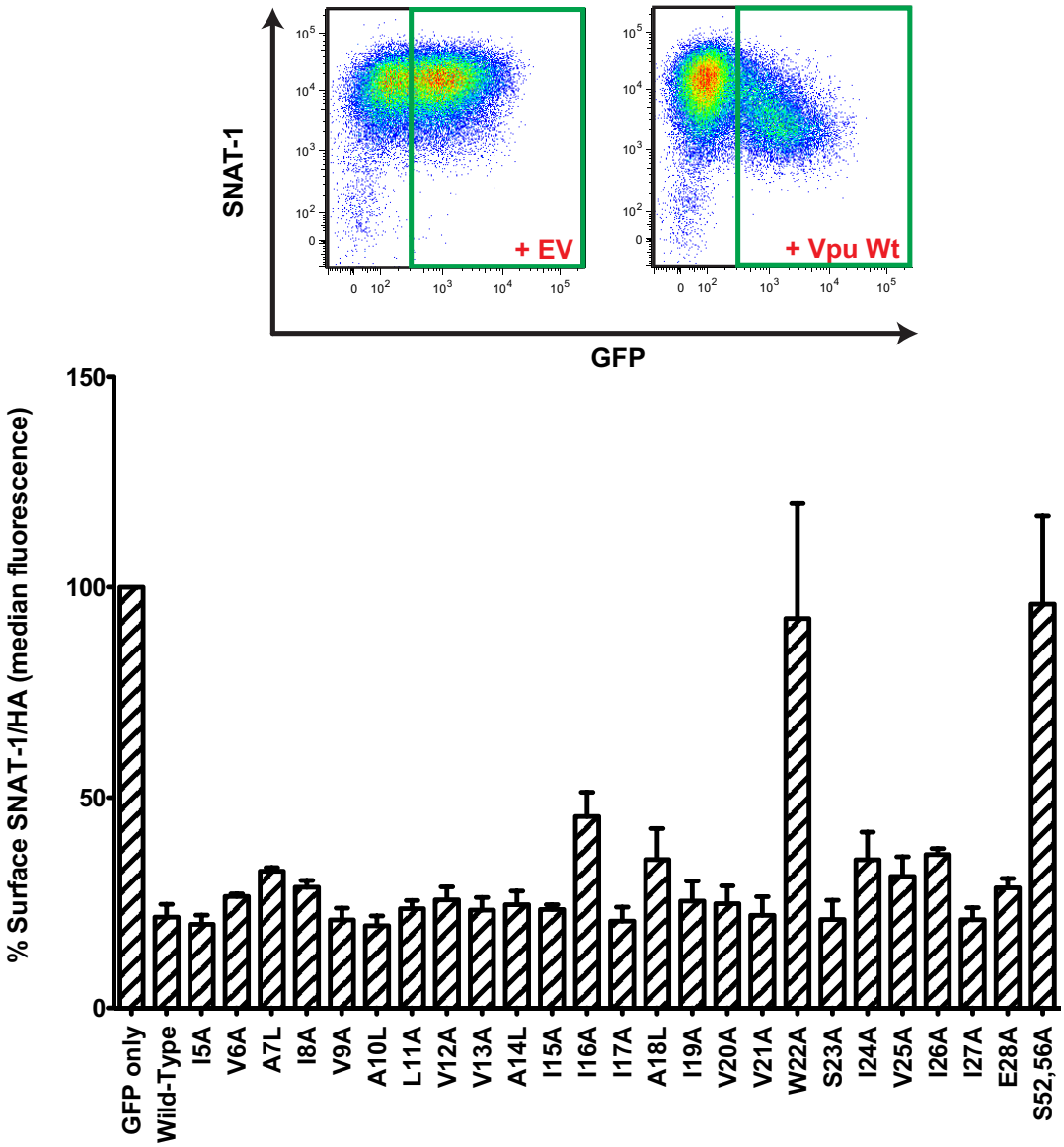

Figure 7.9: The transmembrane residue W22 and the phosphorylation site S52, S56 in the cytoplasmic tail are required for Vpu-mediated SNAT-1 cell surface downregulation.

Screening of the Vpu TMD residues for SNAT-1 downregulation in 293T SNAT-1/HA cells. 293T SNAT-1/HA cells were transduced with VLPs bearing Vpu Wt or the indicated Vpu mutant. After two days in culture, cells were harvested and immunostained for HA before flow cytometry analysis. Cell surface levels of SNAT-1/HA were measured in GFP positive cells (green gate, top panel). For each indicated Vpu mutant, the median fluorescence of SNAT-1/HA is normalized on the surface levels of SNAT-1/HA in Vpu-negative cells (bottom panel). The histograms display the average of the percentage of surface SNAT-1/HA levels obtained from three independent experiments. Errors bars represent the standard error of the mean (SEM).

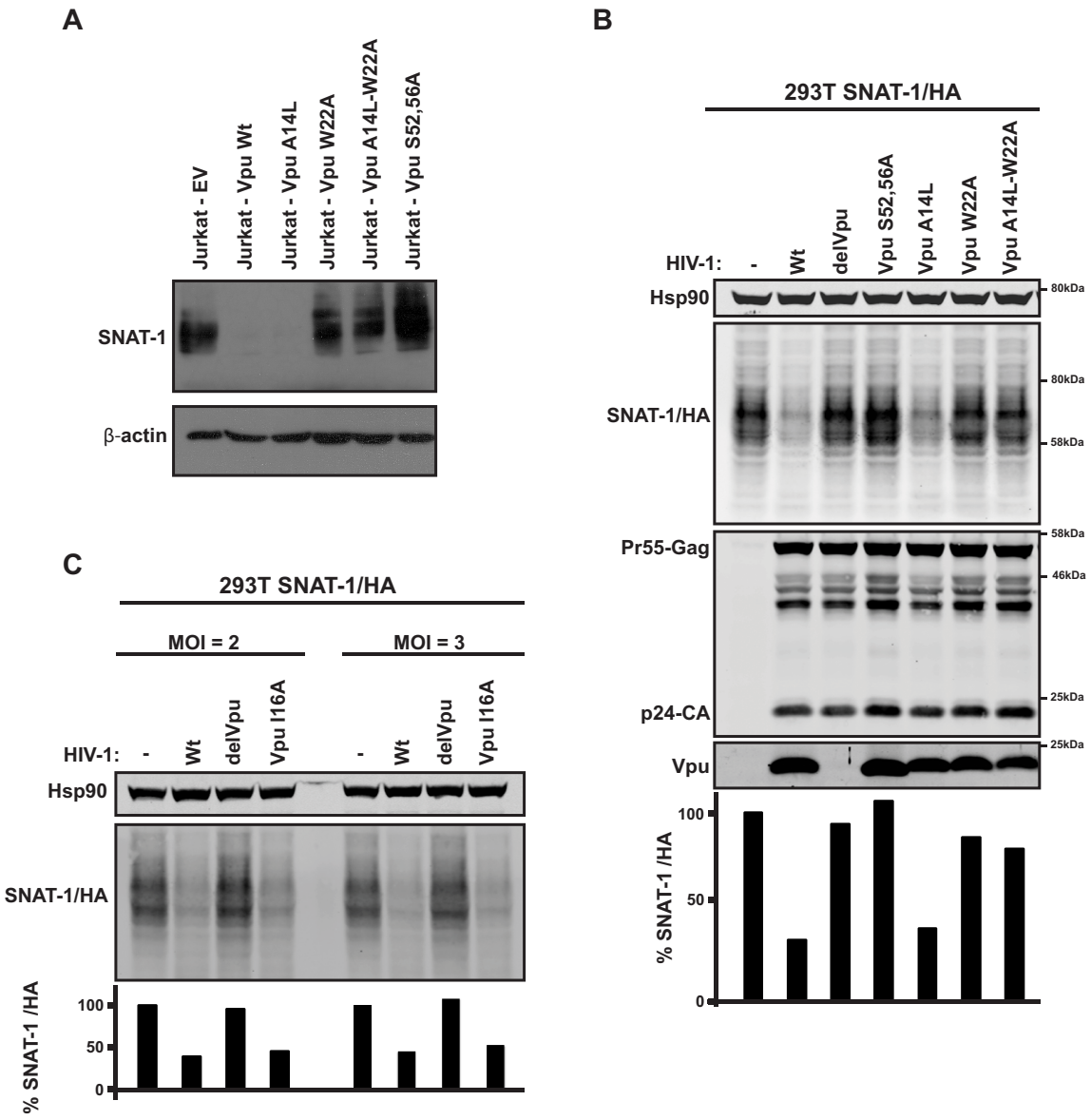

Figure 7.10: Mutations W22A and S52,56A abolish Vpu-mediated SNAT-1 degradation.

A: Equivalent number of the indicated cell lines were harvested and blotted for endogenous SNAT-1 and β-actin as a loading control. Cell lines were prepared by myself and our collaborators performed Western blots. **B:** SNAT-1 degradation by Vpu TMD and phosphorylation mutants in HIV-1 infected 293T SNAT-1/HA cells. 293T SNAT-1/HA were infected with pseudotyped HIV-1 Wt or delVpu (MOI=2) and 48 hours later, cells were blotted for Hsp90, HA, Gag and Vpu. The histograms represent the percentage of total cellular SNAT-1/HA levels normalized to Hsp90. **C:** Ability of Vpu I16A to induce SNAT-1 degradation when expressed in the context of the proviral plasmid. Same experimental procedure as in B.

7.2.3 Vpu mediated SNAT-1 degradation is sensitive to lysosomal and proteasomal inhibitors

Vpu induces SNAT-1 degradation but the nature of the degradation mechanism remains to be determined. To this end, 293T SNAT-1/HA cells were infected with VSV-G pseudotyped HIV-1 Wt or HIV-1 delVpu and 36 hours later the cells were treated with different class of inhibitors or with DMSO as a control for untreated cells. Treatment with Bafilomycin A or Concanamycin A blocks the endolysosomal degradation through inhibition of vacuole-type H^+-ATPase whereas MG132 inhibits directly the proteasome pathway. After 16 hours in the presence of the drugs, cells were harvested and blotted for SNAT-1/HA (Figure 7.11). Both Bafilomycin and concanamycin inhibitors rescued SNAT-1 expression levels in cells lysates from HIV-1 Wt infected cells suggesting that Vpu degrades SNAT-1 via an endolyzosomal process. A prolonged MG132 treatment also restored SNAT-1 expression suggesting a ubiquitin-dependent mechanism mediated by Vpu. Thus, Vpu might use the ubiquitin-tag machinery to direct SNAT-1 for endosomal destruction. Since ubiquitinated-proteins targeted for degradation via the endolysomal pathway are recruited and sorted by components of the ESCRT machinery, we investigated the role of two ESCRT subunits, UBAP1 and Tsg101. Ubiquitin associated-protein 1 (UBAP1) is a subunit of ESCRT-I that forms a complex by interacting with Tsg101, Vps28 and Vps37 and has been shown recently to be involved in the degradation of tetherin mediated by both K5 and Vpu (390). Tsg101 is a core ESCRT-I component required for all ESCRT functions. Depletion of cellular Tsg101 arrests HIV-1 budding at a late stage (140, 141). 293T SNAT-1/HA cells were transfected once with siRNA against UBAP1 or Tsg101 and transfected again 48 hours later with the same siRNA oligos before being infected at a multiplicity of infection of 2 with pseudotyped HIV-1 Wt or HIV-1 delVpu virus particles. Two days post-infection, cells were harvested and subjected to SDS-PAGE and Western blotting to quantify SNAT-1/HA expression (Figure 7.12A). Vpu was found to achieve similar levels of degradation of SNAT-1 in UBAP1-depleted cells as in cells transfected with non-targeting siRNA oligos. Similar to UBAP1 depletion, silencing of Tsg101 also had no impact on the ability of Vpu to induce SNAT-1 degradation. As expected, Tsg101 knockdown also reduced UBAP1 expression (Figure 7.12A), induced accumulation of Gag-p25 in cell lysates and decreased viral particle release by 10 fold compared to control cells (Figure 7.12B). Interestingly, in Tsg101-depleted cells, SNAT-1 expression was decreased likely due to toxicity. These data suggest that Vpu-mediated SNAT-1 degradation is lysosomal and ubiquitin dependent but ESCRT independent, unless there are ESCRT functions that do not involve Tsg101. However, this is unlikely because it is known that Tsg101 is tightly regulated and when its expression is inhibited no ESCRT complexes can form because the others subunits become unstable (441). This likely accounts for the associated decrease of UBAP1 expression in Tsg101-silenced cells.

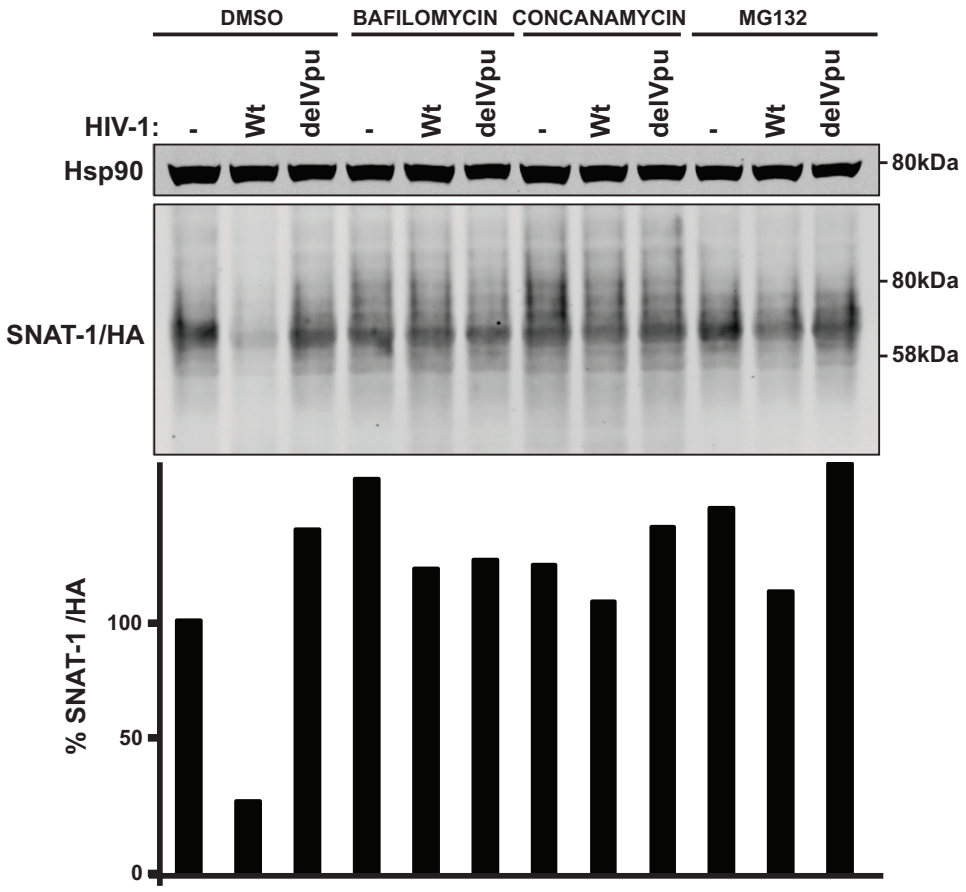

Figure 7.11: Effects of endolysosomal and proteasomal inhibitors on Vpu-mediated SNAT-1 degradation.

293T SNAT-1/HA cells, initially transfected with VSV-G HIV-1 WT or HIV-1 delVpu viruses, were treated for 16 hours with Bafilomycin A1 (100nM), concanamycin A, MG132 (1μg/ml) or DMSO as a control, before being lysed and Western blotted for HA and Hsp90. The histograms represent the percentage of total cellular SNAT-1/HA levels normalized to Hsp90.

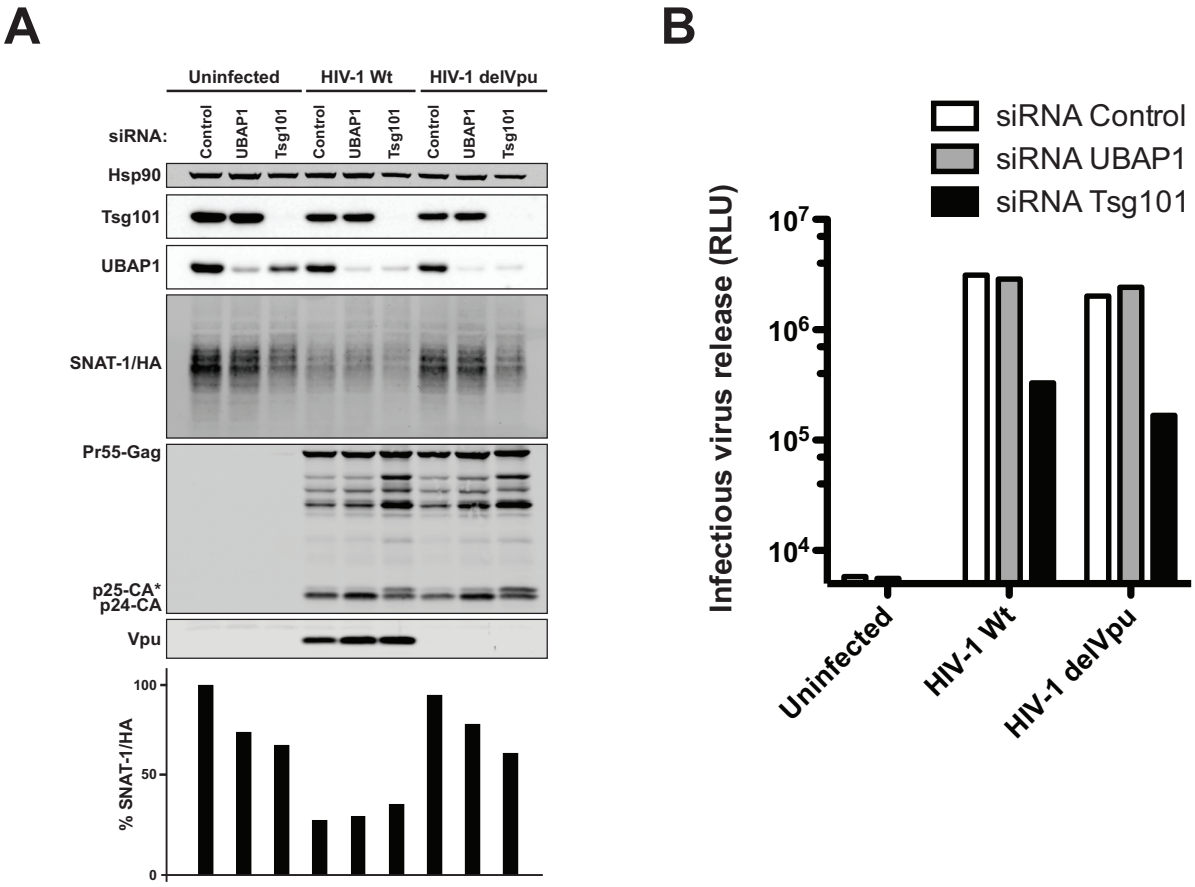

Figure 7.12: siRNA-mediated silencing of UBAP1 and Tsg101 do not impact Vpu-mediated SNAT-1 degradation.

A: 293T SNAT-1/HA cells were transfected twice (cf. chapter 2) with siRNA oligos against UBAP1, Tsg101 or control siRNA and infected with HIV-1 Wt or delVpu. A total of 48 hours later cells were lysed in loading buffer and processed for Western blotting. The total cellular SNAT-1/HA levels normalized to Hsp90 are indicated. **B:** Viral supernatants from A were titrated on HeLa-TZMbl cells. As described in the literature depletion of UBAP1 does not affect HIV-1 particle release.

7.2.4 SNAT-1 sensitivity to Vpu is not determined by its cytoplasmic tail

Vpu-mediated tetherin antagonism requires interaction of both proteins via their transmembrane domains. Recently, Vpu TM domain has also been shown to be essential to retain CD4 molecules in the endoplasmic reticulum before their subsequent degradation via ERAD (370). We then examined the importance of the region formed of 11 membrane-traversing segments, 5 intracellular loops, 5 extracellular loops and a short extracellular C-terminus, in the SNAT-1 sequence for the ability of Vpu to degrade SNAT-1. Importantly, SNAT-2 (SLC38A2), another member of the SLC38 family of solute carrier acting also as an amino acid transporter, was not

found to be downregulated by Vpu in the SILAC screen, although it was identified. This characteristic provides a useful tool to map the determinants in SNAT-1 that confer its sensitivity to Vpu. SNAT-1 and SNAT-2 display the same predicted topology and share 52% of sequence homology facilitating the design of chimera SNAT-1/SNAT-2 proteins (Figure 7.13).

The cytoplasmic tails of SNAT-1 and SNAT-2 were swapped resulting in two chimeras (Figure 7.14A). SNAT 1-2 chimera is mainly identical to SNAT-2 but has the cytoplasmic tail of SNAT-1 whereas SNAT 2-1 chimera is the SNAT-1 protein with SNAT-2 cytoplasmic domain. 293T cells stably expressing SNAT-2/HA, SNAT 1-2/HA and SNAT 2-1/HA were made and tested for Vpu-mediated degradation. The cells were infected with VSV-G pseudotyped HIV-1 Wt or HIV-1delVpu viruses at a MOI of 2. 48 hours later, cells were lysed in loading buffer and processed by Western blot for anti-HA (Figure 7.14B). In contrast to 293T SNAT-1/HA, infection of 293T SNAT-2/HA cells with HIV-1Wt or HIV-1 delVpu does not affect SNAT-2 expression levels demonstrating that Vpu is unable to target SNAT-2 for degradation. Therefore, Vpu displays specificity in its ability to target SNAT-1. Comparison between SNAT-1 and SNAT-2 reveals a high degree of sequence divergence (Figure 7.13). Similarly, expression levels of SNAT 1-2 is also not affected by Vpu expression indicating that the cytoplasmic tail of SNAT-1 by itself does not confer sensitivity for Vpu. However, chimeric SNAT-1 bearing the SNAT-2 cytoplasmic tail (SNAT 2-1) remained sensitive to Vpu-mediated depletion. These results suggest that Vpu-mediated SNAT-1 degradation requires essentially the region outside the cytoplasmic tail in SNAT-1 sequence. Presumably, Vpu is likely to mediate interactions within this region of SNAT-1, but this region not only encompasses transmembrane domains but also five loops facing the cytoplasm and five extracellular loops. It is possible that these loops function to maintain the overall conformation of SNAT-1, thus stabilizing the incorporation of SNAT-1 into the membrane lipid bilayer. Moreover, it cannot be excluded that the intracellular loops might also provide a recognition signal for Vpu docking.

```
SNAT-1   1 MMHFKSGLELTELQNMTVPEDDNISNDSNDFTEVENGQINSKFISDRESRRSLTNSHLEKKKCDEYIPGTTSLGMSVFNLSNAIMGSGILGLAFALANTG   100
SNAT-2   1 MKKAEMGRFSISPDEDSSSYSSNSDFNYSYPTKQAALKSHYADVDPENQNFLLESNLGKKKYETEFHPGTTSFGMSVFNLSNAIVGSGILGLSYAMANTG   100

       101 ILLFLVLLTSVTLLSIYSINLLLICSKETGCMVYEKLGEQVFGTTGKFVIFGATSLQNTGAMLSYLFIVKNELPSAIKFLMGKEETFSAWYVDGRVLVVI   200
       101 IALFIILLTFVSIFSLYSVHLLLKTANEGGSLLYEQLGYKAFGLVGKLAASGSITMQNIGAMSSYLFIVKYELPLVIQALTNIEDKTGLWYLNGNYLVLL   200

       201 VTFGIILPLCLLKNLGYLGYTSGFSLSCMVFFLIVVIYKKFQIPCIVPELN-----------------STISANSTNADTCTPKYVTFNSKTVYALPTIA   283
       201 VSLVVILPLSLFRNLGYLGYTSGLSLLCMVFFLIVVICKKFQVPCPVEAALIINETINTTLTQPTALVPALSHNVTENDSCRPHYFIFNSQTVYAVPILI   300

       284 FAFVCHPSVLPIYSELKDRSQKKMQMVSNISFFAMFVMYFLTAIFGYLTFYDNVQSDLLHKYQSK--DDILILTVRLAVIVAVILTVPVLFFTVRSSLFE   381
       301 FSFVCHPAVLPIYEELKDRSRRRMMNVSKISFFAMFLMYLLAALFGYLTFYEHVESELLHTYSSILGTDILLLIVRLAVLMAVTLTVPVVIFPIRSSVTH   400

       382 LAKKT-KFNLCRHTVVTCILLVVINLLVIFIPSMKDIFGVVGVTSANMLIFILPSSLYLKITDQDGDKGTQRIWAALFLGLGVLFSLVSIPLVIYDWACS   480
       401 LLCASKDFSWWRHSLITVSILAFTNLLVIFVPTIRDIFGFIGASAASMLIFILPSAFYIKLVKKEPMKSVQKIGALFFLLSGVLVMTGSMALIVLDWVHN   500

       481 SSSDEGH   487
       501 APGGGHX   507
```

Figure 7.13: Alignment of protein sequences between SNAT-1 and SNAT-2.

Comparison of SNAT-1 and SNAT-2 protein sequences. The conserved residues are shown in red. The alignment was performed using the alignment tool FFAS03.

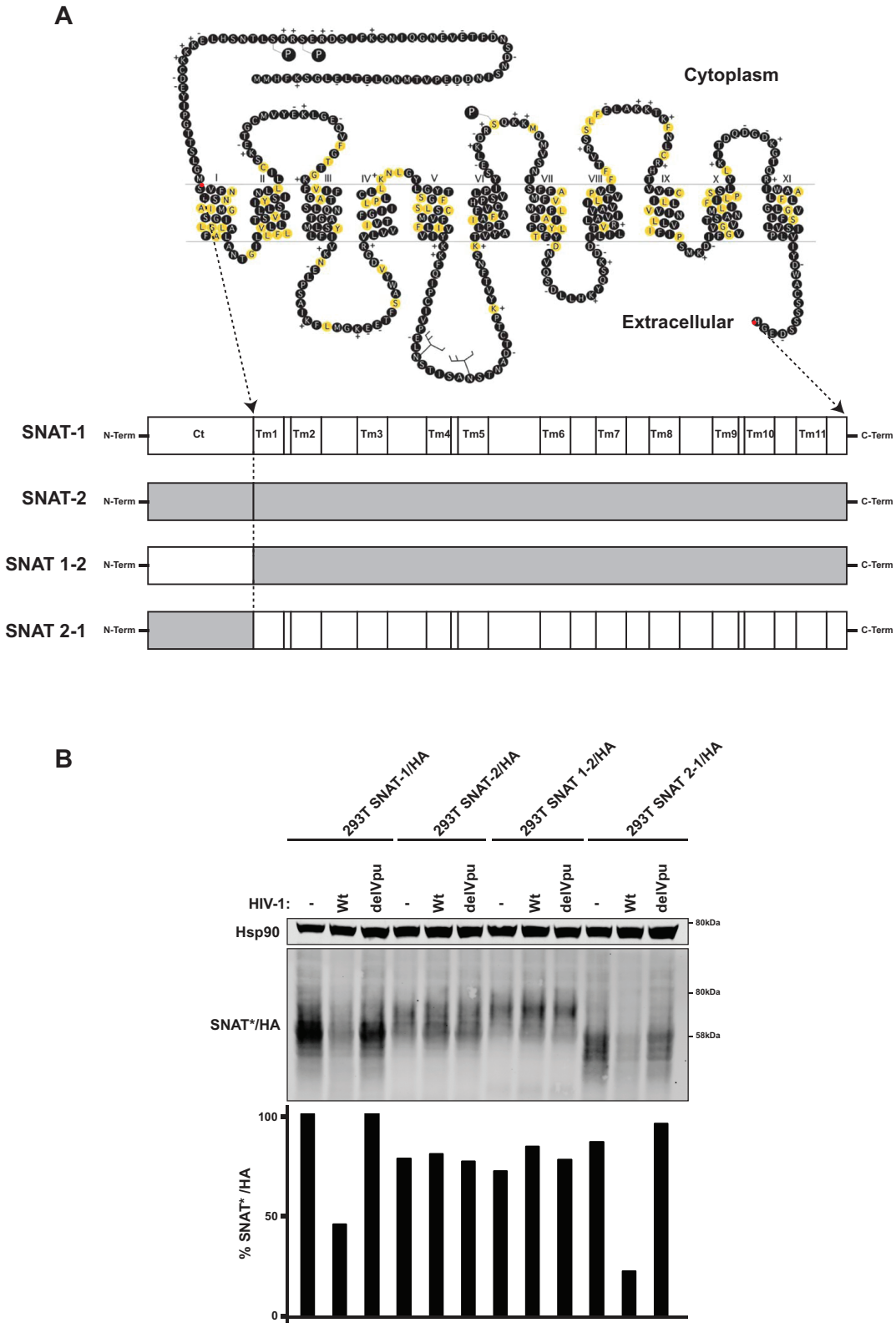

Figure 7.14: SNAT-1 transmembrane region confers sensitivity to Vpu.

A: Schematic representation of SNAT-1/SNAT-2 chimera. **B:** SNAT-1 cytoplasmic tail is not required for Vpu-mediated SNAT-1 degradation. 293T cells stably expressing the indicated SNAT chimera were infected with HIV-1 Wt or the Vpu-defective HIV-1 counterpart at a multiplicity of infection of 2. After two days of incubation, cells were lysed and proteins expression quantified by Western blot. The total cellular levels of SNAT*/HA are normalized to Hsp90 and displayed on histograms.

7.2.5 Vpu physically associates with SNAT-1

We then assessed the ability of Vpu to immunoprecipitate SNAT-1 molecules as an indicator of potential direct or indirect interaction between the two proteins. 293T SNAT-1/HA were transiently transfected with a pCRV1 expression vector encoding Wt Vpu, Vpu A14L-W22A or Vpu S52,56A. Two days later, cells were lysed, HA-tagged proteins immunoprecipitated and Western blotted for Vpu expression (Figure 7.15). We found that Wt Vpu and Vpu S52,56A but not Vpu A14L-W22A were co-immunoprecipitated with SNAT-1/HA molecules. The Vpu A14L-W22A mutant is likely to be defective for tetherin interactions because of the missing tryptophan residue, which was previously shown to be also required to reduce cell-surface levels of SNAT-1. Since Vpu bearing the mutation S52,56A is defective for mediating SNAT-1 degradation but not for interaction, this suggests that SNAT-1 binding to Vpu is likely to be necessary but not sufficient to mediate SNAT-1 degradation. This observation is similar to the tetherin study where physical interaction and degradation are separable events, for which the determinants differ but for both Vpu's targets, initial interaction is always required for subsequent processes.

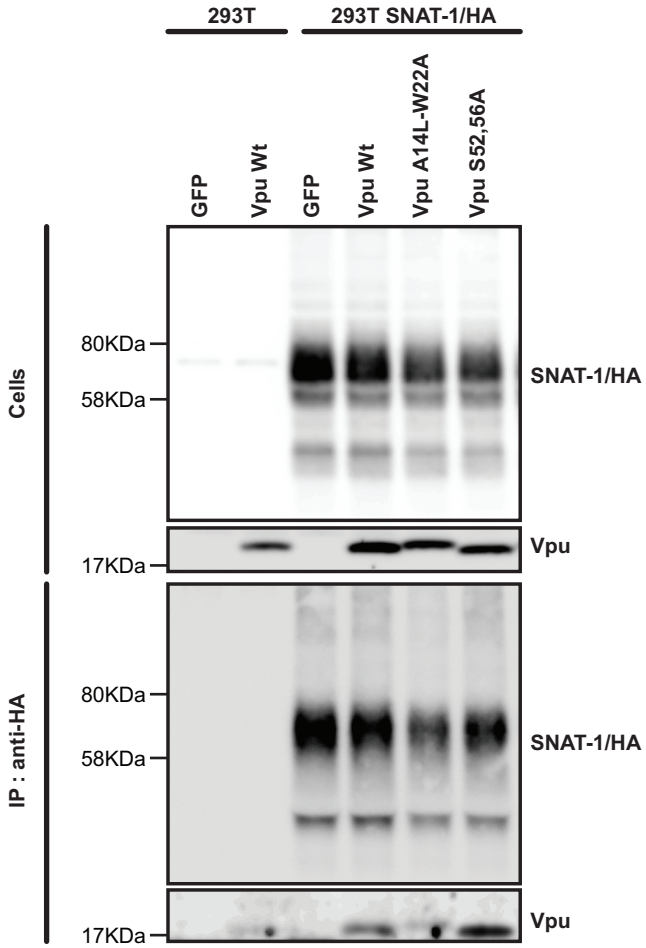

Figure 7.15: Vpu interacting with SNAT-1 involves the residues W22 but not the phosphorylation motif.

293T SNAT-1/HA were transfected with pCRV1 Vpu Wt, Vpu A14L-W22A or Vpu S52,56A. 48 hours post-transfection, cells were lysed and proteins immunoprecipitated with an anti-HA antibody. Lysates and precipitates were subjected to SDS-PAGE and Western blotted for Vpu and SNAT-1/HA.

7.2.6 SNAT-1 and Vpu colocalize into intracellular compartments

In the absence of Vpu expression, SNAT-1 localizes at the plasma membrane and in intracellular compartments that mainly overlay with TGN46 positive compartments suggesting a *trans*-golgi network localization (Figure 7.16A). But despite its localization in the TGN and at the plasma membrane a large proportion of SNAT-1 staining appears to be associated with small vesicles likely to be endosomes. Interestingly, it has been shown that after T cell stimulation there was an increase in surface expression of glutamine transporters (436) consistent with the idea that increased glutamine transport might be due to a combination of increased protein expression and relocation of transporters from intracellular stores to the cell surface. Since Vpu and SNAT-1 can co-immunoprecipitate, it is likely that these two proteins are expressed into similar subcellular compartments. HeLa cells were transiently transfected with a Vpu-Cherry encoding vector and a plasmid encoding SNAT-1/HA. 24 hours post-transfection, cells were fixed in 4% paraformaldehyde, immunostained for SNAT-1/HA and observed by confocal microscopy (Figure 7.16B). Vpu and SNAT-1 colocalize in intracellular compartments that resemble vesicles. Alternatively, 293T SNAT-1/HA were infected with HIV-1 Wt or HIV-1 delVpu and stained for SNAT-1 and Vpu detection (Figure 7.16C). In HIV-1 Wt infected cells SNAT-1 expression is not detected at the cell surface in comparison to uninfected control cells. Similar to tetherin, for the majority of infected cells no residual traces of SNAT-1 expression were detected in intracellular compartments. Only in transiently-transfected cells, we could observe residual amount of SNAT-1 colocalizing with Vpu, most likely due to over-expression of SNAT-1.

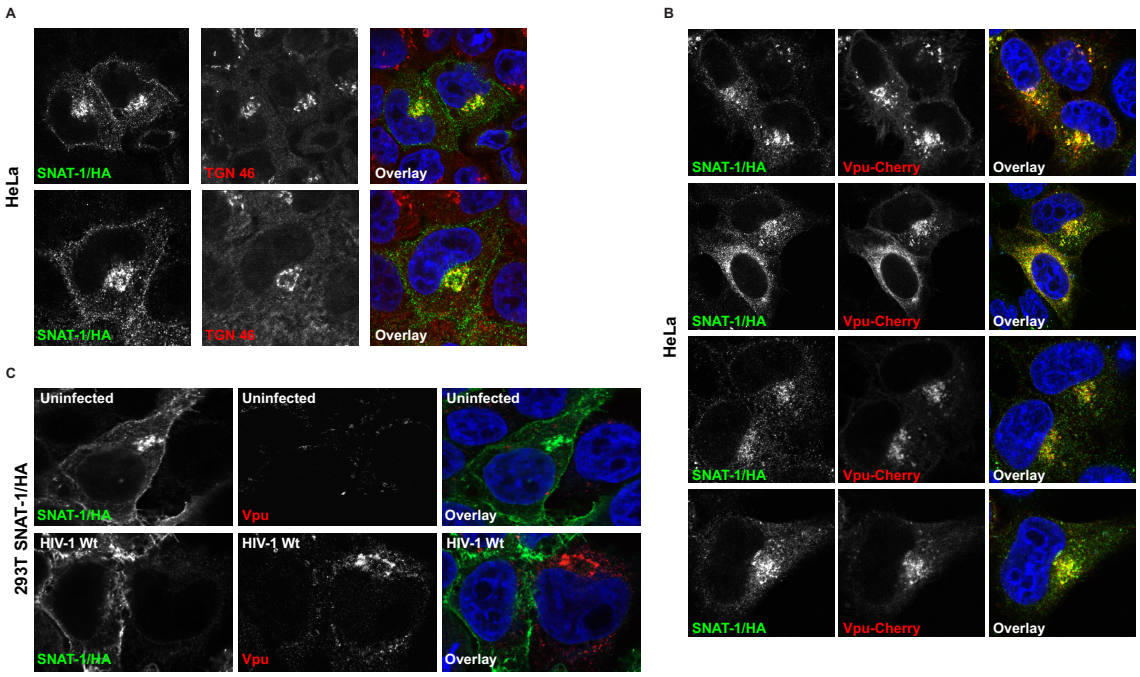

Figure 7.16: Subcellular localization of SNAT-1/HA.

A: SNAT-1/HA subcellular distribution in the absence of Vpu in HeLa cells. HeLa cells were transfected with 100 ng of pCR3.1 SNAT-1/HA expression vector alone or in combination with

100ng of a cherry fused Vpu construct. 24 hours later, the cells were fixed in 4% paraformaldehyde, immunostained with anti-HA antibody, anti-TGN46 (cellular marker of TGN) and fluorescence signals observed by confocal microscopy. Images are representative examples of SNAT-1 expressing cells. **B:** Cherry-fused Vpu and SNAT-1/HA colocalize in transfected HeLa cells. **C:** Depletion of SNAT-1 from the cell surface in infected 293T SNAT-1/HA cells. 293T SNAT-1/HA cells were infected with HIV-1 Wt at a multiplicity of infection of 1 and fixed 48 hours later. Cells were then stained for Vpu and SNAT-1 detection with respectively anti-HA antibody (green) anti-Vpu antibody (red) and examined by confocal microscope. Nuclei were counterstained with DAPI (blue). Images are representative examples of HIV-1 infected 293T SNAT-1/HA.

7.2.7 Effects of SNAT-1-depletion by HIV-1 Vpu in primary $CD4^+$ T lymphocytes

Glutamine is the most abundant amino acid in the plasma and is essential for various biochemical functions including protein synthesis, cellular energy, inter-organ transfer of nitrogen, amine group donor for nucleotide synthesis and other important cellular processes. Recently, its role during $CD4^+$ T lymphocyte activation has been demonstrated (436). Recognition of antigen presented by MHC-II molecules on APCs by the TCR complex triggers a succession of reactions ultimately leading to the activation of the naïve T cell. This activation leads to the secretion of cytokines, clonal expansion of the naïve T cell concerned, and differentiation into a given type of T cell subset. All these processes require a high energetic demand and force the cellular machinery to increase its metabolic activity. In these conditions, nutrients such as glutamine are essential to provide the basic building blocks of protein synthesis and also serve as substrates for many other metabolic processes.

T cell activation is absolutely dependent on extracellular glutamine (436). Removal of glutamine from activated T cells (anti-CD3/CD28 stimulation) in culture consistently inhibits T cell proliferation, blocks secretion of IL-2 and IFN-γ. In that sense, T cell activation is coupled to an increase in glutamine uptake. A 5 to 10 fold induction of glutamine uptake in activated T cells is observed comparatively to unstimulated control cells. Concomitantly to glutamine uptake increase, T cell activation also induces expression of glutamine transporters such as SNAT-1 and SNAT-2.

Given the importance of glutamine for T cell function (436, 442-444), glutamine utilization might be regulated by T Cell Receptor (TCR)-initiated signals. TCR activation triggers multiple signal transduction pathways, including the members of the mitogen-activated protein kinase (MAPK) family. ERK 1/2 (extracellular signal regulated kinase) belongs to this family and was shown to increase expression of amino acid transporters from the system A (445). Consistent with this, treatment of stimulated T cells with ERK inhibitors completely blocks the increased glutamine uptake. This suggests that ERK acts downstream of TCR complex signaling to control SNAT expression, transport activity and positively regulates glutamine uptake (436). The high demand on glutamine during T cell activation suggests that glutamine might not only be used for protein synthesis. Indeed, the activity of the enzyme glutaminase, that catalyzes the conversion of glutamine into glutamate, is enhanced during T cell activation. Activities of enzymes ensuring conversion of glutamate into α-ketoglutarate, which then, can serve as a

substrate to enter the Krebs cycle, are also upregulated by T cell activation (436). In accordance with these published data, our collaborators showed that at glutamine concentrations lower than 1mM the number of cell divisions was severely impaired (Figure 7.17A). At a glutamine concentration of 1mM, T cells displayed high proliferative capacity; nevertheless glutamine concentrations higher than 1mM did not significantly enhance the proliferation. By comparison, the physiological concentration of glutamine *in vivo* is approximately 0.6 mM and *in vitro*, normal culture media are supplemented with 2-4 mM final glutamine concentration. Similar to Carr *et al*, our collaborators demonstrated that expression of the SNAT-1 transporter was induced in activated primary human $CD4^+$ T cell but not in resting T cells (Figure 7.17B). SNAT-1 expression was detectable from 48 hours post-activation and was found to be maximal four days post-stimulation with anti-CD3/CD28. Although SNAT-1 knockdown in immortalized cells, such as Jurkat, does not affect cell growth, in primary human $CD4^+$ T cells, depletion of SNAT-1 expression by RNAi strongly inhibits T cell proliferation despite increasing input of extracellular glutamine provided in the culture medium (Figure 7.17C-D).

These results suggest that Vpu might, by degrading the transporter SNAT-1, block T cell proliferation through limiting the glutamine availability in infected T cells. To test this hypothesis several aspects will need to be addressed. Does Vpu expression affect the proliferative capacity of infected $CD4^+$ T cells? And in that situation is HIV-1 replication more productive? The next part aims to understand the physiological implications of Vpu targeting SNAT-1 for HIV-1 replication.

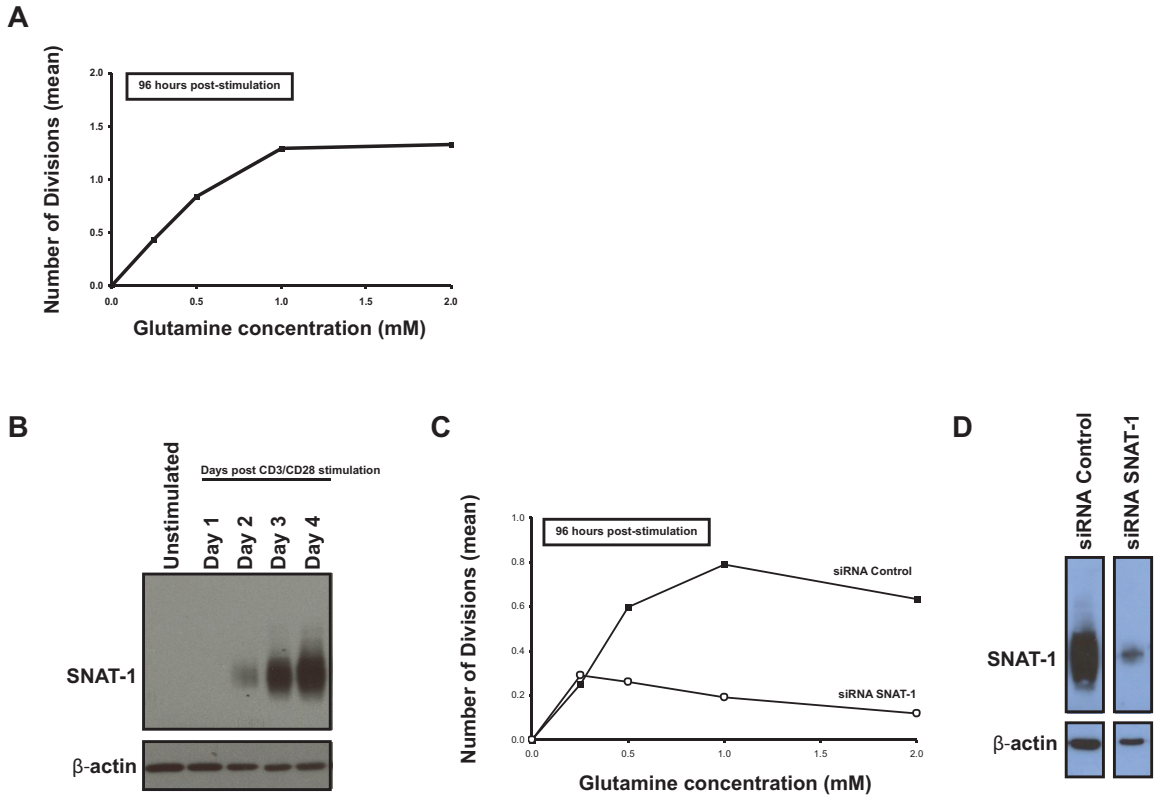

Figure 7.17: CD4$^+$ T cell proliferation is SNAT-1 and glutamine dependent.

These experiments were performed by Paul Lehner's group. **A:** Dependence on glutamine of primary human CD4$^+$ T cell proliferation. CD4$^+$ T cells isolated from PBMCs were labelled with CFSE as a proliferation marker and stimulated with anti-CD3/CD28 beads and placed in culture medium containing the indicated glutamine concentration. 96 hours post-stimulation, cells were harvested and mean number of cell divisions quantified by flow cytometry. **B:** SNAT-1 expression in activated primary human CD4$^+$ T cells. CD4$^+$ T cells were extracted as above and harvested at 24, 48, 72 and 96 hours post-stimulation. Endogenous SNAT-1 expression levels were then analysed by Western blot with anti-SNAT-1 antibody. **C:** Effects of SNAT-1 silencing on CD4$^+$ T cell proliferation. As in A but CD4$^+$ T lymphocytes were electroporated with siRNA control or siRNA against SNAT-1. The cells were grown in media supplemented with different glutamine concentrations and the mean number of cell generations enumerated 96 hours post-isolation. **D:** SNAT-1 knockdown in primary human CD4$^+$ T cells. CD4$^+$ T cells from C were subjected to SDS-PAGE and Western blotted for SNAT-1.

7.2.7.1 Effects of Vpu expression on primary CD4$^+$ T cells proliferative capacity

Since SNAT-1 knockdown and limiting glutamine concentrations impaired T cell proliferation, we investigated whether Vpu expression could also directly cause inhibition of T cell proliferation. Untouched primary human CD4$^+$ T cells were isolated from PBMCs, labelled with CellTrace Violet dye as a proliferation tracer, stimulated with anti-CD3/CD28 antibodies coupled to magnetic beads and cultured in 1mM glutamine-RPMI medium (Figure 7.18A). Since SNAT-1 expression was detectable from 48 hours post-activation, at that time cells were infected with VSV-G pseudotyped HIV-1 Wt or HIV-1 delVpu at a multiplicity of infection of 1. This timing

permits synchronized expression of Vpu and SNAT-1 (Figure 7.17B and Figure 7.18B). Over the following 3 days, cells were harvested every day, and proliferation (via Violet dye) versus intracellular p24 staining (as a marker of infection) were then monitored by flow cytometry for each time point (Figure 7.19). Importantly, because Vpr can induce a G2 cell-cycle arrest of HIV-infected T cells, we used a Vpr mutant (Vpr L64P) that cannot mediate binding with the damage-specific DNA binding protein DDB1 required for Vpr-induced cell-cycle arrest and apoptosis (271).

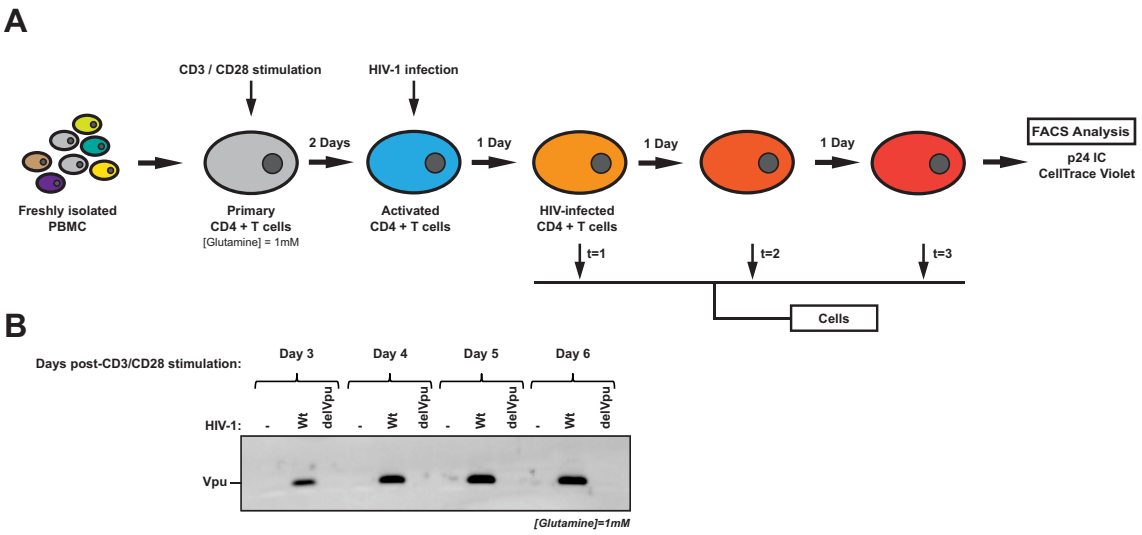

Figure 7.18: Monitoring the proliferation of HIV-1 infected primary human CD4$^+$ T lymphocytes.

A: Schematic representation of the experimental procedure. Primary human CD4$^+$ T lymphocytes were isolated from PBMCs using a negative selection kit, labelled with CellTrace Violet dye and stimulated with anti-CD3/CD28 beads. CD4$^+$ T lymphocytes were then cultured for two days in medium containing 1mM concentration of glutamine before being infected with VSV-G pseudotyped HIV-1 Wt or delVpu. Cells were collected at 24, 48, 72 hours post-infection, stored in staining buffer. All the cells were stained at the same time for intracellular p24 and proliferation was measured by flow cytometry. **B:** Time course of Vpu expression in HIV-1 infected primary CD4$^+$ T cells. CD4$^+$ T cells were purified and infected as above. At day 3, 4, 5 and 6 post-CD3/CD28 stimulation, cells were harvested in SDS-PAGE loading buffer and Vpu expression detected by Western blot.

24 hours post-infection 30% of T cells were p24 positive for both Wt and Vpu-defective HIV-1 and approximately 40% the following day. Uninfected cells from the uninfected sample accumulated 4 divisions with approximately 25% of cells in the third generation, 43% in the second generation and 26% in the first generation (Figure 7.19A). Only a few cells were detected in the fourth generation. In contrast, infected T cells gated on the p24 positive gate displayed a reduced proliferation capacity. A proportion of 10% HIV-1 Wt (Vpr L64P) infected cells were detected in the third generation whereas twice as many Vpu-defective HIV-1 (Vpr L64P-delVpu) infected cells were present in the same generation. A similar delay was observed at day 2 and day 3 post-infection in the presence of Vpu. Indeed, at day 2 post-infection, 31% of

p24 positive HIV-1 Vpr L64P infected cells were detected in the second generation and 5% in the third generation whereas 38% and 14% of p24 positive HIV-1 L64P delVpu infected cells accumulated respectively in the same divisions. This delay seems to result from the fact that more cells accumulated in the first generation when infected with a Vpu-encoding HIV-1 (50%) while only 38% of HIV-1 delVpu infected cells were measured in the first division. These results were then confirmed by an additional experiment performed from a different blood donor (Figure 7.19B). A similar pattern of proliferation was found. In all cases the expression of Vpu induced a delay of T cell proliferation. Cells infected with Vpu-expressing HIV-1 always displayed accumulation of cells in the early generations resulting in less cells counted in the last generations whereas Vpu-defective HIV-1 infected T cells had the opposite proliferation profile. However, the delay observed might be due to the cytopathic effects of Vpu rather than its role in regulating T cell proliferation. Indeed, Vpu has been suggested to promote T cell apoptosis by interfering with NF-κB activation in a manner dependent on β-TRCP interaction (350). Preliminary data showed that SNAT-1 degradation might be β-TRCP dependent, it is therefore possible that Vpu targeting SNAT-1 might also contribute to apoptosis. It would be interesting to determine whether Vpu-mediated degradation of tetherin, CD4 or SNAT-1 participate differentially to apoptosis or if there are any competitive pressures between these three degradation pathways.

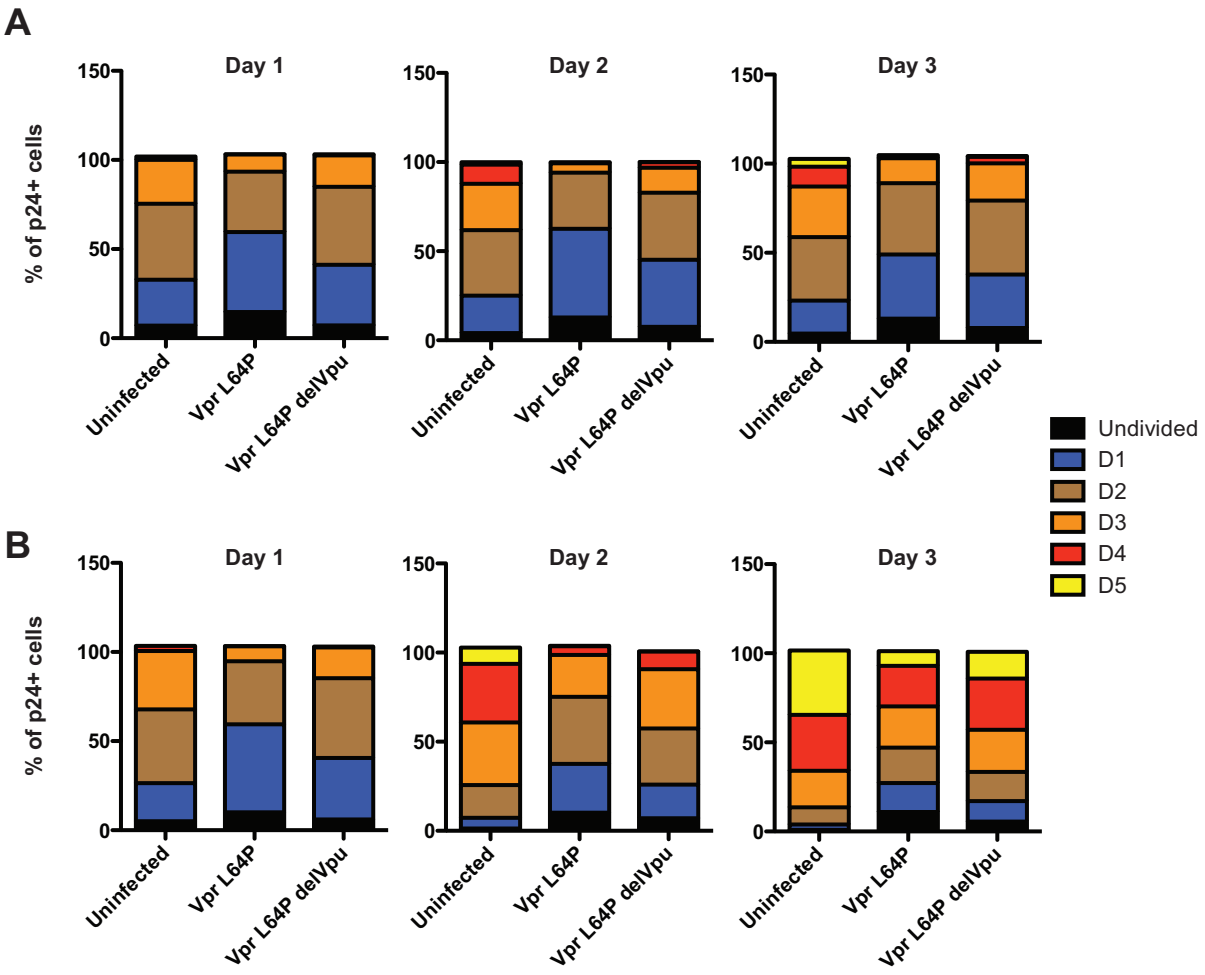

Figure 7.19: Proliferation profile of primary human CD4$^+$ T cells under HIV-1 infection.

A: Primary human CD4$^+$ T cells were isolated and infected as above. Proliferation in p24 positive cells was measured at 24 (day 1), 72 (day 2) and 96 hours (day 3) post-infection by flow cytometry using Violet dye as a cell division tracer. Each histograms display the proportion of p24 positive CD4$^+$ T cells in the indicated cell division (generation). Generations are indicated in colors. **B:** Similar experiment as in A but with a different blood donor. In that experiment, the infection levels were higher than in A.

7.2.7.2 Influence of glutamine levels on HIV-1 replication

Based on the hypothesis that Vpu degrades SNAT-1 to modulate the intracellular glutamine levels, we then asked whether HIV-1 replication was enhanced in glutamine concentrations (< 1mM) that were shown to limit T cell proliferation. To address this, we examined HIV-1 replication in infected cells maintained in different glutamine concentrations (Figure 7.20A). Untouched human CD4$^+$ T cells were isolated from peripheral blood mononuclear cells (PBMC), stimulated with anti-CD3/CD28 antibodies and maintained in culture medium supplemented with minimal glutamine concentration (1mM). Two days later, the cells were infected with VSV-G pseudotyped NL4.3 HIV-1 Wt or HIV-1 delVpu at an MOI of 0.1 to allow the virus to replicate

through the culture over-time via multiple cycles of infection. Three hours post-infection, cells were washed to eliminate viruses in suspension and excess of glutamine. The cells were then placed in media containing dialyzed serum and a dilution range of glutamine concentrations (0-0.2-0.5-1mM). Then, several time points were collected and at which the infectivity of viral supernatants was assayed on TZMbl cells (Figure 7.20B) and cells stained for intracellular p24 (Figure 7.20C). Firstly, we found, based on the infectivity assay of viral supernatants, that virus production was maximal at 3 days post-infection for HIV-1 Wt in all concentrations of glutamine tested. Virus production of HIV-1 delVpu reaches its peak one day later compared to HIV-1 Wt, at day 4 post-infection, for all the conditions tested with the exception of cells maintained in 1mM extracellular glutamine concentration for which the maximal virus production is almost reached at day 3. This observation does not validate our hypothesis, as we would expect to have a lower virus replication rate in high glutamine levels when Vpu is not expressed. Unsurprisingly, HIV-1 delVpu viral titers were 1 log lower than those of HIV-1 Wt due to tetherin-mediated particle release retention. Importantly, no defect in HIV-1 replication was observed at subphysiological glutamine concentrations (0.2; 0.5mM) suggesting that limited cell proliferation is not detrimental for virus replication. In the absence of extracellular glutamine (0mM), the replication rate of HIV-1 Wt was much slower with virus production reaching its peak 7 days post-infection. Since a similar delay was observed in HIV-1 delVpu infected cells, those effects could not be attributed to Vpu. Presumably, this delay reflects the fact that in such conditions fewer virus-producer cells are being generated due to limited cell proliferation thus impairing virus replication but HIV-1 might still manage to replicate in glutamine-free medium by acquiring the nutrients via autophagy. Replication rate analysed by examining the percentage of cells that became p24 positive over time revealed a similar picture (Figure 7.20C). These observations were confirmed by an additional experiment involving a second donor and two different experimental setups (Figure 7.21). Therefore, HIV-1 does not replicate more efficiently in low glutamine concentrations, such concentrations that limit T cell proliferation. In addition, HIV-1 delVpu virus production does not seem to be significantly affected by varying doses of extracellular glutamine. Importantly, even at sub-physiological glutamine concentration (0, 0.2, 0.5 mM) HIV-1 replicates efficiently. The differential effects of glutamine on HIV-1 replication is likely due to the fact that in lower glutamine concentrations T cell proliferation is decreased and consequently fewer T cells are available for rounds of re-infection and viral production. Taken together these data suggest that HIV-1 replication is not positively modulated by Vpu through the regulation of glutamine levels.

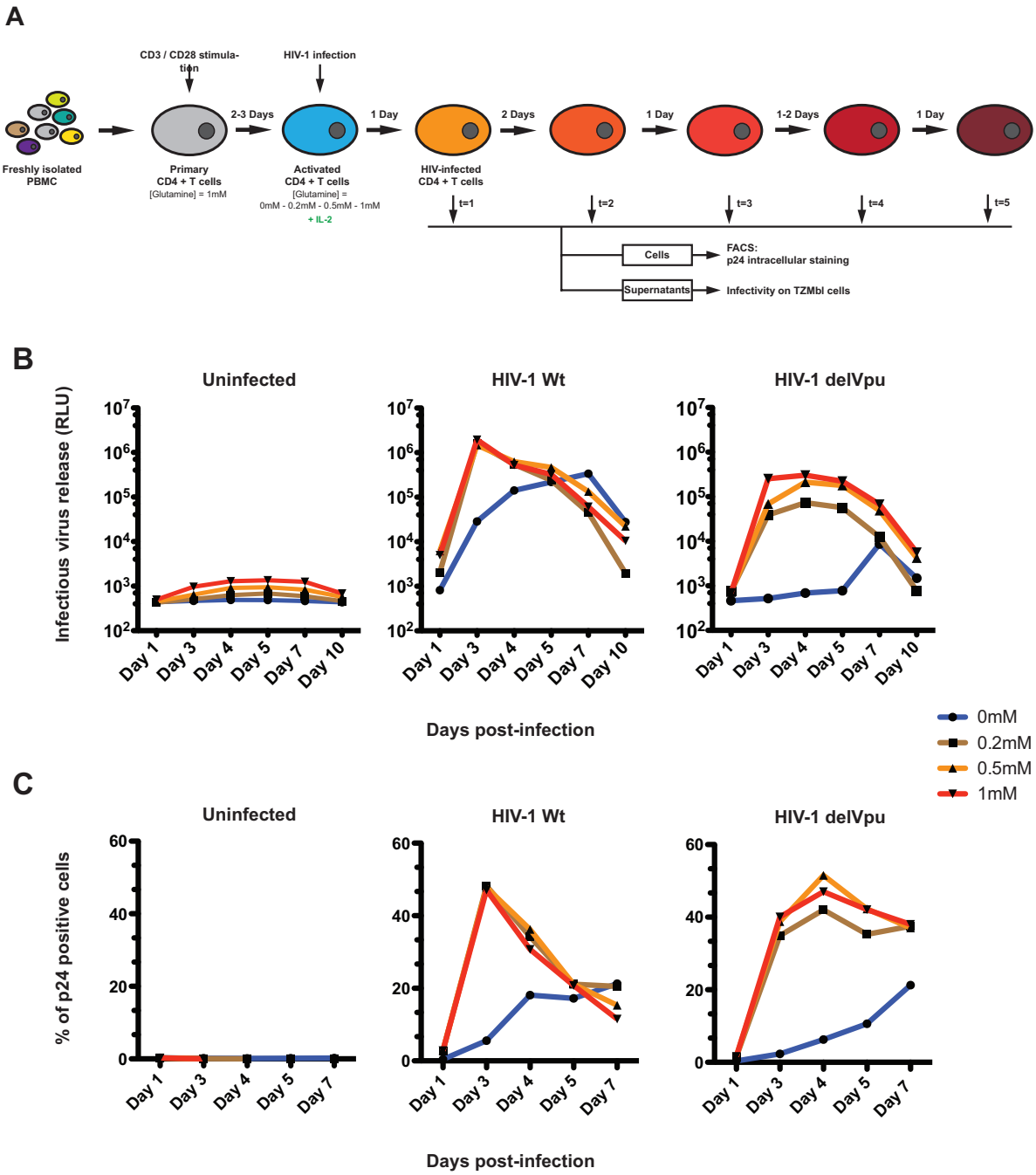

Figure 7.20: Effects of extracellular glutamine levels on HIV-1 replication in primary human CD4$^+$ T cells (DONOR A).

A: Schematic representation of the experimental procedure. CD4$^+$ T cells were negatively isolated from fresh PBMCs and stimulated with anti-CD3/CD28 activator Dynabeads and cultured with medium containing 1mM concentration of glutamine. Two days later, cells were infected as above (MOI=0.1), washed 3 times and placed in medium containing the indicated concentration of glutamine (0, 0.2, 0.5 or 1mM). Time points were collected at the indicated time post-infection. For each time point, both cell lysates and supernatants were harvested. Virus production was determined by measuring the infectivity of viral supernatants via quantification of β-galactosidase activity on HeLa-TZMbl reporter cell lines (**B**). Cells lysates were stored in staining buffer, stained with PE-conjugated anti-p24 and analysed by flow cytometry (**C**). The p24 positive gate was set up using uninfected cells.

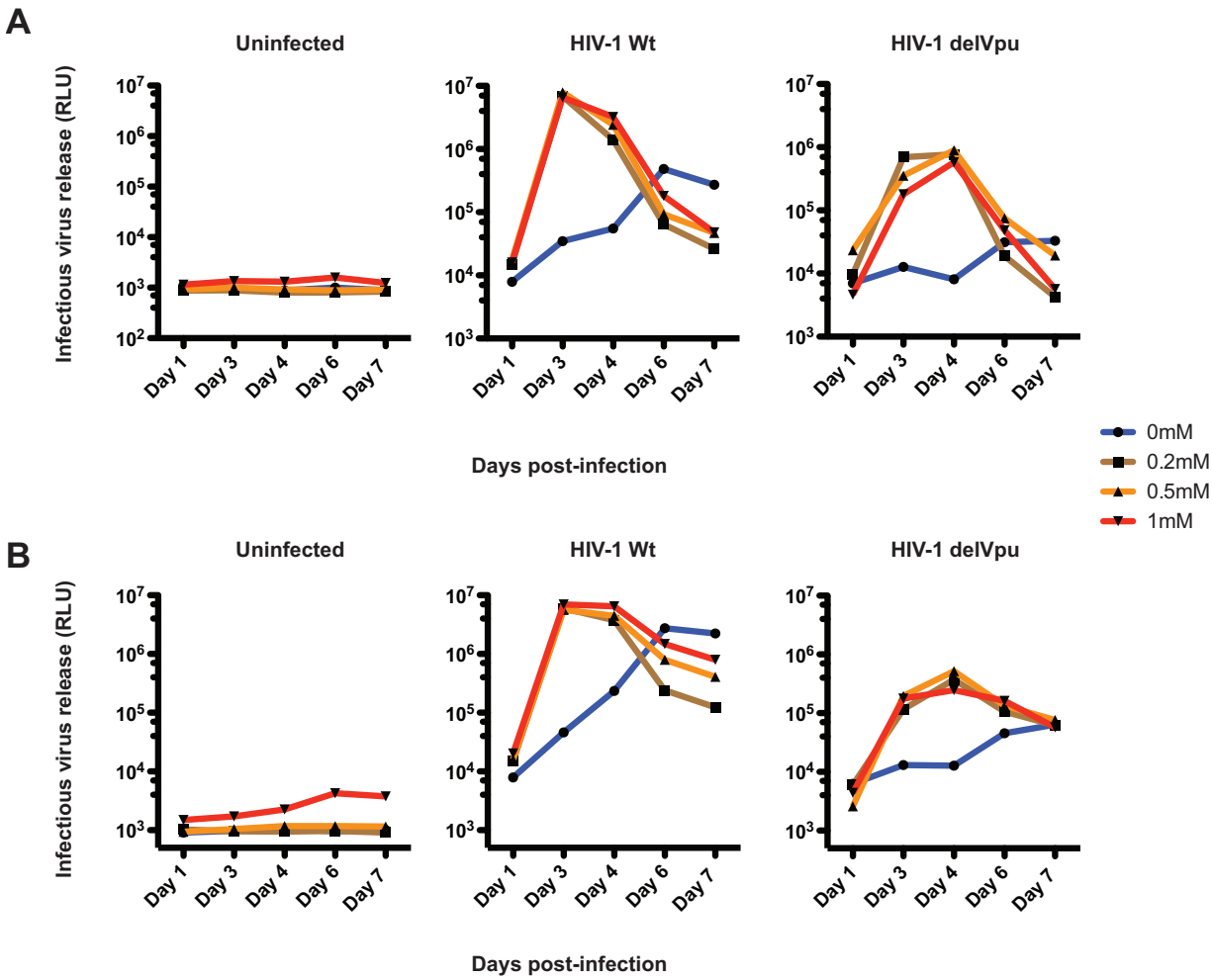

Figure 7.21: Effects of extracellular glutamine levels on HIV-1 replication in primary human CD4$^+$ T cells (DONOR B).

Same experimental procedure than the figure above but with blood from a different donor. **A:** Profile of HIV-1 replication via titration of viral supernatants on TZMbl cells. In this experimental setup, at each time point cells were centrifuged, viral supernatants collected and the same cells were cultured by adding fresh medium containing the appropriate glutamine concentration. **B:** In this experimental setup, cells were not passaged several times by replacing harvested-supernatant. These two experiments involve the same donor. Viral supernatants were assayed on HeLa-TZMbl indicator cells as described before.

We then examined whether the infectivity of viral particles produced was impaired in limiting glutamine levels, conditions that Vpu might create through the degradation of SNAT-1. Primary CD4$^+$ T cells were isolated and infected as mentioned above, at a MOI of 2. 48 hours post-infection, the viral supernatants were titrated on HeLa-TZMbl cells and cell lysates Western-blotted for Gag (Figure 7.22). We found no differences between the amounts of particles released from infected cells maintained in limiting or high glutamine levels, and this, for both HIV-1 Wt and delVpu viruses. Gag was indifferently processed in 0.2, 0.5, 1mM or 0mM glutamine concentrations. Therefore, one single round of HIV-1 replication in CD4$^+$ T lymphocytes does not provide evidence that Vpu influences HIV-1 replication by regulating/limiting glutamine access.

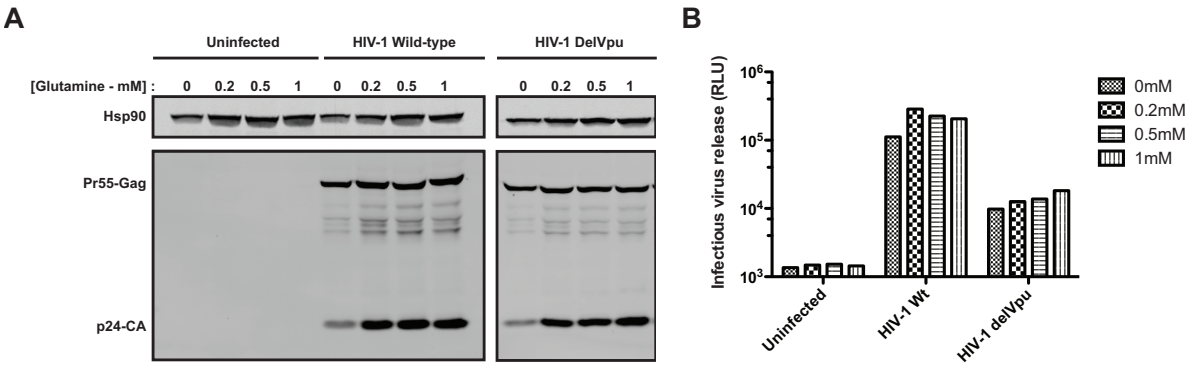

Figure 7.22: Limiting glutamine levels do not affect intracellular Gag processing and single round viral particle release.

A: $CD4^+$ T cells were extracted, infected (MOI=2) with the indicated VSV-G pseudotyped HIV-1 and cultured with different doses of extracellular glutamine. Cells were lysed 48 post-infection in SDS-PAGE loading buffer and Western blotted for gag and Hsp90. **B:** Viral supernatants from A were titrated on HeLa-TZMbl cells.

7.3 Discussion

In this study we have, in collaboration with Paul Lehner's lab, identified a new target of HIV-1 Vpu by proteomics analysis. SNAT-1 was, after tetherin, the second most downregulated plasma membrane protein by Vpu expression in the SILAC assay. Beyond that aspect, this technique provides a picture of the signature printed by Vpu on its host cell and might be used to determine fingerprints of many other viral components. So far, viral proteins have been shown to target several major components of the immune system such as restriction factors, cell-surface immune receptors, pathogens sensors, in order to escape recognition by the immune system. In that sense, SNAT-1 is particularly interesting and challenging since this protein acts as a glutamine transporter and thus represents a major component of cell metabolism, but it is unlikely to be a direct effector of immune responses. Vpu targets a cellular protein, which is not directly harmful for HIV-1, but its depletion might provide a better cellular environment for HIV-1 replication. The physiological implications of SNAT-1-depletion by Vpu have yet to be determined. Since T cell proliferation was shown to be glutamine and SNAT-1-dependent we thought that Vpu could interfere with the glutamine uptake pathway to inhibit T cell proliferation. Additional experiments will need to be done to confirm whether, as expected, glutamine uptake of T cells infected with HIV-1 Wt is decreased compared to T cells infected with Vpu-defective HIV-1. Preliminary data suggest that T cells infected with Vpu-defective HIV-1 undergo more cell divisions than those infected with HIV-1 Wt.

In the attempt to elucidate the benefits for the virus to inhibit T cell proliferation, we have not found any evidence that Vpu could, through the regulation of intracellular glutamine levels, positively affect HIV-1 replication. HIV-1 replication displayed a similar pattern of replication under either low or high glutamine inputs. The virus growth curves of all the glutamine concentrations tested always peak at the same time. Therefore, HIV-1 can cope with subphysiological glutamine levels. In the absence of glutamine, the replication rate was delayed but ultimately the virus managed to achieve efficient virus production in a Vpu-independent manner. With our collaborators we are currently setting up an assay to silence SNAT-1 expression in primary human $CD4^+$ T cells in order to mimic Vpu's effects. It would be interesting to study in such conditions the profiles of HIV-1 replication and T cell proliferation.

It is tempting to speculate that Vpu interferes with T cell metabolism as a means to regulate their activity. By limiting glutamine access Vpu could inhibit T cell proliferation and dampen T cell activation. This scenario is intriguing since T cell activation is a process that generally stimulates virus replication, however this mechanism might, at a late stage of infection, allow the survival of infected cells and avoid activation-induced cell death (AICD). Through the action of Vpu, infected T cells might during HIV-1 infection return to a resting mode as latently infected cells. These cells may constitute an HIV-1 reservoir because they contain in their genome a transcriptionally silenced proviral genome, therefore remaining protected from immune detection. Vpu might play an important role in balancing the T cell activation state and HIV-1 replication. This mechanism may also be linked to the mTOR pathway (mammalian target of rapamycin). Indeed, the mTOR-signaling pathway has also been shown to be involved in T cell

metabolism and function (reviewed in (446)). It is currently thought that T cell activation requires a two-signal model. Signal 1 is the recognition of the antigen by the TCR complex and signal 2 is the co-stimulation mediated by the engagement of CD28. But in that configuration, there is nothing to inform the T cell to differentiate into a T helper (Th1), Th2 or Th17 cell, a regulatory cell or a memory cell. This instruction comes from the presence of environmental cues (amino acids, energy, growth factors, cytokines) integrated by the PI3-kinase family members, mTOR. In that context, mTOR acts as an environmental sensor able to interpret signals from the extracellular compartment to dictate the course of T cell differentiation and function upon antigen recognition. In the context of our study, mTOR might be a key component able to sense the availability of glutamine in the microenvironment and drive, in consequence, the T cell fate. The lack of intracellular glutamine generated by Vpu expression might be sensed by components of the mTOR pathway, leading to their inactivation. So in that configuration, Vpu would inhibit mTOR ("turn-off") and direct the cell towards the appropriate cellular response, for instance autophagy. Moreover, it cannot be excluded that glutamine transporters such as SNAT-1 might also be perfect candidates for glutamine sensing. Indeed, such proteins detected at the cell surface would have access to both intracellular and extracellular stores of glutamine.

Alternatively, we will also investigate the effects of SNAT-1 depletion and limiting glutamine levels on pro-inflammatory responses from HIV-1 infected dendritic cells and macrophages. In those cells, by degrading SNAT-1, Vpu might interfere with the glutamine metabolism required for cytokine production such as interferons (436). In that case, depletion of SNAT-1 in HIV-1 infected cells would be an additional immuno-evasion strategy.

We also examined the molecular mechanism by which Vpu achieves SNAT-1 degradation. We found that SNAT-1 was degraded in HIV-1 infected cells and depleted from the cell surface in a Vpu-dependent manner. We have identified some residues in Vpu sequence important to mediate SNAT-1 downregulation and degradation. The tryptophan residue W22 in Vpu transmembrane domain and the phosphorylation site in the cytoplasmic tail were found to be required for SNAT-1 degradation. Mutation on W22 impaired the ability of Vpu to interact with SNAT-1 in co-immunoprecipitation studies while Vpu S52,56A was still able to pull-down SNAT-1 suggesting that Vpu-mediating SNAT-1 binding was not sufficient for its ultimate degradation. By analogy, these two determinants are also required for Vpu-mediating CD4 and tetherin degradation suggesting that Vpu achieves SNAT-1 depletion by a similar mechanism involving the E3 ubiquitin ligase $SCF^{b\text{-}TRCP}$. Importantly, the recruitment of β-TRCP by Vpu was shown to indirectly inhibit the NF-κB activation pathway and cause apoptotic effects (cf. introduction) (350). Vpu targeting SNAT-1 could therefore be an additional cause of T cell apoptosis. Since degradation of tetherin, CD4 and potentially SNAT-1 are all dependent on β-TRCP interaction, it would be interesting to investigate whether there are competitive pressures to maintain the degradation of one substrate over another in the context of infected cell. Treatment with endolysosomal inhibitors and MG132 rescues SNAT-1 expression from Vpu-mediating degradation suggesting an ubiquitin-dependent endolysosomal degradation pathway. However, depletion of two ESCRT-I components TSg101 and UBAP1 did not impact Vpu's ability to degrade SNAT-1, potentially suggesting an ESCRT-independent mode of lysosomal

degradation. We also showed that the cytoplasmic tail of SNAT-1 did not confer sensitivity to Vpu-mediated interaction and degradation. The determinants in SNAT-1 transmembrane region including the intra/extra cellular loops will be mapped by examining chimeric proteins bearing a truncated region of the SNAT-1 TMD and sequences from species SNAT-1 orthologues. In addition, Vpu colocalized with SNAT-1 into intracellular compartments.

Another important aspect of this project aims to screen Vpus from different HIV-1 and SIV strains for their ability to degrade SNAT-1. We know that tetherin antagonism is largely conserved in all primate lentiviruses even though most of the SIVs overcome tetherin from their corresponding host via the action of Nef. Bearing this in mind, it would be interesting to determine whether SNAT-1 counteraction is also an essential barrier to overcome for lentiviruses. If this was the case, we would expect to detect residues under positive selection in the regions of SNAT-1 targeted by Vpu. Preliminary data from our collaborators indicate that Group O Vpu proteins have not acquired the capacity to target SNAT-1 but Vpus from SIVPtt that gave rise to pandemic HIV-1 showed the ability to downregulate SNAT-1 from the cell surface. SIV Nef's ability to downregulate CD3 and CD28 was linked to reduced activation-induced death in SIV-infected monkeys (316), therefore, we could speculate that HIV-1 Vpu might achieve the same purpose through the degradation of SNAT-1.

Chapter 8 General Conclusion

24 years since the isolation of Vpu, understanding its role in HIV-1 infection is still a challenge. Vpu must be important for HIV-1 replication and/or pathogenesis since macaques infected with a Vpu-defective chimeric SHIV variant was found to revert back to a functional *vpu* open reading frame during the course of infection. Through the targeting of several cellular membrane-associated proteins, Vpu allows HIV-1 to escape recognition by the innate immune system and creates the optimal host cell conditions for virus replication and spread. It is intriguing that Vpu can interact with such a broad range of diverse cellular targets sharing little sequence homology. One of the best examples to illustrate the role of Vpu in counteracting defences developed by the cellular machinery, is the antagonism of the restriction factor, tetherin. Studying the mechanism by which Vpu overcomes tetherin's antiviral activity provides a powerful tool to understand the complex interactions between HIV-1 and its host.

In the chapter 3, we present evidence that Kaposi's sarcoma-associated herpesvirus (KSHV) has also evolved a countermeasure to alleviate tetherin-mediated restriction of virus particle release. KSHV encodes a ubiquitin ligase, K5 that mediates tetherin ubiquitination on its cytoplasmic tail lysines (210). This triggers tetherin removal from the cell-surface and its subsequent routing towards the endosomal compartments for degradation. In this study we compared the mechanisms of tetherin degradation between K5 and Vpu. While for K5, tetherin degradation is sufficient to overcome the antiviral function, we showed for Vpu that final destruction of tetherin did not account for the full antagonistic effect. This was evidenced by the tetherin lysine mutants that appeared to be resistant to degradation but were still sensitive to Vpu-mediated enhancement of virus release. The Vpu S52,56A mutant also illustrates that degradation of tetherin and its inactivation are two decoupled events. Indeed, this mutant fails to reduce intracellular levels of tetherin but displays some activity to enhance virus particle release. Based on recent studies, we now better understand this duality (383). All the data tend towards a model in which Vpu prevents tetherin from being expressed at the sites of virus budding to allow optimal virus release. But this is not strictly linked to Vpu's ability to mediate degradation *per se* but rather to its capacity to engage tetherin into a degradative pathway from which it cannot reach the cell-surface. Because residual tetherin colocalizes with Vpu in the trans-Golgi network, it was therefore initially thought that Vpu, by interacting with tetherin, mediated its sequestration in the TGN. We now think that this is likely to be pools of tetherin/Vpu complexes that accumulate in the TGN before being routed to the endosomal pathway. Presumably, in fixed cells, mainly the Vpu/tetherin complexes that accumulate in the slowest cellular pathway are visualized. Those complexes found in the TGN are likely queuing for delivery into the endosomal pathway. Their subsequent trafficking into endosomes is clathrin-dependent and has been proposed to be governed by a motif in the second alpha helix of Vpu cytoplasmic tail (ExxxLV). Therefore, K5 mediates tetherin downregulation from the cell surface whereas Vpu blocks transit to the surface (378, 382). In both cases, K5 and Vpu block tetherin incorporation into membranes of budding virions by reducing the levels of tetherin on the cell surface.

Several studies have investigated the nature of this degradation mechanism. Components of the ESCRT machinery were found to be required for Vpu-mediated tetherin degradation. Phosphorylation of Vpu on two conserved residues allows Vpu to bind the SCF-β-TrCP1/2 E3 ubiquitin ligase that ubiquitinates the tetherin cytoplasmic tail on multiple residues. In this regard, the residues targeted by Vpu for ubiquitination are still unclear. Not only the lysines but also a motif of serine/threonine/serine residues appear to be required for Vpu-mediated ubiquitination, and in some instance they may contribute to the antagonistic process. Ubiquitination of tetherin by Vpu triggers the recruitment of ESCRT subunits that then, sort tetherin molecules to the lysosomes for degradation.

The basis of the mechanism by which Vpu counteracts tetherin is linked to its capacity to interact via its transmembrane with tetherin. In chapter 4, by mutational analyses of HIV-1 Group M Vpu transmembrane domain, we have identified three amino acid residues that form one face of the transmembrane region of Vpu essential for tetherin interaction and antagonism. This face of Vpu transmembrane domain was also found to be important for mediating interaction with tetherin in a recent study. The data suggest that adaptation of this face of Vpu TMD might have been a prerequisite for virus zoonosis into the human host. This face includes a sequence of three alanines and a tryptophan spaced at four residue intervals within the Vpu TMD helix. It is thought that hydrophobic residues in the C-terminal region of the tetherin transmembrane domain might fit into the grooves formed by the alanines in the Vpu TMD. In that configuration, the tryptophan is thought to stabilize the overall structure of the Vpu TMD domain embedded into the lipid bilayer. These residues might also be involved in regulating the oligomerization state of Vpu. But more studies will need to be done to determine, first the driving force for multimerization and secondly whether Vpu acts on tetherin as a monomer or if higher order Vpu structures are required to neutralize tetherin's function.

Although M-Vpu and O-Vpu derive from an SIVcpz precursor, Vpu from group O HIV-1 has not acquired an anti-tetherin function. In chapter 5, we studied the molecular biology of HIV-1 group O Vpu to understand the reasons that render this protein unable to counteract human tetherin. O-Vpu is defective both for tetherin binding and TGN-associated subcellular localization. These defects map to the transmembrane and the region in the membrane proximal of O-Vpu cytoplasmic, respectively. Only O-Vpu chimera bearing these determinants displayed activity against tetherin. Since tetherin antagonism is conserved in all primate lentiviruses tested so far, in HIV-1 group O the anti-tetherin function might be supported by another viral component. As suggested by the study with Group P HIV-1, it cannot be excluded that some lentiviruses have not acquired such a function. Whether this reflects the lack of efficient spread into the human population as compared to the Group M, is unknown.

In addition to inducing CD4 and tetherin degradation, recently published studies revealed a role for Vpu in downregulating immuno-modulatory surface molecules such as CD1d, NTB-A and PVR possibly to avoid antigen-recognition by the immune system. Other cellular proteins might also be targeted by Vpu. Chapter 6 presents evidence that the glutamine transporter SNAT-1 is an additional cellular substrate of HIV-1 Vpu. While we do not yet understand the physiological implications of SNAT-1 depletion for viral replication, we have shown that $CD4^+$ T

cells infected with Vpu-defective HIV-1 proliferate more than wild-type infected cells. The magnitude of the phenotype is, however, weak and more experiments are required to confirm our hypothesis. Alternatively, SNAT-1 might be essential during viral infection to actively participate in the production of pro-inflammatory cytokines. It would be interesting to investigate whether in Vpu expression conditions such immune responses are attenuated.

Therefore, Vpu promotes HIV-1 replication at different stages; first, during virus assembly, Vpu allows the production of infectious virions. Then, as these nascent virions are budding through the host cell surface, the absence of tetherin allows them to be released into the extracellular milieu. Finally, downregulation of activator ligands prevents the infected cell from being recognized by immune cells, and thus viral replication can persist. Therefore, Vpu plays a pivotal role in the progression of HIV-1 infection; abrogation of this protein's functions is then a viable antiviral strategy.

References

1. **Barré-Sinoussi F**, **Chermann JC**, **Rey F**, **Nugeyre MT**, **Chamaret S**, **Gruest J**, **Dauguet C**, **Axler-Blin C**, **Vézinet-Brun F**, **Rouzioux C**, **Rozenbaum W**, **Montagnier L**. 1983. Isolation of a T-lymphotropic retrovirus from a patient at risk for acquired immune deficiency syndrome (AIDS). Science **220**:868–871.
2. **Gallo RC**, **Salahuddin SZ**, **Popovic M**, **Shearer GM**, **Kaplan M**, **Haynes BF**, **Palker TJ**, **Redfield R**, **Oleske J**, **Safai B**. 1984. Frequent detection and isolation of cytopathic retroviruses (HTLV-III) from patients with AIDS and at risk for AIDS. Science **224**:500–503.
3. **Popovic M**, **Sarngadharan MG**, **Read E**, **Gallo RC**. 1984. Detection, isolation, and continuous production of cytopathic retroviruses (HTLV-III) from patients with AIDS and pre-AIDS. Science **224**:497–500.
4. **Clavel F**, **Guétard D**, **Brun-Vézinet F**, **Chamaret S**, **Rey M-A**, **Santos-Ferreira MO**, **Laurent AG**, **Dauguet C**, **Katlama C**, **Rouzioux C**, **Klatzmann D**, **Champalimaud JL**, **Montagnier L**. 1986. Isolation of a New Human Retrovirus from West African Patients with AIDS 1–5. Science **233**:343–346.
5. **Chakrabarti L**, **Guyader M**, **Alizon M**, **Daniel MD**, **Desrosiers RC**, **Tiollais P**, **Sonigo P**. 1987. Sequence of simian immunodeficiency virus from macaque and its relationship to other human and simian retroviruses. Nature **328**:543–547.
6. **Guyader M**, **Emerman M**, **Sonigo P**, **Clavel F**, **Montagnier L**, **Alizon M**. 1987. Genome organization and transactivation of the human immunodeficiency virus type 2. Nature **326**:662–669.
7. **Huet T**, **Cheynier R**, **Meyerhans A**, **Roelants G**, **Wain-Hobson S**. 1990. Genetic organization of a chimpanzee lentivirus related to HIV-1. Nature **345**:356–359.
8. **Gao F**, **Bailes E**, **Robertson DL**, **Chen Y**, **Rodenburg CM**, **Michael SF**, **Cummins LB**, **Arthur LO**, **Peeters M**, **Shaw GM**, **Sharp PM**, **Hahn BH**. 1999. Origin of HIV-1 in the chimpanzee Pan troglodytes troglodytes. Nature **397**:436–441.
9. **Santiago ML**, **Rodenburg CM**, **Kamenya S**, **Bibollet-Ruche F**, **Gao F**, **Bailes E**, **Meleth S**, **Soong S-J**, **Kilby JM**, **Moldoveanu Z**, **Fahey B**, **Muller MN**, **Ayouba A**, **Nerrienet E**, **McClure HM**, **Heeney JL**, **Pusey AE**, **Collins DA**, **Boesch C**, **Wrangham RW**, **Goodall J**, **Sharp PM**, **Shaw GM**, **Hahn BH**. 2002. SIVcpz in wild chimpanzees. Science **295**:465.
10. **Keele BF**, **Van Heuverswyn F**, **Li Y**, **Bailes E**, **Takehisa J**, **Santiago ML**, **Bibollet-Ruche F**, **Chen Y**, **Wain LV**, **Liegeois F**, **Loul S**, **Ngole EM**, **Bienvenue Y**, **Delaporte E**, **Brookfield JFY**, **Sharp PM**, **Shaw GM**, **Peeters M**, **Hahn BH**. 2006. Chimpanzee reservoirs of pandemic and nonpandemic HIV-1. Science **313**:523–526.
11. **Sharp PM**, **Hahn BH**. 2011. Origins of HIV and the AIDS Pandemic. Cold Spring Harb Perspect Med **1**:a006841.
12. **Bailes E**, **Gao F**, **Bibollet-Ruche F**, **Courgnaud V**, **Peeters M**, **Marx PA**, **Hahn BH**, **Sharp PM**. 2003. Hybrid origin of SIV in chimpanzees. Science **300**:1713.
13. **De Leys R**, **Vanderborght B**, **Vanden Haesevelde M**, **Heyndrickx L**, **van Geel A**, **Wauters C**, **Bernaerts R**, **Saman E**, **Nijs P**, **Willems B**. 1990. Isolation and partial characterization of an unusual human immunodeficiency retrovirus from two persons of west-central African origin. Journal of Virology **64**:1207–1216.
14. **Gürtler LG**, **Hauser PH**, **Eberle J**, **Brunn von A**, **Knapp S**, **Zekeng L**, **Tsague JM**, **Kaptue L**. 1994. A new subtype of human immunodeficiency virus type 1 (MVP-5180) from Cameroon. Journal of Virology **68**:1581–1585.
15. **Mauclère P**, **Loussert-Ajaka I**, **Damond F**, **Fagot P**, **Souquières S**, **Monny Lobe M**, **Mbopi Keou FX**, **Barré-Sinoussi F**, **Saragosti S**, **Brun-Vézinet F**, **Simon F**. 1997. Serological and virological characterization of HIV-1 group O infection in Cameroon. AIDS **11**:445–453.
16. **Simon F**, **Mauclère P**, **Roques P**, **Loussert-Ajaka I**, **Müller-Trutwin MC**, **Saragosti S**, **Georges-Courbot MC**, **Barré-Sinoussi F**, **Brun-Vézinet F**. 1998. Identification of a new human immunodeficiency virus type 1 distinct from group M and group O. Nat Med **4**:1032–1037.
17. **Plantier J-C**, **Leoz M**, **Dickerson JE**, **De Oliveira F**, **Cordonnier F**, **Lemée V**, **Damond F**, **Robertson DL**, **Simon F**. 2009. A new human immunodeficiency virus derived from gorillas. Nat Med **15**:871–872.
18. **Worobey M**, **Gemmel M**, **Teuwen DE**, **Haselkorn T**, **Kunstman K**, **Bunce M**,

Muyembe J-J, **Kabongo J-MM**, **Kalengayi RM**, **Van Marck E**, **Gilbert MTP**, **Wolinsky SM**. 2008. Direct evidence of extensive diversity of HIV-1 in Kinshasa by 1960. Nature **455**:661–664.

19. **Zhu T**, **Korber BT**, **Nahmias AJ**, **Hooper E**, **Sharp PM**, **Ho DD**. 1998. An African HIV-1 sequence from 1959 and implications for the origin of the epidemic. Nature **391**:594–597.
20. **Korber B**, **Muldoon M**, **Theiler J**, **Gao F**, **Gupta R**, **Lapedes A**, **Hahn BH**, **Wolinsky S**, **Bhattacharya T**. 2000. Timing the ancestor of the HIV-1 pandemic strains. Science **288**:1789–1796.
21. **Sharp PM**, **Hahn BH**. 2008. AIDS: prehistory of HIV-1. Nature **455**:605–606.
22. **Gilbert MTP**, **Rambaut A**, **Wlasiuk G**, **Spira TJ**, **Pitchenik AE**, **Worobey M**. 2007. The emergence of HIV/AIDS in the Americas and beyond. Proc Natl Acad Sci USA **104**:18566–18570.
23. **Popper SJ**, **Sarr AD**, **Gueye-Ndiaye A**, **Mboup S**, **Essex ME**, **Kanki PJ**. 2000. Low Plasma Human Immunodeficiency Virus Type 2 Viral Load Is Independent of Proviral Load: Low Virus Production In Vivo. Journal of Virology **74**:1554–1557.
24. **Hirsch VM**, **Olmsted RA**, **Murphey-Corb M**, **Purcell RH**, **Johnson PR**. 2002. An African primate lentivirus (SIVsm) closely related to HIV-2. Nature **339**:389–392.
25. **Gao F**, **Yue L**, **White AT**, **Pappas PG**, **Barchue J**, **Hanson AP**, **Greene BM**, **Sharp PM**, **Shaw GM**, **Hahn BH**. 2002. Human infection by genetically diverse SIVSM-related HIV-2 in west Africa. Nature **358**:495–499.
26. **Chen Z**, **Telfier P**, **Gettie A**, **Reed P**, **Zhang L**, **Ho DD**, **Marx PA**. 1996. Genetic characterization of new West African simian immunodeficiency virus SIVsm: geographic clustering of household-derived SIV strains with human immunodeficiency virus type 2 subtypes and genetically diverse viruses from a single feral sooty mangabey troop. Journal of Virology **70**:3617–3627.
27. **Apetrei C**, **Kaur A**, **Lerche NW**, **Metzger M**, **Pandrea I**, **Hardcastle J**, **Falkenstein S**, **Bohm R**, **Koehler J**, **Traina-Dorge V**, **Williams T**, **Staprans S**, **Plauche G**, **Veazey RS**, **McClure H**, **Lackner AA**, **Gormus B**, **Robertson DL**, **Marx PA**. 2005. Molecular epidemiology of simian immunodeficiency virus SIVsm in U.S. primate centers unravels the origin of SIVmac and SIVstm. Journal of Virology **79**:8991–9005.
28. **Schuitemaker H**, **Koot M**, **Kootstra NA**, **Dercksen MW**, **de Goede RE**, **van Steenwijk RP**, **Lange JM**, **Schattenkerk JK**, **Miedema F**, **Tersmette M**. 1992. Biological phenotype of human immunodeficiency virus type 1 clones at different stages of infection: progression of disease is associated with a shift from monocytotropic to T-cell-tropic virus population. Journal of Virology **66**:1354–1360.
29. **Douek DC**, **Picker LJ**, **Koup RA**. 2003. T cell dynamics in HIV-1 infection. Annu. Rev. Immunol. **21**:265–304.
30. **Coffin JM**, **Hughes SH**, **Varmus HE**, **Fauci AS**, **Desrosiers RC**. 1997. Pathogenesis of HIV and SIV. Cold Spring Harbor Laboratory Press, Cold Spring Harbor (NY).
31. **Stevenson M**. 2003. HIV-1 pathogenesis. Nat Med **9**:853–860.
32. **McCune JM**. 2001. The dynamics of CD4+ T-cell depletion in HIV disease. Nature **410**:974–979.
33. **Doitsh G**, **Cavrois M**, **Lassen KG**, **Zepeda O**, **Yang Z**, **Santiago ML**, **Hebbeler AM**, **Greene WC**. 2010. Abortive HIV infection mediates CD4 T cell depletion and inflammation in human lymphoid tissue. Cell **143**:789–801.
34. **Hirsch VM**. 2004. What can natural infection of African monkeys with simian immunodeficiency virus tell us about the pathogenesis of AIDS? AIDS Rev **6**:40–53.
35. **Silvestri G**. 2005. Naturally SIV-infected sooty mangabeys: are we closer to understanding why they do not develop AIDS? Journal of Medical Primatology **34**:243–252.
36. **Arts EJ**, **Hazuda DJ**. 2012. HIV-1 Antiretroviral Drug Therapy. Cold Spring Harb Perspect Med **2**:a007161.
37. **Autran B**, **Carcelain G**, **Li TS**, **Blanc C**, **Mathez D**, **Tubiana R**, **Katlama C**, **Debré P**, **Leibowitch J**. 1997. Positive effects of combined antiretroviral therapy on CD4+ T cell homeostasis and function in advanced HIV disease. Science **277**:112–116.
38. **Komanduri KV**, **Viswanathan MN**, **Wieder ED**, **Schmidt DK**, **Bredt BM**, **Jacobson MA**, **McCune JM**. 1998. Restoration of cytomegalovirus-specific CD4+ T-lymphocyte responses after ganciclovir and highly active antiretroviral therapy in individuals infected with HIV-1. Nat Med **4**:953–956.
39. **Siliciano RF**, **Greene WC**. 2011. HIV Latency. Cold Spring Harb Perspect Med **1**:a007096.

40. **Hütter G**, **Nowak D**, **Mossner M**, **Ganepola S**, **Müssig A**, **Allers K**, **Schneider T**, **Hofmann J**, **Kücherer C**, **Blau O**, **Blau IW**, **Hofmann WK**, **Thiel E**. 2009. Long-term control of HIV by CCR5 Delta32/Delta32 stem-cell transplantation. N. Engl. J. Med. **360**:692–698.
41. **Hütter G**, **Thiel E**. 2011. Allogeneic transplantation of CCR5-deficient progenitor cells in a patient with HIV infection: an update after 3 years and the search for patient no. 2. AIDS **25**:273–274.
42. **Holt N**, **Wang J**, **Kim K**, **Friedman G**, **Wang X**, **Taupin V**, **Crooks GM**, **Kohn DB**, **Gregory PD**, **Holmes MC**, **Cannon PM**. 2010. Human hematopoietic stem/progenitor cells modified by zinc-finger nucleases targeted to CCR5 control HIV-1 in vivo. Nat. Biotechnol. **28**:839–847.
43. **Rerks-Ngarm S**, **Pitisuttithum P**, **Nitayaphan S**, **Kaewkungwal J**, **Chiu J**, **Paris R**, **Premsri N**, **Namwat C**, **de Souza M**, **Adams E**, **Benenson M**, **Gurunathan S**, **Tartaglia J**, **McNeil JG**, **Francis DP**, **Stablein D**, **Birx DL**, **Chunsuttiwat S**, **Khamboonruang C**, **Thongcharoen P**, **Robb ML**, **Michael NL**, **Kunasol P**, **Kim JH**, **MOPH-TAVEG Investigators**. 2009. Vaccination with ALVAC and AIDSVAX to prevent HIV-1 infection in Thailand. N. Engl. J. Med. **361**:2209–2220.
44. **Frankel AD**, **Young JA**. 1998. HIV-1: fifteen proteins and an RNA. Annu Rev Biochem **67**:1–25.
45. **Malim MH**, **Emerman M**. 2008. HIV-1 accessory proteins--ensuring viral survival in a hostile environment. Cell Host Microbe **3**:388–398.
46. **Swanson CM**, **Malim MH**. 2008. SnapShot: HIV-1 proteins. Cell **133**:742, 742.e1.
47. **Engelman A**, **Cherepanov P**. 2012. The structural biology of HIV-1: mechanistic and therapeutic insights. Nature Reviews Microbiology **10**:279–290.
48. **Klatzmann D**, **Barré-Sinoussi F**, **Nugeyre MT**, **Danquet C**, **Vilmer E**, **Griscelli C**, **Brun-Veziret F**, **Rouzioux C**, **Gluckman JC**, **Chermann JC**. 1984. Selective tropism of lymphadenopathy associated virus (LAV) for helper-inducer T lymphocytes. Science **225**:59–63.
49. **Klatzmann D**, **Champagne E**, **Chamaret S**, **Gruest J**, **Guetard D**, **Hercend T**, **Gluckman JC**, **Montagnier L**. 1984. T-lymphocyte T4 molecule behaves as the receptor for human retrovirus LAV. Nature **312**:767–768.
50. **Sattentau QJ**, **Weiss RA**. 1988. The CD4 antigen: physiological ligand and HIV receptor. Cell **52**:631–633.
51. **Maddon PJ**, **Dalgleish AG**, **McDougal JS**, **Clapham PR**, **Weiss RA**, **Axel R**. 1986. The T4 gene encodes the AIDS virus receptor and is expressed in the immune system and the brain. Cell **47**:333–348.
52. **Feng Y**, **Broder CC**, **Kennedy PE**, **Berger EA**. 1996. HIV-1 entry cofactor: functional cDNA cloning of a seven-transmembrane, G protein-coupled receptor. Science **272**:872–877.
53. **Alkhatib G**, **Combadiere C**, **Broder CC**, **Feng Y**, **Kennedy PE**, **Murphy PM**, **Berger EA**. 1996. CC CKR5: a RANTES, MIP-1alpha, MIP-1beta receptor as a fusion cofactor for macrophage-tropic HIV-1. Science **272**:1955–1958.
54. **Choe H**, **Farzan M**, **Sun Y**, **Sullivan N**, **Rollins B**, **Ponath PD**, **Wu L**, **Mackay CR**, **LaRosa G**, **Newman W**, **Gerard N**, **Gerard C**, **Sodroski J**. 1996. The beta-chemokine receptors CCR3 and CCR5 facilitate infection by primary HIV-1 isolates. Cell **85**:1135–1148.
55. **Deng H**, **Liu R**, **Ellmeier W**, **Choe S**, **Unutmaz D**, **Burkhart M**, **Di Marzio P**, **Marmon S**, **Sutton RE**, **Hill CM**, **Davis CB**, **Peiper SC**, **Schall TJ**, **Littman DR**, **Landau NR**. 1996. Identification of a major co-receptor for primary isolates of HIV-1. Nature **381**:661–666.
56. **Doranz BJ**, **Rucker J**, **Yi Y**, **Smyth RJ**, **Samson M**, **Peiper SC**, **Parmentier M**, **Collman RG**, **Doms RW**. 1996. A dual-tropic primary HIV-1 isolate that uses fusin and the beta-chemokine receptors CKR-5, CKR-3, and CKR-2b as fusion cofactors. Cell **85**:1149–1158.
57. **Dragic T**, **Litwin V**, **Allaway GP**, **Martin SR**, **Huang Y**, **Nagashima KA**, **Cayanan C**, **Maddon PJ**, **Koup RA**, **Moore JP**, **Paxton WA**. 1996. HIV-1 entry into CD4+ cells is mediated by the chemokine receptor CC-CKR-5. Nature **381**:667–673.
58. **McDougal JS**, **Kennedy MS**, **Sligh JM**, **Cort SP**, **Mawle A**, **Nicholson JK**. 1986. Binding of HTLV-III/LAV to T4+ T cells by a complex of the 110K viral protein and the T4 molecule. Science **231**:382–385.
59. **Kwong PD**, **Wyatt R**, **Robinson J**, **Sweet RW**, **Sodroski J**, **Hendrickson WA**. 1998. Structure of an HIV gp120 envelope glycoprotein in complex with the CD4 receptor

and a neutralizing human antibody. Nature **393**:648–659.
60. **Berger EA**, **Doms RW**, **Fenyö EM**, **Korber BT**, **Littman DR**, **Moore JP**, **Sattentau QJ**, **Schuitemaker H**, **Sodroski J**, **Weiss RA**. 1998. A new classification for HIV-1. Nature **391**:240.
61. **Chan DC**, **Fass D**, **Berger JM**, **Kim PS**. 1997. Core structure of gp41 from the HIV envelope glycoprotein. Cell **89**:263–273.
62. **Weissenhorn W**, **Dessen A**, **Harrison SC**, **Skehel JJ**, **Wiley DC**. 1997. Atomic structure of the ectodomain from HIV-1 gp41. Nature **387**:426–430.
63. **Wilen CB**, **Tilton JC**, **Doms RW**. 2012. HIV: Cell Binding and Entry. Cold Spring Harb Perspect Med **2**.
64. **Fassati A**, **Goff SP**. 2001. Characterization of intracellular reverse transcription complexes of human immunodeficiency virus type 1. Journal of Virology **75**:3626–3635.
65. **Nermut MV**, **Fassati A**. 2003. Structural analyses of purified human immunodeficiency virus type 1 intracellular reverse transcription complexes. Journal of Virology **77**:8196–8206.
66. **Bukrinsky MI**, **Haggerty S**, **Dempsey MP**, **Sharova N**, **Adzhubel A**, **Spitz L**, **Lewis P**, **Goldfarb D**, **Emerman M**, **Stevenson M**. 1993. A nuclear localization signal within HIV-1 matrix protein that governs infection of non-dividing cells. Nature **365**:666–669.
67. **Haffar OK**, **Popov S**, **Dubrovsky L**, **Agostini I**, **Tang H**, **Pushkarsky T**, **Nadler SG**, **Bukrinsky M**. 2000. Two nuclear localization signals in the HIV-1 matrix protein regulate nuclear import of the HIV-1 pre-integration complex. Journal of Molecular Biology **299**:359–368.
68. **Freed EO**, **Englund G**, **Maldarelli F**, **Martin MA**. 1997. Phosphorylation of Residue 131 of HIV-1 Matrix Is Not Required for Macrophage Infection. Cell **88**:171–173.
69. **Reil H**, **Bukovsky AA**, **Gelderblom HR**, **Gottlinger HG**. 1998. Efficient HIV-1 replication can occur in the absence of the viral matrix protein. EMBO J. **17**:2699–2708.
70. **Feng YX**, **Copeland TD**, **Henderson LE**, **Gorelick RJ**, **Bosche WJ**, **Levin JG**, **Rein A**. 1996. HIV-1 nucleocapsid protein induces “maturation” of dimeric retroviral RNA in vitro. Proc Natl Acad Sci USA **93**:7577–7581.
71. **Thomas JA**, **Gagliardi TD**, **Alvord WG**, **Lubomirski M**, **Bosche WJ**, **Gorelick RJ**. 2006. Human immunodeficiency virus type 1 nucleocapsid zinc-finger mutations cause defects in reverse transcription and integration. Virology **353**:41–51.
72. **Thomas JA**, **Bosche WJ**, **Shatzer TL**, **Johnson DG**, **Gorelick RJ**. 2008. Mutations in human immunodeficiency virus type 1 nucleocapsid protein zinc fingers cause premature reverse transcription. Journal of Virology **82**:9318–9328.
73. **Forshey BM**, **Schwedler von U**, **Sundquist WI**, **Aiken C**. 2002. Formation of a human immunodeficiency virus type 1 core of optimal stability is crucial for viral replication. Journal of Virology **76**:5667–5677.
74. **Dismuke DJ**, **Aiken C**. 2006. Evidence for a functional link between uncoating of the human immunodeficiency virus type 1 core and nuclear import of the viral preintegration complex. Journal of Virology **80**:3712–3720.
75. **Arhel NJ**, **Souquere-Besse S**, **Munier S**, **Souque P**, **Guadagnini S**, **Rutherford S**, **Prévost M-C**, **Allen TD**, **Charneau P**. 2007. HIV-1 DNA Flap formation promotes uncoating of the pre-integration complex at the nuclear pore. EMBO J. **26**:3025–3037.
76. **Hu WS**, **Hughes SH**. 2012. HIV-1 Reverse Transcription. Cold Spring Harb Perspect Med **2**:a006916.
77. **Charneau P**, **Alizon M**, **Clavel F**. 1992. A second origin of DNA plus-strand synthesis is required for optimal human immunodeficiency virus replication. Journal of Virology **66**:2814–2820.
78. **Fassati A**. 2006. HIV infection of non-dividing cells: a divisive problem. Retrovirology **3**:74.
79. **Goff SP**. 2001. Intracellular trafficking of retroviral genomes during the early phase of infection: viral exploitation of cellular pathways. J Gene Med **3**:517–528.
80. **Yamashita M**, **Emerman M**. 2004. Capsid is a dominant determinant of retrovirus infectivity in nondividing cells. Journal of Virology **78**:5670–5678.
81. **Fassati A**, **Goff SP**. 1999. Characterization of intracellular reverse transcription complexes of Moloney murine leukemia virus. Journal of Virology **73**:8919–8925.
82. **Fassati A**, **Görlich D**, **Harrison I**, **Zaytseva L**, **Mingot J-M**. 2003. Nuclear import of HIV-1 intracellular reverse transcription complexes is mediated by importin 7. EMBO J. **22**:3675–3685.

83. **Zaitseva L**, **Myers R**, **Fassati A**. 2006. tRNAs promote nuclear import of HIV-1 intracellular reverse transcription complexes. Plos Biol **4**:e332.
84. **Goff SP**. 2008. Knockdown Screens to Knockout HIV-1. Cell **135**:417–420.
85. **Brass AL**, **Dykxhoorn DM**, **Benita Y**, **Yan N**, **Engelman A**, **Xavier RJ**, **Lieberman J**, **Elledge SJ**. 2008. Identification of Host Proteins Required for HIV Infection Through a Functional Genomic Screen. Science **319**:921–926.
86. **Christ F**, **Thys W**, **De Rijck J**, **Gijsbers R**, **Albanese A**, **Arosio D**, **Emiliani S**, **Rain J-C**, **Benarous R**, **Cereseto A**, **Debyser Z**. 2008. Transportin-SR2 imports HIV into the nucleus. Curr. Biol. **18**:1192–1202.
87. **König R**, **Zhou Y**, **Elleder D**, **Diamond TL**, **Bonamy GMC**, **Irelan JT**, **Chiang C-Y**, **Tu BP**, **De Jesus PD**, **Lilley CE**, **Seidel S**, **Opaluch AM**, **Caldwell JS**, **Weitzman MD**, **Kuhen KL**, **Bandyopadhyay S**, **Ideker T**, **Orth AP**, **Miraglia LJ**, **Bushman FD**, **Young JA**, **Chanda SK**. 2008. Global analysis of host-pathogen interactions that regulate early-stage HIV-1 replication. Cell **135**:49–60.
88. **Zhou L**, **Sokolskaja E**, **Jolly C**, **James W**, **Cowley SA**, **Fassati A**. 2011. Transportin 3 promotes a nuclear maturation step required for efficient HIV-1 integration. PLoS Pathog **7**:e1002194.
89. **Lee K**, **Ambrose Z**, **Martin TD**, **Oztop I**, **Mulky A**, **Julias JG**, **Vandegraaff N**, **Baumann JG**, **Wang R**, **Yuen W**, **Takemura T**, **Shelton K**, **Taniuchi I**, **Li Y**, **Sodroski J**, **Littman DR**, **Coffin JM**, **Hughes SH**, **Unutmaz D**, **Engelman A**, **KewalRamani VN**. 2010. Flexible use of nuclear import pathways by HIV-1. Cell Host Microbe **7**:221–233.
90. **Schaller T**, **Ocwieja KE**, **Rasaiyaah J**, **Price AJ**, **Brady TL**, **Roth SL**, **Hué S**, **Fletcher AJ**, **Lee K**, **KewalRamani VN**, **Noursadeghi M**, **Jenner RG**, **James LC**, **Bushman FD**, **Towers GJ**. 2011. HIV-1 Capsid-Cyclophilin Interactions Determine Nuclear Import Pathway, Integration Targeting and Replication Efficiency. PLoS Pathog **7**:e1002439.
91. **Craigie R**, **Bushman FD**. 2012. HIV DNA Integration. Cold Spring Harb Perspect Med **2**:a006890.
92. **Schröder ARW**, **Shinn P**, **Chen H**, **Berry C**, **Ecker JR**, **Bushman F**. 2002. HIV-1 integration in the human genome favors active genes and local hotspots. Cell **110**:521–529.
93. **Emiliani S**, **Mousnier A**, **Busschots K**, **Maroun M**, **Van Maele B**, **Tempé D**, **Vandekerckhove L**, **Moisant F**, **Ben-Slama L**, **Witvrouw M**, **Christ F**, **Rain J-C**, **Dargemont C**, **Debyser Z**, **Benarous R**. 2005. Integrase mutants defective for interaction with LEDGF/p75 are impaired in chromosome tethering and HIV-1 replication. J Biol Chem **280**:25517–25523.
94. **Llano M**, **Saenz DT**, **Meehan A**, **Wongthida P**, **Peretz M**, **Walker WH**, **Teo W**, **Poeschla EM**. 2006. An essential role for LEDGF/p75 in HIV integration. Science **314**:461–464.
95. **De Rijck J**, **Bartholomeeusen K**, **Ceulemans H**, **Debyser Z**, **Gijsbers R**. 2010. High-resolution profiling of the LEDGF/p75 chromatin interaction in the ENCODE region. Nucleic Acids Research **38**:6135–6147.
96. **Cherepanov P**, **Maertens G**, **Proost P**, **Devreese B**, **Van Beeumen J**, **Engelborghs Y**, **De Clercq E**, **Debyser Z**. 2003. HIV-1 integrase forms stable tetramers and associates with LEDGF/p75 protein in human cells. J Biol Chem **278**:372–381.
97. **Turlure F**, **Devroe E**, **Silver PA**, **Engelman A**. 2004. Human cell proteins and human immunodeficiency virus DNA integration. Front. Biosci. **9**:3187–3208.
98. **Llano M**, **Vanegas M**, **Hutchins N**, **Thompson D**, **Delgado S**, **Poeschla EM**. 2006. Identification and characterization of the chromatin-binding domains of the HIV-1 integrase interactor LEDGF/p75. Journal of Molecular Biology **360**:760–773.
99. **Chen H**, **Engelman A**. 1998. The barrier-to-autointegration protein is a host factor for HIV type 1 integration. Proc Natl Acad Sci USA **95**:15270–15274.
100. **Rittner K**, **Churcher MJ**, **Gait MJ**, **Karn J**. 1995. The human immunodeficiency virus long terminal repeat includes a specialised initiator element which is required for Tat-responsive transcription. Journal of Molecular Biology **248**:562–580.
101. **Jones KA**, **Kadonaga JT**, **Luciw PA**. 1986. Activation of the AIDS retrovirus promoter by the cellular transcription factor, Sp1. Science **232**:755–759.
102. **Garcia JA**, **Harrich D**, **Soultanakis E**, **Wu F**, **Mitsuyasu R**, **Gaynor RB**. 1989. Human immunodeficiency virus type 1 LTR TATA and TAR region sequences required for transcriptional regulation. EMBO J. **8**:765–778.
103. **Zenzie-Gregory B**, **Sheridan P**, **Jones KA**, **Smale ST**. 1993. HIV-1 core promoter

lacks a simple initiator element but contains a bipartite activator at the transcription start site. J Biol Chem **268**:15823–15832.
104. **Nabel G**, **Baltimore D**. 1987. An inducible transcription factor activates expression of human immunodeficiency virus in T cells. Nature **326**:711–713.
105. **Liu J**, **Perkins ND**, **Schmid RM**, **Nabel GJ**. 1992. Specific NF-kappa B subunits act in concert with Tat to stimulate human immunodeficiency virus type 1 transcription. Journal of Virology **66**:3883–3887.
106. **Kinoshita S**, **Chen BK**, **Kaneshima H**, **Nolan GP**. 1998. Host control of HIV-1 parasitism in T cells by the nuclear factor of activated T cells. Cell **95**:595–604.
107. **Yankulov K**, **Bentley D**. 1998. Transcriptional control: Tat cofactors and transcriptional elongation. Curr. Biol. **8**:R447–9.
108. **Karn J**, **Stoltzfus CM**. 2012. Transcriptional and Posttranscriptional Regulation of HIV-1 Gene Expression. Cold Spring Harb Perspect Med **2**:a006916.
109. **Feng S**, **Holland EC**. 1988. HIV-1 tat trans-activation requires the loop sequence within tar. Nature **334**:165–167.
110. **Dingwall C**, **Ernberg I**, **Gait MJ**, **Green SM**, **Heaphy S**, **Karn J**, **Lowe AD**, **Singh M**, **Skinner MA**, **Valerio R**. 1989. Human immunodeficiency virus 1 tat protein binds trans-activation-responsive region (TAR) RNA in vitro. Proc Natl Acad Sci USA **86**:6925–6929.
111. **Wei P**, **Garber ME**, **Fang SM**, **Fischer WH**, **Jones KA**. 1998. A novel CDK9-associated C-type cyclin interacts directly with HIV-1 Tat and mediates its high-affinity, loop-specific binding to TAR RNA. Cell **92**:451–462.
112. **Mancebo HS**, **Lee G**, **Flygare J**, **Tomassini J**, **Luu P**, **Zhu Y**, **Peng J**, **Blau C**, **Hazuda D**, **Price D**, **Flores O**. 1997. P-TEFb kinase is required for HIV Tat transcriptional activation in vivo and in vitro. Genes & Development **11**:2633–2644.
113. **Bieniasz PD**, **Grdina TA**, **Bogerd HP**, **Cullen BR**. 1998. Recruitment of a protein complex containing Tat and cyclin T1 to TAR governs the species specificity of HIV-1 Tat. EMBO J. **17**:7056–7065.
114. **Pollard VW**, **Malim MH**. 1998. The HIV-1 Rev protein. Annu. Rev. Microbiol. **52**:491–532.
115. **Sodroski J**, **Goh WC**, **Rosen C**, **Dayton A**, **Terwilliger E**, **Haseltine W**. 1986. A second post-transcriptional trans-activator gene required for HTLV-III replication. Nature **321**:412–417.
116. **Malim MH**, **Hauber J**, **Le SY**, **Maizel JV**, **Cullen BR**. 1989. The HIV-1 rev trans-activator acts through a structured target sequence to activate nuclear export of unspliced viral mRNA. Nature **338**:254–257.
117. **Malim MH**, **Cullen BR**. 1991. HIV-1 structural gene expression requires the binding of multiple Rev monomers to the viral RRE: Implications for HIV-1 latency. Cell **65**:241–248.
118. **Fornerod M**, **Ohno M**, **Yoshida M**, **Mattaj IW**. 1997. CRM1 is an export receptor for leucine-rich nuclear export signals. Cell **90**:1051–1060.
119. **Fischer U**, **Huber J**, **Boelens WC**, **Mattaj IW**, **Lührmann R**. 1995. The HIV-1 Rev activation domain is a nuclear export signal that accesses an export pathway used by specific cellular RNAs. Cell **82**:475–483.
120. **Henderson BR**, **Percipalle P**. 1997. Interactions between HIV rev and nuclear import and export factors: the rev nuclear localisation signal mediates specific binding to human importin-β. Journal of Molecular Biology **274**:693–707.
121. **Bolinger C**, **Boris-Lawrie K**. 2009. Mechanisms employed by retroviruses to exploit host factors for translational control of a complicated proteome. Retrovirology **6**:8.
122. **Swanson CM**, **Sherer NM**, **Malim MH**. 2010. SRp40 and SRp55 promote the translation of unspliced human immunodeficiency virus type 1 RNA. Journal of Virology **84**:6748–6759.
123. **Krummheuer J**, **Johnson AT**, **Hauber I**, **Kammler S**, **Anderson JL**, **Hauber J**, **Purcell DFJ**, **Schaal H**. 2007. A minimal uORF within the HIV-1 vpu leader allows efficient translation initiation at the downstream env AUG. Virology **363**:261–271.
124. **Gheysen D**, **Jacobs E**, **de Foresta F**, **Thiriart C**, **Francotte M**, **Thines D**, **De Wilde M**. 1989. Assembly and release of HIV-1 precursor Pr55gag virus-like particles from recombinant baculovirus-infected insect cells. Cell **59**:103–112.
125. **Gottlinger HG**. 2001. The HIV-1 assembly machine. AIDS **15 Suppl 5**:S13–20.
126. **Jouvenet N**, **Bieniasz PD**, **Simon SM**. 2008. Imaging the biogenesis of individual HIV-1 virions in live cells. Nature **454**:236–240.
127. **Bieniasz PD. 2009. The cell biology of HIV-1 virion genesis. Cell Host Microbe**

5:550–558.

128. **Jouvenet N**, **Neil SJD**, **Bess C**, **Johnson MC**, **Virgen CA**, **Simon SM**, **Bieniasz PD**. 2006. Plasma Membrane Is the Site of Productive HIV-1 Particle Assembly. Plos Biol **4**:e435.
129. **Saad JS**, **Miller J**, **Tai J**, **Kim A**, **Ghanam RH**, **Summers MF**. 2006. Structural basis for targeting HIV-1 Gag proteins to the plasma membrane for virus assembly. Proc Natl Acad Sci USA **103**:11364–11369.
130. **Ono A**, **Ablan SD**, **Lockett SJ**, **Nagashima K**, **Freed EO**. 2004. Phosphatidylinositol (4,5) bisphosphate regulates HIV-1 Gag targeting to the plasma membrane. Proc Natl Acad Sci USA **101**:14889–14894.
131. **D'Souza V**, **Summers MF**. 2005. How retroviruses select their genomes. Nature Reviews Microbiology **3**:643–655.
132. **Jouvenet N**, **Simon SM**, **Bieniasz PD**. 2009. Imaging the interaction of HIV-1 genomes and Gag during assembly of individual viral particles. Proc Natl Acad Sci USA **106**:19114–19119.
133. **Kutluay SB**, **Bieniasz PD**. 2010. Analysis of the initiating events in HIV-1 particle assembly and genome packaging. PLoS Pathog **6**:e1001200.
134. **Ono A**, **Freed EO**. 2001. Plasma membrane rafts play a critical role in HIV-1 assembly and release. Proc Natl Acad Sci USA **98**:13925–13930.
135. **Ganser-Pornillos BK**, **Yeager M**, **Sundquist WI**. 2008. The structural biology of HIV assembly. Current Opinion in Structural Biology **18**:203–217.
136. **Kondo E**, **Mammano F**, **Cohen EA**, **Gottlinger HG**. 1995. The p6gag domain of human immunodeficiency virus type 1 is sufficient for the incorporation of Vpr into heterologous viral particles. Journal of Virology **69**:2759–2764.
137. **Kleiman L**, **Jones CP**, **Musier-Forsyth K**. 2010. Formation of the tRNALys packaging complex in HIV-1. FEBS Lett. **584**:359–365.
138. **Freed EO**, **Martin MA**. 1995. The role of human immunodeficiency virus type 1 envelope glycoproteins in virus infection. J Biol Chem **270**:23883–23886.
139. **Martin-Serrano J**, **Neil SJD**. 2011. Host factors involved in retroviral budding and release. Nature Reviews Microbiology **9**:519–531.
140. **Garrus JE**, **Schwedler von UK**, **Pornillos OW**, **Morham SG**, **Zavitz KH**, **Wang HE**, **Wettstein DA**, **Stray KM**, **Côté M**, **Rich RL**, **Myszka DG**, **Sundquist WI**. 2001. Tsg101 and the vacuolar protein sorting pathway are essential for HIV-1 budding. Cell **107**:55–65.
141. **Martin-Serrano J**, **Zang T**, **Bieniasz PD**. 2001. HIV-1 and Ebola virus encode small peptide motifs that recruit Tsg101 to sites of particle assembly to facilitate egress. Nat Med **7**:1313–1319.
142. **Strack B**, **Calistri A**, **Craig S**, **Popova E**, **Göttlinger HG**. 2003. AIP1/ALIX is a binding partner for HIV-1 p6 and EIAV p9 functioning in virus budding. Cell **114**:689–699.
143. **Chung H-Y**, **Morita E**, **Schwedler von U**, **Müller B**, **Kräusslich H-G**, **Sundquist WI**. 2008. NEDD4L overexpression rescues the release and infectivity of human immunodeficiency virus type 1 constructs lacking PTAP and YPXL late domains. Journal of Virology **82**:4884–4897.
144. **Hurley JH**, **Hanson PI**. 2010. Membrane budding and scission by the ESCRT machinery: it's all in the neck. Nat Rev Mol Cell Biol **11**:556–566.
145. **Carlton JG**, **Martin-Serrano J**. 2007. Parallels between cytokinesis and retroviral budding: a role for the ESCRT machinery. Science **316**:1908–1912.
146. **Lata S**, **Schoehn G**, **Jain A**, **Pires R**, **Piehler J**, **Gottlinger HG**, **Weissenhorn W**. 2008. Helical Structures of ESCRT-III Are Disassembled by VPS4. Science **321**:1354–1357.
147. **Weissenhorn W**, **Göttlinger H**. 2011. Essential ingredients for HIV-1 budding. Cell Host Microbe **9**:172–174.
148. **Yeager M**. 2011. Design of in Vitro Symmetric Complexes and Analysis by Hybrid Methods Reveal Mechanisms of HIV Capsid Assembly. Journal of Molecular Biology **410**:534–552.
149. **Pettit SC**, **Sheng N**, **Tritch R**, **Erickson-Viitanen S**, **Swanstrom R**. 1998. The regulation of sequential processing of HIV-1 Gag by the viral protease. Adv. Exp. Med. Biol. **436**:15–25.
150. **Ganser BK**, **Li S**, **Klishko VY**, **Finch JT**, **Sundquist WI**. 1999. Assembly and analysis of conical models for the HIV-1 core. Science **283**:80–83.
151. **Briggs JAG**, **Grünewald K**, **Glass B**, **Förster F**, **Kräusslich HG**, **Fuller SD**. 2006.

The mechanism of HIV-1 core assembly: insights from three-dimensional reconstructions of authentic virions. Structure **14**:15–20.

152. **Pornillos O**, **Ganser-Pornillos BK**, **Yeager M**. 2011. Atomic-level modelling of the HIV capsid. Nature **469**:424–427.
153. **Abbas AHLAK**. 2005. Cellular and Molecular Immunology Updated 5th Edition (Updated Fifth Edition). Elsevier.
154. **Moore JP**, **Cao Y**, **Ho DD**, **Koup RA**. 1994. Development of the anti-gp120 antibody response during seroconversion to human immunodeficiency virus type 1. Journal of Virology **68**:5142–5155.
155. **Richman DD**, **Wrin T**, **Little SJ**, **Petropoulos CJ**. 2003. Rapid evolution of the neutralizing antibody response to HIV type 1 infection. Proc Natl Acad Sci USA **100**:4144–4149.
156. **Wei X**, **Decker JM**, **Wang S**, **Hui H**, **Kappes JC**, **Wu X**, **Salazar-Gonzalez JF**, **Salazar MG**, **Kilby JM**, **Saag MS**, **Komarova NL**, **Nowak MA**, **Hahn BH**, **Kwong PD**, **Shaw GM**. 2003. Antibody neutralization and escape by HIV-1. Nature **422**:307–312.
157. **Overbaugh J**, **Morris L**. 2012. The Antibody Response against HIV-1. Cold Spring Harb Perspect Med **2**:a007039.
158. **Fauci AS**, **Johnston MI**, **Dieffenbach CW**, **Burton DR**, **Hammer SM**, **Hoxie JA**, **Martin M**, **Overbaugh J**, **Watkins DI**, **Mahmoud A**, **Greene WC**. 2008. HIV vaccine research: the way forward. Science **321**:530–532.
159. **Goonetilleke N**, **Liu MKP**, **Salazar-Gonzalez JF**, **Ferrari G**, **Giorgi E**, **Ganusov VV**, **Keele BF**, **Learn GH**, **Turnbull EL**, **Salazar MG**, **Weinhold KJ**, **Moore S**, **CHAVI Clinical Core B**, **Letvin N**, **Haynes BF**, **Cohen MS**, **Hraber P**, **Bhattacharya T**, **Borrow P**, **Perelson AS**, **Hahn BH**, **Shaw GM**, **Korber BT**, **McMichael AJ**. 2009. The first T cell response to transmitted/founder virus contributes to the control of acute viremia in HIV-1 infection. Journal of Experimental Medicine **206**:1253–1272.
160. **Lichterfeld M**, **Yu XG**, **Cohen D**, **Addo MM**, **Malenfant J**, **Perkins B**, **Pae E**, **Johnston MN**, **Strick D**, **Allen TM**, **Rosenberg ES**, **Korber B**, **Walker BD**, **Altfeld M**. 2004. HIV-1 Nef is preferentially recognized by CD8 T cells in primary HIV-1 infection despite a relatively high degree of genetic diversity. AIDS **18**:1383–1392.
161. **Turnbull EL**, **Wong M**, **Wang S**, **Wei X**, **Jones NA**, **Conrod KE**, **Aldam D**, **Turner J**, **Pellegrino P**, **Keele BF**, **Williams I**, **Shaw GM**, **Borrow P**. 2009. Kinetics of expansion of epitope-specific T cell responses during primary HIV-1 infection. The Journal of Immunology **182**:7131–7145.
162. **Kaslow RA**, **Carrington M**, **Apple R**, **Park L**, **Muñoz A**, **Saah AJ**, **Goedert JJ**, **Winkler C**, **O'Brien SJ**, **Rinaldo C**, **Detels R**, **Blattner W**, **Phair J**, **Erlich H**, **Mann DL**. 1996. Influence of combinations of human major histocompatibility complex genes on the course of HIV-1 infection. Nat Med **2**:405–411.
163. **Fellay J**, **Shianna KV**, **Ge D**, **Colombo S**, **Ledergerber B**, **Weale M**, **Zhang K**, **Gumbs C**, **Castagna A**, **Cossarizza A**, **Cozzi-Lepri A**, **De Luca A**, **Easterbrook P**, **Francioli P**, **Mallal S**, **Martinez-Picado J**, **Miro JM**, **Obel N**, **Smith JP**, **Wyniger J**, **Descombes P**, **Antonarakis SE**, **Letvin NL**, **McMichael AJ**, **Haynes BF**, **Telenti A**, **Goldstein DB**. 2007. A whole-genome association study of major determinants for host control of HIV-1. Science **317**:944–947.
164. **Kiepiela P**, **Leslie AJ**, **Honeyborne I**, **Ramduth D**, **Thobakgale C**, **Chetty S**, **Rathnavalu P**, **Moore C**, **Pfafferott KJ**, **Hilton L**, **Zimbwa P**, **Moore S**, **Allen T**, **Brander C**, **Addo MM**, **Altfeld M**, **James I**, **Mallal S**, **Bunce M**, **Barber LD**, **Szinger J**, **Day C**, **Klenerman P**, **Mullins J**, **Korber B**, **Coovadia HM**, **Walker BD**, **Goulder PJR**. 2004. Dominant influence of HLA-B in mediating the potential co-evolution of HIV and HLA. Nature **432**:769–775.
165. **International HIV Controllers Study**, **Pereyra F**, **Jia X**, **McLaren PJ**, **Telenti A**, **de Bakker PIW**, **Walker BD**, **Ripke S**, **Brumme CJ**, **Pulit SL**, **Carrington M**, **Kadie CM**, **Carlson JM**, **Heckerman D**, **Graham RR**, **Plenge RM**, **Deeks SG**, **Gianniny L**, **Crawford G**, **Sullivan J**, **Gonzalez E**, **Davies L**, **Camargo A**, **Moore JM**, **Beattie N**, **Gupta S**, **Crenshaw A**, **Burtt NP**, **Guiducci C**, **Gupta N**, **Gao X**, **Qi Y**, **Yuki Y**, **Piechocka-Trocha A**, **Cutrell E**, **Rosenberg R**, **Moss KL**, **Lemay P**, **O'Leary J**, **Schaefer T**, **Verma P**, **Toth I**, **Block B**, **Baker B**, **Rothchild A**, **Lian J**, **Proudfoot J**, **Alvino DML**, **Vine S**, **Addo MM**, **Allen TM**, **Altfeld M**, **Henn MR**, **Le Gall S**, **Streeck H**, **Haas DW**, **Kuritzkes DR**, **Robbins GK**, **Shafer RW**, **Gulick RM**, **Shikuma CM**, **Haubrich R**, **Riddler S**, **Sax PE**, **Daar ES**, **Ribaudo HJ**, **Agan B**, **Agarwal S**, **Ahern RL**, **Allen BL**, **Altidor S**, **Altschuler EL**, **Ambardar S**, **Anastos K**, **Anderson B**, **Anderson V**, **Andrady U**, **Antoniskis D**, **Bangsberg D**, **Barbaro D**, **Barrie W**,

Bartczak J, **Barton S**, **Basden P**, **Basgoz N**, **Bazner S**, **Bellos NC**, **Benson AM**, **Berger J**, **Bernard NF**, **Bernard AM**, **Birch C**, **Bodner SJ**, **Bolan RK**, **Boudreaux ET**, **Bradley M**, **Braun JF**, **Brndjar JE**, **Brown SJ**, **Brown K**, **Brown ST**, **Burack J**, **Bush LM**, **Cafaro V**, **Campbell O**, **Campbell J**, **Carlson RH**, **Carmichael JK**, **Casey KK**, **Cavacuiti C**, **Celestin G**, **Chambers ST**, **Chez N**, **Chirch LM**, **Cimoch PJ**, **Cohen D**, **Cohn LE**, **Conway B**, **Cooper DA**, **Cornelson B**, **Cox DT**, **Cristofano MV**, **Cuchural G**, **Czartoski JL**, **Dahman JM**, **Daly JS**, **Davis BT**, **Davis K**, **Davod SM**, **DeJesus E**, **Dietz CA**, **Dunham E**, **Dunn ME**, **Ellerin TB**, **Eron JJ**, **Fangman JJW**, **Farel CE**, **Ferlazzo H**, **Fidler S**, **Fleenor-Ford A**, **Frankel R**, **Freedberg KA**, **French NK**, **Fuchs JD**, **Fuller JD**, **Gaberman J**, **Gallant JE**, **Gandhi RT**, **Garcia E**, **Garmon D**, **Gathe JC**, **Gaultier CR**, **Gebre W**, **Gilman FD**, **Gilson I**, **Goepfert PA**, **Gottlieb MS**, **Goulston C**, **Groger RK**, **Gurley TD**, **Haber S**, **Hardwicke R**, **Hardy WD**, **Harrigan PR**, **Hawkins TN**, **Heath S**, **Hecht FM**, **Henry WK**, **Hladek M**, **Hoffman RP**, **Horton JM**, **Hsu RK**, **Huhn GD**, **Hunt P**, **Hupert MJ**, **Illeman ML**, **Jaeger H**, **Jellinger RM**, **John M**, **Johnson JA**, **Johnson KL**, **Johnson H**, **Johnson K**, **Joly J**, **Jordan WC**, **Kauffman CA**, **Khanlou H**, **Killian RK**, **Kim AY**, **Kim DD**, **Kinder CA**, **Kirchner JT**, **Kogelman L**, **Kojic EM**, **Korthuis PT**, **Kurisu W**, **Kwon DS**, **LaMar M**, **Lampiris H**, **Lanzafame M**, **Lederman MM**, **Lee DM**, **Lee JML**, **Lee MJ**, **Lee ETY**, **Lemoine J**, **Levy JA**, **Llibre JM**, **Liguori MA**, **Little SJ**, **Liu AY**, **Lopez AJ**, **Loutfy MR**, **Loy D**, **Mohammed DY**, **Man A**, **Mansour MK**, **Marconi VC**, **Markowitz M**, **Marques R**, **Martin JN**, **Martin HL**, **Mayer KH**, **McElrath MJ**, **McGhee TA**, **McGovern BH**, **McGowan K**, **McIntyre D**, **Mcleod GX**, **Menezes P**, **Mesa G**, **Metroka CE**, **Meyer-Olson D**, **Miller AO**, **Montgomery K**, **Mounzer KC**, **Nagami EH**, **Nagin I**, **Nahass RG**, **Nelson MO**, **Nielsen C**, **Norene DL**, **O'Connor DH**, **Ojikutu BO**, **Okulicz J**, **Oladehin OO**, **Oldfield EC**, **Olender SA**, **Ostrowski M**, **Owen WF**, **Pae E**, **Parsonnet J**, **Pavlatos AM**, **Perlmutter AM**, **Pierce MN**, **Pincus JM**, **Pisani L**, **Price LJ**, **Proia L**, **Prokesch RC**, **Pujet HC**, **Ramgopal M**, **Rathod A**, **Rausch M**, **Ravishankar J**, **Rhame FS**, **Richards CS**, **Richman DD**, **Rodes B**, **Rodriguez M**, **Rose RC**, **Rosenberg ES**, **Rosenthal D**, **Ross PE**, **Rubin DS**, **Rumbaugh E**, **Saenz L**, **Salvaggio MR**, **Sanchez WC**, **Sanjana VM**, **Santiago S**, **Schmidt W**, **Schuitemaker H**, **Sestak PM**, **Shalit P**, **Shay W**, **Shirvani VN**, **Silebi VI**, **Sizemore JM**, **Skolnik PR**, **Sokol-Anderson M**, **Sosman JM**, **Stabile P**, **Stapleton JT**, **Starrett S**, **Stein F**, **Stellbrink H-J**, **Sterman FL**, **Stone VE**, **Stone DR**, **Tambussi G**, **Taplitz RA**, **Tedaldi EM**, **Telenti A**, **Theisen W**, **Torres R**, **Tosiello L**, **Tremblay C**, **Tribble MA**, **Trinh PD**, **Tsao A**, **Ueda P**, **Vaccaro A**, **Valadas E**, **Vanig TJ**, **Vecino I**, **Vega VM**, **Veikley W**, **Wade BH**, **Walworth C**, **Wanidworanun C**, **Ward DJ**, **Warner DA**, **Weber RD**, **Webster D**, **Weis S**, **Wheeler DA**, **White DJ**, **Wilkins E**, **Winston A**, **Wlodaver CG**, **van't Wout A**, **Wright DP**, **Yang OO**, **Yurdin DL**, **Zabukovic BW**, **Zachary KC**, **Zeeman B**, **Zhao M**. 2010. The major genetic determinants of HIV-1 control affect HLA class I peptide presentation. Science **330**:1551–1557.

166. **Martinez-Picado J**, **Prado JG**, **Fry EE**, **Pfafferott K**, **Leslie A**, **Chetty S**, **Thobakgale C**, **Honeyborne I**, **Crawford H**, **Matthews P**, **Pillay T**, **Rousseau C**, **Mullins JI**, **Brander C**, **Walker BD**, **Stuart DI**, **Kiepiela P**, **Goulder P**. 2006. Fitness cost of escape mutations in p24 Gag in association with control of human immunodeficiency virus type 1. Journal of Virology **80**:3617–3623.
167. **Murphy KM**, **Travers P**, **Walport M**, **Janeway C**. 2011. Janeway's Immunobiology. Garland Pub.
168. **Diebold SS**, **Kaisho T**, **Hemmi H**, **Akira S**, **Reis e Sousa C**. 2004. Innate antiviral responses by means of TLR7-mediated recognition of single-stranded RNA. Science **303**:1529–1531.
169. **Heil F**, **Hemmi H**, **Hochrein H**, **Ampenberger F**, **Kirschning C**, **Akira S**, **Lipford G**, **Wagner H**, **Bauer S**. 2004. Species-Specific Recognition of Single-Stranded RNA via Toll-like Receptor 7 and 8. Science Signaling **303**:1526.
170. **Beignon A-S**, **McKenna K**, **Skoberne M**, **Manches O**, **DaSilva I**, **Kavanagh DG**, **Larsson M**, **Gorelick RJ**, **Lifson JD**, **Bhardwaj N**. 2005. Endocytosis of HIV-1 activates plasmacytoid dendritic cells via Toll-like receptor-viral RNA interactions. J. Clin. Invest. **115**:3265–3275.
171. **Fitzgerald-Bocarsly P**, **Jacobs ES**. 2010. Plasmacytoid dendritic cells in HIV infection: striking a delicate balance. J. Leukoc. Biol. **87**:609–620.
172. **Yan N**, **Regalado-Magdos AD**, **Stiggelbout B**, **Lee-Kirsch MA**, **Lieberman J**. 2010. The cytosolic exonuclease TREX1 inhibits the innate immune response to human immunodeficiency virus type 1. Nat. Immunol. **11**:1005–1013.

173. **Laguette N**, **Sobhian B**, **Casartelli N**, **Ringeard M**, **Chable-Bessia C**, **Ségéral E**, **Yatim A**, **Emiliani S**, **Schwartz O**, **Benkirane M**. 2011. SAMHD1 is the dendritic- and myeloid-cell-specific HIV-1 restriction factor counteracted by Vpx. Nature **474**:654–657.
174. **Manel N**, **Hogstad B**, **Wang Y**, **Levy DE**, **Unutmaz D**, **Littman DR**. 2010. A cryptic sensor for HIV-1 activates antiviral innate immunity in dendritic cells. Nature **467**:214–217.
175. **Martin MP**, **Gao X**, **Lee J-H**, **Nelson GW**, **Detels R**, **Goedert JJ**, **Buchbinder S**, **Hoots K**, **Vlahov D**, **Trowsdale J**, **Wilson M**, **O'Brien SJ**, **Carrington M**. 2002. Epistatic interaction between KIR3DS1 and HLA-B delays the progression to AIDS. Nat. Genet. **31**:429–434.
176. **Cerboni C**, **Neri F**, **Casartelli N**, **Zingoni A**, **Cosman D**, **Rossi P**, **Santoni A**, **Doria M**. 2007. Human immunodeficiency virus 1 Nef protein downmodulates the ligands of the activating receptor NKG2D and inhibits natural killer cell-mediated cytotoxicity. J Gen Virol **88**:242–250.
177. **Sydow von M**, **Sönnerborg A**, **Gaines H**, **Strannegård Ö**. 1991. Interferon-Alpha and Tumor Necrosis Factor-Alpha in Serum of Patients in Various Stages of HIV-1 Infection. AIDS Res Hum Retroviruses **7**:375–380.
178. **Meyerson NR**, **Sawyer SL**. 2011. Two-stepping through time: mammals and viruses. Trends Microbiol **19**:286–294.
179. **Terwilliger EF**, **Cohen EA**, **Lu YC**, **Sodroski JG**, **Haseltine WA**. 1989. Functional role of human immunodeficiency virus type 1 vpu. Proc Natl Acad Sci USA **86**:5163–5167.
180. **Klimkait T**, **Strebel K**, **Hoggan MD**, **Martin MA**, **Orenstein JM**. 1990. The human immunodeficiency virus type 1-specific protein vpu is required for efficient virus maturation and release. Journal of Virology **64**:621–629.
181. **Gottlinger HG**, **Dorfman T**, **Cohen EA**, **Haseltine WA**. 1993. Vpu protein of human immunodeficiency virus type 1 enhances the release of capsids produced by gag gene constructs of widely divergent retroviruses. Proc Natl Acad Sci USA **90**:7381–7385.
182. **Geraghty RJ**, **Talbot KJ**, **Callahan M**, **Harper W**, **Panganiban AT**. 2011. Cell type-dependence for Vpu function. Journal of Medical Primatology **23**:146–150.
183. **Neil SJD**, **Eastman SW**, **Jouvenet N**, **Bieniasz PD**. 2006. HIV-1 Vpu promotes release and prevents endocytosis of nascent retrovirus particles from the plasma membrane. PLoS Pathog **2**:e39.
184. **Varthakavi V**, **Smith RM**, **Bour SP**, **Strebel K**, **Spearman P**. 2003. Viral protein U counteracts a human host cell restriction that inhibits HIV-1 particle production. Proc Natl Acad Sci USA **100**:15154–15159.
185. **Neil SJD**, **Sandrin V**, **Sundquist WI**, **Bieniasz PD**. 2007. An interferon-alpha-induced tethering mechanism inhibits HIV-1 and Ebola virus particle release but is counteracted by the HIV-1 Vpu protein. Cell Host Microbe **2**:193–203.
186. **Neil SJD**, **Zang T**, **Bieniasz PD**. 2008. Tetherin inhibits retrovirus release and is antagonized by HIV-1 Vpu. Nature **451**:425–430.
187. **Van Damme N**, **Goff D**, **Katsura C**, **Jorgenson RL**, **Mitchell R**, **Johnson MC**, **Stephens EB**, **Guatelli J**. 2008. The interferon-induced protein BST-2 restricts HIV-1 release and is downregulated from the cell surface by the viral Vpu protein. Cell Host Microbe **3**:245–252.
188. **Goto T**, **Kennel SJ**, **Abe M**, **Takishita M**, **Kosaka M**, **Solomon A**, **Saito S**. 1994. A novel membrane antigen selectively expressed on terminally differentiated human B cells. Blood **84**:1922–1930.
189. **Ishikawa J**, **Kaisho T**, **Tomizawa H**, **Lee BO**. 1995. Molecular cloning and chromosomal mapping of a bone marrow stromal cell surface gene, BST2, that may be involved in pre-B-cell growth. Genomics **26**:527–534.
190. **Blasius AL**, **Giurisato E**, **Cella M**, **Schreiber RD**, **Shaw AS**, **Colonna M**. 2006. Bone marrow stromal cell antigen 2 is a specific marker of type I IFN-producing cells in the naive mouse, but a promiscuous cell surface antigen following IFN stimulation. J. Immunol. **177**:3260–3265.
191. **Bartee E**, **McCormack A**, **Früh K**. 2006. Quantitative membrane proteomics reveals new cellular targets of viral immune modulators. PLoS Pathog **2**:e107.
192. **Le Tortorec A**, **Willey S**, **Neil SJD**. 2011. Antiviral Inhibition of Enveloped Virus Release by Tetherin/BST-2: Action and Counteraction. Viruses **3**:520–540.
193. **Kupzig S**, **Korolchuk V**, **Rollason R**, **Sugden A**, **Wilde A**, **Banting G**. 2003. Bst-

2/HM1.24 is a raft-associated apical membrane protein with an unusual topology. Traffic **4**:694–709.

194. **Ohtomo T**, **Sugamata Y**, **Ozaki Y**, **Ono K**, **Yoshimura Y**, **Kawai S**, **Koishihara Y**, **Ozaki S**, **Kosaka M**, **Hirano T**. 1999. Molecular cloning and characterization of a surface antigen preferentially overexpressed on multiple myeloma cells **258**:583–591.
195. **Moore RC**, **Lee IY**, **Silverman GL**, **Harrison PM**, **Strome R**, **Heinrich C**, **Karunaratne A**, **Pasternak SH**, **Chishti MA**, **Liang Y**, **Mastrangelo P**, **Wang K**, **Smit AF**, **Katamine S**, **Carlson GA**, **Cohen FE**, **Prusiner SB**, **Melton DW**, **Tremblay P**, **Hood LE**, **Westaway D**. 1999. Ataxia in prion protein (PrP)-deficient mice is associated with upregulation of the novel PrP-like protein doppel. Journal of Molecular Biology **292**:797–817.
196. **Nakamura N**, **Inoue N**, **Watanabe R**, **Takahashi M**, **Takeda J**, **Stevens VL**, **Kinoshita T**. 1997. Expression cloning of PIG-L, a candidate N-acetylglucosaminyl-phosphatidylinositol deacetylase. J Biol Chem **272**:15834–15840.
197. **Perez-Caballero D**, **Zang T**, **Ebrahimi A**, **McNatt MW**, **Gregory DA**, **Johnson MC**, **Bieniasz PD**. 2009. Tetherin inhibits HIV-1 release by directly tethering virions to cells. Cell **139**:499–511.
198. **Andrew AJ**, **Miyagi E**, **Kao S**, **Strebel K**. 2009. The formation of cysteine-linked dimers of BST-2/tetherin is important for inhibition of HIV-1 virus release but not for sensitivity to Vpu. Retrovirology **6**:80.
199. **Hinz A**, **Miguet N**, **Natrajan G**, **Usami Y**, **Yamanaka H**, **Renesto P**, **Hartlieb B**, **McCarthy AA**, **Simorre J-P**, **Göttlinger H**, **Weissenhorn W**. 2010. Structural basis of HIV-1 tethering to membranes by the BST-2/tetherin ectodomain. Cell Host Microbe **7**:314–323.
200. **Schubert HL**, **Zhai Q**, **Sandrin V**, **Eckert DM**, **Garcia-Maya M**, **Saul L**, **Sundquist WI**, **Steiner RA**, **Hill CP**. 2010. Structural and functional studies on the extracellular domain of BST2/tetherin in reduced and oxidized conformations. Proc Natl Acad Sci USA **107**:17951–17956.
201. **Yang H**, **Wang J**, **Jia X**, **McNatt MW**, **Zang T**, **Pan B**, **Meng W**, **Wang H-W**, **Bieniasz PD**, **Xiong Y**. 2010. Structural insight into the mechanisms of enveloped virus tethering by tetherin. Proc Natl Acad Sci USA **107**:18428–18432.
202. **Swiecki M**, **Scheaffer SM**, **Allaire M**, **Fremont DH**, **Colonna M**, **Brett TJ**. 2011. Structural and biophysical analysis of BST-2/tetherin ectodomains reveals an evolutionary conserved design to inhibit virus release. J Biol Chem **286**:2987–2997.
203. **Rollason R**, **Korolchuk V**, **Hamilton C**, **Jepson M**, **Banting G**. 2009. A CD317/tetherin-RICH2 complex plays a critical role in the organization of the subapical actin cytoskeleton in polarized epithelial cells. J Cell Biol **184**:721–736.
204. **Jouvenet N**, **Neil SJD**, **Zhadina M**, **Zang T**, **Kratovac Z**, **Lee Y**, **McNatt M**, **Hatziioannou T**, **Bieniasz PD**. 2009. Broad-spectrum inhibition of retroviral and filoviral particle release by tetherin. Journal of virology **83**:1837–1844.
205. **Lehmann M**, **Rocha S**, **Mangeat B**, **Blanchet F**, **Uji-i H**, **Hofkens J**, **Piguet V**. 2011. Quantitative multicolor super-resolution microscopy reveals tetherin HIV-1 interaction. PLoS Pathog **7**:e1002456.
206. **Masuyama N**, **Kuronita T**, **Tanaka R**, **Muto T**, **Hirota Y**, **Takigawa A**, **Fujita H**, **Aso Y**, **Amano J**, **Tanaka Y**. 2009. HM1.24 is internalized from lipid rafts by clathrin-mediated endocytosis through interaction with alpha-adaptin. J Biol Chem **284**:15927–15941.
207. **Rollason R**, **Korolchuk V**, **Hamilton C**, **Schu P**, **Banting G**. 2007. Clathrin-mediated endocytosis of a lipid-raft-associated protein is mediated through a dual tyrosine motif. Journal of Cell Science **120**:3850–3858.
208. **Kaletsky RL**, **Francica JR**, **Agrawal-Gamse C**, **Bates P**. 2009. Tetherin-mediated restriction of filovirus budding is antagonized by the Ebola glycoprotein. Proc Natl Acad Sci USA **106**:2886–2891.
209. **Mansouri M**, **Viswanathan K**, **Douglas JL**, **Hines J**, **Gustin J**, **Moses AV**, **Früh K**. 2009. Molecular mechanism of BST2/tetherin downregulation by K5/MIR2 of Kaposi's sarcoma-associated herpesvirus. Journal of Virology **83**:9672–9681.
210. **Pardieu C**, **Vigan R**, **Wilson SJ**, **Calvi A**, **Zang T**, **Bieniasz P**, **Kellam P**, **Towers GJ**, **Neil SJD**. 2010. The RING-CH ligase K5 antagonizes restriction of KSHV and HIV-1 particle release by mediating ubiquitin-dependent endosomal degradation of tetherin. PLoS Pathog **6**:e1000843.
211. **Sakuma T**, **Noda T**, **Urata S**, **Kawaoka Y**, **Yasuda J**. 2009. Inhibition of Lassa and

Marburg virus production by tetherin. Journal of virology **83**:2382–2385.

212. **Bruce EA**, **Abbink TE**, **Wise HM**, **Rollason R**, **Galão RP**, **Banting G**, **Neil SJ**, **Digard P**. 2012. Release of filamentous and spherical influenza A virus is not restricted by tetherin. J Gen Virol **93**:963–969.
213. **Mangeat B**, **Cavagliotti L**, **Lehmann M**, **Gers-Huber G**, **Kaur I**, **Thomas Y**, **Kaiser L**, **Piguet V**. 2012. Influenza virus partially counteracts restriction imposed by tetherin/BST-2. Journal of Biological Chemistry **287**:22015–22029.
214. **Hammonds J**, **Wang J-J**, **Yi H**, **Spearman P**. 2010. Immunoelectron microscopic evidence for Tetherin/BST2 as the physical bridge between HIV-1 virions and the plasma membrane. PLoS Pathog **6**:e1000749.
215. **Fitzpatrick K**, **Skasko M**, **Deerinck TJ**, **Crum J**, **Ellisman MH**, **Guatelli J**. 2010. Direct restriction of virus release and incorporation of the interferon-induced protein BST-2 into HIV-1 particles. PLoS Pathog **6**:e1000701.
216. **Jolly C**, **Booth NJ**, **Neil SJD**. 2010. Cell-cell spread of human immunodeficiency virus type 1 overcomes tetherin/BST-2-mediated restriction in T cells. Journal of Virology **84**:12185–12199.
217. **Douglas JL**, **Gustin JK**, **Viswanathan K**, **Mansouri M**, **Moses AV**, **Früh K**. 2010. The great escape: viral strategies to counter BST-2/tetherin. PLoS Pathog **6**:e1000913.
218. **Iwabu Y**, **Fujita H**, **Kinomoto M**, **Kaneko K**, **Ishizaka Y**, **Tanaka Y**, **Sata T**, **Tokunaga K**. 2009. HIV-1 accessory protein Vpu internalizes cell-surface BST-2/tetherin through transmembrane interactions leading to lysosomes. Journal of Biological Chemistry **284**:35060–35072.
219. **Douglas JL**, **Viswanathan K**, **McCarroll MN**, **Gustin JK**, **Früh K**, **Moses AV**. 2009. Vpu directs the degradation of the human immunodeficiency virus restriction factor BST-2/Tetherin via a {beta}TrCP-dependent mechanism. Journal of Virology **83**:7931–7947.
220. **Mitchell RS**, **Katsura C**, **Skasko MA**, **Fitzpatrick K**, **Lau D**, **Ruiz A**, **Stephens EB**, **Margottin-Goguet F**, **Benarous R**, **Guatelli JC**. 2009. Vpu antagonizes BST-2-mediated restriction of HIV-1 release via beta-TrCP and endo-lysosomal trafficking. PLoS Pathog **5**:e1000450.
221. **Vigan R**, **Neil SJD**. 2010. Determinants of tetherin antagonism in the transmembrane domain of the human immunodeficiency virus type 1 Vpu protein. Journal of Virology **84**:12958–12970.
222. **Kobayashi T**, **Ode H**, **Yoshida T**, **Sato K**, **Gee P**, **Yamamoto SP**, **Ebina H**, **Strebel K**, **Sato H**, **Koyanagi Y**. 2011. Identification of amino acids in the human tetherin transmembrane domain responsible for HIV-1 Vpu interaction and susceptibility. Journal of Virology **85**:932–945.
223. **Gupta RK**, **Hué S**, **Schaller T**, **Verschoor E**, **Pillay D**, **Towers GJ**. 2009. Mutation of a single residue renders human tetherin resistant to HIV-1 Vpu-mediated depletion. PLoS Pathog **5**:e1000443.
224. **McNatt MW**, **Zang T**, **Hatziioannou T**, **Bartlett M**, **Fofana IB**, **Johnson WE**, **Neil SJD**, **Bieniasz PD**. 2009. Species-specific activity of HIV-1 Vpu and positive selection of tetherin transmembrane domain variants. PLoS Pathog **5**:e1000300.
225. **Jia B**, **Serra-Moreno R**, **Neidermyer W**, **Rahmberg A**, **Mackey J**, **Fofana IB**, **Johnson WE**, **Westmoreland S**, **Evans DT**. 2009. Species-specific activity of SIV Nef and HIV-1 Vpu in overcoming restriction by tetherin/BST2. PLoS Pathog **5**:e1000429.
226. **Sauter D**, **Schindler M**, **Specht A**, **Landford WN**, **Münch J**, **Kim K-A**, **Votteler J**, **Schubert U**, **Bibollet-Ruche F**, **Keele BF**. 2009. Tetherin-Driven Adaptation of Vpu and Nef Function and the Evolution of Pandemic and Nonpandemic HIV-1 Strains. Cell Host Microbe **6**:409–421.
227. **Zhang F**, **Wilson SJ**, **Landford WC**, **Virgen B**, **Gregory D**, **Johnson MC**, **Münch J**, **Kirchhoff F**, **Bieniasz PD**, **Hatziioannou T**. 2009. Nef proteins from simian immunodeficiency viruses are tetherin antagonists. Cell Host Microbe **6**:54–67.
228. **Zhang F**, **Landford WN**, **Ng M**, **McNatt MW**, **Bieniasz PD**, **Hatziioannou T**. 2011. SIV Nef proteins recruit the AP-2 complex to antagonize Tetherin and facilitate virion release. PLoS Pathog **7**:e1002039.
229. **Bour S**, **Schubert U**, **Peden K**, **Strebel K**. 1996. The envelope glycoprotein of human immunodeficiency virus type 2 enhances viral particle release: a Vpu-like factor? Journal of Virology **70**:820–829.
230. **Le Tortorec A**, **Neil SJD**. 2009. Antagonism to and intracellular sequestration of human tetherin by the human immunodeficiency virus type 2 envelope glycoprotein.

Journal of Virology **83**:11966–11978.
231. **Gupta RK**, **Mlcochova P**, **Pelchen-Matthews A**, **Petit SJ**, **Mattiuzzo G**, **Pillay D**, **Takeuchi Y**, **Marsh M**, **Towers GJ**. 2009. Simian immunodeficiency virus envelope glycoprotein counteracts tetherin/BST-2/CD317 by intracellular sequestration. Proc Natl Acad Sci USA **106**:20889–20894.
232. **Abada P**, **Noble B**, **Cannon PM**. 2005. Functional domains within the human immunodeficiency virus type 2 envelope protein required to enhance virus production. Journal of Virology **79**:3627–3638.
233. **Noble B**, **Abada P**, **Nunez-Iglesias J**, **Cannon PM**. 2006. Recruitment of the adaptor protein 2 complex by the human immunodeficiency virus type 2 envelope protein is necessary for high levels of virus release. Journal of Virology **80**:2924–2932.
234. **Alexander L**, **Illyinskii PO**, **Lang SM**, **Means RE**, **Lifson J**, **Mansfield K**, **Desrosiers RC**. 2003. Determinants of increased replicative capacity of serially passaged simian immunodeficiency virus with nef deleted in rhesus monkeys. Journal of Virology **77**:6823–6835.
235. **Serra-Moreno R**, **Jia B**, **Breed M**, **Alvarez X**, **Evans DT**. 2011. Compensatory Changes in the Cytoplasmic Tail of gp41 Confer Resistance to Tetherin/BST-2 in a Pathogenic Nef-Deleted SIV. Cell Host Microbe **9**:46–57.
236. **Neil SJD**. 2011. SIV envelope acquires a nefarious habit. Cell Host Microbe **9**:3–5.
237. **Yang SJ**, **Lopez LA**, **Hauser H**, **Exline CM**, **Haworth KG**, **Cannon PM**. 2010. Anti-tetherin activities in Vpu-expressing primate lentiviruses. Retrovirology **7**:13.
238. **Lopez LA**, **Yang SJ**, **Hauser H**, **Exline CM**, **Haworth KG**, **Oldenburg J**, **Cannon PM**. 2010. Ebola virus glycoprotein counteracts BST-2/tetherin restriction in a sequence-independent manner that does not require tetherin surface removal. Journal of Virology **84**:7243–7255.
239. **Francica JR**, **Varela-Rohena A**, **Medvec A**, **Plesa G**, **Riley JL**, **Bates P**. 2010. Steric Shielding of Surface Epitopes and Impaired Immune Recognition Induced by the Ebola Virus Glycoprotein. PLoS Pathog **6**:e1001098.
240. **Simmons G**, **Wool-Lewis RJ**, **Baribaud F**, **Netter RC**, **Bates P**. 2002. Ebola virus glycoproteins induce global surface protein down-modulation and loss of cell adherence. Journal of Virology **76**:2518–2528.
241. **Lehner PJ**, **Hoer S**, **Dodd R**, **Duncan LM**. 2005. Downregulation of cell surface receptors by the K3 family of viral and cellular ubiquitin E3 ligases. Immunol Rev **207**:112–125.
242. **Sattentau Q**. 2008. Avoiding the void: cell-to-cell spread of human viruses. Nat Rev Microbiol **6**:815–826.
243. **Chen P**, **Hübner W**, **Spinelli MA**, **Chen BK**. 2007. Predominant mode of human immunodeficiency virus transfer between T cells is mediated by sustained Env-dependent neutralization-resistant virological synapses. Journal of Virology **81**:12582–12595.
244. **Durham ND**, **Yewdall AW**, **Chen P**, **Lee R**, **Zony C**, **Robinson JE**, **Chen BK**. 2012. Neutralization resistance of virological synapse-mediated HIV-1 Infection is regulated by the gp41 cytoplasmic tail. Journal of Virology **86**:7484–7495.
245. **Martin N**, **Welsch S**, **Jolly C**, **Briggs JAG**, **Vaux D**, **Sattentau QJ**. 2010. Virological synapse-mediated spread of human immunodeficiency virus type 1 between T cells is sensitive to entry inhibition. Journal of Virology **84**:3516.
246. **Murooka TT**, **Deruaz M**, **Marangoni F**, **Vrbanac VD**, **Seung E**, **Andrian von UH**, **Tager AM**, **Luster AD**, **Mempel TR**. 2012. HIV-infected T cells are migratory vehicles for viral dissemination. Nature.
247. **Jolly C**, **Kashefi K**, **Hollinshead M**, **Sattentau QJ**. 2004. HIV-1 cell to cell transfer across an Env-induced, actin-dependent synapse. J. Exp. Med. **199**:283–293.
248. **Igakura T**, **Stinchcombe JC**, **Goon PKC**, **Taylor GP**, **Weber JN**, **Griffiths GM**, **Tanaka Y**, **Osame M**, **Bangham CRM**. 2003. Spread of HTLV-I between lymphocytes by virus-induced polarization of the cytoskeleton. Science **299**:1713–1716.
249. **Hübner W**, **McNerney GP**, **Chen P**, **Dale BM**, **Gordon RE**, **Chuang FYS**, **Li X-D**, **Asmuth DM**, **Huser T**, **Chen BK**. 2009. Quantitative 3D video microscopy of HIV transfer across T cell virological synapses. Science **323**:1743–1747.
250. **Jolly C**, **Mitar I**, **Sattentau QJ**. 2007. Adhesion molecule interactions facilitate human immunodeficiency virus type 1-induced virological synapse formation between T cells. Journal of Virology **81**:13916–13921.
251. **Llewellyn GN**, **Hogue IB**, **Grover JR**, **Ono A**. 2010. Nucleocapsid promotes localization of HIV-1 gag to uropods that participate in virological synapses between T

cells. PLoS Pathog **6**:e1001167.

252. **Casartelli N**, **Sourisseau M**, **Feldmann J**, **Guivel-Benhassine F**, **Mallet A**, **Marcelin A-G**, **Guatelli J**, **Schwartz O**. 2010. Tetherin restricts productive HIV-1 cell-to-cell transmission. PLoS Pathog **6**:e1000955.
253. **Kuhl BD**, **Sloan RD**, **Donahue DA**, **Bar-Magen T**, **Liang C**, **Wainberg MA**. 2010. Tetherin restricts direct cell-to-cell infection of HIV-1. Retrovirology **7**:115.
254. **Schindler M**, **Rajan D**, **Banning C**, **Wimmer P**, **Koppensteiner H**, **Iwanski A**, **Specht A**, **Sauter D**, **Dobner T**, **Kirchhoff F**. 2010. Vpu serine 52 dependent counteraction of tetherin is required for HIV-1 replication in macrophages, but not in ex vivo human lymphoid tissue. Retrovirology **7**:1.
255. **Cao W**, **Bover L**, **Cho M**, **Wen X**, **Hanabuchi S**, **Bao M**, **Rosen DB**, **Wang Y-H**, **Shaw JL**, **Du Q**, **Li C**, **Arai N**, **Yao Z**, **Lanier LL**, **Liu Y-J**. 2009. Regulation of TLR7/9 responses in plasmacytoid dendritic cells by BST2 and ILT7 receptor interaction. Journal of Experimental Medicine **206**:1603–1614.
256. **Matsuda A**, **Suzuki Y**, **Honda G**, **Muramatsu S**, **Matsuzaki O**, **Nagano Y**, **Doi T**, **Shimotohno K**, **Harada T**, **Nishida E**, **Hayashi H**, **Sugano S**. 2003. Large-scale identification and characterization of human genes that activate NF-kappaB and MAPK signaling pathways. Oncogene **22**:3307–3318.
257. **Liberatore RA**, **Bieniasz PD**. 2011. Tetherin is a key effector of the antiretroviral activity of type I interferon in vitro and in vivo. Proc Natl Acad Sci USA **108**:18097–18101.
258. **Barrett BS**, **Smith DS**, **Li SX**, **Guo K**, **Hasenkrug KJ**, **Santiago ML**. 2012. A Single Nucleotide Polymorphism in Tetherin Promotes Retrovirus Restriction In Vivo. PLoS Pathog **8**:e1002596.
259. **Kestler HW**, **Ringler DJ**, **Mori K**, **Panicali DL**, **Sehgal PK**, **Daniel MD**, **Desrosiers RC**. 1991. Importance of the nef gene for maintenance of high virus loads and for development of AIDS. Cell **65**:651–662.
260. **Deacon NJ**, **Tsykin A**, **Solomon A**, **Smith K**, **Ludford-Menting M**, **Hooker DJ**, **McPhee DA**, **Greenway AL**, **Ellett A**, **Chatfield C**, **Lawson VA**, **Crowe S**, **Maerz A**, **Sonza S**, **Learmont J**, **Sullivan JS**, **Cunningham A**, **Dwyer D**, **Dowton D**, **Mills J**. 1995. Genomic structure of an attenuated quasi species of HIV-1 from a blood transfusion donor and recipients. Science **270**:988–991.
261. **Kirchhoff F**, **Greenough TC**, **Brettler DB**, **Sullivan JL**, **Desrosiers RC**. 1995. Brief report: absence of intact nef sequences in a long-term survivor with nonprogressive HIV-1 infection. N. Engl. J. Med. **332**:228–232.
262. **Hoch J**, **Lang SM**, **Weeger M**, **Stahl-Hennig C**, **Coulibaly C**, **Dittmer U**, **Hunsmann G**, **Fuchs D**, **Müller J**, **Sopper S**. 1995. vpr deletion mutant of simian immunodeficiency virus induces AIDS in rhesus monkeys. Journal of Virology **69**:4807–4813.
263. **Lang SM**, **Weeger M**, **Stahl-Hennig C**, **Coulibaly C**, **Hunsmann G**, **Müller J**, **Müller-Hermelink H**, **Fuchs D**, **Wachter H**, **Daniel MM**. 1993. Importance of vpr for infection of rhesus monkeys with simian immunodeficiency virus. Journal of virology **67**:902–912.
264. **Gibbs JS**, **Lackner AA**, **Lang SM**, **Simon MA**, **Sehgal PK**, **Daniel MD**, **Desrosiers RC**. 1995. Progression to AIDS in the absence of a gene for vpr or vpx. Journal of Virology **69**:2378–2383.
265. **Hirsch VM**, **Sharkey ME**, **Brown CR**, **Brichacek B**, **Goldstein S**, **Wakefield J**, **Byrum R**, **Elkins WR**, **Hahn BH**, **Lifson JD**, **Stevenson M**. 1998. Vpx is required for dissemination and pathogenesis of SIV(SM) PBj: evidence of macrophage-dependent viral amplification. Nat Med **4**:1401–1408.
266. **Zimmerman ES**, **Sherman MP**, **Blackett JL**, **Neidleman JA**, **Kreis C**, **Mundt P**, **Williams SA**, **Warmerdam M**, **Kahn J**, **Hecht FM**, **Grant RM**, **de Noronha CMC**, **Weyrich AS**, **Greene WC**, **Planelles V**. 2006. Human immunodeficiency virus type 1 Vpr induces DNA replication stress in vitro and in vivo. Journal of Virology **80**:10407–10418.
267. **Wen X**, **Duus KM**, **Friedrich TD**, **de Noronha CMC**. 2007. The HIV1 protein Vpr acts to promote G2 cell cycle arrest by engaging a DDB1 and Cullin4A-containing ubiquitin ligase complex using VprBP/DCAF1 as an adaptor. J Biol Chem **282**:27046–27057.
268. **Belzile J-P**, **Duisit G**, **Rougeau N**, **Mercier J**, **Finzi A**, **Cohen EA**. 2007. HIV-1 Vpr-mediated G2 arrest involves the DDB1-CUL4AVPRBP E3 ubiquitin ligase. PLoS Pathog **3**:e85.
269. **Tan L**, **Ehrlich E**, **Yu X-F**. 2007. DDB1 and Cul4A are required for human

immunodeficiency virus type 1 Vpr-induced G2 arrest. Journal of virology **81**:10822–10830.

270. **Hrecka K**, **Gierszewska M**, **Srivastava S**, **Kozaczkiewicz L**, **Swanson SK**, **Florens L**, **Washburn MP**, **Skowronski J**. 2007. Lentiviral Vpr usurps Cul4-DDB1[VprBP] E3 ubiquitin ligase to modulate cell cycle. Proc Natl Acad Sci USA **104**:11778–11783.
271. **Schröfelbauer B**, **Hakata Y**, **Landau NR**. 2007. HIV-1 Vpr function is mediated by interaction with the damage-specific DNA-binding protein DDB1. Proc Natl Acad Sci USA **104**:4130–4135.
272. **Roshal M**, **Kim B**, **Zhu Y**, **Nghiem P**, **Planelles V**. 2003. Activation of the ATR-mediated DNA damage response by the HIV-1 viral protein R. J Biol Chem **278**:25879–25886.
273. **Hrecka K**, **Hao C**, **Gierszewska M**, **Swanson SK**, **Kesik-Brodacka M**, **Srivastava S**, **Florens L**, **Washburn MP**, **Skowronski J**. 2011. Vpx relieves inhibition of HIV-1 infection of macrophages mediated by the SAMHD1 protein. Nature **474**:658–661.
274. **Goujon C**, **Rivière L**, **Jarrosson-Wuilleme L**, **Bernaud J**, **Rigal D**, **Darlix J-L**, **Cimarelli A**. 2007. SIVSM/HIV-2 Vpx proteins promote retroviral escape from a proteasome-dependent restriction pathway present in human dendritic cells. Retrovirology **4**:2.
275. **Sharova N**, **Wu Y**, **Zhu X**, **Stranska R**, **Kaushik R**, **Sharkey M**, **Stevenson M**. 2008. Primate lentiviral Vpx commandeers DDB1 to counteract a macrophage restriction. PLoS Pathog **4**:e1000057.
276. **Li N**, **Zhang W**, **Cao X**. 2000. Identification of human homologue of mouse IFN-gamma induced protein from human dendritic cells. Immunol. Lett. **74**:221–224.
277. **Srivastava S**, **Swanson SK**, **Manel N**, **Florens L**, **Washburn MP**, **Skowronski J**. 2008. Lentiviral Vpx accessory factor targets VprBP/DCAF1 substrate adaptor for cullin 4 E3 ubiquitin ligase to enable macrophage infection. PLoS Pathog **4**:e1000059.
278. **Goldstone DC**, **Ennis-Adeniran V**, **Hedden JJ**, **Groom HCT**, **Rice GI**, **Christodoulou E**, **Walker PA**, **Kelly G**, **Haire LF**, **Yap MW**, **de Carvalho LPS**, **Stoye JP**, **Crow YJ**, **Taylor IA**, **Webb M**. 2011. HIV-1 restriction factor SAMHD1 is a deoxynucleoside triphosphate triphosphohydrolase. Nature **480**:379–382.
279. **Crow YJ**, **Livingston JH**. 2008. Aicardi-Goutières syndrome: an important Mendelian mimic of congenital infection. Developmental Medicine & Child Neurology **50**:410–416.
280. **Dussaix E**, **Lebon P**, **Ponsot G**, **Huault G**, **Tardieu M**. 1985. Intrathecal synthesis of different alpha-interferons in patients with various neurological diseases. Acta Neurol. Scand. **71**:504–509.
281. **Berger A**, **Sommer AFR**, **Zwarg J**, **Hamdorf M**, **Welzel K**, **Esly N**, **Panitz S**, **Reuter A**, **Ramos I**, **Jatiani A**, **Mulder LCF**, **Fernandez-Sesma A**, **Rutsch F**, **Simon V**, **König R**, **Flory E**. 2011. SAMHD1-deficient CD14+ cells from individuals with Aicardi-Goutières syndrome are highly susceptible to HIV-1 infection. PLoS Pathog **7**:e1002425.
282. **Lim ES**, **Fregoso OI**, **McCoy CO**, **Matsen FA**, **Malik HS**, **Emerman M**. 2012. The ability of primate lentiviruses to degrade the monocyte restriction factor SAMHD1 preceded the birth of the viral accessory protein Vpx. Cell Host Microbe **11**:194–204.
283. **Laguette N**, **Rahm N**, **Sobhian B**, **Chable-Bessia C**, **Münch J**, **Snoeck J**, **Sauter D**, **Switzer WM**, **Heneine W**, **Kirchhoff F**, **Delsuc F**, **Telenti A**, **Benkirane M**. 2012. Evolutionary and functional analyses of the interaction between the myeloid restriction factor SAMHD1 and the lentiviral Vpx protein. Cell Host Microbe **11**:205–217.
284. **Sheehy AM**, **Gaddis NC**, **Choi JD**, **Malim MH**. 2002. Isolation of a human gene that inhibits HIV-1 infection and is suppressed by the viral Vif protein. Nature **418**:646–650.
285. **Bogerd HP**, **Cullen BR**. 2008. Single-stranded RNA facilitates nucleocapsid: APOBEC3G complex formation. RNA **14**:1228–1236.
286. **Mangeat B**, **Turelli P**, **Caron G**, **Friedli M**, **Perrin L**, **Trono D**. 2003. Broad antiretroviral defence by human APOBEC3G through lethal editing of nascent reverse transcripts. Nature **424**:99–103.
287. **Zhang H**, **Yang B**, **Pomerantz RJ**, **Zhang C**, **Arunachalam SC**, **Gao L**. 2003. The cytidine deaminase CEM15 induces hypermutation in newly synthesized HIV-1 DNA. Nature **424**:94–98.
288. **Bishop KN**, **Holmes RK**, **Sheehy AM**, **Davidson NO**, **Cho S-J**, **Malim MH**. 2004. Cytidine deamination of retroviral DNA by diverse APOBEC proteins. Curr. Biol. **14**:1392–1396.
289. **Newman ENC**, **Holmes RK**, **Craig HM**, **Klein KC**, **Lingappa JR**, **Malim MH**, **Sheehy AM**. 2005. Antiviral function of APOBEC3G can be dissociated from cytidine

deaminase activity. Curr. Biol. **15**:166–170.
290. **Kaiser SM**, **Emerman M**. 2006. Uracil DNA glycosylase is dispensable for human immunodeficiency virus type 1 replication and does not contribute to the antiviral effects of the cytidine deaminase Apobec3G. Journal of Virology **80**:875–882.
291. **Langlois M-A**, **Neuberger MS**. 2008. Human APOBEC3G can restrict retroviral infection in avian cells and acts independently of both UNG and SMUG1. Journal of Virology **82**:4660–4664.
292. **Bishop KN**, **Verma M**, **Kim E-Y**, **Wolinsky SM**, **Malim MH**. 2008. APOBEC3G inhibits elongation of HIV-1 reverse transcripts. PLoS Pathog **4**:e1000231.
293. **Sheehy AM**, **Gaddis NC**, **Malim MH**. 2003. The antiretroviral enzyme APOBEC3G is degraded by the proteasome in response to HIV-1 Vif. Nat Med **9**:1404–1407.
294. **Marin M**, **Rose KM**, **Kozak SL**, **Kabat D**. 2003. HIV-1 Vif protein binds the editing enzyme APOBEC3G and induces its degradation. Nat Med **9**:1398–1403.
295. **Yu X**, **Yu Y**, **Liu B**, **Luo K**, **Kong W**, **Mao P**, **Yu X-F**. 2003. Induction of APOBEC3G ubiquitination and degradation by an HIV-1 Vif-Cul5-SCF complex. Science **302**:1056–1060.
296. **Jäger S**, **Kim DY**, **Hultquist JF**, **Shindo K**, **LaRue RS**, **Kwon E**, **Li M**, **Anderson BD**, **Yen L**, **Stanley D**, **Mahon C**, **Kane J**, **Franks-Skiba K**, **Cimermancic P**, **Burlingame A**, **Sali A**, **Craik CS**, **Harris RS**, **Gross JD**, **Krogan NJ**. 2012. Vif hijacks CBF-β to degrade APOBEC3G and promote HIV-1 infection. Nature **481**:371–375.
297. **Mariani R**, **Chen D**, **Schröfelbauer B**, **Navarro F**, **König R**, **Bollman B**, **Münk C**, **Nymark-McMahon H**, **Landau NR**. 2003. Species-specific exclusion of APOBEC3G from HIV-1 virions by Vif. Cell **114**:21–31.
298. **Schröfelbauer B**, **Chen D**, **Landau NR**. 2004. A single amino acid of APOBEC3G controls its species-specific interaction with virion infectivity factor (Vif). Proc Natl Acad Sci USA **101**:3927–3932.
299. **Wiegand HL**, **Doehle BP**, **Bogerd HP**, **Cullen BR**. 2004. A second human antiretroviral factor, APOBEC3F, is suppressed by the HIV-1 and HIV-2 Vif proteins. EMBO J. **23**:2451–2458.
300. **Malim MH**, **Bieniasz PD**. 2012. HIV Restriction Factors and Mechanisms of Evasion. Cold Spring Harb Perspect Med **2**:a006940.
301. **Chaudhuri R**, **Lindwasser OW**, **Smith WJ**, **Hurley JH**, **Bonifacino JS**. 2007. Downregulation of CD4 by human immunodeficiency virus type 1 Nef is dependent on clathrin and involves direct interaction of Nef with the AP2 clathrin adaptor. Journal of Virology **81**:3877–3890.
302. **Roeth JF**, **Collins KL**. 2006. Human immunodeficiency virus type 1 Nef: adapting to intracellular trafficking pathways. Microbiol. Mol. Biol. Rev. **70**:548–563.
303. **Lama J**, **Mangasarian A**, **Trono D**. 1999. Cell-surface expression of CD4 reduces HIV-1 infectivity by blocking Env incorporation in a Nef-and Vpu-inhibitable manner. Curr. Biol. **9**:622–631.
304. **Ross TM**, **Oran AE**, **Cullen BR**. 1999. Inhibition of HIV-1 progeny virion release by cell-surface CD4 is relieved by expression of the viral Nef protein. Curr. Biol. **9**:613–621.
305. **Goulder PJR**, **Watkins DI**. 2004. HIV and SIV CTL escape: implications for vaccine design. Nat. Rev. Immunol. **4**:630–640.
306. **Roeth JF**, **Williams M**, **Kasper MR**, **Filzen TM**, **Collins KL**. 2004. HIV-1 Nef disrupts MHC-I trafficking by recruiting AP-1 to the MHC-I cytoplasmic tail. J Cell Biol **167**:903–913.
307. **Lubben NB**, **Sahlender DA**, **Motley AM**, **Lehner PJ**, **Benaroch P**, **Robinson MS**. 2007. HIV-1 Nef-induced down-regulation of MHC class I requires AP-1 and clathrin but not PACS-1 and is impeded by AP-2. Mol. Biol. Cell **18**:3351–3365.
308. **Noviello CM**, **Benichou S**, **Guatelli JC**. 2008. Cooperative binding of the class I major histocompatibility complex cytoplasmic domain and human immunodeficiency virus type 1 Nef to the endosomal AP-1 complex via its mu subunit. Journal of Virology **82**:1249–1258.
309. **Atkins KM**, **Thomas L**, **Youker RT**, **Harriff MJ**, **Pissani F**, **You H**, **Thomas G**. 2008. HIV-1 Nef binds PACS-2 to assemble a multikinase cascade that triggers major histocompatibility complex class I (MHC-I) down-regulation: analysis using short interfering RNA and knock-out mice. J Biol Chem **283**:11772–11784.
310. **Stumptner-Cuvelette P**, **Morchoisne S**, **Dugast M**, **Le Gall S**, **Raposo G**, **Schwartz O**, **Benaroch P**. 2001. HIV-1 Nef impairs MHC class II antigen presentation and surface expression. Proc Natl Acad Sci USA **98**:12144–12149.

311. **Schindler M**, **Wildum S**, **Casartelli N**, **Doria M**, **Kirchhoff F**. 2007. Nef alleles from children with non-progressive HIV-1 infection modulate MHC-II expression more efficiently than those from rapid progressors. AIDS **21**:1103–1107.
312. **Stumptner-Cuvelette P**, **Jouve M**, **Helft J**, **Dugast M**, **Glouzman A-S**, **Jooss K**, **Raposo G**, **Benaroch P**. 2003. Human immunodeficiency virus-1 Nef expression induces intracellular accumulation of multivesicular bodies and major histocompatibility complex class II complexes: potential role of phosphatidylinositol 3-kinase. Mol. Biol. Cell **14**:4857–4870.
313. **Pizzato M**, **Helander A**, **Popova E**, **Calistri A**, **Zamborlini A**, **Palu G**, **Göttlinger HG**. 2007. Dynamin 2 is required for the enhancement of HIV-1 infectivity by Nef. Proc Natl Acad Sci USA **104**:6812–6817.
314. **Wolf D**, **Witte V**, **Laffert B**, **Blume K**, **Stromer E**, **Trapp S**, **d'Aloja P**, **Schürmann A**, **Baur AS**. 2001. HIV-1 Nef associated PAK and PI3-kinases stimulate Akt-independent Bad-phosphorylation to induce anti-apoptotic signals. Nat Med **7**:1217–1224.
315. **Sol-Foulon N**, **Moris A**, **Nobile C**, **Boccaccio C**, **Engering A**, **Abastado J-P**, **Heard J-M**, **van Kooyk Y**, **Schwartz O**. 2002. HIV-1 Nef-induced upregulation of DC-SIGN in dendritic cells promotes lymphocyte clustering and viral spread. Immunity **16**:145–155.
316. **Schindler M**, **Münch J**, **Kutsch O**, **Li H**, **Santiago ML**, **Bibollet-Ruche F**, **Müller-Trutwin MC**, **Novembre FJ**, **Peeters M**, **Courgnaud V**, **Bailes E**, **Roques P**, **Sodora DL**, **Silvestri G**, **Sharp PM**, **Hahn BH**, **Kirchhoff F**. 2006. Nef-mediated suppression of T cell activation was lost in a lentiviral lineage that gave rise to HIV-1. Cell **125**:1055–1067.
317. **Matusali G**, **Potestà M**, **Santoni A**, **Cerboni C**, **Doria M**. 2012. The human immunodeficiency virus type 1 Nef and Vpu proteins downregulate the natural killer cell-activating ligand PVR. Journal of Virology **86**:4496–4504.
318. **Stremlau M**, **Owens CM**, **Perron MJ**, **Kiessling M**, **Autissier P**, **Sodroski J**. 2004. The cytoplasmic body component TRIM5alpha restricts HIV-1 infection in Old World monkeys. Nature **427**:848–853.
319. **Besnier C**, **Takeuchi Y**, **Towers G**. 2002. Restriction of lentivirus in monkeys. Proc Natl Acad Sci USA **99**:11920–11925.
320. **Cowan S**, **Hatziioannou T**, **Cunningham T**, **Muesing MA**, **Göttlinger HG**, **Bieniasz PD**. 2002. Cellular inhibitors with Fv1-like activity restrict human and simian immunodeficiency virus tropism. Proc Natl Acad Sci USA **99**:11914–11919.
321. **Hatziioannou T**, **Perez-Caballero D**, **Yang A**, **Cowan S**, **Bieniasz PD**. 2004. Retrovirus resistance factors Ref1 and Lv1 are species-specific variants of TRIM5alpha. Proc Natl Acad Sci USA **101**:10774–10779.
322. **Hofmann W**, **Schubert D**, **LaBonte J**, **Munson L**, **Gibson S**, **Scammell J**, **Ferrigno P**, **Sodroski J**. 1999. Species-specific, postentry barriers to primate immunodeficiency virus infection. Journal of Virology **73**:10020–10028.
323. **Sayah DM**, **Sokolskaja E**, **Berthoux L**, **Luban J**. 2004. Cyclophilin A retrotransposition into TRIM5 explains owl monkey resistance to HIV-1. Nature **430**:569–573.
324. **Towers GJ**. 2007. The control of viral infection by tripartite motif proteins and cyclophilin A. Retrovirology **4**:40.
325. **Cohen EA**, **Terwilliger EF**, **Sodroski JG**, **Haseltine WA**. 1988. Identification of a protein encoded by the vpu gene of HIV-1. Nature **334**:532–534.
326. **Strebel K**, **Klimkait T**, **Martin MA**. 1988. A novel gene of HIV-1, vpu, and its 16-kilodalton product. Science **241**:1221–1223.
327. **Maldarelli F**, **Chen MY**, **Willey RL**, **Strebel K**. 1993. Human immunodeficiency virus type 1 Vpu protein is an oligomeric type I integral membrane protein. Journal of virology **67**:5056–5061.
328. **Park SH**, **Opella SJ**. 2005. Tilt angle of a trans-membrane helix is determined by hydrophobic mismatch. Journal of Molecular Biology **350**:310–318.
329. **Park SH**, **Mrse AA**, **Nevzorov AA**, **Mesleh MF**, **Oblatt-Montal M**, **Montal M**, **Opella SJ**. 2003. Three-dimensional structure of the channel-forming trans-membrane domain of virus protein “u” (Vpu) from HIV-1. Journal of Molecular Biology **333**:409–424.
330. **Wray V**, **Kinder R**, **Federau T**, **Henklein P**, **Bechinger B**, **Schubert U**. 1999. Solution structure and orientation of the transmembrane anchor domain of the HIV-1-encoded virus protein U by high-resolution and solid-state NMR spectroscopy. Biochemistry **38**:5272–5282.
331. **Hussain A**, **Das SR**, **Tanwar C**, **Jameel S**. 2007. Oligomerization of the human immunodeficiency virus type 1 (HIV-1) Vpu protein--a genetic, biochemical and

biophysical analysis. Virol. J. **4**:81.

332. **Schubert U**, **Ferrer-Montiel AV**, **Oblatt-Montal M**, **Henklein P**, **Strebel K**, **Montal M**. 1996. Identification of an ion channel activity of the Vpu transmembrane domain and its involvement in the regulation of virus release from HIV-1-infected cells. FEBS Lett. **398**:12–18.
333. **Ewart GD**, **Sutherland T**, **Gage PW**, **Cox GB**. 1996. The Vpu protein of human immunodeficiency virus type 1 forms cation-selective ion channels. Journal of Virology **70**:7108–7115.
334. **Schubert U**, **Henklein P**, **Boldyreff B**, **Wingender E**, **Strebel K**, **Porstmann T**. 1994. The human immunodeficiency virus type 1 encoded Vpu protein is phosphorylated by casein kinase-2 (CK-2) at positions Ser52 and Ser56 within a predicted alpha-helix-turn-alpha-helix-motif. Journal of Molecular Biology **236**:16–25.
335. **Henklein P**, **Schubert U**, **Kunert O**, **Klabunde S**, **WRAY V**, **Klöppel KD**, **Kiess M**, **Portsmann T**, **Schomburg D**. 1993. Synthesis and characterization of the hydrophilic C-terminal domain of the human immunodeficiency virus type 1-encoded virus protein U (Vpu). Pept. Res. **6**:79–87.
336. **Wray V**, **Federau T**, **Henklein P**, **Klabunde S**, **Kunert O**, **Schomburg D**, **Schubert U**. 1995. Solution structure of the hydrophilic region of HIV-1 encoded virus protein U (Vpu) by CD and 1H NMR spectroscopy. International Journal of Peptide and Protein Research **45**:35–43.
337. **Federau T**, **Schubert U**, **Flossdorf J**, **Henklein P**, **Schomburg D**, **Wray V**. 1996. Solution structure of the cytoplasmic domain of the human immunodeficiency virus type 1 encoded virus protein U (Vpu). International Journal of Peptide and Protein Research **47**:297–310.
338. **Bour S**, **Strebel K**. 2003. The HIV-1 Vpu protein: a multifunctional enhancer of viral particle release. Microbes Infect **5**:1029–1039.
339. **Schwartz S**, **Felber BK**, **Fenyö EM**, **Pavlakis GN**. 1990. Env and Vpu proteins of human immunodeficiency virus type 1 are produced from multiple bicistronic mRNAs. Journal of Virology **64**:5448–5456.
340. **Varthakavi V**, **Smith RM**, **Martin KL**, **Derdowski A**, **Lapierre LA**, **Goldenring JR**, **Spearman P**. 2006. The pericentriolar recycling endosome plays a key role in Vpu-mediated enhancement of HIV-1 particle release. Traffic **7**:298–307.
341. **Dubé M**, **Roy BB**, **Guiot-Guillain P**, **Mercier J**, **Binette J**, **Leung G**, **Cohen EA**. 2009. Suppression of Tetherin-restricting activity upon human immunodeficiency virus type 1 particle release correlates with localization of Vpu in the trans-Golgi network. Journal of Virology **83**:4574–4590.
342. **Ruiz A**, **Hill MS**, **Schmitt K**, **Stephens EB**. 2010. Membrane raft association of the Vpu protein of human immunodeficiency virus type 1 correlates with enhanced virus release. Virology **408**:89–102.
343. **Fritz JV**, **Tibroni N**, **Keppler OT**, **Fackler OT**. 2012. HIV-1 Vpu's lipid raft association is dispensable for counteraction of the particle release restriction imposed by CD317/Tetherin. Virology **424**:33–44.
344. **Lopez LA**, **Yang SJ**, **Exline CM**, **Rengarajan S**, **Haworth KG**, **Cannon PM**. 2012. Anti-tetherin activities of HIV-1 Vpu and Ebola virus glycoprotein do not involve removal of tetherin from lipid rafts. Journal of Virology **86**:5467–5480.
345. **Pacyniak E**, **Gomez ML**, **Gomez LM**, **Mulcahy ER**, **Jackson M**, **Hout DR**, **Wisdom BJ**, **Stephens EB**. 2005. Identification of a Region within the Cytoplasmic Domain of the Subtype B Vpu Protein of Human Immunodeficiency Virus Type 1 (HIV-1) That Is Responsible for Retention in the Golgi Complex and Its Absence in the Vpu Protein from a Subtype C HIV-1.
346. **Ruiz A**, **Hill MS**, **Schmitt K**, **Guatelli J**, **Stephens EB**. 2008. Requirements of the membrane proximal tyrosine and dileucine-based sorting signals for efficient transport of the subtype C Vpu protein to the plasma membrane and in virus release. Virology **378**:58–68.
347. **Dubé M**, **Bego MG**, **Paquay C**, **Cohen ÉA**. 2010. Modulation of HIV-1-host interaction: role of the Vpu accessory protein. Retrovirology **7**:114.
348. **Moll M**, **Andersson SK**, **Smed-Sörensen A**, **Sandberg JK**. 2010. Inhibition of lipid antigen presentation in dendritic cells by HIV-1 Vpu interference with CD1d recycling from endosomal compartments. Blood **116**:1876–1884.
349. **Shah AH**, **Sowrirajan B**, **Davis ZB**, **Ward JP**, **Campbell EM**, **Planelles V**, **Barker E**. 2010. Degranulation of natural killer cells following interaction with HIV-1-infected cells is hindered by downmodulation of NTB-A by Vpu. Cell Host Microbe **8**:397–409.

350. **Akari H**, **Bour S**, **Kao S**, **Adachi A**, **Strebel K**. 2001. The human immunodeficiency virus type 1 accessory protein Vpu induces apoptosis by suppressing the nuclear factor kappaB-dependent expression of antiapoptotic factors. J. Exp. Med. **194**:1299–1311.
351. **daSilva LLP**, **Sougrat R**, **Burgos PV**, **Janvier K**, **Mattera R**, **Bonifacino JS**. 2009. Human immunodeficiency virus type 1 Nef protein targets CD4 to the multivesicular body pathway. Journal of Virology **83**:6578–6590.
352. **Wildum S**, **Schindler M**, **Münch J**, **Kirchhoff F**. 2006. Contribution of Vpu, Env, and Nef to CD4 down-modulation and resistance of human immunodeficiency virus type 1-infected T cells to superinfection. Journal of Virology **80**:8047–8059.
353. **Cortés MJ**, **Wong-Staal F**, **Lama J**. 2002. Cell surface CD4 interferes with the infectivity of HIV-1 particles released from T cells. J Biol Chem **277**:1770–1779.
354. **Levesque K**, **Zhao Y-S**, **Cohen EA**. 2003. Vpu exerts a positive effect on HIV-1 infectivity by down-modulating CD4 receptor molecules at the surface of HIV-1-producing cells. J Biol Chem **278**:28346–28353.
355. **Tanaka M**, **Ueno T**, **Nakahara T**, **Sasaki K**, **Ishimoto A**, **Sakai H**. 2003. Downregulation of CD4 is required for maintenance of viral infectivity of HIV-1. Virology **311**:316–325.
356. **Bour S**, **Perrin C**, **Strebel K**. 1999. Cell surface CD4 inhibits HIV-1 particle release by interfering with Vpu activity. J Biol Chem **274**:33800–33806.
357. **Bour S**, **Schubert U**, **Strebel K**. 1995. The human immunodeficiency virus type 1 Vpu protein specifically binds to the cytoplasmic domain of CD4: implications for the mechanism of degradation. Journal of Virology **69**:1510–1520.
358. **Lenburg ME**, **Landau NR**. 1993. Vpu-induced degradation of CD4: requirement for specific amino acid residues in the cytoplasmic domain of CD4. Journal of Virology **67**:7238–7245.
359. **Vincent MJ**, **Raja NU**, **Jabbar MA**. 1993. Human immunodeficiency virus type 1 Vpu protein induces degradation of chimeric envelope glycoproteins bearing the cytoplasmic and anchor domains of CD4: role of the cytoplasmic domain in Vpu-induced degradation in the endoplasmic reticulum. Journal of Virology **67**:5538–5549.
360. **Willey RL**, **Buckler-White A**, **Strebel K**. 1994. Sequences present in the cytoplasmic domain of CD4 are necessary and sufficient to confer sensitivity to the human immunodeficiency virus type 1 Vpu protein. Journal of Virology **68**:1207–1212.
361. **Yao XJ**, **Friborg J**, **Checroune F**, **Gratton S**, **Boisvert F**, **Sékaly RP**, **Cohen EA**. 1995. Degradation of CD4 induced by human immunodeficiency virus type 1 Vpu protein: a predicted alpha-helix structure in the proximal cytoplasmic region of CD4 contributes to Vpu sensitivity. Virology **209**:615–623.
362. **Schubert U**, **Bour S**, **Ferrer-Montiel AV**, **Montal M**, **Maldarell F**, **Strebel K**. 1996. The two biological activities of human immunodeficiency virus type 1 Vpu protein involve two separable structural domains. Journal of Virology **70**:809–819.
363. **Margottin F**, **Benichou S**, **Durand H**, **Richard V**, **Liu LX**, **Gomas E**, **Benarous R**. 1996. Interaction between the cytoplasmic domains of HIV-1 Vpu and CD4: role of Vpu residues involved in CD4 interaction and in vitro CD4 degradation. Virology **223**:381–386.
364. **Tiganos E**, **Yao XJ**, **Friborg J**, **Daniel N**, **Cohen EA**. 1997. Putative alpha-helical structures in the human immunodeficiency virus type 1 Vpu protein and CD4 are involved in binding and degradation of the CD4 molecule. Journal of Virology **71**:4452–4460.
365. **Schubert U**, **Strebel K**. 1994. Differential activities of the human immunodeficiency virus type 1-encoded Vpu protein are regulated by phosphorylation and occur in different cellular compartments. Journal of Virology **68**:2260–2271.
366. **Paul M**, **Jabbar MA**. 1997. Phosphorylation of both phosphoacceptor sites in the HIV-1 Vpu cytoplasmic domain is essential for Vpu-mediated ER degradation of CD4. Virology **232**:207–216.
367. **Margottin F**, **Bour SP**, **Durand H**, **Selig L**, **Benichou S**, **Richard V**, **Thomas D**, **Strebel K**, **Benarous R**. 1998. A novel human WD protein, h-beta TrCp, that interacts with HIV-1 Vpu connects CD4 to the ER degradation pathway through an F-box motif. Mol Cell **1**:565–574.
368. **Meusser B**, **Sommer T**. 2004. Vpu-mediated degradation of CD4 reconstituted in yeast reveals mechanistic differences to cellular ER-associated protein degradation. Mol Cell **14**:247–258.
369. **Binette J**, **Dubé M**, **Mercier J**, **Halawani D**, **Latterich M**, **Cohen EA**. 2007.

Requirements for the selective degradation of CD4 receptor molecules by the human immunodeficiency virus type 1 Vpu protein in the endoplasmic reticulum. Retrovirology **4**:75.

370. **Magadán JG**, **Pérez-Victoria FJ**, **Sougrat R**, **Ye Y**, **Strebel K**, **Bonifacino JS**. 2010. Multilayered mechanism of CD4 downregulation by HIV-1 Vpu involving distinct ER retention and ERAD targeting steps. PLoS Pathog **6**:e1000869.
371. **Schubert U**, **Antón LC**, **Bačík I**, **Cox JH**, **Bour S**, **Bennink JR**, **Orlowski M**, **Strebel K**, **Yewdell JW**. 1998. CD4 glycoprotein degradation induced by human immunodeficiency virus type 1 Vpu protein requires the function of proteasomes and the ubiquitin-conjugating pathway. Journal of Virology **72**:2280–2288.
372. **Fujita K**, **Omura S**, **Silver J**. 1997. Rapid degradation of CD4 in cells expressing human immunodeficiency virus type 1 Env and Vpu is blocked by proteasome inhibitors. J Gen Virol **78 (Pt 3)**:619–625.
373. **Hill MS**, **Ruiz A**, **Schmitt K**, **Stephens EB**. 2010. Identification of amino acids within the second alpha helical domain of the human immunodeficiency virus type 1 Vpu that are critical for preventing CD4 cell surface expression. Virology **397**:104–112.
374. **Magadán JG**, **Bonifacino JS**. 2012. Transmembrane domain determinants of CD4 Downregulation by HIV-1 Vpu. Journal of Virology **86**:757–772.
375. **Meusser B**, **Hirsch C**, **Jarosch E**, **Sommer T**. 2005. ERAD: the long road to destruction. Nat Cell Biol **7**:766–772.
376. **Miyagi E**, **Andrew AJ**, **Kao S**, **Strebel K**. 2009. Vpu enhances HIV-1 virus release in the absence of Bst-2 cell surface down-modulation and intracellular depletion. Proc Natl Acad Sci USA **106**:2868–2873.
377. **Dubé M**, **Roy BB**, **Guiot-Guillain P**, **Binette J**, **Mercier J**, **Chiasson A**, **Cohen EA**. 2010. Antagonism of tetherin restriction of HIV-1 release by Vpu involves binding and sequestration of the restriction factor in a perinuclear compartment. PLoS Pathog **6**:e1000856.
378. **Dubé M**, **Paquay C**, **Roy BB**, **Bego MG**, **Mercier J**, **Cohen EA**. 2011. HIV-1 Vpu antagonizes BST-2 by interfering mainly with the trafficking of newly synthesized BST-2 to the cell surface. **12**:1714–1729.
379. **Habermann A**, **Krijnse-Locker J**, **Oberwinkler H**, **Eckhardt M**, **Homann S**, **Andrew A**, **Strebel K**, **Kräusslich H-G**. 2010. CD317/tetherin is enriched in the HIV-1 envelope and downregulated from the plasma membrane upon virus infection. Journal of Virology **84**:4646–4658.
380. **Lau D**, **Kwan W**, **Guatelli J**. 2011. Role of the endocytic pathway in the counteraction of BST-2 by human lentiviral pathogens. Journal of Virology **85**:9834–9846.
381. **Andrew AJ**, **Miyagi E**, **Strebel K**. 2011. Differential effects of human immunodeficiency virus type 1 Vpu on the stability of BST-2/tetherin. Journal of Virology **85**:2611–2619.
382. **Schmidt S**, **Fritz JV**, **Bitzegeio J**, **Fackler OT**, **Keppler OT**. 2011. HIV-1 Vpu blocks recycling and biosynthetic transport of the intrinsic immunity factor CD317/tetherin to overcome the virion release restriction. mBio **2**:e00036–11–e00036–11.
383. **Kueck T**, **Neil SJD**. 2012. A Cytoplasmic Tail Determinant in HIV-1 Vpu Mediates Targeting of Tetherin for Endosomal Degradation and Counteracts Interferon-Induced Restricti. PLoS Pathog **8**:e1002609.
384. **Paul M**, **Mazumder S**, **Raja N**, **Jabbar MA**. 1998. Mutational analysis of the human immunodeficiency virus type 1 Vpu transmembrane domain that promotes the enhanced release of virus-like particles from the plasma membrane of mammalian cells. Journal of Virology **72**:1270–1279.
385. **Tiganos E**, **Friborg J**, **Allain B**, **Daniel NG**, **Yao XJ**, **Cohen EA**. 1998. Structural and functional analysis of the membrane-spanning domain of the human immunodeficiency virus type 1 Vpu protein. Virology **251**:96–107.
386. **Skasko M**, **Wang Y**, **Tian Y**, **Tokarev A**, **Munguia J**, **Ruiz A**, **Stephens EB**, **Opella SJ**, **Guatelli J**. 2012. HIV-1 Vpu protein antagonizes innate restriction factor BST-2 via lipid-embedded helix-helix interactions. Journal of Biological Chemistry **287**:58–67.
387. **Goffinet C**, **Allespach I**, **Homann S**, **Tervo H-M**, **Habermann A**, **Rupp D**, **Oberbremer L**, **Kern C**, **Tibroni N**, **Welsch S**, **Krijnse-Locker J**, **Banting G**, **Kräusslich H-G**, **Fackler OT**, **Keppler OT**. 2009. HIV-1 antagonism of CD317 is species specific and involves Vpu-mediated proteasomal degradation of the restriction factor. Cell Host Microbe **5**:285–297.
388. **Mangeat B**, **Gers-Huber G**, **Lehmann M**, **Zufferey M**, **Luban J**, **Piguet V**. 2009. HIV-1 Vpu neutralizes the antiviral factor Tetherin/BST-2 by binding it and directing its beta-

TrCP2-dependent degradation. PLoS Pathog **5**:e1000574.
389. **Janvier K**, **Pelchen-Matthews A**, **Renaud J-B**, **Caillet M**, **Marsh M**, **Berlioz-Torrent C**. 2011. The ESCRT-0 Component HRS is Required for HIV-1 Vpu-Mediated BST-2/Tetherin Down-Regulation. PLoS Pathog **7**:e1001265.
390. **Agromayor M**, **Soler N**, **Caballe A**, **Kueck T**, **Freund SM**, **Allen MD**, **Bycroft M**, **Perisic O**, **Ye Y**, **McDonald B**, **Scheel H**, **Hofmann K**, **Neil SJD**, **Martin-Serrano J**, **Williams RL**. 2012. The UBAP1 Subunit of ESCRT-I Interacts with Ubiquitin via a SOUBA Domain. Structure **20**:414–428.
391. **Caillet M**, **Janvier K**, **Pelchen-Matthews A**, **Delcroix-Genête D**, **Camus G**, **Marsh M**, **Berlioz-Torrent C**. 2011. Rab7A is required for efficient production of infectious HIV-1. PLoS Pathog **7**:e1002347.
392. **Goffinet C**, **Homann S**, **Ambiel I**, **Tibroni N**, **Rupp D**, **Keppler OT**, **Fackler OT**. 2010. Antagonism of CD317 restriction of human immunodeficiency virus type 1 (HIV-1) particle release and depletion of CD317 are separable activities of HIV-1 Vpu. Journal of Virology **84**:4089–4094.
393. **Tokarev AA**, **Munguia J**, **Guatelli JC**. 2011. Serine-threonine ubiquitination mediates downregulation of BST-2/tetherin and relief of restricted virion release by HIV-1 Vpu. Journal of Virology **85**:51–63.
394. **Chu H**, **Wang J-J**, **Qi M**, **Yoon J-J**, **Chen X**, **Wen X**, **Hammonds J**, **Ding L**, **Spearman P**. 2012. Tetherin/BST-2 Is Essential for the Formation of the Intracellular Virus-Containing Compartment in HIV-Infected Macrophages. Cell Host Microbe **12**:360–372.
395. **Lanier LL**. 2008. Evolutionary struggles between NK cells and viruses. **8**:259–268.
396. **Bonaparte MI**, **Barker E**. 2003. Inability of natural killer cells to destroy autologous HIV-infected T lymphocytes. AIDS **17**:487–494.
397. **Cohen GB**, **Gandhi RT**, **Davis DM**, **Mandelboim O**, **Chen BK**, **Strominger JL**, **Baltimore D**. 1999. The selective downregulation of class I major histocompatibility complex proteins by HIV-1 protects HIV-infected cells from NK cells. Immunity **10**:661–671.
398. **Ward J**, **Bonaparte M**, **Sacks J**, **Guterman J**, **Fogli M**, **Mavilio D**, **Barker E**. 2007. HIV modulates the expression of ligands important in triggering natural killer cell cytotoxic responses on infected primary T-cell blasts. Blood **110**:1207–1214.
399. **Ward J**, **Davis Z**, **DeHart J**, **Zimmerman E**, **Bosque A**, **Brunetta E**, **Mavilio D**, **Planelles V**, **Barker E**. 2009. HIV-1 Vpr triggers natural killer cell-mediated lysis of infected cells through activation of the ATR-mediated DNA damage response. PLoS Pathog **5**:e1000613.
400. **Richard J**, **Sindhu S**, **Pham TNQ**, **Belzile J-P**, **Cohen EA**. 2010. HIV-1 Vpr up-regulates expression of ligands for the activating NKG2D receptor and promotes NK cell-mediated killing. Blood **115**:1354–1363.
401. **Richard J**, **Cohen EA**. 2010. HIV-1 Vpu disarms natural killer cells. Cell Host Microbe **8**:389–391.
402. **Stewart SA**, **Poon B**, **Jowett JB**, **Chen IS**. 1997. Human immunodeficiency virus type 1 Vpr induces apoptosis following cell cycle arrest. Journal of Virology **71**:5579–5592.
403. **Bour S**, **Perrin C**, **Akari H**, **Strebel K**. 2001. The human immunodeficiency virus type 1 Vpu protein inhibits NF-kappa B activation by interfering with beta TrCP-mediated degradation of Ikappa B. J Biol Chem **276**:15920–15928.
404. **O'Doherty U**, **Swiggard WJ**, **Malim MH**. 2000. Human immunodeficiency virus type 1 spinoculation enhances infection through virus binding. Journal of Virology **74**:10074–10080.
405. **Fields BN**, **Knipe DM**, **Howley PM**. 2007. Fields' virology. Lippincott Williams & Wilkins.
406. **Coscoy L**, **Ganem D**. 2000. Kaposi's sarcoma-associated herpesvirus encodes two proteins that block cell surface display of MHC class I chains by enhancing their endocytosis. Proc Natl Acad Sci USA **97**:8051–8056.
407. **Rhodes DA**, **Boyle LH**, **Boname JM**, **Lehner PJ**, **Trowsdale J**. 2010. Ubiquitination of lysine-331 by Kaposi's sarcoma-associated herpesvirus protein K5 targets HFE for lysosomal degradation. Proc Natl Acad Sci USA **107**:16240–16245.
408. **Mansouri M**, **Rose PP**, **Moses AV**, **Früh K**. 2008. Remodeling of endothelial adherens junctions by Kaposi's sarcoma-associated herpesvirus. Journal of Virology **82**:9615–9628.
409. **Ishido S**, **Choi JK**, **Lee BS**, **Wang C**, **DeMaria M**, **Johnson RP**, **Cohen GB**, **Jung JU**. 2000. Inhibition of natural killer cell-mediated cytotoxicity by Kaposi's sarcoma-

associated herpesvirus K5 protein. Immunity **13**:365–374.
410. **Sanchez DJ**, **Gumperz JE**, **Ganem D**. 2005. Regulation of CD1d expression and function by a herpesvirus infection. **115**:1369–1378.
411. **Thomas M**, **Boname JM**, **Field S**, **Nejentsev S**, **Salio M**, **Cerundolo V**, **Wills M**, **Lehner PJ**. 2008. Down-regulation of NKG2D and NKp80 ligands by Kaposi's sarcoma-associated herpesvirus K5 protects against NK cell cytotoxicity. Proc Natl Acad Sci USA **105**:1656–1661.
412. **Li Q**, **Means R**, **Lang S**, **Jung JU**. 2007. Downregulation of gamma interferon receptor 1 by Kaposi's sarcoma-associated herpesvirus K3 and K5. Journal of Virology **81**:2117–2127.
413. **Durrington HJ**, **Upton PD**, **Hoer S**, **Boname J**, **Dunmore BJ**, **Yang J**, **Crilley TK**, **Butler LM**, **Blackbourn DJ**, **Nash GB**, **Lehner PJ**, **Morrell NW**. 2010. Identification of a lysosomal pathway regulating degradation of the bone morphogenetic protein receptor type II. J Biol Chem **285**:37641–37649.
414. **Sanchez DJ**, **Coscoy L**, **Ganem D**. 2002. Functional organization of MIR2, a novel viral regulator of selective endocytosis. J Biol Chem **277**:6124–6130.
415. **Bartee E**, **Mansouri M**, **Hovey Nerenberg BT**, **Gouveia K**, **Früh K**. 2004. Downregulation of major histocompatibility complex class I by human ubiquitin ligases related to viral immune evasion proteins. Journal of Virology **78**:1109–1120.
416. **Hewitt EW**, **Duncan L**, **Mufti D**, **Baker J**, **Stevenson PG**, **Lehner PJ**. 2002. Ubiquitylation of MHC class I by the K3 viral protein signals internalization and TSG101-dependent degradation. EMBO J. **21**:2418–2429.
417. **Mansouri M**. 2006. Kaposi sarcoma herpesvirus K5 removes CD31/PECAM from endothelial cells. Blood **108**:1932–1940.
418. **Boname JM**, **Lehner PJ**. 2011. What has the study of the K3 and K5 viral ubiquitin E3 ligases taught us about ubiquitin-mediated receptor regulation? Viruses **3**:118–131.
419. **Randow F**, **Lehner PJ**. 2009. Viral avoidance and exploitation of the ubiquitin system. Nat Cell Biol **11**:527–534.
420. **Lim ES**, **Malik HS**, **Emerman M**. 2010. Ancient adaptive evolution of tetherin shaped the functions of Vpu and Nef in human immunodeficiency virus and primate lentiviruses. Journal of Virology **84**:7124–7134.
421. **Mehnert T**, **Routh A**, **Judge PJ**, **Lam YH**, **Fischer D**, **Watts A**, **Fischer WB**. 2008. Biophysical characterization of Vpu from HIV-1 suggests a channel-pore dualism. Proteins **70**:1488–1497.
422. **Sharpe HJ**, **Stevens TJ**, **Munro S**. 2010. A comprehensive comparison of transmembrane domains reveals organelle-specific properties. Cell **142**:158–169.
423. **Marassi FM**, **Ma C**, **Gratkowski H**, **Straus SK**, **Strebel K**, **Oblatt-Montal M**, **Montal M**, **Opella SJ**. 1999. Correlation of the structural and functional domains in the membrane protein Vpu from HIV-1. Proc Natl Acad Sci USA **96**:14336–14341.
424. **Vigan R**, **Neil SJD**. 2011. Separable determinants of subcellular localization and interaction account for the inability of group O HIV-1 Vpu to counteract tetherin. Journal of Virology **85**:9737–9748.
425. **Van Heuverswyn F**, **Li Y**, **Neel C**, **Bailes E**, **Keele BF**, **Liu W**, **Loul S**, **Butel C**, **Liegeois F**, **Bienvenue Y**, **Ngolle EM**, **Sharp PM**, **Shaw GM**, **Delaporte E**, **Hahn BH**, **Peeters M**. 2006. Human immunodeficiency viruses: SIV infection in wild gorillas. Nature **444**:164.
426. **Sauter D**, **Specht A**, **Kirchhoff F**. 2010. Tetherin: holding on and letting go. Cell **141**:392–398.
427. **Goepfert PA**, **Shaw K**, **Wang G**, **Bansal A**, **Edwards BH**, **Mulligan MJ**. 1999. An endoplasmic reticulum retrieval signal partitions human foamy virus maturation to intracytoplasmic membranes. Journal of Virology **73**:7210–7217.
428. **Skasko M**, **Tokarev A**, **Chen C-C**, **Fischer WB**, **Pillai SK**, **Guatelli J**. 2011. BST-2 is rapidly down-regulated from the cell surface by the HIV-1 protein Vpu: evidence for a post-ER mechanism of Vpu-action. Virology **411**:65–77.
429. **Petit SJ**, **Blondeau C**, **Towers GJ**. 2011. Analysis of the human immunodeficiency virus type 1 M group Vpu domains involved in antagonizing tetherin. J Gen Virol **92**:2937–2948.
430. **Takehisa J**, **Kraus MH**, **Ayouba A**, **Bailes E**, **Van Heuverswyn F**, **Decker JM**, **Li Y**, **Rudicell RS**, **Learn GH**, **Neel C**, **Ngole EM**, **Shaw GM**, **Peeters M**, **Sharp PM**, **Hahn BH**. 2009. Origin and biology of simian immunodeficiency virus in wild-living western gorillas. Journal of Virology **83**:1635–1648.
431. **Van Heuverswyn F**, **Li Y**, **Bailes E**, **Neel C**, **Lafay B**, **Keele BF**, **Shaw KS**, **Takehisa**

J, **Kraus MH**, **Loul S**, **Butel C**, **Liegeois F**, **Yangda B**, **Sharp PM**, **Mpoudi-Ngole E**, **Delaporte E**, **Hahn BH**, **Peeters M**. 2007. Genetic diversity and phylogeographic clustering of SIVcpzPtt in wild chimpanzees in Cameroon. Virology **368**:155–171.

432. **Schubert U**, **Bour S**, **Willey RL**, **Strebel K**. 1999. Regulation of virus release by the macrophage-tropic human immunodeficiency virus type 1 AD8 isolate is redundant and can be controlled by either Vpu or Env. Journal of Virology **73**:887–896.
433. **Sauter D**, **Hué S**, **Petit SJ**, **Plantier J-C**, **Towers GJ**, **Kirchhoff F**, **Gupta RK**. 2011. HIV-1 Group P is unable to antagonize human tetherin by Vpu, Env or Nef. Retrovirology **8**:103.
434. **Weekes MP**, **Antrobus R**, **Talbot S**, **Hör S**, **Simecek N**, **Smith DL**, **Bloor S**, **Randow F**, **Lehner PJ**. 2012. Proteomic plasma membrane profiling reveals an essential role for gp96 in the cell surface expression of LDLR family members, including the LDL receptor and LRP6. J. Proteome Res. **11**:1475–1484.
435. **Mackenzie B**, **Erickson JD**. 2004. Sodium-coupled neutral amino acid (System N/A) transporters of the SLC38 gene family. Pflugers Arch. **447**:784–795.
436. **Carr EL**, **Kelman A**, **Wu GS**, **Gopaul R**, **Senkevitch E**, **Aghvanyan A**, **Turay AM**, **Frauwirth KA**. 2010. Glutamine Uptake and Metabolism Are Coordinately Regulated by ERK/MAPK during T Lymphocyte Activation. The Journal of Immunology **185**:1037–1044.
437. **Varoqui H**, **Zhu H**, **Yao D**, **Ming H**, **Erickson JD**. 2000. Cloning and functional identification of a neuronal glutamine transporter. J Biol Chem **275**:4049–4054.
438. **Mackenzie B**. 2003. Functional Properties and Cellular Distribution of the System A Glutamine Transporter SNAT1 Support Specialized Roles in Central Neurons. J Biol Chem **278**:23720–23730.
439. **Ardawi MS**, **Newsholme EA**. 1983. Glutamine metabolism in lymphocytes of the rat. Biochem. J. **212**:835–842.
440. **Ardawi MS**. 1988. Glutamine and glucose metabolism in human peripheral lymphocytes. Metab. Clin. Exp. **37**:99–103.
441. **McDonald B**, **Martin-Serrano J**. 2008. Regulation of Tsg101 expression by the steadiness box: a role of Tsg101-associated ligase. Mol. Biol. Cell **19**:754–763.
442. **Hörig H**, **Spagnoli GC**, **Filgueira L**, **Babst R**, **Gallati H**, **Harder F**, **Juretic A**, **Heberer M**. 1993. Exogenous glutamine requirement is confined to late events of T cell activation. J Cell Biochem **53**:343–351.
443. **Yaqoob P**, **Calder PC**. 1997. Glutamine requirement of proliferating T lymphocytes. Nutrition **13**:646–651.
444. **Yaqoob P**, **Calder PC**. 1998. Cytokine production by human peripheral blood mononuclear cells: differential senstivity to glutamine availability. **10**:790–794.
445. **Franchi-Gazzola R**. 1999. Adaptive Increase of Amino Acid Transport System A Requires ERK1/2 Activation. Journal of Biological Chemistry **274**:28922–28928.
446. **Powell JD**, **Delgoffe GM**. 2010. The Mammalian Target of Rapamycin: Linking T Cell Differentiation, Function, and Metabolism. Immunity **33**:301–311.

Publications

1. The RING-CH ligase K5 antagonizes restriction of KSHV and HIV-1 particle release by mediating ubiquitin-dependent endosomal degradation of tetherin.
Claire Pardieu, Raphaël Vigan, Sam J. Wilson, Alessandra Calvi, Trinity Zang, Paul Bieniasz, Paul Kellam, Greg J. Towers, Stuart J. D. Neil.
Plos Pathogens. April 2010.

2. Determinants of tetherin antagonism in the transmembrane domain of the human immunodeficiency virus type 1 Vpu protein.
Vigan, R. & Neil, S. J. D.
Journal of Virology. December 2010.

3. Separable determinants of subcellular localization and interaction account for the inability of group O HIV-1 Vpu to counteract tetherin.
Vigan, R. & Neil, S. J. D.
Journal of Virology. October 2011.

OPEN ACCESS Freely available online

PLoS PATHOGENS

The RING-CH Ligase K5 Antagonizes Restriction of KSHV and HIV-1 Particle Release by Mediating Ubiquitin-Dependent Endosomal Degradation of Tetherin

Claire Pardieu[1☯], Raphaël Vigan[2☯], Sam J. Wilson[1,3], Alessandra Calvi[2], Trinity Zang[3], Paul Bieniasz[3], Paul Kellam[1,4], Greg J. Towers[1]*, Stuart J. D. Neil[2]*

1 MRC Centre for Medical Molecular Virology, University College London, London, United Kingdom, **2** Department of Infectious Disease, King's College London School of Medicine, Guy's Hospital, London, United Kingdom, **3** Howard Hughes Medical Institute, Aaron Diamond AIDS Research Center and Laboratory of Retrovirology, The Rockefeller University, New York, New York, United States of America, **4** Wellcome Trust Sanger Institute, Hinxton, Cambridge, United Kingdom

Abstract

Tetherin (CD317/BST2) is an interferon-induced membrane protein that inhibits the release of diverse enveloped viral particles. Several mammalian viruses have evolved countermeasures that inactivate tetherin, with the prototype being the HIV-1 Vpu protein. Here we show that the human herpesvirus Kaposi's sarcoma-associated herpesvirus (KSHV) is sensitive to tetherin restriction and its activity is counteracted by the KSHV encoded RING-CH E3 ubiquitin ligase K5. Tetherin expression in KSHV-infected cells inhibits viral particle release, as does depletion of K5 protein using RNA interference. K5 induces a species-specific downregulation of human tetherin from the cell surface followed by its endosomal degradation. We show that K5 targets a single lysine (K18) in the cytoplasmic tail of tetherin for ubiquitination, leading to relocalization of tetherin to CD63-positive endosomal compartments. Tetherin degradation is dependent on ESCRT-mediated endosomal sorting, but does not require a tyrosine-based sorting signal in the tetherin cytoplasmic tail. Importantly, we also show that the ability of K5 to substitute for Vpu in HIV-1 release is entirely dependent on K18 and the RING-CH domain of K5. By contrast, while Vpu induces ubiquitination of tetherin cytoplasmic tail lysine residues, mutation of these positions has no effect on its antagonism of tetherin function, and residual tetherin is associated with the trans-Golgi network (TGN) in Vpu-expressing cells. Taken together our results demonstrate that K5 is a mechanistically distinct viral countermeasure to tetherin-mediated restriction, and that herpesvirus particle release is sensitive to this mode of antiviral inhibition.

Citation: Pardieu C, Vigan R, Wilson SJ, Calvi A, Zang T, et al. (2010) The RING-CH Ligase K5 Antagonizes Restriction of KSHV and HIV-1 Particle Release by Mediating Ubiquitin-Dependent Endosomal Degradation of Tetherin. PLoS Pathog 6(4): e1000843. doi:10.1371/journal.ppat.1000843

Editor: Jae U. Jung, University of Southern California School of Medicine, United States of America

Received April 22, 2009; **Accepted** March 3, 2010; **Published** April 15, 2010

Funding: This work was funded by a Wellcome Trust Research Career Development Fellowship to SJDN (WT082274MA) and a Wellcome Trust Senior Research Fellowship to GJT (076608). The funders had no role in study design, data collection and analysis, decision to publish, or preparation of the manuscript.

Competing Interests: The authors have declared that no competing interests exist.

* E-mail: g.towers@ucl.ac.uk (GJT); stuart.neil@kcl.ac.uk (SJDN)

☯ These authors contributed equally to this work.

Introduction

The inhibitory effect of type 1 interferons (type 1 IFN) on the replication of mammalian viruses has been documented for over 50 years. However the effecter mechanisms that interfere with virus replication have not been well characterized. While many IFN response genes are known, few definitive antiviral functions have been ascribed to them. Amongst the best characterized are PKR/2′5′oligoadenylate synthetase, MxA and ISG15, all of which have broad activity against a variety of mammalian RNA viruses [1]. Recently the identification of retroviral restriction factors including members of the APOBEC3 family of cytidine deaminases, as well as TRIM5 and other members of the tripartite motif protein family, has highlighted innate intracellular defense mechanisms as key determinants of tropism for human and primate immunodeficiency viruses [2,3]. Moreover, these antiviral activities have driven the acquisition of viral countermeasures [2,4] and thus interferon-inducible restriction factors are now thought to represent an important arm of the antiviral innate immune system [3].

Tetherin, (BST2/CD317) has recently been shown to inhibit the release of HIV-1 particles that are defective for the accessory protein Vpu [5,6]. In the absence of Vpu expression, nascent HIV-1 particles assemble at the plasma membrane but remain tethered to the surface of tetherin expressing cells via a protease-sensitive linkage. Tethered virions are then endocytosed leading to their accumulation in late endosomes [5,7,8]. Tetherin colocalization with restricted viral particles on cell surfaces and in endosomes is well documented [5,6,9]. Strikingly, it is tetherin's unusual topology that is thought to be directly responsible for its mode of action [10]. Tetherin is a dimeric type-II membrane protein consisting of an N-terminal cytoplasmic tail, an extracellular domain with a putative coiled coil, and a C-terminal GPI anchor which is required for its antiviral function [5,11]. It forms dimers which are thought to cross-link viral and cellular membranes during viral budding [10]. Tetherin appears to have no direct association with any viral structural proteins and is therefore able to restrict a range of unrelated viruses including retroviruses, filoviruses and arenaviruses [9,12,13]. It is expressed on mature B cells and plasmacytoid dendritic cells, but can be

Author Summary

To replicate efficiently in their hosts, viruses must avoid antiviral cellular defenses that comprise part of the innate immune system. Tetherin, an antiviral membrane protein that inhibits the release of several enveloped viruses from infected cells, is antagonized by the HIV-1 Vpu protein. The K5 protein of the human pathogen Kaposi's sarcoma-associated herpesvirus (KSHV) modulates the cell surface levels of several host proteins including tetherin. We show that KSHV release is sensitive to tetherin, and that K5 expression is required for efficient virus production in tetherin-expressing cells. K5 is also capable of rescuing Vpu-defective HIV-1 virus release from tetherin. K5 expression induces a down-regulation of cell-surface tetherin levels and degradation in late endosomes, which depends on a single lysine residue in the tetherin cytoplasmic tail. Finally, we show that the ESCRT pathway, which promotes the trafficking of cell surface receptors for degradation, is required for K5-mediated tetherin removal from the plasma membrane. Thus, we demonstrate that herpesviruses are sensitive to the antiviral effects of tetherin and that KSHV has evolved a mechanism for its destruction. These findings extend the list of viruses sensitive to tetherin, suggesting that tetherin counter-measures are widespread defense mechanisms amongst enveloped viruses.

induced in many cell types by type-I interferon (IFN) [8,14,15,16,17]. Sequence analysis of orthologues of tetherin from primates indicates high levels of positive selection during their evolution suggesting selective pressure from pathogenic viral infections [18,19]. Together, these observations suggest that tetherin may be an important antiviral defense against enveloped virus replication, necessitating the acquisition of viral counter-measures to antagonize its activity.

Interestingly, other potential viral countermeasures to tetherin may exist. Kaposi's sarcoma-associated herpesvirus (KSHV), also known as Human herpesvirus 8 (HHV8), encodes two immuno-modulatory membrane associated RING-CH (MARCH) E3 ubiquitin ligases named K3 and K5 [20]. K5 has been shown to mediate the down-regulation of a variety of cell surface markers including MHC class I, PE-CAM-1, CD80/CD86, ICAM-1, IFNγ receptor and NKG2D [21,22,23,24,25,26,27]. In a recent proteomics screen Bartee and colleagues used a methodology called stable isotope labeling of amino acids in cultured cells (SILAC) to identify proteins that are removed from the plasma membrane on K5 expression. One of the novel K5 targets found was tetherin (BST2) [28]. Here we have tested the hypothesis that tetherin restricts assembly/release of KSHV particles and that an important function of K5 is to overcome this process.

Results

KSHV particle release is sensitive to tetherin-mediated restriction

Tetherin has the capacity to restrict the release of diverse enveloped viruses including filoviruses and arenaviruses [9,12,13]. Given the capacity of the KSHV protein K5 to reduce cell surface expression of tetherin [28] we tested whether KSHV could be restricted by the expression of increasing amounts of exogenous human tetherin. We reasoned that the complex envelopment strategy of herpesviruses [29] and the tropism of KSHV for tetherin-positive mature B cells made this virus potentially sensitive to restriction by tetherin. To test this we generated a HeLa cell line harboring latent recombinant rKSHV.219 episomes under puromycin selection which encode eGFP driven by the human EF-1α promoter and DsRed driven by the KSHV PAN promoter that responds to the KSHV immediate early protein RTA [30]. Transfection of these cells with an RTA encoding plasmid (pCMV RTA) induces KSHV transcription, lytic replication and the release of KSHV particles, the efficiency of which can be assessed by measurement of RFP expression. The amount of virus released 48h post-RTA induction can be measured by quantitative PCR (Q-PCR) detecting DNAse-I protected genomes in the supernatant or by titration of infectious virus onto 293T cells and enumeration of GFP expressing cells by flow cytometry.

We first determined whether transfecting a plasmid expressing tetherin together with pCMV-RTA would impact on the amount of infectious virions released into the supernatant. Figure 1A clearly demonstrates a linear decrease in release of KSHV infectious virus when increasing amounts of the tetherin-expressing plasmid are transfected with a constant amount of pCMV-RTA. Similarly, Q-PCR performed on DNAse-I resistant genomes showed a greater than 10-fold decrease in total virions released for the highest dose of tetherin-expressing plasmid used (Figure 1B). To control for transfection efficiency, cells were recovered after virus collection and cell lysates subjected to western blotting (Figure 1C). As expected, increasing amounts of tetherin were detected as increasing amounts of tetherin-expressing plasmid was transfected. Importantly, equal RTA expression was found in all samples confirming that RTA levels were not impacted by tetherin expression. To further rule out an effect of tetherin expression on KSHV reactivation we also measured lytic viral RNA production by quantitative RT-PCR. Ct values for ORF37 were normalized to those obtained for cellular GAPDH. Figure 1D shows very similar ORF37/GAPDH ratios for each condition. Whilst unlikely, it is also possible that exogenous expression of increasing amounts of tetherin might lower genomic replication, thus leading to a reduced amount of virions and/or DNase-I resistant genomes in the supernatant. To rule this out we measured intracellular episomes in DNA extracts by Q-PCR. Figure 1E clearly demonstrates that episome copy number was similar across all conditions and could not account for reduced viral production.

Reduction of K5 expression using K5 specific shRNA reduces KSHV release

We then tested whether K5 expression was required for efficient KSHV release from r219-HeLa cells. We reasoned that if K5 is a KSHV antagonist for tetherin then reducing its expression by RNA interference (RNAi) should inhibit KSHV release. Three shRNA hairpins were designed and expressed in 293T cells together with a HA-tagged K5 protein. Reduction of K5 expression by the hairpins was assessed by recovering the cells 48 hours after transfection and subjecting the lysates to western blot (Figure 2A). Blots probed with the anti-HA antibody were stripped and re-probed for alpha tubulin to control for equal loading (Figure 2A). All three hairpins reduced K5 expression with hairpin 3 (sh-K5iii) being the most potent. We then expressed the hairpins in r219-HeLa cells using lentiviral vectors [31]. 72 hours later the cells were re-seeded and transfected with RTA to induce KSHV lytic replication. Release of infectious KSHV was measured by titration of supernatants on 293T as before (Figure 2B). We found that expression of specific anti-K5 shRNA reduced KSHV titer in the supernatant whereas expression of an empty shRNA vector did not (Figure 2B). The number of DNAse-I resistant KSHV genomes in the supernatant was also reduced by all three shRNA vectors, as shown by taqman Q-PCR (Figure 2C). Messenger RNA for the late gene ORF37 was measured by quantitative RT-PCR in each sample and values were corrected

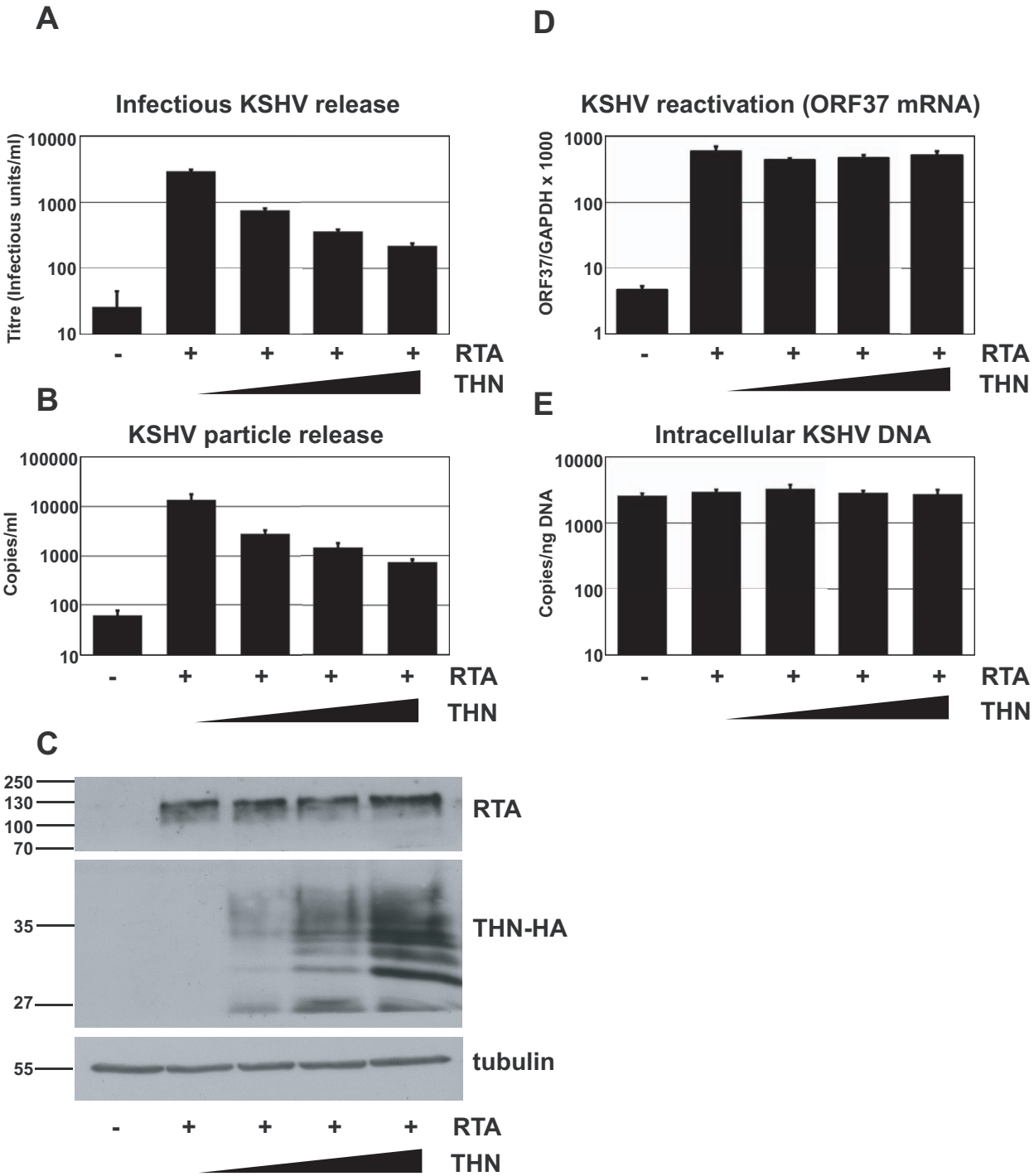

Figure 1. Over-expression of human tetherin restricts KSHV particle release. HeLa KSHV cells were transfected with an expression vector encoding the KSHV early transcriptional activator RTA and increasing doses of pCR3.1 encoding human tetherin. Plasmid dose was kept constant using pcDNA3.1. 48 hours after transfection supernatants were harvested, filtered and used to infect 293T cells (**A**) and infectious virus titer determined by GFP expression in the target cells by flow cytometry. Values are presented as infectious units/ml. (**B**) Parallel supernatants were treated for 2 hours with DNase-I and viral genomic DNA isolated and supernatant genome copy number enumerated by quantitative Taqman PCR specific for ORF37. Values are presented as copies/ml. (**C**) Western blot analysis for RTA protein (top panel) performed on r219-HeLa cells after virus collection indicates that RTA expression levels were equivalent in each sample. Blots were stripped and detection of tetherin using an anti-HA antibody performed (middle panel) shows increasing tetherin levels across samples, as expected. Alpha tubulin was detected concomitantly to RTA to demonstrate equal loading (bottom panel). (**D**) KSHV reactivation was equivalent in all samples as evidenced by measurement of ORF37 mRNA levels by quantitative Taqman PCR and after normalization to GAPDH levels. (**E**) KSHV genome levels remained constant in all samples as evidenced by equivalent numbers of intracellular KSHV episomes per nanogram of total cellular DNA. Results are the mean of 2 independent experiments and errors are standard error of the mean.
doi:10.1371/journal.ppat.1000843.g001

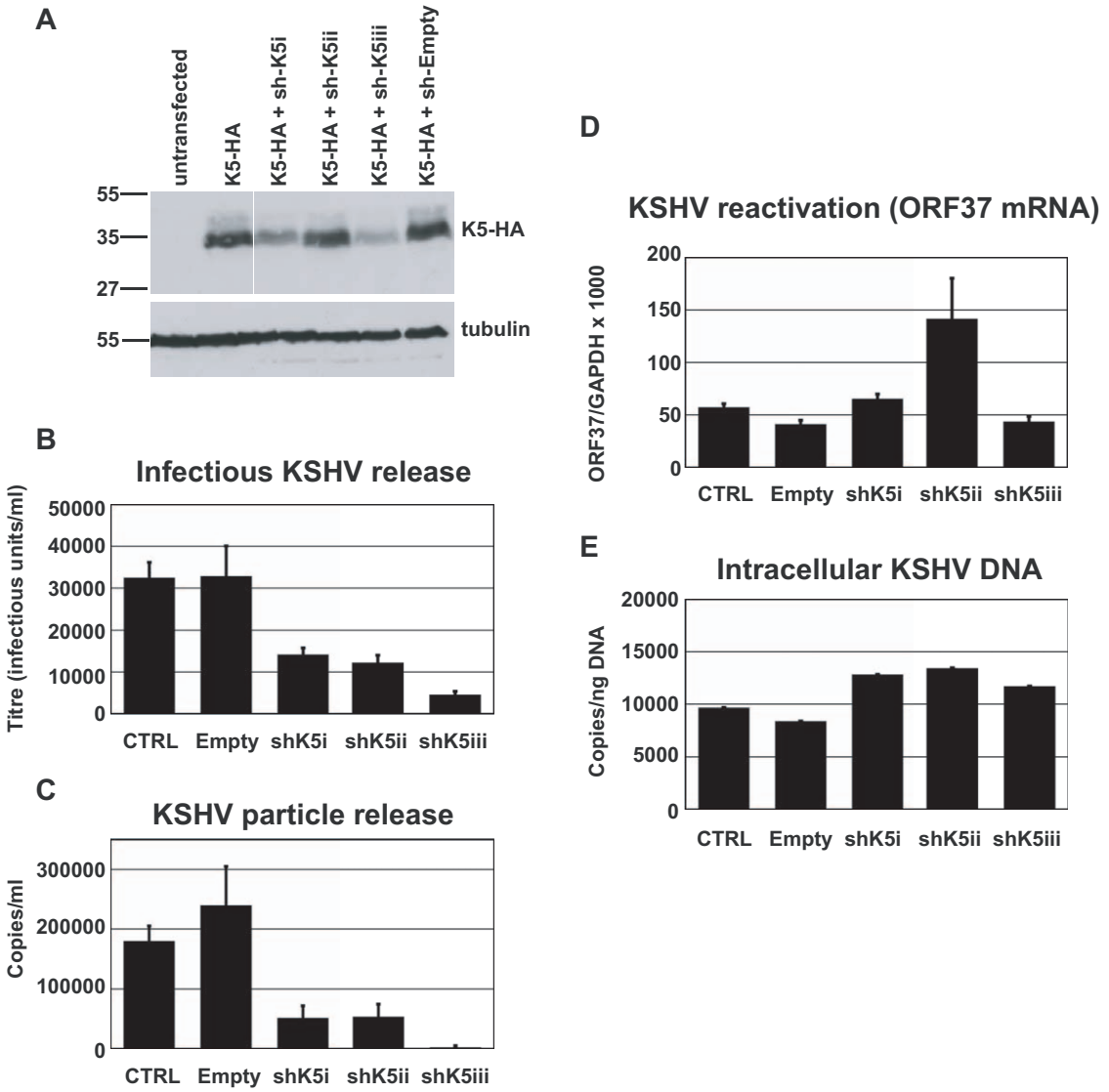

Figure 2. RNAi-depletion of K5 during lytic replication suppresses KSHV particle release. (**A**) Three shRNA hairpins were designed to target K5 and co-expressed with K5-HA in 293T cells. The efficiency of reduction of K5 expression was assessed 48 hours later by western blot of total cell lysates detecting the HA tag. Stripped blots were re-probed for alpha tubulin to demonstrate equal loading. (**B & C**) r219-HeLa cells were transduced by lentiviral vectors encoding K5 shRNAs at an MOI of 5, reseeded 72 hours later and transfected with RTA expression plasmid the following day. Supernatants were harvested 48 hours post-RTA transfection and KSHV titer expressed as infectious unit/ml (**B**) and DNase-I resistant genome copies/ml (**C**) were determined as in Figure 1. At the time of harvest (48 hours post RTA transfection), ORF37 and GAPDH mRNA were measured in the cell lysates by Taqman Q-RT-PCR to assess effect of the hairpins on KSHV reactivation and ORF37 expression (**D**). At the time of harvest, cells were also kept to assess the effect of the hairpins on genome replication. Cellular DNA was extracted and KSHV episomes measured by QPCR for ORF37 (**E**). Results are expressed as KSHV genomes per nanogram of total cellular DNA. Results are the mean of 2 independent experiments and errors are standard error of the mean.
doi:10.1371/journal.ppat.1000843.g002

for cellular GAPDH mRNA levels. This demonstrated that hairpin expression did not significantly inhibit KSHV reactivation (Figure 2D). In fact hairpin 2 appeared to stimulate ORF37 expression in one experiment leading to the large error bar. However, this experiment shows that inhibition of reactivation cannot account for the loss of KSHV in the supernatant. To further rule out an effect of hairpin expression on genomic replication we also measured intracellular KSHV episomes by DNA Q-PCR for ORF37 (Figure 2E) This control confirmed that the number of KSHV episomes in the cells did not account for the K5 hairpin induced defect in KSHV release and supports the notion that K5 antagonizes tetherin.

These results suggest that K5 is required for efficient KSHV particle release in a cell line that constitutively expresses tetherin and that expressing increasing amounts of exogenous tetherin further inhibits KSHV release. Together our data suggest that tetherin has antiviral activity against KSHV and that K5 has an important role in overcoming tetherin-mediated restriction.

K5 can substitute for Vpu in rescuing HIV-1 particle release from tetherin-mediated restriction

Having established a role for K5 in counteracting tetherin during KSHV release we then tested whether K5 expression could functionally substitute for the HIV-1 encoded tetherin antagonist

Vpu and rescue the release of tetherin restricted HIV-1(delVpu) particles [5]. We transfected HeLa cells with the HIV-1 molecular clone NL4.3, or a Vpu-defective counterpart, together with expression vectors for HA-tagged K5 or Vpu. As predicted, K5 expression potently rescued HIV-1(delVpu) release to levels achieved by Vpu expression (Figure 3A). This was evidenced both by measurement of HIV-1 p24 capsid protein released into the supernatant by western blots as well as by titration of infectious HIV-1 virus released into the supernatant on sensitive indicator cells (Figure 3A, B and C). Importantly K5 expression had no effect on wild-type HIV-1 particle release or on HIV-1 structural protein expression. These data demonstrate that K5 is a functional homolog of HIV-1 Vpu and that KSHV encodes a tetherin countermeasure.

The fact that K5 has been demonstrated to be a RING dependent E3 ligase for ubiquitin [20] suggested that the RING-CH domain is important for its function. We therefore made a RING deletion mutant of K5 (K5delRING) and tested its ability to counteract tetherin restriction in an HIV-1 release assay as above. Despite similar expression levels of the mutant and wild type K5 proteins (Figure 3B), the RING-defective K5 was unable to rescue HIV-1(del Vpu) release from HeLa cells (Figure 3A and C). To confirm that K5 can antagonize tetherin function we repeated the experiment but in a tetherin-deficient cell line (HT1080) [5] stably expressing a tetherin protein in which an HA-tag had been inserted into the ectodomain at amino acid position 154 [9]. HT/THN-HA cells were then transduced with retroviral vectors co-expressing DsRed and Vpu, or K5 or K5delRING at doses sufficient to give >90% DsRED-positive cells as demonstrated by flow cytometry 48 hours later. The cells were then re-seeded and infected with VSV-G pseudotyped HIV-1(wt) or HIV-1(del Vpu) at a multiplicity of infection of 0.2. Since HT1080 cells are devoid of CD4, VSV-G pseudotyping allows the measurement of a single round of viral replication. Similar to the experiment in HeLa cells, HT/THN-HA released HIV-1(del Vpu) particles approximately 20 fold less efficiently than they released wild type virus. Furthermore, expression of either K5 or Vpu, but not K5delRING, could rescue the tetherin mediated defect in virus release (Figure 3D and E). Measurement of gag levels in supernatants and extracts of infected cells by western blot indicated that the effects of

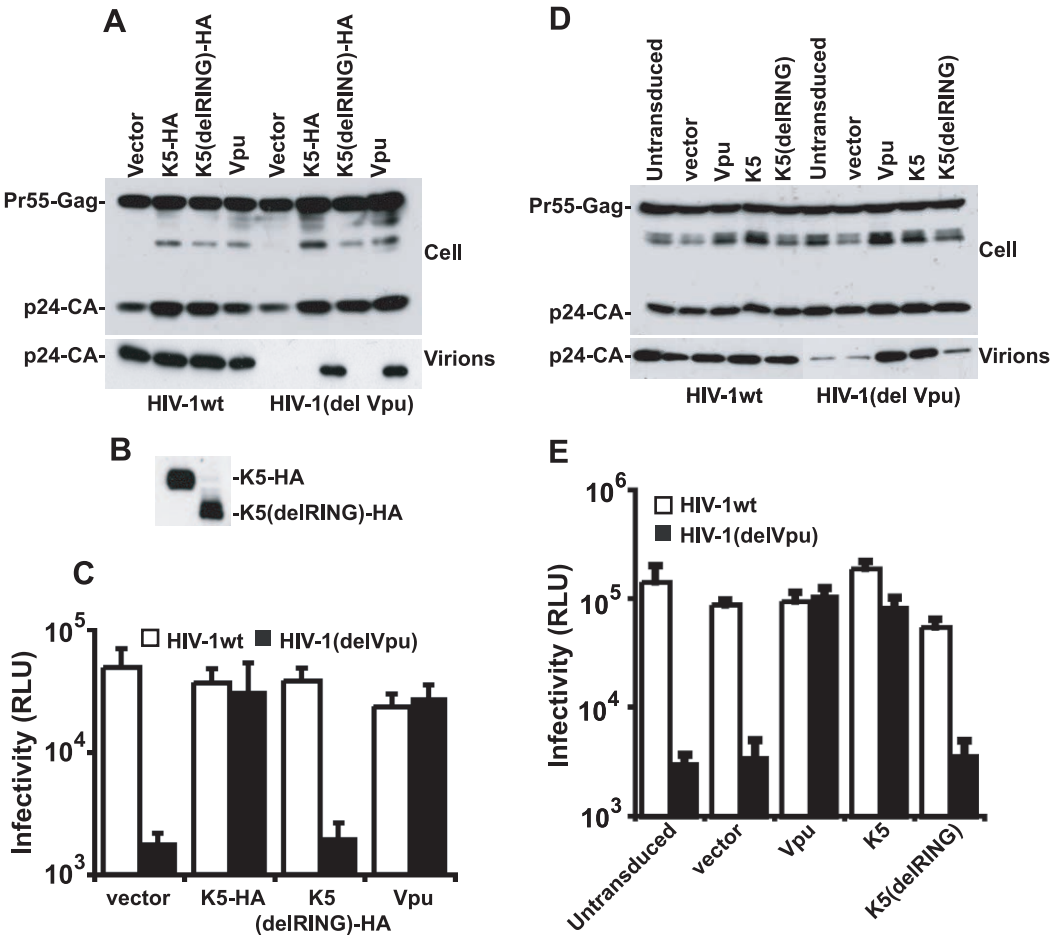

Figure 3. K5 rescues Vpu-defective HIV-1 particle release from tetherin mediated restriction. (**A, B and C**) HeLa cells were co-transfected with HIV-1wt or HIV-1(del Vpu) proviral plasmids in combination with empty vector, or expression vector encoding Vpu, HA-tagged K5 or K5 lacking the N-terminal RING domain. 48h post-transfection cell lysates and pelleted supernatants were analysed for HIV-1 Gag proteins by western blot using an anti-p24CA monoclonal antibody (**A**) or an anti-HA monoclonal (**B**). Viral supernatants were also used to infect HeLa-TZM indicator cells and infectious viral release determined by relative beta-galactosidase activity 48h later (**C**). (**D and E**) HT1080 cells stably expressing human tetherin (HT1080/THN-HA) were transduced with retroviral vectors encoding both dsRED and either Vpu, K5 or K5(del RING) at doses sufficient to give >90% transduction as determined by flow cytometry. Cells were then infected with HIV-1wt or HIV-1(del Vpu) pseudotyped with VSV-G at an MOI of 0.2. Cell lysates and supernatants were processed as in (**A**) 48h later.
doi:10.1371/journal.ppat.1000843.g003

tetherin, Vpu and K5 were on HIV-1 release and not gag protein expression. Intriguingly, K5 could not antagonize tetherin function in transiently-transfected 293T cells, even when tetherin expression was titrated to vary its expression level (Figure S1). We propose that 293T cells lack a co-factor essential for K5's antagonism of tetherin, but not for Vpu function. Interestingly, 293T cells are also unable to support HIV-2 Env's anti-tetherin activity [32], suggesting that this particular cell line might be poorly suited for characterization of some tetherin antagonists.

Species-specific down-regulation of cell surface tetherin by K5

Vpu has been shown to remove tetherin from the cell surface after transfection [6] and in HIV-1-infected cells [32]. We therefore tested whether K5 expression had the same effect on surface tetherin levels in HT/THN-HA cells by expressing K5 via retroviral transduction. Both K5 (Figure 4A) and HIV-1 Vpu (Figure S2) expression led to a marked reduction of tetherin from the cell surface. Importantly, the K5delRING protein was inactive in this assay as predicted by data in Figure 3. HIV-1 Vpu-mediated tetherin antagonism displays distinct species specificity for primate tetherin genes with non-human primate orthologues being largely insensitive to HIV-1 Vpu [18,19,33]. Sensitivity to HIV-1 Vpu maps to the tetherin transmembrane domain and mutation of the T residue at position 45 to the I present in Rhesus macaques (T45I) coupled with an in frame deletion of a GI pair at the N-terminus of the human tetherin protein's TM (delGI-T45I) results in a human tetherin that is completely resistant to HIV-1 Vpu [18] (Figure S2). We therefore examined whether K5 also displays similar species–specific effects (Figure 4B). Unlike HIV-1 Vpu, K5 was able to down-regulate the THN(delGI-T45I) mutant human tetherin. However, K5 was unable to down-regulate the rhesus macaque tetherin protein. Thus K5 also displays species-specificity in its antagonism of primate tetherins but the determinants of this specificity are distinct from those of HIV-1 Vpu.

We then examined whether K5 could also down regulate human tetherin from the surface of a B cell line carrying KSHV (Figures 4C and D). Body-cavity-based lymphoma (BCBL) 1 cells were transduced with a lentiviral vector encoding K5 or with an empty vector and surface tetherin expression assessed by flow cytometry analysis, using a specific antibody against human tetherin. K5 expression led to a reduction of cell surface tetherin as compared to the levels on cells treated with the empty vector or levels detected on un-transduced cells (Figure 4C). The mean of mean fluorescence intensity (MFI) values for 3 representative experiments are also shown (Figure 4D).

K5 induces ubiquitin-dependent endolysozomal degradation of tetherin

We next examined the fate of tetherin in K5-expressing cells. HT/THN-HA cells were transduced to stably express K5 or Vpu and intracellular levels of tetherin were compared to levels in unmanipulated cells. Tetherin appears in western blots as a heterogeneous smear of glycosylated species that varies between cell types [10,17]. After K5 and Vpu expression, tetherin levels in the modified cell lysates were decreased (to 4% of wildtype in the case of K5 and to 31% of wildtype for Vpu), suggesting that, like Vpu, K5 induces tetherin degradation (Figure 5A). At present it is unclear whether Vpu induces tetherin degradation via a proteasomal-dependent [19,34,35] or lysozomal pathway [36,37]. This is further complicated by the fact that endolysozomal degradative pathways are often also dependent on ubiquitin, and thus proteasomal inhibition can inhibit them through depletion of free cytoplasmic ubiquitin levels. We addressed the K5 mechanism of action by examining the role of lysozomal degradation using the vacuolar ATPase inhibitor bafilomycin A1 or by inhibiting proteasomal degradation using MG132. We then measured steady state levels of tetherin in K5 or Vpu expressing cells. A 16h treatment with BafA1 or MG132 substantially rescued tetherin levels from both Vpu and K5 expression. BafA1 treatment rescued not only mature tetherin species, but also lower molecular weight fragments that are likely to be partially degraded tetherin molecules. This suggested that K5 degrades tetherin via an endolysozomal process, similar to that by which it degrades Class I MHC [38]. The rescue of tetherin degradation products in HT/THN-HA cells that do not express HIV-1 Vpu or K5 suggested that endosomal processing of tetherin contributes to its natural turnover. In contrast, whilst MG132 treatment also rescued partially tetherin levels in HT/THN-HA-K5 cells, mature species were predominant. In Vpu-expressing cells MG132 appeared more potent for tetherin rescue than BafA1, and again differential tetherin species were rescued by each inhibitor. Together, these data suggest that while tetherin degradation by K5 and Vpu are sensitive to both classes of inhibitor, the stages of degradation that are affected are different.

Next we determined whether we could observe differences in the cellular localization of tetherin induced by K5 or Vpu. In HT/THN-HA cells, tetherin localized predominantly to the plasma membrane with a small amount of the intracellular localizations coincident with the late endosomal marker CD63 (Figure 5B) This is consistent with the notion of natural tetherin turnover in endolysozomal compartments. In K5 expressing cells, while tetherin levels are markedly reduced, remaining tetherin was much more often found associated with CD63+ late endosomes than in controls (Figure 5B), implicating K5-induced endosomal degradation. In contrast, in Vpu-expressing cells, tetherin was never observed in CD63+ endosomes, but instead localized predominantly to compartments that stain positive for the Trans-Golgi marker TGN46 (Figure 5B and C). This localization is similar to that observed after expression of the HIV-2 and SIVtan envelope glycoproteins [32,39]. Thus, the subcellular localization of tetherin after K5 expression suggests that K5 causes it to be delivered to late endosomes for degradation. Importantly, this distinguishes K5 and Vpu-induced tetherin antagonism and implies distinct mechanisms.

Since the RING domain of K5 is required for tetherin down-regulation from the cell surface, and degradation is sensitive to the drug MG132, which also causes ubiquitin depletion, we hypothesized that K5 mediated ubiquitination might drive tetherin delivery to late endosomes. We therefore examined whether proteasomal or lysozomal inhibition could rescue cell-surface tetherin levels (Figure 5D). We found that whilst endosomal inhibition with BafA1 treatment rescued tetherin protein in the cell extracts of K5 expressing cells (Figure 5A) neither BafA1 or concanamycin A could rescue tetherin levels at the cell surface (Figure 5D). However, consistent with a role for ubiquitination in the delivery of tetherin for endosomal degradation, MG132 treatment of tetherin-expressing cells did substantially rescue tetherin levels at the surface of K5-expressing cells (Figure 5D and E). In contrast, none of the inhibitors significantly rescued tetherin surface expression in Vpu-expressing cells. These observations demonstrate that K5-induces an endosomal degradation of tetherin and suggest that an ubiquitin dependent process is required for its delivery into this pathway. Conversely, HIV-1 Vpu causes tetherin degradation by a distinct mechanism that is associated with its localization to the TGN (Figure 5B–C).

Next we asked whether the double-tyrosine based endocytic motif in the tetherin cytoplasmic tail was required for K5-

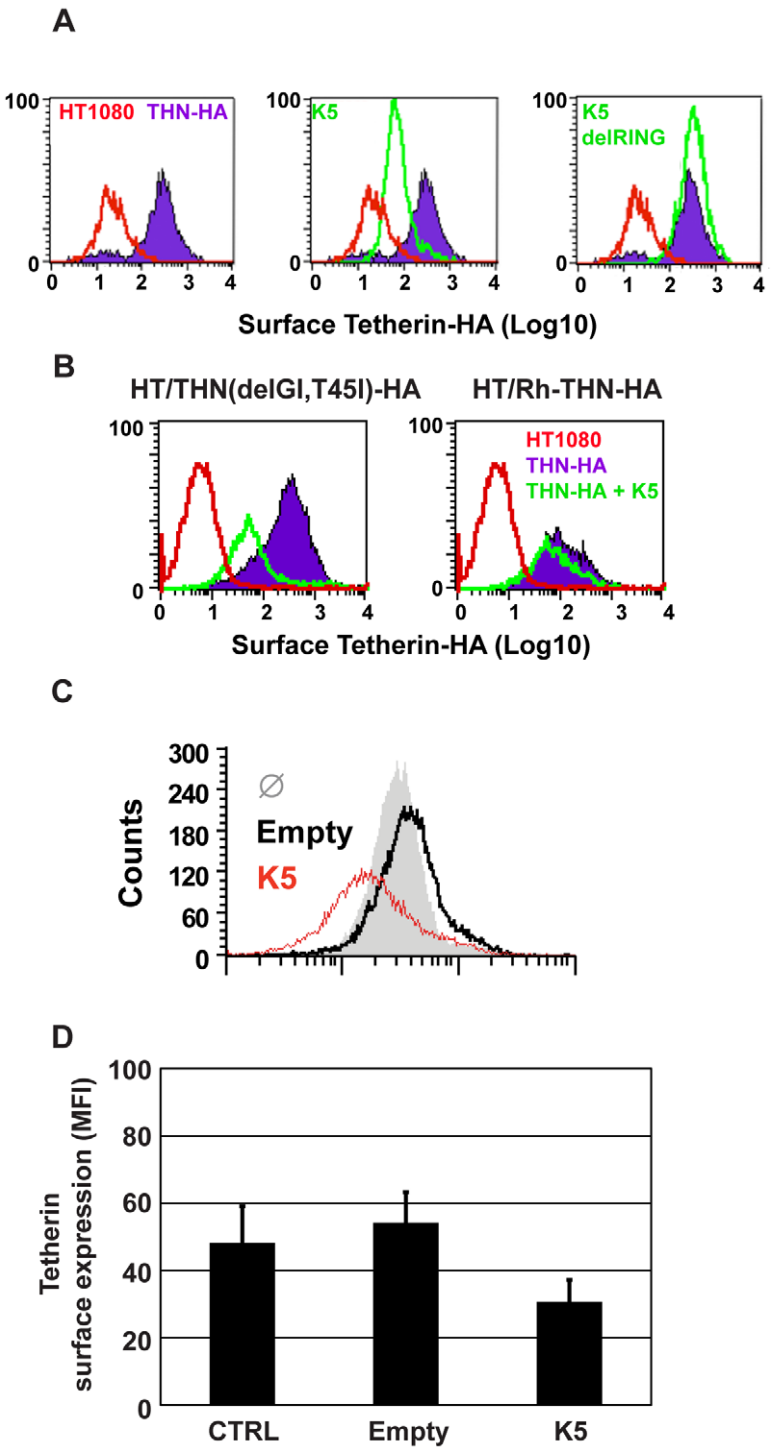

Figure 4. K5 mediates cell-surface down-regulation tetherin. (**A**) HT1080/THN-HA cells were transduced with retroviral vectors encoding dsRED and either K5 or K5(del RING). 48h post-transduction the cells were immunostained for surface tetherin using an anti-HA monoclonal antibody and an Alexa-488-conjugated goat-anti-mouse secondary antibody. Surface expression of tetherin was then analyzed in the dsRED positive population by flow cytometry. Parental HT1080 cells were used as a control for background antibody binding and are represented by the red line. Tetherin levels in HT1080 cells expressing tetherin alone are indicated by the purple line and levels of tetherin after K5 expression is represented by the green line. (**B**) The same analyses were performed on HT1080 cells expressing the HA-tagged Vpu-resistant human tetherin (delGI,T45I) and rhesus tetherin. Labeling is similar to panel A. (**C**) BCBL1 were transduced with a lentiviral vector expressing K5 (red line), an empty vector (black line), or left untreated (grey peak), and cell surface expression of tetherin detected by flow cytometry 48 hours later as described above. (**D**) Mean fluorescence intensity (MFI) values from (**C**) are also shown.
doi:10.1371/journal.ppat.1000843.g004

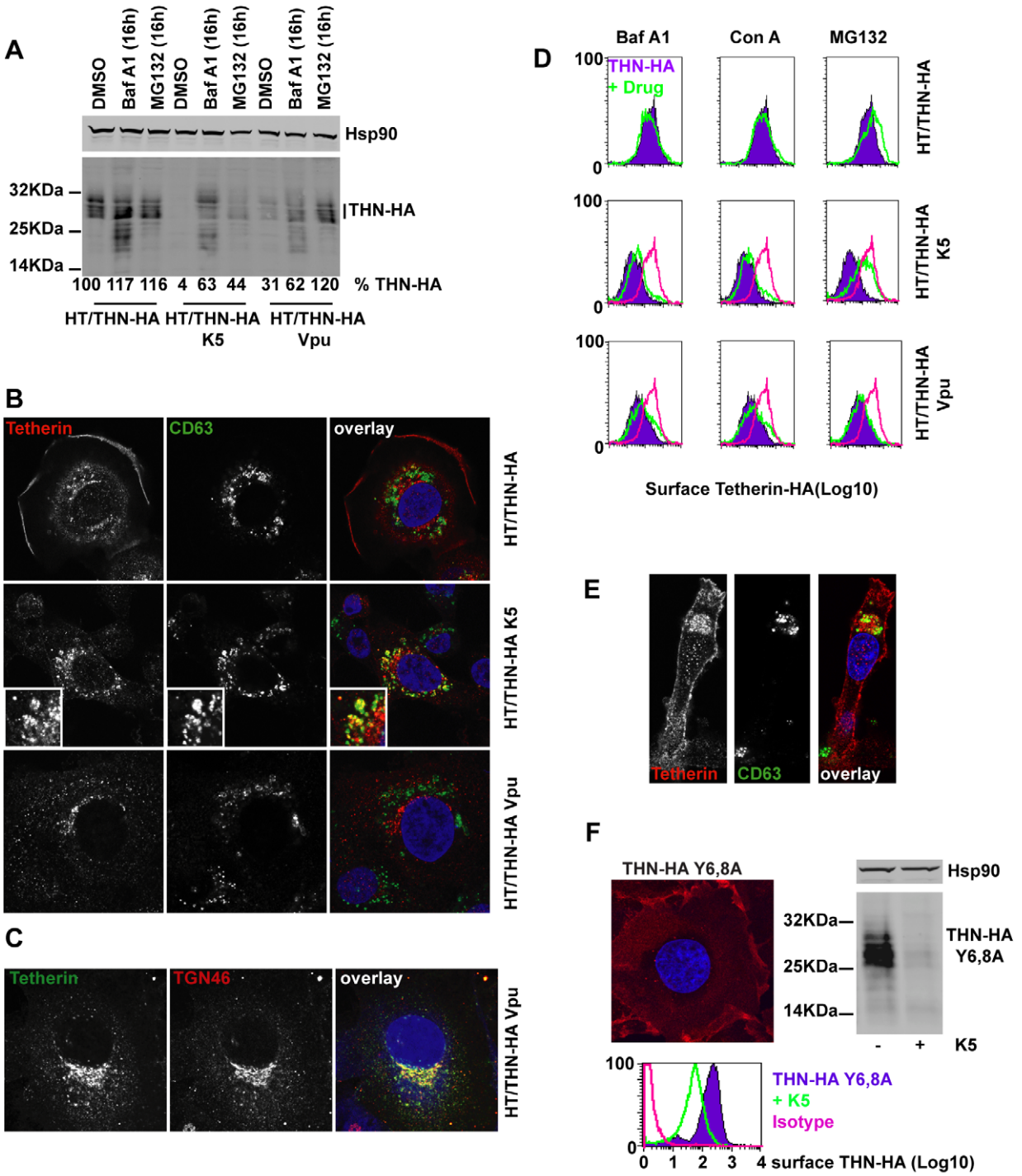

Figure 5. Effects of proteasomal and endosomal inhibitors on tetherin levels and localization in cells expressing K5 and Vpu. (**A**) Western blots of cell lysates from HT/THN-HA cells and isogenic pools stably expressing K5 or Vpu from retroviral vectors. Cells were treated for 16h with BafA1 (100nM), MG132 (1μg/ml) or DMSO as a control, lysed and separated by SDS-PAGE. THN-HA was detected by anti-HA polyclonal antibody, with Hsp90 serving as a loading control and visualized using Licor fluorescently coupled 650 and 800 nm secondary antibodies. Percent mature tetherin levels, normalized to Hsp90 loading are displayed below each lane. (**B**) Representative examples of HT/THN, HT/THN-HA K5 and HT/THN-HA Vpu cells immunostained for tetherin with a rabbit anti-HA antibody (red) and an antibody for the late endosomal marker CD63 (green). Nuclei were counterstained with DAPI (blue) and cells examined by confocal microscopy. (**C**) HT/THN-HA Vpu cells stained for THN-HA (green) and the trans-Golgi marker TGN46 (red) were processed as above. (**D**) Cells from A were surface stained for tetherin levels and analyzed by flow cytometry. Purple histograms represent tetherin levels on DMSO treated cells. Green overlays indicate tetherin levels after treatment with the indicated drug. The pink histogram overlays show the levels of tetherin on untreated HT/THN-HA from the upper row for comparison. (**E**) Confocal image of a representative HT/THN-HA K5 cell treated with MG132 and stained for THN-Ha (red) and CD63 (green). (**F**) HT/THN-HA Y6,8A were imaged by confocal microscopy for tetherin (red). The cells were then manipulated to express K5 and analyzed by flow cytometry for surface tetherin and by western blot for total cellular tetherin levels.

doi:10.1371/journal.ppat.1000843.g005

mediated degradation. This motif binds the clathrin adaptors AP1 and AP2 and has been reported to be important for tetherin endocytosis and recycling [40]. HT1080 cells expressing THN-HA Y6,8A were generated and tetherin localization determined by immunofluorescence microscopy. As expected this mutant tetherin was found almost exclusively at the plasma membrane (Figure 5F). Interestingly, expression of K5 in these cells still led to significant tetherin down-regulation and degradation (Figure 5F) as demonstrated by flow cytometry and western blot. Thus tetherin trafficking to late endosomes induced by K5 is independent of its endocytic motif, suggesting that K5 targets tetherin for degradation via a pathway that is independent from its normal subcellular trafficking.

Delivery to late endosomes and antagonism of antiviral activity by K5 is dependent on a single lysine residue in the tetherin cytoplasmic tail

K5 targeting of class I MHC molecules depends on membrane proximal lysine residues in their cytoplasmic tails [20]. Tetherin also has two membrane proximal lysines, K18 and K21. To seek a role for these residues we mutated them to arginine, singly or in combination, in THN/HA and stably expressed these mutant tetherins in HT1080 cells. We then stained the cell surface tetherin via the HA tag and measured cell surface tetherin levels by flow cytometry (Figure 6A). All tetherins were expressed at the cell surface, but the lysine mutants were expressed at enhanced levels as compared to the wild-type protein. This suggested that these two lysines might be involved in natural tetherin turnover. When K5 was expressed in the mutant tetherin cell lines, tetherin down-regulation was almost completely prevented for proteins bearing a K18R substitution. In contrast, K21R mutation had no effect on K5-induced cell surface down-regulation. Furthermore, K21R but not K18R or K18,21R mutants were consistently redistributed to CD63+ compartments upon K5 expression (Figure 6B). We then further examined whether K5 retained the ability to disrupt tetherin function in the absence of cell-surface tetherin down-regulation, as has been suggested for Vpu [17]. HT/THN-HA and HT/THN-HA K18R cells expressing either K5 or Vpu were infected with HIV-1wt and HIV-1(delVpu) VSV-G pseudotyped

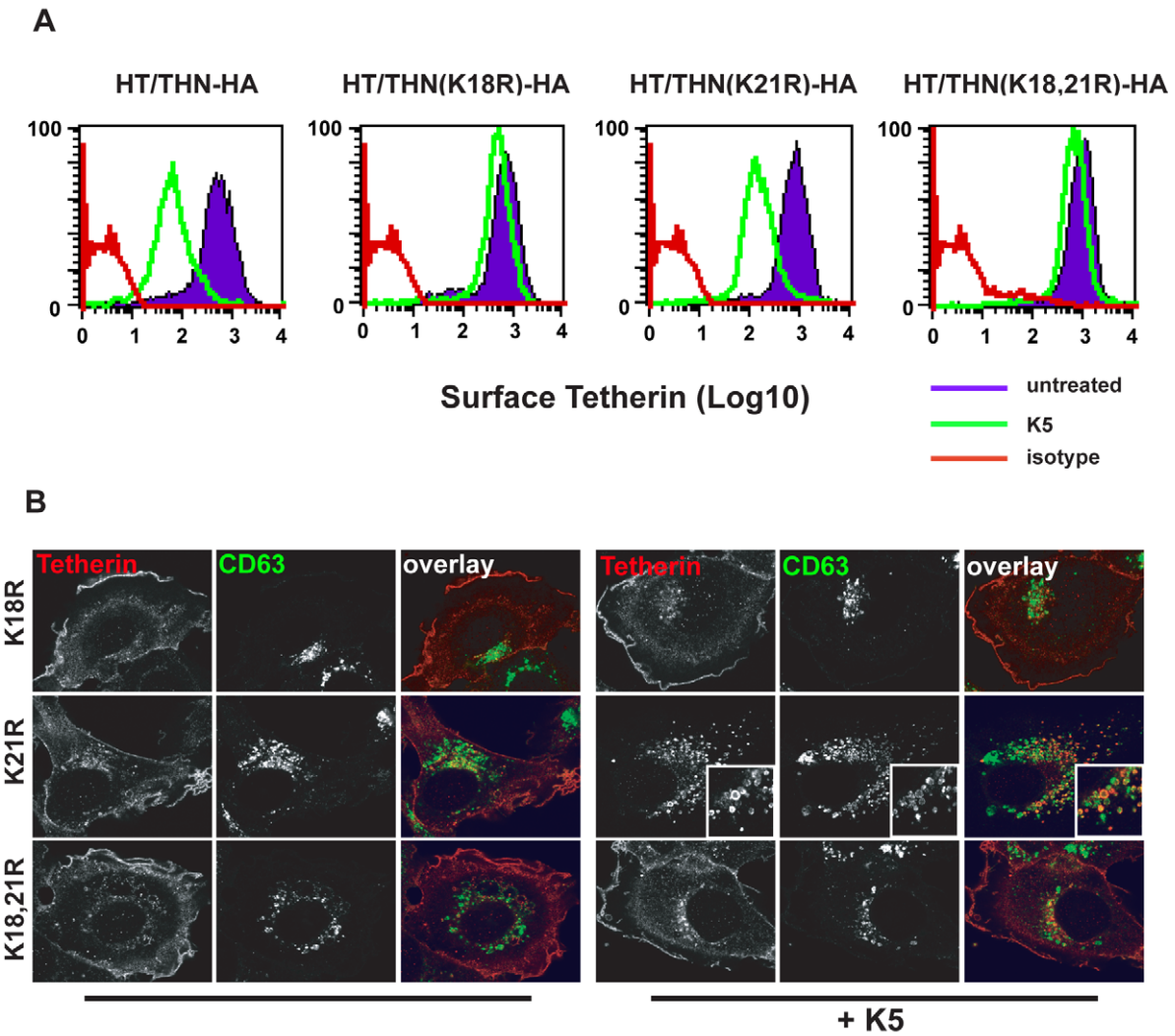

Figure 6. K18 in the tetherin cytoplasmic tail is required for K5-mediated cell surface down-regulation and delivery to endosomes. (**A**) Flow cytometry analyses of HT1080 cells expressing wild type tetherin or the indicated mutant. Purple histograms represent THN-HA levels on unmanipulated cells, with the green overlay showing tetherin levels in the equivalent cells stably expressing K5. Red histograms represent the antibody isotype control. (**B**) Representative examples the cells from (**A**) were stained for THN-HA (red) and CD63 (green) and examined by confocal microscopy.
doi:10.1371/journal.ppat.1000843.g006

viruses at an MOI of 0.2. Supernatants were collected 48h later and infectious virus output was measured on HeLa-TZM cells. THN-HA K18R expressing cells restricted Vpu-defective HIV-1 release similarly to the wild type protein, however expression of K5 failed to rescue the release of HIV-1(delVpu) from HT/THN-HA-K18R cells (Figure 7A). By contrast Vpu-mediated antagonism of tetherin was unaffected by mutation of K18 in HT1080 cells (Figure 7A) or indeed either of the lysine residues in 293T cells (Figure 7B). Thus, removal of tetherin from the cell surface and delivery to late endosomes is required for K5-mediated antagonism of its antiviral action and this is dependent on the lysine at position 18. Measurement of gag levels in cell extracts and supernatants by western blot demonstrated that tetherin expression did not impact on gag expression (Figure 7C). Measurement

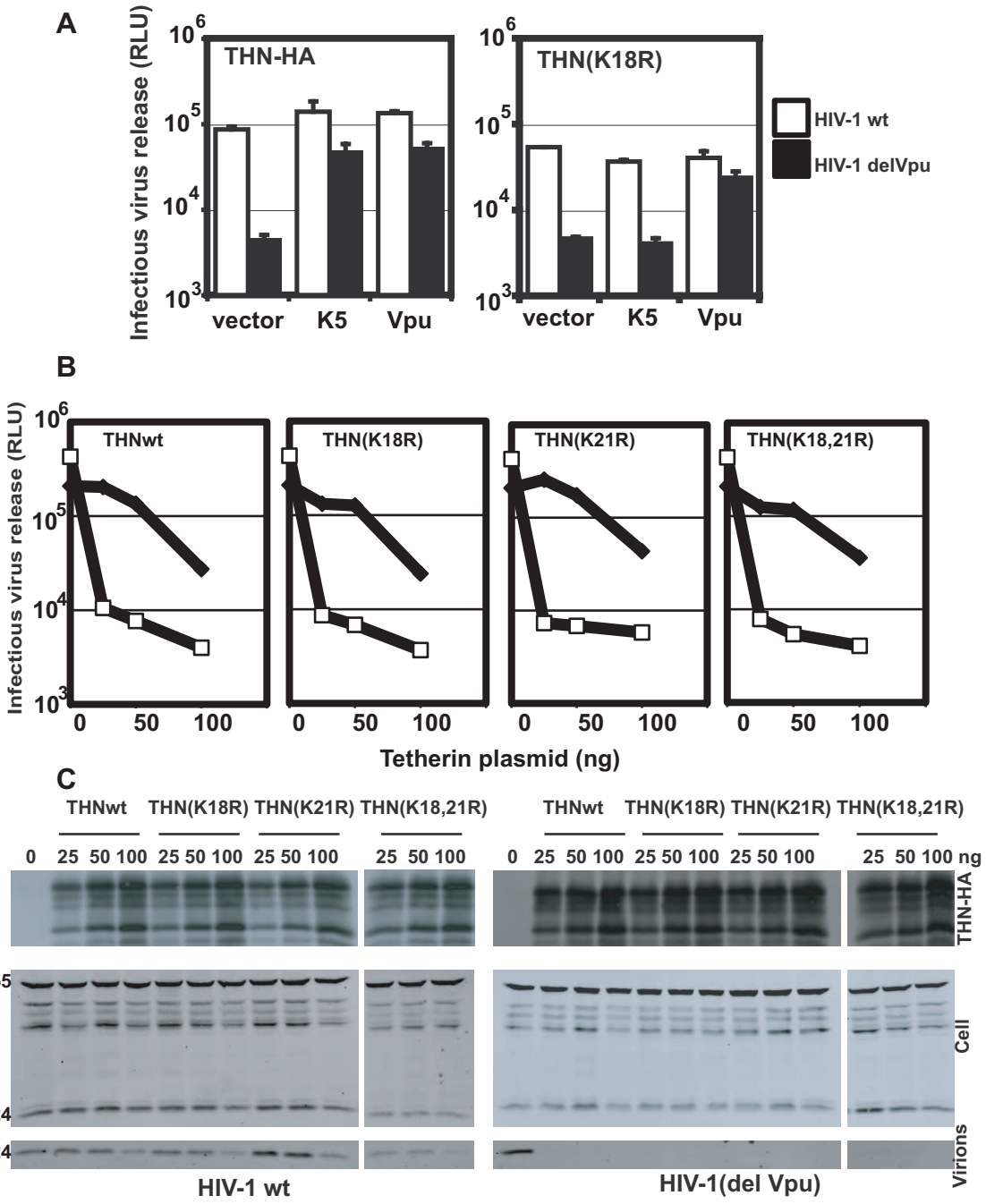

Figure 7. K18 is required for tetherin antagonism by K5 but both cytoplasmic tail lysines are dispensable for Vpu-mediated antagonism. (**A**) HT/THN-HA and HT/THN-HA(K18R) or derivatives stably expressing K5 or Vpu were infected with wild type HIV-1 or HIV-1(delVpu) VSV-G pseudotypes at an MOI of 0.2. 48h after infection cell supernatants were harvested and the released infectivity determined on HeLa-TZM cells. (**B and C**) The effect of tetherin lysine mutants on HIV-1 release in 293T cells. Cells were transiently transfected with wild type HIV-1 or HIV-1(delVpu) proviruses with increasing doses of the indicated THN-HA mutant. 48h after transfection viral supernatants were assayed for infectivity on HeLa-TZM cells (**B**) and cell lysates and pelleted virions analyzed by western blot for HIV-1 p24 CA and THN-HA expression (**C**).
doi:10.1371/journal.ppat.1000843.g007

of tetherin levels ensured that tetherin was expressed as expected (Figure 7C).

Since lysine residues serve as targets for ubiquitination we next sought evidence for tetherin ubiquitination in the presence of K5. HeLa cells were transfected with THN-HA or THN-HA K18, 21R in the presence of an ubiquitin bearing a 6-histidine tag. The cells were treated for 8h with BafA1 to block tetherin degradation and ubiquitinated proteins were isolated by incubating whole cell lysates with nickel-agarose beads. In the presence of either co-transfected K5 or Vpu, THN-HA molecules could be isolated from the transfected cells (Figure 8). The tetherin predominantly formed a single species at a size suggestive of mono-ubiquitination. Interestingly, we failed to pull down ubiquitinated tetherin molecules when their cytoplasmic lysine residues had been mutated, after either K5 or Vpu transfection. This implies that the action of both K5 and Vpu leads to ubiquitination of the tetherin cytoplasmic tail. In the case of K5, this suggests that ubiquitination of K18 antagonizes tetherin-mediated restriction and directs it to endosomal compartments for degradation. Intriguingly, mutating the lysine residues does not make tetherin insensitive to Vpu suggesting that tetherin becomes ubiquitinated as a consequence of tetherin antagonism by HIV-1 Vpu but that this ubiquitination is not required for the antagonistic process.

K5-mediated down-regulation of tetherin is sensitive to inhibition of the ESCRT pathway

There are several ubiquitin-dependent mechanisms by which K5 might achieve tetherin degradation. For example, ubiquitination of tetherin's cytoplasmic tail could stimulate its internalization and mediate classical recruitment of the ESCRT pathway through engagement of TSG101, as has been shown for K3 targeting of MHC I [41]. This would lead to the budding of tetherin containing vesicles into the lumen of multivesicular bodies for degradation in lysozomes [42]. To examine the role of the ESCRT pathway in K5-mediated tetherin degradation, we tested whether K5-mediated loss of tetherin from the cell surface was sensitive to expression of a dominant negative form of VPS4. VPS4 is the essential AAA-ATPase that provides the energy for ESCRT disassembly and recycling during the final membrane scission event in the sorting of cell surface receptors for endosomal degradation [43]. Co-transfection of HeLa cells with GFP-dnVPS4(E228Q) [44] substantially rescued cell surface tetherin levels from K5 as assessed by flow-cytometry (Figure 9A and B). Expression of K5delRING has no effect on THN cell surface expression, concordant with Figure 4, and neither does the dominant negative VPS4 protein when expressed with the tetherin RING mutant. Together with the demonstration that K5 leads to tetherin ubiquitination and degradation, these observations strongly suggest that K5 induces a VPS4 and ubiquitination-dependent trafficking of tetherin from the cell surface to late endosomes for destruction. Importantly, this mechanism is similar to that used by K3 to down-regulate Class I MHC molecules [38,41].

Discussion

Tetherin has emerged as a potent inhibitor of enveloped virus release [5,6,9,12,13]. Recent evidence has demonstrated that tetherin dimers act as a physical linkage between the membranes of the infected cell and nascent virions [10]. This mechanism lends itself well to a general non-specific antiviral inhibition that restricts virus release and thereby interferes with viral spread to new target cells. It also suggests that mammalian viruses may not be able to easily mutate to avoid tetherin because tetherin does not directly interact with any viral structural proteins. Sensitive viruses must therefore evolve specific ways of counteracting it. In the case of primate lentiviruses, several tetherin antagonists have now been identified. The Vpu accessory protein antagonizes tetherin in HIV-1 infected cells [5,6], whereas in a variety of SIVs that do not encode a Vpu gene, the Nef protein can overcome the tetherin orthologues from their host species [33,45]. Interestingly, HIV-2 [32] and at least one strain of SIV [39] have acquired the ability to

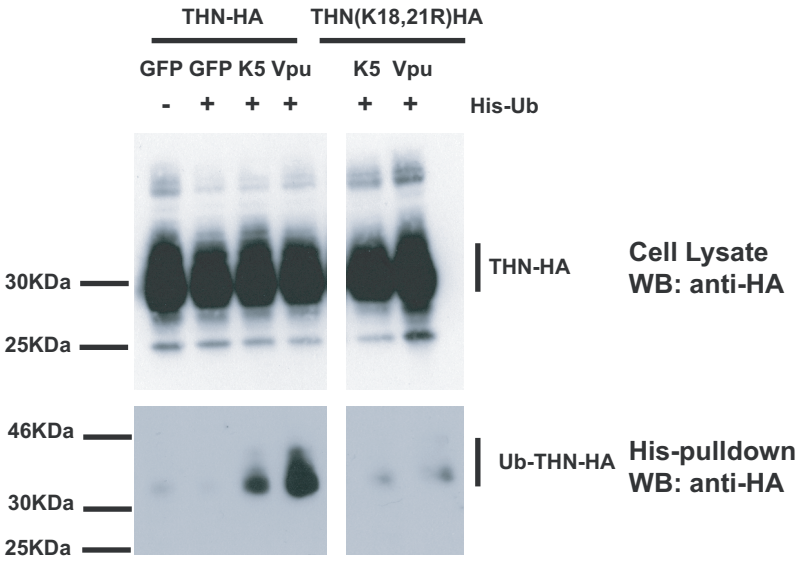

Figure 8. Tetherin cytoplasmic tail lysine residues are ubiquitinated in the presence of K5 and Vpu. HeLa cells were transiently transfected with the indicated THN-HA expression vector in combination with K5, Vpu or GFP and in the presence or absence of 6His-tagged ubiquitin. 48h after transfection, cells were treated for 8 hours with BafA1 (100nM) to prevent tetherin degradation. Cell lysates were then harvested and ubiquitinated proteins were isolated by binding to Ni-Nti-agarose. Cell lysates and pull-downs were analyzed by western blot for THN-HA detecting the HA tag.
doi:10.1371/journal.ppat.1000843.g008

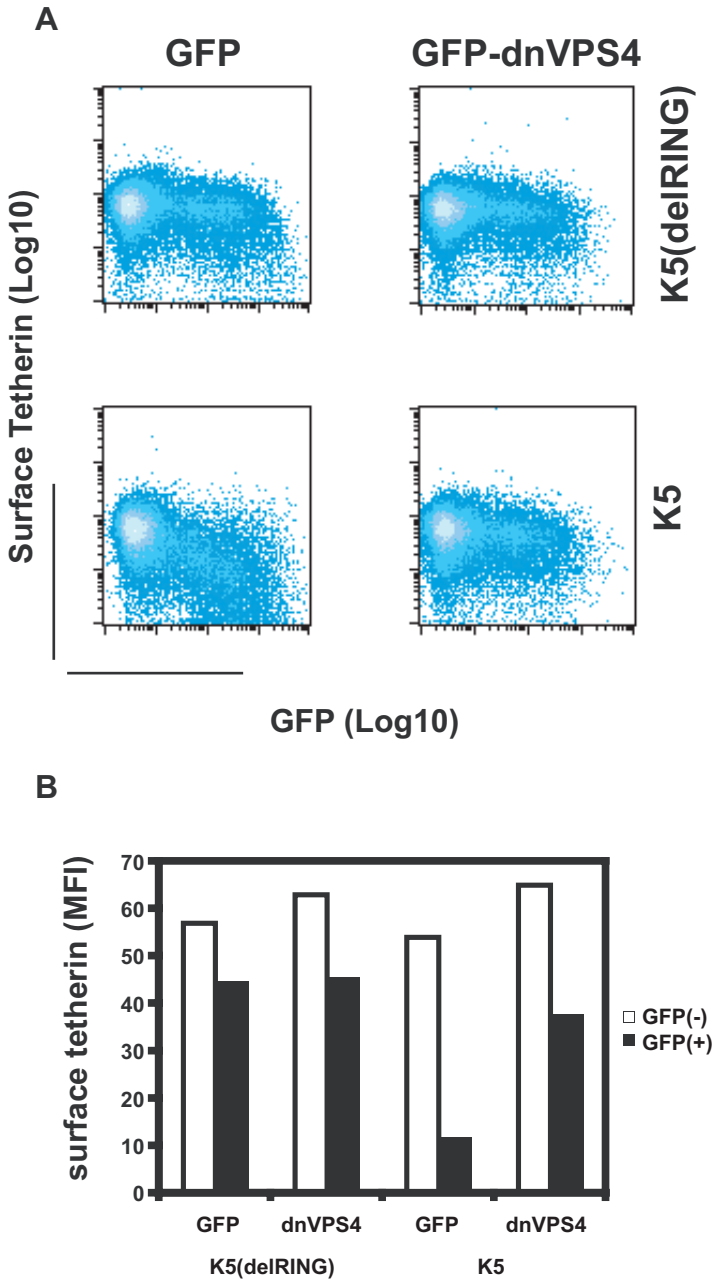

Figure 9. Cell-surface down-regulation of tetherin by K5 is inhibited by dominant-negative VPS4. (**A**) HeLa cells were transfected with wild type K5 or K5(del RING) expression vectors in combination with either GFP or a dominant negative mutant of VPS4 fused to GFP (VPS4 E228Q). 24h later cells were stained for cell surface tetherin using anti-BST2 monoclonal antibody and a goat-anti-mouse Alexa633 secondary antibody. Flow cytometry dot plots are shown. (**B**) The mean florescent intensities (MFI) of surface tetherin expression in GFP positive and GFP negative populations from the samples in panel A are plotted.
doi:10.1371/journal.ppat.1000843.g009

antagonize tetherin with their envelope glycoproteins. Outside the *Retroviridae*, the ebolavirus glycoprotein has anti-tetherin activity [13] and here we propose that human herpesvirus KSHV antagonizes tetherin with K5.

While this study was in revision, a study from Mansouri and colleagues showed that tetherin could be degraded by K5 in an ubiquitin-dependent manner [46]. Our data demonstrate that K5 can fully substitute for Vpu in mediating the efficient release of HIV-1 particles from tetherin-expressing cells. This requires the K5 RING domain and leads to a cell-surface down-regulation of tetherin followed by its degradation in endosomal compartments. Down-regulation of tetherin by K5 and its targeting to endosomes requires the membrane proximal lysine residue K18 in the cytoplasmic tail, and this process is sensitive to inhibition of the proteasome with MG132. Since K5-induced ubiquitination of tetherin is dependent on its cytoplasmic tail lysines, the effects of proteasomal inhibition are likely to be due to depletion of cytoplasmic ubiquitin levels, rather than blocking proteasomal degradation of tetherin. Furthermore, K5-mediated tetherin degradation requires a functional ESCRT pathway as shown by the rescue of surface tetherin levels after expression of a dominant negative VPS4 protein. These observations suggest that

K5 targets tetherin by inducing an ubiquitin-dependent sorting of tetherin to multivesicular bodies where it is destroyed in a lysozomal compartment, a similar mechanism to that of K3-mediated degradation of Class I MHC molecules [41]. K3 targets MHCI for ESCRT-dependent sorting and destruction via addition of a single ubiquitin moiety to the molecule's cytoplasmic tail through recruitment of the E2 enzymes UbcH5B and/or C [38]. Lysine-63 poly-ubiquitination is then induced through the subsequent recruitment of Ubc13 [38]. While we cannot rule out that K5 induces poly-ubiquitination of tetherin, we were only able to observe species consistent with mono-ubiquitination. Thus, while K5 induces ESCRT-dependent tetherin degradation, the precise molecular details of the endosomal targeting may differ between K3 and K5 targets. Whether endocytosis of tetherin is stimulated by K5, or whether it is routed to endosomes from the Golgi, bypassing the cell surface remains an interesting question. Our observation that surface down-regulation of tetherin is independent of its tyrosine-based endocytic-sorting signal [40] suggests the latter. Since K5 localizes mainly to the ER [47], tetherin ubiquitination could happen very early after synthesis leading to endosomal routing independently of the cell surface. Similarly, Mansouri and colleagues suggested that in K5-expressing cells, little tetherin reaches the PM, based on surface biotinylation experiments [46]. However, neither of these results is unambiguous, especially if cell surface turnover is fast. Further studies of the molecular details of K5 mechanism are required to fully dissect its effects on tetherin trafficking.

An important aspect of our study is the comparative analysis of the mechanisms by which Vpu and K5 achieve tetherin antagonism. Both proteins lead to cell surface down-regulation and degradation of tetherin but the mechanism of Vpu remains unclear. Several studies have shown that tetherin degradation is blocked by proteasomal inhibition [19,34,35], whereas others suggest endosomal degradation [36,37]. It is clear that whilst Vpu-mutants that cannot interact with βTRCP2 cannot mediate tetherin degradation [36,37], they can nonetheless antagonize tetherin and rescue viral release [17]. Thus, the SCF-Skp1-cullin 1 ubiquitin ligase complex and perhaps an ER-associated degradative pathway are implicated in tetherin degradation and this process presumably follows tetherin antagonism at the cell surface [35,36]. Tetherin down-regulation and degradation might therefore not be as strictly linked during Vpu-mediated antagonism as it is during K5 mediated antagonism of tetherin. Furthermore, proteasomal inhibition appeared to be more potent than endosomal inhibition in rescuing cellular levels of tetherin in Vpu-expressing cells. Unlike K5, we saw no evidence of tetherin redistribution to endosomes in response to Vpu. Rather, residual tetherin can be seen in the TGN, consistent with a recent study suggesting that Vpu localization to the TGN is important for tetherin antagonism [48]. Similarly, proteasomal inhibition does not restore tetherin to the surface of Vpu-expressing cells, and neither does dominant negative VPS4 (not shown). Also consistent with these observations, is our observation that Vpu can induce ubiquitination of tetherin cytoplasmic tail lysine residues, but these are dispensable for Vpu sensitivity. Thus their ubiquitination appears to be a consequence of tetherin antagonism rather than the absolute requirement for K18 demonstrated for K5 sensitivity. In this respect, we suggest tetherin antagonism by Vpu precedes, and may not be dependent on, degradation, but rather results in the sequestration of tetherin away from budding virions, preventing incorporation. Thus there are more parallels with the mechanism by which HIV-2 and SIVtan envelopes antagonize tetherin through sequestration in TGN-associated compartments [32,39]. K5's apparent inability to antagonize tetherin in 293T cells, cells that support Vpu's antagonism of tetherin, suggests that Vpu and K5 may require different cellular cofactors. Clearly, further comparative mechanistic studies will allow us to dissect the differences and similarities in the mode of action of these two very different proteins.

We, and others [46], have also shown that productive KSHV release is restricted by tetherin expression and knockdown of K5 expression imparted a block to virus release. Furthermore, tetherin expression is reduced on B cells after K5 expression. Importantly, this indicates that herpesvirus particle assembly is sensitive to the antiviral effects of tetherin. The mechanism of herpesvirus assembly and envelopment is complex and controversial, most studies have focused on herpes simplex virus type 1 (HSV-1). Immature HSV-1 capsids may bud through nuclear membrane, re-entering the cytoplasm, and then bud again into secretory vesicles [29] via an ESCRT dependent process [49]. Our data suggest that in the case of KSHV, at least one budding stage is through a membrane accessible to tetherin. Tetherin is highly expressed in terminally differentiated B cells and plasma cells, important cellular targets for KSHV [50]. B cell to plasma cell differentiation activates KSHV lytic replication through the activation of XBP-1 and the unfolded protein response [51]. Therefore the virus undergoes productive replication in cells that express high levels of tetherin. This cellular tropism may have provided the selective pressure for K5 evolution to target tetherin. K5 has the ability to modulate the expression of a variety of cell surface molecules involved in immuno-recognition (MHC and NK receptors) and cell adhesion, suggesting targeting of tetherin is part of a wider immuno-evasion strategy by KSHV [52]. Is tetherin antagonism found in other mammalian herpesviruses? B cell expression of tetherin would certainly suggest that this might be the case for Epstein Barr Virus (EBV). Removal of MHC and related molecules is certainly a common feature of several human herpesvirus immune evasion strategies [52,53,54], and it is likely that if other herpesviruses are sensitive to tetherin-mediated restriction, proteins with analogous function to K5 might also target tetherin. MARCH ligase homologues are also found in a variety of poxviruses [20], which also have highly complex envelopment strategies [55].

Aside from the cytoplasmic tail lysine residue K18, we do not yet fully understand the determinants of sensitivity for tetherin's antagonism by K5. Data presented herein show that while K5, like Vpu [18,19], cannot target tetherin from Rhesus macaques, the TM domain positions that determine the difference in Vpu-sensitivity do not confer resistance to K5. Tetherin has been under high levels of positive selection during mammalian evolution, particularly in the cytoplasmic tail and TM domain, areas of the protein likely to be topologically accessible to viral antagonists [18,19]. Several residues in the TM domain are responsible for the species-specific activity of Vpu. However, positive selection in other parts of tetherin may be due to selective pressure exerted by distinct viral countermeasures. We speculate that some mammalian herpesviruses, which show strong co-evolution with their hosts, may have contributed to this evolutionary pressure. Tetherin may therefore represent an extremely interesting case study in the evolution of an antiviral gene under regular assault by unrelated viral pathogens, as has been suggested for PKR [56].

In conclusion, here we have demonstrated that tetherin is capable of restricting a human herpesvirus and show that in the case of KSHV, the virus has co-opted an immuno-modulatory ubiquitin ligase to target this antiviral effector.

Materials and Methods

Plasmids, cells and antibodies

All adherent cells were maintained in Dulbecco's Modified Eagle Medium (DMEM) supplemented with 10% fetal calf serum and antibiotics. BCBL-1 cells were maintained in Roswell Park Memorial Institute (RPMI) medium supplemented with 10% FCS and antibiotics. HeLa, 293T and HT1080 cells were obtained from the ATCC. The HIV-1 indicator cell line, HeLa-TZM, that expresses HIV-1 receptors and an integrated HIV-1-LTR controlling expression of a beta-galactosidase reporter gene were kindly provided by John Kappes and Xiaoyun Wu via the NIH AIDS reagents program. HT1080/THN-HA is a clonal cell line expressing human tetherin with an internal HA tag inserted at nucleotide position 463 [18] expressed from an integrated MLV proviral vector, pLHCX (Clontech). Mutants of tetherin were constructed by standard methods and expressed from pCR3.1 and pLHCX. Vpu, K5 and a K5 mutant lacking amino acids 1–62 encompassing the RING domain (K5delRING) were amplified by PCR and inserted into pCR3.1 with C-terminal HA and mCherry fusion tags and the retroviral vectors pCxCR, which also encodes dsRED express as a marker gene, and pCMS28, a pMigR1 derivative encoding puromycin under control of an Internal Ribosome Entry Site (IRES). The molecular clones of HIV-1 NL4.3 and the Vpu-defective counterpart have been described previously [7]. Anti-HA monoclonal antibody HA1.11 was obtained from Covance, rabbit anti-HA polyclonal was obtained from Rockland and anti-BST2 monoclonal antibody was obtained from Abnova. Secondary Alexa Fluor 488, 594 and 633 antibodies for flow cytometry and microscopy were obtained from Molecular Probes. For quantitative western blotting, Licor 680 and 800nm secondary abs were used and blots scanned using a Licor scanner.

Production of KSHV

HeLa cells infected with KSHV were made by infecting HeLa with rKSHV.219 a recombinant KSHV virus encoding RFP, GFP and puromycin resistance, a gift from Jeff Vieira [30]. Cells were selected and kept under puromycin selection. To induce rKSHV.219 into the lytic cycle, r219-Hela cells were seeded at 3.10^5 cells/well onto 6-well plates and transfected with 1.5 μg of an expression factor for RTA (pCMV-RTA) (a gift from Adrian Whitehouse) using Fugene-6. RFP expression was visible a day after transfection. The transfection mix was removed and replaced with 2 ml of fresh medium. Virus was recovered another 24 hours later, i.e. 48 hours after transfection, and filtered through 0.45 μM device (Millipore) to remove any cellular debris. Infectious virus was measured by titration of supernatants onto 293T cells and total virus by QPCR on DNAse-I resistant genomes. To assay for KSHV release in the presence of tetherin, r219-Hela cells were transfected with pCMV-RTA and increasing doses of tetherin expression vector pCR3.1-THN [5]. Plasmid dose was kept constant using empty vector (pCDNA3.1). To assay for KSHV release under conditions where K5 expression is reduced, r219-Hela cells were seeded at 10^5 cells per well in 6-well plates 24 hours prior to transduction with the lentiviral vectors encoding the K5 specific hairpins, or the empty vector, at a multiplicity of infection (MOI) of 5. 72 hours post-transduction, cells were counted, re-seeded into 6-well plates and transfected with RTA encoding plasmid as above.

Quantitation of KSHV infectious particles by titration onto 293T

293T cells were seeded at 10^5 cells/well in 12-well plates 24 hours prior to titration. For each viral collection 250 μl (a sixth) of the final volume of filtered virus was added to fresh medium to a final volume of 1 ml and used to infect 293T cells. Titrations were performed in duplicate using polybrene (4μg/ml). 12-well plates were subjected to spinoculation at 500 g for 1 hour at RT before being returned to the incubator. Cells were analyzed by flow cytometry 48 hours post-inoculation.

Quantitation of KSHV genomes by Taqman PCR against KSHV early gene ORF37

KSHV genomes were quantified by extracting total DNA (QIAamp, QIAGEN) from DNAse-I treated supernatant (70 units/ml for 2 hours, RQ1 Promega, UK) with 40μg of salmon sperm DNA as a carrier (Sigma, Poole UK). 5μg of purified DNA was subjected to quantitative Taqman PCR for KSHV early gene ORF37 as described [57]. Absolute copy number was determined with reference to a standard curve derived by QPCR against serial dilutions of an ORF37 amplicon encoding plasmid, a gift from David Bibby and Duncan Clark, as described [58].

Quantification of mRNA levels for the late gene ORF37 in r219-HeLa cell lysates by Q-RT-PCR

Total mRNA was extracted from r219-HeLa cells after virus collection, 48 hours post-RTA transfection (RNeasy, QIAGEN). cDNA syntheses were performed on 4 μl of the RNA (SuperScript II Reverse Transcriptase, Invitrogen) according to manufacturer's instructions. cDNAs were treated with 2 units of RNAse H (Invitrogen) for 20 minutes at 37°C before being used in taqman Q-PCR reactions for ORF37 and GAPDH. GAPDH primers were GAPDH forward primer, 5′-GGCTGAGAACGGGAAGCTT-3′; GAPDH reverse primer, 5′-AGGGATCTCGCTCCTGGAA-3′; GAPDH probe, 5′-FAM-TCATCAATGGAAATCCCATCACC-A-TAMRA-3′. Absolute copy number was determined with reference to a standard curve derived by QPCR against serial dilutions of a GAPDH amplicon encoding plasmid. QPCR for ORF37 was performed as described above.

Quantification of the number of episomes per nanogram of total DNA in r219-HeLa cells

Cellular DNA was extracted from r219-HeLa cells after virus collection, 48 hours post-RTA transfection (QIAamp, QIAGEN) and QPCR for ORF37 performed, as described above, on cellular associated episomes. Copy numbers were normalized to quantities of DNA used for each reaction.

Production of retroviral vectors and infectious HIV-1 (VSV-G pseudotypes)

Semi-confluent 293T cells on 6-well dishes were transfected with 1μg of vector plasmid, 1μg of pMLVgag-pol or p8.91 (HIV-1 gag-pol, tat and rev expression vector) and 0.2μg pCMV-VSVG. For full length replication competent HIV-1 (VSV-G) pseudotypes, 293T cells were transfected with 2μg of pNL4.3 or pNL4.3(del Vpu) and 0.2μg of VSV-G. This leads to production of replication competent HIV-1 that has both VSV-G and HIV-1 gp160 envelope proteins on its surface. Virus and vector stocks were harvested 48h post-transfection. Those encoding florescent markers were titrated on HT1080 cells and analyzed by flow cytometry; lentiviral vectors encoding shRNA hairpins were titered by Q-PCR on 293T cells with primers specific for the HIV-1 LTR; and the endpoint titer of full length HIV-1 pseudotypes was determined on HeLa-TZM cells by staining infected foci with X-Gal 48h post-infection.

HIV-1 release assays

Subconfluent HeLa cells were transfected with 500ng of HIV-1 proviral plasmid and 100ng of pCR3.1-Vpu or pCR3.1-K5-HA/K5delRING-HA using lipofectamine 2000 (Invitrogen). Viral supernatants and cell lysates were harvested 48h later. Supernatant virions were filtered and pelleted at 30000g through 20% sucrose/PBS cushion for 90 minutes. Lysates and virions were then separated by SDS-PAGE and HIV-1 Gag proteins detected using an anti-p24 monoclonal antibody CA183 (provided by B Chesboro through the NIH AIDS Reagents repository). In parallel, harvested supernatants were titered onto HeLa-TZM indicator cells and 48 hours later beta-gal activity was determined in cell lysates using a Tropix Beta-galactosidase activity kit (Molecular Probes). For assays involving stable HT1080/THN-HA cell lines, 10^5 cells were plated per well in a 12 well plate and infected with 2×10^4 infectious units (MOI 0.2) of HIV-1 (VSV-G) or HIV-1(del Vpu)(VSV-G) viral stocks. 48h later cell lysates and viral supernatants were treated as above.

Flow cytometry and confocal microscopy

Cell surface staining for tetherin and THN-HA was performed using the appropriate antibodies by standard methods and analyzed on a FACS-Calibur (Becton-Dickinson). Cells for microscopy were grown on glass coverslips and transfected or treated with BafA1 (100nM), concanamycin A (100nM) or MG132 (1μg/ml) (Sigma, UK) for 10h. The cells were then fixed in 4% paraformaldehyde, permeabilized with 0.1% Triton-×100 and stained with the required primary and secondary antibody. Cells were then examined using a Zeiss confocal microscope.

Tetherin ubiquitination assay

HeLa cells seeded on 10cm plates were transiently transfected with the indicated THN-HA expression vector (5ug) in combination with K5, Vpu or GFP (2μg) expression vectors and in the presence or absence of a 6-His-tagged ubiquitin encoding plasmid (2μg). 48h after transfection, cells were treated for 8h with BafA1 (Sigma) to prevent further tetherin degradation. Cells were lysed in 5M guanidinium hydrochloride, sonicated and ubiquitinated proteins were isolated by binding to 50μl of Ni2+ Nti-agarose (Invitrogen) for 3h at room temperature. The beads were eluted with 100mM imidazole. Lysates and pull-downs were then analyzed by western blot for THN-HA.

Supporting Information

Figure S1 K5 does not antagonize tetherin-mediated restriction of HIV-1(del Vpu) in 293T cells. 293T cells were transfected with wild type HIV-1 or HIV-1(del Vpu) proviral plasmids in combination with either Vpu or K5 expression vectors and increasing doses of pCR3.1 THN-HA. 48h later supernatant infectivity was determined on HeLa-TZM cells and is shown plotted against tetherin input.
Found at: doi:10.1371/journal.ppat.1000843.s001 (0.26 MB EPS)

Figure S2 Vpu mediates the surface down-regulation of THN-HA but not THN-HA(delGI-T45I) or Rh-THN-HA in HT1080 cells. Surface expression levels of stably transduced HT1080 cells expressing THN-HA, THN-HA(delGI-T45I) or Rh-THN-HA and Vpu were measured by flow cytometry. The red line represents staining in unmodified HT1080 cells, the purple histogram represents tetherin expression levels in tetherin expressing cells and the green line represents tetherin levels after HIV-1 Vpu expression.
Found at: doi:10.1371/journal.ppat.1000843.s002 (0.29 MB EPS)

Acknowledgments

We thank Jeff Vieira, Adrian Whitehouse, David Bibby, Duncan Clark and Paul Lehner for reagents and Bruce Chesebro, John Kappes and Xiaoyun Wu for reagents via the NIH AIDS reagents program and members of the Towers and Kellam labs, particularly Ed Tsao, for advice.

Author Contributions

Conceived and designed the experiments: RV PK GJT SJDN. Performed the experiments: CP RV SJW SJDN. Analyzed the data: CP RV GJT SJDN. Contributed reagents/materials/analysis tools: RV SJW AC TZ PB PK GJT SJDN. Wrote the paper: CP GJT SJDN.

References

1. Haller O, Kochs G, Weber F (2006) The interferon response circuit: induction and suppression by pathogenic viruses. Virology 344: 119–130.
2. Wolf D, Goff SP (2008) Host restriction factors blocking retroviral replication. Annu Rev Genet 42: 143–163.
3. Neil S, Bieniasz P (2009) Human immunodeficiency virus, restriction factors, and interferon. J Interferon Cytokine Res 29: 569–580.
4. Malim MH, Emerman M (2008) HIV-1 accessory proteins–ensuring viral survival in a hostile environment. Cell Host Microbe 3: 388–398.
5. Neil SJ, Zang T, Bieniasz PD (2008) Tetherin inhibits retrovirus release and is antagonized by HIV-1 Vpu. Nature 451: 425–430.
6. Van Damme N, Goff D, Katsura C, Jorgenson RL, Mitchell R, et al. (2008) The interferon-induced protein BST-2 restricts HIV-1 release and is downregulated from the cell surface by the viral Vpu protein. Cell Host Microbe 3: 245–252.
7. Neil SJ, Eastman SW, Jouvenet N, Bieniasz PD (2006) HIV-1 Vpu promotes release and prevents endocytosis of nascent retrovirus particles from the plasma membrane. PLoS Pathog 2: e39. doi:10.1371/journal.ppat.0020039.
8. Neil SJ, Sandrin V, Sundquist WI, Bieniasz PD (2007) An interferon-alpha-induced tethering mechanism inhibits HIV-1 and Ebola virus particle release but is counteracted by the HIV-1 Vpu protein. Cell Host Microbe 2: 193–203.
9. Jouvenet N, Neil SJ, Zhadina M, Zang T, Kratovac Z, et al. (2009) Broad-spectrum inhibition of retroviral and filoviral particle release by tetherin. J Virol 83: 1837–1844.
10. Perez-Caballero D, Zang T, Ebrahimi A, McNatt MW, Gregory DA, et al. (2009) Tetherin inhibits HIV-1 release by directly tethering virions to cells. Cell 139: 499–511.
11. Kupzig S, Korolchuk V, Rollason R, Sugden A, Wilde A, et al. (2003) Bst-2/HM1.24 is a raft-associated apical membrane protein with an unusual topology. Traffic 4: 694–709.
12. Sakuma T, Noda T, Urata S, Kawaoka Y, Yasuda J (2009) Inhibition of Lassa and Marburg virus production by tetherin. J Virol 83: 2382–2385.
13. Kaletsky RL, Francica JR, Agrawal-Gamse C, Bates P (2009) Tetherin-mediated restriction of filovirus budding is antagonized by the Ebola glycoprotein. Proc Natl Acad Sci U S A 106: 2886–2891.
14. Blasius AL, Giurisato E, Cella M, Schreiber RD, Shaw AS, et al. (2006) Bone marrow stromal cell antigen 2 is a specific marker of type I IFN-producing cells in the naive mouse, but a promiscuous cell surface antigen following IFN stimulation. J Immunol 177: 3260–3265.
15. Kawai S, Azuma Y, Fujii E, Furugaki K, Ozaki S, et al. (2008) Interferon-alpha enhances CD317 expression and the antitumor activity of anti-CD317 monoclonal antibody in renal cell carcinoma xenograft models. Cancer Sci 99: 2461–2466.
16. Ohtomo T, Sugamata Y, Ozaki Y, Ono K, Yoshimura Y, et al. (1999) Molecular cloning and characterization of a surface antigen preferentially overexpressed on multiple myeloma cells. Biochem Biophys Res Commun 258: 583–591.
17. Miyagi E, Andrew AJ, Kao S, Strebel K (2009) Vpu enhances HIV-1 virus release in the absence of Bst-2 cell surface down-modulation and intracellular depletion. Proc Natl Acad Sci U S A 106: 2868–2873.
18. McNatt MW, Zang T, Hatziioannou T, Bartlett M, Fofana IB, et al. (2009) Species-specific activity of HIV-1 Vpu and positive selection of tetherin transmembrane domain variants. PLoS Pathog 5: e1000300. doi:10.1371/journal.ppat.1000300.
19. Gupta RK, Hue S, Schaller T, Verschoor E, Pillay D, et al. (2009) Mutation of a single residue renders human tetherin resistant to HIV-1 Vpu-mediated depletion. PLoS Pathog 5: e1000443. 10.1371/journal.ppat.1000443.
20. Lehner PJ, Hoer S, Dodd R, Duncan LM (2005) Downregulation of cell surface receptors by the K3 family of viral and cellular ubiquitin E3 ligases. Immunol Rev 207: 112–125.
21. Stevenson PG, Efstathiou S, Doherty PC, Lehner PJ (2000) Inhibition of MHC class I-restricted antigen presentation by gamma 2-herpesviruses. Proc Natl Acad Sci U S A 97: 8455–8460.

22. Coscoy L, Ganem D (2000) Kaposi's sarcoma-associated herpesvirus encodes two proteins that block cell surface display of MHC class I chains by enhancing their endocytosis. Proc Natl Acad Sci U S A 97: 8051–8056.
23. Ishido S, Wang C, Lee BS, Cohen GB, Jung JU (2000) Downregulation of major histocompatibility complex class I molecules by Kaposi's sarcoma-associated herpesvirus K3 and K5 proteins. J Virol 74: 5300–5309.
24. Coscoy L, Ganem D (2001) A viral protein that selectively downregulates ICAM-1 and B7-2 and modulates T cell costimulation. J Clin Invest 107: 1599–1606.
25. Mansouri M, Douglas J, Rose PP, Gouveia K, Thomas G, et al. (2006) Kaposi sarcoma herpesvirus K5 removes CD31/PECAM from endothelial cells. Blood 108: 1932–1940.
26. Thomas M, Boname JM, Field S, Nejentsev S, Salio M, et al. (2008) Down-regulation of NKG2D and NKp80 ligands by Kaposi's sarcoma-associated herpesvirus K5 protects against NK cell cytotoxicity. Proc Natl Acad Sci U S A 105: 1656–1661.
27. Li Q, Means R, Lang S, Jung JU (2007) Downregulation of gamma interferon receptor 1 by Kaposi's sarcoma-associated herpesvirus K3 and K5. J Virol 81: 2117–2127.
28. Bartee E, McCormack A, Fruh K (2006) Quantitative membrane proteomics reveals new cellular targets of viral immune modulators. PLoS Pathog 2: e107. doi:10.1371/journal.ppat.0020107.
29. Mettenleiter TC, Klupp BG, Granzow H (2006) Herpesvirus assembly: a tale of two membranes. Curr Opin Microbiol 9: 423–429.
30. Vieira J, O'Hearn PM (2004) Use of the red fluorescent protein as a marker of Kaposi's sarcoma-associated herpesvirus lytic gene expression. Virology 325: 225–240.
31. Ylinen LM, Keckesova Z, Wilson SJ, Ranasinghe S, Towers GJ (2005) Differential restriction of human immunodeficiency virus type 2 and simian immunodeficiency virus SIVmac by TRIM5alpha alleles. J Virol 79: 11580–11587.
32. Le Tortorec A, Neil SJ (2009) Antagonism to and intracellular sequestration of human tetherin by the human immunodeficiency virus type 2 envelope glycoprotein. J Virol 83: 11966–11978.
33. Jia B, Serra-Moreno R, Neidermyer W, Rahmberg A, Mackey J, et al. (2009) Species-specific activity of SIV Nef and HIV-1 Vpu in overcoming restriction by tetherin/BST2. PLoS Pathog 5: e1000429. doi:10.1371/journal.ppat.1000429.
34. Goffinet C, Allespach I, Homann S, Tervo HM, Habermann A, et al. (2009) HIV-1 antagonism of CD317 is species specific and involves Vpu-mediated proteasomal degradation of the restriction factor. Cell Host Microbe 5: 285–297.
35. Mangeat B, Gers-Huber G, Lehmann M, Zufferey M, Luban J, et al. (2009) HIV-1 Vpu neutralizes the antiviral factor Tetherin/BST-2 by binding it and directing its beta-TrCP2-dependent degradation. PLoS Pathog 5: e1000574. doi:10.1371/journal.ppat.1000574.
36. Douglas JL, Viswanathan K, McCarroll MN, Gustin JK, Fruh K, et al. (2009) Vpu directs the degradation of the human immunodeficiency virus restriction factor BST-2/Tetherin via a {beta}TrCP-dependent mechanism. J Virol 83: 7931–7947.
37. Mitchell RS, Katsura C, Skasko MA, Fitzpatrick K, Lau D, et al. (2009) Vpu antagonizes BST-2-mediated restriction of HIV-1 release via beta-TrCP and endo-lysosomal trafficking. PLoS Pathog 5: e1000450. doi:10.1371/journal.ppat.1000450.
38. Duncan LM, Piper S, Dodd RB, Saville MK, Sanderson CM, et al. (2006) Lysine-63-linked ubiquitination is required for endolysosomal degradation of class I molecules. EMBO J 25: 1635–1645.
39. Gupta RK, Mlcochova P, Pelchen-Matthews A, Petit SJ, Mattiuzzo G, et al. (2009) Simian immunodeficiency virus envelope glycoprotein counteracts tetherin/BST-2/CD317 by intracellular sequestration. Proc Natl Acad Sci U S A.
40. Rollason R, Korolchuk V, Hamilton C, Schu P, Banting G (2007) Clathrin-mediated endocytosis of a lipid-raft-associated protein is mediated through a dual tyrosine motif. J Cell Sci 120: 3850–3858.
41. Hewitt EW, Duncan L, Mufti D, Baker J, Stevenson PG, et al. (2002) Ubiquitylation of MHC class I by the K3 viral protein signals internalization and TSG101-dependent degradation. EMBO J 21: 2418–2429.
42. Hurley JH (2008) ESCRT complexes and the biogenesis of multivesicular bodies. Curr Opin Cell Biol 20: 4–11.
43. Wollert T, Wunder C, Lippincott-Schwartz J, Hurley JH (2009) Membrane scission by the ESCRT-III complex. Nature 458: 172–177.
44. Martin-Serrano J, Eastman SW, Chung W, Bieniasz PD (2005) HECT ubiquitin ligases link viral and cellular PPXY motifs to the vacuolar protein-sorting pathway. J Cell Biol 168: 89–101.
45. Zhang F, Wilson SJ, Landford WC, Virgen B, Gregory D, et al. (2009) Nef Proteins from Simian Immunodeficiency Viruses Are Tetherin Antagonists. Cell Host Microbe.
46. Mansouri M, Viswanathan K, Douglas JL, Hines J, Gustin J, et al. (2009) Molecular mechanism of BST2/tetherin downregulation by K5/MIR2 of Kaposi's sarcoma-associated herpesvirus. J Virol 83: 9672–9681.
47. Haque M, Chen J, Ueda K, Mori Y, Nakano K, et al. (2000) Identification and analysis of the K5 gene of Kaposi's sarcoma-associated herpesvirus. J Virol 74: 2867–2875.
48. Dube M, Roy BB, Guiot-Guillain P, Mercier J, Binette J, et al. (2009) Suppression of Tetherin-Restricting Activity on HIV-1 Particle Release Correlates with Localization of Vpu in the trans-Golgi Network. J Virol.
49. Pawliczek T, Crump CM (2009) Herpes simplex virus type 1 production requires a functional ESCRT-III complex but is independent of TSG101 and ALIX expression. J Virol 83: 11254–11264.
50. Jenner RG, Maillard K, Cattini N, Weiss RA, Boshoff C, et al. (2003) Kaposi's sarcoma-associated herpesvirus-infected primary effusion lymphoma has a plasma cell gene expression profile. Proc Natl Acad Sci U S A 100: 10399–10404.
51. Wilson SJ, Tsao EH, Webb BL, Ye H, Dalton-Griffin L, et al. (2007) X box binding protein XBP-1s transactivates the Kaposi's sarcoma-associated herpesvirus (KSHV) ORF50 promoter, linking plasma cell differentiation to KSHV reactivation from latency. J Virol 81: 13578–13586.
52. Areste C, Blackbourn DJ (2009) Modulation of the immune system by Kaposi's sarcoma-associated herpesvirus. Trends Microbiol 17: 119–129.
53. Powers C, DeFilippis V, Malouli D, Fruh K (2008) Cytomegalovirus immune evasion. Curr Top Microbiol Immunol 325: 333–359.
54. Zuo J, Currin A, Griffin BD, Shannon-Lowe C, Thomas WA, et al. (2009) The Epstein-Barr virus G-protein-coupled receptor contributes to immune evasion by targeting MHC class I molecules for degradation. PLoS Pathog 5: e1000255. doi:10.1371/journal.ppat.1000255.
55. Roberts KL, Smith GL (2008) Vaccinia virus morphogenesis and dissemination. Trends Microbiol 16: 472–479.
56. Elde NC, Child SJ, Geballe AP, Malik HS (2009) Protein kinase R reveals an evolutionary model for defeating viral mimicry. Nature 457: 485–489.
57. Stamey FR, Patel MM, Holloway BP, Pellett PE (2001) Quantitative, fluorogenic probe PCR assay for detection of human herpesvirus 8 DNA in clinical specimens. J Clin Microbiol 39: 3537–3540.
58. Towers GJ, Stockholm D, Labrousse-Najburg V, Carlier F, Danos O, et al. (1999) One step screening of retroviral producer clones by real time quantitative PCR. J Gene Med 1: 352–359.

JOURNAL OF VIROLOGY, Dec. 2010, p. 12958–12970 Vol. 84, No. 24
0022-538X/10/$12.00 doi:10.1128/JVI.01699-10

Determinants of Tetherin Antagonism in the Transmembrane Domain of the Human Immunodeficiency Virus Type 1 Vpu Protein[▽]

Raphaël Vigan and Stuart J. D. Neil*

Department of Infectious Disease, King's College London School of Medicine, Guy's Hospital, London SE1 9RT, United Kingdom

Received 11 August 2010/Accepted 28 September 2010

Tetherin (BST2/CD317) potently restricts the particle release of human immunodeficiency virus type 1 (HIV-1) mutants defective in the accessory gene *vpu*. Vpu antagonizes tetherin activity and induces its cell surface downregulation and degradation in a manner dependent on the transmembrane (TM) domains of both proteins. We have carried out extensive mutagenesis of the HIV-1 NL4.3 Vpu TM domain to identify three amino acid positions, A14, W22, and, to a lesser extent, A18, that are required for tetherin antagonism. Despite the mutants localizing indistinguishably from the wild-type (wt) protein and maintaining the ability to multimerize, mutation of these positions rendered Vpu incapable of coimmunoprecipitating tetherin or mediating its cell surface downregulation. Interestingly, these amino acid positions are predicted to form one face of the Vpu transmembrane alpha helix and therefore potentially contribute to an interacting surface with the transmembrane domain of tetherin either directly or by modulating the conformation of Vpu oligomers. While the equivalent of W22 is invariant in HIV-1/SIVcpz Vpu proteins, the positions of A14 and A18 are highly conserved among Vpu alleles from HIV-1 groups M and N, but not those from group O or SIVcpz that lack human tetherin (huTetherin)-antagonizing activity, suggesting that they may have contributed to the adaption of HIV-1 to human tetherin.

Tetherin (CD317/BST2) is an interferon-induced type II membrane glycoprotein of unusual topology (4, 25, 44) that potently restricts the release of diverse mammalian enveloped viral particles from infected cells (24, 33, 42, 45, 49, 52, 63). The protein consists of a short 21-amino-acid cytoplasmic tail, a transmembrane (TM) domain, a predominantly helical extracellular domain containing three cysteine residues that mediate tetherin dimerization (1, 44, 48) and an extended parallel coiled-coil (18), and a C-terminal glycophosphatidylinositol anchor that links it back to the cellular membrane (25). These structural features are key to the mode of tetherin activity (48). Tetherin is localized to the plasma membrane (PM) and constitutively recycles through intracellular compartments (25, 50). It is incorporated into budding virions and acts as a physical tether, cross-linking the virion and cellular membranes, thereby preventing virus particle release from the host cell (11, 15, 16, 48). Strong evidence suggests that the dual membrane anchor of tetherin allows it to form parallel dimers with one terminal in the virion membrane and the other in the cell (48). The result of this is that mature viral particles are retained on cell surfaces by protease-sensitive linkages that contain tetherin, and virions can then be endocytosed and accumulate in endosomal compartments (41, 42, 48). This relatively nonspecific inhibition of virus release does not require that tetherin interact directly with any virally encoded structural protein; thus, several mammalian viruses have evolved to encode proteins that specifically inactivate tetherin function (5), the prototype being the human immunodeficiency virus type 1 (HIV-1) accessory protein Vpu (42, 63).

Tetherin antagonism is a highly conserved attribute among primate immunodeficiency viruses (14, 23, 27, 53, 68), implying that modulating tetherin activity is essential for these viruses *in vivo*. While the Vpu protein overcomes tetherin-mediated restriction of HIV-1, simian immunodeficiency viruses (SIVs) and HIV-2 that lack a *vpu* gene counteract tetherin through their Nef protein (23, 68) or envelope glycoproteins (14, 23, 27). Primate tetherin antagonism by both Vpu and Nef is species specific (13, 23, 36, 68). HIV-1 Vpu can counteract only human, gorilla, and chimpanzee tetherins, whereas SIV Nef proteins can target multiple primate tetherins but not the human protein (23, 36, 53, 67, 68). This specificity maps to residues in tetherin's TM domain for Vpu (13, 36, 51) and a cytoplasmic tail motif for Nef (23, 28, 68). It has been suggested that both the cytoplasmic tail (28, 36) and the TM domain (13, 36) have been subjected to high positive selection during primate evolution. To add more complexity, SIVcpz, the direct precursor of HIV-1, is a recombinant virus derived from SIVs that encoded either a Vpu or a Nef with tetherin-antagonizing activity (54). The SIVcpz Nef targeting of chimpanzee tetherin was maintained, while the Vpu activity was apparently lost (53). Since the Nef target sequence in the cytoplasmic tail of human tetherin (huTetherin) has been deleted, the Vpu protein appears to have readapted to tetherin antagonism in HIV-1, leading to speculation that Vpu-mediated antagonism of tetherin may have been a prerequisite for efficient human-to-human transmission (28, 53, 67).

Vpu is a 16-kDa membrane protein consisting of an N-terminal TM domain and a C-terminal cytoplasmic tail made up of two amphipathic alpha helices separated by a conserved casein kinase II phosphorylation motif that mediates binding

* Corresponding author. Mailing address: Department of Infectious Disease, King's College London School of Medicine, Guy's Hospital, London SE1 9RT, United Kingdom. Phone: 44 207 188 8279. Fax: 44 207 188 3385. E-mail: stuart.neil@kcl.ac.uk.

▽ Published ahead of print on 6 October 2010.

to βTRCP1 and -2 (reviewed in reference 61). Vpu forms multimers in infected cells (30), with the TM domains forming a cation-permeable channel (10, 57), although the functional relevance of this for counteracting tetherin is unclear at present. In addition to antagonizing tetherin, a conserved function of most HIV-1/SIV Vpu proteins is to induce βTRCP-dependent ER-associated degradation of CD4 (3, 35, 38, 55, 65) to facilitate HIV-1 envelope maturation (66). In contrast, Vpu antagonizes tetherin in a post-ER compartment (58). Vpu localizes predominantly to the *trans*-Golgi network (TGN) and recycling endosomes (8, 64). In response to Vpu, tetherin is downregulated from the cell surface (63). Several reports also demonstrate that Vpu induces tetherin degradation dependent on the recruitment of a βTRCP2-SCF-Cullin1 ubiquitin ligase complex (6, 12, 22, 32, 39). While tetherin degradation is ubiquitin dependent, it is unclear whether it occurs in lysosomes (6, 22, 39) or proteasomally following an ERAD-like process (12, 13, 32). Furthermore, evidence suggests that degradation and, to some extent, cell surface downregulation of tetherin are dispensable events in tetherin antagonism by Vpu (40). Vpu localization to the TGN correlates with its ability to overcome tetherin (8), and recent studies demonstrate that tetherin also accumulates in the TGN in response to both Vpu and the envelope glycoproteins of HIV-2 and SIVtan (7, 14, 17, 27, 45). The TM domain of Vpu is essential for its antitetherin activity, and early studies demonstrated that deletion of parts of the TM (47), scrambling (56), or multiple amino acid replacements (62) blocked Vpu-enhanced virus release. Vpu coimmunoprecipitates with human, but not monkey, tetherin, suggesting that direct interaction between the two proteins is essential for antagonism (7, 22). However, the determinants in the Vpu TM domain required for this interaction have not been identified fully. In this study, we carried out extensive mutagenesis of the HIV-1 NL4.3 Vpu TM domain to show that a conserved face of the HIV-1 group M Vpu transmembrane helix is required for tetherin interaction and antagonism.

MATERIALS AND METHODS

Cells and plasmids. All cells were maintained at 37°C/5% CO_2 in Dulbecco's modified Eagle's medium (DMEM) (Invitrogen, United Kingdom) supplemented with 10% fetal calf serum (FCS) and gentamicin. HEK293T cells and HeLa cells were obtained from the American Tissue Culture Collection (ATCC), and the HIV-1 reporter cell line HeLa-TZMbl was kindly provided by John Kappes through the NIH AIDS Reagents Repository Program (ARRP); HeLa/CD4 cells were provided by A. Akrigg through the National Institute of Biological Standards and Controls (NIBSC) Centre for AIDS Reagents (Potters Bar, United Kingdom). Human HT1080 cells stably expressing human tetherin tagged extracellularly with an HA epitope have been described previously (45). The HIV-1 molecular clone plasmid pNL4.3 was obtained from the NIH ARRP, and the Vpu-defective counterpart has been described previously (41). pCR3.1 encoding codon-optimized HIV-1 NL4.3 Vpu tagged at the C terminus with a hemagglutinin (HA) epitope was derived from pVphu (43) (kindly provided by K. Strebel through the NIH ARRP). All transmembrane domain mutants of Vpu (Fig. 1A) were generated by QuikChange site-directed mutagenesis PCR by standard methods using the Phusion-II polymerase (New England Biolabs), and sequences were confirmed. pCR3.1 expression vectors encoding tagged or untagged human tetherins have been described elsewhere (24, 36, 42).

Virus release assays. Subconfluent HEK293T cells were transfected with 500 ng of proviral plasmid in combination with 50 ng of pCR3.1-huTetherin and variable concentrations of pCR3.1-Vpu-HA or mutants thereof using polyethyleneimine (1 mg/ml; Polysciences). The medium was replaced 16 h after transfection, and viral supernatants and cell lysates were harvested 48 h posttransfection. The infectivity of viral supernatants was determined by infecting HeLa-TZMbl and analyzing chemiluminescent beta-galactosidase activity 48 h later using Tropix beta-galactosidase reagent (Applied Biosystems). To analyze physical particle release, filtered supernatants were pelleted through a 20% sucrose-PBS cushion in a bench-top microcentrifuge at 20,000 × g for 90 min at 4°C, and pellets were resuspended in SDS-PAGE loading buffer. Virion and cell lysates were then subjected to SDS-PAGE and Western blotting for HIV-1 p24-CA using the monoclonal antibody (MAb) 187 (kindly provided by B. Chesebro through the NIH ARRP), Vpu-HA using mouse anti-HA monoclonal Ab (Covance), Hsp90 (rabbit polyclonal; Santa Cruz Biotechnologies), or Vpu (rabbit polyclonal; kindly provided by K. Strebel through the NIH ARRP [30]) and visualized by LiCor apparatus using secondary antibodies conjugated to fluorophores (IRDye 800 goat anti-rabbit and IRDye 680 goat anti-mouse antibodies).

Flow cytometry. Subconfluent HeLa cells in 6-well dishes were transfected with 400 ng pCR3.1-enhanced green fluorescent protein (eGFP) and 400 ng pCR3.1-Vpu-HA or TM mutant. At 48 h posttransfection, the cells were harvested and stained for surface tetherin using a specific anti-BST2 monoclonal IgG2a antibody (Abnova) and goat anti-mouse IgG2a Alexa633-conjugated secondary antibody (Molecular Probes, Invitrogen, United Kingdom). Tetherin expression on GFP^+ cells was then analyzed using a FACSCalibur flow cytometer (Becton Dickinson) and FlowJo software. Alternatively Jurkat cells were infected with vesicular stomatitis virus G (VSV-G)-pseudotyped HIV-1 at a multiplicity of infection (MOI) of 0.2. Forty-eight hours later, cells were stained for surface tetherin expression as described above, fixed and permeabilized for 20 min (Cytofix/Cytoperm fixation/permeabilization kit; BD Biosciences), and stained for intracellular HIV-1 Gag using the KC57 antibody conjugated to phycoerythrin (PE) (Beckman-Coulter).

Immunofluorescence microscopy. HeLa cells plated on glass coverslips were transfected with 100 ng of Vpu-HA expression vector or TM domain mutants. At 24 h posttransfection, the cells were fixed in 4% paraformaldehyde, permeabilized in 0.1% Triton X-100, and immunostained using a mouse anti-HA monoclonal antibody (Covance) and sheep anti-human TGN46 (Serotec) followed by the appropriate donkey secondary antibodies coupled to Alexa 488 and 594 fluorophores (Molecular Probes, Invitrogen, United Kingdom). The coverslips were then mounted on slides using ProLong Antifade containing DAPI (4′,6-diamidino-2-phenylindole) (Molecular Probes, Invitrogen, United Kingdom) and examined on a Leica DM-IRE2 confocal microscope. Similarly, HT1080-tetherin-HA cells were plated on coverslips and infected with VSV-G-pseudotyped HIV-1 NL4.3 or Vpu mutant at an MOI of 0.2. Forty-eight hours later, the cells were fixed and stained with Vpu-, HA-, and TGN46-specific antibodies with the appropriate donkey secondary antibodies linked to Alexa 488, 647, and 594 dyes, respectively.

Immunoprecipitation. Subconfluent HEK293T cells were transfected with 500 ng of Vpu-HA, the appropriate TM mutant or pCR3.1-YFP, and 500 ng of pCR3.1-huTetherin or pCR3.1-Vpu-YFP. At 48 h posttransfection, the cells were lysed on ice for 30 min on ice in buffer containing 50 mM Tris-HCl (pH 7.4), 150 mM NaCl, complete protease inhibitors (Roche), and 1% digitonin (Calbiochem). After removal of the nuclei, the resulting supernatants were precleared for 30 min at 4°C with 60 μl of protein G-agarose (Invitrogen). The supernatants were then incubated with 5 μg/ml mouse anti-HA (Covance) for 2 h at 4°C before addition of 50 μl of fresh protein G-agarose for a further 3 h. The beads were then washed 4 times in lysis buffer containing 0.1% digitonin and resuspended in SDS-PAGE loading buffer. Cell lysates and immunoprecipitates were then Western blotted for Vpu using mouse anti-HA and for tetherin using rabbit anti-BST2 (40) (kindly provided by K. Strebel through the NIH ARRP).

RESULTS

Identification and characterization of point mutations in the Vpu transmembrane domain that inhibit tetherin antagonism. The TM domain of Vpu is an absolute requirement for enhancing virus particle release (56). Recent studies have demonstrated that Vpu and tetherin coimmunoprecipitate with each other in a species-specific manner, strongly suggesting a direct interaction (7). To better characterize the determinants of tetherin antagonism in the Vpu TM domain, we conducted scanning mutagenesis through this region (residues 5 to 28) of a codon-optimized HIV-1 NL4.3 Vpu bearing a C-terminal HA tag (Fig. 1A). All nonalanine residues were mutated individually to alanines, while bulkier hydrophobic leucine residues replaced those that were alanines. These Vpu TM

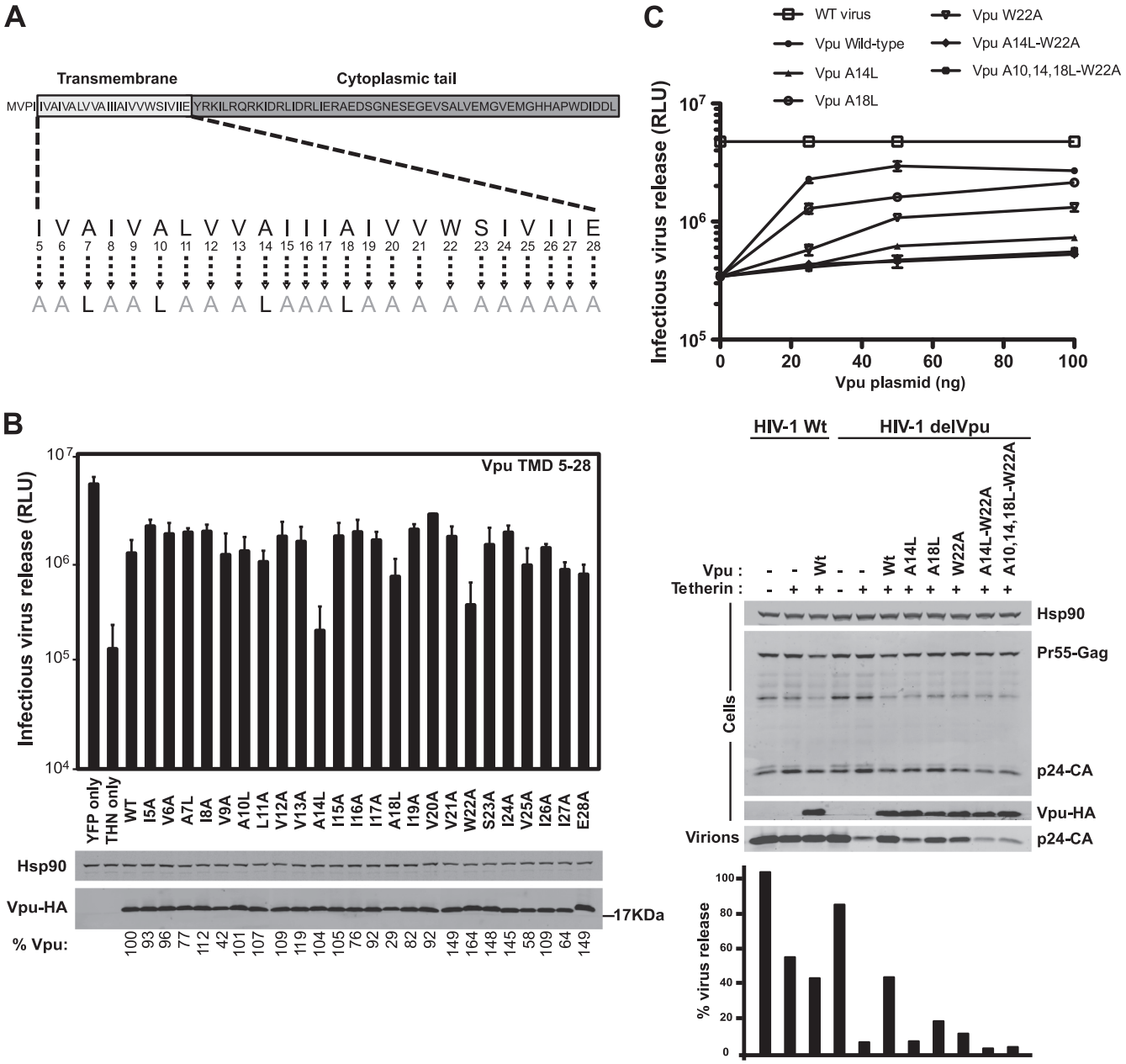

FIG. 1. Scanning mutagenesis of the HIV-1 NL4.3 Vpu TM domain and tetherin antagonism. (A) A schematic representation of point mutations made in the TM domain of a codon-optimized HIV-1 NL4.3 Vpu protein. (B) 293T cells were transiently transfected with 500 ng of HIV-1 delVpu provirus, 50 ng of tetherin plasmid, and 25 ng of the indicated Vpu expression vector. At 48 h after transfection, the resulting viral supernatants were assayed for infectivity on HeLa-TZM indicator cells by measuring beta-galactosidase activity (top). Error bars are ± standard error of the mean (SEM) for three independent experiments. 293T cell lysates from one replicate of the assay were subjected to SDS-PAGE, blotted for Vpu-HA, with the 90-kDa heat shock protein (Hsp90) serving as a loading control (bottom), and analyzed by a LiCor quantitative imager. Numbers below the lanes indicate the percentages of relative Vpu expression compared to that of the wild-type protein. (C) 293T cells transfected with 500 ng of HIV-1 wt or HIV-1 delVpu and 50 ng of tetherin expression vectors with increasing doses of the indicated Vpu-HA mutant. The resulting infectivity was determined as described in the legend to panel B, and error bars represent ± SEM for three independent experiments. (D) Cell lysates and pelleted virions from one replicate of that shown in panel C were subjected to SDS-PAGE and LiCor Western blotting was performed for HIV-1 p24-CA, Vpu-HA, and Hsp90 (top). The histogram (bottom) indicates supernatant virion yield (p24 band intensity) relative to the release of HIV-1 wt in the absence of tetherin. RLU, relative light unit; YFP, yellow fluorescent protein; THN, tetherin.

mutants were then screened for their ability to rescue Vpu-defective HIV-1 from tetherin-mediated restriction. Human 293T cells, which lack endogenous tetherin expression, were transfected with HIV-1 NL4.3 delVpu proviruses in the presence of a fixed dose of a human tetherin expression vector and either a plasmid encoding HA-tagged wild-type (wt) Vpu or the TM domain mutants. At 48 h posttransfection, cell lysates and viral supernatants were harvested and analyzed by West-

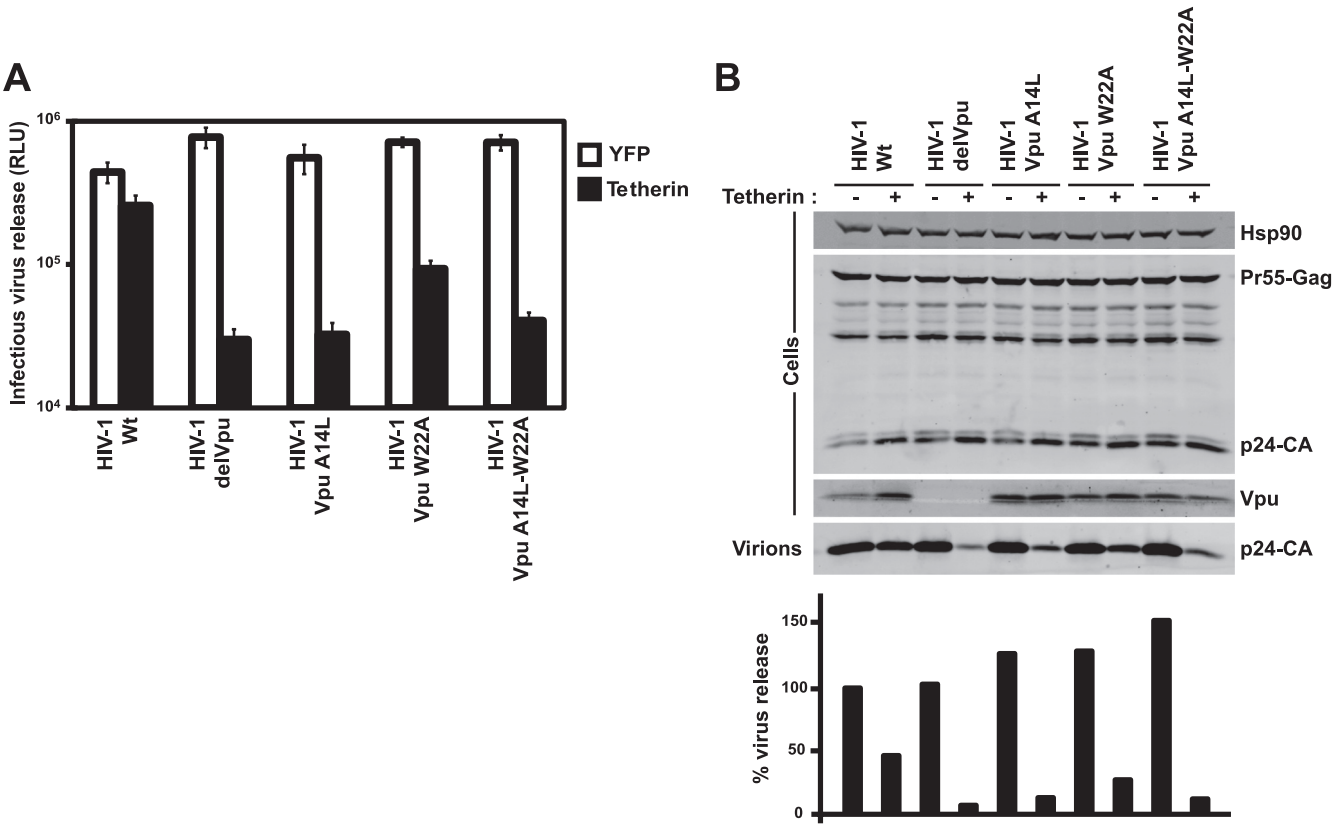

FIG. 2. The effect of A14 and W22 mutations in the context of full-length proviral clones. HIV-1 wt, HIV-1 delVpu, HIV-1 Vpu A14L, HIV-1 Vpu W22A, and HIV-1 Vpu A14L/W22A proviral clones were transfected into 293T cells in the presence or absence of 50 ng of tetherin expression vector. Forty-eight hours later, the supernatants were assayed for infectivity on HeLa-TZM cells (A) and pelleted virions (B), and cell lysates were processed for Western blotting as described in the legend to Fig. 1.

ern blotting or titrated on HeLa-TZM indicator cells (Fig. 1B). As expected, in the presence of human tetherin, the release of infectious HIV-1 delVpu was reduced approximately 50-fold, as determined by the infectivity of harvested supernatants on HeLa-TZM indicator cells, and expression of wild-type Vpu in *trans* rescued the majority of this defect. Two mutants, the A14L and W22A mutants, were markedly defective in viral rescue compared to the control, with a third, the A18L mutant, displaying a minor defect. Furthermore, several mutants (the V9A, V25A, and I27A mutants) also displayed slight (approximately 2-fold) defects compared to the wild type, but this appeared due to expression levels of the proteins rather than a functional defect *per se*. Interestingly mutation of S23, which has been shown previously to completely abolish the ion channel activity of Vpu (37), or V13, I17, and V21, which would line the pore of a putative channel (46), conferred no defect in tetherin antagonism, suggesting that formation of an ion conducting pore may not be required to relieve the restriction.

To characterize the functional mutants further, the A14L, A18L, and W22A mutants or two combined mutants, the A14L/W22A and A10L/A14L/A18L/W22A mutants, were rescreened against a fixed dose of tetherin, but with various levels of Vpu expression and virus release characterized by both infectious titer release and physical particle yield by quantitative Western blotting (Fig. 1C and D). Despite equivalent expression levels of Vpu and HIV-1 Gag in producer cells, neither the A14L mutant nor the W22A mutant could fully rescue HIV-1 delVpu from tetherin, and both remained defective compared to the wild-type Vpu, even at the highest inputs. The A18L mutant was the least defective and regained most of its function at higher plasmid inputs. Combining the A14L and W22A mutants into a single mutant, either in the context of the A14L/W22A or A10L/A14L/A18L/W22A mutant, rendered Vpu effectively unable to counteract tetherin at any level of expression.

Finally we engineered A14L and W22A mutants back into the HIV-1 NL4.3 genome to place them under wild-type Vpu expression conditions and tested virus release from 293T cells transfected with tetherin (Fig. 2A and B). Consistent with expression of the mutants in *trans*, we found that the mutant carrying A14L alone and the combined mutant had a defect in release equivalent to a full Vpu deletion, whereas W22A retained a low level of tetherin antagonism. Thus, positions A14, W22, and, to a lesser extent, A18, appear to be key residues required for tetherin antagonism in the Vpu TM domain.

The A14 and W22 mutants fail to downregulate tetherin from the cell surface. To further characterize the nature of the Vpu TM mutants, we first determined their effects on cell surface tetherin levels. Vpu expression leads to a downregulation of cell surface tetherin and subsequently a degradation step which itself may be dispensable for Vpu activity (12, 40, 63). Tetherin-positive HeLa cells were cotransfected with an

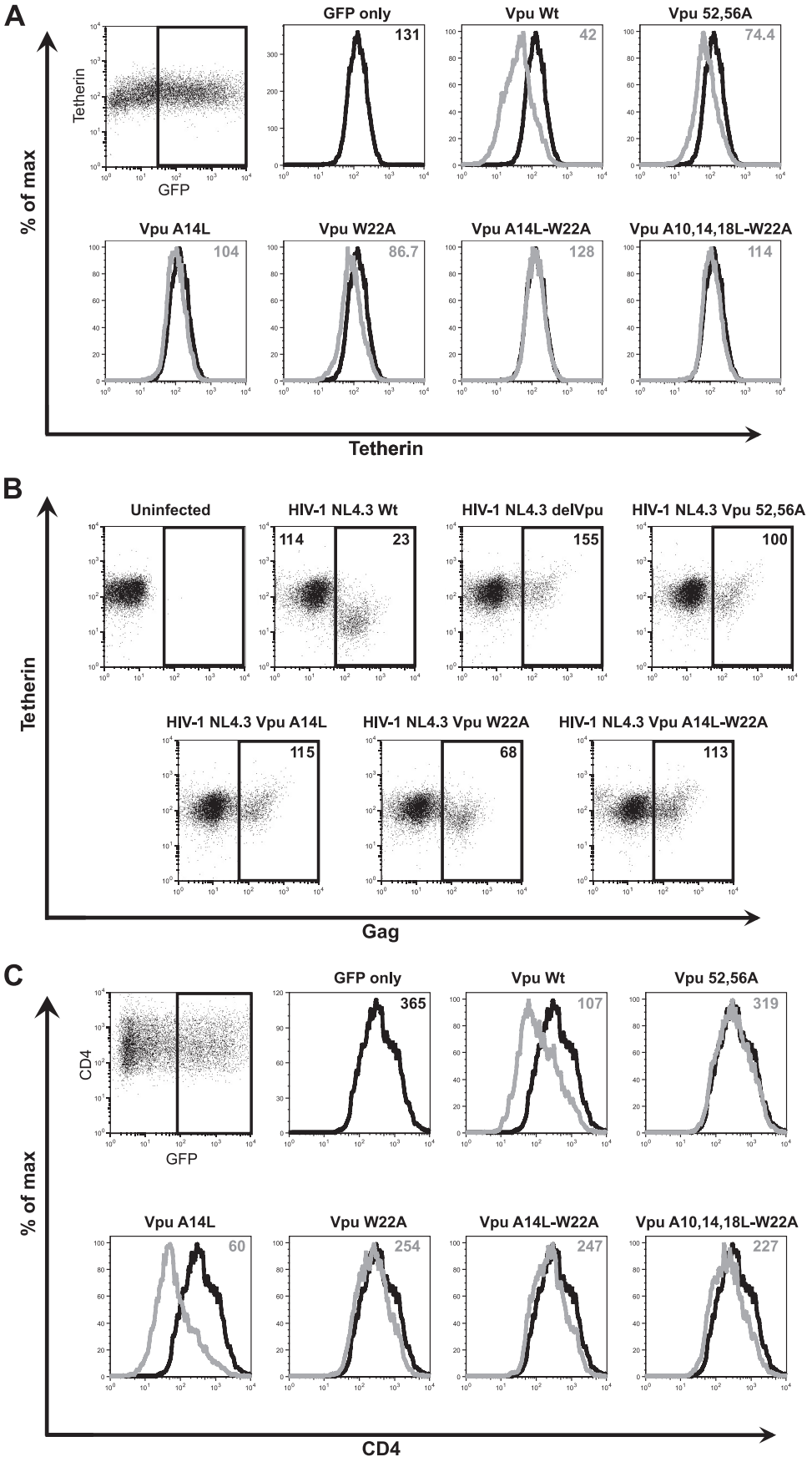
A
GFP only
Vpu Wt
Vpu 52,56A
Tetherin
GFP
131
42
74.4
Vpu A14L
Vpu W22A
Vpu A14L-W22A
Vpu A10,14,18L-W22A
104
86.7
128
114
% of max
Tetherin
B
Uninfected
HIV-1 NL4.3 Wt
HIV-1 NL4.3 delVpu
HIV-1 NL4.3 Vpu 52,56A
114
23
155
100
HIV-1 NL4.3 Vpu A14L
HIV-1 NL4.3 Vpu W22A
HIV-1 NL4.3 Vpu A14L-W22A
115
68
113
Tetherin
Gag
C
GFP only
Vpu Wt
Vpu 52,56A
CD4
GFP
365
107
319
Vpu A14L
Vpu W22A
Vpu A14L-W22A
Vpu A10,14,18L-W22A
60
254
247
227
% of max
CD4

empty vector control or Vpu expression vector in combination with a GFP marker plasmid. At 48 h posttransfection, the cells were harvested, stained for cell surface tetherin using a specific monoclonal antibody, and analyzed by flow cytometry (Fig. 3A). Tetherin was downregulated from the cell surface of GFP^+ cells expressing Vpu, and as expected, downregulation was reduced in the presence of a Vpu mutant that does not interact with βTRCP1/2 and Vpu S52 56A (12, 39, 63). Both the A14L and W22A mutants failed to fully downregulate tetherin, and either multiple mutant containing both A14L and W22A mutations was completely defective for downregulation. To confirm this with relevant infected cells, $CD4^+$ Jurkat T cells were infected with VSV-G-pseudotyped wild-type HIV-1, HIV-1 delVpu, HIV-1 Vpu2/6, HIV-1 Vpu A14L, HIV-1 Vpu W22A, or HIV-1 A14L/W22A, and 48 h later cells were stained for surface tetherin and intracellular Gag (Fig. 3B). As expected, Gag-positive cells in cultures infected with wild-type HIV-1, but not with HIV-1 delVpu or HIV-1 Vpu2/6, showed loss of tetherin expression at the cell surface. However, in line with our findings for transfected cells, Jurkat cells infected with viruses bearing an A14L mutation showed little cell surface tetherin reduction. The W22A mutant retained a residual ability to downregulate cell surface tetherin, again in line with our above observations. Thus, Vpu TM mutants that cannot antagonize tetherin function are concomitantly defective for cell surface tetherin downregulation and, by extension, degradation.

We also tested our Vpu mutants for their ability to downregulate CD4. Although CD4 and Vpu have been shown to interact through cytoplasmic tail interactions, a role for the TM domain has been implicated by some (62), but not others (56). HeLa/CD4 cells were transfected as described above, and cell surface CD4 levels were measured 48 h later (Fig. 3B). As expected, Vpu expression led to a reduction in surface CD4 that again was blocked in the presence of an S52 56A mutant. Vpu A14L retained the ability to downregulate CD4, indicating that this mutant is specifically defective for tetherin antagonism. In contrast, and consistent with the work of Tiganos et al. (62), the Vpu W22A mutant and multiple mutants bearing this lesion were also defective for CD4 downregulation. Thus, both tetherin and CD4 downmodulation require residues in the Vpu TM, but these determinants only partially overlap.

Defective Vpu TM mutants localize to the TGN. While CD4 degradation occurs in the endoplasmic reticulum (ER), Vpu-mediated virus release is sensitive to brefeldin A (58), suggesting that tetherin antagonism takes place outside the ER. Vpu localizes to the TGN and endosomal compartments, and the ability to localize to the TGN has been shown to be important for tetherin antagonism (8). Moreover, tetherin itself recycles via the TGN (25, 50), and recent data for both Vpu and HIV-2/SIV envelopes suggest that sequestration of tetherin in the TGN is associated with antagonism (7, 14, 17, 27). Since the TM domain(s) of integral membrane proteins may be involved in subcellular localization (59), we next sought to rule out whether our Vpu TM mutants were aberrantly localized. HeLa cells transfected with Vpu-HA or TM mutants were grown on coverslips, fixed 24 h later, immunostained for Vpu (anti-HA) and the TGN marker TGN46, and examined by confocal microscopy. As expected, wild-type Vpu-HA localizes predominantly to perinuclear and punctate structures, with much of the perinuclear signal overlapping with the TGN (Fig. 4A), consistent with previous studies. We found that all of our Vpu TM mutants localized similarly, with TGN accumulation visible in all cases. These data suggest that Vpu localization to the TGN is independent of the ability to counteract tetherin, and similarly, Vpu localizes to $TGN46^+$ compartments in tetherin-negative cells (data not shown). We then examined Vpu and tetherin localization in infected HT1080 cells expressing tetherin bearing an extracellular HA tag (HT1080/tetherin-HA) (Fig. 4B). As expected, in these cells tetherin localizes to the plasma membrane (PM) as well as the TGN since both newly synthesized tetherin and that which recycles passes through the Golgi network en route to the PM (25, 50). Consistent with reports of TGN accumulation of tetherin in HIV-1-infected cells (7), we found that wild-type Vpu and tetherin colocalized in the TGN with a concomitant reduction in cell surface expression. In contrast, and consistent with the flow cytometry data presented in Fig. 3, cells infected with a virus bearing the A14L/W22A mutation showed no evidence of tetherin relocalization from the PM to the TGN. This indicates that the defect in tetherin antagonism for A14L and W22A mutants of Vpu is likely not due to gross subcellular mislocalization and that Vpu localization to the TGN and Vpu-induced accumulation of tetherin in TGN46-positive compartments are independent events.

Tetherin poorly coimmunoprecipitates with Vpu TM mutants. We then assessed the ability of Vpu TM mutants to coimmunoprecipitate tetherin as an indicator of direct interaction between the proteins. 293T cells were transfected with a human tetherin expression vector and wild-type Vpu-HA or the TM mutant. At 48 h after transfection, cell lysates were immunoprecipitated with an anti-HA antibody. As shown in Fig. 5A, tetherin (both precursor mannosylated and mature complex glycosylated forms) was efficiently coimmunoprecipitated with wild-type Vpu, despite total cellular tetherin levels being lower in cell lysates due to Vpu-induced degradation (Fig. 5A, low-exposure lysate panel). The A14L and W22A mutants displayed little or no tetherin degradation and only poorly coimmunoprecipitated the protein. Furthermore, combined mutants containing both A14L and W22A were further

FIG. 3. Effects of Vpu TM mutations on cell surface levels of tetherin and CD4. (A) HeLa cells were transfected with a wild-type Vpu (Vpu Wt)-encoding vector or the indicated mutant and a GFP-expressing construct. Cell surface staining for endogenous tetherin was analyzed by flow cytometry 48 h later. Histograms show the tetherin levels on GFP^+ cells in empty vector control cells (black) or Vpu/Vpu mutant-expressing cells (gray). The median fluorescent intensities indicated in the top corner of each histogram are representative examples of 3 independent experiments. (B) Jurkat cells were infected with the indicated VSV-G-pseudotyped viral stocks at an MOI of 0.2. Forty-eight hours later, cells were stained for surface tetherin expression and intracellular Gag and analyzed by flow cytometry. Gag-positive infected cells were gated (black square), and surface tetherin levels were compared. Numbers indicate median fluorescence intensities of surface tetherin on the infected cells. (C) As shown in panel A, but the effects of Vpu-wt or Vpu-TM mutants on surface CD4 were examined in transfected HeLa/CD4 cells.

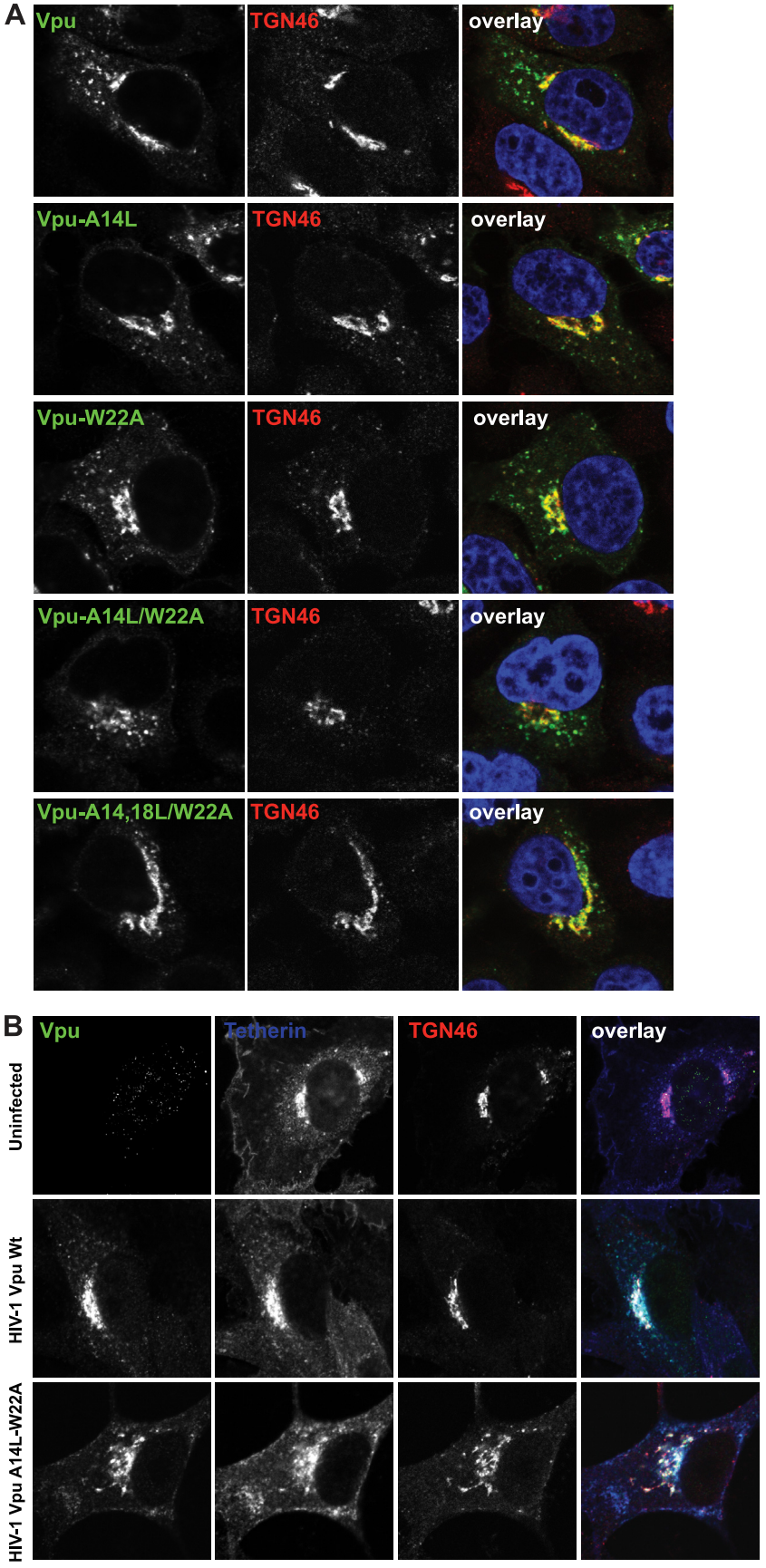
A
Vpu
TGN46
overlay
Vpu-A14L
TGN46
overlay
Vpu-W22A
TGN46
overlay
Vpu-A14L/W22A
TGN46
overlay
Vpu-A14,18L/W22A
TGN46
overlay
B
Vpu
Tetherin
TGN46
overlay
Uninfected
HIV-1 Vpu Wt
HIV-1 Vpu A14L-W22A

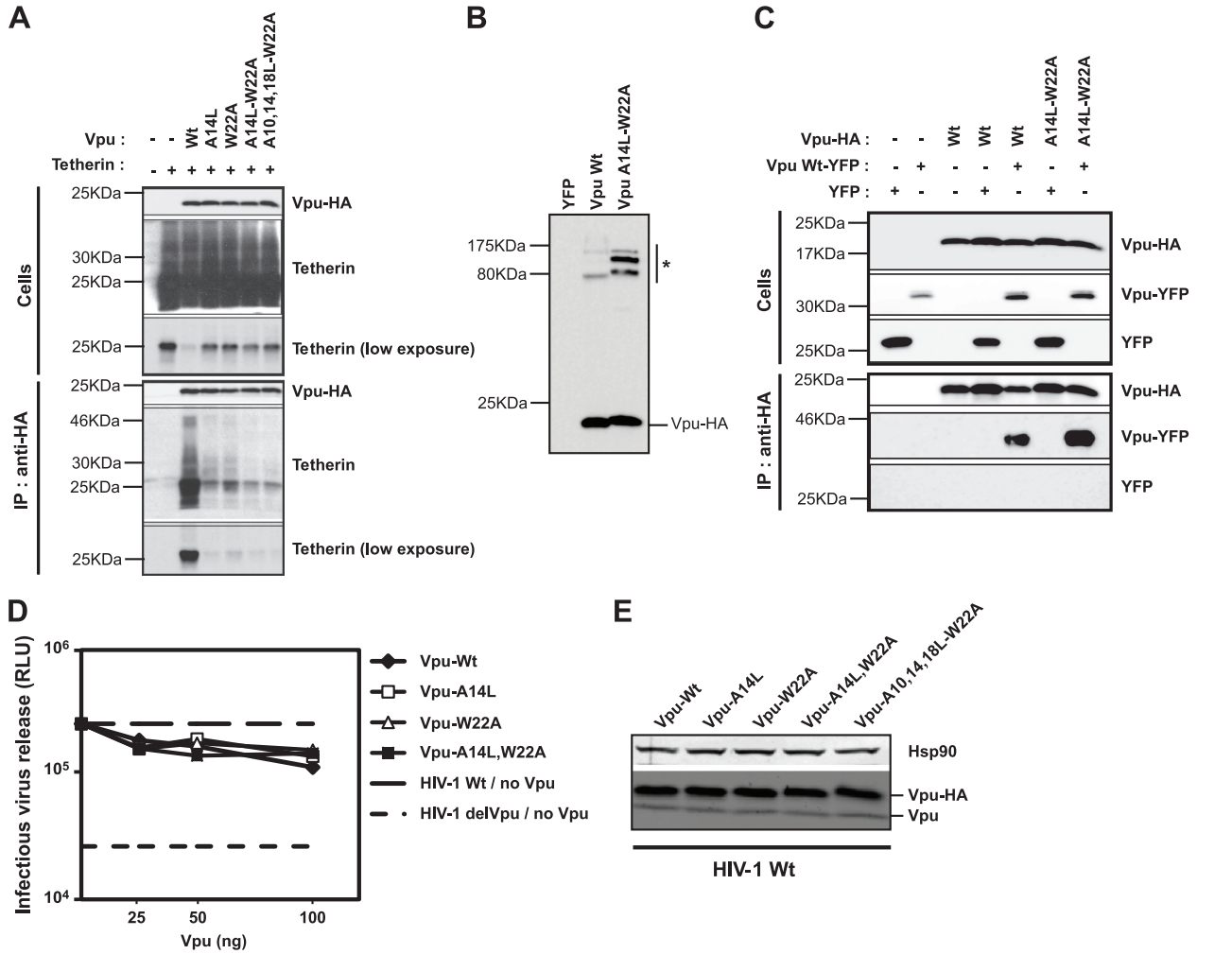

FIG. 5. Vpu TM mutants are unable to coimmunoprecipitate tetherin but maintain the ability to multimerize with wild-type Vpu. (A) 293T cells were transfected with the indicated plasmid Vpu vectors or the indicated mutant and with tetherin. YFP only or tetherin only served as negative controls. Forty-eight hours later, Vpu was immunoprecipitated (IP) via the HA tag from cell lysates and subjected to SDS-PAGE. Total lysates and immunoprecipitates were then Western blotted for tetherin and Vpu-HA. Molecular mass markers are indicated, and blots are a representative example of three independent experiments. (B) 293T cells transfected with HA-tagged Vpu or Vpu A14L/W22A were lysed in 1% digitonin after 48 h, subjected to nonreducing SDS-PAGE without prior boiling, and Western blotted with an anti-HA monoclonal Ab. (C) 293T cells were transfected with Vpu-YFP and either Vpu-HA or Vpu A14L/W22A-HA. Forty-eight hours later, cell lysates were immunoprecipitated with anti-HA Abs as described in the legend to Fig. 5A, and whole lysates and IP fractions Western blotted for Vpu-HA and Vpu-YFP with anti-HA and anti-GFP antibodies, respectively. (D) 293T cells were transfected with wild-type HIV-1 NL4.3 proviral plasmid, 50 ng of tetherin, and the indicated amount of Vpu-HA or mutant, and infectious release was determined on HeLa-TZM cells 48 h later. Dotted lines represent wild-type and Vpu-defective viral titers in the absence of any expression of Vpu in *trans*. (E) Cell lysates of the 100-ng input described in the legend to panel D blotted with an anti-Vpu polyclonal Ab to allow simultaneous detection of the Vpu-HA expressed in *trans* and the wild-type Vpu expressed from the NL4.3 provirus.

reduced in their ability to coimmunoprecipitate tetherin. Thus, the defect in tetherin antagonism in the A14L and W22A mutants correlates directly with their failure to interact with tetherin. Coupled with the observation that these mutants localize identically to wild-type Vpu, these data strongly suggest that these positions in the Vpu TM domain are critical for the interaction with tetherin. Interestingly, the fact that we coimmunoprecipitated the lower-molecular-weight, immature form of tetherin with Vpu may suggest that while Vpu exerts its effect on tetherin in a post-ER compartment, interaction may occur prior to further carbohydrate modification.

Oligomers of Vpu can be detected in infected cells (21, 30),

FIG. 4. Subcellular localization and multimerization of Vpu TM mutants. (A) HeLa cells were transfected by either 100 ng Vpu wt-HA or the indicated mutant. A total of 24 h later, the cells were fixed and stained for Vpu localization with anti-HA antibody (green) and a TGN marker (TGN46; red) and examined by confocal microscopy. (B) HT1080/THN-HA cells were infected with HIV-1 wt or HIV-1 Vpu A14L/W22A at an MOI of 0.2. Forty-eight hours later, the cells were fixed and stained for Vpu (green), TGN46 (red), and tetherin-HA (blue) and examined by confocal microscopy.

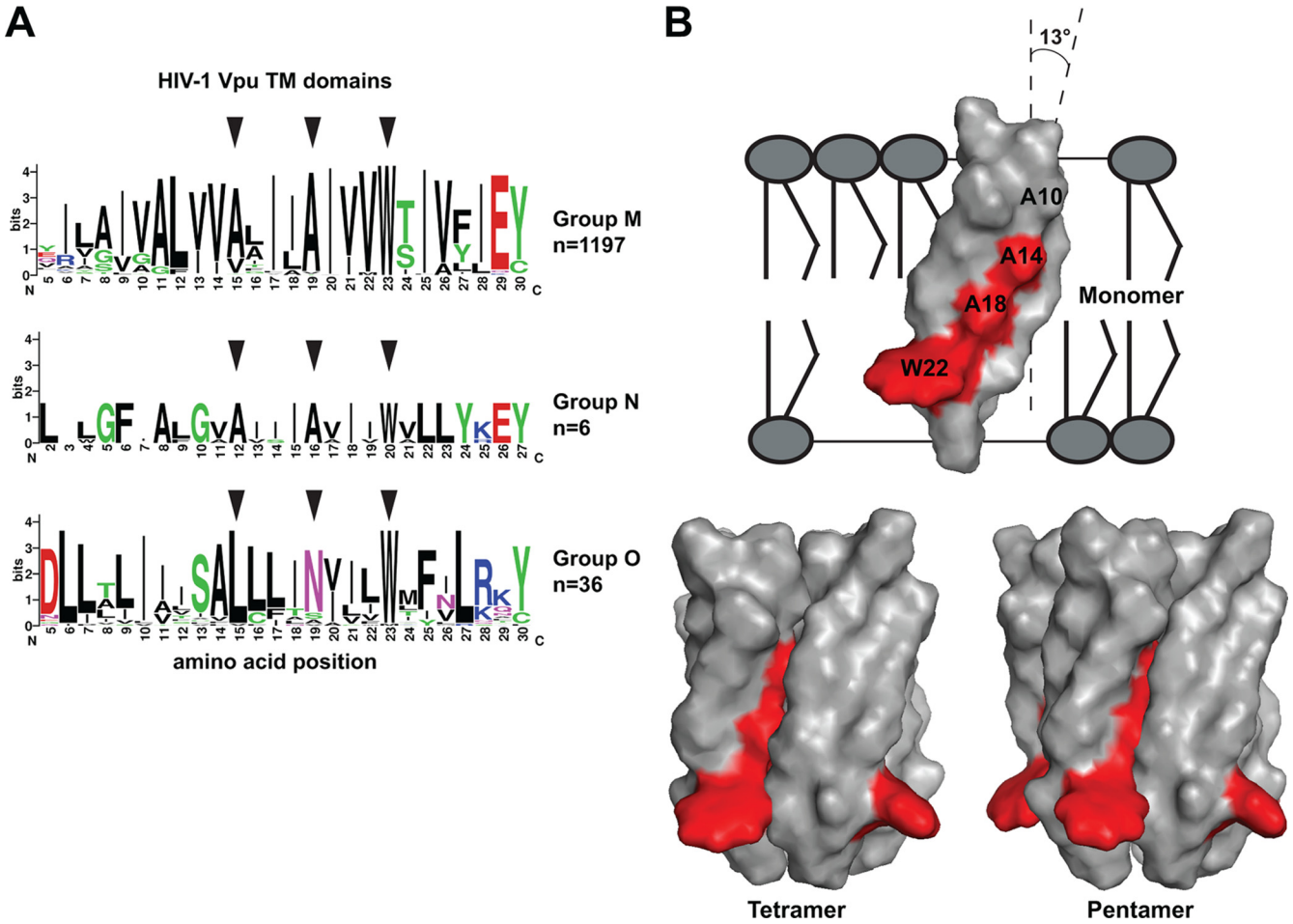

FIG. 6. Residues A14, A18, and W22 form one face of the TM helix and are conserved in HIV-1 groups M and N, but not O. (A) Logo plots of the TM domains of Vpu sequences drawn from the HIV Sequence Database (www.hiv.lanl.gov). Group M comprises 500 clade B, 200 clade C, 200 clade A, 200 clade D, 42 clade F, 48 clade G, and 7 clade H TM sequences. Arrows indicate the equivalent positions of NL4.3 Vpu A14, A18, and W22 residues. (B) Positions of A14, A18, and W22 (red) in the solid-state NMR structure of the NL4.3 Vpu TM domain determined in membranes and the modeled tetrameric and pentameric assemblies based on it, as determined by Park et al. (46). Images were generated in PyMol from the RSCB protein database entries 1PI7 (pentamer) and 1PI8 (tetramer).

although their functional significance for tetherin antagonism is not known. We next asked whether we could detect Vpu mutants in multimeric forms in transfected cells. Western blots of postnuclear lysates of Vpu-HA-transfected 293T cells run under nonreducing conditions without prior boiling displayed a higher-molecular-mass form of Vpu (approximately 80 kDa) in addition to a monomer (Fig. 5B), consistent with previous observations (30). This species of Vpu was also detected for the Vpu A14L/W22A mutant, suggesting that our TM mutants did not abolish Vpu multimerization. In addition, this mutant also formed a larger (approximately 100- to 120-kDa) form. Furthermore, under the same immunoprecipitation conditions in which Vpu TM mutants failed to interact with tetherin, we could show that wild-type Vpu tagged with GFP could coimmunoprecipitate with both Vpu-HA and Vpu A14L/W22A-HA (Fig. 5C). Therefore, the defect in tetherin antagonism by our TM mutants was not due to an inability of the proteins to self-associate, although whether the nature or stability of these mutant oligomers is different or whether other cellular factors contribute to them is unknown. To characterize this further, we reasoned that if tetherin antagonism was mediated by functional Vpu multimers, Vpu A14L/W22A mutants might be dominant-negative inhibitors of tetherin antagonism. However, titration of Vpu TM mutants into HIV-1 wt viral release assays did not induce any enhanced sensitivity to tetherin, despite estimated mutant Vpu levels 10-fold over that expressed from the provirus (Fig. 5D and E). Thus, while not ruling out that Vpu acts as a multimer to target tetherin, these data show that the ability of Vpu-TM mutants to associate with wild-type Vpu does not compromise its function.

A14, A18, and W22 form a face of the TM helix that is conserved in group M and N, but not O, Vpu proteins. We next looked at the conservation of the above TM positions in Vpu sequences deposited in the HIV Sequence Database (www.hiv.lanl.gov) (Fig. 6A). Aligning the TM domains of 1,197 group M Vpu sequences shows that the positions equivalent to A18 and W22 are highly conserved. The majority of sequences also have the equivalent of position 14 as A, but in many cases this can be V. Notably we did not find an L at this position in naturally occurring group M sequences. The same was ob-

served with the small number of group N Vpu sequences available; the equivalents of positions 14, 18, and 22 were A, A, and W, respectively. Interestingly, this was not the case for HIV-1 group O Vpu proteins, which have recently been shown to be defective in tetherin antagonism (53). Here the position 14 equivalent is almost always L, and the majority of sequences have an N at position 18. Again the W is invariant, which, since group O Vpu proteins retain CD4 degradation activity (53), is consistent with W22A mutants of NL4.3 Vpu being defective for both tetherin and CD4 downregulation. Thus, the residues we have identified as important for tetherin antagonism in HIV-1 NL4.3 Vpu are conserved in viruses that can antagonize human tetherin, but not in those that cannot.

The solid-state nuclear magnetic resonance (NMR) structure of the NL4.3 Vpu TM domain in lipid membranes has been determined previously (34, 46). The core TM domain (residues 8 to 25) forms a slightly kinked alpha helix tilted at approximately 13 degrees to the vertical. Residues A10, A14, A18, and W22 form one diagonal face of the helix (Fig. 6B). Because Vpu can form ion-permeable channels, this structure was further modeled to account for this, and the most favorable conformations that would allow channel function were predicted to be a tetramer or a pentamer (46) (Fig. 6B). In this conformation, W22 is predicted to protrude outward from the pentamer and may give stability to the structure in the membrane. A14 and A18 are positioned at the interface with the adjacent monomers, and therefore, their replacement with bulkier leucine residues may impinge on this interaction and, although not sufficient to block Vpu multimerization, alter the conformation or stoichiometry of Vpu oligomers. Alternatively, or in addition to contributing to interhelical contacts or stability, A14, A18, and W22 might also contribute to a conserved binding surface for interaction with another protein, potentially tetherin.

DISCUSSION

The mechanism by which Vpu antagonizes tetherin activity is unclear at present. While Vpu expression leads to either endosomal or proteasomal degradation of tetherin (6, 12, 13, 22, 32, 39), the ultimate destruction of tetherin appears dispensable (7, 40). Moreover, tetherin accumulation in the TGN in response to Vpu suggests that removal of tetherin from the cell surface is a result of Vpu inhibiting tetherin recycling/transport to the plasma membrane, and Vpu localization to the TGN, mediated by determinants in its cytoplasmic tail, correlates with this activity (7, 8). Furthermore, in $CD4^+$ T cells, removal of tetherin itself from the cell surface may not be strictly required to block its antiviral activity (40). In this study we have characterized transmembrane domain mutants of HIV-1 NL4.3 Vpu that cannot antagonize tetherin-mediated restriction of virion release, with major defects associated with changes at positions A14 and W22. Vpu TM mutants defective for tetherin antagonism are concomitantly defective for tetherin downregulation from the cell surface and, by extension, degradation. This directly correlates with the inability of these mutants to interact with tetherin in coimmunoprecipitations. Since these residues are conserved in group M and N Vpu proteins and their mutation does not grossly affect Vpu localization to the TGN or prevent Vpu from interacting with itself, we propose that A14, W22, and, to a lesser extent, A18 contribute to the interaction between tetherin and Vpu. In the absence of this interaction, antagonism of the antiviral activity of tetherin, its cell surface downregulation, and its ultimate degradation are all impaired.

While it cannot be ruled out that a cellular cofactor mediates Vpu-tetherin interactions, the genetic evidence for direct binding between their TM domains is strong. First, the species specificity of HIV-1 NL4.3 Vpu maps to positively selected residues in the tetherin TM domain, suggesting that viral countermeasures that target the tetherin TM may have acted as a selective pressure on tetherin evolution (13, 36). In particular, a GI deletion toward the N terminus (cytoplasmic) and a T45I change at the C terminus (extracellular) of the tetherin TM account for the sensitivity of human, but not macaque, tetherin to NL4.3 Vpu, although additional residues can contribute to Vpu sensitivity (36). Moreover, the Vpu proteins from other HIV-1 group M strains have a more expanded tropism for other primate tetherins (53). However, in the case of HIV-1 NL4.3, this species specificity correlates with the lack of coimmunoprecipitation with insensitive primate tetherin variants (7). Second, a recent study demonstrated fluorescence resonance energy transfer (FRET) between Vpu and human tetherin that was dependent on the Vpu TM domain (2). Finally, deletion mutations within the Vpu TM that encompass W22 or the complete scrambling of its sequence have long been known to inhibit Vpu-mediated virus release (47, 56, 62). Our data build on these observations, implicating specific Vpu TM residues in the interaction with tetherin that do not affect TGN localization or block self-association.

Modeling of the Vpu TM structure has historically been done on the basis that it forms a multimeric cation-permeable channel in cellular membranes (10, 57). Since scrambling the TM domain blocks both ion channel activity and efficient virus release, it was thought that these activities were related (10, 57). Indeed, amiloride-based drugs that block Vpu channel function have been shown to display antiviral activity against HIV-1 in (tetherin-positive) macrophages (9), and other studies report that chimeric Vpu proteins bearing the TM domain of the influenza A virus proton channel M2 were functional for virus release and sensitive to rimantadine (19, 20). However, since we found that mutation of S23, known to be required for channel activity (60) and the potential target for amilorides (26), had no effect on tetherin inactivation in our assays, there appears to be a discrepancy in directly correlating cation transport and virus release (tetherin antagonism). The role of ion transport in Vpu function is therefore unclear, but given the multifunctional nature of HIV-1 accessory proteins (31), it is possible that the ion channel activity is related to a yet-to-be-defined role of Vpu in HIV-1 replication.

We do not know the stoichiometry of the Vpu-tetherin interaction or indeed whether Vpu multimerization is required for its antagonism. Oligomers of Vpu can be detected in infected cells (30). NMR structures of the Vpu TM have been used to predict the conformation of Vpu multimers; however, as discussed above, these have revolved around its ion channel activity. More recent data suggest that there might be an equilibrium of Vpu monomers and different multimeric forms (29), while another FRET-based study provided evidence that Vpu-Vpu interactions could be detected in Golgi-related structures

but not in the ER (21), suggesting that Vpu multimerization may occur differentially in subcellular compartments. Based on the NMR structural model of a Vpu pentamer shown in Fig. 6 (46), an A14L mutation might disrupt interhelical interactions in Vpu multimers and a W22A mutant might lose the stability imparted by the tryptophan side chain. However, neither mutation disrupts the ability of Vpu to interact with itself nor alters its subcellular distribution, although they may lead to additional multimeric forms at steady state (Fig. 5B). Furthermore, V13A and I16A mutants, which in the predicted multimers would be associated with A14 on the adjacent helix, lack significant defects in tetherin antagonism. A14 and W22 might also contribute to a direct tetherin-interacting surface formed upon Vpu multimerization. However, one piece of data from our study is not consistent with Vpu targeting tetherin as a functional multimer. Despite overexpressing Vpu mutants in excess, we were unable to observe any dominant-negative activity of A14L and W22A mutants against wild-type HIV-1 virion release in the presence of tetherin, as might be expected if A14L/W22A mutations were disrupting the integrity or conformation of functional Vpu multimers. While not itself demonstrating that Vpu acts on tetherin as a monomer, this observation shows that despite being unable to mediate tetherin interaction, the ability of the A14L/W22A mutant to multimerize with the wild-type protein does not block its inactivation of tetherin. Alternatively, if Vpu did act on tetherin as a monomer, the fact that A14, A18, and W22 form a face of the TM helix might be indicative of the residues forming a binding surface. If so, they could directly interact with residues in the tetherin TM domain known to be required for sensitivity to Vpu. Further in-depth structure/function analyses are required to distinguish between these possibilities. Such studies will be essential for the design of any potential Vpu inhibitors.

The ability to counteract tetherin is conserved among primate lentiviruses, indicating that this attribute is essential for replication/transmission of these viruses *in vivo* (14, 23, 27, 42, 53, 68). Recent studies have suggested that the ability of HIV-1 Vpu to counteract human tetherin is a "reacquisition" of an ancestral Vpu function in the SIVgsn/SIVmon/SIVmus lineage that was lost in SIVcpz presumably due to redundancy with the tetherin antagonism function of Nef (53). The selective pressures that lead to the specific deletion of the SIV Nef target sequence (G/DDIWK) in the cytoplasmic tail of human tetherin are unclear (23, 28, 68), although prehistoric human exposure to Nef-like proteins from pathogenic viruses is a possible explanation. Regardless, the spread of SIVcpz to humans to become HIV-1 presented the virus with a problem; the tetherin countermeasure was ineffective (54). Recent data from the Emerman group have demonstrated that swapping the majority of the TM domain of HIV-1 Vpu, including the residues identified herein, renders SIVcpz Vpu active against human tetherin (28). The differences between the HIV-1 Vpu and SIVcpz Vpu TM domains indicate that multiple changes occurred during the adaption of HIV-1 Vpu to humans. Interestingly, in terms of acquiring tetherin antagonism and maintaining CD4 downregulation, there is evidence that this was fully achieved only by HIV-1 group M, derived from the SIVcpz zoonosis that gave rise to the HIV/AIDS pandemic (53). Data from the small number of group N Vpu proteins available suggest that tetherin antagonism has developed to some extent here too, although these proteins now do not target CD4. HIV-1 group O Vpu proteins, by contrast, are devoid of tetherin antagonistic activity, while remaining capable of targeting CD4 (53). We note with interest that the conservation of an A and, to a lesser extent a V, at the equivalent to position 14 in the Vpu TM is found only in Vpu proteins from groups M and N, whereas in group O it is invariably L and is often acidic in SIVcpz. In our hands, an A14L mutation was selectively defective for tetherin and had no effect on CD4 downregulation. In contrast, the W residue is invariant in all HIV-1/SIVcpz Vpu TMs, consistent with its role in both tetherin antagonism and CD4 degradation. Position 18, which when mutated to a leucine has a lesser effect on tetherin antagonism in NL4.3 Vpu, is also highly conserved in groups M and N but in group O is most often a polar residue (N or S). Thus, the residues identified in our screen are associated with Vpu proteins that can antagonize tetherin, but not those that cannot. Whether these residues are sufficient to confer tetherin antagonism to group O Vpu or whether they are necessary only in the context of other differences in the TM domains, as suggested by the data of Lim et al. (28), remains to be determined. As shown in Fig. 6A, several other positions in the group M Vpu TMs are highly conserved, particularly surrounding A14 and W22, and when mutated individually, they had little or no effect on tetherin antagonism in our transfection assays but may have subtle context-dependent roles. Additional features of the cytoplasmic tail that modulate Vpu localization to the TGN also play a role in tetherin antagonism (8), and it is at present unknown whether these are functional in group O Vpu proteins.

In summary, we have identified conserved determinants in the HIV-1 Vpu TM domain that contribute to tetherin interaction and antagonism. Further studies will determine the structural implications of these mutations on tetherin binding and the role of Vpu multimerization in the process and potentially allow the design of antiviral candidates to disrupt Vpu-tetherin interactions.

ACKNOWLEDGMENTS

We thank Paul Bieniasz, Greg Towers, Klaus Strebel, John Kappes, Bruce Chesebro, the NIH AIDS Reagents Repository, and the NIBSC Centre for AIDS Reagents for the kind gift of reagents. We are especially grateful to Michael Linden and Julian Bergeron for helpful discussions, Anna Le Tortorec for reagents, and other members of the Neil lab for support and encouragement.

This work was supported by a Wellcome Research Career Development Fellowship (WT082274MA) and an MRC project grant (G0801937) to S.J.D.N.

Author contributions: R.V. and S.J.D.N. designed the experiments; R.V. performed the experiments; R.V. and S.J.D.N. analyzed the data and wrote the paper.

REFERENCES

1. **Andrew, A. J., E. Miyagi, S. Kao, and K. Strebel.** 2009. The formation of cysteine-linked dimers of BST-2/tetherin is important for inhibition of HIV-1 virus release but not for sensitivity to Vpu. Retrovirology **6:**80.
2. **Banning, C., J. Votteler, D. Hoffmann, H. Koppensteiner, M. Warmer, R. Reimer, F. Kirchhoff, U. Schubert, J. Hauber, and M. Schindler.** 2010. A flow cytometry-based FRET assay to identify and analyse protein-protein interactions in living cells. PLoS One **5:**e9344.
3. **Binette, J., M. Dube, J. Mercier, D. Halawani, M. Latterich, and E. A. Cohen.** 2007. Requirements for the selective degradation of CD4 receptor molecules by the human immunodeficiency virus type 1 Vpu protein in the endoplasmic reticulum. Retrovirology **4:**75.
4. **Blasius, A. L., E. Giurisato, M. Cella, R. D. Schreiber, A. S. Shaw, and M.**

Colonna. 2006. Bone marrow stromal cell antigen 2 is a specific marker of type I IFN-producing cells in the naive mouse, but a promiscuous cell surface antigen following IFN stimulation. J. Immunol. **177:**3260–3265.
5. **Douglas, J. L., J. K. Gustin, K. Viswanathan, M. Mansouri, A. V. Moses, and K. Fruh.** 2010. The great escape: viral strategies to counter BST-2/tetherin. PLoS Pathog. **6:**e1000913.
6. **Douglas, J. L., K. Viswanathan, M. N. McCarroll, J. K. Gustin, K. Fruh, and A. V. Moses.** 2009. Vpu directs the degradation of the human immunodeficiency virus restriction factor BST-2/tetherin via a βTrCP-dependent mechanism. J. Virol. **83:**7931–7947.
7. **Dubé, M., B. B. Roy, P. Guiot-Guillain, J. Binette, J. Mercier, A. Chiasson, and E. A. Cohen.** 2010. Antagonism of tetherin restriction of HIV-1 release by Vpu involves binding and sequestration of the restriction factor in a perinuclear compartment. PLoS Pathog. **6:**e1000856.
8. **Dubé, M., B. B. Roy, P. Guiot-Guillain, J. Mercier, J. Binette, G. Leung, and E. A. Cohen.** 2009. Suppression of tetherin-restricting activity upon human immunodeficiency virus type 1 particle release correlates with localization of Vpu in the *trans*-Golgi network. J. Virol. **83:**4574–4590.
9. **Ewart, G. D., K. Mills, G. B. Cox, and P. W. Gage.** 2002. Amiloride derivatives block ion channel activity and enhancement of virus-like particle budding caused by HIV-1 protein Vpu. Eur. Biophys. J. **31:**26–35.
10. **Ewart, G. D., T. Sutherland, P. W. Gage, and G. B. Cox.** 1996. The Vpu protein of human immunodeficiency virus type 1 forms cation-selective ion channels. J. Virol. **70:**7108–7115.
11. **Fitzpatrick, K., M. Skasko, T. J. Deerinck, J. Crum, M. H. Ellisman, and J. Guatelli.** 2010. Direct restriction of virus release and incorporation of the interferon-induced protein BST-2 into HIV-1 particles. PLoS Pathog. **6:**e1000701.
12. **Goffinet, C., I. Allespach, S. Homann, H. M. Tervo, A. Habermann, D. Rupp, L. Oberbremer, C. Kern, N. Tibroni, S. Welsch, J. Krijnse-Locker, G. Banting, H. G. Krausslich, O. T. Fackler, and O. T. Keppler.** 2009. HIV-1 antagonism of CD317 is species specific and involves Vpu-mediated proteasomal degradation of the restriction factor. Cell Host Microbe **5:**285–297.
13. **Gupta, R. K., S. Hue, T. Schaller, E. Verschoor, D. Pillay, and G. J. Towers.** 2009. Mutation of a single residue renders human tetherin resistant to HIV-1 Vpu-mediated depletion. PLoS Pathog. **5:**e1000443.
14. **Gupta, R. K., P. Mlcochova, A. Pelchen-Matthews, S. J. Petit, G. Mattiuzzo, D. Pillay, Y. Takeuchi, M. Marsh, and G. J. Towers.** 30 October 2009. Simian immunodeficiency virus envelope glycoprotein counteracts tetherin/BST-2/CD317 by intracellular sequestration. Proc. Natl. Acad. Sci. U. S. A. [Epub ahead of print.] doi:10.1073/pnas.0907075106.
15. **Habermann, A., J. Krijnse Locker, H. Oberwinkler, M. Eckhardt, S. Homann, A. Andrew, K. Strebel, and H. G. Krausslich.** 2010. CD317/tetherin is enriched in the HIV-1 envelope and downregulated from the plasma membrane upon virus infection. J. Virol. **84:**4646–4658.
16. **Hammonds, J., J. J. Wang, H. Yi, and P. Spearman.** 2010. Immunoelectron microscopic evidence for tetherin/BST2 as the physical bridge between HIV-1 virions and the plasma membrane. PLoS Pathog. **6:**e1000749.
17. **Hauser, H., L. A. Lopez, S. J. Yang, J. E. Oldenburg, C. M. Exline, J. C. Guatelli, and P. M. Cannon.** 2010. HIV-1 Vpu and HIV-2 Env counteract BST-2/tetherin by sequestration in a perinuclear compartment. Retrovirology **7:**51.
18. **Hinz, A., N. Miguet, G. Natrajan, Y. Usami, H. Yamanaka, P. Renesto, B. Hartlieb, A. A. McCarthy, J. P. Simorre, H. Gottlinger, and W. Weissenhorn.** 2010. Structural basis of HIV-1 tethering to membranes by the BST-2/tetherin ectodomain. Cell Host Microbe **7:**314–323.
19. **Hout, D. R., L. M. Gomez, E. Pacyniak, J. M. Miller, M. S. Hill, and E. B. Stephens.** 2006. A single amino acid substitution within the transmembrane domain of the human immunodeficiency virus type 1 Vpu protein renders simian-human immunodeficiency virus (SHIV(KU-1bMC33)) susceptible to rimantadine. Virology **348:**449–461.
20. **Hout, D. R., M. L. Gomez, E. Pacyniak, L. M. Gomez, B. Fegley, E. R. Mulcahy, M. S. Hill, N. Culley, D. M. Pinson, W. Nothnick, M. F. Powers, S. W. Wong, and E. B. Stephens.** 2006. Substitution of the transmembrane domain of Vpu in simian-human immunodeficiency virus (SHIVKU1bMC33) with that of M2 of influenza A results in a virus that is sensitive to inhibitors of the M2 ion channel and is pathogenic for pig-tailed macaques. Virology **344:**541–559.
21. **Hussain, A., S. R. Das, C. Tanwar, and S. Jameel.** 2007. Oligomerization of the human immunodeficiency virus type 1 (HIV-1) Vpu protein–a genetic, biochemical and biophysical analysis. Virol. J. **4:**81.
22. **Iwabu, Y., H. Fujita, M. Kinomoto, K. Kaneko, Y. Ishizaka, Y. Tanaka, T. Sata, and K. Tokunaga.** 2009. HIV-1 accessory protein Vpu internalizes cell-surface BST-2/tetherin through transmembrane interactions leading to lysosomes. J. Biol. Chem. **284:**35060–35072.
23. **Jia, B., R. Serra-Moreno, W. Neidermyer, A. Rahmberg, J. Mackey, I. B. Fofana, W. E. Johnson, S. Westmoreland, and D. T. Evans.** 2009. Species-specific activity of SIV Nef and HIV-1 Vpu in overcoming restriction by tetherin/BST2. PLoS Pathog. **5:**e1000429.
24. **Jouvenet, N., S. J. Neil, M. Zhadina, T. Zang, Z. Kratovac, Y. Lee, M. McNatt, T. Hatziioannou, and P. D. Bieniasz.** 2009. Broad-spectrum inhibition of retroviral and filoviral particle release by tetherin. J. Virol. **83:**1837–1844.
25. **Kupzig, S., V. Korolchuk, R. Rollason, A. Sugden, A. Wilde, and G. Banting.** 2003. Bst-2/HM1.24 is a raft-associated apical membrane protein with an unusual topology. Traffic **4:**694–709.
26. **Lemaitre, V., R. Ali, C. G. Kim, A. Watts, and W. B. Fischer.** 2004. Interaction of amiloride and one of its derivatives with Vpu from HIV-1: a molecular dynamics simulation. FEBS Lett. **563:**75–81.
27. **Le Tortorec, A., and S. J. Neil.** 2009. Antagonism to and intracellular sequestration of human tetherin by the human immunodeficiency virus type 2 envelope glycoprotein. J. Virol. **83:**11966–11978.
28. **Lim, E. S., H. S. Malik, and M. Emerman.** 2010. Ancient adaptive evolution of tetherin shaped the functions of Vpu and Nef in human immunodeficiency virus and primate lentiviruses. J. Virol. **84:**7124–7134.
29. **Lu, J. X., S. Sharpe, R. Ghirlando, W. M. Yau, and R. Tycko.** 2010. Oligomerization state and supramolecular structure of the HIV-1 Vpu protein transmembrane segment in phospholipid bilayers. Protein Sci. **19:**1877–1896.
30. **Maldarelli, F., M. Y. Chen, R. L. Willey, and K. Strebel.** 1993. Human immunodeficiency virus type 1 Vpu protein is an oligomeric type I integral membrane protein. J. Virol. **67:**5056–5061.
31. **Malim, M. H., and M. Emerman.** 2008. HIV-1 accessory proteins–ensuring viral survival in a hostile environment. Cell Host Microbe **3:**388–398.
32. **Mangeat, B., G. Gers-Huber, M. Lehmann, M. Zufferey, J. Luban, and V. Piguet.** 2009. HIV-1 Vpu neutralizes the antiviral factor tetherin/BST-2 by binding it and directing its beta-TrCP2-dependent degradation. PLoS Pathog. **5:**e1000574.
33. **Mansouri, M., K. Viswanathan, J. L. Douglas, J. Hines, J. Gustin, A. V. Moses, and K. Fruh.** 2009. Molecular mechanism of BST2/tetherin downregulation by K5/MIR2 of Kaposi's sarcoma-associated herpesvirus. J. Virol. **83:**9672–9681.
34. **Marassi, F. M., C. Ma, H. Gratkowski, S. K. Straus, K. Strebel, M. Oblatt-Montal, M. Montal, and S. J. Opella.** 1999. Correlation of the structural and functional domains in the membrane protein Vpu from HIV-1. Proc. Natl. Acad. Sci. U. S. A. **96:**14336–14341.
35. **Margottin, F., S. P. Bour, H. Durand, L. Selig, S. Benichou, V. Richard, D. Thomas, K. Strebel, and R. Benarous.** 1998. A novel human WD protein, h-beta TrCp, that interacts with HIV-1 Vpu connects CD4 to the ER degradation pathway through an F-box motif. Mol. Cell **1:**565–574.
36. **McNatt, M. W., T. Zang, T. Hatziioannou, M. Bartlett, I. B. Fofana, W. E. Johnson, S. J. Neil, and P. D. Bieniasz.** 2009. Species-specific activity of HIV-1 Vpu and positive selection of tetherin transmembrane domain variants. PLoS Pathog. **5:**e1000300.
37. **Mehnert, T., A. Routh, P. J. Judge, Y. H. Lam, D. Fischer, A. Watts, and W. B. Fischer.** 2008. Biophysical characterization of Vpu from HIV-1 suggests a channel-pore dualism. Proteins **70:**1488–1497.
38. **Meusser, B., and T. Sommer.** 2004. Vpu-mediated degradation of CD4 reconstituted in yeast reveals mechanistic differences to cellular ER-associated protein degradation. Mol. Cell **14:**247–258.
39. **Mitchell, R. S., C. Katsura, M. A. Skasko, K. Fitzpatrick, D. Lau, A. Ruiz, E. B. Stephens, F. Margottin-Goguet, R. Benarous, and J. C. Guatelli.** 2009. Vpu antagonizes BST-2-mediated restriction of HIV-1 release via beta-TrCP and endo-lysosomal trafficking. PLoS Pathog. **5:**e1000450.
40. **Miyagi, E., A. J. Andrew, S. Kao, and K. Strebel.** 2009. Vpu enhances HIV-1 virus release in the absence of Bst-2 cell surface down-modulation and intracellular depletion. Proc. Natl. Acad. Sci. U. S. A. **106:**2868–2873.
41. **Neil, S. J., S. W. Eastman, N. Jouvenet, and P. D. Bieniasz.** 2006. HIV-1 Vpu promotes release and prevents endocytosis of nascent retrovirus particles from the plasma membrane. PLoS Pathog. **2:**e39.
42. **Neil, S. J., T. Zang, and P. D. Bieniasz.** 2008. Tetherin inhibits retrovirus release and is antagonized by HIV-1 Vpu. Nature **451:**425–430.
43. **Nguyen, K. L., M. llano, H. Akari, E. Miyagi, E. M. Poeschla, K. Strebel, and S. Bour.** 2004. Codon optimization of the HIV-1 vpu and vif genes stabilizes their mRNA and allows for highly efficient Rev-independent expression. Virology **319:**163–175.
44. **Ohtomo, T., Y. Sugamata, Y. Ozaki, K. Ono, Y. Yoshimura, S. Kawai, Y. Koishihara, S. Ozaki, M. Kosaka, T. Hirano, and M. Tsuchiya.** 1999. Molecular cloning and characterization of a surface antigen preferentially overexpressed on multiple myeloma cells. Biochem. Biophys. Res. Commun. **258:**583–591.
45. **Pardieu, C., R. Vigan, S. J. Wilson, A. Calvi, T. Zang, P. Bieniasz, P. Kellam, G. J. Towers, and S. J. Neil.** 2010. The RING-CH ligase K5 antagonizes restriction of KSHV and HIV-1 particle release by mediating ubiquitin-dependent endosomal degradation of tetherin. PLoS Pathog. **6:**e1000843.
46. **Park, S. H., A. A. Mrse, A. A. Nevzorov, M. F. Mesleh, M. Oblatt-Montal, M. Montal, and S. J. Opella.** 2003. Three-dimensional structure of the channel-forming trans-membrane domain of virus protein "u" (Vpu) from HIV-1. J. Mol. Biol. **333:**409–424.
47. **Paul, M., S. Mazumder, N. Raja, and M. A. Jabbar.** 1998. Mutational analysis of the human immunodeficiency virus type 1 Vpu transmembrane domain that promotes the enhanced release of virus-like particles from the plasma membrane of mammalian cells. J. Virol. **72:**1270–1279.

48. **Perez-Caballero, D., T. Zang, A. Ebrahimi, M. W. McNatt, D. A. Gregory, M. C. Johnson, and P. D. Bieniasz.** 2009. Tetherin inhibits HIV-1 release by directly tethering virions to cells. Cell **139:**499–511.
49. **Radoshitzky, S. R., L. Dong, X. Chi, J. C. Clester, C. Retterer, K. Spurgers, J. H. Kuhn, S. Sandwick, G. Ruthel, K. Kota, D. Boltz, T. Warren, P. J. Kranzusch, S. P. Whelan, and S. Bavari.** 2010. Infectious Lassa virus, but not filoviruses, is restricted by Bst-2/tetherin. J. Virol. **84:**10569–10580.
50. **Rollason, R., V. Korolchuk, C. Hamilton, P. Schu, and G. Banting.** 2007. Clathrin-mediated endocytosis of a lipid-raft-associated protein is mediated through a dual tyrosine motif. J. Cell Sci. **120:**3850–3858.
51. **Rong, L., J. Zhang, J. Lu, Q. Pan, R. P. Lorgeoux, C. Aloysius, F. Guo, S. L. Liu, M. A. Wainberg, and C. Liang.** 2009. The transmembrane domain of BST-2 determines its sensitivity to down-modulation by human immunodeficiency virus type 1 Vpu. J. Virol. **83:**7536–7546.
52. **Sakuma, T., T. Noda, S. Urata, Y. Kawaoka, and J. Yasuda.** 2009. Inhibition of Lassa and Marburg virus production by tetherin. J. Virol. **83:**2382–2385.
53. **Sauter, D., M. Schindler, A. Specht, W. N. Landford, J. Munch, K. A. Kim, J. Votteler, U. Schubert, F. Bibollet-Ruche, B. F. Keele, J. Takehisa, Y. Ogando, C. Ochsenbauer, J. C. Kappes, A. Ayouba, M. Peeters, G. H. Learn, G. Shaw, P. M. Sharp, P. Bieniasz, B. H. Hahn, T. Hatziioannou, and F. Kirchhoff.** 2009. Tetherin-driven adaptation of Vpu and Nef function and the evolution of pandemic and nonpandemic HIV-1 strains. Cell Host Microbe **6:**409–421.
54. **Sauter, D., A. Specht, and F. Kirchhoff.** 2010. Tetherin: holding on and letting go. Cell **141:**392–398.
55. **Schubert, U., L. C. Anton, I. Bacik, J. H. Cox, S. Bour, J. R. Bennink, M. Orlowski, K. Strebel, and J. W. Yewdell.** 1998. CD4 glycoprotein degradation induced by human immunodeficiency virus type 1 Vpu protein requires the function of proteasomes and the ubiquitin-conjugating pathway. J. Virol. **72:**2280–2288.
56. **Schubert, U., S. Bour, A. V. Ferrer-Montiel, M. Montal, F. Maldarell, and K. Strebel.** 1996. The two biological activities of human immunodeficiency virus type 1 Vpu protein involve two separable structural domains. J. Virol. **70:**809–819.
57. **Schubert, U., A. V. Ferrer-Montiel, M. Oblatt-Montal, P. Henklein, K. Strebel, and M. Montal.** 1996. Identification of an ion channel activity of the Vpu transmembrane domain and its involvement in the regulation of virus release from HIV-1-infected cells. FEBS Lett. **398:**12–18.
58. **Schubert, U., and K. Strebel.** 1994. Differential activities of the human immunodeficiency virus type 1-encoded Vpu protein are regulated by phosphorylation and occur in different cellular compartments. J. Virol. **68:**2260–2271.
59. **Sharpe, H. J., T. J. Stevens, and S. Munro.** 2010. A comprehensive comparison of transmembrane domains reveals organelle-specific properties. Cell **142:**158–169.
60. **Sharpe, S., W. M. Yau, and R. Tycko.** 2006. Structure and dynamics of the HIV-1 Vpu transmembrane domain revealed by solid-state NMR with magic-angle spinning. Biochemistry **45:**918–933.
61. **Strebel, K.** 2007. HIV accessory genes Vif and Vpu. Adv. Pharmacol. **55:**199–232.
62. **Tiganos, E., J. Friborg, B. Allain, N. G. Daniel, X. J. Yao, and E. A. Cohen.** 1998. Structural and functional analysis of the membrane-spanning domain of the human immunodeficiency virus type 1 Vpu protein. Virology **251:**96–107.
63. **Van Damme, N., D. Goff, C. Katsura, R. L. Jorgenson, R. Mitchell, M. C. Johnson, E. B. Stephens, and J. Guatelli.** 2008. The interferon-induced protein BST-2 restricts HIV-1 release and is downregulated from the cell surface by the viral Vpu protein. Cell Host Microbe **3:**245–252.
64. **Varthakavi, V., R. M. Smith, K. L. Martin, A. Derdowski, L. A. Lapierre, J. R. Goldenring, and P. Spearman.** 2006. The pericentriolar recycling endosome plays a key role in Vpu-mediated enhancement of HIV-1 particle release. Traffic **7:**298–307.
65. **Willey, R. L., F. Maldarelli, M. A. Martin, and K. Strebel.** 1992. Human immunodeficiency virus type 1 Vpu protein induces rapid degradation of CD4. J. Virol. **66:**7193–7200.
66. **Willey, R. L., F. Maldarelli, M. A. Martin, and K. Strebel.** 1992. Human immunodeficiency virus type 1 Vpu protein regulates the formation of intracellular gp160-CD4 complexes. J. Virol. **66:**226–234.
67. **Yang, S. J., L. A. Lopez, H. Hauser, C. M. Exline, K. G. Haworth, and P. M. Cannon.** 2010. Anti-tetherin activities in Vpu-expressing primate lentiviruses. Retrovirology **7:**13.
68. **Zhang, F., S. J. Wilson, W. C. Landford, B. Virgen, D. Gregory, M. C. Johnson, J. Munch, F. Kirchhoff, P. D. Bieniasz, and T. Hatziioannou.** 2009. Nef proteins from simian immunodeficiency viruses are tetherin antagonists. Cell Host Microbe **6:**54–67.

JOURNAL OF VIROLOGY, Oct. 2011, p. 9737–9748 Vol. 85, No. 19
0022-538X/11/$12.00 doi:10.1128/JVI.00479-11

Separable Determinants of Subcellular Localization and Interaction Account for the Inability of Group O HIV-1 Vpu To Counteract Tetherin[▽]

Raphaël Vigan and Stuart J. D. Neil*

Department of Infectious Disease, King's College London School of Medicine, Guy's Hospital, London SE1 9RT, United Kingdom

Received 9 March 2011/Accepted 7 July 2011

Tetherin (BST-2/CD317) is thought to restrict retroviral particle release by cross-linking nascent viral and cellular membranes. Unlike the Vpu proteins encoded by human immunodeficiency virus type 1 (HIV-1) group M strains (M-Vpu), those from the nonpandemic HIV-1 group O (O-Vpu) are not able to counteract tetherin activity. Here, we characterized the basis of this defect in O-Vpu. O-Vpu differs from M-Vpu in that it fails to interact with tetherin and downregulate it from the cell surface. Unlike M-Vpu, O-Vpu localizes to the endoplasmic reticulum (ER) rather than the *trans*-Golgi network (TGN). Interestingly M-Vpu bearing an ER retention signal at the C terminus localizes similarly to O-Vpu. While it still interacts with tetherin, it fails to promote virus release, suggesting that O-Vpu deficiency correlates with its cellular distribution in the endoplasmic reticulum as well as its failure to bind tetherin. O-Vpu–M-Vpu chimeras were designed to identify the minimal changes required to restore tetherin antagonism. While several chimeric proteins bearing residues of the M-Vpu transmembrane domain into the O-Vpu transmembrane domain recovered tetherin binding in coimmunoprecipitation studies, efficient antagonism required an additional glutamic acid-to-lysine change in the membrane-proximal hinge region of the O-Vpu cytoplasmic tail that was sufficient to abolish ER retention and permit TGN localization.

Tetherin is a recently identified antiviral factor that interferes with the late stages of the human immunodeficiency virus type 1 (HIV-1) replication cycle by preventing the release of nascent viral particles from infected cells (38, 59). It is an interferon-induced type II membrane glycoprotein (3, 25, 40) composed of a short cytoplasmic tail (CT), a transmembrane domain (TMD), and an extracellular domain mainly consisting of a coiled-coil region (19, 47, 56, 64), followed by a putative glycophosphatidylinositol (GPI) lipid anchor at the C terminus embedded in cholesterol-rich microdomains at the cellular membrane (25). Tetherin localizes to the plasma membrane (PM) and multiple membrane compartments, including the *trans*-Golgi network (TGN), and recycles via the clathrin-adaptor complex (AP-1 and AP-2) endocytosis machinery (25, 43). The protein's function essentially relies on its unusual structural topology, underscored by the ability to create a completely artificial tetherin-like protein from unrelated protein subunits with similar restriction activity (42). Tetherin is thought to inhibit virus release by being incorporated into nascent virions and directly cross-linking the viral and the cellular membranes (11, 16, 42), leading to the accumulation of fully mature virions at the plasma membrane, followed by internalization and subsequent lysosomal degradation (37, 38). Interestingly, since tetherin does not directly interact with any virally encoded structural protein, it can block a broad spectrum of mammalian enveloped viruses, including retroviruses, Ebola virus, Marburg virus, Lassa fever virus, and Kaposi's sarcoma-associated herpesvirus (KSHV; human herpesvirus 8) (22, 23, 30, 41, 44). Concomitantly, many of these viruses have evolved countermeasures that target tetherin function (5). The prototype of these antagonists is the HIV-1 accessory protein Vpu (38, 59).

Vpu is a 16-kDa phosphoprotein consisting of an N-terminal transmembrane domain and a cytoplasmic tail that forms two alpha helices linked by a conserved DGSNES motif that can be phosphorylated by casein kinase II (55). The interaction of this motif with β-TrCP1 and -2 is required to mediate endoplasmic reticulum (ER)-associated degradation of CD4 (2, 31, 48, 63). The Vpu TM domain is thought to oligomerize to form pentameric cation channels (10, 28, 50) and localizes predominantly to internal membrane structures, including the TGN and endosomes (9, 61). Vpu is not incorporated into HIV-1 particles and therefore must perform its functions within the infected cells. Vpu induces tetherin to be downregulated from the cell surface (59) and degraded (6, 13, 20, 29, 34), although whether this degradation is an absolute requirement to overcome tetherin restriction is still unclear (35). The large fraction of Vpu colocalization with tetherin in the TGN suggests that newly synthesized or recycled tetherin from the cell surface might be sequestered in the TGN (8), similarly to what has been observed with HIV-2 Env (17, 26). Consistent with this, TGN localization of Vpu correlates with antitetherin function (9). Tetherin and Vpu interact with each other via their transmembrane domains (8, 20, 24, 62). Some of the determinants required for the interaction have recently been mapped and form single faces of both proteins' respective TM domains. In the tetherin TM domain, mutations on residues I34, L37, and L41 affect its sensitivity for Vpu (24). In the viral protein, residues A14, W22, and, to a lesser extent, A18 that form one

* Corresponding author. Mailing address: Department of Infectious Disease, King's College London School of Medicine, Guy's Hospital, 2nd Floor, Borough Wing, London SE1 9RT, United Kingdom. Phone: 44 (0)207 188 8279. Fax: 44 (0)207 188 3385. E-mail: stuart.neil@kcl.ac.uk.

▽ Published ahead of print on 20 July 2011.

face of the Vpu TMD are required for tetherin interaction and antagonism (62).

The HIV-1 Vpu protein is able to counteract only human, chimpanzee, and gorilla tetherins. This species specificity resides in the aforementioned TM domain interactions, and several of the determinants in the tetherin TM domain have been subjected to positive selection during primate evolution (14, 33). In simian immunodeficiency virus (SIV) cpz, the direct precursor of HIV-1, the Nef protein rather than Vpu antagonizes chimpanzee tetherin, and the ability of Vpu to target human tetherin is an adaptation that presumably occurred during the zoonosis of this virus to humans (21, 33, 45, 65, 66). To add further to this complexity, only Vpu proteins from HIV-1 group M, the viruses predominantly responsible for the HIV-1 pandemic, can both antagonize tetherin efficiently and degrade CD4. In HIV-1 group O, Vpu proteins are unable to target tetherin but still retain the ability to degrade CD4, whereas this situation is reversed in HIV-1 group N, with Vpu retaining some level of tetherin antagonism but losing activity against CD4 (45). HIV-1 group O infections are limited mainly to Cameroon. While HIV-1 group O-infected individuals can progress to AIDS, the spread of this virus appears to be inefficient compared to group M (32). It has recently been speculated that Vpu adaptation to human tetherin may have therefore been important for the pandemic spread of HIV/AIDS (46).

In this study, we characterized the cell biological basis for the defects in the Vpu proteins from HIV-1 group O (O-Vpu) that impair its ability to antagonize tetherin. We found that O-Vpu is defective both for tetherin binding and also in its subcellular localization to the TGN. These attributes are separable to the TM domain and the membrane-proximal hinge region of the first alpha helix of the cytoplasmic tail, respectively. Simultaneous replacement of these domains in O-Vpu with those from Vpu proteins encoded by HIV-1 group M strains (M-Vpu) are required to reconstitute tetherin antagonism.

MATERIALS AND METHODS

Cells and plasmids. All cells were maintained at 37°C with 5% CO_2 in Dulbecco's modified Eagle's medium (DMEM; Invitrogen, United Kingdom) supplemented with 10% fetal calf serum (FCS) and gentamicin. HEK293T (293T) cells and HeLa cells were obtained from the American Type Culture Collection (ATCC), and the HIV-1 reporter cell line HeLa-TZMbl was kindly provided by John Kappes through the NIH AIDS Reagents Repository Program (ARRP). HeLa/CD4 cells were provided by A. Akrigg through the National Institute of Biological Standards and Controls (NIBSC) Centre for AIDS Reagents (Potters Bar, United Kingdom). The HIV-1 molecular clone plasmid pNL4.3 was obtained from the NIH ARRP, and the Vpu-defective counterpart has been described previously (37). pCR3.1, encoding a codon-optimized HIV-1 NL4.3 Vpu tagged at the C terminus with an HA epitope (pCR3.1-Vpu-HA), mentioned in this study as M-Vpu Wt, was derived from pVphu (kindly provided by K. Strebel through the NIH ARRP) (39). Codon-optimized Vpu group O (O-Vpu) genes derived from HIV-1 group O strains 9435 and HJ001 as well as a consensus sequence assembled from 32 full-length O-Vpu sequences available in the HIV Sequence Database (http://www.hiv.lanl.gov) were synthesized by multiple overlapping PCRs and cloned into the expression vector pCR3.1. O-Vpu mutants and chimeras were generated by QuikChange site-directed mutagenesis and overlapping PCR, respectively, by standard methods using Phusion II polymerase (New England BioLabs). All the sequences were confirmed.

Virus release assays. Subconfluent HEK293T cells were transfected with 500 ng of proviral plasmid in combination with 50 ng of pCR3.1 human tetherin and variable concentrations of pCR3.1-Vpu-HA or mutants thereof using polyethylenimine (1 mg/ml; Polysciences). The medium was replaced 16 h after transfection, and viral supernatants and cell lysates were harvested at 48 h posttransfection and analyzed for infectivity using HeLa-TZMbl indicator cells and particle production by Western blotting and as described previously (62).

Flow cytometry. Subconfluent HeLa cells in 6-well dishes were transfected with 400 ng pCR3.1 encoding enhanced green fluorescent protein (pCR3.1-EGFP) and 400 ng pCR3.1-Vpu-HA. At 48 h posttransfection, the cells were harvested and stained for surface tetherin using a specific anti-BST2 monoclonal IgG2a antibody (Abnova) and a goat anti-mouse IgG2a-allphycocyanin Alexa 633 conjugated as a secondary antibody (Molecular Probes, Invitrogen, United Kingdom). Tetherin expression in green fluorescent protein (GFP)-positive cells was then analyzed using a FACSCalibur flow cytometer (Becton Dickinson) and FlowJo software.

Immunofluorescence microscopy. HeLa cells plated on glass coverslips were transfected with 100 ng of Vpu-HA expression vector. At 24 h posttransfection, the cells were fixed in 4% paraformaldehyde, permeabilized in 0.1% Triton X-100, and immunostained using mouse or rabbit anti-HA antibodies (Covance), a sheep anti-human TGN46 (Serotec), and a mouse anti-protein disulfide isomerase (anti-PDI; Molecular Probes, Invitrogen), followed by the appropriate donkey secondary antibodies coupled to Alexa 488 and 594 fluorophores (Molecular Probes, Invitrogen, United Kingdom). The coverslips were then mounted on slides using ProLong antifade reagent containing 4′,6-diamidino-2-phenylindole (Molecular Probes, Invitrogen, United Kingdom) and examined on a Leica DM-IRE2 confocal microscope.

Immunoprecipitation. Coimmunoprecipitation of tetherin with Vpu-HA from transfected HEK293T cells was performed as described previously (62). Cell lysates and immunoprecipitates were Western blotted for Vpu using mouse anti-HA and tetherin using rabbit anti-BST2 (kindly provided by K. Strebel through the NIH ARRP).

RESULTS

O-Vpu 9435 fails to interact with tetherin or mediate its cell surface downregulation and localizes to ER-associated compartments. HIV-1 group O Vpu has been shown to lack the ability to counteract human tetherin but can still induce CD4 degradation (45). To confirm this, a Vpu gene from HIV-1 group O strain 9435 was synthesized with a C-terminal HA tag and tested for its ability to block tetherin antiviral function. 293T cells were cotransfected with a fixed dose of tetherin plasmid, increasing amounts of Vpu expression vectors, and a proviral plasmid of HIV-1 NL4.3 deleted for the Vpu gene [HIV-1(Vpu^-)]. At 48 h posttransfection, cells were lysed and supernatants were analyzed by Western blotting for p24 and Vpu detection or titrated on HeLa-TZMbl indicator cells (Fig. 1A). As expected, a prototype M-Vpu (NL4.3) efficiently rescues virus production in the presence of tetherin. In contrast, O-Vpu of strain 9435 (O-Vpu 9435) was unable to rescue particle release from tetherin restriction, even at higher plasmid inputs, and was equivalent to an M-Vpu A14L-W22A TM mutant that we have shown previously to be defective for tetherin antagonism (62). All proteins were expressed at comparable levels, and O-Vpu 9435 expression did not affect intracellular Gag protein synthesis (Fig. 1A). Whereas M-Vpu runs on a Western blot as a single species, O-Vpu 9435 appears as a doublet. M-Vpu overcomes human tetherin by mediating its removal from the cell surface and blocking its incorporation into nascent virions. To address whether O-Vpu fails to antagonize tetherin because it cannot induce its downregulation, tetherin-positive HeLa cells were cotransfected with an empty vector control or a Vpu expression vector in combination with a GFP marker plasmid. At 48 h posttransfection, cells were harvested and stained for surface tetherin levels (Fig. 1B). As expected in GFP-positive cells, expression of M-Vpu Wt but not M-Vpu A14L-W22A leads to a decrease of tetherin levels at the cell surface. Expression of O-Vpu 9435 had little effect

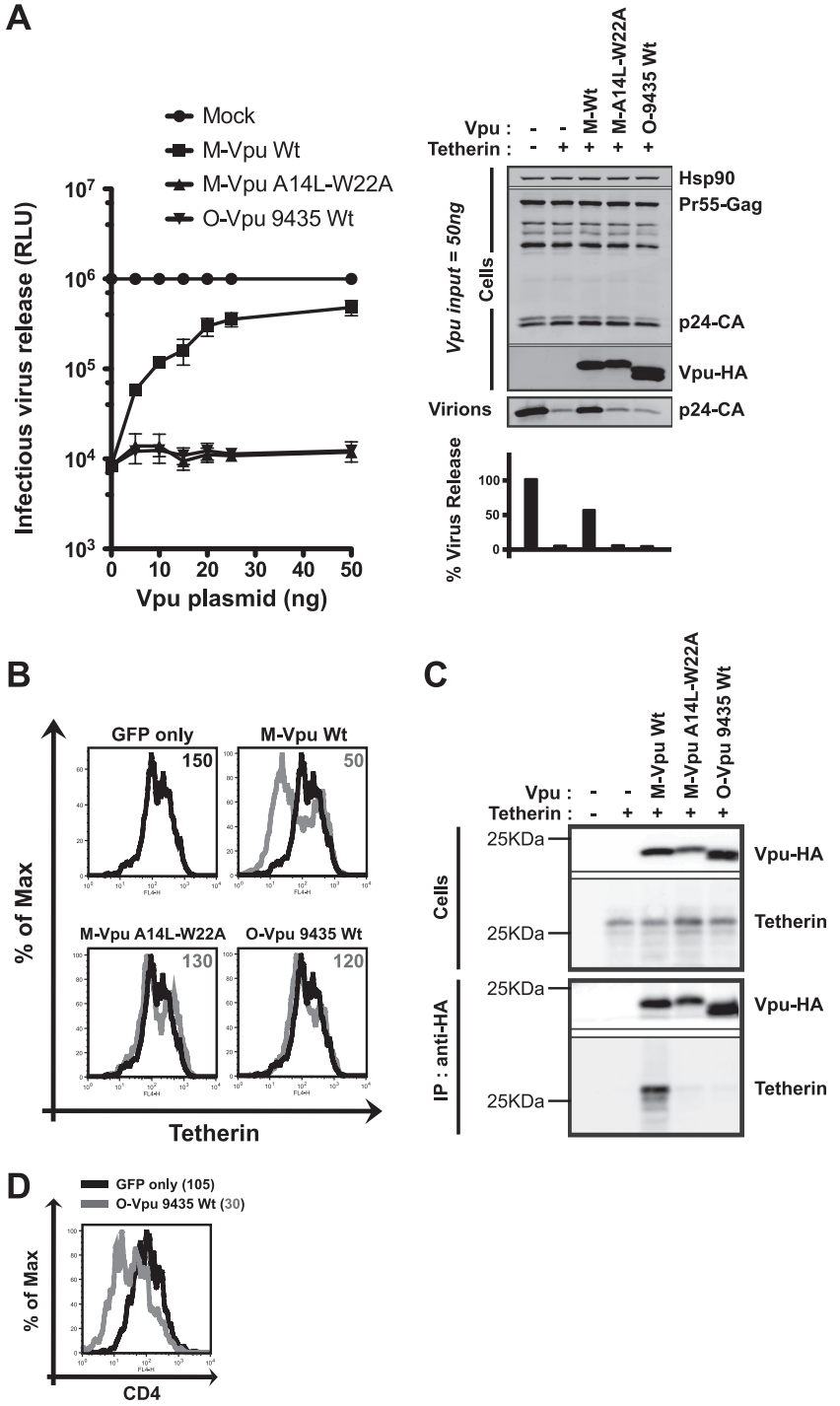

FIG. 1. Defects in tetherin antagonism, binding, and downregulation by O-Vpu 9435. (A) 293T cells were transiently transfected with 500 ng of HIV-1(Vpu$^-$) provirus, 50 ng of tetherin plasmid, and increasing doses of the indicated Vpu expression vector. At 48 h posttransfection, the resulting viral supernatants were assayed for infectivity on HeLa-TZMbl indicator cells by measuring beta-galactosidase activity at 48 h postinfection. Cell lysates and pelleted virions from cells transfected with 50 ng of Vpu plasmid were subjected to SDS-PAGE and blotted for Vpu-HA, p24-CA, and Hsp90 protein, which served as a loading control, and analyzed by a LiCor quantitative imager. Relative virus release was calculated as a percentage of the virion p24 band intensity of the no-tetherin control. RLU, relative light units. (B) HeLa cells were cotransfected with 400 ng of GFP marker plasmid and the indicated Vpu expression vector. At 48 h posttransfection, endogenous surface tetherin was immunostained and expression levels were quantified by flow cytometry. Histograms represent the tetherin levels on GFP-positive gated cells in empty vector control cells (black peak) or in Vpu-expressing cells (overlaid gray peak). Median fluorescence intensities of the overlaid histogram are indicated in the top right corner. (C) 293T cells were transiently transfected with 500 ng of human tetherin-encoding plasmid and 500 ng of the indicated Vpu expression vector. After 2 days of incubation at 37°C, Vpu was immunoprecipitated (IP) via the HA tag from cell lysates and subjected to SDS-PAGE. Total cell lysates and immunoprecipitates were then Western blotted for tetherin and Vpu-HA. Molecular mass markers are indicated, and blots are a representative example of three independent experiments. (D) As in panel B, but the effects of O-Vpu on surface CD4 were examined in transfected HeLa/CD4 cells.

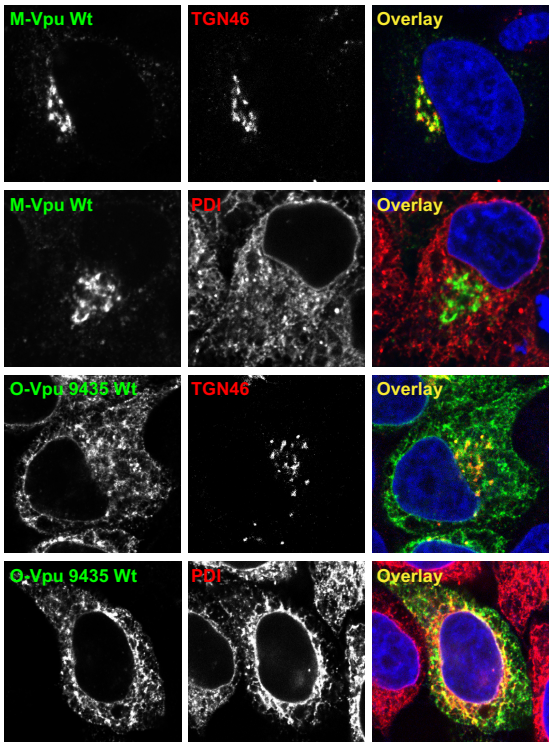

FIG. 2. O-Vpu 9435 localizes to the ER. HeLa cells were transfected by either 100 ng of M-Vpu Wt-HA or O-Vpu Wt-HA plasmid. Twenty-four hours later, the cells were fixed and stained for Vpu detection with anti-HA antibody (green), a TGN marker (TGN46; red), or an ER marker antibody (PDI; red) and examined by confocal microscopy.

on surface tetherin levels. Finally, Vpu mediates tetherin downregulation through interaction via their transmembrane domains. Mutations impairing this interaction render the viral protein incapable of allowing coimmunoprecipitation of tetherin from cell lysates (62). We then assessed the ability of O-Vpu 9435 to interact with tetherin in this assay. 293T cells were cotransfected with tetherin and Vpu-HA expression vectors. Two days after transfection, cells were lysed and Vpu proteins were immunoprecipitated via the HA epitope and analyzed by Western blotting (Fig. 1C). As expected, tetherin coimmunoprecipitates with M-Vpu Wt and not with the transmembrane Vpu mutant (M-Vpu A14L-W22A). Similarly, tetherin also failed to coimmunoprecipitate with O-Vpu 9435, suggesting the lack of a direct interaction between the tetherin TMD and O-Vpu TMD. Finally, despite these defects in tetherin antagonism, as expected, this O-Vpu construct retained the ability to induce CD4 downregulation (Fig. 1D).

Vpu localization in the TGN has been shown to be important to suppress tetherin restriction activity, consistent with Vpu inducing sequestration of tetherin in the TGN (8, 9). Here we addressed whether the O-Vpu 9435 cellular localization accounts for its inability to block tetherin function. HeLa cells were transfected with a Vpu-HA-encoding vector. Twenty-four hours later cells were fixed and immunostained for Vpu-HA and either the ER marker, protein disulfide isomerase (PDI), or the *trans*-Golgi network marker, TGN46 (Fig. 2). As expected, M-Vpu localized in perinuclear compartments that mainly overlay with TGN46-positive compartments but not with PDI. However, although a minor fraction of O-Vpu protein 9435 localizes in the TGN, the majority forms a reticular staining pattern that partially overlays with PDI-positive compartments, suggesting that, unlike M-Vpu, O-Vpu 9435 localizes to ER-associated compartments. Thus, the failure of O-Vpu 9435 to antagonize tetherin correlates both with its inability to interact directly with tetherin and with its lack of accumulation in the TGN.

Retention of M-Vpu in the endoplasmic reticulum prevents tetherin antagonism but does not block their interaction. We next investigated the functional consequences of restricting Vpu expression to the ER. Vpu-induced virus release in T cells is sensitive to brefeldin A (51), suggesting that Vpu function requires post-ER trafficking. However, the broad inhibition of the secretory pathway will also affect tetherin trafficking, potentially confounding this conclusion. To circumvent this, we made a M-Vpu protein bearing an ER retention signal derived from the bovine foamy virus envelope protein (-KKDQ) at the C terminus (12). As expected, M-Vpu KKDQ shows a reticular staining overlapping with PDI-positive compartments, indicative of an ER localization (Fig. 3A), with only a minor fraction of M-Vpu KKDQ proteins localizing with the TGN marker. M-Vpu KKDQ displays weak activity against tetherin restriction, despite increasing doses of plasmid (Fig. 3B), indicating that post-ER trafficking of Vpu is essential for tetherin antagonism. Similarly, transfection of tetherin-positive HeLa cells reveals that M-Vpu KKDQ fails to downregulate tetherin from the plasma membrane (Fig. 3C). However, preventing M-Vpu from leaving the ER does not impair its ability to interact with tetherin in coimmunoprecipitates from transient transfections (Fig. 3D). This was not due to tetherin-Vpu interactions occurring during the immunoprecipitation, as subsequent mixing of cell lysates from 293T cells transfected with either Vpu or tetherin individually failed to yield tetherin coimmunoprecipitating with Vpu-HA (see supplemental Fig. 1 [http://www.kcl.ac.uk/schools/medicine/research/diiid/depts/infectious/groups/neil/]). These data therefore suggest that Vpu and tetherin may interact early in the secretory pathway, but only after exit from the ER is Vpu able to exert its inhibitory effect on tetherin activity. Furthermore, these results suggest that O-Vpu 9435 localization in the endoplasmic reticulum may contribute to its deficiency in tetherin antagonism but does not account for its lack of tetherin interaction.

Defects in tetherin interaction and TGN localization map to the TM domain and first alpha helix of O-Vpu, respectively. We then went on to assess the minimal changes needed in O-Vpu 9435 to allow it to antagonize human tetherin. O-Vpu 9435 and M-Vpu proteins derive from distinct SIVcpz zoonoses and as such are very diverse at the amino acid level. However, they do have basic features known to be important for CD4 degradation (7) (Fig. 4A): first, the conserved W residue in the TM domain (58, 62) and, second, the dual serine motif phosphorylated by CKII that binds to β-TrCP (7). After the TM domain in Vpu is a putative hinge region followed by an amphipathic alpha helix (H1) which has been proposed to lie along the face of the membrane with the nonpolar residues partially submerged and the charged residues interacting with the polar phospholipid heads (4). In contrast, in H1 of O-Vpu the TM-proximal part of the helix is extended by a run of

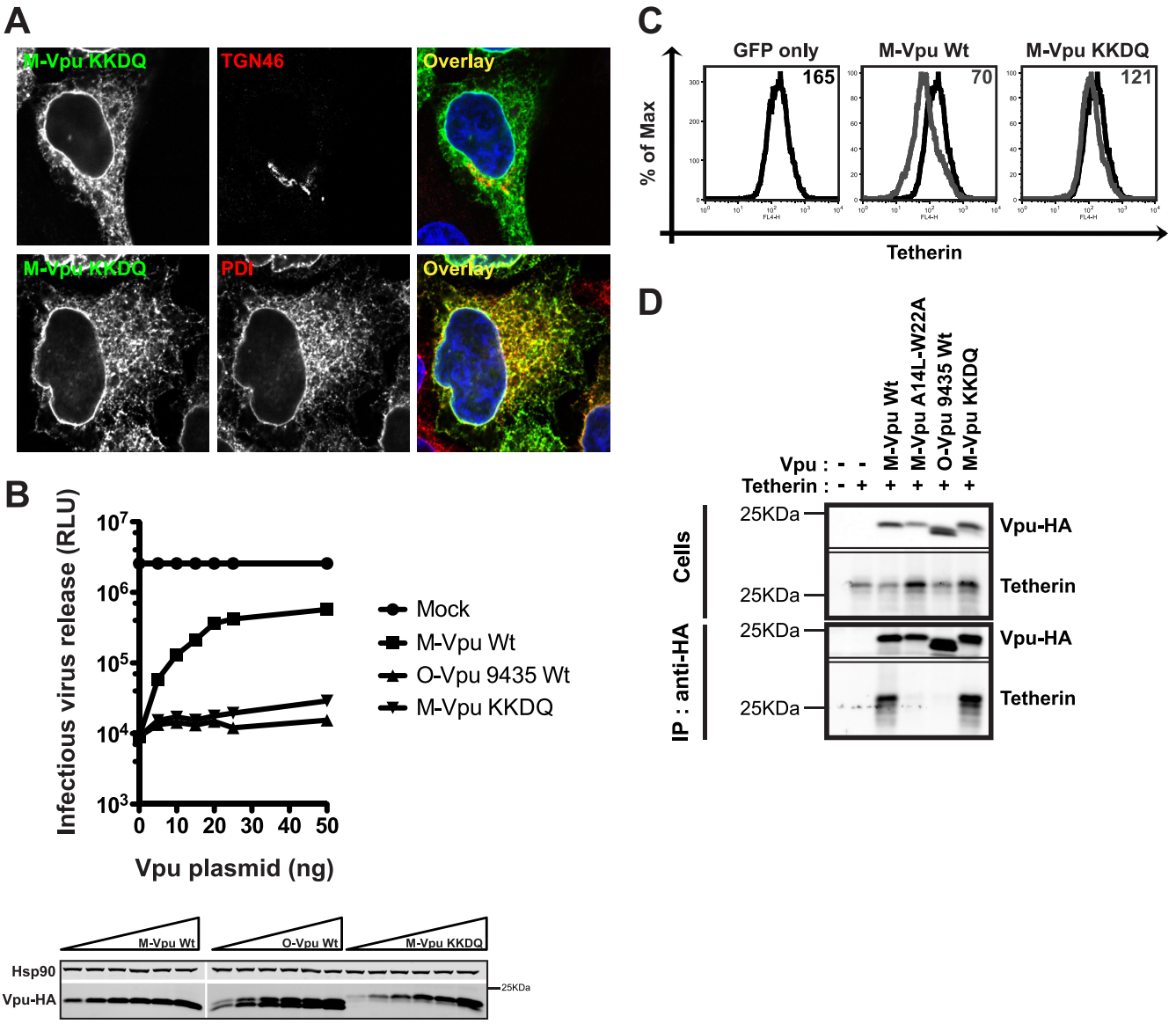

FIG. 3. Retention of M-Vpu in the ER inhibits tetherin antagonism but does not block interaction. (A) HeLa cells were transfected by 100 ng of M-Vpu KKDQ-HA plasmid. Twenty-four hours later, the cells were fixed and stained for Vpu detection with anti-HA antibody (green), a TGN marker (TGN46; red), or an ER marker antibody (PDI; red) and the appropriate secondary antibodies and examined by confocal microscopy. (B) 293T cells were transiently transfected with 500 ng of HIV-1(Vpu$^-$) provirus, 50 ng of tetherin-encoding plasmid, and increasing amounts of the indicated Vpu expression vector. Cells and supernatant-containing viral particles were harvested at 48 h posttransfection. The resulting infectious virions in culture supernatants were titrated on HeLa-TZMbl indicator cells by measuring beta-galactosidase activity at 48 h postinfection. Vpu protein expression in cell lysates was analyzed by Western blotting using an anti-HA antibody. (C) The indicated Vpu constructs were cotransfected in HeLa cells with a GFP-encoding vector, and surface tetherin levels were quantified by flow cytometry at 48 h posttransfection. (D) 293T cells were transiently transfected with 500 ng of human tetherin-encoding plasmid and 500 ng of the indicated Vpu expression vector. After 2 days of incubation at 37°C, Vpu was immunoprecipitated via the HA tag from cell lysates and subjected to SDS-PAGE. Total cell lysates and immunoprecipitates were then Western blotted for tetherin and Vpu-HA detection. Molecular mass markers are indicated, and blots are a representative example of three independent experiments.

alternating basic and acidic residues that breaks its amphipathicity. Chimeric proteins, combining M-Vpu TMD and O-Vpu CT or vice versa, were designed (Fig. 4A). 293T cells were cotransfected with a fixed amount of tetherin, Vpu, and the HIV-1(Vpu$^-$) proviral plasmid. Forty-eight hours later cells were analyzed by Western blotting and titrated on HeLa-TZMbl indicator cells (Fig. 4B). Substitution of the two key residues from M-Vpu TMD, A14 and A18, essential for tetherin interaction (62), into O-Vpu TMD did not result in a functional O-Vpu mutant (O-Vpu B), demonstrating that these residues are not sufficient to confer tetherin antagonism. Although they localized to the TGN (data not shown), chimeras composed of O-Vpu TMD and M-Vpu CT were unable to enhance particle release in tetherin-expressing cells. The same mutant designed by adding the equivalent determinants of M-Vpu TMD into O-Vpu TMD (Vpu OBTM-MCT) did not

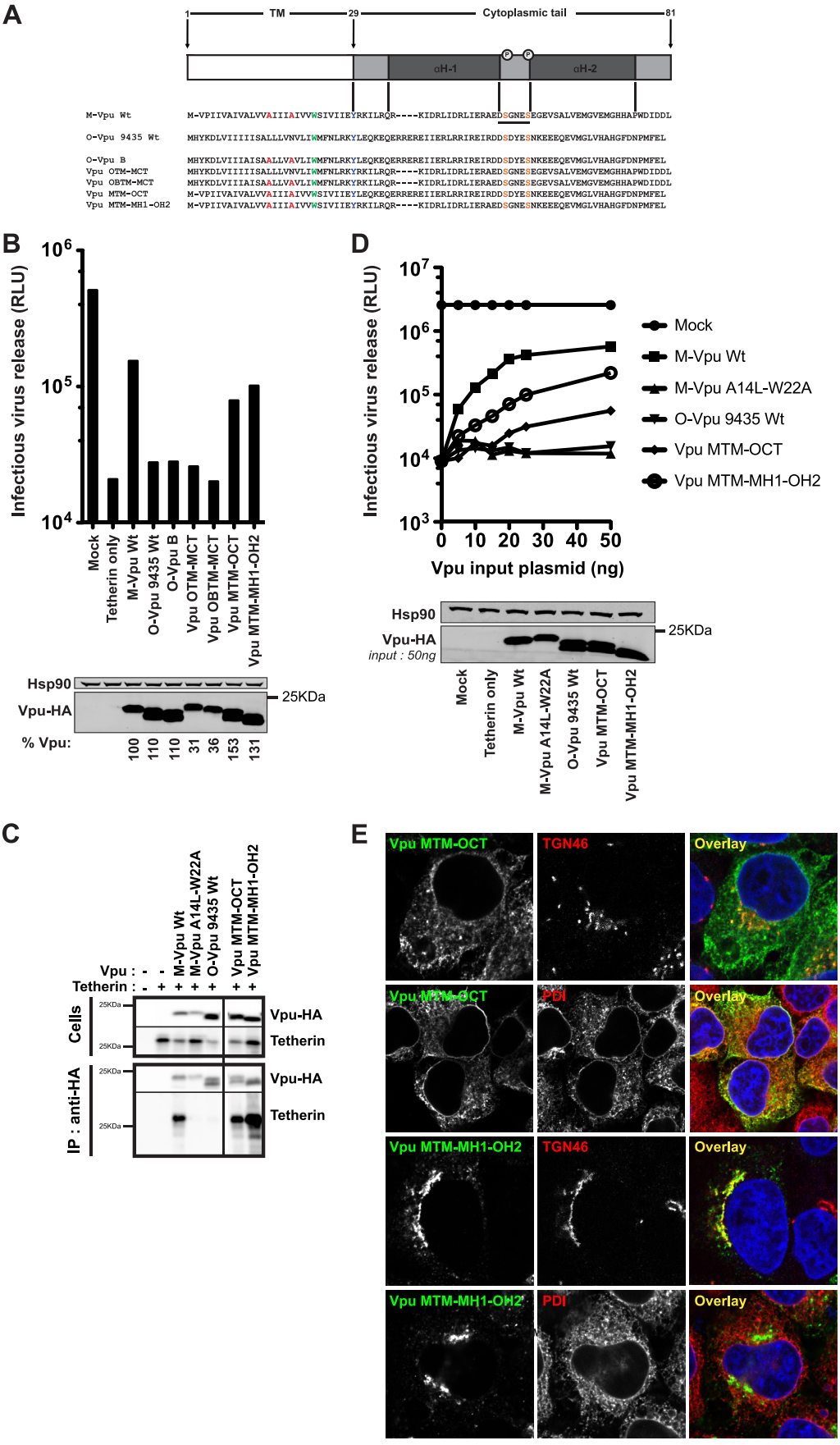
A
TM
Cytoplasmic tail
αH-1
αH-2
M-Vpu Wt
O-Vpu 9435 Wt
O-Vpu B
Vpu OTM-MCT
Vpu OBTM-MCT
Vpu MTM-OCT
Vpu MTM-MH1-OH2
B
Infectious virus release (RLU)
Mock
Tetherin only
M-Vpu Wt
O-Vpu 9435 Wt
O-Vpu B
Vpu OTM-MCT
Vpu OBTM-MCT
Vpu MTM-OCT
Vpu MTM-MH1-OH2
Hsp90
Vpu-HA
25KDa
% Vpu:
100 110 110 31 36 153 131
C
Vpu :
Tetherin :
M-Vpu Wt
M-Vpu A14L-W22A
O-Vpu 9435 Wt
Vpu MTM-OCT
Vpu MTM-MH1-OH2
Cells
IP : anti-HA
Vpu-HA
Tetherin
25KDa
D
Infectious virus release (RLU)
Vpu input plasmid (ng)
Mock
M-Vpu Wt
M-Vpu A14L-W22A
O-Vpu 9435 Wt
Vpu MTM-OCT
Vpu MTM-MH1-OH2
Hsp90
Vpu-HA
input : 50ng
25KDa
E
Vpu MTM-OCT
TGN46
Overlay
PDI
Vpu MTM-MH1-OH2

gain function to suppress tetherin restriction. However, two chimeras that were both composed of an intact M-Vpu TMD gained function against tetherin either in the context of the O-Vpu cytoplasmic tail (Vpu MTM-OCT) or with the M-Vpu first alpha helix (Vpu MTM-MH1-OH2). To characterize these proteins further, Vpu MTM-OCT and Vpu MTM-MH1-OH2 mutants were rescreened against a fixed dose of tetherin but with various expression levels of Vpu. Despite both chimeras being effective at coimmunoprecipitating tetherin (Fig. 4C), only Vpu MTM-MH1-OH2 gained function against tetherin restriction at lower plasmid inputs (Fig. 4D) and at higher expression had activity almost to the levels of M-Vpu Wt. In contrast Vpu MTM-OCT achieved only a low efficiency of tetherin antagonism, even at the highest plasmid inputs. Consistent with the importance of Vpu association with the TGN for tetherin antagonism (9), Vpu MTM-MH1-OH2 but not Vpu MTM-OCT localized predominantly to the TGN rather than the ER (Fig. 4E). Together these data suggest that amino acid differences in the first alpha helix between O-Vpu 9435 and M-Vpu retain the former in ER-like compartments. Thus, the simultaneous replacement of the tetherin interaction domain (TM) in the context of the first alpha helix of M-Vpu sequences that permit TGN localization is required for full antagonism of tetherin.

A single glutamic acid-to-lysine change in the putative hinge region of O-Vpu proteins confers localization to the TGN. We next investigated the determinants in the H1 domain of O-Vpu that account for its localization to the ER. First, we assessed whether ER retention of our O-Vpu 9435 was representative of the known available sequences. To this end, we synthesized an HA-tagged consensus O-Vpu (O-Vpu cons) from all the full-length sequences available in the HIV Sequence Database (http://www.hiv.lanl.gov) ($n = 32$) and, additionally, the Vpu from strain HJ001 (45). As expected, both proteins were defective for counteracting tetherin from transiently transfected 293T cells (Fig. 5A) and failed to interact in coimmunoprecipitations (Fig. 5B), consistent with our previous observations. When we examined the subcellular localization, however, we observed that while Vpu-O cons was again retained in the ER, HJ001 Vpu displayed more prominent localization to the TGN (Fig. 5C). Alignment of the H1 domains of these proteins revealed that a major difference in HJ001 was a membrane-proximal K residue at position 32 instead of an E in Vpu-O cons and 9435 (Fig. 6A). This lysine was present in only a minority of O-Vpu sequences, suggesting that the acidic residue is representative of HIV-1 group O (Fig. 6A). Interestingly, position 32 in O-Vpu is equivalent to K31 in M-Vpu, which is embedded within the putative membrane-proximal hinge YRKILR. Mutation of R30-K31 to alanines in HIV-1 NL4.3 Vpu was previously shown to lead to an endosomal localization and a concomitant decrease in antitetherin activity (9). To determine whether this residue also plays a role in O-Vpu localization, we replaced the hinge region with the equivalent part of M-Vpu in the context of the M-Vpu TM domain (MTM-RKILR-OCT). In addition, we also made the E32K point mutation in O-Vpu 9435 and MTM-OCT. When transfected into 293T cells with tetherin, MTM-RKILR-OCT and MTM-OCT E32K both regained function equivalent to that of the MTM-MH1-OH2 chimera, indicating that this single amino acid change was sufficient to enhance tetherin antagonism (Fig. 6B). As expected, the E32K change on its own did not confer tetherin antagonism to O-Vpu due to its TM domain's inability to interact with tetherin (data not shown). Examination of the localization of these Vpu proteins revealed that unlike the parental O-Vpu, MTM-RKILR-OCT, MTM-OCT E32K, and O-Vpu E32K all displayed localization to TGN46-positive compartments (Fig. 6C). In contrast, the reciprocal mutation, K31E, in the context of M-Vpu was not sufficient to restrict the protein's localization to ER-associated compartments (data not shown). Thus, a single acidic residue present in the hinge region of the majority of O-Vpu sequences precludes the protein from leaving ER-associated compartments and is responsible for their poor activity against human tetherin even when TM-mediated interaction is restored.

DISCUSSION

The ability to counteract tetherin is a conserved attribute of primate lentiviruses, although the viral protein that performs this function varies (46). While tetherin antagonism is associated with the Vpu proteins of the SIVgsn/mon/mus lineage, their descendant, SIVcpz Vpu, lacks this activity, probably due to redundancy with a Nef protein acquired via recombination from a SIVrcm-related virus (45). Adaptation of HIV-1 Vpu to human tetherin is therefore associated with the genetic changes that accompanied the zoonosis of SIVcpz to humans, which has happened at least four times in the last century, giving rise to groups M, N, O, and P (18). The Vpu proteins of most group M viruses tested can counteract tetherin (45). In contrast, group O Vpu proteins are defective for this attribute, and in the few sequences from group N, Vpu counteraction of tetherin is variable (45). In this study, we have addressed the molecular and cell biological basis for the difference between M-Vpu and O-Vpu proteins. We have shown that O-Vpu is defective for tetherin antagonism for two reasons. First and most important, its TM domain lacks the capacity to interact

FIG. 4. Defects in O-Vpu can be rescued by replacement of the TM domain in the context of the M-Vpu first alpha helix. (A) Schematic representation of the Vpu topology and alignments comparing Vpu sequences from HIV-1 group M and group O or the indicated mutants. (B) 293T cells were transfected with the HIV-1(Vpu$^-$) provirus, a fixed dose of tetherin plasmid, and the indicated Vpu construct. After 2 days, viral supernatants were assayed on HeLa-TZMbl indicator cells and cells lysates were analyzed by Western blotting for Vpu-HA and Hsp90. Numbers below indicate the Vpu expression levels normalized with Hsp90 expression levels compared to the M-Vpu Wt protein expression. (C) The indicated Vpu constructs were coexpressed in 293T cells with 500 ng of human tetherin-encoding plasmid. At 48 h posttransfection, cells were lysed and Vpu proteins were isolated via immunoprecipitation and subjected to SDS-PAGE. Both tetherin and Vpu-HA expressions were visualized on a Western blot using the appropriate antibodies. (D) Same as in panel B but with various doses of the indicated Vpu mutants added in *trans*. (E) The indicated Vpu-HA chimeras (green) were transiently expressed in HeLa cells and coimmunostained either with a TGN marker (TGN46; red) or with an ER marker (PDI; red).

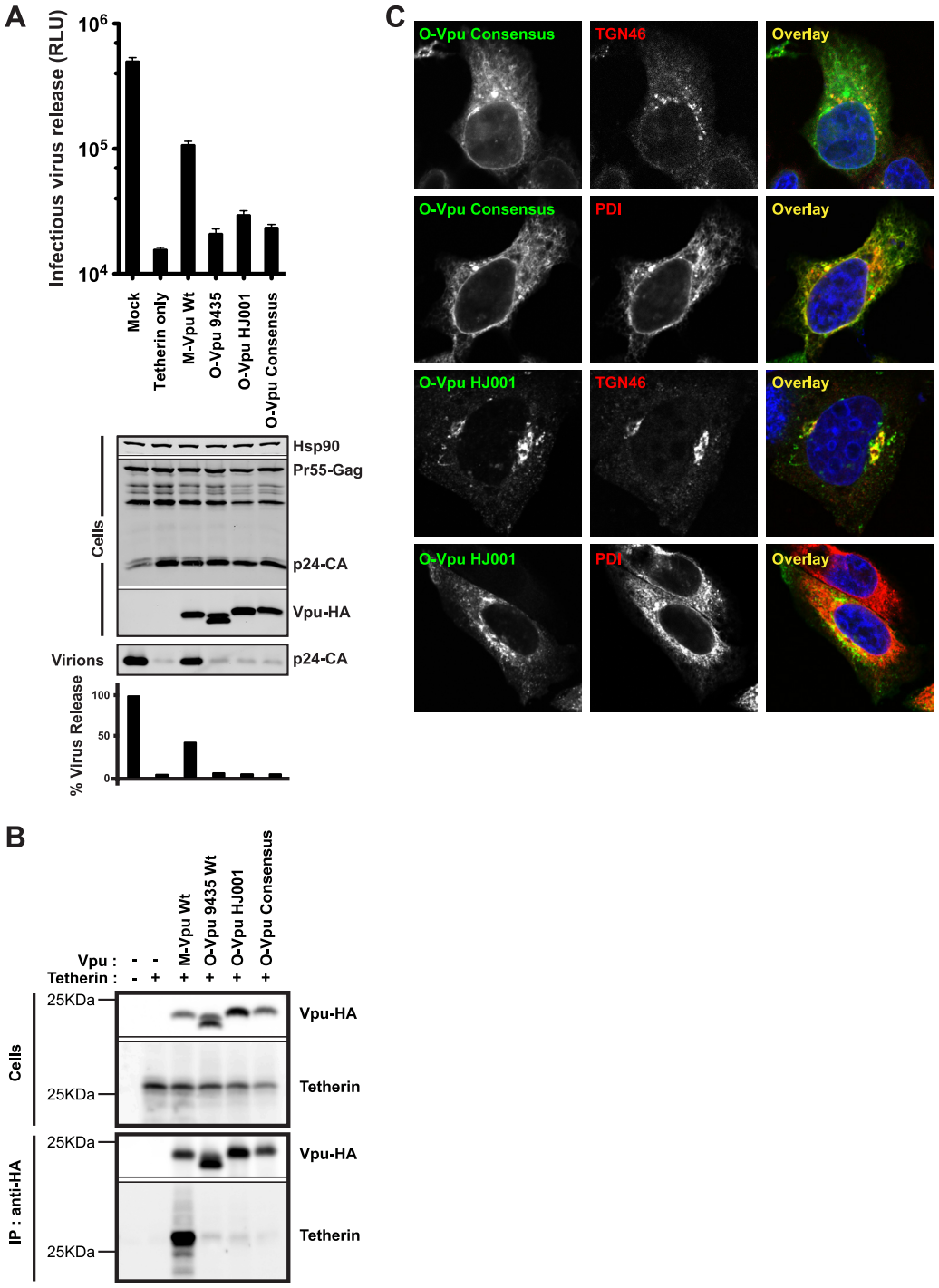

FIG. 5. Antitetherin activities and subcellular localizations of a consensus O-Vpu and O-Vpu HJ001. (A) Counteraction of tetherin-mediated restriction of HIV-1(Vpu$^-$) from transfected 293T cells by the indicated O-Vpu-HA construct and corresponding Western blots of cell lysates and pelleted virions as described in the legend to Fig. 1. (B) Coimmunoprecipitation of O-Vpu-HA proteins with tetherin from transiently transfected 293T cells as described in the text. (C) Subcellular localization of the indicated O-Vpu-HA (green) in transfected HeLa cells costained either with a TGN marker (TGN46; red) or with an ER marker (PDI; red).

with tetherin in coimmunoprecipitations. However, the ability to bind tetherin is not sufficient to confer antagonism to O-Vpu. O-Vpu appears to be retained in the ER and fails to localize to the TGN. This maps to the first alpha helix of the cytoplasmic tail, specifically, a glutamic acid residue at position 32, found in the majority of O-Vpu sequences. Replacement of this region is also required for efficient tetherin antagonism. Second, we further show that ER retention of M-Vpu fails to antagonize tetherin, despite maintaining the ability to interact with tetherin.

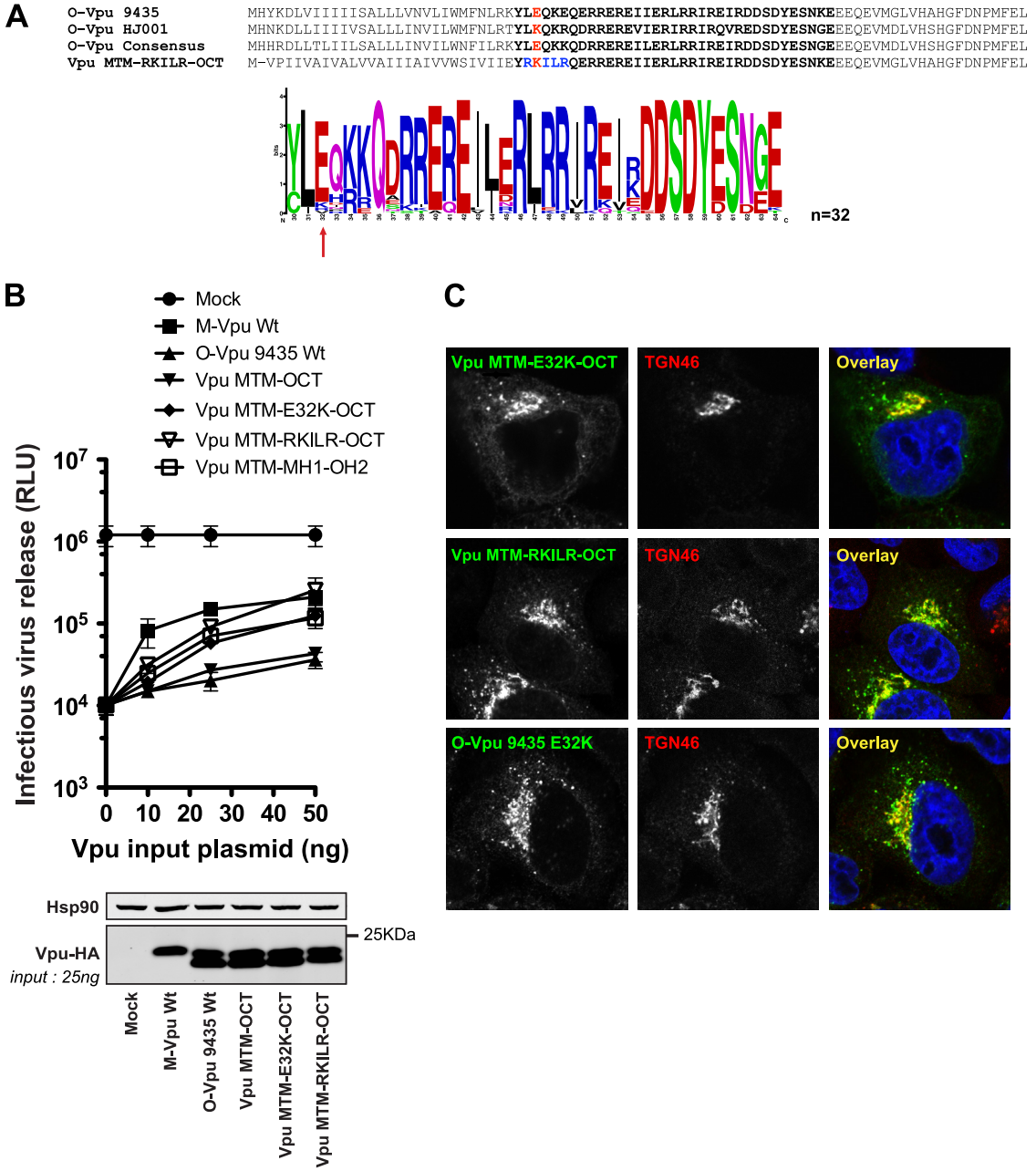

FIG. 6. An E32K point mutation confers TGN localization and tetherin antagonism to O-Vpu bearing the group M TM domain. (A) Alignment of the consensus O-Vpu, O-Vpu 9435, and O-Vpu HJ001 sequences (above) and expanded logoplot of the amino acid sequences of the first alpha helix of publicly available O-Vpu sequences ($n = 32$) (below). Position E32 is indicated (red arrow). (B) 293T cells were transfected with 500 ng of HIV-1(Vpu$^-$), 50 ng of tetherin, and various doses of the indicated Vpu-HA construct and processed as described in the legend to Fig. 4. (C) Subcellular localization of the indicated O-Vpu-HA (green) in transfected HeLa cells costained with a TGN marker (TGN46; red).

We showed previously that mutation of conserved residues A14, A18, and W22, which form one face of the M-Vpu TM domain, impairs tetherin interaction and antagonism (62). The A14 and A18 positions are conserved in M- and N-Vpu proteins but not in group O or SIVcpz Vpu proteins, suggesting that changes to this face of the TM domain helix may have been driven by adaptation of HIV-1 Vpu to human tetherin. The O-Vpu TM domain failed to interact with human tetherin in coimmunoprecipitations; however, replacement of these residues is not sufficient to confer tetherin interaction to O-Vpu. Moreover, in attempts to delineate the minimal requirements to render the O-Vpu TM domain capable of mediating tetherin antagonism in the context of MTM-MH1, no chimeric TM domain gained function (data not shown). These results suggest that the functional binding interface of Vpu with tetherin is likely to be contextually dependent on the entire conformation of the TM domain.

The retention of O-Vpu in ER-associated compartments

confers a defect to antagonism even when interaction with tetherin is mediated through a chimeric TM domain. This can be partially overcome by increased Vpu expression, which we interpret as being due to minor amounts of O-Vpu being observable in the TGN at high expression levels. Several years ago Schubert and Strebel demonstrated that brefeldin A inhibited Vpu-mediated HIV-1 release from infected T cells (51), and the same laboratory has recently confirmed these data, in the light of the discovery of tetherin (1). However, because brefeldin A blocks the bulk flow of secretory proteins from the ER, including tetherin, we attempted to alleviate any potential confounding factors by appending a strong ER retention signal to M-Vpu. ER-retained M-Vpu was clearly defective for tetherin antagonism, but unlike O-Vpu, it was still able to interact with tetherin in coimmunoprecipitates, in contrast to a recent report (54). This suggests that while tetherin and Vpu can interact in the ER, antagonism of tetherin function requires trafficking of Vpu-tetherin complexes into TGN compartments. Recent data from the Strebel group have further shown that under overexpression conditions, Vpu can induce ER-associated degradation of newly synthesized tetherin, but this does not happen in virus-infected cells (1). Thus, if Vpu and tetherin do interact prior to ER exit, the appending of the -KKDQ motif leads to disruption of this interaction when the Vpu is retrieved from the *cis*-Golgi network. However, to definitively show whether this is the case will require further fluorescence resonance energy transfer-based microscopy studies of Vpu-tetherin interactions in living cells.

The inability of O-Vpu to exit the ER maps to the membrane-proximal region of the first alpha helix of the cytoplasmic tail. The amphipathic nature of helix 1 is thought to allow it to lie partially buried along the face of the membrane with the basic residues in contact with the phospholipid heads (4). Between the TM domain and the first alpha helix is a putative hinge region, the basic residues of which in subtype B Vpu proteins have been implicated in endosome-to-TGN localization when mutated to hydrophobic residues (9). We found that replacement of the hinge region in O-Vpu 9435 with the corresponding RKILR of M-Vpu conferred both TGN localization and efficient tetherin antagonism when combined with the M-Vpu TM domain. This phenotype mapped to an acidic residue (E32) in the position equivalent to M-Vpu K31 that is conserved in the majority of O-Vpu proteins. Since the reverse mutation in M-Vpu did not lead to its ER retention, these data suggest to us that it is unlikely that this is a specific TGN-targeting motif itself. Rather, we suggest that the distribution of basic and acidic residues in the membrane-proximal region of the O-Vpu may influence the overall conformation of the cytoplasmic tail in relation to the membrane and that the retention of O-Vpu in ER-associated compartments may be related to such a structural change. It is interesting to note that O-Vpu 9435 and chimeric molecules bearing its first alpha-helical region run as a doublet on SDS-polyacrylamide gels, perhaps suggesting potential differences in conformation or phosphorylation. Since O-Vpu still downmodulates CD4, a process that requires interaction with the Vpu cytoplasmic tail and its phosphorylation, such putative conformational differences do not affect this ER-associated process. However, they do preclude tetherin antagonism without high overexpression. Interestingly, while the majority of O-Vpu proteins have an E at position 32, a minority of sequences has K at this position and hence display increased TGN localization (exemplified by O-Vpu HJ001). The lack of a TMD-mediated interaction still precludes tetherin antagonism in this case.

The Vpu protein of SIVcpz is able to downregulate CD4 but cannot target tetherin, presumably because this function became redundant when the ancestral virus acquired a tetherin-antagonizing Nef protein from the SIVrcm lineage (45). Unlike the result with the TM domain of O-Vpu, replacement of the TM domain of consensus SIVcpzUS Vpu with that of HIV-1 M-Vpu is sufficient to confer tetherin antagonism (27). Groups M, N, O, and P represent four distinct zoonoses of SIVcpz strains to humans. Group O is also highly related to SIVgor, suggesting that both viruses have derived from the same SIVcpz strain relatively recently (less than 200 years) (57, 60). Whether group O was acquired directly from gorillas or whether these are separate zoonoses of the same virus from chimpanzees is not clear. However, they were transmitted to humans, and in each case the zoonotic virus would have initially been unable to target human tetherin due to the loss of the Nef-targeting determinant in the human protein's cytoplasmic tail (21, 45, 66). In the case of groups M and N, it is likely that the TM adaptation of the SIVcpz Vpu proteins was sufficient to adapt to tetherin antagonism, although N-Vpu proteins appear to have lost the ability to degrade CD4, the reason for which is unclear at present (45). CD4 targeting is conserved in all other known HIV-1/SIV Vpu proteins, indicating that this is also an essential function and is maintained, despite Nef performing a similar role, further suggesting spatial and temporal differences for CD4 targeting. It is interesting to speculate that the competing pressure to maintain CD4 degradation in the more distantly related SIVcpz that gave rise to HIV-1 group O precluded its adaptation to human tetherin because of its ER retention. In SIVcpz infections in chimpanzees, the requirement of the protein to leave the ER efficiently may have been under less pressure to be maintained because SIVcpz Nef antagonized tetherin in this species and was lost. Alternatively, if group O was primarily derived from SIVgor, these differences in Vpu may be a reflection of the SIVcpz Vpu process of adaptation to new hosts in relatively quick succession. To understand this further, more detailed molecular and cellular characterization of SIV Vpu proteins is required. Furthermore, Vpu, like Nef, may have other targets, in addition to CD4 and tetherin. Recent studies have implicated a role for Vpu in downregulating CD1d and NTB-A to avoid killing of infected cells by NK T cells and NK cells, respectively (36, 53). Therefore, the adaptation of any SIV Vpu in a new species is liable to be subject to further pressure to maintain functions against these and other yet-to-be-identified immunomodulatory targets.

It has recently become clear that primate lentiviruses are under evolutionary pressure to maintain an activity that counteracts tetherin. That O-Vpu and at least some N-Vpu proteins have no such activity has led to speculation that this Vpu function may account for the lack of efficient spread of groups N and O in humans compared to group M (46). Furthermore, evidence from HIV-2 in human and Nef-defective SIVmac-infected macaques suggests that when tetherin antagonism is compromised, viruses that restore the activity in their envelope glycoproteins can emerge (15, 26, 52). It should be borne in

mind that group N and O viruses still retain the capacity to cause AIDS in infected individuals, and at present, it is not known whether the failure of O-Vpu to adapt to human tetherin has forced the acquisition of tetherin antagonism on the O-group Env. This is all the more plausible given that there is at least one documented case of an HIV-1 envelope glycoprotein with Vpu-like activity (49).

ACKNOWLEDGMENTS

We thank the members of the Neil lab for support and are grateful to Klaus Strebel, John Kappes, and Bruce Chesebro for reagents supplied through the NIH AIDS Research and Reference Reagent Program.

This work was funded by Wellcome Research Career Development Fellowship WTO82274MA and MRC grant G0801937 to S.J.D.N.

R.V. and S.J.D.N. designed the experiments; R.V. performed the experiments; R.V. and S.J.D.N. analyzed the data and wrote the paper.

REFERENCES

1. **Andrew, A. J., E. Miyagi, and K. Strebel.** 2010. Differential effects of human immunodeficiency virus type 1 Vpu on the stability of BST-2/tetherin. J. Virol. **85:**2611–2619.
2. **Binette, J., et al.** 2007. Requirements for the selective degradation of CD4 receptor molecules by the human immunodeficiency virus type 1 Vpu protein in the endoplasmic reticulum. Retrovirology **4:**75.
3. **Blasius, A. L., et al.** 2006. Bone marrow stromal cell antigen 2 is a specific marker of type I IFN-producing cells in the naive mouse, but a promiscuous cell surface antigen following IFN stimulation. J. Immunol. **177:**3260–3265.
4. **Bour, S., and K. Strebel.** 2003. The HIV-1 Vpu protein: a multifunctional enhancer of viral particle release. Microbes Infect. **5:**1029–1039.
5. **Douglas, J. L., et al.** 2010. The great escape: viral strategies to counter BST-2/tetherin. PLoS Pathog. **6:**e1000913.
6. **Douglas, J. L., et al.** 2009. Vpu directs the degradation of the human immunodeficiency virus restriction factor BST-2/tetherin via a β-TrCP-dependent mechanism. J. Virol. **83:**7931–7947.
7. **Dube, M., M. G. Bego, C. Paquay, and E. A. Cohen.** 2010. Modulation of HIV-1-host interaction: role of the Vpu accessory protein. Retrovirology **7:**114.
8. **Dube, M., et al.** 2010. Antagonism of tetherin restriction of HIV-1 release by Vpu involves binding and sequestration of the restriction factor in a perinuclear compartment. PLoS Pathog. **6:**e1000856.
9. **Dube, M., et al.** 2009. Suppression of tetherin-restricting activity upon human immunodeficiency virus type 1 particle release correlates with localization of Vpu in the trans-Golgi network. J. Virol. **83:**4574–4590.
10. **Ewart, G. D., T. Sutherland, P. W. Gage, and G. B. Cox.** 1996. The Vpu protein of human immunodeficiency virus type 1 forms cation-selective ion channels. J. Virol. **70:**7108–7115.
11. **Fitzpatrick, K., et al.** 2010. Direct restriction of virus release and incorporation of the interferon-induced protein BST-2 into HIV-1 particles. PLoS Pathog. **6:**e1000701.
12. **Goepfert, P. A., et al.** 1999. An endoplasmic reticulum retrieval signal partitions human foamy virus maturation to intracytoplasmic membranes. J. Virol. **73:**7210–7217.
13. **Goffinet, C., et al.** 2009. HIV-1 antagonism of CD317 is species specific and involves Vpu-mediated proteasomal degradation of the restriction factor. Cell Host Microbe **5:**285–297.
14. **Gupta, R. K., et al.** 2009. Mutation of a single residue renders human tetherin resistant to HIV-1 Vpu-mediated depletion. PLoS Pathog. **5:**e1000443.
15. **Gupta, R. K., et al.** 2009. Simian immunodeficiency virus envelope glycoprotein counteracts tetherin/BST-2/CD317 by intracellular sequestration. Proc. Natl. Acad. Sci. U. S. A. **106:**20889–20894.
16. **Hammonds, J., J. J. Wang, H. Yi, and P. Spearman.** 2010. Immunoelectron microscopic evidence for tetherin/BST2 as the physical bridge between HIV-1 virions and the plasma membrane. PLoS Pathog. **6:**e1000749.
17. **Hauser, H., et al.** 2010. HIV-1 Vpu and HIV-2 Env counteract BST-2/tetherin by sequestration in a perinuclear compartment. Retrovirology **7:**51.
18. **Heeney, J. L., A. G. Dalgleish, and R. A. Weiss.** 2006. Origins of HIV and the evolution of resistance to AIDS. Science **313:**462–466.
19. **Hinz, A., et al.** 2010. Structural basis of HIV-1 tethering to membranes by the BST-2/tetherin ectodomain. Cell Host Microbe **7:**314–323.
20. **Iwabu, Y., et al.** 2009. HIV-1 accessory protein Vpu internalizes cell-surface BST-2/tetherin through transmembrane interactions leading to lysosomes. J. Biol. Chem. **284:**35060–35072.
21. **Jia, B., et al.** 2009. Species-specific activity of SIV Nef and HIV-1 Vpu in overcoming restriction by tetherin/BST2. PLoS Pathog. **5:**e1000429.
22. **Jouvenet, N., et al.** 2009. Broad-spectrum inhibition of retroviral and filoviral particle release by tetherin. J. Virol. **83:**1837–1844.
23. **Kaletsky, R. L., J. R. Francica, C. Agrawal-Gamse, and P. Bates.** 2009. Tetherin-mediated restriction of filovirus budding is antagonized by the Ebola glycoprotein. Proc. Natl. Acad. Sci. U. S. A. **106:**2886–2891.
24. **Kobayashi, T., et al.** 2011. Identification of amino acids in the human tetherin transmembrane domain responsible for HIV-1 Vpu interaction and susceptibility. J. Virol. **85:**932–945.
25. **Kupzig, S., et al.** 2003. Bst-2/HM1.24 is a raft-associated apical membrane protein with an unusual topology. Traffic **4:**694–709.
26. **Le Tortorec, A., and S. J. Neil.** 2009. Antagonism to and intracellular sequestration of human tetherin by the human immunodeficiency virus type 2 envelope glycoprotein. J. Virol. **83:**11966–11978.
27. **Lim, E. S., H. S. Malik, and M. Emerman.** 2010. Ancient adaptive evolution of tetherin shaped the functions of Vpu and Nef in human immunodeficiency virus and primate lentiviruses. J. Virol. **84:**7124–7134.
28. **Maldarelli, F., M. Y. Chen, R. L. Willey, and K. Strebel.** 1993. Human immunodeficiency virus type 1 Vpu protein is an oligomeric type I integral membrane protein. J. Virol. **67:**5056–5061.
29. **Mangeat, B., et al.** 2009. HIV-1 Vpu neutralizes the antiviral factor tetherin/BST-2 by binding it and directing its beta-TrCP2-dependent degradation. PLoS Pathog. **5:**e1000574.
30. **Mansouri, M., et al.** 2009. Molecular mechanism of BST2/tetherin downregulation by K5/MIR2 of Kaposi's sarcoma-associated herpesvirus. J. Virol. **83:**9672–9681.
31. **Margottin, F., et al.** 1998. A novel human WD protein, h-beta TrCp, that interacts with HIV-1 Vpu connects CD4 to the ER degradation pathway through an F-box motif. Mol. Cell **1:**565–574.
32. **Mauclere, P., et al.** 1997. Serological and virological characterization of HIV-1 group O infection in Cameroon. AIDS **11:**445–453.
33. **McNatt, M. W., et al.** 2009. Species-specific activity of HIV-1 Vpu and positive selection of tetherin transmembrane domain variants. PLoS Pathog. **5:**e1000300.
34. **Mitchell, R. S., et al.** 2009. Vpu antagonizes BST-2-mediated restriction of HIV-1 release via beta-TrCP and endo-lysosomal trafficking. PLoS Pathog. **5:**e1000450.
35. **Miyagi, E., A. J. Andrew, S. Kao, and K. Strebel.** 2009. Vpu enhances HIV-1 virus release in the absence of Bst-2 cell surface down-modulation and intracellular depletion. Proc. Natl. Acad. Sci. U. S. A. **106:**2868–2873.
36. **Moll, M., S. K. Andersson, A. Smed-Sorensen, and J. K. Sandberg.** 2010. Inhibition of lipid antigen presentation in dendritic cells by HIV-1 Vpu interference with CD1d recycling from endosomal compartments. Blood **116:**1876–1884.
37. **Neil, S. J., S. W. Eastman, N. Jouvenet, and P. D. Bieniasz.** 2006. HIV-1 Vpu promotes release and prevents endocytosis of nascent retrovirus particles from the plasma membrane. PLoS Pathog. **2:**e39.
38. **Neil, S. J., T. Zang, and P. D. Bieniasz.** 2008. Tetherin inhibits retrovirus release and is antagonized by HIV-1 Vpu. Nature **451:**425–430.
39. **Nguyen, K. L., et al.** 2004. Codon optimization of the HIV-1 vpu and vif genes stabilizes their mRNA and allows for highly efficient Rev-independent expression. Virology **319:**163–175.
40. **Ohtomo, T., et al.** 1999. Molecular cloning and characterization of a surface antigen preferentially overexpressed on multiple myeloma cells. Biochem. Biophys. Res. Commun. **258:**583–591.
41. **Pardieu, C., et al.** 2010. The RING-CH ligase K5 antagonizes restriction of KSHV and HIV-1 particle release by mediating ubiquitin-dependent endosomal degradation of tetherin. PLoS Pathog. **6:**e1000843.
42. **Perez-Caballero, D., et al.** 2009. Tetherin inhibits HIV-1 release by directly tethering virions to cells. Cell **139:**499–511.
43. **Rollason, R., V. Korolchuk, C. Hamilton, P. Schu, and G. Banting.** 2007. Clathrin-mediated endocytosis of a lipid-raft-associated protein is mediated through a dual tyrosine motif. J. Cell Sci. **120:**3850–3858.
44. **Sakuma, T., T. Noda, S. Urata, Y. Kawaoka, and J. Yasuda.** 2009. Inhibition of Lassa and Marburg virus production by tetherin. J. Virol. **83:**2382–2385.
45. **Sauter, D., et al.** 2009. Tetherin-driven adaptation of Vpu and Nef function and the evolution of pandemic and nonpandemic HIV-1 strains. Cell Host Microbe **6:**409–421.
46. **Sauter, D., A. Specht, and F. Kirchhoff.** 2010. Tetherin: holding on and letting go. Cell **141:**392–398.
47. **Schubert, H. L., et al.** 2010. Structural and functional studies on the extracellular domain of BST2/tetherin in reduced and oxidized conformations. Proc. Natl. Acad. Sci. U. S. A. **107:**17951–17956.
48. **Schubert, U., et al.** 1998. CD4 glycoprotein degradation induced by human immunodeficiency virus type 1 Vpu protein requires the function of proteasomes and the ubiquitin-conjugating pathway. J. Virol. **72:**2280–2288.
49. **Schubert, U., S. Bour, R. L. Willey, and K. Strebel.** 1999. Regulation of virus release by the macrophage-tropic human immunodeficiency virus type 1 AD8 isolate is redundant and can be controlled by either Vpu or Env. J. Virol. **73:**887–896.
50. **Schubert, U., et al.** 1996. Identification of an ion channel activity of the Vpu transmembrane domain and its involvement in the regulation of virus release from HIV-1-infected cells. FEBS Lett. **398:**12–18.
51. **Schubert, U., and K. Strebel.** 1994. Differential activities of the human immunodeficiency virus type 1-encoded Vpu protein are regulated by phos-

phorylation and occur in different cellular compartments. J. Virol. **68:**2260–2271.
52. **Serra-Moreno, R., B. Jia, M. Breed, X. Alvarez, and D. T. Evans.** 2011. Compensatory changes in the cytoplasmic tail of gp41 confer resistance to tetherin/BST-2 in a pathogenic Nef-deleted SIV. Cell Host Microbe **9:**46–57.
53. **Shah, A. H., et al.** 2010. Degranulation of natural killer cells following interaction with HIV-1-infected cells is hindered by downmodulation of NTB-A by Vpu. Cell Host Microbe **8:**397–409.
54. **Skasko, M., et al.** 2011. BST-2 is rapidly down-regulated from the cell surface by the HIV-1 protein Vpu: evidence for a post-ER mechanism of Vpu-action. Virology **411:**65–77.
55. **Strebel, K.** 2007. HIV accessory genes Vif and Vpu. Adv. Pharmacol. **55:**199–232.
56. **Swiecki, M., et al.** 2011. Structural and biophysical analysis of BST-2/tetherin ectodomains reveals an evolutionary conserved design to inhibit virus release. J. Biol. Chem. **286:**2987–2997.
57. **Takehisa, J., et al.** 2009. Origin and biology of simian immunodeficiency virus in wild-living western gorillas. J. Virol. **83:**1635–1648.
58. **Tiganos, E., et al.** 1998. Structural and functional analysis of the membrane-spanning domain of the human immunodeficiency virus type 1 Vpu protein. Virology **251:**96–107.
59. **Van Damme, N., et al.** 2008. The interferon-induced protein BST-2 restricts HIV-1 release and is downregulated from the cell surface by the viral Vpu protein. Cell Host Microbe **3:**245–252.
60. **Van Heuverswyn, F., et al.** 2007. Genetic diversity and phylogeographic clustering of SIVcpzPtt in wild chimpanzees in Cameroon. Virology **368:**155–171.
61. **Varthakavi, V., et al.** 2006. The pericentriolar recycling endosome plays a key role in Vpu-mediated enhancement of HIV-1 particle release. Traffic **7:**298–307.
62. **Vigan, R., and S. J. Neil.** 2010. Determinants of tetherin antagonism in the transmembrane domain of the human immunodeficiency virus type 1 Vpu protein. J. Virol. **84:**12958–12970.
63. **Willey, R. L., F. Maldarelli, M. A. Martin, and K. Strebel.** 1992. Human immunodeficiency virus type 1 Vpu protein induces rapid degradation of CD4. J. Virol. **66:**7193–7200.
64. **Yang, H., et al.** 2010. Structural insight into the mechanisms of enveloped virus tethering by tetherin. Proc. Natl. Acad. Sci. U. S. A. **107:**18428–18432.
65. **Yang, S. J., et al.** 2010. Anti-tetherin activities in Vpu-expressing primate lentiviruses. Retrovirology **7:**13.
66. **Zhang, F., et al.** 2009. Nef proteins from simian immunodeficiency viruses are tetherin antagonists. Cell Host Microbe **6:**54–67.